CONFORMATIONALLY PREORGANIZED CARBOCYCLIC AND BACKBONE EXTENDED PYRROLIDINE PEPTIDE NUCLEIC ACIDS: CHEMICAL SYNTHESIS AND BIOPHYSICAL STUDIES

THESIS SUBMITTED TO

THE UNIVERSITY OF PUNE

FOR THE DEGREE OF

DOCTOR OF PHILOSOPHY

IN CHEMISTRY

BY

GOVINDARAJU, T

DIVISION OF ORGANIC CHEMISTRY (SYNTHESIS)

NATIONAL CHEMICAL LABORATORY

PUNE 411 008

February 2005

DEDICATED TO MY MOTHER

National Chemical Laboratory

Division of Organic Chemistry (Synthesis)

Pune - 411 008. INDIA
Telefax: 91 (20) 2589 3153

Email: kng@ems.ncl.res.in

Dr. K. N. Ganesh, FNA, FASc

Head
Organic Chemistry Synthesis

CERTIFICATE

This is to certify that the work presented in the thesis entitled **"CONFORMATIONALLY PREORGANIZED CARBOCYCLIC AND BACKBONE EXTENDED PYRROLIDINE PEPTIDE NUCLEIC ACIDS: CHEMICAL SYNTHESIS AND BIOPHYSICAL STUDIES"** submitted by Govindaraju, T. was carried out by the candidate at National Chemical Laboratory, Pune, under my supervision. Such materials as obtained from other sources have been duly acknowledged in the thesis.

February 2005

Dr. K. N. Ganesh

Research Guide

Head, Division of Organic Chemistry (synthesis)

National Chemical Laboratory

Pune 411 008.

CANDIDATE'S DECLARATION

I here by declare that the thesis entitled "**CONFORMATIONALLY PREORGANIZED CARBOCYCLIC AND BACKBONE EXTENDED PYRROLIDINE PEPTIDE NUCLEIC ACIDS: CHEMICAL SYNTHESIS AND BIOPHYSICAL STUDIES**" submitted for the degree of Doctor of Philosophy in Chemistry to the University of Pune has not been submitted by me to any other university or institution. This work was carried out at the National Chemical Laboratory, Pune, India.

National Chemical Laboratory **Govindaraju, T**

Pune 411 008.

February 2005

ACKNOWLEDGEMENT

It gives me an immense pleasure to express my deep sense of gratitude towards my research guide Dr. K. N. Ganesh for all the advice, guidance, support and encouragement during every stage of this work. He made me realize the importance of doing quality research, in a better way at crucial stage of my career, of coarse is a turning point. He taught me each and every aspect of research, from working table to formulation of ideas to presentation of results. Although this eulogy is insufficient, I preserve an everlasting gratitude for him.

I am very much grateful to Dr. V. A. Kumar for her constant support and the fruitful discussion we had throughout the coarse of my thesis work. The confidence she had in me, willingness to share new ideas, excitements helped me in a real sense to shape my research career.

I take this opportunity to thank my teachers Suresh and Dr. Hari Prasad, Bangalore University, for their encouragement and motivation.

My special thanks to Mrs.Anita Gunjal and Dr.A. A. Natu for their help and encouragement during the coarse of this work.

I am also thankful to Mrs. M. V. Mane and Mrs. S. S. Kunte for HPLC analysis, Mrs. Shantakumari, for mass analysis. The kind support from NMR group is greatly acknowledged and thanks to Dr. Rajmohanan and Dr. usha palgune.

My thanks are also due to Dr. Mohan Bhadbhade and Mr. Rajesh Gonnade for their help in X-ray analysis. I also thank Dr. Srinivas Hotha for his kind cooperation at the last stage of my thesis work.

I would like to place on record my thanks to Dr. Vairamani, IICT, Hyderabad and Dr. K. P. Madhusudanan, SAIF, CDRI, Lucknow for their help in recording MALDI-TOF spectra.

I sincerely thank my seniors and colleagues for their help in various capacities, co-operation and maintaining cheerful atmosphere in the lab. Thank you Pradeep, Ramesh, Meena, Moneesha, Nagamani, Dinesh, Nagendra, Raman, Praveen, Umashankara, Gourishankar, Khirud, Sridher, Madhuri, Smita, Patwa, Ashwini, geetali and rupa. I also thank Pawar and Bhumkar for their assistance.

I have no words to express my gratitude to my mother, without knowing where and what I am doing, just wishing me all the time with no expectations. My father would have been happiest man today, but I feel his blessings and dreams are definitely everlasting motivation for me. I also thank all my family members; their expectations and hope kept me awake all along.

My heartfelt thanks go to Vasanth and Manju, Bangalore for being so helpful as link between me and my family and……Without their support, life would have become worse for me.

I thank Shamasundar, Dr. K. N. Rao, Dr. Kumbar, Dr. Yenjarappa, Dr. Bennur, Bhoje Gowda, Ravi, Prasanna, Sumanth, Sachin, Prakash, Suresh, Manish, Sathya, Girish, Tiwari, Subha Rao, Sushil, Jadab, Manas, Rajendra, Sanki, Sudhir, Ashish, Shashi, Shankar, Thiru, Devraj, Muruli, Manoj and Gourav for their cheerful company and making my NCL life very lively and enjoyable.

I take this opportunity to thank each and every person who have helped and supported me throughout my education period.

I thank director NCL, for allowing me to work in this premier institute, providing the infrastructure and his great sense of appreciation and recognition is highly inspirational.

It is my sincere thanks to CSIR, New Delhi, for the financial support. In fact the fellowship was the seeding to take up research career at that time and not the curiosity or interest I had in doing science.

Govindaraju, T

CONTENTS

PUBLICATIONS

1. Govindaraju, T.; Gonnade, R. G.; Bhadbhade, M. M.; Kumar, V. A.; Ganesh, K. N: (1*S,*2*R/*1*R,*2*S*)-Aminocyclohexyl Glycyl Thymine PNA: Synthesis, Monomer Crystal Structures, and DNA/RNA Hybridization Studies. ***Org. Lett***. **2003**, *5*, 3013-3016.

2. Govindaraju, T.; Kumar, V. A.; Ganesh, K. N: Synthesis and Evaluation of (1*S*,2*R*/1*R*,2*S*)-Aminocyclohexyl-glycyl PNAs as Conformationally Pre-organized PNA Analogues for DNA/RNA Recognition. ***J. Org. Chem***. **2004**, *69*, 1858-1865

3. Govindaraju, T.; Kumar, V. A.; Ganesh, K. N: *cis*-Cyclopentyl PNA (*cp*PNA) as constrained chiral PNA analogues: Stereochemical dependence of DNA/RNA hybridization. ***Chem. Commun***. **2004**, 860-861.

4. Govindaraju, T.; Kumar, V. A.; Ganesh, K. N: (1*S*,2*R*/1*R*,2*S*)-*cis*-Cyclopentyl PNA (*cp*PNA) as constrained PNA analogues: Synthesis and Evaluation of *aeg-cp*PNA chimera and Stereopreferences in hybridization with DNA/RNA**.** ***J. Org. Chem***. **2004**, *69*, 5725-5734.

5. Govindaraju, T.; Kumar, V. A: Backbone Extended Pyrrolidine Peptide Nucleic Acids (*bep*PNA): Synthesis, Characterization and DNA/RNA binding Studies. ***Chem. Commun***. **2005**, 495-497.

6. Govindaraju, T.; Kumar, V. A. Ganesh, K. N: Cyclohexanyl and Cyclopentanyl PNAs: Conformationally preorganized PNAs with steric filters for selective binding of RNA. **2004**, (***J. Am. Chem. Soc***. Revised submitted).

7. Govindaraju, T: Microwave assisted fast and clean conversion of mesylate to azide: Synthesis of (1*S*,2*R/*1*R,*2*S*)-1-azido-2-carbocyclic amines, immediate precursor to vicinal-1,2- *cis*-diamines. ***Indian J. Chem. B*** **2005**, (in press).

Symposia attended/Poster presentations

1. **Seventh National Symposium in Bio-Organic Chemistry**, Guru Nanak Dev University, Amritsar, India, 9th–10th November, 2001. Poster, PP-21; Pyrrolidine Peptide Nucleic Acids: Oligonucleotide Analogues with Chiral Peptide Backbone: Meena, Govindaraju, T.; Kumar, V. A.; Ganesh, K. N.

2. **Fourth National Symposium of the Chemical Research Society of India**, National Chemical Laboratory, Pune, India, 2002.

3. **XXXIII National Seminar on Crystallography** during 8-10 January 2004 held at National Chemical Laboratory, Pune 411 008, India. Poster, P-41: Design, Synthesis and X-ray Crystal structures of *cis*-Cyclohexyl and Cyclopentyl PNA monomers: Govindaraju, T.; Gonnade, R. G.; Bhadbhade, M. M.; Kumar, V. A.; Ganesh, K. N.

4. **IUPAC International Conference on Biodiversity and Natural products**: Chemistry and Medical Applications (ICOB-4 & ISCNP-24)-BNP-2004, Delhi, India, 26-31 Jan. 2004, Poster, P-107: Backbone extended Pyrrolidine Peptide Nucleic Acid: Synthesis, Characterization and cDNA Binding Studies: Govindaraju, T.; Kumar, V. A.; Ganesh, K. N: Selected for **Best poster award**.

Oral presentations

1. **RSC-student symposium**, West India section, held at IIT-Bombay from 24th-25th Sept 2004. Govindaraju, T.; Kumar, V. A.; Ganesh, K. N. Title: Designed carbocyclic peptide nucleic acids for DNA/RNA discrimination.

2. **J-NOST, National level symposium** for junior organic chemists held at National chemical Laboratory, Pune from 8th-10th Nov 2004. Govindaraju, T.; Kumar, V. A.; Ganesh, K. N. Title: Carbocyclic and backbone extended pyrrolidine peptide nucleic acids for DNA/RNA discrimination.

Awards

1. The "**Keerti Sangoram Endowment Award**" for best research scholar, 2004: National Chemical Laboratory, Pune 411008, India.

2. The "**Best Poster Award**": Poster, P-107: Backbone extended Pyrrolidine Peptide Nucleic Acid: Synthesis, Characterization and cDNA Binding Studies: Govindaraju, T.; Kumar, V. A.; Ganesh, K. N: presented at **IUPAC International Conference** on Biodiversity and Natural products: Chemistry and Medical Applications BNP-2004, Delhi, India, on 26-31 Jan. 2004.

ABSTRACT

The thesis entitled "**CONFORMATIONALLY PREORGANIZED CARBOCYCLIC AND BACKBONE EXTENDED PYRROLIDINE PEPTIDE NUCLEIC ACIDS: CHEMICAL SYNTHESIS AND BIOPHYSICAL STUDIES**" is divided into 5 chapters as follows

Chapter 1: **Introduction**: In the area of modified nucleic acids, there have been several modified molecules reported to date. However, the unmodified oligonucleotides are rapidly identified and cleaved by the action of nucleases that primarily hydrolyze the phosphodiester of the internucleoside backbone. Furthermore, the ability of the negatively charged DNA to cross phospholipid cell membrane is poor. Hence structural modifications are needed to enable oligonucleotides to be used as antisense therapeutic agents in biological systems and also to understand the structural changes that they introduce in the oligonucleotides incorporating them. The structural changes include the modifications in nucleobase, phosphodiester linkage and/or the sugar moiety (Figure 1). Among all these, peptide nucleic acids (PNA) are found to mimic many of the oligonucleotide properties, composed of *N*-(2-aminoethyl)glycine units to which natural nucleobases are attached *via* methylenecarbonyl linker (Figure 1, *aeg*PNA), an acyclic sugar-phosphate backbone modification. PNA binds to complementary DNA and RNA to form duplexes *via* Watson-crick base pairs and triplexes through Watson-crick base pair and Hoogsteen hydrogen bonding that exhibit thermal stability higher than that of DNA:DNA and DNA:RNA complexes. Because of higher thermal stability of PNA hybrids and stability to proteases and nucleases, PNAs are of great interest in medicinal chemistry, with potential for the development as gene-targeted drugs (antigene and antisense) and as reagents in molecular biology and diagnostics. However, the use PNA in antisense drug design limited because of its equal affinity in binding to both DNA as well as RNA. This non-discrimination of identical DNA and RNA sequences, important problem from application perspective has not been addressed.

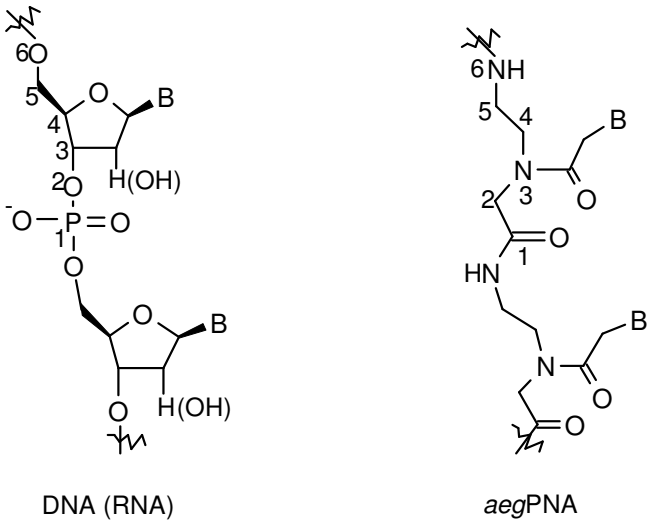

Figure 1. Chemical structures of DNA (RNA) and PNA.

An analysis of the X-ray structural data of PNA_2:DNA triplex, PNA:DNA duplex and NMR data of PNA:RNA duplex suggests that the dihedral angle β could be a key factor (Figure 2). The preferred values for the PNA_2:DNA triplex and PNA:RNA duplex is in the range 65-70°

while that for the PNA:DNA duplex is about ~140°, suggesting that it may be possible to impart DNA/RNA binding selectivity by restricting β to 65-70° range through suitable modification.

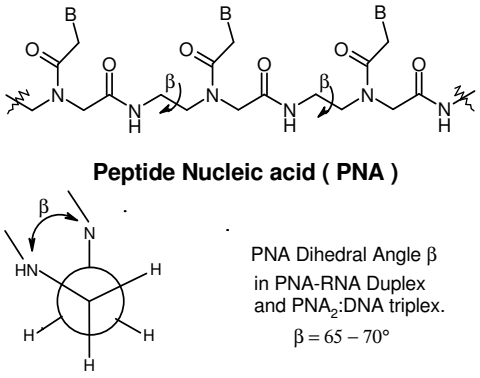

Figure 2. Dihedral angle β in PNA:DNA (RNA) complexes

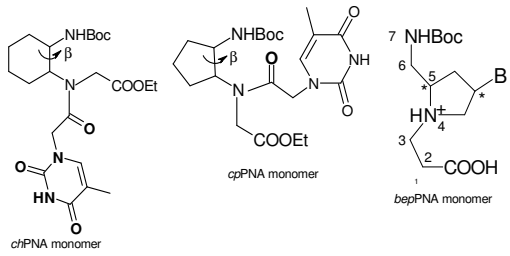

Figure 3. Designed target monomers

Objective: It occurred to us that in (1*S*,2*R*) and (1*R*,2*S*) cyclohexyl (pentyl) PNAs with *cis* stereochemistry, the dihedral angle β would be around 65° and hence these may be more suitable analogs for incorporation into PNA backbone. Particularly in *cis*-cyclohexyl system the dihedral angle over the axial-equatorial substituents will be in the required range and will slightly less in *cis*-cyclopentyl system. The PNAs derived from two enantiomeric units will provide entropic advantage as well as the chirality introduces the orientation in binding to DNA/RNA. The cyclohexyl and cyclopentyl monomers as shown in Figure 3 were designed, synthesized and the torsion angles were determined from their single crystal X-ray structures of both enantiomers.

<u>Chapter 2</u>: Synthesis and Evaluation of (1*S*,2*R*)-and (1*R*,2*S*)-Aminocyclohexylglycyl PNAs (*ch*PNA) as conformationally Preorganized PNA Analogues for DNA/RNA Recognition

Through the *cis*-cyclohexyl modification (Figure 4), chirality and conformational constraint are simultaneously conferred on the classical PNA backbone to influence the orientation of binding, strike a balance between entropy and enthalpy and more importantly to introduce discrimination in binding to RNA and DNA. These properties will influence the over all physico-chemical and biological properties of the so derived PNAs. The two enantiomers of the *cis*-cyclohexyl PNA monomer were synthesized from the chirally pure (1*S*,2*R*) and (1*R*,2*S*)-cyclohexyl-1,2-diamines in their optically pure form. Unlike the *trans*-cyclohexyl-1,2-diamines which are available commercially, *cis*-cyclohexyl-1,2-diamines are not available because of the difficulty involved or no viable route available to synthesize them in their chirally pure form. We have selected the enzymatic route for the synthesis of target monomers because of their fascinating substrate selectivity and activity. The optical purities of enantiomers obtained from the enzymatic resolution are always better than from any other method.

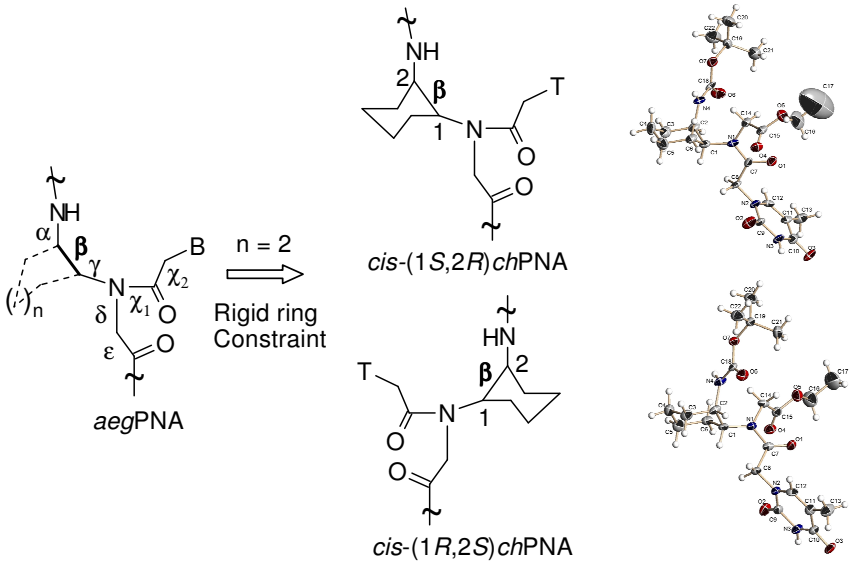

Figure 4. Structures of *aeg*PNA and designed chiral *cis*-(1*S*,2*R*)- and (1*R*,2*S*)-amino cyclohexyl PNAs (*ch*PNA) with crystal structures of corresponding monomers

Synthesis of *cis*-(1*S*,2*R*)-11a and (1*R*,2*S*)-11b aminocyclohexyl thymine monomers: The synthesis started with the resolution of mixture of (+) and (-)-*trans*-2-azido cyclohexanol **2** (Scheme 1) using enzyme *Pseudomonas Cepacia* lipase (Amano-PS). The enantiopurity of both (*1R,2R*) **2a** and (1*S,2S*) **2b** isomers was confirmed by comparing with known values for the optical rotations reported in the literature and by ^{13}C NMR using the chiral chemical shift reagent Eu *(hfc)*$_3$. The target monomers were synthesized from optically pure azido alcohols following the reaction steps shown in Scheme 2. The torsion angles β as deduced from the X-ray crystal structure (Figure 4) for **10a**(1*S,2R*) and **10b**(1*R*,2*S*) are –63^o and +66^o respectively which are closer in magnitude to that found in PNA$_2$:DNA and PNA:RNA complexes, with difference in their relative signs as expected for the enantiomeric pairs (Table 1, Chapter 3). *aeg*PNA monomers were synthesized according to literature procedure.

Biophysical Studies of *ch*PNAs: Various *ch*PNA decamers (**13**-**19**, Table 1) incorporating one or two *cis*-(1*S*,2*R*/1*R*,2*S*)-amino cyclohexyl glycyl thymine PNA monomers in different positions were synthesized. To investigate the binding selectivity, specificity and discrimination of *ch*PNAs towards complementary DNA and RNA, first the stoichiometry of the *ch*PNA:DNA was determined using Job's method. The UV-melting studies were carried out with all the synthesized oligomers and the T_m data was compared with the control *aeg*PNA T$_{10}$ (Table 1). The stability of the *ch*PNA duplexes with DNA/RNA was also studied (Table 1). The CD spectra of single strands and corresponding complexes with complementary DNA were recorded. Finally the complexation of these *ch*PNAs to complementary DNA was confirmed by gel electrophoretic shift assay. Due to a higher binding affinity of PNA:DNA complexes compared

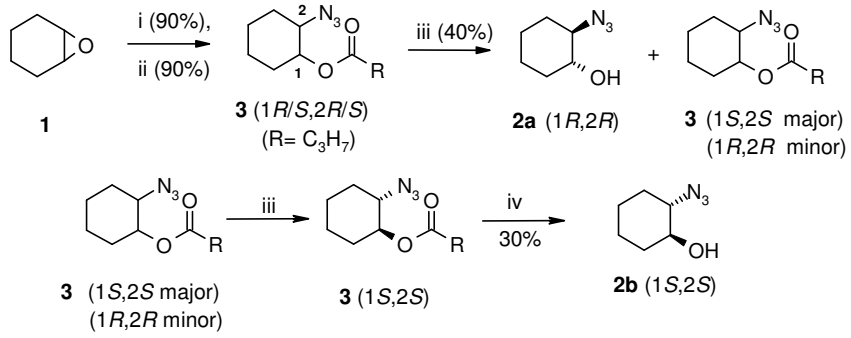

Scheme 1: Reagents and conditions: (i) NaN_3, NH_4Cl, *aq*-Ethanol, reflux, 18 h. (ii) n-Butyric anhydride, dry pyridine, DMAP (cat), rt, 16 h. (iii) *Pseudomonas cepacia* (Lipase), phosphate buffer, pH 7.2, 2.5 h. (iv) NaOMe in MeOH

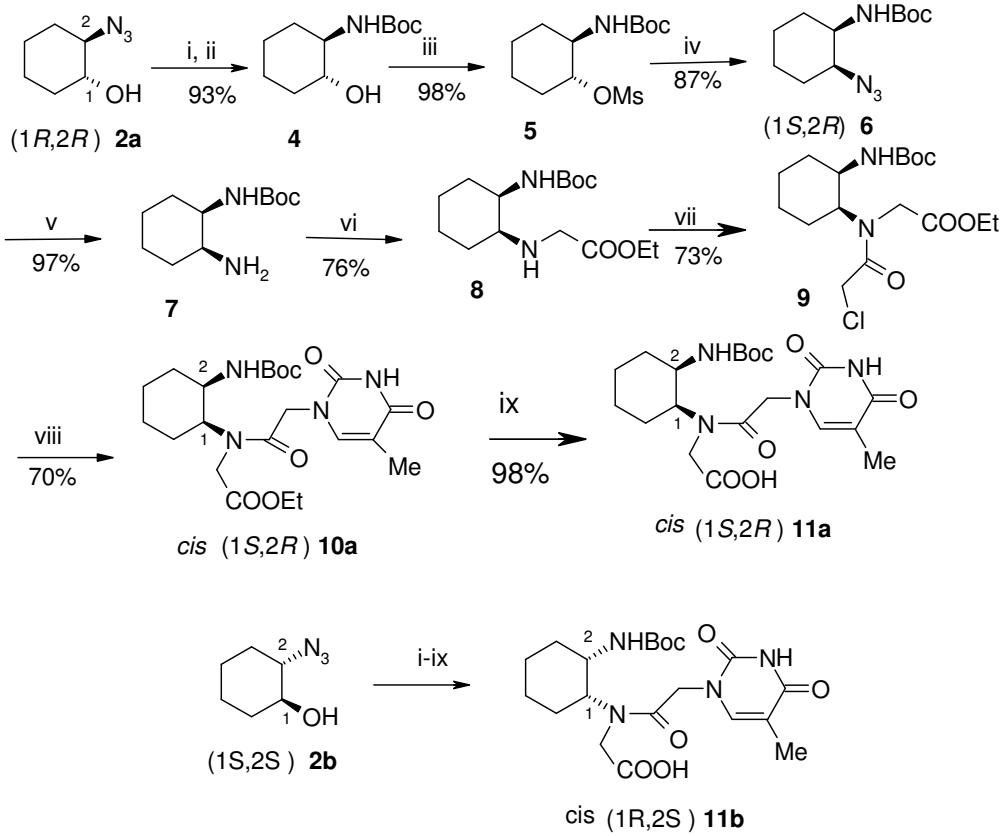

Scheme 2: Reagent and conditions (i) PtO_2, dry EtOAc, H_2, 35-40 psi, rt, 3.5 h; (ii) $Boc)_2O$ (iii) MsCl, dry Pyridine, DMAP, 0-5°C, 5 h; (iv) NaN_3, dry DMF, 72°C, 8 h; (v) PtO_2, MeOH, H_2, 35-40 psi, rt, 3.5 h; (vi) $BrCH_2COOEt$, KF-Celite, dry CH_3CN, rt, 4 h; vii) $ClCH_2COCl$, Na_2CO_3, Dioxan: H_2O (1:1), 0°C, 30 min.; (viii) Thymine, K_2CO_3 dry DMF, 60-65°C, 3.5 h.; (ix) 0.5 M LiOH, aq. THF, 0.5 h.

with DNA:DNA complexes, the added PNA binds to the complementary DNA strand (d(GCGA$_{10}$GCG) in the DNA complex, releasing the DNA strand (d(GCGT$_{10}$GCG).

The *ch*PNA imparts an unprecedented selectivity for binding RNA over DNA for duplex and triplex formation. An interesting difference in duplex formation by the mixed base sequence of *ch*PNA and triplex formation by homopyrimidine *ch*PNA oligomers is in the stereochemical preferences: *RS*>*SR* in duplex stabilization while *SR* > *RS* in triplex stabilization.

Table 1. Melting temperatures (T_m, °C) of PNA:DNA/RNA hybrids[a]

Entry	PNA sequences	DNA	RNA
1	*aeg*PNA **12** H-TTTTTTTTTT-Lys-NH_2	69.2	>80.0
2	*ch*PNA **13** H-TTTTT$_{SR}$TTTTT-Lys-NH_2	41.1	77.2
3	*ch*PNA **14** H-TTTTT$_{RS}$TTTTT-Lys-NH_2	45.0	70.7
4	*ch*PNA **15** H-T$_{SR}$TTTT$_{SR}$TTTTT-Lys-NH_2	34.4	64.4
5	*ch*PNA **16** H-T$_{RS}$TTTT$_{RS}$TTTTT-Lys-NH_2	37.5	58.6
6	*aeg*PNA **17**. H-G T AGATCACT-LysNH_2	55.0	55.4
7	*ch*PNA **18**. H-G T$_{SR}$ AGAT$_{SR}$CACT$_{SR}$-LysNH_2	25.0	58.0
8	*ch*PNA **19**. H-G T$_{RS}$ AGAT$_{RS}$CACT$_{RS}$-LysNH_2	35.0	>85

a T_m = melting temperature (measured in Buffer. 10 mM Sodium phosphate, pH 7.0 with 100 mM NaCl and 0.1 mM EDTA). Measured from 10 to 90° C at ramp 0.2° C/min. UV-absorbance measured at 260 nm. All values are an average of 3 independent experiments and accurate to within ± 50.5° C. RNA = poly rA/ 5' AGUGAUCUAC. nd = not detected. DNA = dCGCA$_{10}$CGC/ 5' AGTGATCTAC

<u>Chapter 3</u>: (1*S*,2*R*)-and (1*R*,2*S*)-*cis*-Aminocyclopentylglycyl PNAs (*cp*PNA) as Conformationally Constrained analogues: Synthesis and Evaluation of *aeg*PNA-*cp*PNA chimera and Stereopreferences in Hybridization with DNA/RNA

In an attempt to tune the dihedral angle β according to our hypothesis and to strike balance between flexibility and rigidity", rather to keep a situation where the PNA:RNA/DNA complex formation should facilitated by "balanced enthalpy and entropic contribution", *cis*-(1*S*,2*R*/1*R*2*S*)-cyclopentyl PNAs (*cp*PNA) were designed. The flexible *cis*-cyclopentane ring in the pre-organized PNA structure makes it to bind complementary DNA/RNA sequence without losing the entropy of the PNA strand during the complexation and represents the study of DNA/RNA discrimination effect, of reduced dihedral angle β in *cp*PNA compare to *ch*PNA with

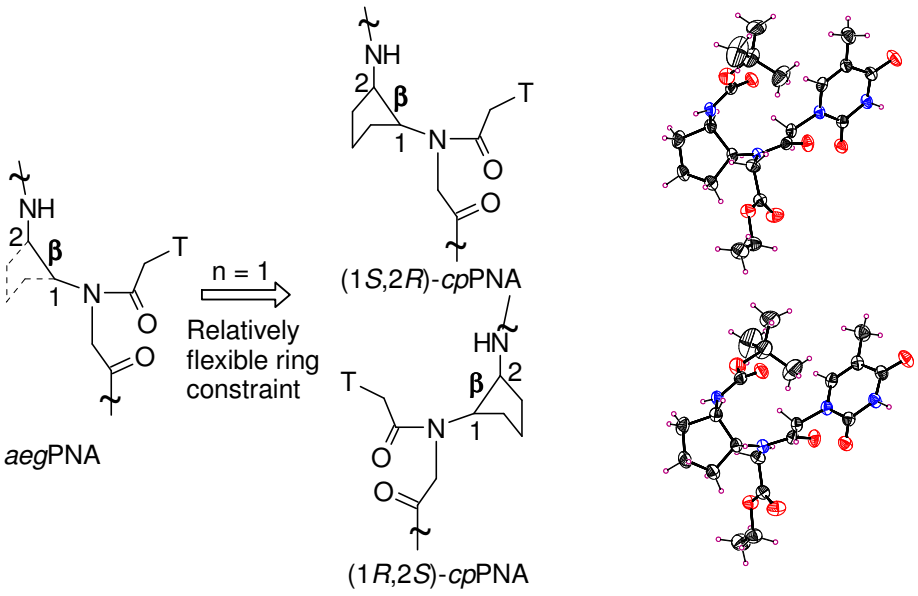

Figure 5. Dihedral angle and ring flexibility based design of *cp*PNA and crystal structures of corresponding monomers

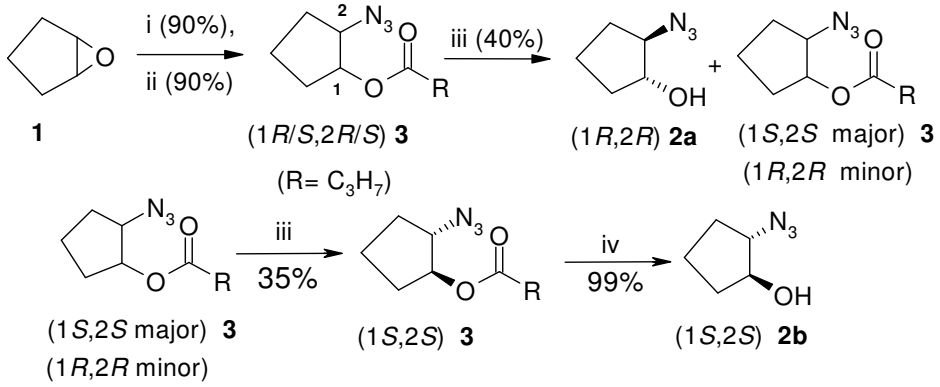

Scheme 3. Reagents and conditions: (i) NaN_3, NH_4Cl, ethanol:water (2:8) reflux, 16 h. (ii) n-Butyric anhydride, dry pyridine, DMAP (cat), rt, 16 h. (iii) *Pseudomonas cepacia* (Lipase), phosphate buffer, pH 7.2, 2.5 h. (iv) NaOMe in MeOH

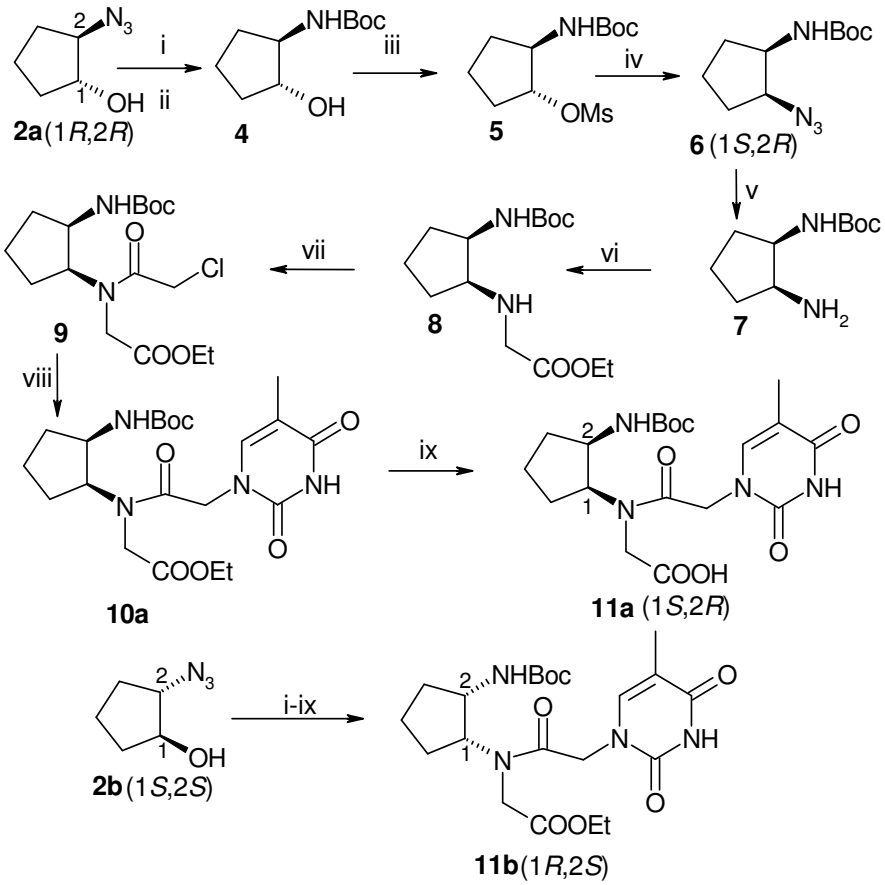

Scheme 4. Reagent and conditions. (i) PtO_2, dry EtOAc, H_2, 35-40 psi, rt, 3.5 h; (ii) $(Boc)_2O$ (iii) MsCl, dry triethyl amine, rt, 0.5 h; (iv) NaN_3, dry DMF, 70°C, 5 h; (v) PtO_2, MeOH, H_2, 35-40 psi, rt, 3.5 h; (vi) $BrCH_2COOEt$, KF-Celite, dry CH_3CN, 65°C, 4 h; vii) $ClCH_2COCl$, Na_2CO_3, Dioxan: H_2O (1:1), 0°C, 5 min.; (viii) Thymine, K_2CO_3 dry DMF, 65°C, 4 h.; (ix) 0.5 M LiOH, aq. THF, 0.5 h.

specificity of complex formation. The *cp*PNA (Figure 5) was designed by constraining the ethylene diamine portion of the *aeg*PNA with hydrocarbon linker having three methylenes and one less than that in *ch*PNA. Imposing a conformational constraint to a flexible aminoethylglycyl PNA using a flexible *cis*-cyclopentane ring.

Synthesis of *cis*-(1*S*,2*R*)- and (1*R*,2*S*)-aminocyclopentyl thymine monomers: The *cis*-cyclopentyl PNA monomer was synthesized as two different enantiomers in their highest optical purity. The synthesis of the *cp*PNA monomers started with the enzymatically resolved azido alcohols (1*R*,2*R*)-**2a** and (1*S*,2*S*)-**2b** (Scheme 3 and 4). The enantiopurity of both (1*R,*2*R*) **2a** and (1*S,*2*S*) **2b** isomers was confirmed by comparing with the known values of optical rotations reported in the literature and by ^{1}H NMR using the chiral chemical shift reagent Eu*(hfc)*$_3$. All new compounds were characterized by ^{1}H, ^{13}C NMR and mass spectral data. The torsion angles **β** as deduced from the X-ray crystal structures for **10a** (1*S,*2*R*) and **10b** (1*R*,2*S*) are –24° and +25° respectively (Table 2).

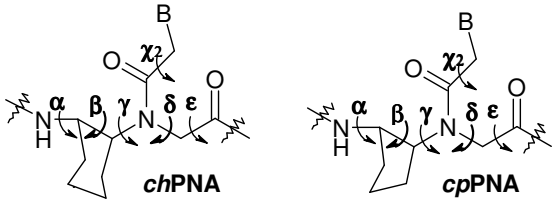

Table 2. Dihedral angles (°) in PNA and PNA:DNA/RNA complexes

Compound	α	β	γ	δ	χ_1	χ_2
PNA_2:DNA	-103	73	70	93	1	-175
PNA:DNA	105	141	78	139	-3	151
PNA:RNA	170	67	79	84	4	-171
*ch*PNA(1*S*,2*R*)*	128	-63	76	119	1.02	-175
*ch*PNA(1*R*,2*S*)*	-129	66	-78	-119	-0.87	174
*cp*PNA(1*S*,2*R*)*	84	-24	86	90	0.89	165
*cp*PNA(1*R*,2*S*)*	-84	25	-86	-90	1.2	-165

* dihedral angles from monomer crystal structures.: *ch*PNA, *cp*PNA

Biophysical Studies of *cp*PNAs: The modified *cis*-(1*S*,2*R*/1*R*,2*S*)-aminocyclopentylglycyl thymine monomers **11a** and **11b** were incorporated into PNA sequences using Boc chemistry on L-lysine-derivatized (4-methylbezhydryl)amine (MBHA) resin, using HBTU/HOBt/DIEA in DMF as the coupling reagent. Various PNA oligomers (**12**-**23**, Table 3)-

Table 3. Melting temperatures (T_m, °C) of PNA:DNA/RNA hybrids[a]

Entry	PNA sequences	DNA	RNA
1	*aeg*PNA **12**, H-TTTTTTTT-$LysNH_2$	45.0	62.0
2	*cp*PNA **13**, H-TTTTTTTt_{SR}-$LysNH_2$	51.0	73.5
3	*cp*PNA **14**, H-TTTt_{SR}TTTT-$LysNH_2$	22.0	76.0
4	*cp*PNA **15**, H-t_{SR}TTTTTTT-$LysNH_2$	44.5	66.0
5	*cp*PNA **16**, H-TTTTTTTt_{RS}-$LysNH_2$	55.0	>85.0
6	*cp*PNA **17**, H-TTTt_{RS}TTTT-$LysNH_2$	62.0	61.0
7	*cp*PNA **18**, H-t_{RS}TTTTTTT-$LysNH_2$	48.7	69.0
8	*cp*PNA **19**, H-$(t_{SR})_8$-$LysNH_2$	66.6	>85.0
9	*cp*PNA **20**, H-$(t_{RS})_8$-$LysNH_2$	72.0	>85.0
10	*aeg*PNA **21**. H-G T AGATCACT-$LysNH_2$	55.0	55.4
11	*cp*PNA **22**. H-G T_{SR} AGAT$_{SR}$CACT$_{SR}$-$LysNH_2$	77.1	84.0
12	*cp*PNA **23**. H-G T_{RS} AGAT$_{RS}$CACT$_{RS}$-$LysNH_2$	78.8	>85.0

a T_m = melting temperature (measured in Buffer. 10 mM Sodium phosphate, pH 7.0 with 100 mM NaCl and 0.1 mM EDTA). Measured from 10 to 90° C at ramp 0.2° C/min. UV-absorbance measured at 260 nm. RNA = poly rA/ 5' AGUGAUCUAC. nd = not detected. DNA = dCGCA$_8$CGC/ 5' AGTGATCTAC

incorporating modified monomers were synthesized. To investigate the binding selectivity, specificity and discriminationof *cp*PNAs towards complementary DNA and RNA, first the stoichiometry of the *cp*PNA:DNA was determined using Job's plot. The UV-melting values of the complexes with complementary DNA and RNA were measured (Table 3). The CD spectra of single strands and corresponding complexes were recorded. Finally the complexation of homothymine *cp*PNAs to complementary DNA was confirmed by gel electrophoretic shift assay and Isothermal titration calorimetry.

The torsional angle β in 1,2–disubstituted *cis*-cyclopentyl system is less than that in *ch*PNA but seems to have significant consequences on the hybridization ability of *cp*PNA oligomers. The higher binding of cyclopentyl PNAs is perhaps a consequence of the relative ease of -conformational adjustments in a cyclopentyl ring as compared to rigid locking of cyclohexane systems. The favorable conformational features of the monomers are co-operatively transmitted to the oligomeric level. *cp*PNA with a lower monomer dihedral angle β (~23^{o}) binds to RNA and DNA with greatly higher avidity compared to *aeg*PNA and *ch*PNA, but lacks the discriminating ability of *ch*PNA.

<u>Chapter 4</u>: Backbone Extended Pyrrolidine Peptide Nucleic Acids (*bep*PNA): Synthesis, Characterization and DNA/RNA binding Studies

A completely different approach from the those discussed above is designing a molecule (DNA or PNA analogue) which could take care most of the PNA draw backs into consideration like poor aqueous solubility and cellular uptake, ambiguity in binding to complementary oligonucleotides both in parallel antiparallel directions and equal affinity for DNA as well as RNA. The pyrrolidine PNA (Figure 1) is the outcome of one of the ways to lock the PNA conformation for this purpose. The mixed results surfacing from different groups infer that the conformational constraint imposed onto PNA backbone in the form of ring structure may not be uniform for various nucleobases or with sequence context. Previous studies on DNA/RNA analogues have shown that the number of bonds in the repetitive DNA/RNA backbone can be varied to five or seven. In view of above discussion, a chiral pyrrolidine PNA with an extended

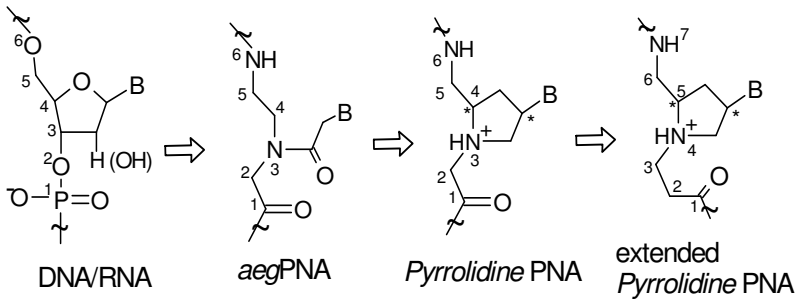

Figure 6. Designed *bep*PNA as DNA/RNA and PNA mimic

backbone (Figure 6) was undertaken that may have potential for selective targeting to DNA or RNA.

Synthesis of *bep*PNA monomer [(*2S,4S*)-2-(*tert*-butoxycarbonylaminomethyl)-4-(thymin-1-yl) pyrolidin-1-yl] propanoic acid: The synthesis of the target monomer was accomplished from *trans*-4-hydroxy-L-proline (1) as shown in Scheme 5. The *bep*PNA thymine monomer **12** was incorporated into PNA sequences at predefined positions (Table 4) and the binding selectivity and discrimination of *bep*PNAs towards complementary DNA and RNA was studied using the UV-melting experiments (Table 4). The CD spectra of single strands and corresponding complexes with complementary DNA were recorded. Finally the complexation of homothymine *bep*PNAs to complementary DNA was confirmed by Gel electrophoretic shift assay (Figure 7).

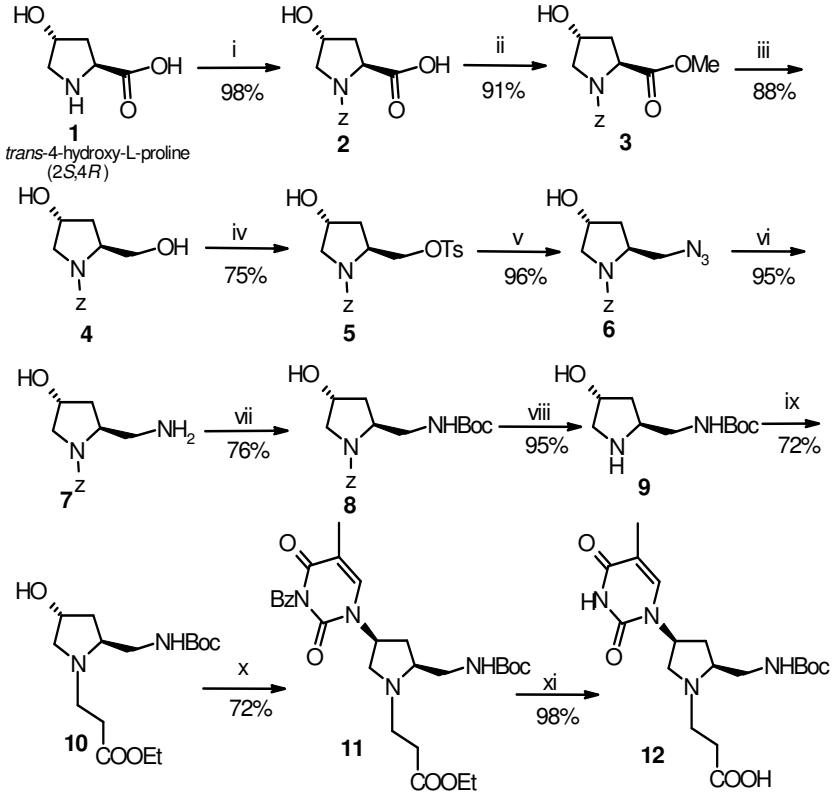

Scheme 5. ***Reagents and conditions***: (i) Cbz-Cl (50% toluene soln.), Et_3N, $NaHCO_3$, water, rt, 8 h. (ii) $SOCl_2$, Et_3N, MeOH, rt, 7 h. (iii) LiCl, $NaBH_4$, ethanol:THF(4:3), rt, 7 h. (iv) TsCl, pyridine, rt, 7 h. (v) NaN_3, DMF, 70°C, 8 h. (vi) Raney Ni, H_2, MeOH, 35 psi, rt, 3 h. (vii) $BocN_3$, DMSO, 50°C, 5 h. (viii) H_2/Pd-C, MeOH, 60 psi, rt, 7 h. (ix) Ethyl acrylate, MeOH, rt, 2.5 h. (x) N3-benzoyl –Thymine, DEAD, PPh_3, benzene, rt, 4 h. (xi) 2N aq. NaOH, Dowex H^+,rt, 5 h.

The C-terminal modified *bep*PNA **14** binds to DNA with slight decrease in T_m (ΔT_m= -1°C) where as *bep*PNA **16** modified at *N*-terminal stabilizes the complex (ΔT_m= +2°C) compare to control *aeg*PNA **13**. Surprisingly *bep*PNA **15**, modified unit at the center not shown any complexation with DNA. Alternate and homooligomeric *bep*PNAs (**17** and **18**) were also not forming complex with DNA. When the complexation studies were performed with RNA (poly rA), all *bep*PNAs bind with approximately same T_m but slightly lower than that of control

*aeg*PNA **13** except *bep*PNA **17** which shown very high binding affinity (ΔT_m= +18°C) (Table 3). The observed transitions are very sharp with RNA compared to that with DNA. UV-T_m data clearly suggest that *bep*PNA monomer introduced the DNA/RNA binding selectivity and affinity depending on the position and the number of units present in the PNA sequence.

Table 4. UV-T_m (°C) of PNA:DNA/RNA hybrids[a]

Sequence	DNA	RNA
*aeg*PNA **13**, H-TTTTTTTT-LysNH$_2$	51.5	65.8
*bep*PNA **14**, H-TTTTTTT**t**-LysNH$_2$	49.0	59.9
*bep*PNA **15**, H-TTT**t**TTTT-LysNH$_2$	nd	59.2
*bep*PNA **16**, H-**t**TTTTTTT-LysNH$_2$	53.0	59.0
*bep*PNA **17**, H-T**t**T**t**T**t**T**t**-LysNH$_2$	nd	84.4
*bep*PNA **18**, H-**t t t t t t t t**-LysNH$_2$	nd	58.9
*bep*PNA **19**, H-G**t** AGA**t**CACt-LysNH$_2$	nd	81.0

a T_m = melting temperature (Buffer. 10 mM Sodium phosphate, pH 7.0 with 100 mM NaCl and 0.1 mM EDTA). Measured from 10 to 90° C at ramp 0.2° C/min. UV-absorbance measured at 260 nm. RNA = poly rA/ 5' AGUGAUCUAC.
nd = not detected. DNA = dCGCA$_8$CGC/ 5' AGTGATCTAC

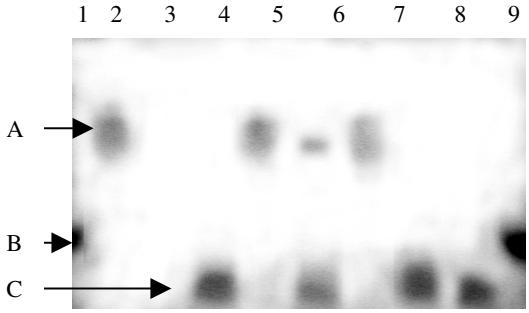

Figure 7. **Gel sift assay**. PNA-DNA complexation: Lane 1, BPB; lane 2, (*aeg*PNA **13**)$_2$:DNA ; lane 3, ss*bep*PNA **14**; lane 4, ssDNA ; lane 5, (*bep*PNA **14**)$_2$+DNA; lane 6, (*bep*PNA **15**)$_2$+DNA; lane 7, (*bep*PNA **16**)$_2$:DNA; lane 8, (*bep*PNA **17**)$_2$+DNA; lane 9, (*bep*PNA **18**)$_2$ + DNA; lane 10, BPB (bromophenol blue). DNA=CGCAAAAAAAACGC. **A**. PNA-DNA complex, **B**. BPB, **C**. Single stranded DNA.

<u>Chapter 5</u>. Synthesis of (1*S*,2*R*/1*R*,2*S*)-1-azido-2-carbocyclic amines, immediate precursor to vicinal-1,2- *cis*-diamines: Microwave assisted fast and clean conversion of mesylate to azide

An efficient and rapid conversion of mesylatye to azide under microwave irradiation has been carried out, which proceed through inversion of configuration from chiral mesylates to provide optically pure *cis*-azides, immediate precursors of vicinal-*cis*-1,2-diamines. These diamines can serve as metal ligands in asymmetric catalysis and their derivatives can be employed as medicinal agents. This represents the efficient, rapid, clean and high yielding process, an alternative to time-consuming conventional method.

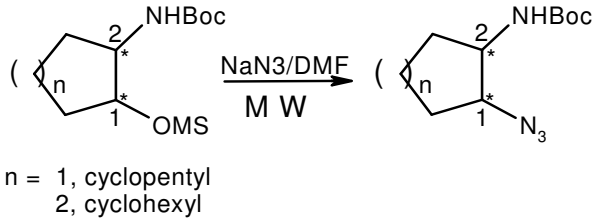

Scheme 6. Azidation of carbocyclic mesylates.

The conventional synthetic procedure involves the heating of the mesylate with NaN_3 (8.0 eq.) taken in DMF for 5-12 h at 65-70°C depending on the substrate. In microwave method the reactions were performed in a microwave reactor. The reaction mixture was irradiated with microwave in 1-6 cycles of 2 mins each followed by 1 min rest until complete conversion of the starting material (Scheme 6).

ABREVIATIONS

β ala	β-alanine
A	Adenine
Ac	Acetyl
Ac_2O	Acetic anhydride
aeg	Aminoethylglycine
aep	Aminoethylprolyl
ala	Alanine
ap	Antiparallel
Arg	Arginine
Aq.	Aqueous
bep	Backbone extended pyrrolidine
BPB	Bromophenol blue
Bz	Benzoyl
C	Cytosine
Calcd.	Calculated
Cat	Catalytic/catalyst
Cbz	Benzyloxycarbonyl
CD	Circular Dichroism
ch	Cyclohexyl
cp	Cyclopentyl
CSR	Chemical shift reagent
D-	Dextro-
dA	2'-Deoxyadenosine
dC	2'-Deoxycytidine
dT	2'-Deoxythymidine
dU	2'-Deoxyuridine
DCC	Dicyclohexylcarbodiimide
DCM	Dichloromethane

DCU	Dicyclohexyl urea
dG	2’-Deoxyguanosine
DEAD	Diethylazodicarboxylate
Dhbt	3-Hydroxy-2,3-dihydro-4-oxo-benzotriazole
DIAD	Diisopropylazodicarboxylate
DIPCDI	Diisopropylcarbodiimide
DIPEA/DIEA	Diisopropylethylamine
DMAP	4’,4’-Dimethylaminopyridine
DMF	N,N-dimethylformamide
DMSO	N,N-Dimethyl sulfoxide
DNA	2’-deoxyribonucleic acid
ds	Double stranded
eda	Ethylenediamine
EDTA	Ethylenediaminetetraacetic acid
ee	Enantiomeric excess
Et	Ethyl
EtOAc	Ethyl acetate
FAB	Fast atom bombardment
Fmoc	9-Fluorenylmethoxycarbonyl
FT	Fourier Transform
g	gram
G	Guanine
gly	Glycine
h	Hours
his	Histidine
HBTU	2-(1H-Benzotriazole-1-yl)-1,1,3,3-tetramethyluronum hexafluorophosphate
HIV	Human Immuno Difficiency Virus
HOBt	1-Hydroxybenzotriazole
HPLC	High Performance Liquid Chromatography

Hz	Hertz
IR	Infra red
ITC	Isothermal Titration Calorimetry
L-	Levo-
LC-MS	Liquid Chromatography-Mass Spectrometry
Lys	Lysine
MALDI-TOF	Matrix Assisted Laser Desorption Ionisation-Time of Flight
MBHA	4-Methyl benzhydryl amine
MF	Molecular formula
mg	milligram
MHz	Megahertz
min	minutes
µl	Microliter
µM	Micromolar
ml	milliliter
mM	millimolar
mmol	millimoles
m.p	melting point
ms	Methanesulfonyl
MS	Mass spectrometry
MW	Molecular weight/Microwave
N	Normal
nm	Nanometer
NMR	Nucler Magnetic Resonance
p	Parallel
PCR	Polymerase chain reaction
pfp	Pentafluorophenyl
ppm	Parts per million
PNA	Peptide Nucleic Acid

Pro	Proline
PS-oligo	Phosphorothioate-oligo
Py	Pyridine
R	Rectus
rA	ribo Adenosine
Rf	Retention factor
RNA	Ribonucleic Acid
RP	Reverse Phase (-HPLC)
r.t.	Room temperature
RT	Retention time
S	Sinister
Ser	Serine
SPPS	Solid Phase Peptide Synthesis
ss	Single strand
T	Thymine
t-Boc	*tert*-Butyloxycarbonyl
TBTU	2-(1H-Benzotriazole-1-yl)-1,1,3,3-tetramethyluronum tetrafluoroborate
TEA/Et_3N	Triethylamine
TBE	Tris-Borate-EDTA
TFA	Trifluoroacetic acid
TFMSA	Trifluoromethane sulfonic acid
THF	Tetrahydrofuran
TLC	Thin layer chromatography
T_m	Melting temperature
TPP	Triphenylphosphine (PPh_3)
Ts	*p*-Toluene sulfonyl
U	Uridine
UV-Vis	Ultraviolet-Visible

Chapter-1

INTRODUCTION

1.1 Nucleic Acids: Chemical Structure and Importance

Nucleic acids are the most important class of biopolymers dominating the modern molecular science after the Watson-Crick discovery of the double helical structure of DNA.[1] Their vital roles are fundamental for the storage and transmission of genetic information within cells and contain all information required for transmission and execution of steps necessary to make proteins which are another important class of biopolymers, important for cellular function. Nucleic acids are made up of a linear array

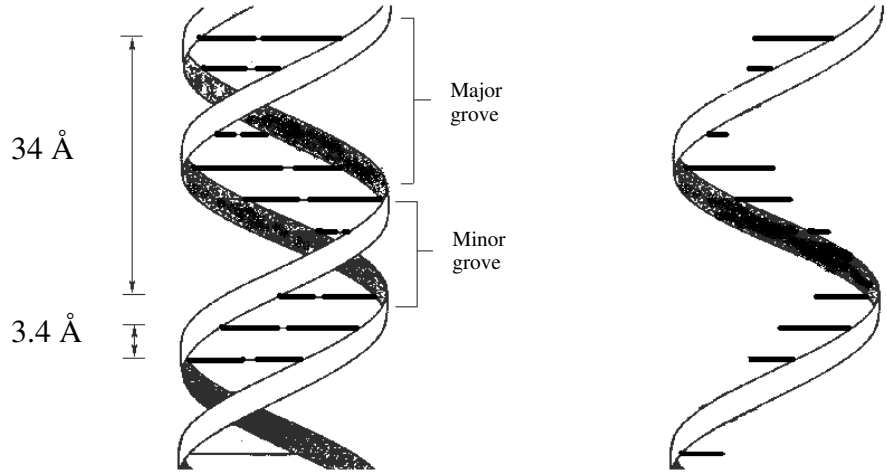

Figure 1. The ribbon model of DNA and RNA. The ribbons represent the sugar phosphate backbone and the horizontal thick lines in RNA and base pairs in DNA, the rise per base-pair and turn 3.4 Å and 34 Å are also shown

of monomers called nucleotides. Nucleotides are the phosphate esters of nucleosides and these are the components of both ribonucleic acid (RNA, Figure 1) and deoxyribonucleic acid (DNA, Figure 1). RNA is made up ribonucleotides while the monomers of DNA are 2'-deoxyribonucleotides. All nucleotides are constructed from three components: a

nitrogen heterocyclic **base**, a pentose **sugar**, and a **phosphate** residue. The major bases are monocyclic pyrimidines or bicyclic purines. The major purines are adenine (A) and guanine (G) and are found in both DNA and RNA. The major pyrimidines are cytosine (C), thymine (T) found in DNA and uracil (U) in RNA instead of T.

In nucleoside, the purine or pyrimidine base is joined from a ring nitrogen to carbon-1' of a pentose sugar. In ribonucleic acid, the pentose is D-ribose which is locked into a five membered furanose ring by the bond from C-1' of sugar to N-1 of C or U or N-9 of A and G. This bond is on the same side of the sugar ring as the C-5 hydroxymethyl group and is defined as a β–glycosidic linkage. In DNA, the pentose sugar is 2'-deoxy-D-ribose and the four nucleic acids are deoxyadenosine, deoxyguanine, deoxycytidine, and deoxythymidine. In DNA, the methylated pyrimidine base takes the place of uracil in RNA (Figure 2).

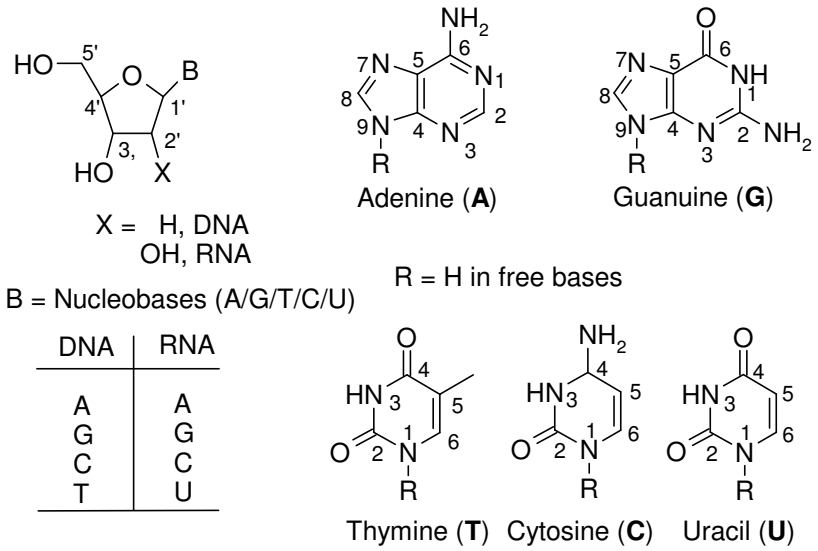

Figure 2. Structures of nucleosides and nucleobases of DNA and RNA

1.1.1 Shapes of nucleotides

Nucleotides have rather compact shapes with several interactions between non-bonded atoms. Their molecular geometry is so closely related to that of the corresponding

nucleotide units in oligomers and nucleic acid helical structure is a consequence of the conformational preferences of individual nucleotides. The details of the conformational structure are accurately defined by the torsional angles α, β, γ, δ, ε, and ζ in the phosphate backbone, θ_o to θ_4, in the furanose ring, and χ for the glycosidic bond (Figure 3c). Because many of these torsional angles are interdependent, one can simply describe the shapes of nucleotides in terms of four parameters: the sugar pucker, the *syn-anti* conformation of the glycosidic bond, the orientation of C4'-C5', and phosphate ester bonds.

1.1.2 Sugar pucker

The furanose rings are twisted out of the plane in order to minimize non-bonded interactions between their substituents. This '*puckering*' is described by identifying the major displacement of carbon C-2' and C-3' from the median plane of C1' –O4' – C4'. Thus, if the *endo*-displacement of C-2' is greater than the *exo*-displacement of C-3', the conformation is called C2'-*endo* and so on for other atoms of the ring (Figure 3a and 3b).

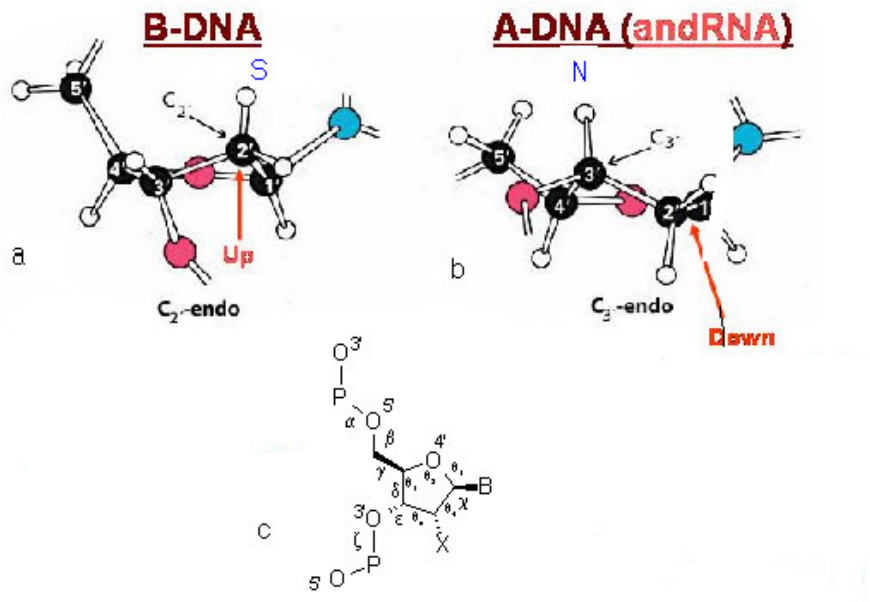

Figure 3. Torsion angle notation for polynucleotide chain and structures of C2'-*endo* and C3'-*endo* sugar puckers.

The *endo*-face of the furanose is on the same side as C5' and the base; the *exo*-face is on the opposite face to the base. The sugar puckers are located in the north (N) and south (S) domains of the pseudorotation cycle of the furanose ring (Figure 4), which also fortuitously reflect the relative shapes of the C-C-C-C bonds in the C2'-*endo*- and -*exo*-forms respectively.[2] In solution, N and S conformations are in rapid equilibrium and are separated by low energy barrier. The average position of the equilibrium is influenced by (i) the preference of the electronegative substituents at C2' and C3' for axial orientation, (as in the case of RNA the C2'-OH interact with backbone phosphate, C3'-*endo* is preferable conformation), (ii) the orientation of the base (*syn* goes with C2'-*endo*), and (iii) the formation of an intra-strand hydrogen-bond from O2' in one RNA residue to O4' in the next, which favors C3'-*endo*-pucker. The rise in the sugar phosphate backbone for each monomeric unit is 5.9 Å in case of RNA and 7.0 Å for DNA.

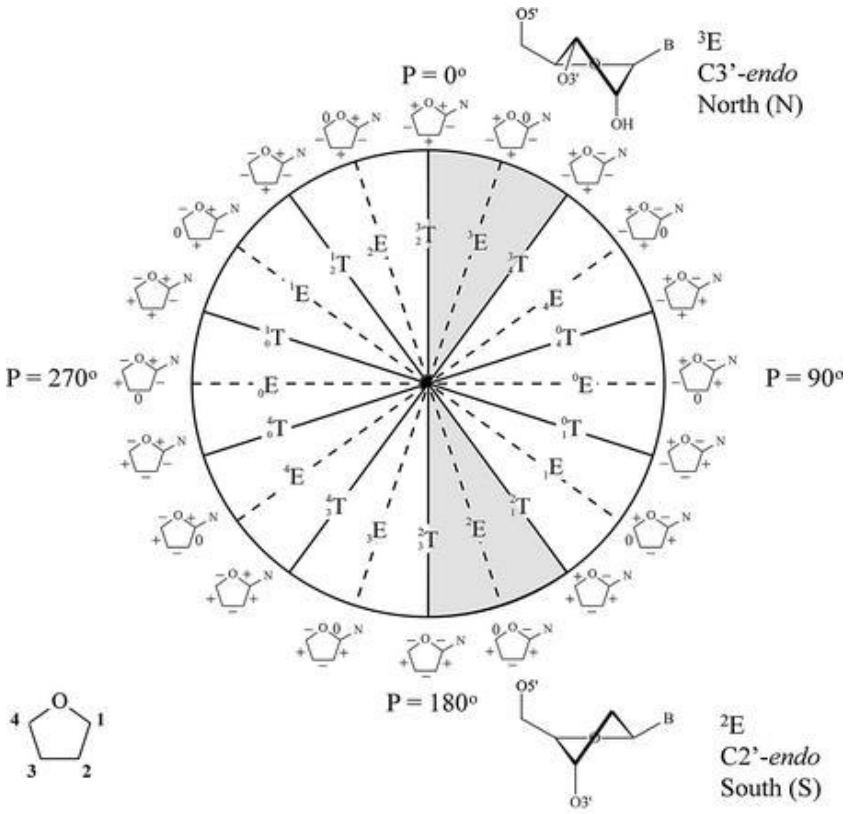

Figure 4. Pseudorotation cycle of the furanose ring and preferred conformation of ribose (top) and deoxyribose nucleotides.[2]

1.1.3 Hydrogen bonding

The N-H groups of the nucleobases are potent hydrogen bond donors, while the sp^2-hybridized electron pairs on the oxygens of the base C=O groups and that on the ring nitrogens are hydrogen bonding acceptors. In Watson-Crick pairing, there are two hydrogen bonds in an A:T base pair and three in a C:G base pair (Figure 5).[1]

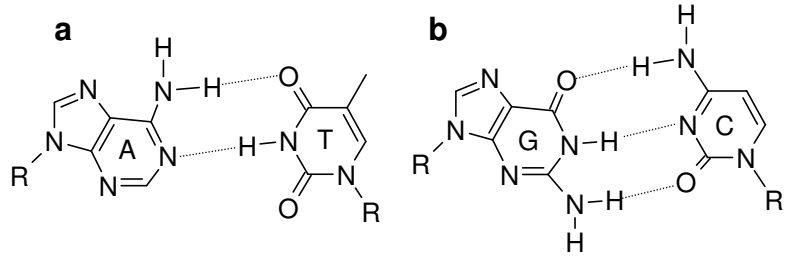

Figure 5. Watson-Crick base pairing scheme for (a) A-T base pair and (b) G-C base pair

While Watson-Crick base pairing is then dominant pattern between the nucleobases, other significant pairings are Hoogsteen (HG)[3a] and Wobble base pairs.[3b]

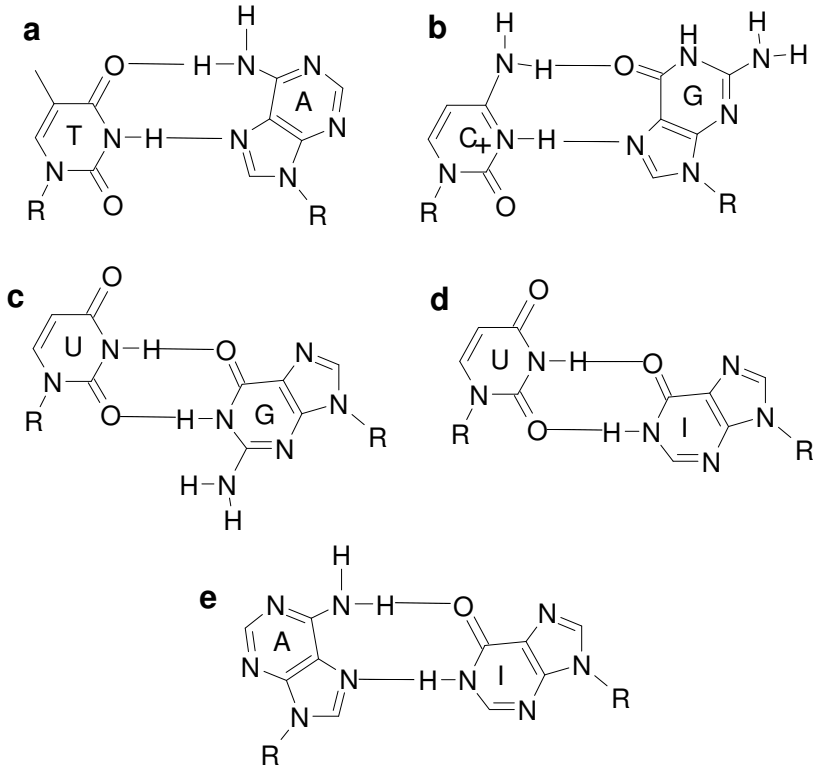

Figure 6. Hoogsteen (a and b) and Wobble (c-e) hydrogen bonding scheme. I = Inosine

Hoogsteen base pairing (Figure 6a and 6b) which is not isomorphous with Watson-Crick base pairing has importance in triple helix formation. In wobble base pairing, a single purine is able to recognize non-complementary pyrimidines (e.g. GU, where U = uracil) and (Figure 6c-e) have importance in the interaction of messenger RNA (*m*-RNA) with transfer RNA (*t*-RNA) on the ribosome during protein synthesis (codon-anticodon interactions). Several mismatched base pairs and anomalous hydrogen bonding patterns have been seen in X-ray studies of synthetic oligodeoxynucleotides.[4]

1.1.4 DNA Secondary Structure

Diffraction studies on heterogeneous DNA fibers have identified two distinct conformations for the DNA double helix.[5] At low humidity (and high salt) the favored form is the highly crystalline A-DNA (Figure 7) while at high humidity (and low salt) the dominant structure is B-DNA (Figure 7). A-DNA follows the Watson-Crick model with anti-parallel, right-handed double helix and the phosphate backbone is on the outside of a cylinder. There are 11 bases in each turn of 28 Å, which gives a vertical rise of 2.56 Å per base pair. In order to maintain the normal van der Waals separation of 3.4 Å, the stacked bases are tilted sideways through 20^{o}. The sugar backbone has skewed phosphate ester P-O bonds and antiperiplanar conformations for the adjacent C-O ester bonds. Finally, the furanose ring has C3'-*endo*-pucker and the glycoside is in the *anti*-conformation. This leaves a 5.4 Å P-P separation between adjacent intrastrand phosphates. A-duplex structure has a very deep major-groove and quite shallow minor-groove. B-DNA has now grown into family of structures encompassing B-, B'-, C-, C'-, C"-, D-, E-, and T-DNAs. B-DNA is a right-handed double helix and is the most predominant conformation in solution, with wide major-groove and a narrow minor-groove. Its bases stack predominantly above their neighbors in the same strand and are perpendicular to the helix

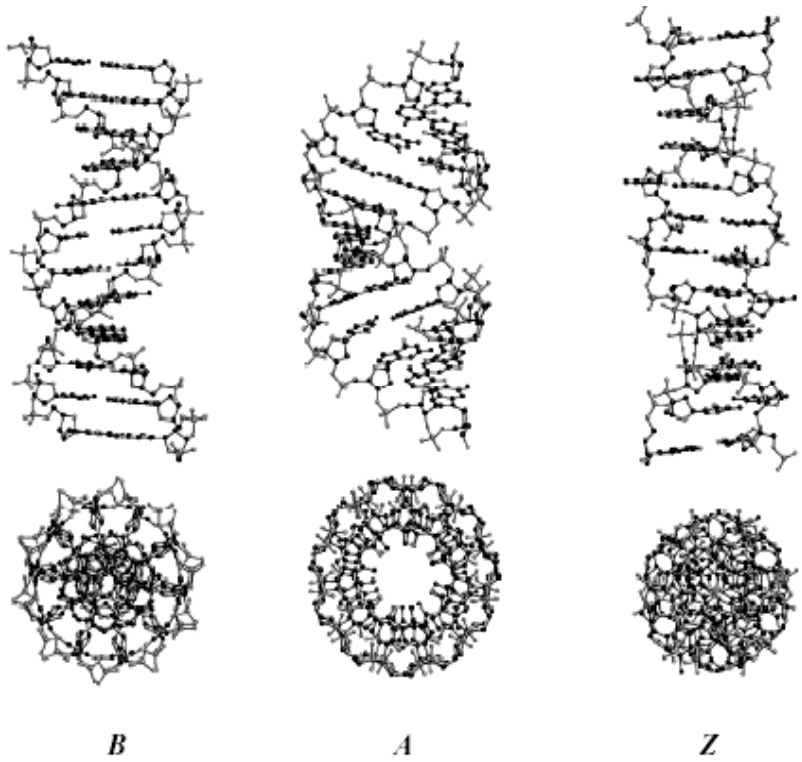

Figure 7. Top: molecular models of B, A, and Z form DNA. Bottom: views along the helical axis.[5-6]

axis. The sugars have the C2'-*endo*-pucker, all the glycosides have *anti*-conformation, and most of the other rotamers have normal populations. Adjacent phosphates in the same chain are little further apart, P-P = 6.7 Å, than in A-DNA. A very unusual form of DNA duplex is the left-handed Z-DNA.[6] The left-handedness of this antiparallel duplex is a result of a switch in the glycosidic torsion angle from the regular anti- to the unusual *syn*-conformation for purine nucleoside in each base pair. This *anti-syn* features alternate regularly along the DNA backbone, causing the phosphorous atoms to follow a zig-zag course: hence the name Z-DNA. At the same time, the sugar pucker alternates from C2'-*endo* for the *anti*-residues to C3'-*endo* for the *syn*-nucleosides. These changes have profound effect on base stacking in Z-DNA. The net result of these changes is that the minor groove of Z-DNA is so deep that it actually contains the helix axis and the major-groove of Z-DNA is a convex surface on which cytosine-C5', guanine-N7, and –C8 are

Table 1. Salient features of major DNA conformations

Parameters	A Form	B Form	Z-Form
Direction of helical rotation	Right	Right	Left
Conditions	Low humidity and high salt	Dilute aqueous solutions	High salt and alternating G-C sequences
Residues per turn of helix	11	10	12 base pairs
Rotation of helix per residue (in degrees)	33	36	-30
Base tilt relative to helix axis (in degrees)	20	6	7
Rise per base pair	2.3 Å	3.4 Å	3.8 Å
Major groove (width)	narrow and deep (11.0 Å)	wide and deep (5.7 Å)	Flat (2.0 Å)
Minor groove (width)	wide and shallow (2.7 Å)	narrow and deep (11.7 Å)	narrow and deep (8.8 Å)
Orientation of N-glycosidic Bond	Anti	Anti	Anti for Py, Syn for Pu
Comments		most prevalent within cells	occurs in stretches of alternating pu-py base pairs

exposed (Figure 7) This conformation of DNA is stabilized by high concentrations of $MgCl_2$, NaCl and alcohol (lower dielectric constant), and is favored for alternating G-C/G-C sequences and there are exceptions. B-DNA changes its conformation to Z-DNA at higher salt concentration. The features of major DNA conformations are summarized in Table 1.

1.1.5 Structures of RNA

Now RNA is recognized to have greater structural versatility than DNA. Its chemical reactivity (instability) arises from the extra complexity of the presence of 2'-OH group in ribonucleosides, capable of intermolecular nucleophilic attack on adjacent phosphate. RNA oligomers are composed of phosphate esters of D-ribose having nucleobases A, G, C and U attached through C1'-N3 (Py)/N9 (Pu) glycosidic bonds.

1.1.6 RNA secondary Structure

RNA is single stranded but can form complex and unusual structures such as stem and bubble structures, due to the chain folding as a consequence of intramolecular base pairing. An example of folded RNA structure is *t*-RNA, which is the key RNA involved in the translation of genetic information from *m*-RNA to proteins. *t*-RNA contains about 70 bases that are folded such that there are base paired stems, bulges and open loops. The overall shape of the completely folded *t*-RNA is L-shaped.

The presence of the 2'-hydroxy group in RNA hinders the formation of a B-type helix but can be accommodated within an A-type helix. At low ionic strength, A-RNA has 11 base pairs per turn in a right-handed, antiparallel double helix. The sugars adopt a C3'-*endo* pucker and other geometric parameters are all very similar to A-DNA. If the salt concentration is raised above 20%, A'-RNA form is observed which has 12 base pairs per turn of the duplex. Both structures have typical Watson-Crick base pairs, which are displaced by 4.4 Å from the helix axis and so form a very deep major-groove and rather shallow minor-groove.

Antisense RNA is defined as a short RNA transcript that lacks coding capacity, but has a high degree of complementarity to structure of coding RNA which enables the two to hybridize. The consequence is that such antisense, or complementary RNA can act as a repressor of the normal function or expression of the targeted RNA. Such a species have been detected in many prokaryotic cells with suggested functions concerning RNA-primed replication of plasmid DNA, transcription of bacterial genes, and messenger translation in bacteria and bacteriophages. Quite clearly, such a regulation of gene expression depends on the integrity of RNA duplexes.

1.1.7 RNA:DNA duplexes

RNA:DNA duplexes are formed i) during DNA replication of the short primer sequences in Okazaki fragments, ii) when RNA polymerase transcribes DNA into complementary messenger RNA and iii) when reverse transcriptase makes a DNA complement to the viral RNA. Such hybrids can also be formed in vitro by annealing together two complementary strands of RNA and DNA. These heteroduplexes adopt the A-conformation common to RNA and DNA, the former giving an 11-fold helix typical of A-RNA and latter a 12-fold helix characteristic of A'-RNA. The greater stability of RNA:DNA heteroduplexes over DNA:DNA homoduplexes is the basis of the construction of **antisense DNA oligomers**.

1.1.8 Molecular Recognition in the Major groove of Duplex DNA

The major and minor grooves of DNA differ significantly in their electrostatic potential, hydrogen bonding character,[4a] steric effects, hydration[5d] and dielectric strength.[7] AT and TA base pairs can accept additional hydrogen bonds from ligands bound in the major groove via the C4 carbonyl of T and N7 of A, while in the minor groove hydrogen bonding occurs through the C2 of carbonyl of T and N3 of A (Figure 8). The only hydrogen bond donor in the major groove for the AT base pair is the N6 amino group of A, while none exits in the minor groove. For CG and GC duplexes, the H-bond acceptors in the major groove are N7 and O6 for G and in the minor groove are O2 of C and N3 of G. The hydrogen bond donor in the major groove for CG is the N4 amino of C and in the minor groove, the N2 amino of G.

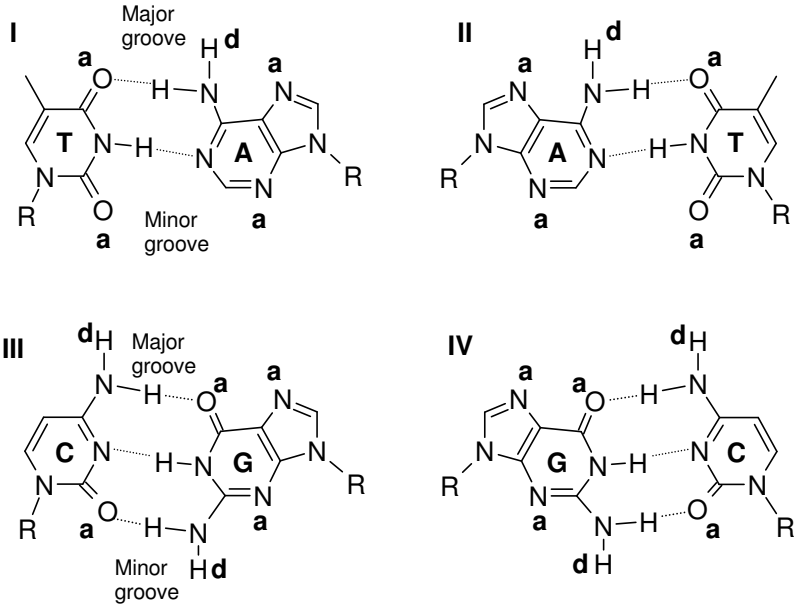

Figure 8. Hydrogen bond donor and acceptor sites in the major groove and minor groove of duplex DNA at I) TA, II) AT, III) CG, and IV) GC base pairs, a= acceptor and d = donor sites

The salient outcome of this pattern of hydrogen bond donors and acceptors in the grooves is that the binding molecules can discriminate the AT base pair from CG efficiently from the major groove side but not so well in the minor groove.[4a] Two further features of molecular discriminations are noteworthy. In AT and TA base pairs, the C5 methyl of T offers substantial hydrophobic recognition in the major groove which is absent for CG and GC base pairs. However, in the CG and GC duplexes, the N2 amino group of G presents a steric block to hydrogen bond formation at N3 of G and the C2 carbonyl of C in the minor groove. It is possible to distinguish AT from TA and GC from CG in the major groove since the horizontally ordered array of hydrogen bonding sites and hydrophobic centers differ among the four pairs (Figure 8). The native electrostatic potential due to phosphate charges is greater in the AT minor groove than in GC-rich regions, and this provides an additional important source for AT-specific minor groove recognition.[5d]

1.1.9 Triple-stranded nucleic acids

The first triple-stranded nucleic acid was described in 1957 when poly rU-poly rA was found to form a stable 2:1 Complex in the presence of $MgCl_2$.[8] A similar complex is formed from 2poly rC as long as the cytosine bases in one strand are protonated to

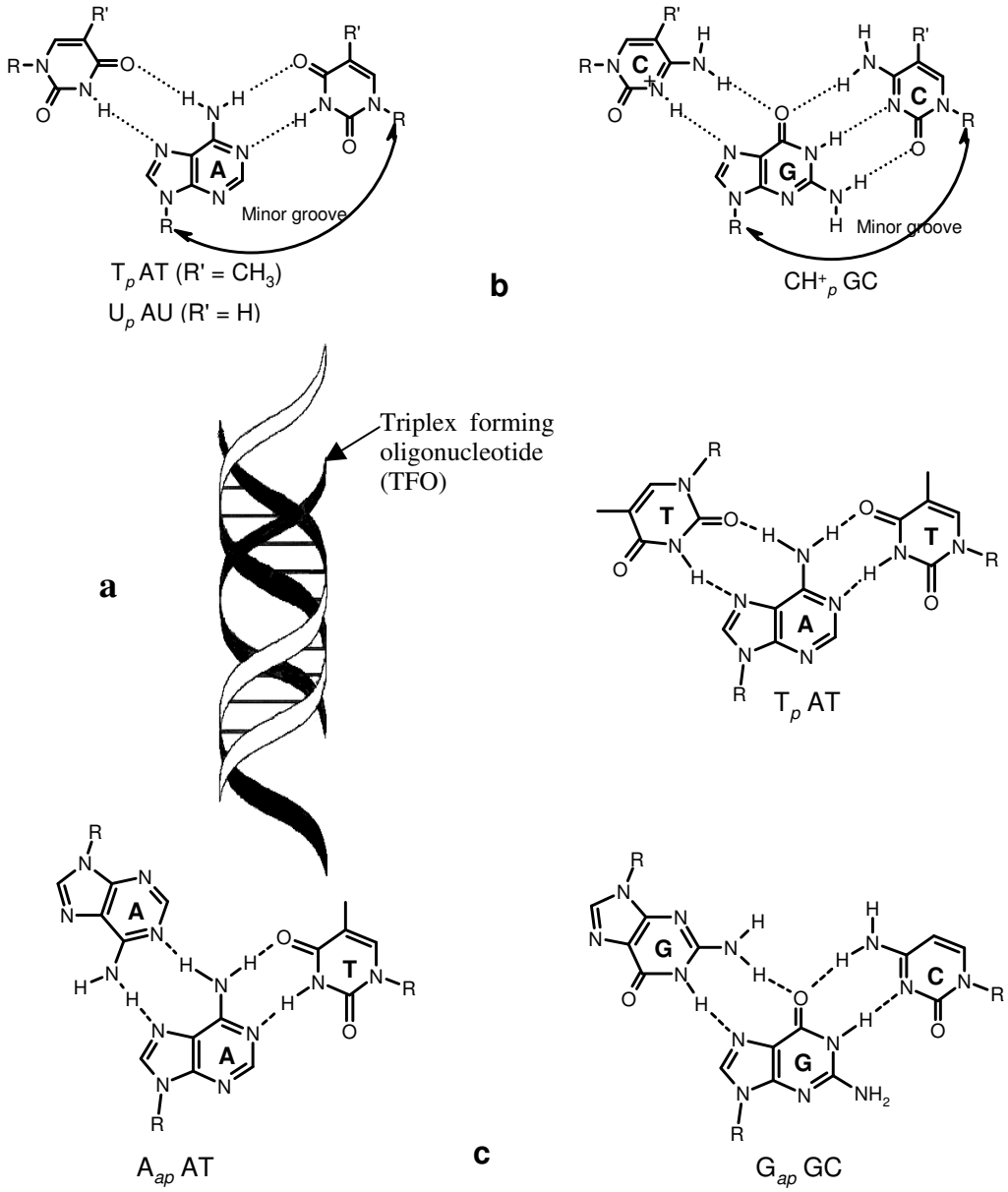

Figure 9. a) A ribbon model demonstrating the relative position of a TFO in the major groove of DNA, **b**) The pyrimidine binding motif- The binding of a TFO in a parallel (*p*) orientation to the polypurine strand of DNA-the two canonical base triplets of this motif, i) involving protonated cytosine in the $CH^+{}_p$G:C triplet and ii) T_pA:T. **c**) The purine motif-the binding of TFO in antiparallel (*ap*) orientation. The three canonical base triplets in this motif: A*ap*AT, G_{ap}GC and T_{ap}AT

complete the hydrogen-bond pattern, CH^+.G:C (Figure 9b). The triplexes formed with synthetic oligonucleotides, remained an obscure part of DNA chemistry until 1987 when it was realized that they offered a means for designing DNA sequence specific agents.[9,10]

DNA triple helix formation results from the major groove binding of a third strand (Figure 9a) ODN that is either pyrimidine (Y)- or purine-rich, in parallel (*p*) or antiparallel (*ap*) orientation respectively to the central purine strand as shown in Figure 10.[11,12] A purine-rich third strand binds in antiparallel orientation to the central strand, while a pyrimidine-rich strand does so in a parallel orientation. The specificity in triplex formation is derived from Hoogsteen (HG) hydrogen bonding. Thus, T recognizes A of A-0T Watson-Crick base pair to form T_pAT triad and protonated C binds to G of G-C base pair to give $CH^+{}_p$GC in the pyrimidines motif (Figure 9b). Similarly in the purine motif, the third strand A binds to A of A-T, leading to a A_{ap}AT triad, while G binds to G of G-C base pair forming G_{ap}GC triad in the reverse Hoogsteen mode (Figure 9c).[13]

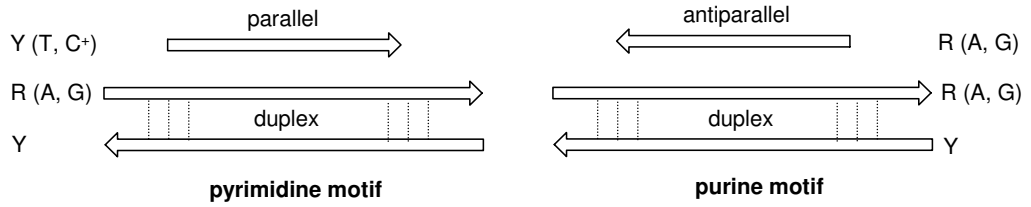

Figure 10. Pyrimidine and purine motifs of triplex formation

The widespread occurrence of polypurine/polypyrimidine tracts in eukaryotic DNA suggest that these sequences may have a biological function and consequently, therapeutic significance. The analysis of eukaryotic sequence databases reveals thousands of polypurine/polypyrimidine tracts, with potential for triple helix formation. Triplex formation obeys precise rules imposed by structural constraints. For a given sequence of DNA it is possible to design therapeutic oligonucleotides (ODNs) that will specifically bind to it and thereby inhibit the gene expression, Different aspects of triple-stranded

structures have been discussed in several reviews.[14] The formation and stabilization of triplexes depends on different types of interactions like electrostatic forces, stacking and hydrophobicity contributions, Hoogsteen hydrogen bonds, and hydration forces.

1.2 Oligonucleotides as Therapeutic Agents

Designing a small organic molecule as a drug against traditional drug target proteins requires structural knowledge of the binding site (target) and the binding forces. Since our understanding of protein folding is incomplete, this way of drug discovery process has serious limitations. In contrast, the nucleotide sequence in RNA and DNA is universal and the understanding of their structure is much better, from the drug-design point of view nucleic acid targets are very appealing. In principle one can design drugs that, like nucleic acids, is repetitive in its primary structure and bind sequence specifically to these drug targets. In order for the sequence specific recognition to happen, the drug should contain nucleobases, which are fundamental units of nucleic acid recognition; in other words, a short piece of oligonucleotide itself can act as a drug. Two innovative strategies are being tested for inhibiting the production of disease related proteins using such sequence specific DNA fragments as gene expression inhibitors (Figure 11).

The triplex approach, also called antigene strategy, aims to stall the production of an unwanted protein by selectively inhibiting the transcription of corresponding gene. In this method, the oligonucleotides target the major groove of DNA where it winds around the double helical DNA to form a triplex (Figure 9a).

The antisense strategy[15] aims to selectively impede the translation process. The sequences of the bases along a messenger RNA molecule spell out the series of amino acids that must be stung together to make a protein. To obtain a molecule that bind to the sense strand, one must construct a string of nucleotides having the complementary

"antisense" sequence. This upon binding to complementary region on *m*-RNA sterically inhibits the protein synthesis machinery.

1.2.1 Antisense Oligonucleotides

The concept behind the antisense therapeutics is simple and rational: to inhibit the expression of a specific gene at the *m*-RNA level by using complementary oligonucleotides, called antisense oligonucleotides, thereby blocking the expression of the protein encoded by the target RNA. In theory, hybridization of the antisense oligonucleotide to its complementary *m*-RNA by Watson-Crick base pairing should provide high specificity and affinity. The use of antisense oligonucleotides was originally postulated in the late 1960s by Grineva and co-workers.[16] In the 1970s, Ts'o and co-workers determined the chemical modification of the native molecule would result in the protection from exo and endonucleases.[17] In 1978, Zamecnik and Stephenson first illustrated the idea of antisense therapeutics by demonstrating that antisense oligonucleotides could inhibit replication of Rous *sarcoma* virus in a cellular system.[18,19] Not much progress was made in this field at that time, primarily because the synthetic methodologies for obtaining relatively larger quantity of oligonucleotides were

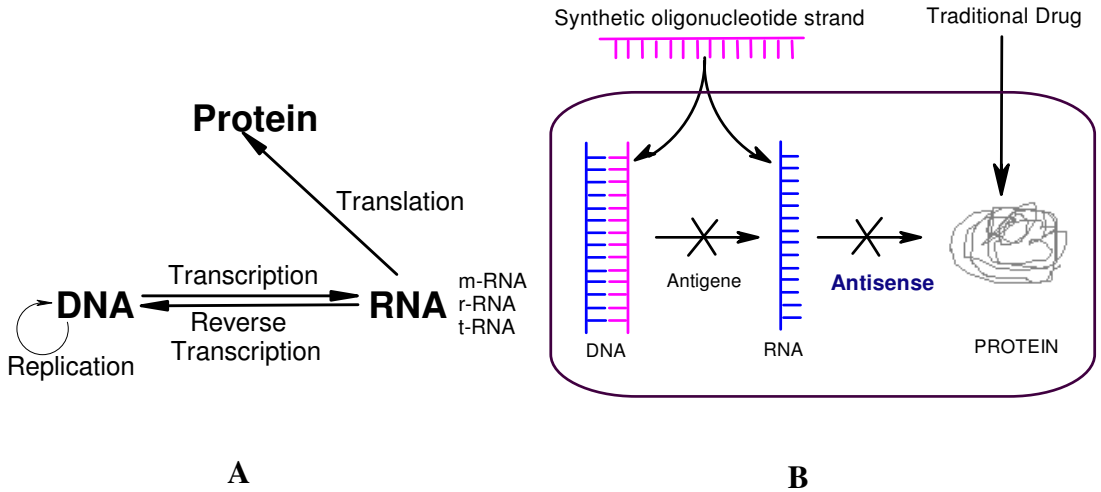

Figure 11. **A**. Central Dogma of cell-displays flow of genetic information from DNA to protein. **B**. Principle of action of antigene and antisense oligonucleotides

unavailable. During past decade, numerous reports in the literature have demonstrated the ability of antisense oligonucleotides to block the function of specific genes. Antisense oligonucleotides are currently being investigated as therapeutic agents for the treatment of viral infections, cancers and inflammatory diseases, and several human clinical trials of such are under way.[20] Vitravene developed by ISIS pharmaceuticals is the first and only antisense drug so far approved by the FDA for the treatment of cytomegalovirus (CMV) retinitis in people with AIDS.

1.2.2 Mechanisms of action of therapeutic oligonucleotides

Antisense oligonucleotide design: The action of antisense oligonucleotides can be rationalized by traditional receptor theory. The affinity of oligonucleotides for their nucleic acid receptors results from hybridization interactions that depend on hydrogen bonding and base stacking in the double helix that is formed. A minimum level of affinity is required for the desired interaction and this can be achieved with an oligonucleotide of at least 17 to 25 nucleotides length.[21] The GC content of the oligonucleotide is an important factor because a high percentage of these nucleotides could result in the formation of secondary or tertiary structures within the oligonucleotide.[22] Several computational approaches have been designed to predict the antisense oligonucleotide efficacy; before its use, it is imperative that every oligonucleotide is checked for similarities with other sequences present in the gene data bases. The mechanisms of potential antisense oligonucleotide interactions with target nucleic acids are complex, as there is a long sequence of events leading from DNA to protein synthesis.

As the target *m*-RNA can exhibit several secondary structures, not all antisense oligonucleotides may be effective because of their inability to access and hybridize with the target sequence. Mechanisms to identify accessible *m*-RNA sequences have been

developed and should prove helpful in antisense oligonucleotide design. Software packages that predict toxicity and nonspecific hybridization have become available, and techniques involving the screening of oligonucleotide libraries for RNase activation have been developed.[23] One has to consider several properties like stability, pharmacokinetics, cellular uptake etc in sequence design of antisense oligonucleotides.[24]

Mechanism of Action: The underlying basis by which antisense oligonucleotides exert their activity is based on Watson and Crick's postulate of hybridization to a complementary sequence.[1] There are a number of mechanisms by which antisense oligonucleotides inhibit the formation of a protein via hybridization in the nucleus with the pre-*m*-RNA, *m*-RNA or chromosomal DNA of a target protein (Figure 14). One of the primary means of inhibiting translation is by the activation of RNase H, which digests the RNA strand of the RNA-DNA complex.[25] Once the RNA strand is degraded, the surviving DNA oligonucleotide is then free to bind to another mRNA strand and hence the antisense DNA will act catalytically for RNase H activity by binding to a new messenger RNA, again inducing RNA hydrolysis and the process repeated (Figure 14c). It has been demonstrated that oligonucleotides can enter the nucleus and interact directly with the gene of interest (as an antigene). Formation of a triple helix would prevent unwinding of DNA strands and thus prevent DNA polymerase-mediated transcription, although it should be noted that this process is dependent on Hoogsteen bonding and not on Watson-Crick hybridization (Figure 14a).[26]

Inhibition of RNA processing by the prevention of intron splicing should occur with oligonucleotides designed to bridge the splice variants.[27] Whether or not this actually occurs has not been clearly demonstrated.[28] Targeting of the initiating start codon with an

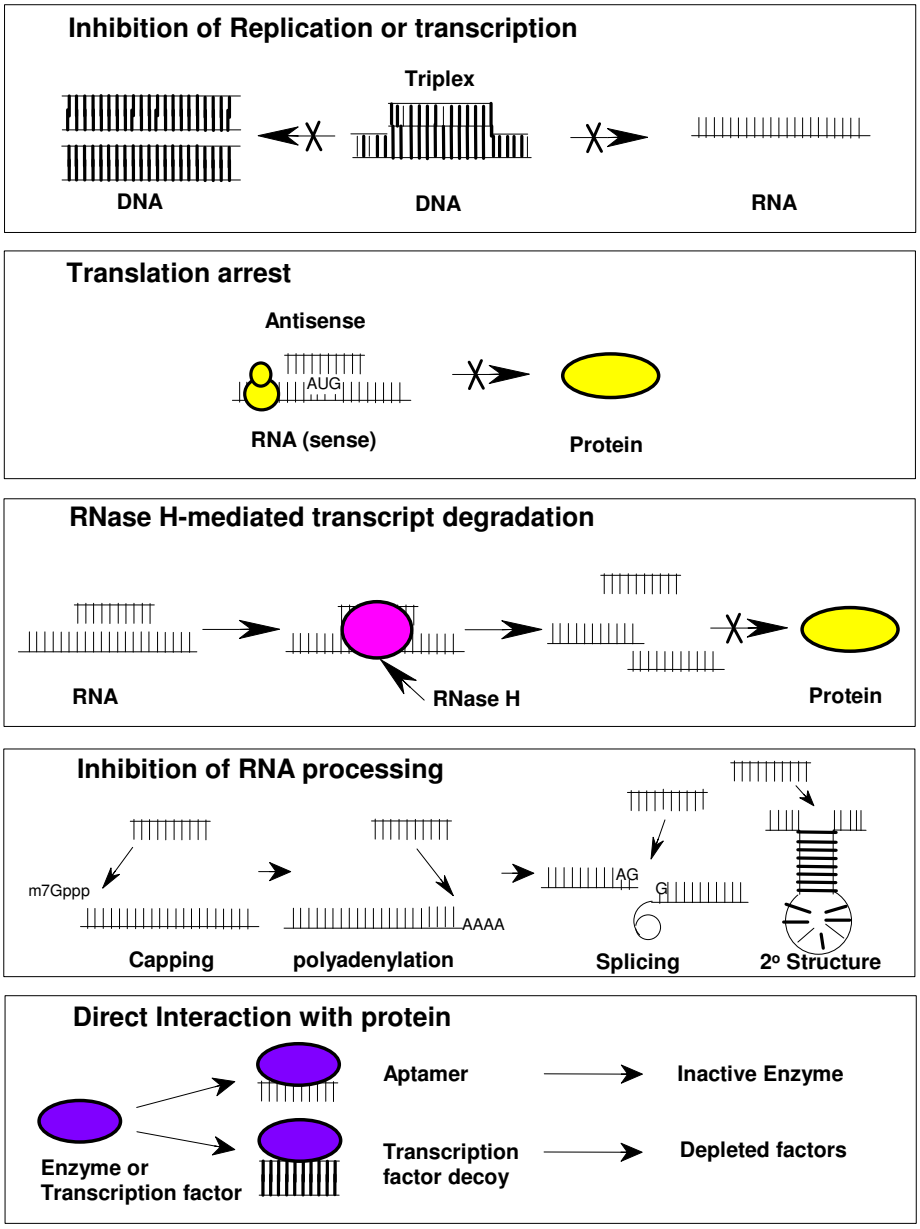

Figure 14. Potential mechanisms of action of antisense oligonucleotides[26-33]

antisense oligonucleotide is hypothesized to cause the arrest of translation (Figure 14b),[29] although, in theory, interaction of an antisense oligonucleotide at any point on the mRNA sequence should also cause translational arrest and perhaps result in the formation of truncated proteins. RNA is known to develop secondary and tertiary structures, such as stem-loop complexes, *via* intramolecular interactions.[30] Disruption of these structures might weaken mRNA stability and cause its degradation (Figure 14d),[31] and also arrest the messenger RNA exportation from the nucleus to the cytoplasm.

Other mechanisms by which to inhibit RNA include the inhibition of 5' capping and the inhibition of 3' polyadenylation, both of which will destabilize the RNA species (Figure 14d).[32] A key early step in RNA processing is capping. This stabilizes pre-*m*-RNA and is important for the stability of mature *m*-RNA. It is also necessary in binding to nuclear matrix and transport of *m*-RNA out of the nucleus, and thus presents an interesting target. Several oligonucleotides that bind near the cap site have been shown to be active, presumably inhibiting the binding of proteins required to cap the RNA. In the 3'-untranslated regions of pre-*m*-RNA molecules are sequences that result in post-transcriptional addition of long (hundreds of nucleotides) tracts of polyadenylate. Polyadenylation stabilizes the *m*-RNA and may play other roles in the intermediatary metabolism of RNA species.[32] Theoretically, interactions in the 3'-terminal region of pre-*m*-RNA could inhibit polyadenylation and destabilize the RNA species. Oligonucleotides can also be used as aptamers to inhibit proteins and other molecules directly and specifically (Figure 14e).[33]

1.2.3 Spectroscopic methods for studying DNA/RNA Interactions

The ability of antisense oligonucleotides to bind in vitro the target DNA/RNA, can be detected by using various biophysical techniques as follows

UV-Spectroscopy: Nucleic acid complexes have lower UV absorption than that predicted from the sum of their constituent base extinction coefficients that is usually measured at 260 nm. This phenomenon known as "hypsochromicity" results from coupling of the transition dipoles between neighboring stacked bases and is larger in amplitude for A-U and A-T pairs.[34] As a result, the UV absorption of a DNA duplex increases typically by 20-30 % when it is denatured. This transition from a helix to an unstacked, strand-separated coil has a strong entropic component and so is temperature

dependent. The mid-point of this thermal transition is known as the **melting temperature** (T_m). Such dissociation of nucleic acid helices in solution to give single stranded DNA/RNA is a function of base composition, sequence, and chain length as well as of temperature, salt concentration, and pH of the solvent (buffer). In particular, early observations of the relationship between T_m and base composition for different DNAs showed that A-T pairs are less stable than G-C pairs, a fact which is now expressed in a linear correlation between T_m and the gross composition of a DNA oligomer by the equation:[35]

$$T_m = X + 0.41\ (\%C+G)\ ^oC$$

The constant X is dependent on salt concentration and pH and has a value of 69.3°C for 0.3 M sodium ions at pH 7.

A second consequence is that the steepness of the transition curve also depends on base sequence. Thus, melting curves for homooligomers have much sharper transitions than those for random-sequence oligomers. This is because A-T rich regions melt first to give unpaired regions which then extend gradually with rising temperature until, finally, even the pure G-C regions have melted. In some cases, the shape of the melting curve can be analyzed to identify several components of defined composition melting in series. Because of end-effects, short homooligomers melt at lower temperatures and with broader transitions than longer homooligomers. For example for poly $(rA)_n$-poly $(rU)_n$, the octamer melts at 9°C, and the undecamer at 20°C, and long oligomers at 49°C in the same sodium cacodylate buffer at pH 6.9. Consequently, in the design of synthetic self-complementary duplexes for crystallization and X-ray structure determination, G-C pairs are often placed at the ends of hexamers and octamers to stop them 'fraying'. Lastly, the marked dependence of T_m on salt concentration is seen for DNA from *Diplococcus*

pneumoniae whose T_m rises from 70°C at 0.01 M KCl to 87°C for 0.1 M KCl and to 98 °C at 1.0 M KCl.

Data from many melting profiles have been analyzed to give a 'stability matrix' for nearest neighbor stacking. This can be used to predict T_m for a B-DNA polymer of known sequence with general accuracy of 2-3°C.

The converse of melting is the renaturation of two, separated, complementary strands to form a correctly paired duplex, In practice, the melting curve for denaturation of DNA is only reversible for relatively short oligomers, where the rate determining process is the formation of a nucleation site of about three base pairs followed by rapid zipping-up of the strands and where there is no competition from other impending processes. However, hysteresis observed in the process of denaturation and renaturation due to negative charge repulsions. When solutions of unpaired, complementary large nucleic acids are incubated at 10-20°C below their T_m, renaturation takes place over a period of time. For short DNAs of upto several hundred base pairs, nucleation is rate limiting at low concentration and each duplex zip to completion almost instantly. The nucleation process is bimolecular, so renaturation is concentration dependent. The annealing of two complementary strands has many applications. For RNA-DNA duplexes, it has provided a tool of fundamental importance for gene identification and is being explored in the applications of antisense DNA.

Duplex melting: Duplexes exhibit a single transition into single strands (melting) accompanied by an increase in UV absorption termed as *hyperchromicity*. According to the 'all or none model'[36] the UV absorbance value at any given temperature is an average of the absorbance of duplex and single strands. A plot of absorbance against temperature gives a sigmoidal curve in case of duplexes and the midpoint of the sigmoidal curve

(Figure 12) called as the 'melting temperature' (T_m) is the temperature (equilibrium point) at which the duplex and the single strands exist in equal proportions.

Triplex melting: In the case of triplexes, the first dissociation leads to melting of triplex generating the duplex (WC duplex) and third strand (Hoogsteen strand), followed by the duplex dissociation to form two single strands.[14d] The DNA triplex melting shows characteristic double sigmoidal transition (Figure 12b) and UV melting temperature for each transition is obtained from the first derivative plots. The lower melting temperature (T_m1) corresponds to triplex to duplex transition while the second higher melting temperature (T_m2) is the transition of duplex to single strands.

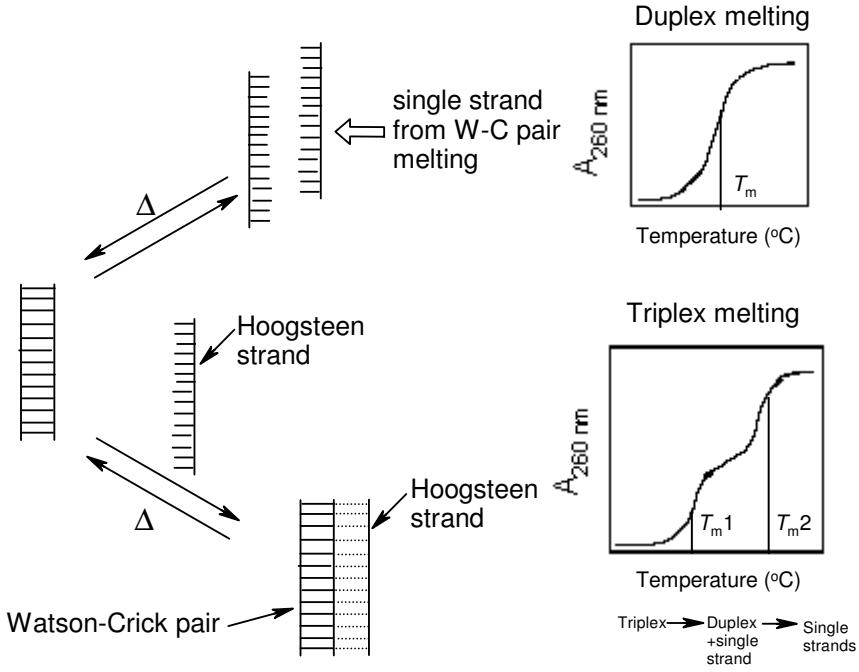

Figure 12. Schematic representation of DNA duplex and Triplex.

Stoichiometry. *The binding stoichiometry of oligonucleotide to target DNA/RNA by UV-titration (mixing)*: This is derived from Job's plot. The two components of the complex are mixed in different molar ratios, so that the total concentration of each mixture should be constant, i.e., as the concentration of one strand decreases,

concentration of the second strand increases and the UV-absorbance of each mixture is recorded. The absorbance decreases in the beginning to a minimum and then again increases. The molar ratio of the two strands at which absorbance reached minimum, indicates the stoichiometry of complexation.

***Circular Dichroism* (CD):** Circular dichroism[37] is a spectroscopic technique that depends on the property of optical activity, i.e., chiral molecules that interact with the right and left circularly polarized lights differently. Circularly polarized light occurs in two non-superimposable right and left circularly polarized forms, which are related to each other as mirror images. CD is particularly useful for studying chiral molecules and has very special significance in the characterization of biomolecules.

Circular dichroism is the measure of difference in absorption, A, of left and right circularly polarized light:

$$\text{CD} = A_l - A_r$$

The Beer-Lambert law relates the absorption, (A) of light to concentration of sample C by the equation

$$A = \varepsilon C l$$

where l is the length of the sample through which the light passes, ε is the extinction coefficient; if l is measured in cm and C in M = mol dm^{-3}, then ε has units of $mol^{-1}\ dm^3\ cm^{-1}$.

Most CD spectropolarimeters, measure difference in absorbance of light and left circularly polarized light to produce CD spectrum in units of ellipticity, θ, in milli-degrees, versus λ, rather than ΔA versus λ. The conversion between these two is:

$$\text{CD} = \Delta A \text{ (absorbance units)} = A_l - A_r$$

$$= 4\pi\theta \text{ (degrees)}/180 \ln 10$$

$$= \theta \text{ (millidegrees)}/32{,}982$$

The CD version of the Beer-Lambert law is:

$$\Delta A = (\Delta \varepsilon) Cl$$

The commonly used units in current literature are the mean residue ellipticity (degree cm^2 $dmol^{-1}$) and molar ellipticity $[\theta]$ the difference in molar extinction coefficients, $[\theta] = 3298\ (\Delta \varepsilon)$.

The most common applications of CD include probing the structure of biological macromolecules, in particular determining the α-helical content of proteins and conformational analysis of nucleic acids and interaction with other ligands.

Single stranded DNAs are structurally less defined than duplex DNAs and their CD signal is smaller. CD spectra of RNAs show that naturally occurring RNAs to be mainly well structured with extensive duplex regions (stem-bulb).

In an isolated nucleotide, the chirality originates from the ribose sugar and influences the base absorption. In the normal spectral region (down to 180 nm), the chiral ribose-phosphate backbone has no transitions and in the CD spectrum of nucleic acids one detects the CD induced into base transitions as a result of their coupling with the backbone transitions.[38] The magnitude of $\Delta \varepsilon_{max}$ is of the order of 2 mol^{-1} dm^3 cm^{-1} at 270 nm and the purine bases have a negative signal whereas the pyrimidines have a positive signal. In the case of CD spectrum of DNA and RNA polynucleotide with stacked bases, the magnitude is larger at 270 nm and significantly larger at 200 nm than that of individual bases. The spectrum is dominated by the induced CD transitions of the bases from their coupling among each other, due to their stacking on top of each other in a chiral (helical) fashion.

The simplest application of CD to DNA structure determination is for identification of polymorph present in sample.[39] The CD signature of the B-form DNA as read from longer to shorter wavelength is a positive band centered at 275 nm, a negative band at 240 nm, with cross over around 258 nm. These two bands arise not from a simple degenerate exciton coupling, but as a result of superimposition of all coupling transitions from all the bases.

If B-DNA is compacted and the bases tilted and radially displaced from the center of the helix (Figure 7, table 1) then A-form DNA results. A-DNA is characterized by a positive CD band centered at 260 nm that is larger than the corresponding B-DNA band, a fairly intense negative band at 210 nm and a very intense positive band at 190 nm. The 250-230 nm region is also usually fairly flat though not necessarily zero. Naturally occurring RNAs adopt the A-form if they are duplex.

The left handed Z-form DNA (Figure 7, table 1) is seen for poly $[(G\text{-}C)_2]$ in the presence of high salt concentrations. It is characterized by a negative CD band at 290 nm and positive band at 260 nm. Care must be taken in using these signatures to identify Z-form DNA, since the same DNA in A-Form has a negative band at 295 nm and a positive band at 270 nm.[40] A more definitive signal is the large negative CD signal in the 195-200 nm region for Z-DNA, where as B-form DNA CD is near zero or positive in this region. For Z-DNA the CD passes through zero between 180 and 185 nm.

The sign of the CD signature tells the handedness of the condensed DNA particle, with a negative signal above 250 nm corresponding to a left handed helix. CD spectra are easy to measure that often the simplest technique to probe DNA conformational changes as a function of ionic strength, solvent, ligand concentration etc. When the twist direction is reversed from B-DNA to Z-DNA,[37d] an inversion of the CD spectrum might be

expected. The salt dependence of DNA CD was correlated with changes in the helix-winding angle (the angle between the neighboring bases) deduced from measurements of super-helicity in closed circular DNA.[41] The CD at 275 nm is highly sensitive to the winding angle.[42] On going from dilute salt to 3.0 M CsCl, for example, the 275 nm band is nearly disappeared.

CD denaturation (melting) and CD-Job's plots are equally important as they give T_m and binding stoichiometry of DNA/RNA complexes respectively.

1.3 Modified oligonucleotides as antisense therapeutic agents

The unmodified antisense oligonucleotides are intended to enter the cell where they can pair with, and so inactivate, the complementary *m*-RNA sequences. But their inability to permeate cell membrane as they carry anionic charge results from repulsive interaction with the cell lipid layer. Further they are degraded by intracellular enzymes such as exo-nucleases. It became very clear that the nuclease susceptibility of natural oligonucleotides based on an unmodified (deoxy)-ribose phosphodiester (PO) backbone, would preclude profound antisense activity in biological systems at concentrations

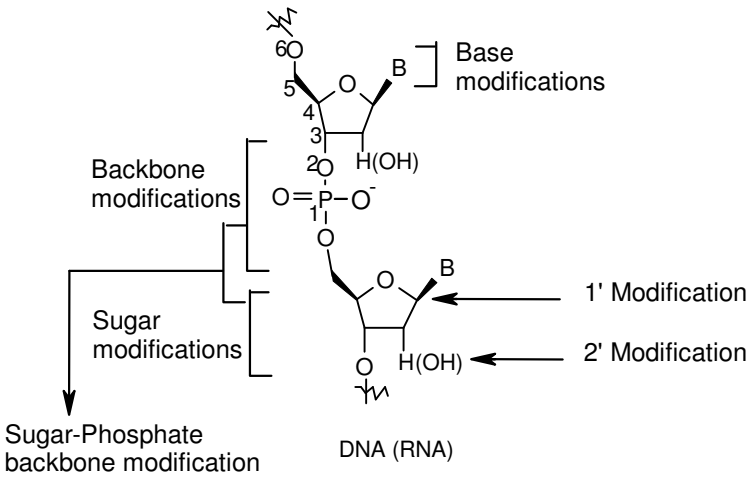

Figure 13. Oligonucleotide modifications

relevant in the context of potential therapeutic applications.[43-46] This necessitated the chemical modification of oligonucleotides (Figure 13) and represents the key element in development of antisense therapeutics. The first generation modifications focused attention on oligonucleotides having phosphorothioates (PS, Figure 14a),[47] phosphorodithioates, methylphosphonates (Figure 14b)[48] and phosphoramidates (Figure 14c)[49] replacing the anionic phosphate diester linkages and to 2'-OH protection of the ribonucleotides as second-generation antisense oligonucleotides.

Phosphorothioates (PS-oligos): The PS-oligos are oligonucleotides in which one of the non-bridged oxygen was replaced by sulfur and the backbone thus retains the negative charge, but with reduced charge density compared to phosphodiester analogue (Figure 14a).[47] PS-oligos can be easily synthesized on a commercial DNA synthesizer,[50] but the avidity of this analog for the complementary DNA was lower than natural oligonucleotide. The non-stereospecific synthesis of phosphorothioates results in the formation of a mixture of diastereomers and the conformational heterogeneity leads to lowering of the melting temperature. As a consequence, the search for a stereocontrolled synthesis has been undertaken,[51] and synthesized P-chiral analogues of PS-oligos were

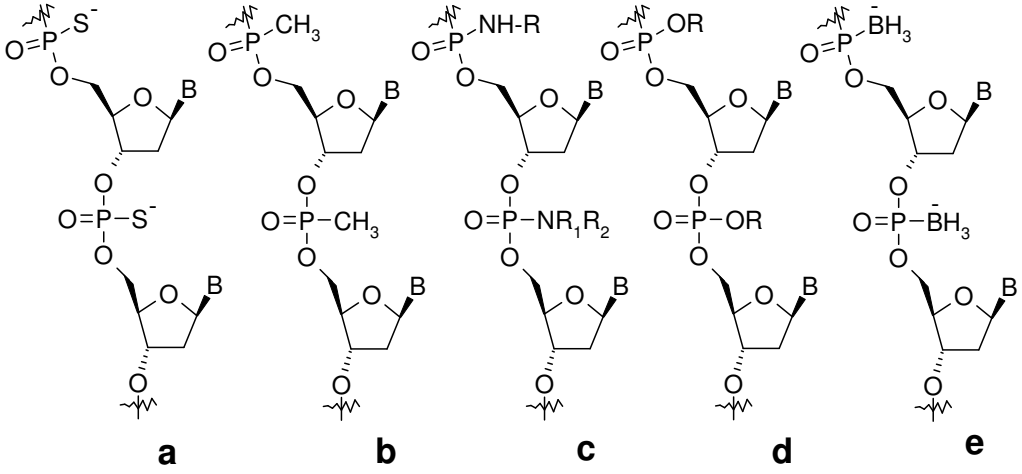

Figure 14. First generation modified antisense oligonucleotide (replacement of 'O' in P-O)

used for the biological studies of antisense targets inside living cells. PS-oligos are substrates to RNase H and these first generation antisense agents have been extensively tested in human clinical trials against numerous targets. The only antisense agent approved by FDA (Vitravene) so far is based on PS-oligos. However, these oligos have tendency to induce non-specific effects, through binding to cellular and extracellular proteins[52] as well as cleavage of non-target *m*-RNAs that are only partially complementary by RNaseH.[53]

Replacement of both non-bridging phosphodiester oxygens leads to non-chiral phosphorodithioates. Compared with the corresponding phosphorothioates, the duplex stability of phosphorodithioate modified oligonucleotides with DNA decreased, and they exhibit less non-specific protein binding and more resistance to nuclease.

Methylphosphonates: Oligonucleoside methylphosphonates are a class of nonionic oligonucleotide analogs (Figure 14b).[48] These oligomers contain deoxyribonucleoside or 2'-O-methylribonucleoside units that are linked in a 3'-5' manner via methylphosphonate groups. The methylphosphonate internucleotide linkage is similar in structure to the natural phosphodiester (PO) internucleotide bond.[54] One of the non esterified oxygens of PO group is replaced with a methyl group, and this substitution results in the loss of the negative charge. Inclusion of methylphosphonate linkage in the oligomer introduces a new center of asymmetry in to the oligonucleotide as Rp or an Sp configuration and consequently the oligomer preparation can contain up to 2^n diastereomers, where *n* is the number of methylphosphonate linkages. Methylphosphonates are resistant to the action of cellular nucleases. The electroneutral methylphosphonate linkage would reduce charge repulsion in methylphosphonate oligos and complementary target nucleic acid more readily penetrate cell membranes, thus

enhancing their internalization by cells (also known by the name MATAGENES, masking tape for gene expression).[55]

Although oligodeoxyribonucleoside methylphosphonates form stable duplexes with single stranded DNA, hybrids formed with complementary RNA of the same nucleotide sequence generally have lower stability.[56] The reduction in melting value has been ascribed to the presence of mixture of diastereomers. In contrast to normal DNA-DNA/RNA duplex, the stability of methylphosphonate-DNA duplexes are not significantly affected by changes in ionic strength. In addition to the poor aqueous solubility, methylphosphonates cannot induce RNase H activity. For these reasons this modification is less useful as antisense molecule but can serve as the platform for the development of effective antisense oligonucleotides.

Oligonucleotide Phosphoramidates (Figure 14c): Phosphoramidates are another well-studied class of backbone modifications.[49] They are resistant to hydrolysis by nucleases. With DNA targets, oligonucleotide phosphoramidates (Figure 13c, R_1 = H, R_2 = -CH_3, -CH_2CH_2OMe, $(CH_2CH_2)_2O$) exhibit rather poor hybridization characteristics (ΔT_m = -0.1 to –2.3°C, at pH 7.2).[49,57] Oligonucleotide phosphoramidates (R_1= H, R_2 = CH_2CH_2N-$(CH_2CH_2)_2O$) form weak duplexes at neutral pH and more stable duplexes under acidic conditions (pH 5.6), due to protonation of the terminal amine. Oligo-phosphoramidate with (R_1 = H, R_2 = $CH_2CH_2NMe_2$), is however reported to hybridize to DNA targets at both neutral and acidic pH. Hybridization of oligonucleotides consisting of alternating phosphoramidite/phosphodiester linkage to RNA targets is similar to the corresponding interaction with wild type oligonucleotides.[58] The T_m of these complexes turned out to be independent of the ionic strength of the buffer, in contrast to the behavior

of unmodified oligonucleotides with DNA or RNA targets, which shows a strong T_m increase, with increasing salt concentration.

Oligo-Phosphotriesters: Eventhough phoshotriesters are common intermediates in oligonucleotide synthesis, little data about their hybridization behavior are available. It has been shown that ethyl phosphotriester (Figure 14d, R = $-CH_2CH_3$) modified oligonucleotides form substantially less stable self-complementary duplexes compared to wild type.[59] A single modification in a self complementary sequence (which therefore had a backbone modification in each strand of the duplex) resulted in a T_m decrease of -4^oC and -11^oC, depending on whether the Sp or the Rp diastereomer was used.

Oligo-boranophosphonates (Figure 14e): These are derived by replacing one of the non-bridging oxygen atoms in the phosphodiester group of DNA with borane (BH_3).[60] The boron phosphate diester is isoelectronic with phosphodiesters, isosteric with methylphosphonate group and is chiral. These negatively charged oligos are highly water soluble, but more liphophilic than DNA. NMR and CD studies show that replacing the phosphodiester linkage in dinucleotides with the boranophosphodiester results in only a slight change in configurational characteristics, such as sugar pucker, acyclic torsional angles and base stacking.[61] Boranophosphate DNA is considerably more stable to various nuclease enzymes than native DNA and overall more stable than phosphorothioate DNA.[60c] The discovery that oligonucleotide boranophosphodiesters can activate *E.coli* RNase H and induce cleavage of RNA is encouraging.[62]

1.3.1 Oligonucleotides with backbone replacement not containing phosphorous

A second generation of backbone replacements for the use of antisense oligonucleotides involves elimination of phosphorous atom from the phosphotriester backbone (Figure 15). A common problem for all anionic analogs is the ineffective

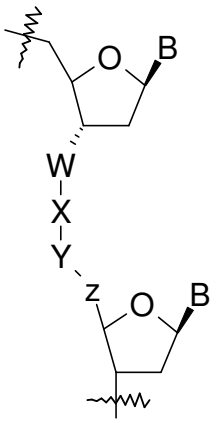

	W	X	Y	Z
1	CH_2	SO_2	CH_2	CH_2
2	NH	SO_2	CH_2	CH_2
3	O	SO_2	NH	CH_2
4	O	CH_2	O	CH_2
5	S	CH_2	O	CH_2
6	CH_2	NCH_3	O	CH_2
7	NR	CO	CH_2	CO
8	CH_2	CH_2	NH	CH_2
9	CH_2	CO	NR	CH_2
10	CH_2	NH	CO	CH_2
11	CO	NH	CH_2	CH_2
12	O	CO	O	CH_2
13	O	CO	NH	CH_2
14	O	CH_2	C	C

Figure 15. Non-phosphorous neutral backbone modifications

permeation of cellular membranes. Anionic ODNs are taken up by endosomes, but are unable to cross the endosomal membrane in the absence of cationic lipids.[63] Based on this observation, neutral isosteres of the phosphodiester linkage (Figure 15) have been devised.[64] An increasing number of neutral ODN analogs have been developed that do not contain stereogenic phosphorous centers.[65] Substitution of the PO linkage with neutral SO_2 group resulted in a series of sulfonyl containing linkages. Sulfones **1**[66a], sulfonamides **2**[66b] and sulfamates **3**[66c] have been prepared as ODN analogs, but very little in vitro and cellular data are available. The formacetal linkage **4** exhibits somewhat inferior sequence-specific binding affinities.[67] Slightly increased RNA binding properties were observed with the 3'-thioformacetal **5**[68] and N-methylhydroxylamine **6**[69] linkages. 5'-thioformacetal containing ODNs do not hybridize as well as the unmodified ODNs to either RNA or DNA. Replacement of the PO backbone by amide groups **7**-**11** resulted in neutral and achiral linkages that were tested for RNA binding and nuclease stability. Analogs **9** and **11** were identified as having good binding affinity to the RNA targets and high stability towards cellular nucleases.[70] Modifications of the 2'-position into OMe

provided ODNs with even greater binding affinity and nuclease stability.[71] Carbonate **12** and carbamate **13** linkages have also been reported as replacements for the PO backbone. The carbonate linkage has been prepared as dimer, but no biochemical data available. The 5'-N-carbamate linkage **13** is chemically stable, and cytidine hexamers were found to bind complementary DNA and RNA with high affinity,[72a] while thymidine hexamer cabamate ODN bound nucleic acid targets with relatively low affinity.[72b] Replacement of the PO linkage with an acetylenic bond **14** resulted in depressed RNA affinity.[73]

Modification of the internucleoside PO linkage: Modifications that do not contain PO linkages as part of the actual backbone structure automatically eliminate the susceptibility to nuclease degradation. They have to be incorporated into oligonucleotides via 3'-activated backbone-modified di-nucleotide analogs. The most promising modification that has emerged from the replacement of PO linkage by a neutral carboxylic amide is **amide** (**A,** Figure 16) from CIBA group.[70,74] Modified oligonucleotides with alternating arrangement of PO and amide **A** linkages exhibit modest increase in RNA binding affinity (0.5°C/modified dimer unit) over the

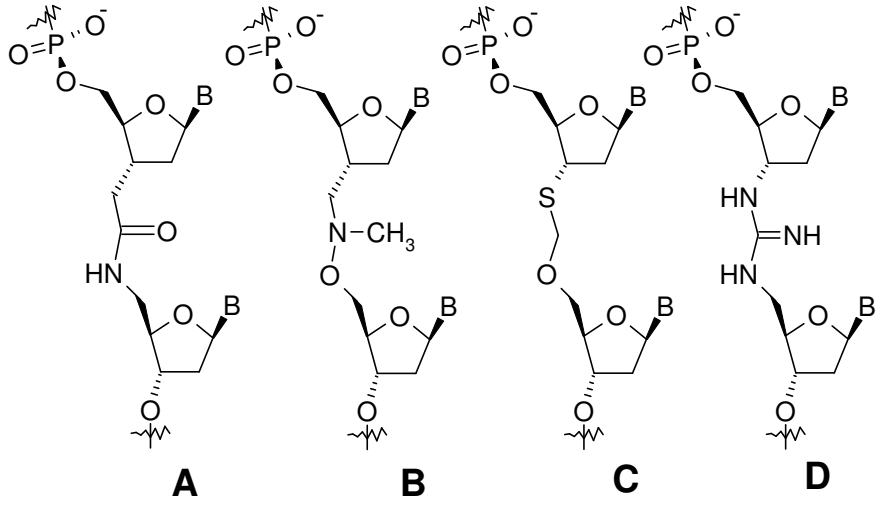

Figure 16. Modification of the internucleoside PO linkage in ODNs

unmodified wild-type duplexes. Various types of hydroxylamine-based internucleoside linkages have been studied by the ISIS group.[75] The most attractive modification appears to be the **methyl (methylimino) (MMI) linkages** (**B,** Figure 16), whose incorporation into oligodeoxynucleotides leads to slight enhanced RNA binding affinity (0.1-0.5^{o}C/modified dimer unit) and increases nuclease resistance. Another successful approach to backbone modified oligonucleotide analogs with enhanced RNA affinity consists in the replacement of phosphodiester group by 3'-thioformacetal (3'-SCH_2)-5') linkages **C** (Figure 16). An increase in T_m of 0.8^{o}C/modified dimer unit has been reported with complementary RNA, in comparison to the unmodified wild type duplex. A novel type of DNA analog, which incorporates internucleoside guanidine groups in place of natural PO linkages, termed **deoxyribonucleic guanidine** [**D**, (DNG), Figure 16], has recently been reported.[76] For fully modified analog DNG-T_5, whose 1:1 complex with poly rA was reported to exhibit incredible thermal stability (T_m = 100^{o}C at ionic strength μ= 0.22).

1.3.2 Sugar Modifications

2'-Modifcations: An important class of second-generation antisense oligonucleotide analogs is 2'-modified oligonucleotides. 2'-O-alkyl substitiuents (**1**-**4**, Figure 17) enhance the RNA binding affinity of the corresponding oligonucleotides[77] and also confer a significant degree of nuclease protection to adjacent PO linkages.[78] The 2'-

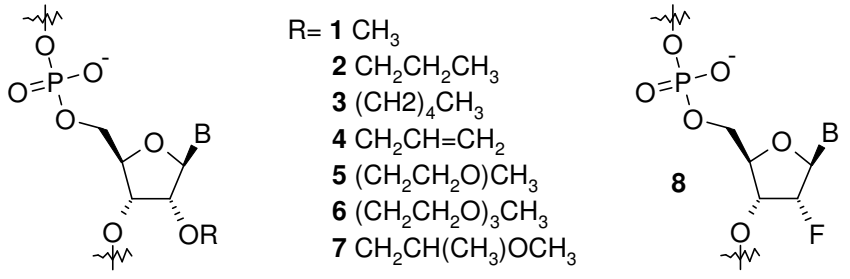

Figure 17. 2'-Modified oligonucleotides

O-methyl sugar 1 (Figure 17) enhances binding to complementary ODNs and confers stability to ssRNA from RNases, but is susceptible to degradation by DNases. It is also clear from the studies that larger 2'-alkyl groups lead to greatly enhanced nuclease stability, while RNA binding affinity gradually decreases with increasing size of the 2'-alkoxy substituents.[79] In contrast, ethylene glycol based 2'-O-substituents (**5**-**7**, Figure 17) promote RNA binding to the same extent as a simple 2'-O-methyl group (~1.0^{o}C/modification) and provides much higher degree of nuclease protection. Other 2'-modifications comprise the 2'-fluoro substituents (**8**, Figure 17) which has shown to have pronounced favorable effect on RNA binding affinity (1.5^{o}C/modification) among all 2'-substituents investigated to date. This phenomenon is generally attributed to a strong preference of the modified sugar moieties for RNA-like-3'-*endo* conformation.[80]

Pentapyranosyl-NA and threofuranosyl-NA (TNA): Pentapyranosyl-nucleic acid system was introduced by Eschenmoser group as depicted in the Figure 18. The 3' to 4' ribopyranosyl-series, having the vicinal phosphodiester groups arranged in 3'-axial 4'-equatorial position, does not produce a competent oligonucleotide pairing system. The 3' to 4' lyxopyranosyl oligonucleotides do not self-pair in the form of Watson-Crick duplexes, as well as triplexes in the case of homoadenine and homothymidine strands.[81] The thermal stabilities of these duplexes are typically weaker and more sequence dependent. These findings lead subsequently to the synthesis and evaluation of TNA (Figure 18), in which the diaxiality of the phosphodiester substituents is maintained, while the ring structure has contracted from pyranose to furanose. TNA is an extraordinary oligonucleotidic system, in that it does not only self-pair into antiparallel duplexes of the W-C type with stabilities similar to RNA, but in that it also efficiently cross pairs with target DNA and RNA.[82] As a conformationally restricted oligonucleotide

analog, Herdewijn group has developed 1,5-anhydrohexitol-NA (HNA).[83] Not only does HNA form self paired duplexes, but it also cross pairs with natural DNA and RNA. Typically, HNA-DNA duplexes show increased thermal stability (ΔT_m/mod = +1.3°C) with DNA as complement and by (ΔT_m/mod = + 3°C) with RNA as complement.

Locked Nucleic Acids (LNA): Another conformationally constrained analog is locked nucleic acids (LNA, Figure 18), introduced in 1998 by Imanishi[84] and Wengel group.[85] Structurally, this modification corresponds to a ribonucleoside in which the 2'-oxygen and the 4'-carbon atoms are linked via methylene unit. This modification locks the ribofuranose subunit into the 3'-*endo* conformation of nucleic acid duplex. Single and multiple LNA substitutions within a mixed sequence DNA oligonucleotide stabilize duplex formation with a complementary RNA typically by ΔT_m/mod = + 4 - 8°C, depending on the sequence and the number of LNA units used.

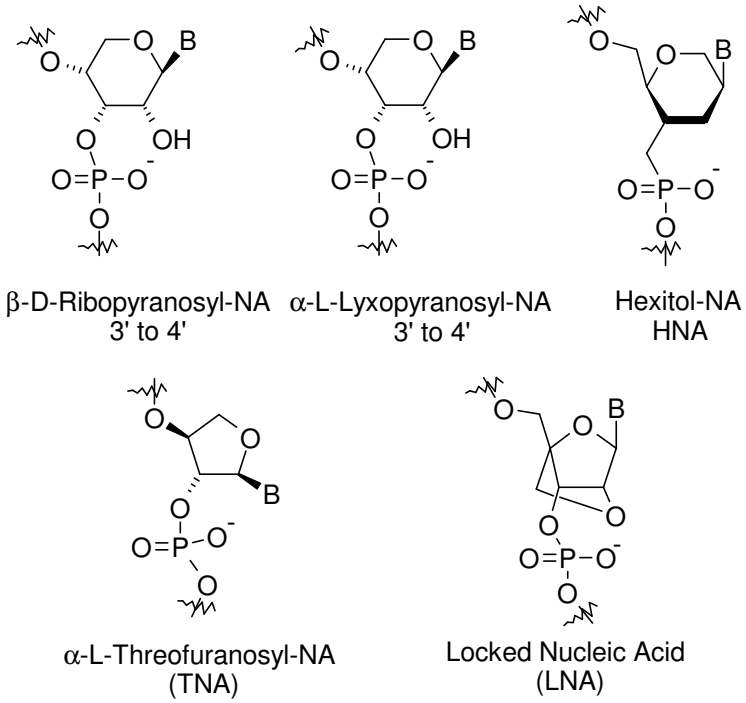

Figure 18. Sugar modifications in oligonucleotides

Six and five membered carbocyclic analogs: In case of carbocyclic pyranosyl analogues, cyclohexanyl-nucleic acid (CNA, Figure 19) was prepared in both enantiomeric (D/L) forms and D-CNA hybridizes to complementary RNA as compared to DNA with reduced affinity.[86] A similar analogue is cyclohexenyl-nucleic acid (CeNA, Figure 19), the dehydrogenated form of CNA. Complementary recognition of RNA by the CeNA is more efficient as pure DNA and half efficient as HNA.[87] Five membered carbocyclic analogs of 2'-deoxyribonucleosides are characterized by the replacement of O-4' of the deoxyribose ring by a carbon atom (Figure 19a).[88] Oligonucleotides incorporating the carbocyclic nucleoside units result in a modest increase in DNA-RNA duplex stability (ΔT_m = 0.3°-0.4°C over unmodified wild-type duplex). Similar effects on RNA binding affinity are observed for hydroxy substituted (Figure 19b) building blocks but showed higher nuclease resistance than the unsubstituted **19a**.[89] Bicyclic thymidine analog (Figure 19c) has been reported to increase the RNA binding affinity to

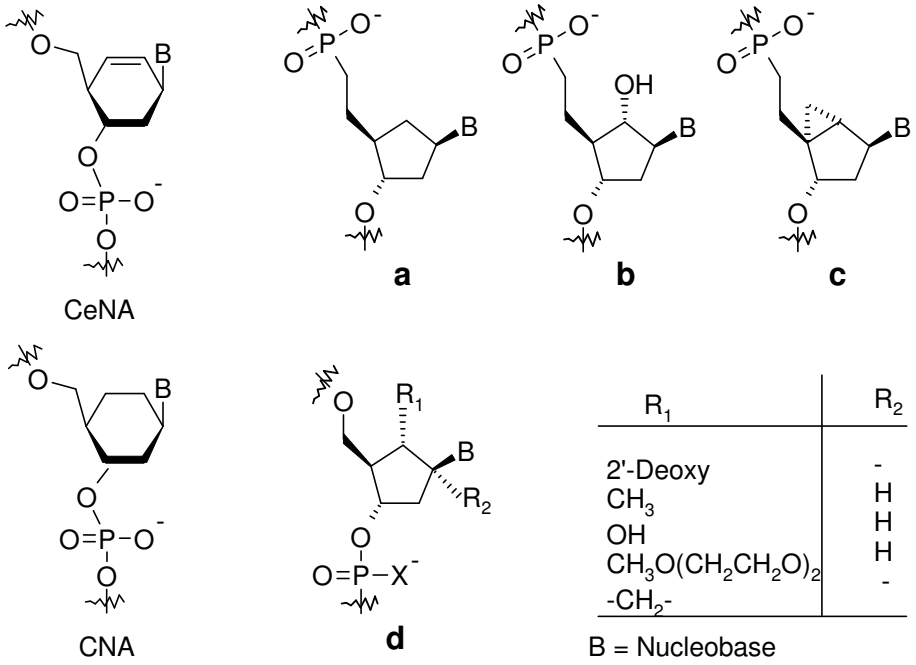

R_1	R_2
2'-Deoxy	-
CH_3	H
OH	H
$CH_3O(CH_2CH_2O)_2$	H
$-CH_2-$	-

Figure 19. Carbocyclic oligonucleotide-analogs

corresponding oligodeoxyribonucleotides to a substantial degree.[90] Altmann *et al.* investigated the effects of a number of differently substituted carbocyclic building blocks (Figure 19d) on the biological activity of antisense oligonucleotides in cell culture. None of these analogs was found to be truly, a more effective inhibitor of mRNA expression than the corresponding phosphorothioates.[91]

1.3.3 Sugar-Phosphate modified oligonucleotide

Morpholinonucleotides and peptide nucleic acids are the most prominent modified nucleic acid mimics that involve the replacement of the sugar-phosphate backbone.

Morpholino nucleotides: Summerton *et al.* prepared novel oligonucleotide analogues from ribonucleotide derived morpholine units, linked by carbamate groups (Figure 20a).[53,92] Cytosine hexamer with stereoregular backbone was prepared in solution phase and was shown to bind poly dG with very high affinity. Solubility characteristics of the resulting oligomer have been improved by terminal conjugation with polyethylene glycol. Fully modified morpholino oligomers where phosphorodiamidate groups are shown to be more effective antisense agents than iso-sequential PS-oligos in cell-free systems and in various cultured cells (Figure 20b). This is attributed to the fact that

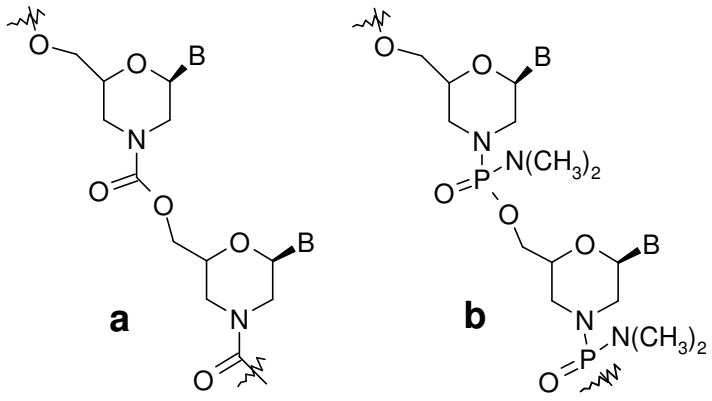

Figure 20. Morpholino ODNs linked by **a**) carbamate, **b**) phosphorodiamidate

morpholino oligos, unlike PS-oligos, do not bind to non-specific proteins and are much more sequence specific in their binding to DNA. In one notable study, morpholino oligos were shown to be more effective than PS-oligos as sequence specific antisense inhibitors of tumor necrosis factor-α (TNF-α) in mouse macrophages, despite poor uptake into these cells.[93]

1.4 Peptide Nucleic Acids

Peptide nucleic acid (PNA), a DNA mimic resulting from the sugar-phosphate backbone replacement by a pseudopeptide backbone, was introduced by Nielsen *et al*. in 1991.[94] The structure of PNA is remarkably simple consisting of repeating *N*-(1-aminoethyl)-glycine units linked by amide bonds (Figure 21). The purine (A, G) and pyrimidines (C,T) bases are attached to the backbone through methylene carbonyl linkages and hence PNA is hybrid of peptides and nucleic acids in a rare structural combination. PNAs do not contain any sugar moieties or phosphate groups. It was therefore a surprise that PNA in many respects mimicked the behavior of DNA, and in some applications demonstrated superior properties. Homopyrimidine PNAs bind to

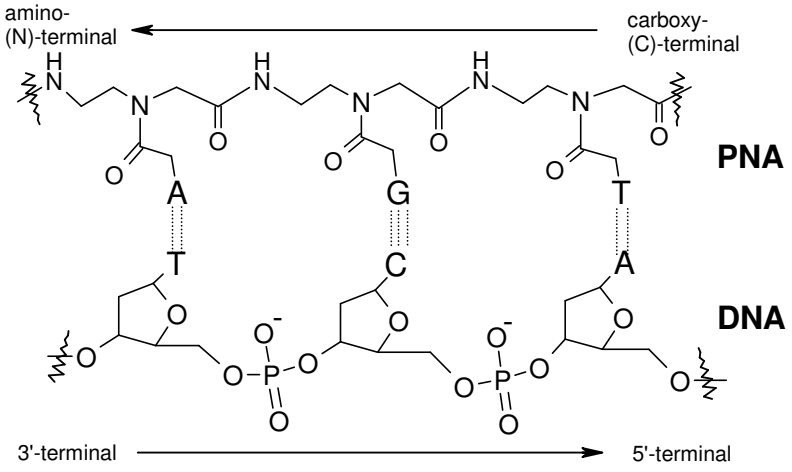

Figure 21. An antiparallel PNA:DNA duplex showing chemical structure of PNA (upper strand) as compare to that DNA (lower

complementary DNA and RNA to form triplexes with slightly increased affinity to RNA over DNA, while PNAs with both pyrimidine and purine bases form very stable duplexes with DNA/RNA, with equal affinity but more than that of either DNA-DNA or DNA-RNA complexes. Interestingly PNA can bind to DNA duplex to form triplex or duplex by displacing one of the DNA strand having same sequence of bases.

By convention, PNAs are depicted like peptides, with the *N*-terminus (corresponding to 5'-end of DNA) at the first (left) position and the *C*-terminus (3'-end of DNA) at the right. PNA is set apart from DNA in that the backbone of PNA is acyclic, achiral and neutral. PNAs can bind to complementary nucleic acids in both antiparallel and parallel orientation (Figure 10), unlike natural DNA which always prefers antiparallel orientation. However, the antiparallel orientation is strongly preferred, and the parallel duplex has been shown to have different structure.[95] Because of very favorable hybridization proprties[95,96] and high chemical and bio-stability,[97] it was regarded as a very promising lead for developing efficient antisense agents and medical drugs.[98]

1.4.1 PNA-DNA complex formation and their structures

Duplex formation with complementary DNA and RNA: PNAs obey Watson-Crick rules of hybridization with complementary DNA and RNA. Antiparallel PNA-DNA hybrids are considerably more stable than the corresponding DNA-DNA complexes.[95] The increased stability results in an increase in T_m of approximately 1^oC/base. Antiparallel PNA-RNA duplexes are even more stable compared to DNA-RNA hybrids, and PNA-DNA duplexes.[96] The stability of parallel PNA-DNA and PNA-RNA duplexes is almost exactly the same as that of (antiparallel) DNA-DNA and DNA-RNA duplexes respectively. An interesting aspect of PNA-DNA duplex formation is, the T_m decreases with increase in salt concentration (ionic strength) which is contrast to that of DNA-DNA

duplex, for which increase in T_m with salt concentration observed.[99] Base pair mismatches result in a reduction of the T_m value of 8-20°C.[95] This discrimination is, in some cases, approximately double that observed for DNA-DNA duplexes.

Triplex formation: Homopyrimidine PNAs and PNAs with high pyrimidine/purine ratio bind to target DNA normally by formation of unusually stable PNA_2-DNA triplexes.[94] However, in case of C-rich PNAs and GC-rich DNA duplexes, PNA-DNA_2 triplexes are observed. Base pairing mismatches result in a drop in melting temperature of 14-25°C.[100] The sequence specificity of triplex formation is based on the selectivity of formation of the intermediate PNA-DNA duplex, whereas binding of the third strand contributes only slightly to selectivity. In contrast, the analogous PNA_2-DNA triplexes are not formed by homopurine PNA.[101] PNAs also form stable PNA_2-RNA triplexes with RNA.[102]

PNA targeting double stranded DNA: Homopyrimidine PNAs complex with target DNA duplexes to form triplexes. An interesting and peculiar property of PNA is that, it can bind to duplex DNA to form triplex by displacing one of the strands of DNA duplex. Other binding modes for PNA have been demonstrated (Figure 22), where it can bind to DNA duplex through unusual mechanism called strand invasion. Strand invasion

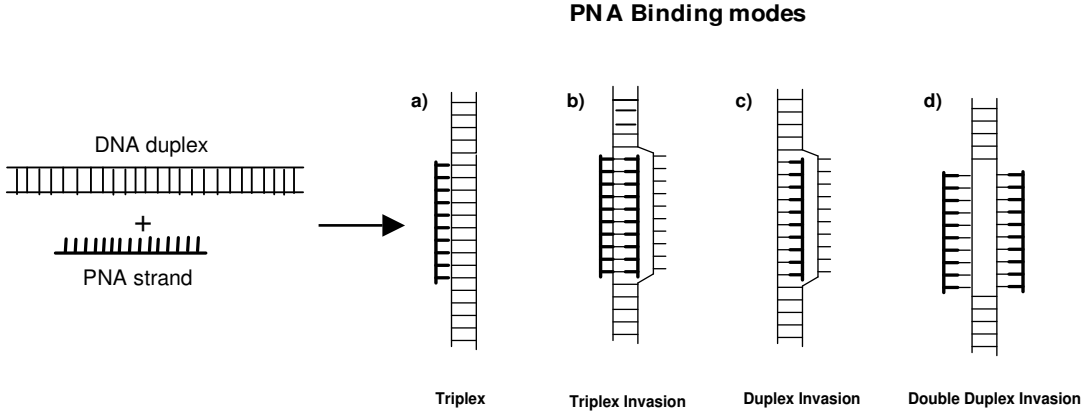

Figure 22. Schematic representation of PNA binding modes for targeting double stranded DNA. Thick structures signify PNA.

based on PNA-DNA formation (Figure 22c) appears to be limited to PNAs that form extremely stable PNA-DNA duplexes, such as very purine rich PNAs.[103] Classical triplex formation with a single PNA Hoogsteen strand (Figure 22a) has been observed as a kinetic intermediate.[104] However, PNA:DNA_2 triplexes are much less stable than the corresponding triplex invasion complexes (Figure 22b). Double duplex invasion complexes (Figure 22d) can also be formed using pseudo-complementary PNA containing diaminopurine-thiouracil 'base pairs' that sterically destabilize the competing PNA-PNA duplex.[105]

Structure of PNA-DNA duplexes: Detailed structural information has been obtained from the NMR spectroscopic study of two antiparallel PNA-DNA duplexes (Figure 23).[106] The DNA strand is in a conformation similar to the B-form, with a glycosidic *anti*-conformation, and the deoxyribose in C2'-*endo* form. A more recent NMR study[107] showed that an octameric antiparallel PNA-DNA duplex contained elements of both A-form and B-form. The primary amide bonds of the backbone are in

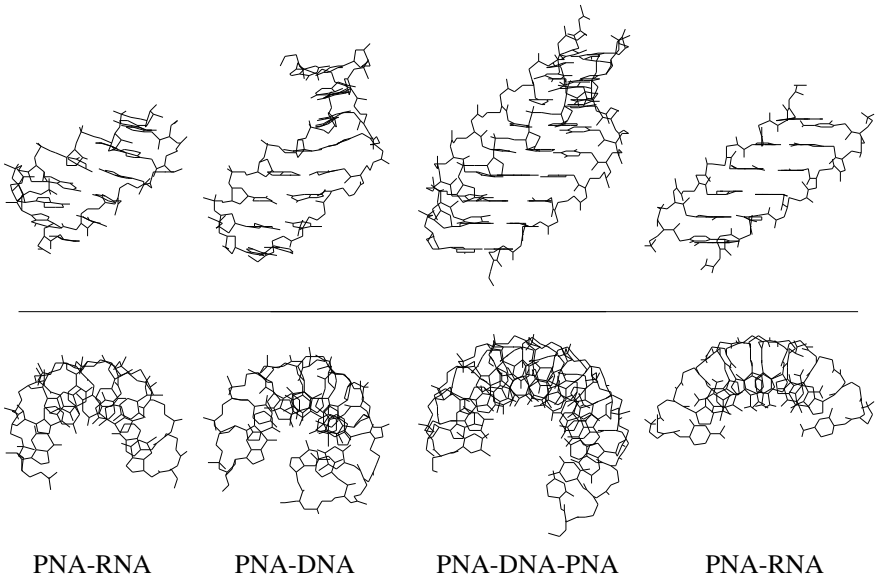

Figure 23. Structures of various PNA complexes shown in side view (upper panel) or top view (lower panel).

trans conformation and the carbonyl oxygen atoms of the backbone-nucleobase linker point towards the carboxy-terminus of the PNA strand. The CD spectra of antiparallel PNA-DNA complexes are similar to DNA-DNA spectra and indicate the formation of right handed helix.[95,106]

Structure of PNA-RNA duplexes: The structural information of PNA-RNA complex has also been obtained from NMR solution structure study (Figure 23).[107] All bases form Watson-Crick base pairs, the glycosidic torsion angle in the RNA strand indicates an *anti*-conformation, and the ribose sugars are in the 3'-*endo* form. The RNA strand thus resembles an A-form structure. The tertiary amide bonds all are in the *cis*-conformation. The carbonyl group of the tertiary amide in PNA backbone is isosteric to the C2'-hydroxyl group, which increases the solvent contact of the carbonyl oxygen atom. The CD spectra of antiparallel PNA-RNA duplexes also indicate the formation of a right-handed helix with geometry similar to the A- or B-form.[95]

Structure of PNA_2-DNA triplexes: The structural information of PNA_2-DNA triple-helix was obtained from the X-ray crystal structure analysis of the complex formed by a bis-(PNA) and its complementary antiparallel DNA (Figure 23).[108] The nucleobases of the PNA strand bind to the DNA by Watson-Crick pairing and Hoogsteen hydrogen bonding. The structure is different, however, from both A-form and B-form DNA, and forms a "P-helix" with 16 bases per turn. The DNA phosphate groups are hydrogen bonded to the PNA backbone amide protons of the Hoogsteen strand. These hydrogen bonds, together with additional van der Waals contact and the lack of electrostatic repulsion are the main factors responsible for the enormous stability of the triplex. The deoxyribose of DNA strand is in C3'-*endo* conformation like A-form and bases lie almost perpendicular to the helix axis, which is characteristic of B-form DNA. The crystal

structure is in agreement with the CD spectra of PNA_2-DNA triple-helices measured in solution.[109] The X-ray structure of self-complementary PNA-PNA duplex bears a strong similarity to the P-form of PNA_2-DNA triplex (Figure 23).[110]

1.4.2 Inhibition of gene expression

Antisense: Unlike antisense oligonucleotides, PNA-RNA hybrids are not substrates for RNase H,[102b,111] and therefore PNAs must exert their antisense effect by other mechanisms, such as direct steric blocking of ribosomes or essential translation factors. The targets around the AUG initiation codon in general seems sensitive.[102b,112] In contrast, it has been found by *in vitro* translation experiments that mixed purine/pyridine sequence PNAs, which form PNA-RNA duplexes with the target, did not arrest translation-elongation, indicating that the PNA was displaced by the moving ribosome.[102b] However, when homopurine targets are present in the translated region of gene, these can be targeted by homopyrimidine bis-(PNA), which forms extremely stable PNA_2-DNA triplexes that are indeed capable of arresting the ribosome during elongation.[102b,111] Therefore, as with general antisense gene targeting a sensible first choice would be targets close to or overlapping the AUG initiation site.

Antigene: Homopurine regions of 8 bp or more in length in double-stranded DNA (dsDNA) can be targeted by homopyrimidine PNAs via the formation of extremely stable PNA triplex strand invasion complexes.[94,113] Because two PNAs-one W-C bound and the other Hoogsteen bound are required to form these complexes, most often bis-PNAs in which the two parts are chemically linked are employed for dsDNA targeting.[114] PNA triplex invasion complexes occlude protein binding (transcription factors, restriction enzymes) to proximal or overlapping DNA sites that have sufficient stability to arrest the elongating RNA polymerase[111,115] or DNA polymerase,[116] thereby making PNAs good

candidates for antigene reagents. [104,117] Binding to dsDNA is, however, very sensitive to even moderate ionic strength,[118a] and by only employing bis-PNAs, stable binding is possible at 140 mM KCl.[118b] Thus the possibilities of using antigene PNAs *in vivo* seems slim.

Inhibition of Replication: The elongation of DNA primers by DNA polymerases can be inhibited by PNAs in cell free systems. Consequently the inhibition of DNA replication by PNAs should be possible via DNA duplex invasion under physiological pH or if the DNA is single stranded during the replication process as in the case of extrachromosomal mitochondrial DNA.[116]

1.4.3 Chemical Modifications of PNA

The structure of the classical PNA monomer (**1**) has been subjected to a variety of rational modifications with the aim of understanding the structure activity relations in this class of DNA mimics. The modifications also address the drawbacks of PNA oligomers and to improve the properties for various applications within medicine, diagnostics, molecular biology etc. These drawbacks include low aqueous solubility, ambiguity in DNA binding orientation and poor membrane permeability. Structurally, the analogues can be derived from modifications in the ethylenediamine or glycine sector of the monomer, linker to the nucleobase, the nucleobase itself or a combination of the above. The strategic rationale behind the modifications[119] are (i) introduction of chirality into the achiral PNA backbone to influence the orientational selectivity in complementary DNA binding, (ii) rigidification of PNA backbone via conformational constrain to pre-organize the PNA structure and entropically drive the duplex formation, (iii) introduction of cationic functional groups directly in the PNA backbone, in a side chain substitution or at the *N* or *C* terminus of the PNA, (iv) modulate nucleobase pairing either by modification

of the linker or the nucleobase itself and (v) conjugation with 'transfer' molecules for effective penetration into cells. In addition to improving the PNA structure as above for therapeutics, several modifications are directed towards their applications in diagnostics.

The earliest and the simplest of the modifications involved extension of the PNA structure with a methylene group individually in each of the structural sub-units (aminoethyl,[120] glycine[121] and base linker[121]) of the PNA monomer. These resulted in PNAs with *N*-(2-aminoethyl)-β-alanine **2** and *N*-(3-aminopropyl)glycine **3** backbone and ethylene carbonyl linked nucleobase **4**. However, these modifications resulted in a significant lowering of T_m of the derived PNA:DNA hybrids. The deleterious consequences of such subtle changes to the PNA structure suggested the high structural organization to which the original PNA structure is inherently tuned for interaction with

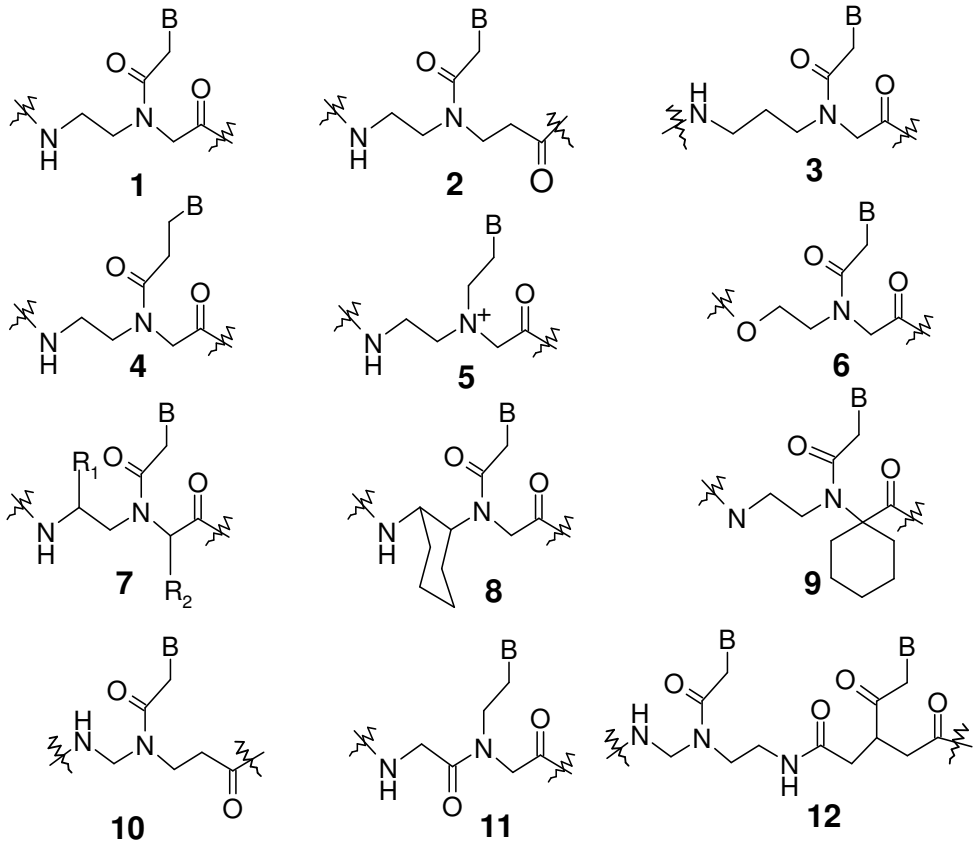

Figure 24. Chemical modifications of PNA

DNA. The replacement of the tertiary amide carbonyl by a methylene group leading to a flexible, cationic tertiary amine monomer **5** resulted in a large destabilization of the PNA:DNA hybrids.[122] The necessity of such a pseudo rigid amide group pointed to the importance of constrained flexibility in the backbone.

Further rigidification of the PNA backbone has been attempted by introduction of alkyl substituents individually or simultaneously in the aminoethyl **7a** or glycine[119,123-125] **7b** segments or in both. Suitable substitutions may also lead to generation of cyclic structures with 1,2-cyclohexylamino- (**8**) and spirocyclohexyl (**9**) rings in monomers.[126,127] While PNAs that bear (*S,S*) cyclohexyl ring in the aminoethyl part hybridize with complement DNA similar to the unmodified PNA, those derived from (*R,R*) cyclohexyl moiety (**8b**) lacked such a property.[126] Thermodynamic data showed that DNA binding of the *SS*-isomer PNA was accompanied by a reduced loss in entropy, but this was counter-balanced by a decreased gain in enthalpy.[126]A number of modifications generated by substitution of glycine component by other α-amino acids, leading to chiral PNA **7** (R_1=H) having hydrophobic, hydrophilic or charged α-substituents have been reported.[124] PNA oligomers incorporating chiral monomers retained the hybridization properties though less efficiently, with tolerance for small and medium substituents at the glycine-α position. Substitution with L/D-alanine showed a slight preference for anti-parallel binding with DNA, with D-alanine being slightly better than L-alanine.[123] Among other replacements, only those derived from D-lysine exhibited DNA hybridization properties as good as that of original PNA. The incorporation of chiral monomers enhanced the sequence selectivity of PNA oligomers in hybridization, with maximum for D-glutamic acid and D-lysine substitutions. The lysine-modified oligomers were also

more readily soluble in aqueous systems. In general, the different substituents caused equal or lower destabilization of PNA:RNA hybrids as compared to PNA:DNA hybrids.

Another type of modification involved interchange of various CO and NH groups on the peptide linkages leading to retro inverse[128] **10**, peptoid[129] **11** and heterodimeric[130] **12** analogues. In all these systems, the inter-base residue separations are similar to the unmodified PNA, but accompanied by inversion of intra and inter residue amide bonds. Except for the heterodimer analogue, these exhibited a lower potency for duplex formation with complementary DNA/RNA suggesting that in addition to geometric factors, other subtle requirements such as hydration and dipole-dipole interactions, etc influencing the microenvironment of the backbone, may be involved in effecting efficient PNA:DNA hybridization.

One of the relatively successful modifications so far are the PNAs derived from monomers based on 4-aminoproline (Figure 25)[131-132] **13**. The two asymmetric centers on the proline core at C2 and C4 lead to four diastereomeric monomers and one can expect different hybridization properties of PNAs composed from such chiral monomers. Synthetically all these can be obtained from L-4-*trans*-hydroxyproline, which is abundantly available. 4-Aminoproline nucleus also offers the flexibility to interchange the positions of the nucleobase and backbone among the different nitrogens, leading to

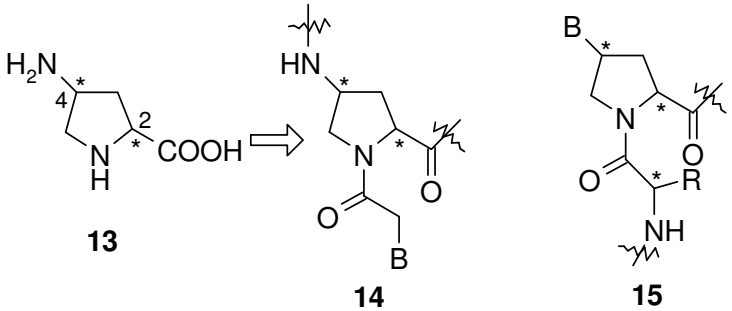

Figure 25. PNA modifications derived from 4-hydroxy-proline

oligomeric PNAs of diverse structures. Prolyl peptide nucleic acids **14** (Figure 25) based on partial substitution of L-4-*trans*-aminoprolyl units exhibited tendency to hybridize nucleic acids similar to that of unmodified PNA.[131,132] In sharp contrast, analogous PNAs derived from L-4-*cis*-aminoprolyl or D-4-*trans*-aminoprolyl units in the backbone, significantly decreased the DNA binding properties as compared to achiral PNA. However, interestingly and significantly, inclusion of even a single 4-aminoproline into a PNA sequence, either at the *N*-terminus or in the interior, not only led to stabilization of the derived PNA-DNA hybrids, but also effected significant discrimination in the orientation of binding. The chirality of the incorporated 4-aminoproline seems to influence the overall orientation selectivity. However, the stability of such PNA:DNA duplexes decreased with increasing number of chiral prolyl substitutions, and the four homooligomers derived from each of the diastereomers completely failed to form duplexes.[132] Negative results were obtained with PNAs derived from 4-nucleobase substituted prolyl-glycyl amide monomeric units[133] **15** (Figure 25). Unlike other PNAs, including the 4-aminoprolyl analogues **14**, this has a tertiary amide group with the amide nitrogen part of a cyclic ring system on the backbone. This leads to highly rigid structures that are not poised for effective duplex formation. There are many modifications derived from five membered pyrrolidine, which are discussed in Chapter 4.

Modified Nucleobases: There is increasing interest in modulating and expanding the recognition motifs of standard base pairs. Employing non-natural nucleobase ligands in place of natural nucleobases would help understand the recognition process in terms of various factors contributing to the event such as hydrogen bonding and internucleobase stacking. Further, new recognition motifs may also have potential applications in diagnostics and nanomaterial chemistry. This when coupled with high affinity and strand

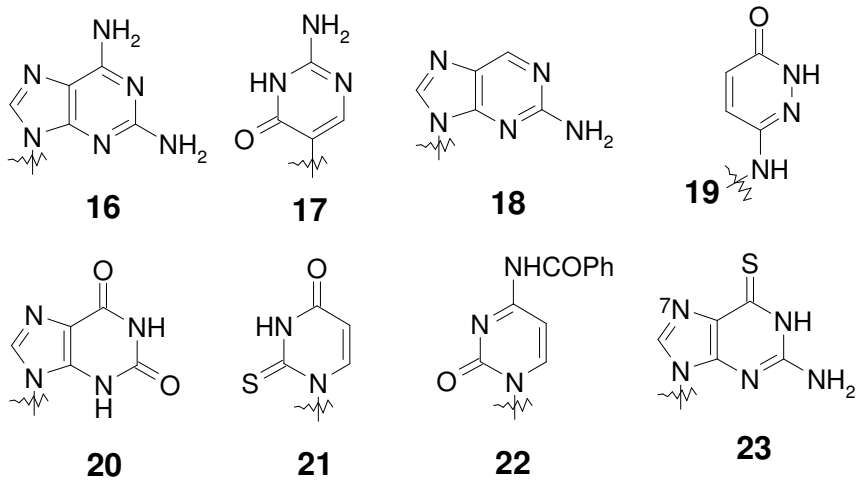

Figure 26. Examples of modified nucleobases in PNA

invasion properties offered by PNA would add a new dimension to PNA applications. The non-standard nucleobases employed so far with PNA are limited, compared to the repertoire of backbone modifications described earlier. 2,6-Diaminopurine[134] **16** (Figure 26) offers increased affinity and selectivity for thymine and pseudoisocytosine[114] **17** is a very efficient mimic of protonated cytosine for triplex formation. 2-Aminopurine[135] **18** hydrogen bonds with U and T in reverse Watson-Crick mode and has the advantage of being inherently fluorescent to enable study of kinetic events associated in hybridization.

The E-base[136] **19** was rationally designed for recognition of T:A base pair in the major groove and form a stable triad with T in the central position. The hypoxanthine base[137] **20** linked to standard PNA backbone binds A most strongly when T is its neighbor and binds C, when A is its neighbor and can thus effectively replace T or G under above circumstances. 2-Thiouracil **21** in a PNA chain opposite to 2,6-diaminopurine **35** in DNA has been effectively used as sterically compromised base pair in a double duplex invasion in PNA context.[105] N^4-Benzoylcytosine **22** present in a PNA chain has been shown to cause inhibition of triplex formation.[138] Another base introduced into PNA oligomers is 6-

thioguanine **23** which effected a characteristic shift in wavelength of absorbance due to hybridization, but decreased the PNA:DNA hybrid stability.[98c]

PNA-DNA Chimerae: The successful applications of the remarkable DNA binding properties of PNAs are sometimes (sequence/length dependent) hampered by their tendency to self-aggregate and poor aqueous solubility. Overcoming these limitations and imparting other abilities for therapeutic applications such as cellular uptake, RNase H activation properties, have been addressed by designing covalent hybrids or chimaeras of PNA with DNA, functional peptides and other effector molecules. Three types of PNA-DNA chimeras (Figure 27) are in place (i) 5'-DNA-linker X- PNA -*pseudo*-3' [98c,139] **24** (ii) *pseudo*-5'-DNA-linker X- DNA-3' [138] **25** and (iii) *pseudo* -5'-PNA-linker X- DNA-3' [98c] **26.** Synthetic protocols have been developed with protecting groups compatible for carrying out on-line synthesis of both PNA and DNA to generate the chimeras. Several interesting properties were noticed in such covalent hybrids such as co-operative stabilizing effects against proteases and nucleases, enhanced water solubility and duplex/triplex stabilities dependent on the structure of chimerae and

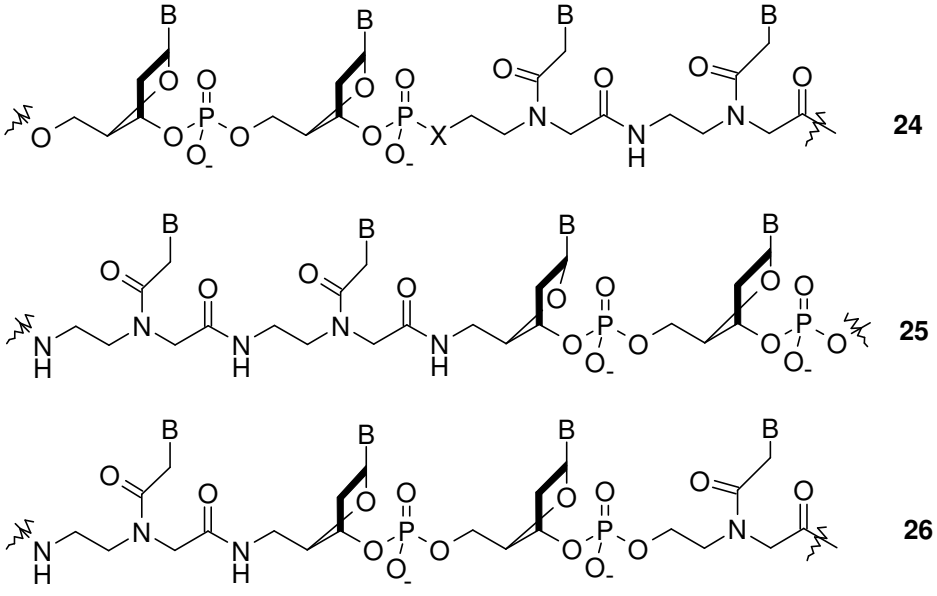

Figure 27. PNA-DNA Chimeras

the linker. The linker can also be a fragment of DNA to generate PNA-(5')-DNA-(3')-PNA chimera which formed stable duplexes with both DNA and RNA with a lower stability than corresponding DNA:DNA and DNA:RNA duplexes.[140]

PNA-peptide chimerae: A PNA pentadecamer with a heptapeptide attached to N-terminus through *tris*-(8-amino-3,6-dioxaoctanoic acid) was found to have a higher T_m on hybridization with DNA perhaps due to the presence of two positively charged arginine units.[141] A PNA-peptide-PNA chimera consisting of two oligopyrimidine PNA nonamers linked by His-Gly-Ser-Ser-Gly-His formed a stable triplex helix with oligopurine DNA strand.[108] Similarly, cationic *tris*-PNA structures involving a positively charged lysine in hairpin region[118b] and PNA's conjugated with Ni-complexing peptide (N-terminal His_6) have been synthesized for affinity chromatographic applications.[142] 2'-5'-Oligoadenylates are known to activate 2-5A dependent RNase L and hence their PNA conjugates have been used to cause degradation of RNA substrates by RNaseL.[143] A PNA peptide chimerae involving linking a 10-mer peptide containing serine, which is a substrate for protein kinase A was used in an assay for phosphorylation of serine by kinase.[141] The 5-mer PNA sequence H_2N-TAGGG-COOH linked to the N-terminus of various homooligomeric peptides of cationic amino acids lysine, ornithine and arginine are shown to inhibit human telomerase.[144]

1.4.4 Cellular Uptake of PNA

Peptide nucleic acids suffer from poor aqueous solubility and cellular uptake, because of its neutral backbone. The solubility problem was solved by selecting lysine amino acid as a spacer chain during the solid phase synthesis of PNAs and also by synthesizing PNA analogues that possesses positive charge in the backbone by default. In an effort to equip PNAs with a lipophilic tail that would confer liposome affinity, PNA-

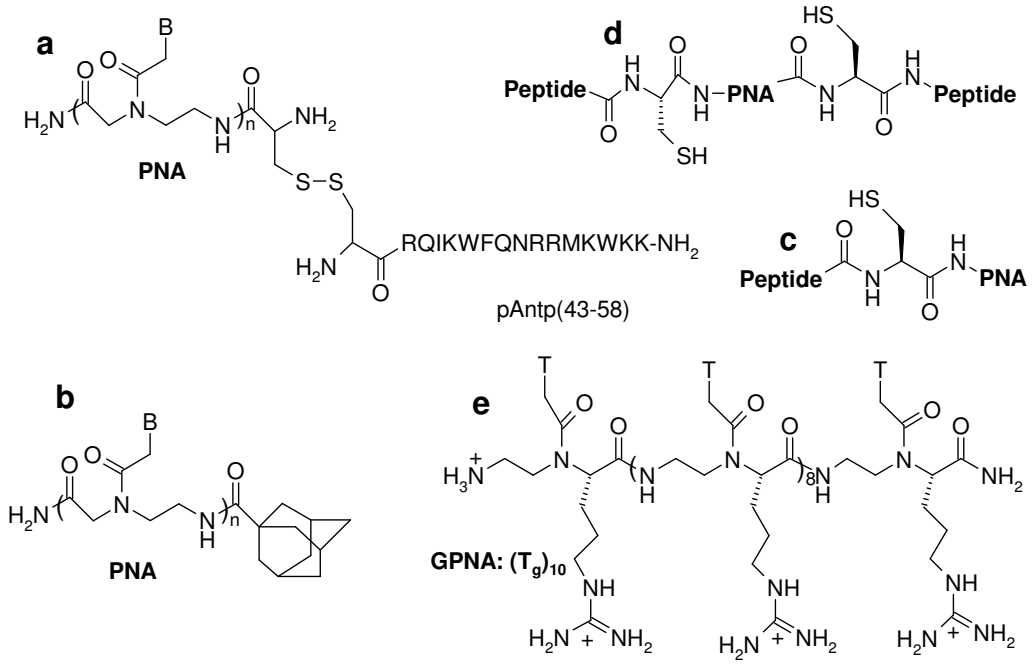

Figure 28. PNA-peptide conjugates (a, c, d). PNA-lipid (adamantly) conjugate (b), Cationic PNAs (GPNA, e).

lipid (adamantyl) conjugates (Figure 28b) have been prepared and studied their liposome mediated cellular uptake.[145] The properties of these conjugates are influenced by PNA sequence and results were encouraging and in several cases diffuse cytoplasmic uptake was observed when using cationic liposomes as carriers. However certain peptides are internalized very efficiently by cells,[146] such as third helix of the homeo domain of the antennepedia protein (Figure 27a) and sequences of tat protein. The remarkable uptake properties of HIV-1 Tat transduction domain is the result of short basic sequences of (GRKKRRQRRR).[147] They are amphiphatic –helices with high content of basic amino acid residues (Lys, Arg). These peptides are conjugated to one or both the end of PNA by an amide or disulfide linker (Figure 28a, c, d).[148] The results on cellular uptake of such PNA-peptide conjugates are impressive. In another strategy PNA containing arginine side chains (GPNA, Figure 28e) exhibited remarkable uptake properties.[149] Interestingly, the

cellular uptake of these GPNAs is not by endocytosis-driven nor receptor mediated perhaps through membrane flipping.

1.4.5 Applications of PNA

Antigene and antisense applications: Peptide nucleic acids have promise as candidates for gene therapeutic drug design. They require well-identified target and well-characterized mechanism for their cellular delivery. PNAs are chemically and biologically stable molecules and have significant effect on replication, transcription (antigene), and translation processes, as revealed from in vitro experiments. Moreover no sign of any general toxicity of PNA has so far been observed. PNA-dsDNA strand displacement complexes can inhibit protein binding and block RNA polymerase elongation. (Section-1.4.2).

Interaction of PNA with enzymes. ***RNase H***: The antisense oligonucleotide with an RNase H activity (e.g., PS-oligos) is considered a better antisense molecule (inhibitor) than one without the activity (methylphosphonates and HNAs).[98c] Despite their

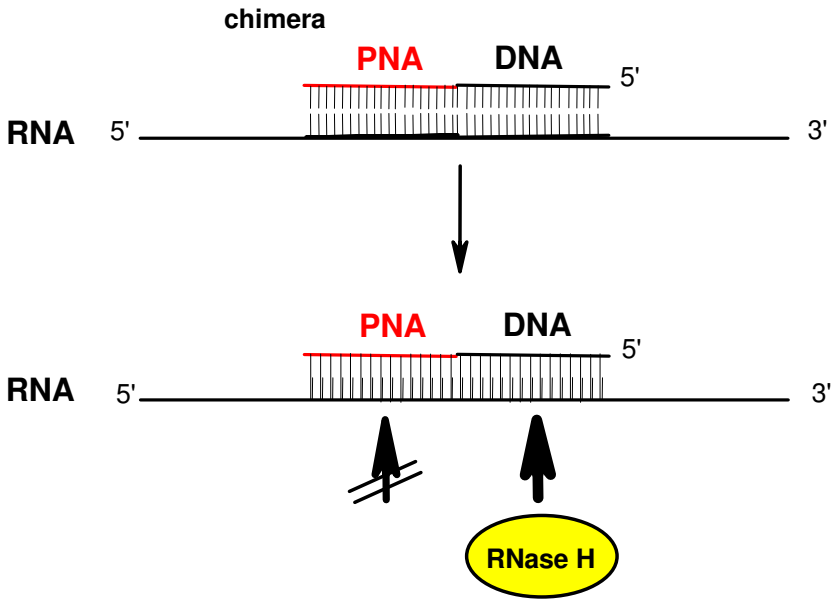

Figure 29. Schematic representation of RNase H-mediated cleavage of activity after the binding of a PNA-DNA chimera to an RNA target.

remarkable DNA binding properties, PNAs generally are not capable of stimulating RNase H activity on duplex formation with RNA. However, recent studies have shown that DNA/PNA chimeras are capable of stimulating RNase H activity. On formation of a chimeric RNA double strand, PNA/DNA can activate the RNA cleavage activity of RNase H (Figure 29). Cleavage occurs at the ribonucleotide parts base-paired to the DNA part of the chimera. Moreover, this cleavage is sequence specific in such a way that certain sequences of DNA/PNA chimerae are preferred over others.[98c] They are also reported to be taken up by cells to a similar extent as corresponding oligonucleotides.[98c] Thus, PNA/DNA chimerae appear by far the best potential candidates for antisense PNA constructs.

Polymerase and reverse transcriptase: In general, there is no direct interaction of PNA with either DNA polymerase or reverse transcriptase. However, different groups have shown indirect involvement of PNA in inhibiting these enzyme activities under *in vitro* conditions. Primer extension by MMLV reverse transcriptase has been shown to be inhibited by introducing a PNA oligomer.[111] In another experiment, it was demonstrated that the primer extension catalyzed by *Taq*-polymerase can be terminated by incorporating a PNA (PNA-$H(t)_{10}$) in to the system.[150] The reverse transcription of *gag* gene of HIV I is also inhibited *in vitro* by PNAs.[151] The inhibition has been achieved by using a bis-PNA construct, which is more efficient than the corresponding mono PNA construct.[112] Human telomerase, a ribonucleoprotein complex consisting of a protein with DNA polymerase activity and an RNA component, synthesizes (TTAGGG)n repeats at the 3' end of DNA strands. PNA oligomers that are complementary to the RNA primer-binding site can inhibit the telomerase activity. Studies have shown that the telomerase inhibition activity of PNA is better than that of corresponding activity of PS-oligos.[152]

Corey et al have demonstrated an efficient inhibition of telomerase after lipid mediated delivery of template- and non-template-directed PNA into cell.[153]

Diagnostics: The properties of PNAs in forming complexes with DNA like, high thermal stability, better sequence discrimination, strand invasion of dsDNA, and more importantly they can alter the gel electrophoretic mobility of complementary nucleic acids considerably on binding on account of their neutral character made them as the choice for the use in diagnostics.

The "**PCR clamping**" method for the detection of point mutations[154] is based on the ability to form strong PNA-DNA complex and inability to function as primers in the polymerase chain reaction (PCR). Targeting the PNA oligomer, even partially, against the primer binding site can block the formation of the PCR product. Skilful choice of the length of the primer can even allow discrimination of alleles, which differ only in one base pair. Discrimination of point mutations in the Ki-*ras* gene has been carried out by PCR clamping, where the amplification of the wild-type DNA is inhibited, relative to mutated gene, which binds with lower affinity (Figure 30).[155] Demers *et al*. have used PNAs to suppress the preferential amplification of small allelic PCR products during copying of VNTR *loci*, which leads to false genotypic patterns.[156] The quantitation of

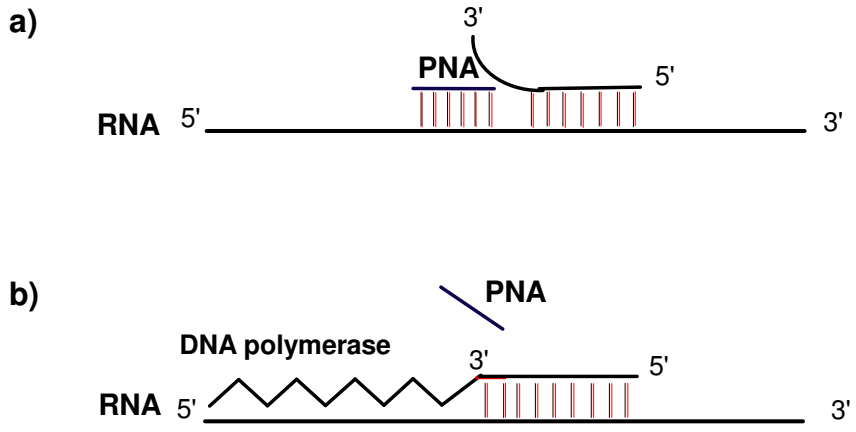

Figure 30. 'PCR clamping' technique. a) inhibition of wild-type DNA amplification and b) amplification of mutated DNA, by PNA.

telomeric repeats is also possible with PNAs.[157] The use of PNAs immobilized on surfaces as sequence specific DNA biosensors.[158]

PNAs as tools in biotechnology: PNAs can be used for the modulation of enzymatic cleavage. After strand displacement by PNA in a DNA duplex, the displaced DNA strand can be selectively cleaved by nuclease S1.[159] The single strand specific nuclease S1, in combination with two PNAs, be transformed into an "artificial restriction enzyme" that cleaves both DNA strands, and whose recognition sequence is determined by the PNA sequences employed (Figure 31). Conversely PNAs can also be used to block DNA cleavage by restriction enzymes.[160]

Furthermore, PNAs can be used to prevent the methylation of DNA sequence specifically. On dissociation of the PNA-DNA complex only the modified recognition sequence can be cleaved by the appropriate methylase sensitive restriction enzyme.[161]

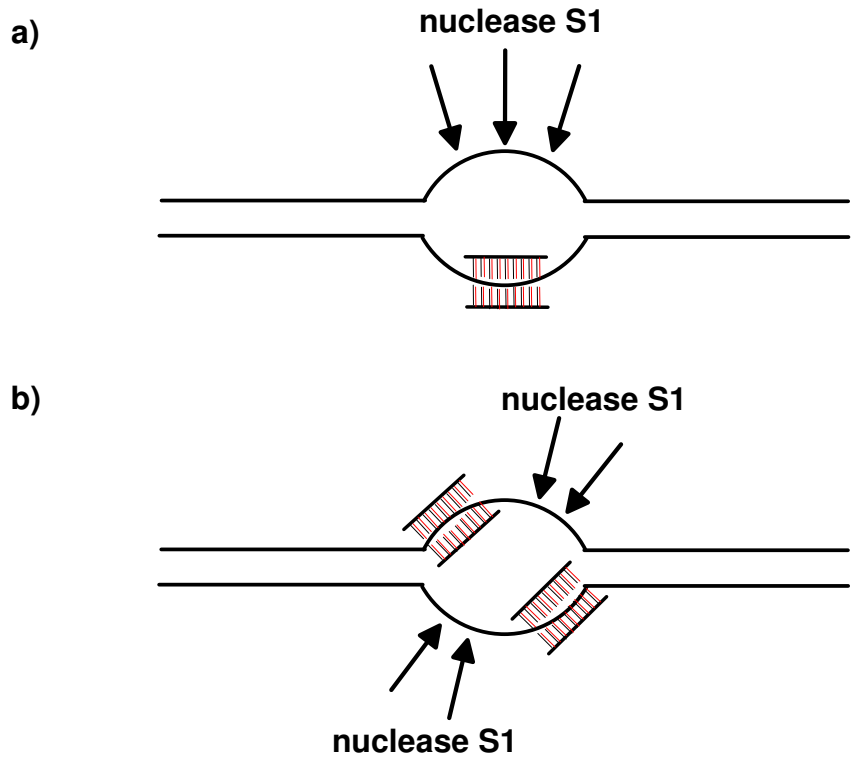

Figure 31. Artificial restriction enzymes: a) single stranded cleavage by PNA; b) double stranded cleavage by double PNA clamping.

This principle of "rare genome-cutters" has been exploited in a similar way with triple-helix forming oligonucleotides.[162]

Nucleic acid purification: Based on its unique hybridization properties, PNAs can also be used to purify target nucleic acids. PNAs carrying six histidine residues have been used to purify target nucleic acids using nickel affinity chromatography.[142] Also, biotinylated PNAs in combination with streptavidin-coated magnetic beads may be used to purify *Chlamydia trachomatis* genomic DNA directly from urine samples. However, it appears that this simple, fast, and straightforward 'purification by hybridization' approach has drawbacks. It requires the knowledge of a target sequence and depends on a capture oligomer to be synthesized for each different target nucleic acid. Such target sequences for the short pyrimidines PNA, i.e., the most efficient probe for strand invasion, are prevalent in large nucleic acids. Thus short PNAs can also be used as generic capture probes for purification of large nucleic acids. It has been shown that a biotin-tagged PNA-thymine heptamer could be used to efficiently purify human genomic DNA from whole blood by a simple and rapid procedure.

1.5 The Present work

The introduction has given an overview on the concept of gene therapeutic techniques, various types of modified antisense oligonucleotides to improve the activity of natural oligonucleotides and in particular polyamide peptide nucleic acids and their applications. Also it has provided an insight into different modifications of PNA to address some of its drawbacks.

Definition of problem: An important problem from application perspective that has not been adequately dealt is that of non-discrimination of identical DNA and RNA sequences. An analysis of the X-ray and NMR structural data suggests that the dihedral angle β

could be a key factor (Table 1). The preferred values for β in PNA_2:DNA triplex and PNA:RNA duplex is in the range 65-70° while that for the PNA:DNA duplex is about ~140°, suggesting that it may be possible to impart DNA/RNA binding selectivity by restricting β to 65-70° range through suitable modification.

Table 1. Dihedral angles (°) in PNA and PNA:DNA/RNA complexes

Entry	Compound	α	β	γ	δ	χ_1	χ_2
1	PNA_2:DNA[108]	-103	73	70	93	1	-175
2	PNA:DNA[106]	105	141	78	139	-3	151
3	PNA:RNA[107]	170	67	79	84	4	-171

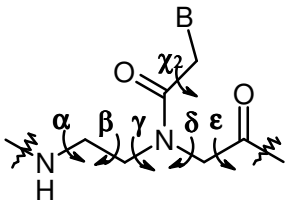

*aeg*PNA

The present work in the thesis focused on introducing RNA/DNA discrimination into PNA by tuning dihedral angle **β** as well as a pyrrolidine modification with extended backbone. The following chapters discuss the synthesis of designed monomers, incorporation into PNA oligomers using solid phase synthesis and study of the discrimination properties using various biophysical techniques.

Chapter 2: In an attempt to tune the dihedral angle **β** and to render the resulting modified PNA to bind selectively to RNA over DNA, *cis*-cyclohexyl PNA (*ch*PNA) with axial-equatorial disposition of *cis*-1,2 substituents were designed as shown in below. This chapter describes the synthesis of *ch*PNA monomers, their incorporation into *aeg*PNA and DNA/RNA discrimination studies.

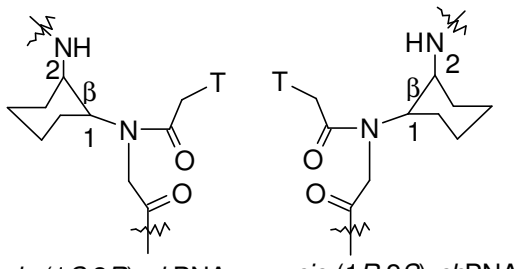

cis-(1*S*,2*R*)-*ch*PNA *cis*-(1*R*,2*S*)-*ch*PNA

Chapter 3: To improve the binding affinity with retained DNA/RNA discrimination, a relatively flexible cyclopentyl PNA (*cp*PNA) with *cis*-pseudoaxial/pseudoequatorial dispositions of substituents were designed, where better torsional adjustments are possible to attain the necessary hybridization competent conformations. This chapter summarizes the synthesis of *cp*PNA monomers, their oligomerization and DNA/RNA binding studies.

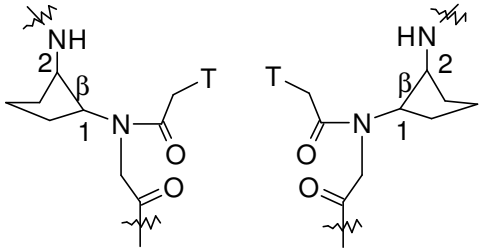

cis-(1*S*,2*R*)-*cp*PNA *cis*-(1*R*,2*S*)-*cp*PNA

Chapter 4: In a different approach, a cationic pyrrolidine based peptide nucleic acid (*bep*PNA) was designed which as an extended backbone compared to *aeg*PNA and natural DNA as well. This *bep*PNA was designed, to address all the drawbacks of classical PNA through a novel monomeric unit. The synthesis of the *bep*PNA monomers, oligomerization and DNA/RNA binding studies of the synthesized oligomers are presented in this chapter.

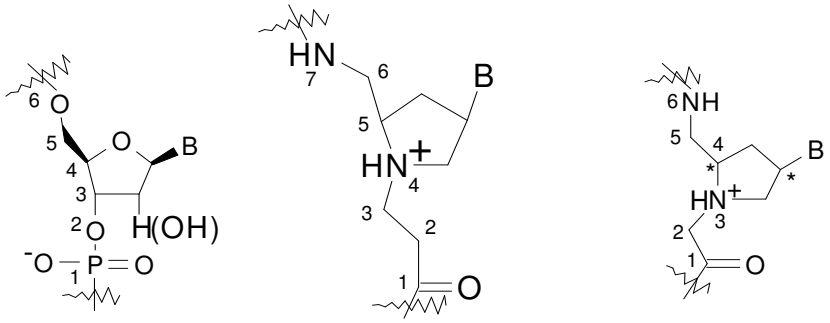

DNA/RNA *bep*PNA *Pyrrolidine* PNA

Chapter 5: An efficient and rapid conversion of mesylatye to azide under microwave irradiation has been carried out, which proceed through inversion of

configuration from chiral mesylates to provide optically pure *cis*-azides, immediate precursors of vicinal-*cis*-1,2-diamines.

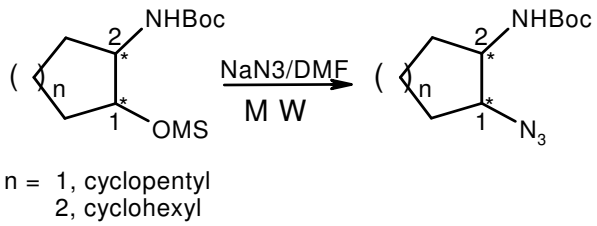

n = 1, cyclopentyl
2, cyclohexyl

Chapter-2

Synthesis and Evaluation of (1*S*,2*R*)-and (1*R*,2*S*)-Aminocyclohexylglycyl PNAs (*ch*PNA) as conformationally Preorganized PNA Analogues for DNA/RNA Recognition

2.1 Introduction

In the area of modified nucleic acids and oligonucleotide analogues, several chemical modifications have been reported to date for applications in antisense therapeutics.[163] Among these, peptide nucleic acids (PNA), composed of *N*-(2-aminoethyl)glycine units to which natural nucleobases are attached *via* methylene-carbonyl linker[94] (Figure 1, *aeg*PNA) are found to mimic many of the oligonucleotide properties. PNA binds to complementary DNA and RNA to form duplexes *via* Watson-

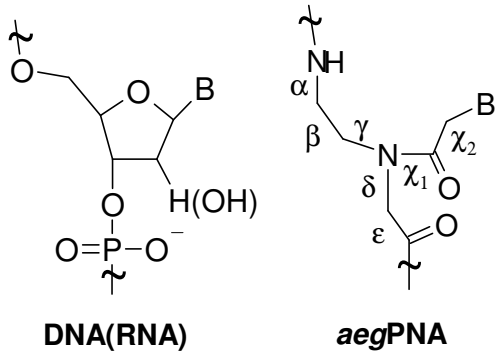

Figure 1. Basic chemical structures of DNA (RNA) and *aeg*PNA

Crick base pairs and triplexes through Watson-crick base pair and Hoogsteen hydrogen bonding. PNA:DNA/RNA hybrids exhibit thermal stability higher than that of analogous DNA:DNA and DNA:RNA complexes.[95,96] Because of this attractive feature and stability to proteases and nucleases, PNAs are of great interest in medicinal chemistry,[98] with potential for developing gene targeted drugs (antigene and antisense) and as reagents in molecular biology and diagnostics.[154-162] Since the development of PNA, there has been

several rational modifications in order to understand the structure-activity relationship.[166] However, PNA suffers from drawbacks such as poor aqueous solubility, cell permeability, ambiguity in directional binding of the complementary DNA/RNA, in both parallel and antiparallel orientations. Attempts to address these shortcomings have lead to several structural modifications of PNA.[164] These comprise ligand conjugation, introduction of chirality into achiral backbone and modifications to conformationally rigidify the PNA strand to entropically drive the duplex formation.[164] An effective way to preorganize the PNA strand for attaining hybridization competent conformation is to introduce ring structures connecting the backbone to side-chain. Some of the strategic rationale behind the modifications is to overcome the ambiguity in DNA/RNA binding orientations, flexibility or lack of rigidity and discrimination between RNA and DNA binding. This can be achieved by several cyclic modifications[164] to preorganize the PNA structure, which entropically drives the duplex formation. One such modification is incorporation of the spirocyclohexyl ring in the glycine part of the *aeg*PNA monomer (Figure 2a).[127]

Introduction of chirality in the achiral PNA backbone influences the orientational selectivity in complementary DNA binding. A number of modifications generated by substitution of glycine component by other α-amino acids, leading to chiral PNA (Figure 2b, R_1=H) having hydrophobic, hydrophilic or charged α-substituents have been reported.[119,123-125] PNA oligomers incorporating chiral monomers retained the hybridization properties though less efficiently, with tolerance for small and medium

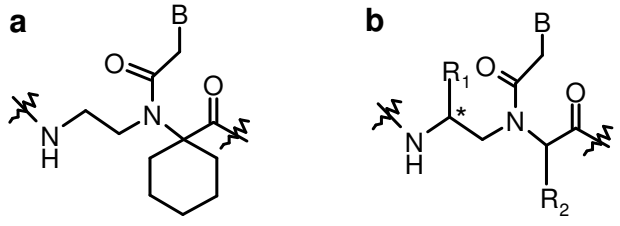

Figure 2. a) Spirocyclohexyl PNA b) α–amino acid substituted PNA.

substituents at the glycine-α position. Substitution with L/D-alanine showed a slight preference for anti-parallel binding with DNA, with D-alanine being slightly better than L-alanine.[123] Among other replacements, only those derived from D-lysine exhibited DNA hybridization properties as good as that of original PNA. The incorporation of chiral monomers enhanced the sequence selectivity of PNA oligomers in hybridization, with maximum for D-glutamic acid and D-lysine substitutions. The lysine modified oligomers were also more readily soluble in aqueous systems. In general, the different substituents caused equal or lower destabilization of PNA:RNA hybrids as compared to PNA:DNA hybrids.

In an another attempt, modification is to constrain the flexibility in ethylene diamine segment of the PNA monomer by imposing a cyclohexyl ring.[126] The (*S*,*S*) cyclohexyl PNA (Figure 3) hybridizes with complementary DNA with slightly lower T_m compared to unmodified PNA, while (*R*,*R*) cyclohexyl PNA lacked such a property. Thermodynamic data has shown that the DNA-binding of the (*S*,*S*) cyclohexyl PNA is accompanied by an entropy gain, but counterbalanced by a decreased enthalpy.

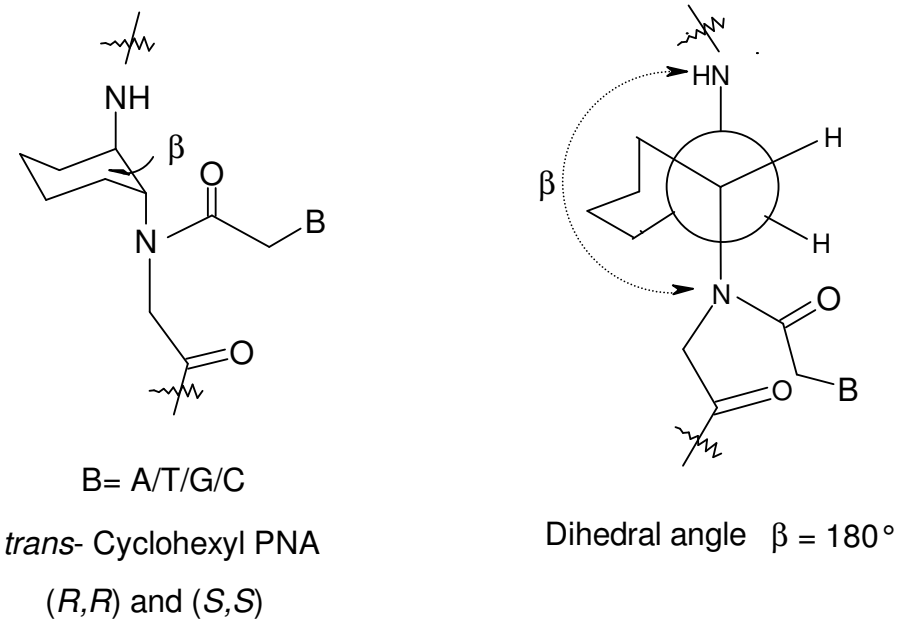

Figure-3. *trans*-(1*S*,2*S*/1*R*,2*R*)-cyclohexyl PNA showing (*e*,*e*) disposition.

Moreover, the Molecular Dynamics simulations performed on the model structure of (*S*,*S*) and (*R*,*R*) cyclohexyl PNAs showed that the dihedral angle β (Figure 3) is close to 180° (1,2-diaxial).[126]

2.2 Rationale and Objective of the Present Work

The rationale for the present work is to design peptide nucleic acid analogues that can bind selectively to RNA or DNA. Classical PNAs are very flexible and are able to adjust their conformations to accommodate binding to both DNA and RNA (Figure 4). While several researchers have made conformationally rigidified analogues of PNAs and accidentally few of them have shown a slight marginal discrimination between DNA and RNA. No systematic attempts have been made to rationally control the PNA conformation such that a modified PNA will have preferential complexation towards one type oligonucleotide compared to another. If the PNA:DNA complex is too stable it may not dissociate inside the cells and the PNA will not be available to bind m-RNA. Therefore, examining new PNAs with differential binding preference for RNA over DNA could lead to PNAs with better cellular uptake properties and antisense activity. The modified PNAs that form stable PNA:RNA complexes compared to regular *aeg*PNAs

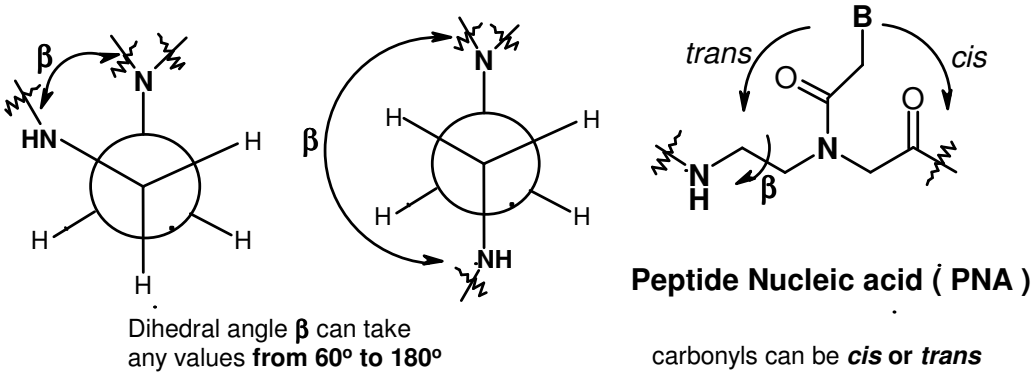

Figure 4. The flexibility of *aeg*PNA is attributed to i) ethylene diamine portion of the backbone (where dihedral angle β can vary from 60° to 180°) and ii) side chain linker connecting nucleobase to main chain (carbonyls can be *cis* or *trans*).

could successfully inhibit protein synthesis by binding to m-RNA sequences. In addition, PNAs that selectively bind RNA over DNA will avoid competitive DNA binding and will ensure that observed antisense activity occurs via binding to RNA.

Analysis of PNA:DNA[106] and PNA:RNA[107] duplexes by solution NMR studies and PNA_2:DNA[108] triplex by X-ray structural studies has revealed distinctive differences in the PNA conformations (Table 1).[165] The most notable difference is in the dihedral angle **β**. In a PNA:RNA duplex and PNA_2:DNA triplex, **β** has values in the range of 65-70° and in a PNA:DNA duplex, **β** is approximately 140°. In regular PNA backbone there are no conformational restrictions for β, therefore this dihedral angle can adopt all necessary values for RNA or DNA binding. But if **β** is restricted to values in the range 65-70°, the resulting PNA should bind to RNA selectively over DNA. This also suggests that the *trans* geometry (**β** ≅ 180°) of the cyclohexyl PNA reported earlier in literature is far from the desired PNA conformation and is not suitable for the hybridization with target DNA/RNA.

Table 1. Dihedral angles (°) in PNA and PNA:DNA/RNA complexes

Entry	Compound	α	β	γ	δ	χ_1	χ_2
1	PNA_2:DNA[108]	-103	73	70	93	1	-175
2	PNA:DNA[106]	105	141	78	139	-3	151
3	PNA:RNA[107]	170	67	79	84	4	-171

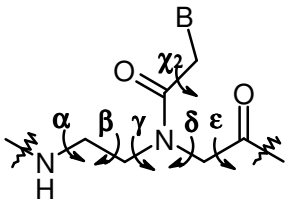

*aeg*PNA

In view of the above observations, it was intended to modulate the conformational rigidity of the ethylene diamine portion of the PNA backbone to attain optimum and selective binding to ribonucleic acid (RNA). The model is conceptually derived by introducing cyclic hydrocarbon constraint on C-C of ethylene diamine portion of *aeg*PNA. The possible number of methylene groups in the hydrocarbon may vary from one to four (Figure 5). Among the four possibilities, hydrocarbon-linkers with one

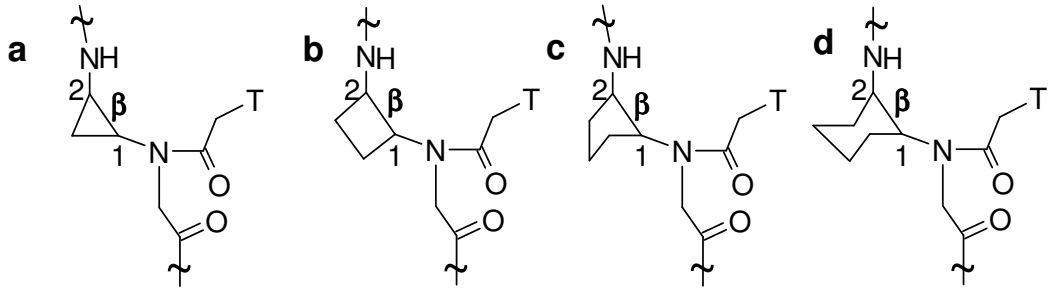

Figure 5. Probable Carbocyclic PNAs.

(cyclopropyl) and two (cyclobutyl) methylenes were excluded from initial trials on the basis of their instability (steric and torsional strain) and greater deviation of **β** is expected. The cyclohexyl ($4xCH_2$) and cyclopentyl ($3xCH_2$) modifications would be more suitable for this purpose. As it was discussed, the *trans*-cyclohexyl constrained PNA is not suitable for either DNA binding or RNA binding, because the dihedral angle β is 180° which is not in the range of angle required for neither DNA nor RNA binding. On the other hand, (1*S*,2*R*) and (1*R*,2*S*) cyclohexyl (pentyl) PNAs with *cis* stereochemistry, have dihedral angle β close to 65° (Figure 6) and hence are more suitable as analogs for incorporation into PNA backbone to achieve differential DNA/RNA binding. Particularly

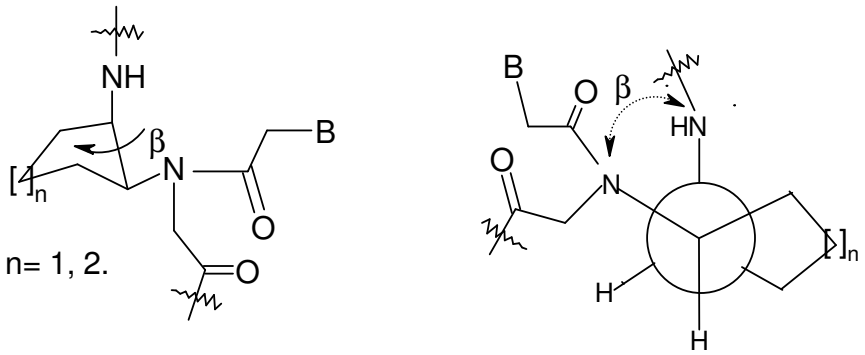

cis-Cyclohexyl (pentyl) PNA

B= A/T/G/C

PNA Dihedral Angle β

in PNA-RNA Duplex.

$\beta = 65 - 70°$

Figure 6. Dihedral angle representation in *ch*PNA (*cp*PNA).

in *cis*-cyclohexyl system, the dihedral angle for 1,2-axial-equatorial substituents will be in the required range of 60° and will be slightly less in *cis*-cyclopentyl system. The PNAs derived from these two enantiomeric units should therefore provide entropic advantage through pre-organization. Further, the chirality may introduce orientation selectivity in binding to DNA/RNA.

This chapter deals with chemical synthesis and biophysical evaluation of PNA oligomers having (1*S*,2*R*) and (1*R*,2*S*)-cyclohexyl monomers incorporated at specific positions into *aeg*PNA backbone (Figure 7).

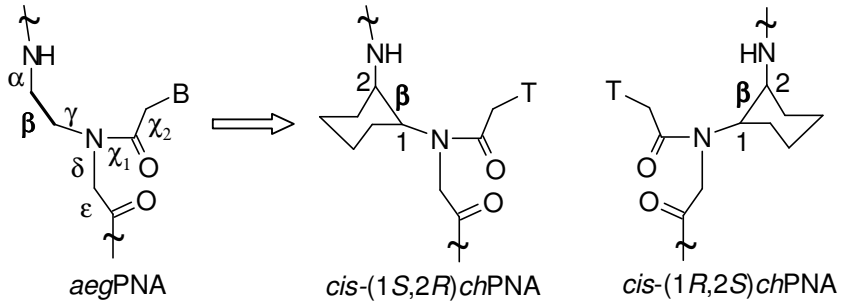

Figure 7. Structures of *aeg*PNA and designed chiral *cis*-(1*S*,2*R*)- and (1*R*,2*S*)-amino cyclohexyl PNAs (*ch*PNA)

The specific objectives of this chapter are

i) Synthesis of *cis*-(1*S*,2*R*) and (1*R*,2*S*)-aminocyclohexylglycyl PNA (*ch*PNA) monomers involving chemo-enzymatic resolution of one of the key intermediates.

ii) Crystallization and X-ray structures of *cis*-(1*S*,2*R*) and (1*R*,2*S*)-*ch*PNA monomers.

iii) Solid phase synthesis of oligomers incorporating *aeg*PNA monomers and *ch*PNA monomer.

iv) Cleavage from the solid support and purification, characterization of the oligomers.

v) The binding studies of *ch*PNA and *aeg*PNA chimeras with DNA/RNA using various biophysical techniques UV, CD and gel electrophoresis.

2.3 Results and Discussion

The two enantiomers of the *cis*-cyclohexyl PNA monomer (Figure 8) were synthesized from the chirally pure (1*S*,2*R*) and (1*R*,2*S*)-cyclohexyl-1,2-diamines in their optically pure form. Unlike the *trans*-cyclohexyl-1,2-diamines (**7a** and **7b**) which are available commercially, *cis*-cyclohexyl-1,2-diamines are not available, perhaps because of the synthetic difficulties or non availability of routes to synthesize them in their chirally pure form. These diamines can be obtained from the corresponding chirally pure 1,2-aminoalcohols (**4a** and **4b**) via stereochemical transformations. The enantiomerically pure 1,2-aminoalcohols (**4a** and **4b**) can be obtained from the ring opening of the cyclohexane-1,2-epoxide using sodium azide and chemoenzymatic resolution of the racemate, reduction of the azide functionality. We have selected the enzymatic route for the synthesis of target monomers because of the accompanying substrate selectivity and activity. The optical purities of enantiomers obtained from the enzymatic resolution are always better than from chemical methods. The target monomers were synthesized starting from simple cyclohexene epoxide as represented schematically in the Figure 9.

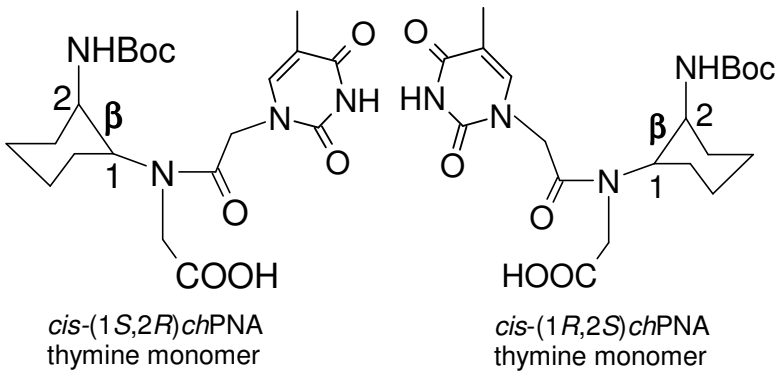

Figure 8. Structures of target *ch*PNA monomers **11a** and **11b**.

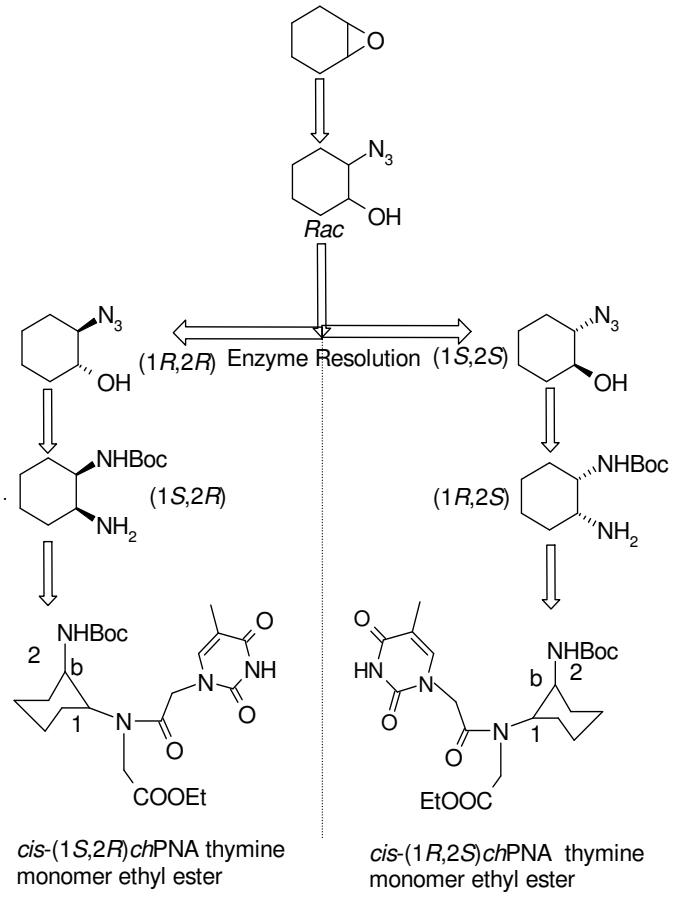

Figure 9. Schematic representation of Synthesis of *ch*PNA-monomer esters **10a** and **10b**

2.3.1 Enzyme Hydrolysis[166]

Today hydrolases are established enzymatic tools for organic synthesis on a laboratory as well as industrial scale. Hydrolases are chiral catalysts, which function without a coenzyme,[166] are commercially available and possess low substrate specificity, but high enantiotropic selectivity and enantiomer selectivity. Catalytic hydrolysis and formation of C-O bond of an ester is amongst the most useful enzyme catalyzed reactions in organic synthesis. Among hydrolases, the most widely used class of enzymes for chemo- and regioselective transformations are the Lipases. Hydrolysis of C-O bonds of esters is usually carried out at room temperature in aqueous solution or in mixtures of water and either water-miscible or water-immiscible solvent. Because of large excess of

water, the equilibrium is more towards the side of carboxylic acid and the alcohol and the reaction is practically irreversible (Note 1). Low solubility of liquid substrates normally presents no problem since lipases are active at the liquid-liquid interface. In aqueous solution, the parameters that most influence the rate of hydrolysis are pH and temperature. In most cases the hydrolysis is done at room temperature and pH 7.0, but at lower temperature, the selectivity of the hydrolysis may be higher.[166] Among the hydrolases, the most widely used are, lipases such *Candida antarctica* lipase, *Candida cylindracea* (*rugosa*) lipase and *Pseudomonas sp*. Lipases (for example *pseudomonas cepacia* lipase).

***Note* 1: Mechanism of hydrolase catalyzed reaction**

R^1-CO-X-R^2 + enzyme ⇌ R^1-CO-X-R^2 · enzyme ⇌ R^1-CO- enzyme · H-X-R^2 ⇌ R^1-CO- enzyme + H-X-R^2 (Eq. 1)

R^1-CO- enzyme + H-Y-R^3 ⇌ R^1-CO- enzyme · H-Y-R^3 ⇌ R^1-CO-Y-R^3 · enzyme ⇌ enzyme + R^1-CO-Y-R^3 (Eq. 2)

R^1-CO-X-R^2 + H-Y-R^3 ⇌ R^1-CO-Y-R^3 + H-X-R^2 (Eq. 3)

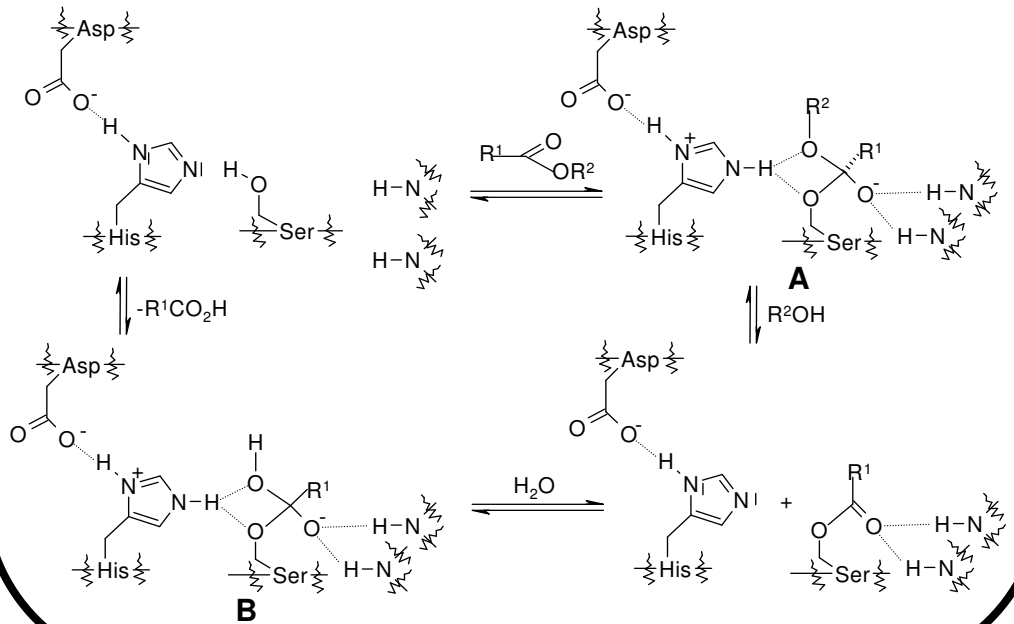

Note *1* *(contd…)*

Enzyme catalysed selective ester hydrolysis: Resolution of racemic alcohols or carboxylic acids:[166] The enzymes used are all serine hydrolases, involves the following steps (Note 1). Formation of an enzyme-substrate complex, attack of the hydroxyl group of the serine residue in the active site of the enzyme on the carbonyl group of the substrate or reagent with formation of a covalent acyl-enzyme-product complex and its transformation to the free acyl-enzyme and H-X-R2 (eq. 1); reaction of the acyl enzyme with nucleophile, as for example water or an alcohol with formation of an acyl-enzyme substrate complex, which reacts with deacylation and formation of an another enzyme product complex, which finally gives the free enzyme and the product (Eq. 2). The overall equilibrium, the attainment of which is catalyzed by the enzyme, is depicted in Eq. 3. All steps are reversible. Formation of the acyl-enzyme and its reaction with a nucleophile involves the enzyme bound tetrahedral intermediates **A** and **B**. In these processes a triad of three amino acids of the active site of the enzyme, Ser, His and Asp (Glu), which are specifically oriented in a three dimensional way, together with other amino acids involved. The stabilization of the oxy anion intermediates A and B and the corresponding transition states through hydrogen bonding from amide bonds or other amino acid residues of the active site is very crucial. Hydrolysis of the C-O bonds of esters [Eq. 1 to 3, X = O and YR3 = OH] is usually carried out at room temperature in aqueous medium or in mixtures of water and either water-miscible or water-immiscible solvent. *Because of the large excess of water, equilibrium usually is mainly if not completely on the side of the carboxylic acid and the alcohol [Eq. 3, X, Y, = O, R3 = H] and the reaction is practically irreversible.*

Lipases: Lipases (triacyl glycerol acyl hydrolases) are a unique class of hydrolases for asymmetric synthesis based on prochiral or racemic substrates. Lipases are induced-fit enzymes, accepting non-natural substrates of enormous structural diversity. The lipases most commonly used are commercially available *pig pancreas lipase* (PPL), *Pseudomonas cepacia* (PCL) or *P. fluorescens* lipase (PFL), *candida cylindracea* (CCL) or *C. rugosa lipase* (CRL), *Pseudomonas sp.* Lipase (PSL), increasingly *Candida antartica* B lipase (CAL-B). About 70 different lipases are commercially available. Most of these are presumably serine hydrolases containing serine residue in their active site and featuring presumably the triad Ser….His….Asp. The crystal structures of 13 different lipases have been determined.

2.3.2 Chemo-enzymatic resolution of *Racemic*, *trans*-2-azido-cyclohexanol.

There have been number of approaches reported to date for the resolution of *trans*-2-aminocyclohexanol or in general amino alcohols, probably due to their importance both as chiral building blocks and as products of biological and pharmacological interest.[167] One of the very early attempt was by fractional crystallization of their respective tartaric acid salts.[168] Eventhough there are many reports for the resolution of *racemic-trans*-2-aminocyclohexanol, enzymatic resolution of these amino alcohols remains scarcely reported. With this background, the resolution of the *trans*-2-azido alcohols which are the precursors of amino alcohols using enzymes, was attempted. Faber *et al* reported a novel method for the resolution of *racemic-trans*-2-

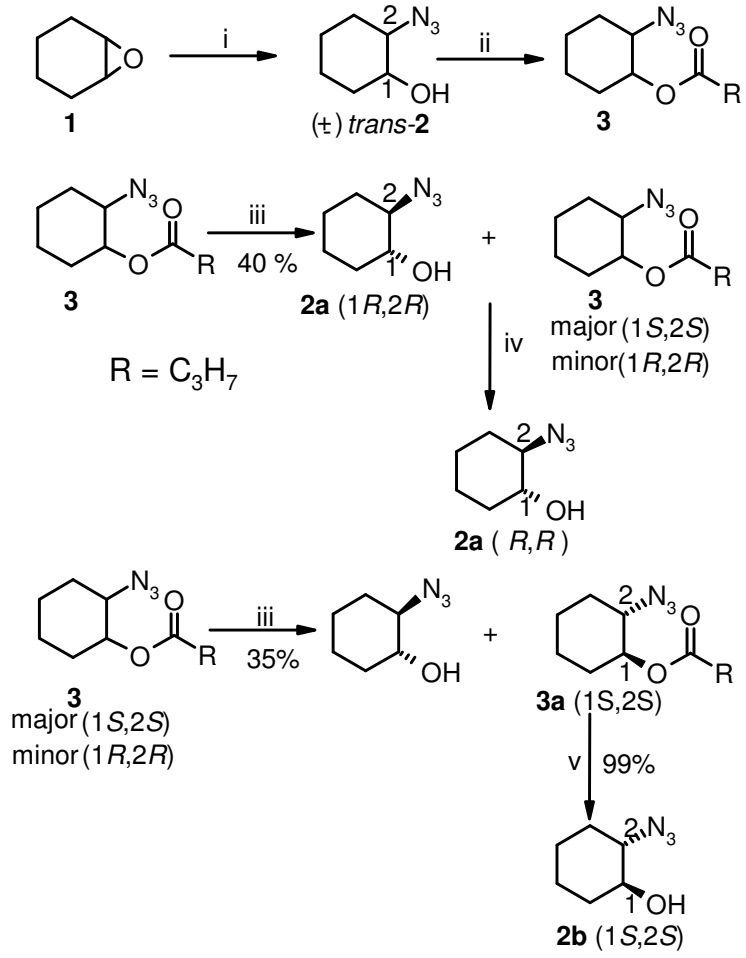

Scheme 1: Reagents and conditions: (i) NaN_3, NH_4Cl, *aq*-Ethanol, reflux, 18 h. (ii) n-Butyric anhydride, dry pyridine, DMAP (cat), rt, 16 h. (iii) *Pseudomonas cepacia* (Lipase), phosphate buffer, pH 7.2, 2.5 h. (iv) Column chromatography separation (v) NaOMe in MeOH 0.5 h.

azido cyclohexanol using enzymatic hydrolysis.[169] The chemo enzymatic resolution of *racemic-trans*-2-azido cyclohexanoate **3** was effected by a slightly modified procedure using lipases well known in literature.[169] The enzyme lipase used in the literature procedures for this resolution is *Candida cylindracea*, which gave ~90-95% *ee* for both enantiomers. The enzyme is substrate selective and shows selectivity to n-butyrate ester than other esters such as acetate, isobutyrate; hence the n-butyrate ester of *racemic-trans*-2-azido cyclohexanol (**3**) was the substrate for enzyme hydrolysis.

The butyrate ester of *racemic trans*-2-azido cyclohexanol (**3**) was synthesized by the oxirane ring opening of the commercially available meso epoxide **1.** Among several reaction conditions available for the ring opening of cyclohexene epoxide with sodium azide,[170] a simple method was used which involve the refluxing of the epoxide with NaN_3, in presence of NH_4Cl as coordinating salt in aqueous ethanol,[170] followed by esterification with butyric anhydride (Scheme 1) in pyridine and DMAP as a catalyst.[171] The *racemic* butyrate ester **3** was resolved by enzymatic enantioselective hydrolysis using the lipase from *Pseudomonas cepacia* (Amano-PS, LPSAA0852814) in 10 mM sodium phosphate buffer (pH 7.2). This reaction proceeded with 40% conversion, and was followed by chromatography, to obtain the optically pure (1*R*,2*R*) azido alcohol **2a**. The earlier reported procedure for this resolution employed the lipase from *Candida cylindracea* (*candida rugosa*), but was found to be less effective as compared to Amano-PS. After a comparative resolution of *racemic* butyrate **3** with both the enzymes, we found that the *Pseudomonas cepacia* lipase gave a better enantiomeric purity of the azido alcohols under identical reaction conditions and in less reaction time. The enzymatic treatment of the mixture of minor (1*R*,2*R*) and major (1*S*,2*S*) butyrate esters **3** was done for a second time to improve the ee, followed by column purification. Subsequent

methanolysis of the **3a** (1*S*,2*S*) ester using NaOMe in methanol gave pure (1*S*,2*S*) **2b** in 35% overall yield. The enantiopurity of both (1*R*,2*R*) **2a** and (1*S*,2*S*) **2b** isomers was confirmed by comparing with known values for the optical rotations reported in the literature[170] and enantiomeric excess was found to be >98% for both the isomers.

The enantiomeric purity of alcohols (1*R*,2*R*)-**2a** and (1*S*,2*S*)-**2b** were confirmed from ^{13}C NMR measurement of their acetyl derivatives utilizing a chiral chemical shift reagent, (+)-*tris*-[3-(heptafluoropropylhydroxymethylene)-d-camphorato]europium (III) [Eu(*hfc*)$_3$, Note 2]. (7.7mole%).[172] Examination of the ^{13}C NMR spectrum of the acetyl derivatives of racemic (1*R*/*S*,2*R*/*S*)-**2** shows the splitting in the methyl carbon and carbonyl signals into clear doublet. But in the corresponding spectra of acetyl derivatives of (1*R*,2*R*)-**2a** and (1*S*,2*S*)-**2b**, the above mentioned signals were singlet and corresponding to respective signal in the spectrum of their racemate (Figure 10).

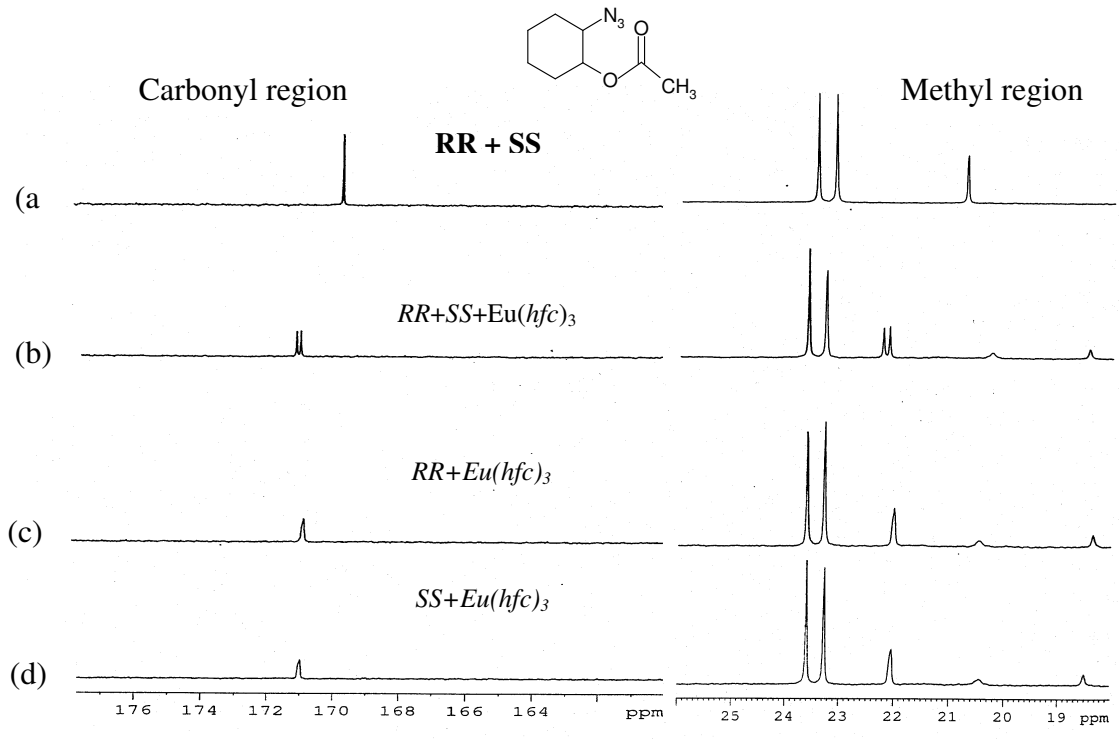

Figure 10. Enantiopurity of alcohols (1*R*,2*R*) **3a** and (1*S*,2*S*) **3b** using ^{13}C NMR of complexes of 3a and **3b** with chiral chemical Shift reagent

***Note* 2**

Determination of enantiopurity by NMR using Chemical shift reagent: Lanthanide complexes can serve as weak Lewis acids. In nonpolar solvents (eg. $CDCl_3$, CCl_4, or CS_2) these paramagnetic salts are able to bind Lewis bases, such as amides, amines, esters, ketones, and sulfoxides. As a result, protons, carbons, and other nuclei are usually deshielded relative to their positions in uncomplexed substrates, and chemical shifts of those nuclei are altered. The extent of this alteration depends on the strength of the complex and the distance

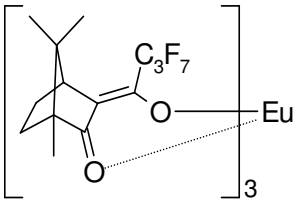

Chiral shift reagent, Eu(*hfc*)$_3$

of the nuclei from paramagnetic metal ion. Therefore, the NMR signals of different types of nuclei are shifted to different extents, and this leads to spectral simplification. The spectral nonequivalence observed in the presence of chiral chemical shift reagents (CSR) can explained by the difference in geometry of the diastereomeric CSR-chiral substrate complexes, as well as different magnetic environment of the coordinated enantiomers that causes the anisochrony.[172] So chiral lanthanide shift reagents [for example, Eu(*hfc*)$_3$, (+)-*tris*-(3-heptafluoropropylhydroxymethylene)-*d*-camphorato)-europium (III), Figure 33] are much more commonly used to quantitatively analyze enantiomer compositions. Sometimes it may be necessary to chemically convert the enantiomer mixtures to their derivatives in order to get reasonable peak separation with chiral shift reagents.

2.3.3 *N*-[(2*R*)-*t*-Boc-Aminocyclohex-(1*S*)-yl]-*N*-(thymin-1-acetyl)-glycine ethyl ester 10a.

The synthesis of the target (1*S*,2*R*) monomer ester **10a** (Scheme 2) started with the reduction of the azide function in (1*R*,2*R*) **2a** by hydrogenation using Adam's catalyst[173] and *in situ* reaction of the resulting amine with Boc-anhydride yielded the N-*Boc*-protected amino alcohol (1*R*,2*R*) **4**. Other hydrogenation catalysts such as Raney Ni, 10%

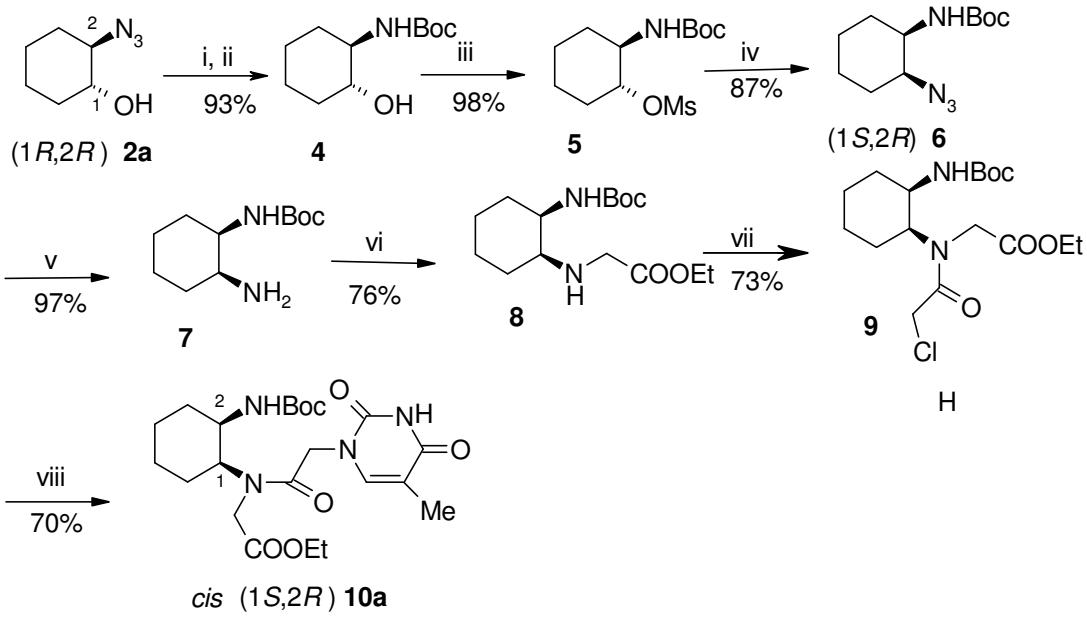

Scheme 2: Reagent and conditions (i) PtO_2, dry EtOAc, H_2, 35-40 psi, rt, 3.5 h; (ii) $(Boc)_2O$ (iii) MsCl, dry Pyridine, DMAP, 0-5°C, 5 h; (iv) NaN_3, dry DMF, 72°C, 18 h; (v) PtO_2, MeOH, H_2, 35-40 psi, rt, 3.5 h; (vi) $BrCH_2COOEt$, KF-Celite, dry CH_3CN, rt, 4 h; vii) $ClCH_2COCl$, Na_2CO_3, Dioxan: H_2O (1:1), 0°C, 30 min.; (viii) Thymine, K_2CO_3 dry DMF, 60-65°C, 3.5 h.;

Pd/C were also effective at catalyzing the reduction of azide, but the product obtained required extensive purification due to the associated side products and consequently lower yields. The alcohol **4** was then converted to corresponding mesylate (1*R,*2*R*) **5**. The mesylate was treated with NaN_3 in dry DMF to yield the azide (1*S*,2*R*) **6** with inversion of configuration at C1. This was confirmed from the crystal structures of mesylate (1*R,*2*R*) **5** and azide (1*S*,2*R*) **6** (Figure 11c and e, Table 3 and 5 respectively). The azide (1*S*,2*R*) **6** was hydrogenated using Adam's catalyst to give the amine (1*S,*2*R*) **7**, which without further purification was alkylated with ethyl bromoacetate in the presence of freshly prepared KF-Celite. This resulted in the monosubstituted *cis*-1,2-diamine (1*S,*2*R*) **8** which on acylation with chloroacetyl chloride gave the compound (1*S*,2*R*) **9.** Chloroacetyl chloide was prepared by distillation of a mixture of chloroacetic acid and benzoyl chloride under vacuum at 70°C. The condensation of (1*S*,2*R*) **9** with thymine in presence of K_2CO_3 in DMF yielded the desired (1*S*,2*R*) aminocyclohexyl (thymin-1-yl-acetyl)

glycyl PNA monomer ethyl ester (1*S*,2*R*) **10a** and was confirmed by X-ray crystal structure (Figure 11a, Table 6). All new compounds were characterized by ^{1}H, ^{13}C NMR and mass spectral data and elemental analysis.

2.3.4 *N*-[(2*S*)-*t*-Boc-Aminocyclohex-(1*R*)-yl]-*N*-(thymin-1-acetyl)-glycine ethyl ester 10b.

The synthesis of the target (1*R*,2*S*)monomer ester **10b** started with the reduction of the azide function in (1*S*,2*S*) **2b** by hydrogenation using Adam's catalyst[173] and in *situ* *t-Boc* protection of the resulting amine function yielded the *Boc*-protected amino alcohol (1*S*,2*S*) **4** (Scheme 3). Following a similar set of reactions as for the synthesis of isomer **10a**, *viz*., mesylation of the alcohol (1*S*,2*S*) **4**, azidation of the mesylate **5** (crystal structure, Figure 11d, Table 4) to get azide (1*R*,2*S*) **6**, reduction of the azide followed by alkylation with ethyl bromoacetate and acylation of the amine to yield chloro compound (1*R*,2*S*) **9**. The condensation of chloro compound with nucleobase thymine afforded the

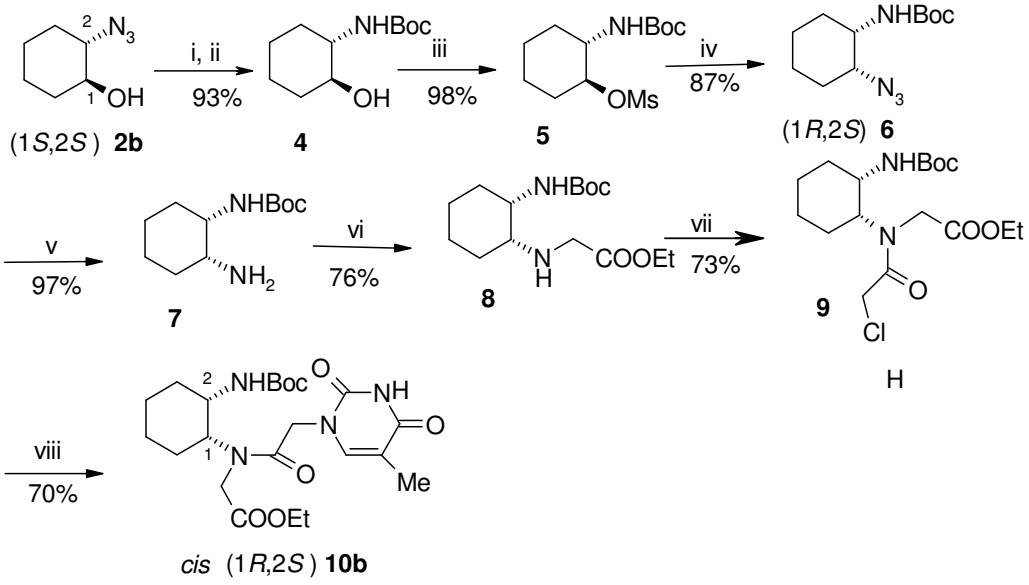

Scheme 3: Reagent and conditions (i) PtO_2, dry EtOAc, H_2, 35-40 psi, rt, 3.5 h; (ii) $(Boc)_2O$ (iii) MsCl, dry Pyridine, DMAP, 0-5°C, 5 h; (iv) NaN_3, dry DMF, 72°C, 18 h; (v) PtO_2, MeOH, H_2, 35-40 psi, rt, 3.5 h; (vi) $BrCH_2COOEt$, KF-Celite, dry CH_3CN, rt, 4 h; vii) $ClCH_2COCl$, Na_2CO_3, Dioxan: H_2O (1:1), 0°C, 30 min.; (viii) Thymine, K_2CO_3 dry DMF, 60-65°C, 3.5 h.;

monomer ethyl ester (1*R*,2*S*) **10b** in very good yield. The structure of **10b** was confirmed by X-ray crystal structure (Figure 11b, Table 7).

All attempts to couple thymine-acetic acid and the amine **8** using coupling reagents like DCC, HBTU and TBTU were unsuccessful (Scheme 4). This is perhaps due to the presence of the bulky *tert*-butyloxycarbonyl (*Boc*-) group in the adjacent position. It is seen that in the crystal structures of the final monomer esters **10a** and **10b** where the thymine base, attached to the main backbone via methylene carbonyl linker, is away from both Boc group and the glycine in chain (Figure 11a and 11b).

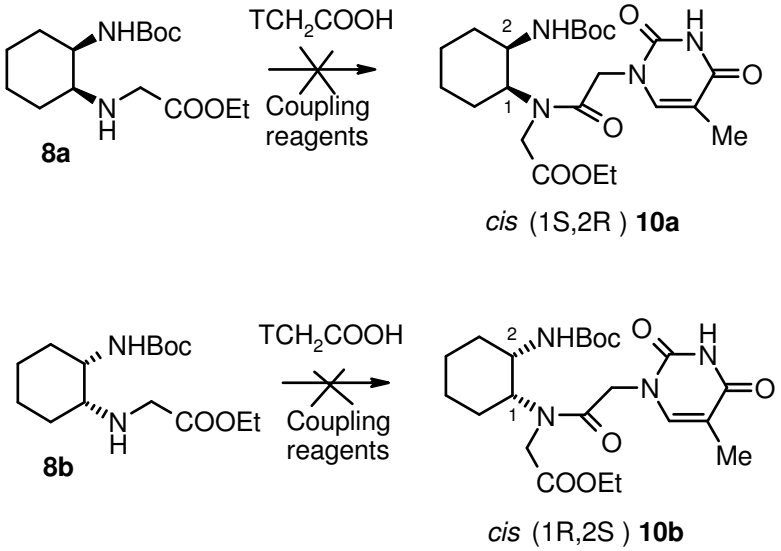

Scheme 4. Direct coupling of amine and thymine acetic acid

2.3.5 Crystal structures *ch*PNA thymine monomer esters 10a and 10b: Comparison of the dihedral angles with that of known values of PNA complexes and Implication.

Single crystals of both **10a** and **10b** were obtained by crystallization from chloroform (with petroleum ether as less polar solvent) and few drops of ethanol. Though the addition of ethanol improves the crystal quality, the exact reason is not known. X-ray intensity data were collected on a Bruker SMART APEX CCD diffractometer at low temperature. Both the enantiomers contain one molecule of ordered chloroform with full

occupancy and another molecule of highly disordered chloroform with occupancy less than unity. The high R-values despite data collection at low temperature could be attributed to the extensive disorder of the solvent molecule in **10a** and **10b** (Figure 12) and extensive disorder of the end methyl group of the side chain in **10a**. This is an excellent example for the C-H….Cl interaction directing the crystallization of compounds in halogenated solvents. The torsion angles β as deduced from the X-ray crystal structures for **10a** (1*S*,2*R*) and **10b** (1*R*,2*S*) are –63° a`nd +66° respectively which are closer in magnitude to that found in PNA_2:DNA and PNA:RNA complexes, with difference in their relative signs as expected for the enantiomeric pairs (Table 2). In solution, the tertiary amide bond in PNA is known to exist as a rotameric mixture.[106-107] In the present structures, the amide bond is *trans* with carbonyl pointing towards the *C*-terminus, similar

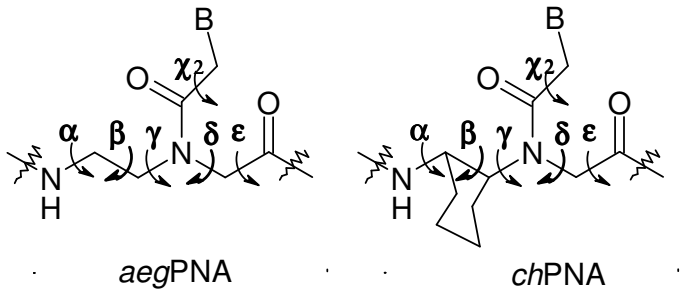

Table 2. Dihedral angles (°) in PNA and PNA:DNA/RNA complexes

Entry	Compound	α	β	γ	δ	χ_1	χ_2
1	PNA_2:DNA[108]	-103	73	70	93	1	-175
2	PNA:DNA[106]	105	141	78	139	-3	151
3	PNA:RNA[107]	170	67	79	84	4	-171
4	*ch*PNA(1*S*,2*R*)*	128	-63	76	119	1.02	-175
5	*ch*PNA(1*R*,2*S*)*	-129	66	-78	-119	-0.87	174

* dihedral angles from monomer crystal structures.: *ch*PNA

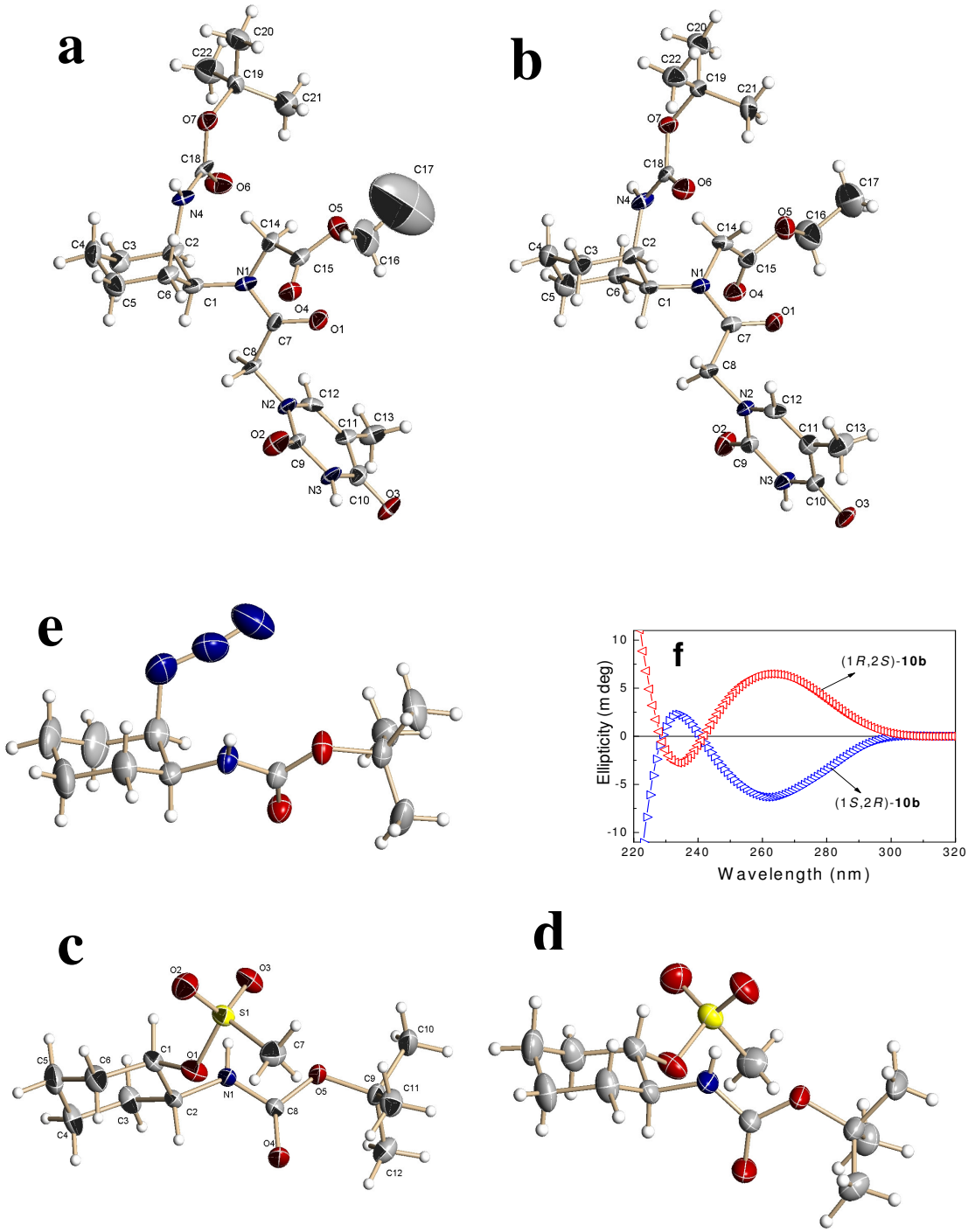

Figure 11. Crystal structures of compounds a) **10a**, b) **10b**, c) **5a**, d) **5b**, e) **6a**, and f) CD signatures of **10a** and **10b** measured in methanol.

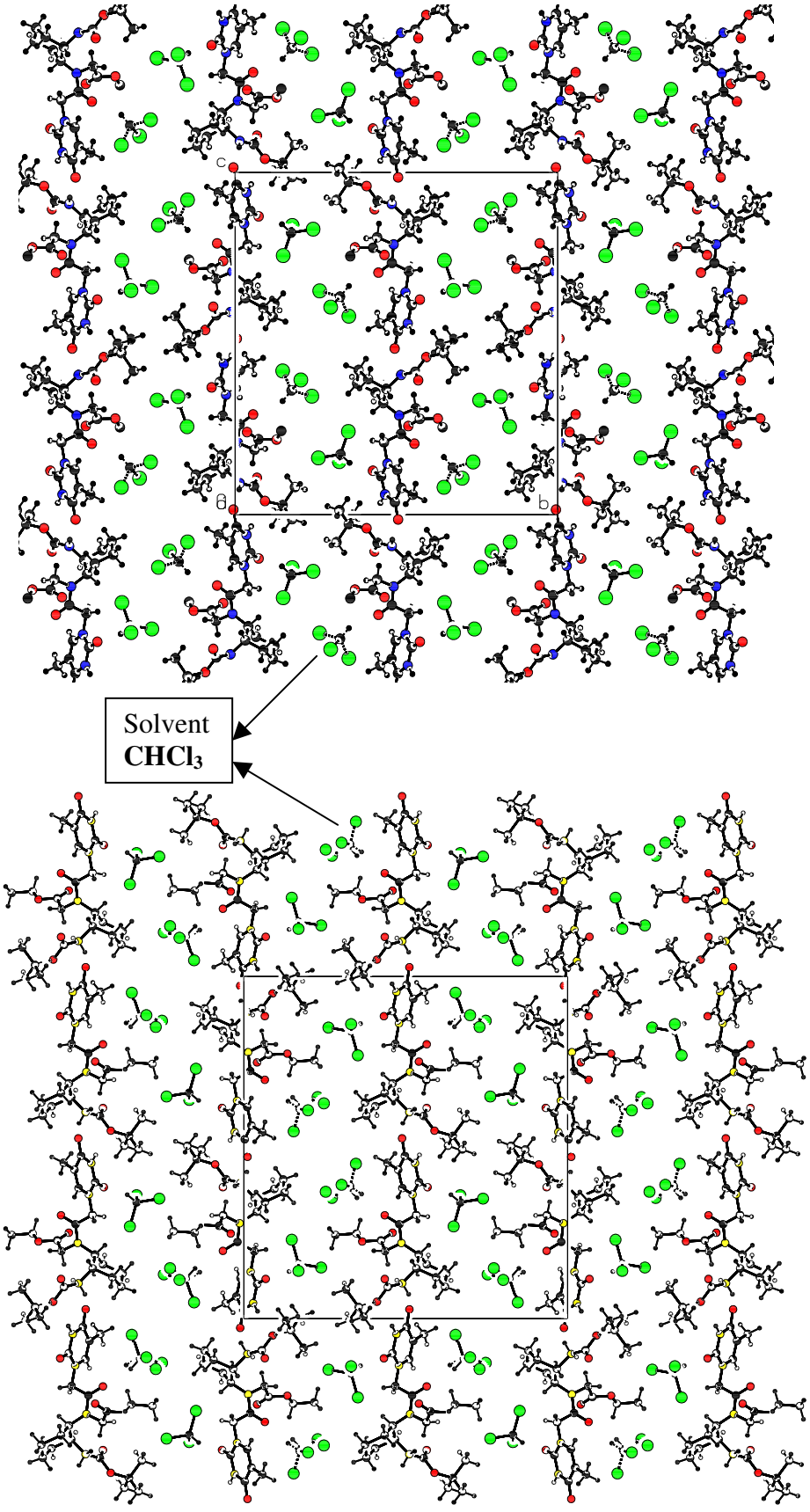

Figure 12. Crystal packing of **10a** (top) and **10b** (bottom).

Table 3. Crystal data and structure refinement for (1*S*,2*R*)-5a.

Identification code	**(1*S*,2*R*)-5a**
Empirical formula	C12 H23 N O5 S
Formula weight	293.37
Temperature	293(2) K
Wavelength	0.71073 Å
Crystal system, space group	Orthorhombic, $P2_12_12_1$
Unit cell dimensions	a = 5.232(3) Å alpha = 90°. b = 9.090(4) Å beta = 90°. c = 32.408(16) Å gamma = 90°.
Volume	1541.4(13) $Å^3$
Z, Calculated density	4, 1.264 Mg/m^3
Absorption coefficient	0.225 mm^{-1}
F(000)	632
Crystal size	0.665 x 0.075 x 0.04 mm
Theta range for data collection	1.26 to 25.00 deg.
Limiting indices	-6<=h<=6, -8<=k<=10, -38<=l<=37
Reflections collected / unique	7601 / 2709 [R(int) = 0.0389]
Completeness to theta = 25.00	99.8 %
Refinement method	Full-matrix least-squares on F^2
Data / restraints / parameters	2709 / 0 / 176
Goodness-of-fit on F^2	1.191
Final R indices [I>2sigma(I)]	R1 = 0.0543, wR2 = 0.1224
R indices (all data)	R1 = 0.0644, wR2 = 0.1370
Absolute structure parameter	0.06(14)

Table 4. Crystal data and structure refinement for (1*R*,2*S*)-5b.

Identification code	(1*R*,2*S*)-5b
Empirical formula	C12 H23 N O5 S
Formula weight	293.37
Temperature	293(2) K
Wavelength	0.71073 Å
Crystal system, space group	Orthorhombic, $P2_12_12_1$
Unit cell dimensions	a = 5.2293(6) Å alpha = 90°. b = 9.0539(10) Å beta = 90°. c = 32.279(4) Å gamma = 90°.
Volume	1528.3(3) $Å^3$
Z, Calculated density	4, 1.275 Mg/m^3
Absorption coefficient	0.227 mm^{-1}
F(000)	632
Crystal size	0.44 x 0.29 x 0.29 mm
Theta range for data collection	2.34 to 24.99 deg.
Limiting indices	-6<=h<=6, -10<=k<=10, -38<=l<=38
Reflections collected / unique	10920 / 2694 [R(int) = 0.0340]
Completeness to theta = 24.99	99.9 %
Max. and min. transmission	0.9365 and 0.9078
Refinement method	Full-matrix least-squares on F^2
Data / restraints / parameters	2694 / 0 / 264
Goodness-of-fit on F^2	1.108
Final R indices [I>2sigma(I)]	R1 = 0.0304, wR2 = 0.0780
R indices (all data)	R1 = 0.0312, wR2 = 0.0787
Absolute structure parameter	0.01(7)

Table 5. Crystal data and structure refinement for (1*S*,2*R*)-6a.

Identification code	**(1*S*,2*R*)-6a**
Empirical formula	C11 H20 N4 O2
Formula weight	240.31
Temperature	293(2) K
Wavelength	0.71073 Å
Crystal system, space group	Tetragonal, $P4_32_12$
Unit cell dimensions	a = 12.159(6) Å alpha = 90°. b = 12.159(6) Å beta = 90°. c = 19.086(13) Å gamma = 90°.
Volume	2821(3) $Å^3$
Z, Calculated density	8, 1.131 Mg/m^3
Absorption coefficient	0.080 mm^{-1}
F(000)	1040
Crystal size	0.66 x 0.36 x 0.18 mm
Theta range for data collection	1.99 to 24.97 deg.
Limiting indices	-14<=h<=12, -14<=k<=14, -22<=l<=21
Reflections collected / unique	14080 / 2493 [R(int) = 0.0866]
Completeness to theta = 24.97	100.0 %
Max. and min. transmission	0.9860 and 0.9491
Refinement method	Full-matrix least-squares on F^2
Data / restraints / parameters	2493 / 0 / 158
Goodness-of-fit on F^2	1.143
Final R indices [I>2sigma(I)]	R1 = 0.0846, wR2 = 0.2069
R indices (all data)	R1 = 0.1179, wR2 = 0.2283
Absolute structure parameter	4(4)
Extinction coefficient	0.0032(15)

Table 6. Crystal data and structure refinement for (1*S*,2*R*)-10a.

Identification code	**(1*S*,2*R*)-10a**
Empirical formula	C23 H33.25 Cl4.50 N4 O7
Formula weight	637.31
Temperature	150(2) K
Wavelength	0.71073 Å
Crystal system, space group	Orthorhombic, P 2_1 2_1 2_1
Unit cell dimensions	a = 6.201(4) Å alpha = 90 deg. b = 22.599(14) Å beta = 90 deg. c = 23.835(14) Å gamma = 90 deg.
Volume	3340(3) Å3
Z, Calculated density	4, 1.267 Mg/m3
Absorption coefficient	0.436 mm-1
F(000)	1327
Crystal size	0.75 x 0.34 x 0.02 mm
Theta range for data collection	1.93 to 25.00 deg.
Limiting indices	-7<=h<=7, -26<=k<=26, -28<=l<=28
Reflections collected / unique	31159 / 5864 [R(int) = 0.0965]
Completeness to theta = 25.00	99.2 %
Max. and min. transmission	0.9913 and 0.7370
Refinement method	Full-matrix least-squares on F2
Data / restraints / parameters	5864 / 30 / 368
Goodness-of-fit on F^2	1.164
Final R indices [I>2sigma(I)]	R1 = 0.1043, wR2 = 0.2477
R indices (all data)	R1 = 0.1197, wR2 = 0.2567
Absolute structure parameter	0.18(17)

Table 7. Crystal data and structure refinement for (1*S*,2*R*)-10b.

Identification code	**(1*S*,2*R*)-10b**
Empirical formula	'C23.50 H35 Cl5.25 N4 O7'
Formula weight	671.67
Temperature	150(2) K
Wavelength	0.71073 Å
Crystal system, space group	Orthorhombic, P 2_1 2_1 2_1
Unit cell dimensions	a = 6.2353(9) Å alpha = 90
	b = 22.617(3) Å beta = 90
	c = 23.988(3) Å gamma = 90
Volume	3382.8(8) $Å^3$
Z, Calculated density	4, 1.319 Mg/m^3
Absorption coefficient	0.492 mm^{-1}
F(000)	1397
Crystal size	1.21 x 0.27 x 0.05 mm
Theta range for data collection	2.83 to 25.00 deg.
Limiting indices	-7<=h<=7, -26<=k<=26, -28<=l<=28
Reflections collected / unique	43174 / 5932 [R(int) = 0.0728]
Completeness to theta = 25.00	99.4 %
Max. and min. transmission	0.9773 and 0.5888
Refinement method	Full-matrix least-squares on F^2
Data / restraints / parameters	5932 / 30 / 371
Goodness-of-fit on F^2	1.046
Final R indices [I>2sigma(I)]	R1 = 0.0723, wR2 = 0.2074
R indices (all data)	R1 = 0.0847, wR2 = 0.2147

to that previously observed for cyanuryl monomer[174] and to that seen in the recently reported crystal structure of the D-lysine based chiral PNA-DNA duplex.[167] The crystal structure data also shows axial-equatorial dispositions for the *cis*-disubstituted (1*S*,2*R*/1*R*,2*S*)-cyclohexyl PNA monomers, with the bulky substituents directed into an equatorial position.

2.3.6 Hydrolysis of *ch*PNA Monomer esters.

To synthesize *ch*PNA oligomers the monomer esters have to be hydrolyzed to get free acids having protected amino group. The *ch*PNA thymine monomer ethyl esters **10a** and **10b** were subjected to ester hydrolysis using very mild base 0.5 M LiOH in THF:Water. The reaction mixture was acidified to pH 3.0 and extracted to ethyl acetate. The organic solvent was evaporated to afford free acids **11a** and **11b** in quantitative yields (Scheme 5). This hydrolysis under mild condition minimizes the racemization.

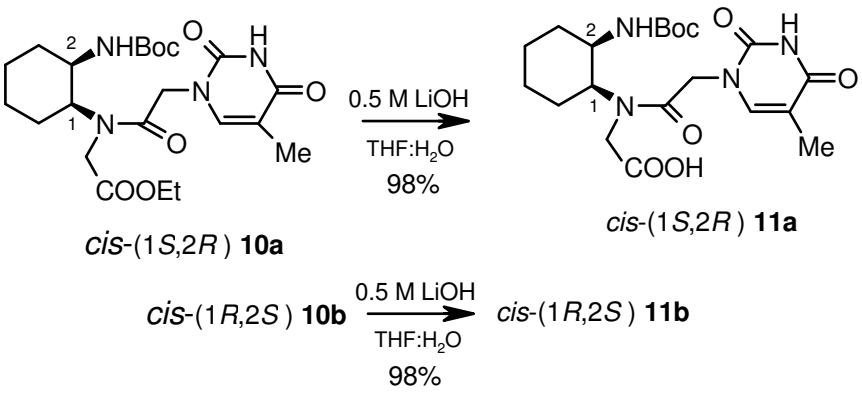

cis-(1*S*,2*R*) **10a**

cis-(1*S*,2*R*) **11a**

cis-(1*R*,2*S*) **10b** $\xrightarrow[\text{THF:H}_2\text{O}]{\text{0.5 M LiOH}}$ *cis*-(1*R*,2*S*) **11b**

98%

Scheme 5. Hydrolysis of ethyl esters of *ch*PNA monomers

2.3.7 Synthesis of Aminoethylglycyl PNA (*aeg*PNA) monomers.

The synthesis was carried out as reported in literature[175-177] starting from the readily available 1,2-diaminoethane (Scheme 5). The monoprotected derivative of **13** was prepared by treating a large excess of 1,2-diaminoethane with *t*-butoxycarbazide in dioxan:water under high dilution conditions to minimize the formation of di-*Boc*

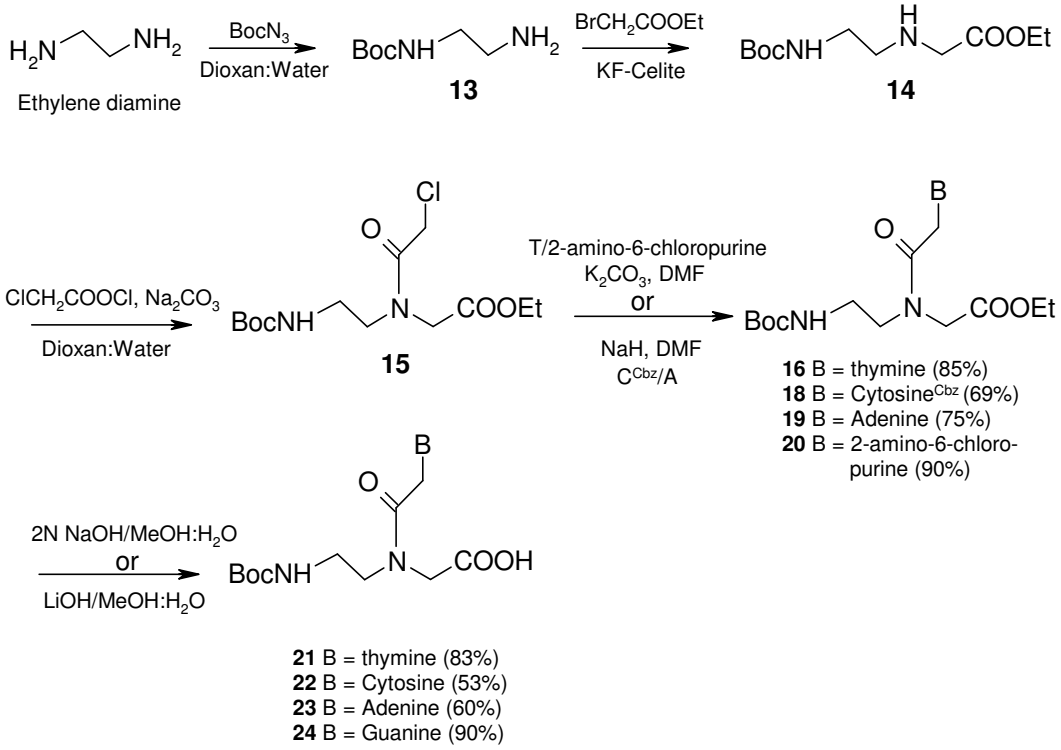

Scheme 6. Synthesis of *aeg*PNA monomers.

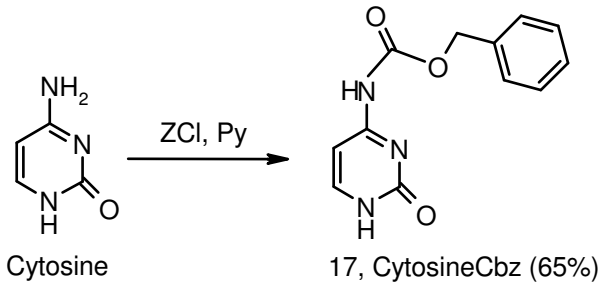

Scheme 7. Exocyclic-amine potection of cytosine.

derivative. The di-*Boc* compound being insoluble in water was removed by filtration after evaporation of dioxan from the reaction mixture. The *N*1-*t*-*Boc*-1,2-diaminoethane was then subjected to *N*-alkylation using equimolar amounts of ethylbromoacetate and KF-Celite as base in acetonitrile to give compound **14**. The use of KF-Celite[178] was found to be advantageous over conventional bases such as K_2CO_3, both in terms of product-yield and ease of work-up.

The compound **14** was not stable for longer time at room temperature. The aminoethylglycine **14** thus obtained was treated with chloroacetyl chloride in aqueous dioxan with Na_2CO_3 as a base to yield the chloro compound **15**. The ethyl *N*-(*t-Boc*-aminoethyl)-*N*-(chloroacetyl)-glycinate (**15**) was used as a common intermediate for the preparation of all the four PNA monomers. Alkylation of the ethyl *N*-(*t-Boc*-aminoethyl)-*N*-(chloroacetyl)-glycinate is regiospecific to *N*1 of thymine. Thymine was reacted with ethyl *N*-(*t-Boc*-aminoethyl)-*N*-(chloroacetyl)-glycinate using K_2CO_3 as a base to obtain *N*-(*t-Boc*-aminoethylglycyl)-thymine ethyl ester (**16**) in high yield. In case of cytosine, the exocyclic-amine N^4 was protected with Cbz (Scheme 6) to obtain **17**,[175] which was used for alkylation employing NaH as the base to provide the *N*1-substituted product **18**. Adenine treated with NaH in DMF to give sodium adenylate, which was then reacted with ethyl *N*-(*t-Boc*-aminoethyl)-*N*-(chloroacetyl)-glycinate to obtain *N*-(*t-Boc*-aminoethylglycyl)-adenine ethyl ester (**19**) in moderate yield. The alkylation of 2-amino-6-chloro purine with ethyl *N*-(*t-Boc*-aminoethyl)-*N*-(chloroacetyl)-glycinate was facile with K_2CO_3 as the base and yielded the corresponding *N*-(*t-Boc*-aminoethylglycyl)-(2-amino-6-chloro purine) ethyl ester (**20**) in excellent yield. All the compounds exhibited ^1H and ^{13}C NMR spectra consistent with the reported data.[175-177]

The ethyl esters except that of cytosine monomer were hydrolyzed in presence of 2N NaOH to give the corresponding acids (**21**, **23**, **24**), which were used for solid phase synthesis. In case of 2-amino-6-chloropurine monomer ester hydrolysis, the chloro group is also oxidized to keto group to give guanine monomer **24**. Cytosine monomer is more susceptible to Cbz deprotection in strong basic conditions, so in this case mild base LiOH was used for hydrolysis to afford the monomer acid **22**. The need for the exocyclic amino

group protection for adenine and guanine was eliminated, as they were found to be unreactive under the conditions used for peptide coupling.

2.3.8 Solid Phase Peptide Synthesis of *aeg*PNA and *aeg-ch*PNA chimera

General principle of Solid Phase Peptide Synthesis (SPPS): In contrast to solution phase method, the solid phase method devised by Merrifield,[179] offers great advantages. In this method, the *C*-terminal amino acid is linked to an insoluble matrix such as polystyrene beads having reactive functional groups, which also acts as a permanent protection for the carboxylic acid (Figure 13). The next N^{α}-protected amino acid is coupled to the resin bound amino acid either by using an active pentaflurophenyl (pfp) or 3-hydroxy-2,3-dihydro-4-oxo-benzotriazole (Dhbt) ester or by an *in situ* activation with carbodiimide reagents. The excess amino acid is washed out and the deprotection and coupling reactions are repeated until the desired peptide is achieved. The

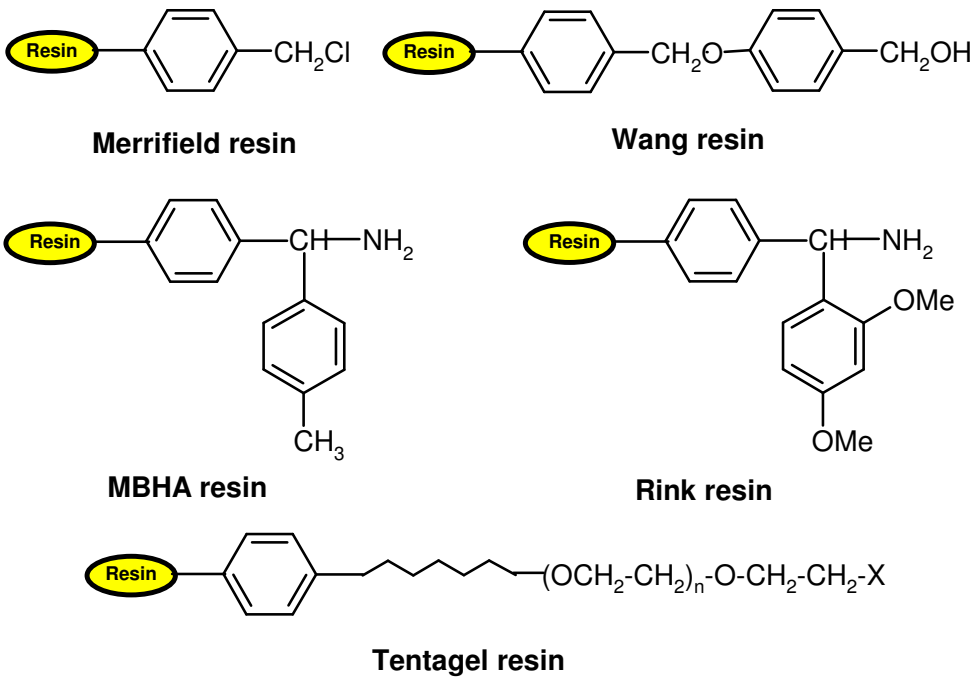

Figure 13. Few representative structures of resins used in SPPS

need to purify intermediates at every step is obviated. Finally, the resin bound peptide and the side chain protecting groups are cleaved in one step.

The advantage of the solid phase synthesis are (i) all the reactions are performed in a single vessel minimizing the loss due to transfer, (ii) large excess of monomer carboxylic acid component can be used resulting in high coupling efficiency, (iii) excess reagents can be removed by simple filtration and washing steps and (iv) the method is amenable to automation and semi micro manipulation.

Currently, two chemistries are available for the routine synthesis of peptides by solid phase method (Figure 14). First method involves the use of *t*-butyloxycarbonyl (*t-Boc*) group as N^{α}-protection that is removed by acidic conditions such as 50% TFA in

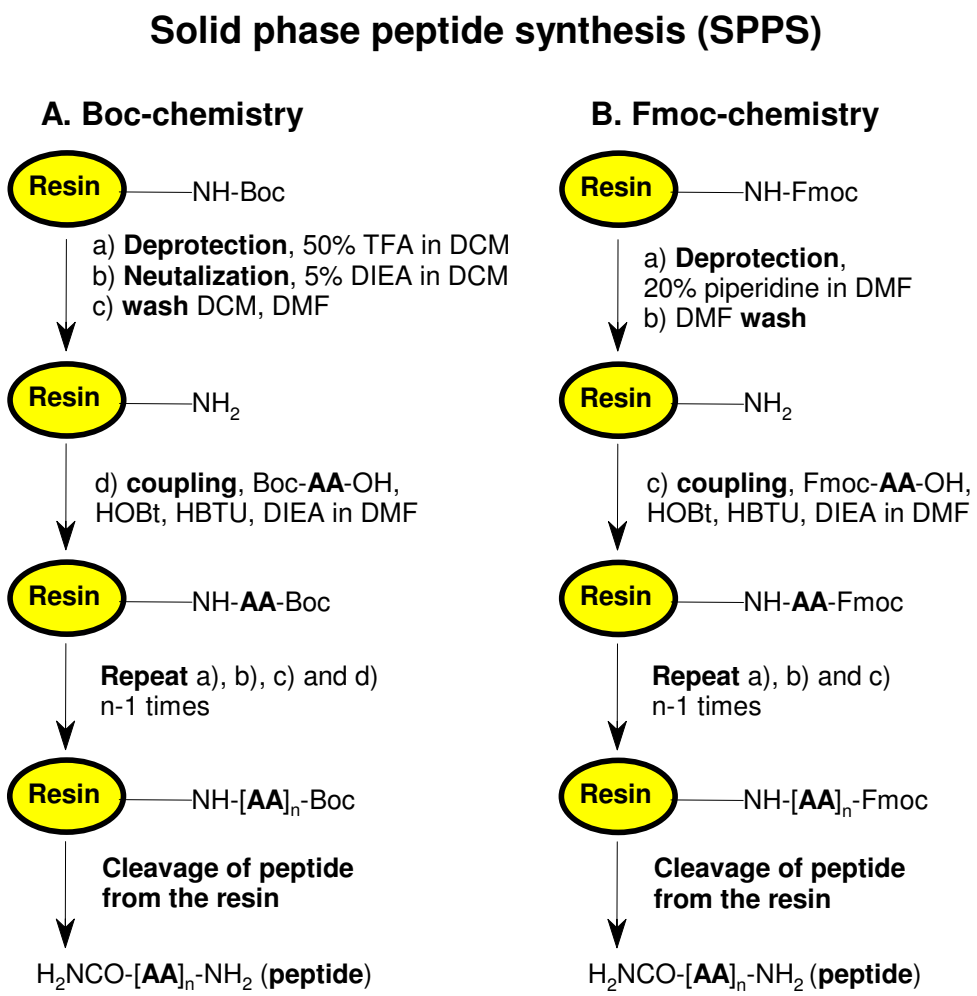

Figure 14. Schematic representation of SSPS **A**) Boc-chemistry and **B**) Fmoc-chemistry

DCM.[180] The reactive side chains of amino acids are protected with groups that are stable to *t-Boc* deprotection conditions and removable under strongly acidic conditions using HF in dimethyl sulfide or TFMSA in TFA. Alternatively a base labile protecting group strategy is used involving fluorenylmethyloxycarbonyl (Fmoc) group for N^{α}-protection, which is stable to acidic conditions but can be cleaved efficiently with a secondary base such as piperidine. Coupled with mild acid sensitive side chain protection, this method offers a second strategy for SPPS. In both chemistries, the linker group that joins the peptide to the resin is chosen such that the side chain protecting groups and the linker are cleaved in one step at the end of the peptide synthesis.

Common methods used to cleave benzyl ester bound peptides are (i) hydrogenolysis or (ii) ammonalysis. A peptide linked to styrene-DVD-copolymer *via* benzyl ester is cleaved by treatment with $Pd(OAc)_2$ in DMF or THF and subsequent hydrogenolysis.[181] In the second method peptide built on Merrifield resin is amidated with NH_3/MeOH. In this case some partial transesterification of the benzyl ester with MeOH gives rise to C-terminal methyl ester of the peptide, which subsequently is amidated with NH_3 to give the peptide-C-terminal amide.[182] In another method, a peptide-*C*-terminal amide is synthesized by treatment of the peptide bound to Wang resin (p-benzyloxy alcohol resin) or Tentagel resin (where PEG spacer is attached to the polystyrene backbone *via* a benzyl ether linkage) with ammonium chloride under ambient conditions to yield peptide-*C*-terminal amides.[183] In case of (4-methyl benzhydryl) amine-resin (MBHA), the peptide bound resin is treated with strong acid TFMSA in TFA to afford peptide with *C*-terminal amide.[184]

Synthesis of PNA Oligomers: Solid phase peptide synthesis protocols can be easily applied to the synthesis of oligomeric PNAs from the *C*-terminus to *N*-terminus.

The Fmoc protection strategy has a drawback in PNA synthesis since a small amount of acyl migration from the tertiary amide to the free amine has been observed during Fmoc deprotection with piperidine.[185] In the present work *t*-Boc protection strategy was selected. MBHA resin (4-methyl–Benzhydryl amine resin) was used as the solid support on which the oligomers were built and the monomers were coupled by *in situ* activation with HBTU / HOBt.[177] In the synthesis of all oligomers, orthogonally protected (*Boc*/Cl-Cbz) L-lysine was selected as the *C*-terminal spacer-amino acid and it is linked to the resin through amide bond.[175] The amine content on the resin was determined by the picrate assay and found to be 0.85 mmol/g and loading was suitably lowered to approximately 0.250 mmol/g by partial acetylation of amine content using calculated amount of acetic anhydride.[185,186] Free -NH_2 on the resin available for coupling was again estimated before starting synthesis. The PNA oligomers were synthesized using repetitive cycles (Figure-15), each comprising the following steps:

(i) Deprotection of the *N*-*t*-Boc group using 50% TFA in CH_2Cl_2.

(ii) Neutralization of the trifluoroacetate salt of amine with diisopropyl ethylamine (DIEA) to liberate the free amine.

(iii) Coupling of the free amine with the free carboxylic acid group of the incoming monomer (3 to 4 equivalents). The coupling reaction was carried out in DMF/ DMSO with HBTU as coupling reagent in the presence of DIEA and HOBt as catalysts. The deprotection of the *N*-*t*-Boc protecting group and the coupling reactions were monitored by Kaiser's test.[187] Alternatively, Chloranil[188] or De Clercq[189] tests can also be used which detects secondary amine. The *t-Boc*-deprotection step leads to a positive Kaiser's test, where in the resin beads as well as the solution are blue in color

(Rheumann's purple). On the other hand, upon completion of the coupling reaction, the Kaiser's test is negative, the resin beads remaining colorless.

(iv) capping of the unreacted amino groups using Ac_2O / Pyridine in CH_2Cl_2 in case coupling does not go to completion. Figure 15 represents a typical Solid phase peptide synthesis cycle.

Various oligomers synthesized for the present study of DNA/RNA recognition are shown in Table 8. The unmodified *aeg*PNA homooligomer T_{10} (Table 8, entry 1, *aeg*PNA **25**) was synthesized using *t-Boc* protected *aeg*PNA monomer **21**. This was used as the control sequence for comparing the hybridization and discrimination properties of *ch*PNA oligomers. The modified *cis*-(1*S*,2*R*/1*R*,2*S*)-aminocyclohexylglycyl thymine monomers **11a** and **11b** were incorporated into PNA oligomers using *Boc* chemistry on L-lysine derivatized (4-methylbenzhydryl) amine (MBHA) resin.[190] Various homothymine PNA

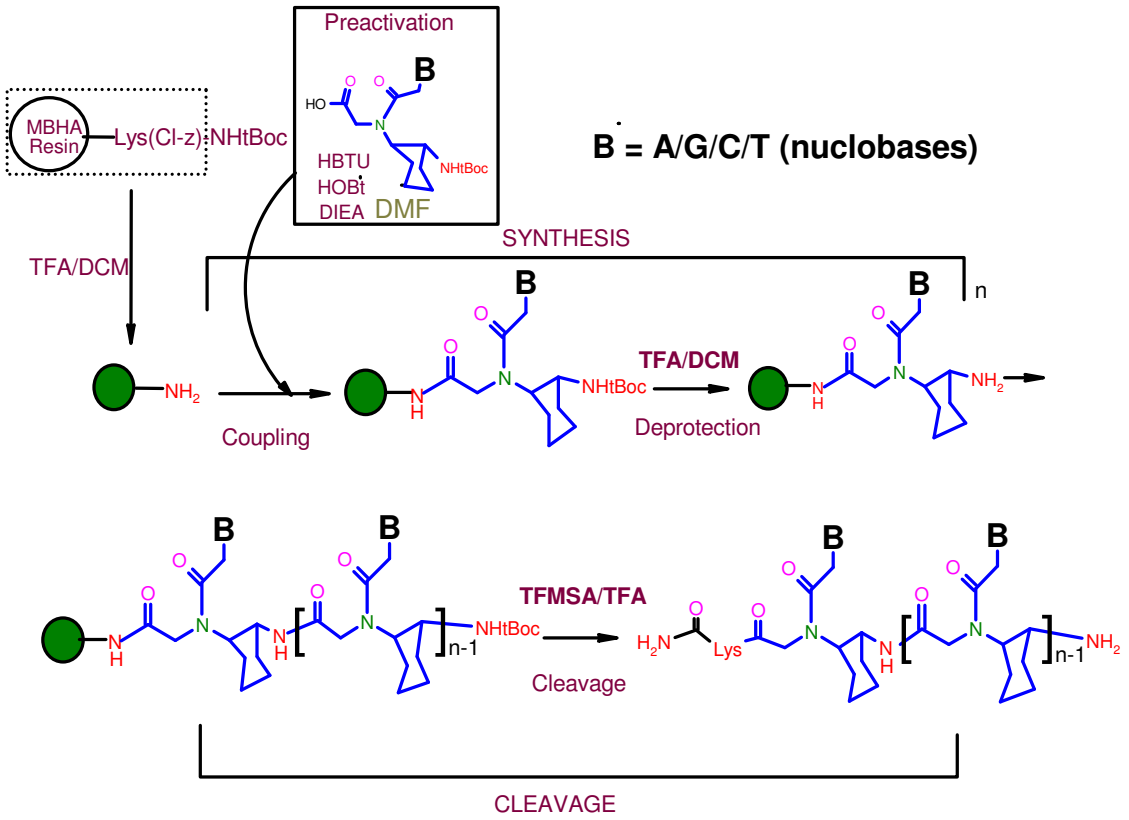

Figure-15. Solid phase peptide Synthesis

decamers (**26-29**, Table 8) incorporating one or two *cis*-(1*S*,2*R*/1*R*,2*S*)-aminocyclohexylglycyl thymine PNA monomers in different positions were synthesized following the *t-Boc* chemistry protocol of SPPS.

Polypyrimidine (thymine) decamers as mentioned above are synthesized to study the effect of the two isomers of *cis*-cyclohexyl units for their triplex-forming ability. The classical homopyrimidine *aeg*PNAs are known to complex with the complementary oligonucleotide DNA/RNA in a 2:1 PNA:DNA/RNA stoichiometry.[102] In order to study the duplex formation potential and in particular DNA/RNA discrimination of the *ch*PNA monomeric units, it was imperative to synthesize mixed sequences incorporating both, purine and pyrimidines. The mixed sequences **31-37** were synthesized by incorporating *ch*PNA thymine monomers **11a** and **11b** and *aep*PNA guanine **24**, adenine **23** and cytosine **22** monomers. Control mixed sequence **30** and **33** were also synthesized by incorporating *aeg*PNA G, A, C, T monomers for the use of comparative studies.

Cleavage of the PNA Oligomers from the Solid Support: The oligomers were cleaved from the solid support, using trifluoromethanesulphonic acid (TFMSA) in the presence of trifluoroacetic acid (TFA) ('Low, High TFMSA-TFA method"),[191] which yields oligomer with amide at their *C*-terminus. The synthesized PNA oligomers were cleaved from the resin (oligomer attached to L-lysine derivatized MBHA resin) using this procedure to obtain sequences bearing L-lysine-amide at their C-termini (Table 8). A cleavage time of 2-2.5 h at room temperature was found to be optimum. The side chain protecting groups were also cleaved during this cleavage process. After cleavage reaction, the oligomer was precipitated from methanol with dry diethylether.

Purification of the PNA Oligomers: All the cleaved oligomers were subjected to initial gel filtration. The purity of the so obtained oligomers was checked by analytical RP

HPLC (C18 column, CH_3CN-H_2O system), which shows more than 65-70% purity. These were subsequently purified by reverse phase HPLC on a semi preparative C18 column. The purity of the oligomers was again ascertained by analytical RP-HPLC and their integrity was confirmed by MALDI-TOF mass spectrometric analysis. Some representative HPLC profiles and mass spectra are shown in Figures 16 and 17 (Table 9).

Table 8. PNA sequences synthesized in the present study

Entry	Sequence code	PNA Sequences
		Homothymine sequences
1	*aeg*PNA **25**	H-T T T T T T T T T T-LysNH_2
2	*ch*PNA **26**	H-T T T T t_{SR} T T T T T-LysNH_2
3	*ch*PNA **27**	H-T T T T t_{RS} T T T T T-LysNH_2
4	*ch*PNA **28**	H-T T T T t_{SR} T T T t_{SR}-LysNH_2
5	*ch*PNA **29**	H-T T T T t_{RS} T T T T t_{RS}-LysNH_2
		Mixed Sequences
6	*aeg*PNA **30**	H-G T A G A T C A C T-LysNH_2
7	*ch*PNA **31**	H-G t_{SR} A G A t_{SR} C A C t_{SR}-LysNH_2
8	*ch*PNA **32**	H-G t_{RS} A G A t_{RS} C A C t_{RS}-LysNH_2
9	*aeg*PNA **33**	H-G G C A G T G C C T-LysNH_2
10	*ch*PNA **34**	H-G G C A G G t_{SR} G C C T-LysNH_2
11	*ch*PNA **35**	H-G G C A G G t_{SR} G C C t_{SR} -LysNH_2
12	*ch*PNA **36**	H-G G C A G G t_{RS} G C C T-LysNH_2
13	*ch*PNA **37**	H-G G C A G G t_{RS} G C C t_{RS} -LysNH_2

A/G/C/T = *aeg*PNA Adenine/Guanine/Cytosine/Thymine monomers, t_{SR} = (1*S*,2*R*)-*ch*PNA Thymine monomer, t_{RS} = (1*R*,2*S*)-*ch*PNA Thymine monomer.

HPLC profile of *ch*PNA **26**

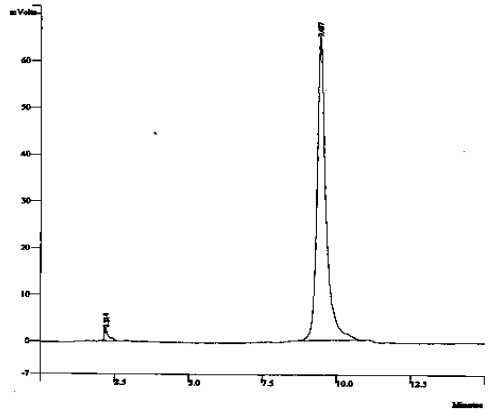

HPLC profile of *ch*PNA **27**

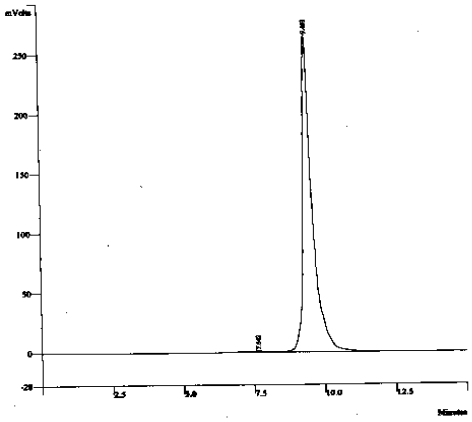

HPLC profile of *ch*PNA **28**

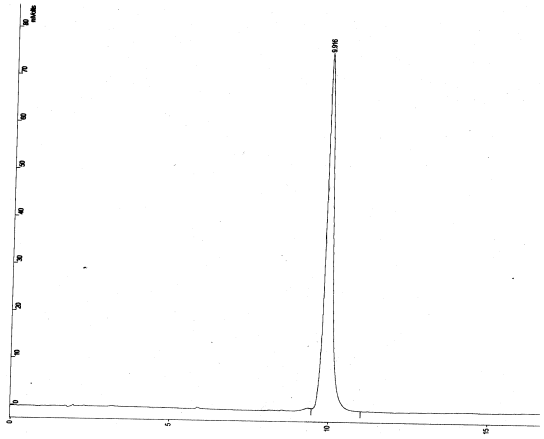

HPLC profile of *ch*PNA **29**

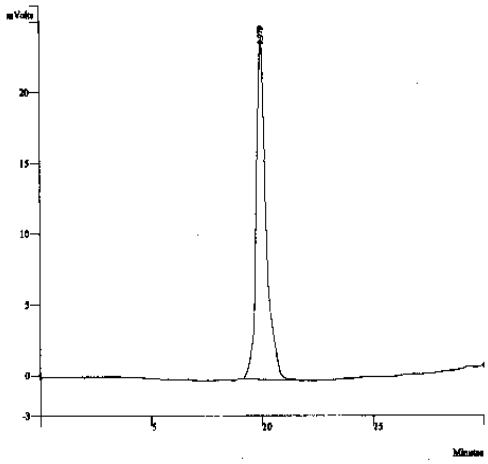

HPLC profile of *ch*PNA **31**

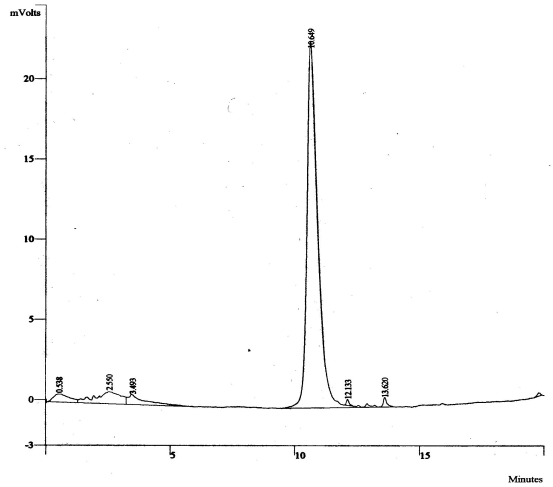

HPLC profile of *ch*PNA **32**

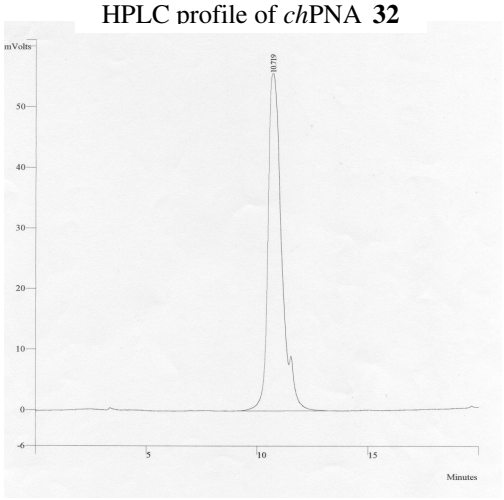

Figure 16a. Reverse phase HPLC profiles of *ch*PNAs. (For HPLC conditions, see experimental section)

HPLC profile of *aeg*PNA **33**

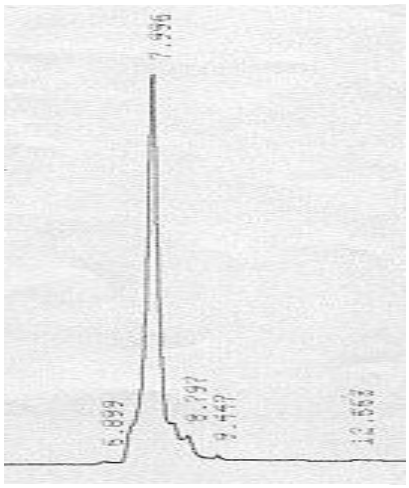

HPLC profile of *ch*PNA **34**

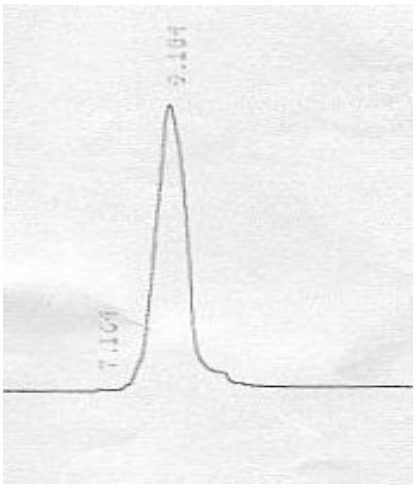

HPLC profile of *ch*PNA **35**

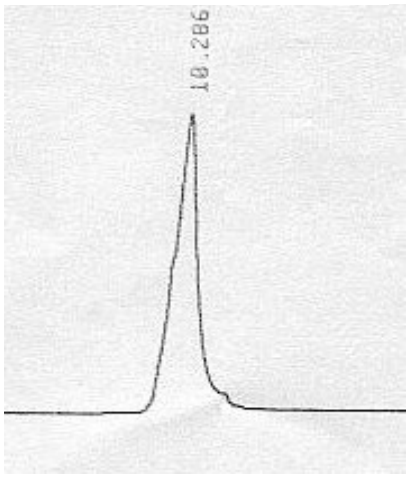

HPLC profile of *ch*PNA **36**

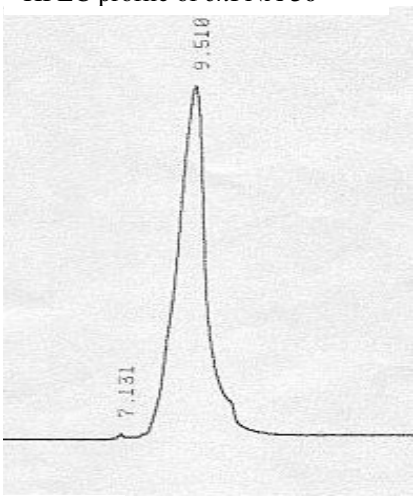

HPLC profile of *ch*PNA **37**

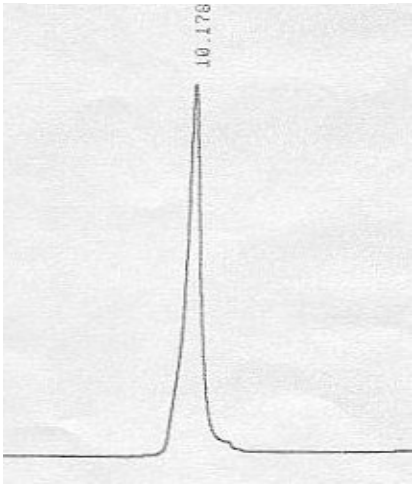

Figure 16b. Reverse phase HPLC profiles of *ch*PNAs **33**-**37**. (For HPLC conditions, see experimental section)

MALDI-TOF of *ch*PNA **26**

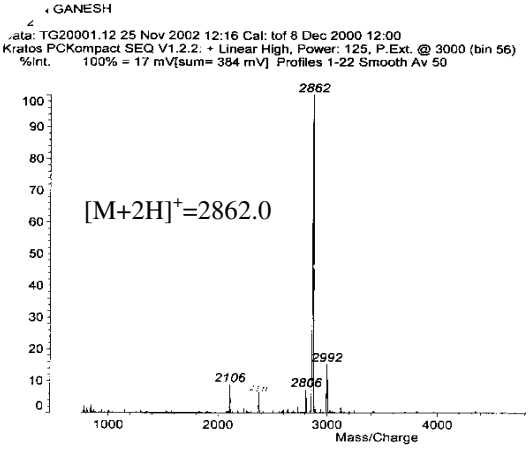

MALDI-TOF of *ch*PNA **27**

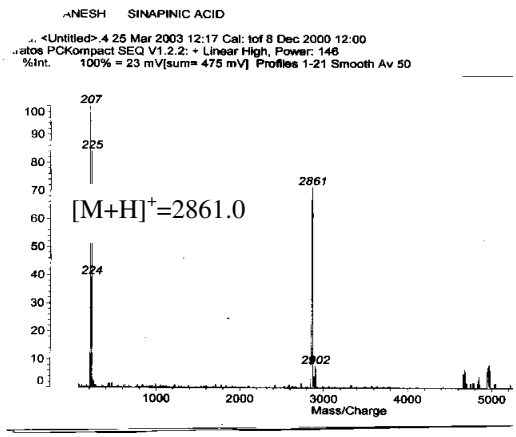

MALDI-TOF of *ch*PNA **28**

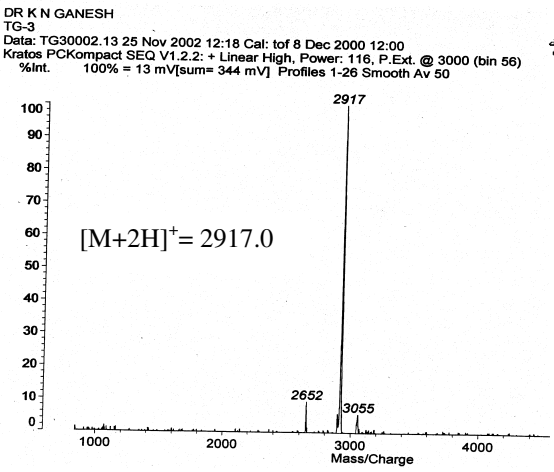

MALDI-TOF of *ch*PNA **29**

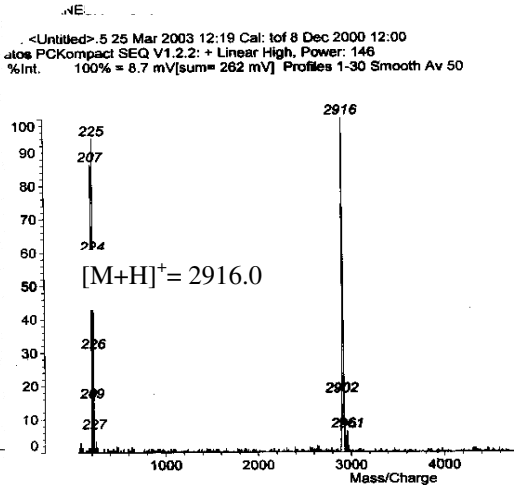

MALDI-TOF of *ch*PNA **31**

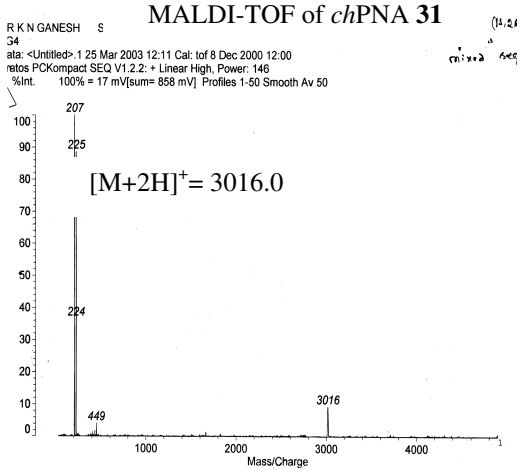

Figure 17a. MALDI-TOF spectra of *ch*PNAs

MALDI-TOF of *aeg*PNA **33**.

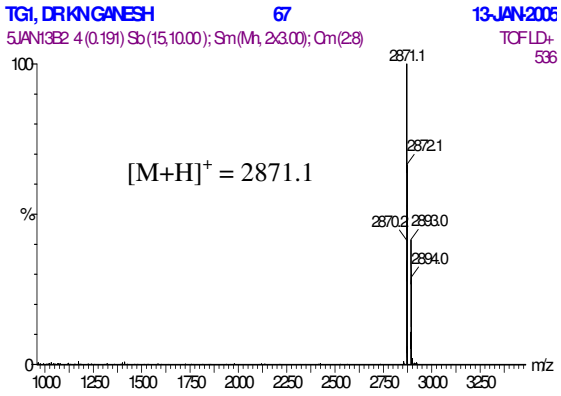

MALDI-TOF of *ch*PNA **34**.

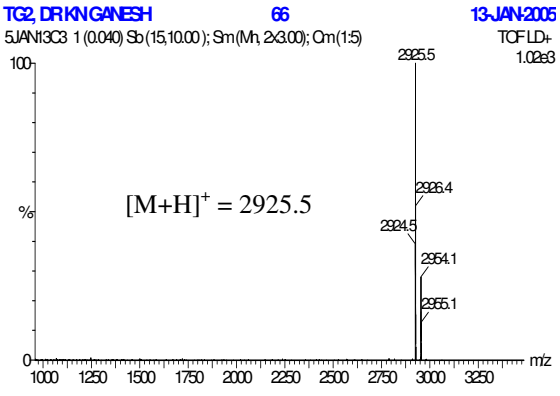

MALDI-TOF of *ch*PNA **35**.

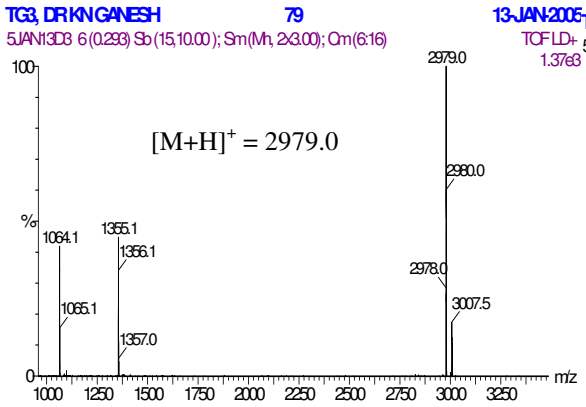

MALDI-TOF of *ch*PNA **36**.

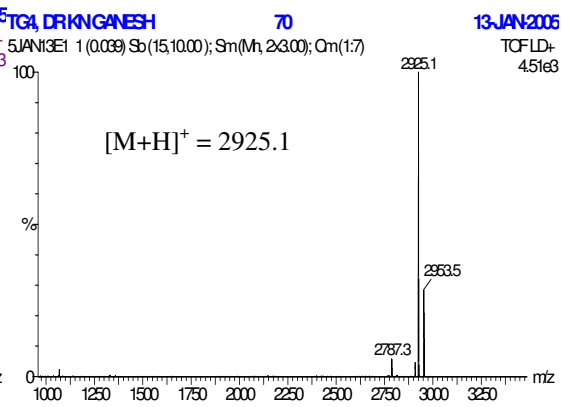

MALDI-TOF of *ch*PNA **37**.

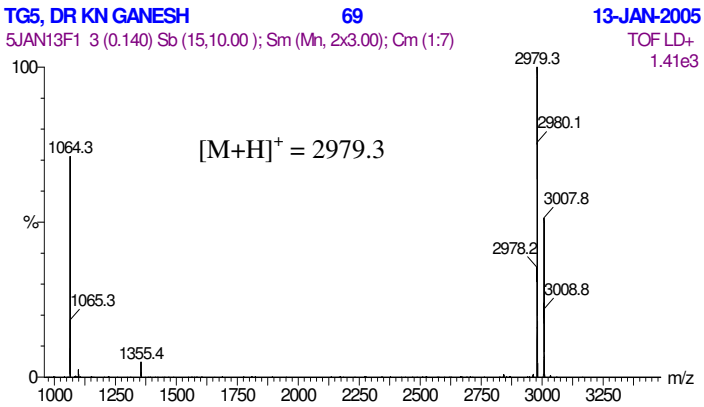

Figure 17a. MALDI-TOF spectra of *ch*PNAs

Table 9. HPLC and MALDI-TOF mass spectral analysis of modified PNAs.

Entry	PNA	Retention time (min)	Calculated MW (mol.formula)	Measured MW
1	*aeg*PNA **25**	8.25	2806.0 ($C_{116}H_{154}N_{42}O_{42}$)	2808.0 $M+2H]^+$
2	*ch*PNA **26**	9.40	2860.0 ($C_{120}H_{160}N_{42}O_{42}$)	2862.0 $[M+2H]^+$
3	*ch*PNA **27**	9.43	2860.0 ($C_{120}H_{160}N_{42}O_{42}$)	2861.0 $[M+H]^+$
4	*ch*PNA **28**	9.91	2915.0 ($C_{124}H_{166}N_{42}O_{42}$)	2917.0 $[M+2H]^+$
5	*ch*PNA **29**	9.97	2915.0 ($C_{124}H_{166}N_{42}O_{42}$)	2916.0 $[M+H]^+$
6	*aeg*PNA **30**	10.50	2852.0 ($C_{114}H_{147}N_{60}O_{31}$)	2853.0 $[M+H]^+$
7	*ch*PNA **31**	10.64	3014.0 ($C_{126}H_{165}N_{60}O_{31}$)	3016.0 $[M+2H]^+$
8	*ch*PNA **32**	10.71	3014.0 ($C_{126}H_{165}N_{60}O_{31}$)	3016.0 $[M+2H]^+$
9	*aeg*PNA **33**	7.99	2870.0 ($C_{113}H_{146}N_{61}O_{32}$)	2871.1 $[M+H]^+$
10	*ch*PNA **34**	9.10	2924.0 ($C_{117}H_{152}N_{61}O_{32}$)	2925.5 $[M+H]^+$
11	*ch*PNA **35**	10.28	2978.0 ($C_{121}H_{158}N_{61}O_{32}$)	2979.0 $[M+H]^+$
12	*ch*PNA **36**	9.51	2924.0 ($C_{117}H_{152}N_{61}O_{32}$)	2925.1 $[M+H]^+$
13	*ch*PNA **37**	10.17	2978.0 ($C_{121}H_{158}N_{61}O_{32}$)	2979.3 $[M+H]^+$

2.3.9 Synthesis of Complementary Oligonucleotides

The DNA oligonucleotides **38**-**48** (Table 10) were synthesized on Applied Biosystems ABI 3900 High Throughput DNA Synthesizer using standard β-cyanoethyl phosphoramidite chemistry.[192] The oligomers were synthesized in the 3' to 5' direction on polystyrene solid support, followed by ammonia treatment. The oligonucleotides were desalted by gel filtration, their purity ascertained by RP HPLC on a C18 column to be more than 98% and were used without further purification in the biophysical studies of PNAs. The RNA oligonucleotides **44-50** (Table 10) were obtained commercially.

Table 10. DNA/RNA Oligonucleotides used in the present work

Entry	Sequence code	Sequences	Type (corresponding PNA)
		DNA sequence 5' to 3'	
1	DNA **38**	C G C A A A A A A A A A A C G C	Match (**25**-**29**)
2	DNA **39**	C G C A A A A A C A A A A C G C	Mismatch (**25**-**29**)
3	DNA **40**	G C G T T T T T T T T T T G C G	Match (**38**)
4	DNA **41**	Poly dA	Match (**25**-**29**)
5	DNA **42**	A G T G A T C T A C	Antiparallel (**31**-**32**)
6	DNA **43**	C A T C T A G T G A	Parallel (**31**-**32**)
		RNA sequences 5' to 3'	
7	RNA **44**	A G U G A U C U A C	Antiparallel (**31**-**32**)
8	RNA **45**	C A U C U A G U G A	Parallel (**31**-**32**)
9	RNA **46**	Poly rA	Match (**25**-**29**)
10	DNA **47**	AGGCACTGCC	Antiparallel (**33**-**37**)
11	DNA **48**	CCGTCACGGA	Parallel (**33**-**37**)
12	RNA **49**	AGGCACUGCC	Antiparallel (**33**-**37**)
13	RNA **50**	CCGUCACGGA	Parallel (**33**-**37**)

2.3.10 Biophysical Studies of *ch*PNA:DNA/RNA Complexes

To investigate the binding selectivity, specificity and discrimination of *ch*PNAs towards complementary DNA and RNA, the stoichiometry of the *ch*PNA:DNA was first determined using Job's method.[193] The UV-melting studies were then carried out with all the synthesized oligomers and the T_m data was compared with the control *aeg*PNA T_{10}. The stability of the *ch*PNA duplexes with DNA/RNA was also studied. The CD spectra of single strands and corresponding complexes with complementary DNA were recorded. Finally the complexation of these *ch*PNAs to complementary DNA was confirmed by gel electrophoretic shift assay (PAGE).

2.3.10.1 Binding Stoichiometry: CD and UV-mixing Curves

Ultraviolet (UV) absorption and circular dichroism (CD) measurements are extremely useful to determine the stoichiometry and stability of duplexes and triplexes. The stoichiometry of the paired strands may be obtained from the mixing curves, in which the optical property at a given wavelength is plotted as a function of the mole

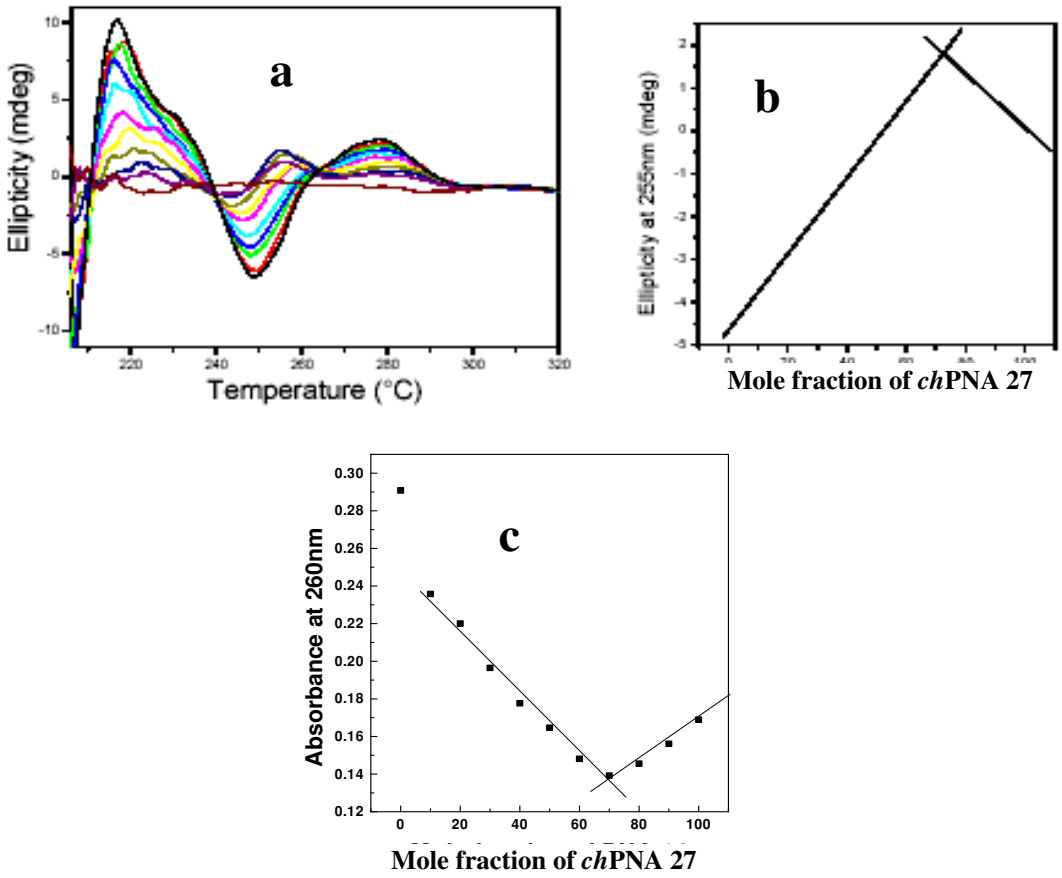

Figure 18. a) CD-curves for *ch*PNA **27** and the complementary DNA **38** d($CGCA_{10}CGC$) mixtures in the molar ratios of 0:100, 10:90, 20:80, 30:70, 40:60, 50:50, 60:40, 70:30, 80:20, 90:10, 100:0 (Buffer, 10 mM Sodium phosphate pH 7.0, 100 mM NaCl, 0.1 mM EDTA), b) CD-Job plot corresponding to 255 nm, c) UV-job plot corresponding to above mixtures of different molar ratios, absorbance recorded at 260 nm.

fraction of each strand from isodichroic and isoabsortive point (Job's plot).[193] The combination of absorption and CD spectra provides unambiguous determination of the complex formation and strand stoichiometry than is provided by absorption spectra alone.

Various stoichiometric mixtures of *ch*PNA **27** and DNA **38** were made with relative molar ratios of (*ch*PNA **27**:DNA **38**) strands of 0:100, 10:90, 20:80, 30:70, 40:60, 50:50, 60:40, 70:30, 80:20, 90:10, 100:0, all at the same strand concentration 2 μM in sodium phosphate buffer, 100 mM NaCl, 0.1 mM EDTA (10 mM, pH 7.0). The samples with the individual strands were annealed and the CD spectra were recorded (Figure 18a). The CD spectra at different molar ratios show a isodichroic point (wavelength of equal

CD magnitude) around 265 nm. CD values around such wavelengths are therefore especially useful for plotting mixing curves. This systematic change in the CD spectral features upon variable stoichiometric mixing of PNA and DNA components can be used to generate Job's plot which was indicated a binding ratio of 2:1 for the cyclohexyl PNA_2:DNA complexes, expected for triplex formation. The mixing curve in Figure 18b was plotted using the CD data at 260 nm from the spectra in Figure 18a, which indicated the formation of triplex of *ch*PNA **27**:DNA **38**. Absorbance spectra were also recorded for the mixtures of *ch*PNA **27**:DNA **38** in different proportions as mentioned above. A mixing curve was plotted, absorbance at fixed wavelength (λ_{max} 260 nm) against mole fractions of *ch*PNA **27**. Figure 18c shows the change in λ_{max} observed for the mixtures of different molar fractions. There is a drastic shift in the λ_{max} value when the concentration of *ch*PNA **27** in the mixtures increased to 60 to 70%, which further increases behind that proportions. This supports the formation of (*ch*PNA **27**)$_2$:DNA **38** triplexes.

2.3.10.2 CD spectroscopic studies of PNA:DNA/RNA complexes.

PNA is non chiral and does not show any significant CD signatures. However PNA:DNA complexes exhibit characteristic CD signatures due to chirality induced by DNA component.[194] It is known that the formation of PNA triplexes is accompanied by appearance of positive CD bands at 258 nm and 285 nm that are not present in DNA. The 258 nm band is slightly sharper and of higher intensity than 285 nm. The presence of chiral centers in cyclohexyl PNAs should further influence the CD patterns of the derived PNA:DNA triplexes. Figure 19A-C shows the CD spectra of individual *ch*PNAs **26**-**29**, DNA **38** and the *ch*PNA:DNA complexes. The single stranded cyclohexyl PNAs (**26**-**29**) show weak CD bands in the 250-290 nm regions that are absent in unmodified PNA **25**. The CD spectra of complexes of *ch*PNA **26**, *ch*PNA **27**, *ch*PNA **28** and *ch*PNA **29** with

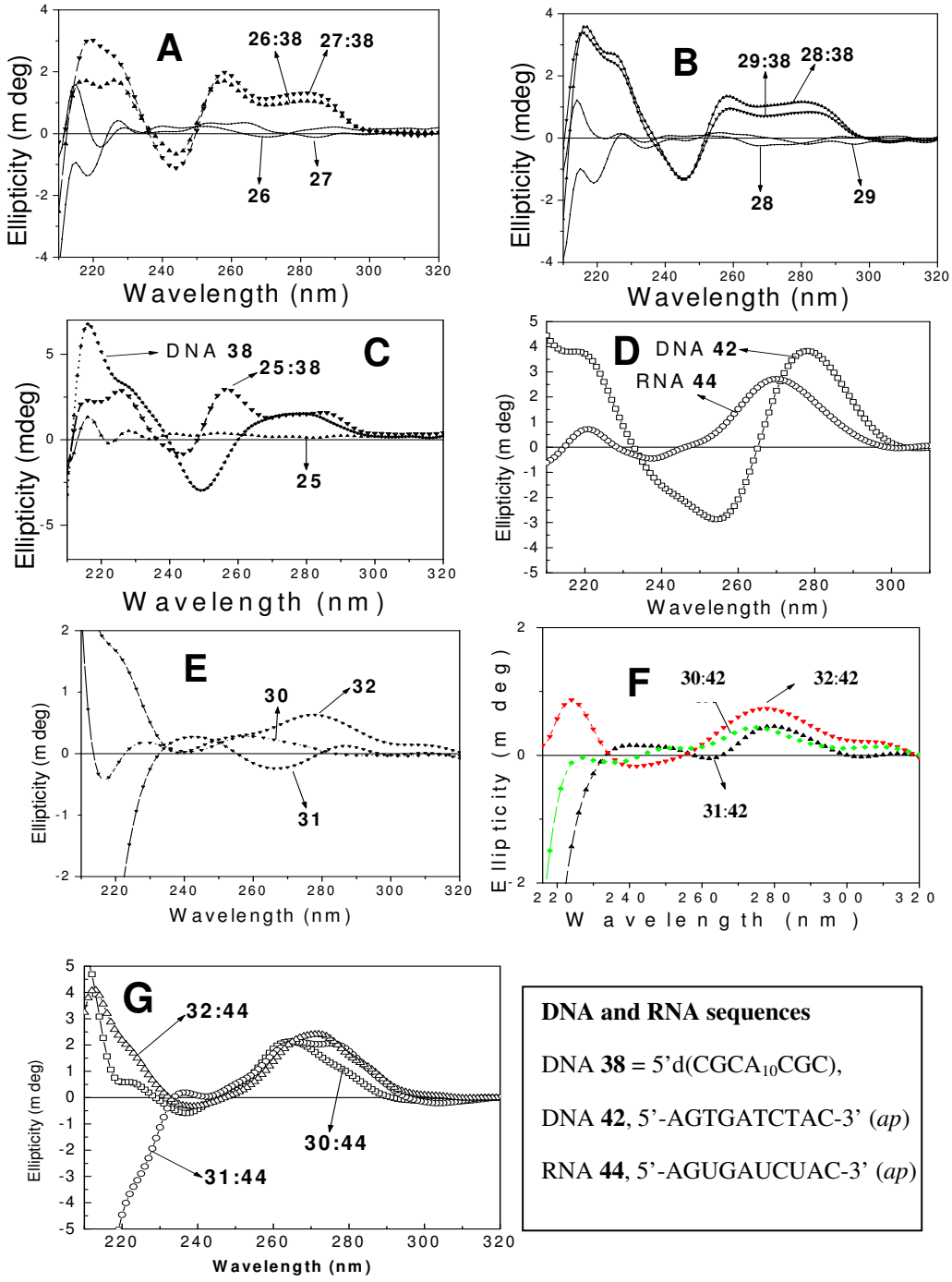

Figure 19. A-C: CD spectra of *aeg*PNA **25**, *SR-ch*PNA **26**, *RS-ch*PNA **27,** *SR-ch*PNA **28,** *RS-ch*PNA **29** and corresponding complexes with DNA **38**. **D-E**: CD spectra of *aeg*PNA **30**, *SR-ch*PNA **31**, *RS-ch*PNA **32** and corresponding complexes with DNA **42** and RNA **44**. (10 mM sodium phosphate buffer, pH=7.0, 100 mM NaCl, 0.1 m M EDTA, 20°C).

$d(A_{10})$ are nearly identical (Figure 19A and 19B) and are similar to the CD spectrum of the unmodified (PNA**12**)$_2$-$d(A_{10})$ triplex (Figure 19C).[109] All PNA:DNA triplexes show

the expected positive bands at 258 and 285 nm, with intensity of the former higher than that of latter. Interestingly the relative intensity ratios of 258/285 nm bands are different for the cyclohexyl PNA:DNA triplexes as compared to the control PNA:DNA triplex. The 285 nm band increased in intensity with the degree of modification, irrespective of the nature of the modification (*RS*/*SR*). These results suggest that the cyclohexyl modifications may alter the base stacking in the modified PNA:DNA complexes. The systematic changes in the CD spectral features upon variable stoichiometric mixing of PNA and DNA components can be used to generate Job's plot which also indicated a binding ratio of 2:1 for the cyclohexyl PNA:DNA complexes, confirming the formation of triplexes.

CD Spectra of duplexes: The *ch*PNA:DNA duplexes (Figure 19F) show CD profiles similar to that of *aeg*-PNA:DNA duplex, with a positive band at 277 nm and a low intensity negative band at 250 nm. Thus near mirror image CD spectra of *ch*PNA **31** and *ch*PNA **32** show that there is no epimerization during the synthesis. The CD profiles of *ch*PNA:RNA duplexes (Figure 19G) consisting of a high intensity positive band (260-270 nm) and a low intensity negative band (245 nm) like that of *aeg*-PNA:RNA duplex (Figure 19G), suggests a high degree of helical identity among the *aeg/ch*-PNA:RNA duplexes. The single stranded PNAs containing chiral (1*S*,2*R*)- and (1*R*,2*S*)-aminocyclohexyl units have weak but distinct CD spectra (Figure 19E). Due to the dominant CD contributions from DNA/RNA strands in the complexes, differences due to *SR*/*RS* are not apparent, although the CD of the two enantiomeric *ch*PNA monomers are mirror images (Figure 11f).

2.3.10.3 UV-Melting studies of *ch*PNA-DNA/RNA complexes.

Thermal Stability of triplexes: The hybridization studies of modified PNAs with complementary DNA (**38**) sequence were done by temperature dependent UV-absorbance experiments. The stoichiometry for homopyrimidine PNA:DNA complexation as established by UV absorbance mixing data at 260 nm (Job' plot),[193] was 2:1 ratio (Figure 17c). The thermal stabilities (T_m) of PNA_2:DNA triplexes were obtained for different PNA modifications with both complementary DNA **38** (Figure 20a, Table 11) and DNA **39** having a single mismatch (Figure 20b, Table 11). The corresponding complexes with poly rA and poly dA were also studied for relative compatibility of the imposed stereochemistry with ribo and deoxyribonucleic acids (Figure 20a and b, Table 12). Unlike DNA triplexes, which shows two distinct transitions corresponding to triplex to duplex melting and later duplex to single strands melting, *ch*PNA_2:DNA triplexes show single transition similar to PNA_2:DNA triplex melting.[100,113,175]

In general, the PNA_2:DNA triplexes were found to be less stable for PNAs containing enantiomeric (1*S*,2*R*) or (1*R*,2*S*) modified cyclohexyl units, as compared to the unmodified PNA. The PNA oligomers **26** and **27** (Table 11, entry 2 and 3) having a modification in the center of the sequence destabilized the complexes with DNA **38** (ΔT_m = -28°C and -24°C respectively) in comparison to the control PNA **25** (Table 1, entry 1). In the case of PNA oligomers **28** and **29** (Table 1, entry 4 and 5) having two modified units (at *N*-terminal and center), a further decrease in T_m (ΔT_m = -35°C and -32°C) was observed. PNAs **27** and **29** modified with (1*R*,2*S*)-isomer were slightly better binding with DNA **38** than the PNAs **26** and **28** with enantiomeric (1*S*,2*R*) isomer. The comparative binding study was also conducted for complexation with poly-rA. For

appropriate comparison of DNA and RNA complex stabilities, UV-experiments were done with poly dA, which exhibited a higher T_m than the DNA oligonucleotide **38**.

Table 11. UV-Melting temperatures (T_m values in °C)[a] of *ch*PNA$_2$:DNA triplexes.

Entry		PNA sequences (homothymine)	DNA **38**	DNA **39**
1	**25**	H-TTTTTTTTTT-Lys-NH_2	69.2	58.0 (- 11.2)[b]
2	**26**	H-TTTTT$_{SR}$TTTTT-Lys-NH_2	41.1	26.1 (-15.0)
3	**27**	H-TTTTT$_{RS}$TTTTT-Lys-NH_2	45.0	29.1 (-16.1)
4	**28**	H-T$_{SR}$TTTT$_{SR}$TTTTT-Lys-NH_2	34.4	23.3 (-11.0)
5	**29**	H-T$_{RS}$TTTT$_{RS}$TTTTT-Lys-NH_2	37.5	25.7 (-12.0)

DNA 38 = 5'd(CGCA$_{10}$CGC); DNA **39 = 5'**d(CGCA$_4$*C*A$_5$CGC), [a] T_m = melting temperature (measured in the buffer 10 mM sodium phosphate, 100 mM Nacl, 0.1 mM EDTA, pH = 7.0), PNA$_2$-DNA complexes. [b] Values in parenthesis indicate the difference in T_m as a result of the mismatch in DNA sequence. [c].Values in parenthesis indicate difference in binding with RNA over DNA. The values reported here are the average of 3 independent experiments and are accurate to ±0.5°C.

The complexes of the modified oligomers with poly rA exhibited lowered T_m, indicating destabilization as compared to the unmodified PNA **25** (Table 12, entry 1), but the magnitudes were relatively small for either poly-rA or poly dA (ΔT_m ~7°C per modification) than observed for the complexes with DNA oligonucleotides. The most interesting observation is that the stereochemistry of the monomeric units is able to direct the DNA verses RNA binding selectivity; thus the (1*S*,2*R*)-PNAs **26** and **28** (Table 12, entry 2 and 4) with one and two modifications show better binding to poly-rA compared to the corresponding (1*R*,2*S*) PNAs **27** and **29** (Table 12, entry 3 and 5). The situation is

Table 12. UV-Melting temperatures (T_m values in °C)[a] of *ch*PNA$_2$:DNA triplexes.

Entry		PNA sequences (homothymine)	Poly rA **46**	Poly dA **41**
1	**25**	H-TTTTTTTTTT-Lys-NH_2	> 80.0	72.4
2	**26**	H-TTTTT$_{SR}$TTTTT-Lys-NH_2	77.2	61.5 (-15.7)[c]
3	**27**	H-TTTTT$_{RS}$TTTTT-Lys-NH_2	70.7	63.5 (-7.2)
4	**28**	H-T$_{SR}$TTTT$_{SR}$TTTTT-Lys-NH_2	64.4	53.7 (-10.7)
5	**29**	H-T$_{RS}$TTTT$_{RS}$TTTTT-Lys-NH_2	58.6	53.5 (-5.1)

[a] T_m = melting temperature (measured in the buffer 10 mM sodium phosphate, 100 mM Nacl, 0.1 mM EDTA, pH = 7.0), PNA$_2$-DNA complexes. [b] Values in parenthesis indicate the difference in T_m as a result of the mismatch in DNA sequence. [c].Values in parenthesis indicate difference in binding with RNA over DNA. The values reported here are the average of 3 independent experiments and are accurate to ±0.5°C.

reverse for binding with DNA, the (1*R*,2*S*) PNAs **27** and **29** bind DNA better compared to (1*S*,2*R*)-PNAs **26** and **28**. In general, all PNA oligomers showed a slightly lower binding with poly dA than with poly rA**.** The observed transitions are sharp for modified PNA complexes with poly rA and poly dA as compared to complexes of unmodified PNA **25**. Introduction of the second modified unit at *N*-terminus actually reduced the overall stability of complexes both with dA_{10}, poly dA and poly rA as well as the differenial RNA over DNA binding stability.

UV-Tm mismatch studies: The thermal stabilities of PNA complexes with DNA **39** [d(A_4CA_5] containing single mismatch at the middle modification site were also measured (Figure 20b, Table 12). The ΔT_m for control PNA **25** (Table 11, entry 1) was –11° while that for modified PNAs **26** and **27** (Table 11, entry 2 and 3) were –15 ^oC when a single modified unit is present. With the second modified unit, this difference also reduced to reduced to –11^oC with a lowering of T_m (Table 11, entry 4 and 5). These results indicated that the cyclohexyl modified PNAs retain the ability of PNAs of sequence specific recognition and binding to cDNA allowing discrimination against mismatch sequences.

Thermal Stability of Duplexes: To study the effect of PNA designs on corresponding duplexes, the mixed sequence decamer PNAs incorporating either the (1*S*,2*R*)- or (1*R*,2*S*)- aminocyclohexyl-T units at three thymine positions of *aeg*PNA **30** decamer (Table 13, *ch*PNA **31** and *ch*PNA **32** respectively) were synthesized. The T_m values of various PNAs hybridized with cDNA/RNA for parallel and antiparallel bindings were determined from temperature–dependent UV absorbance or CD plots (Figure 17 and 18) and summarized in Table 13 (Figure 21a and b).

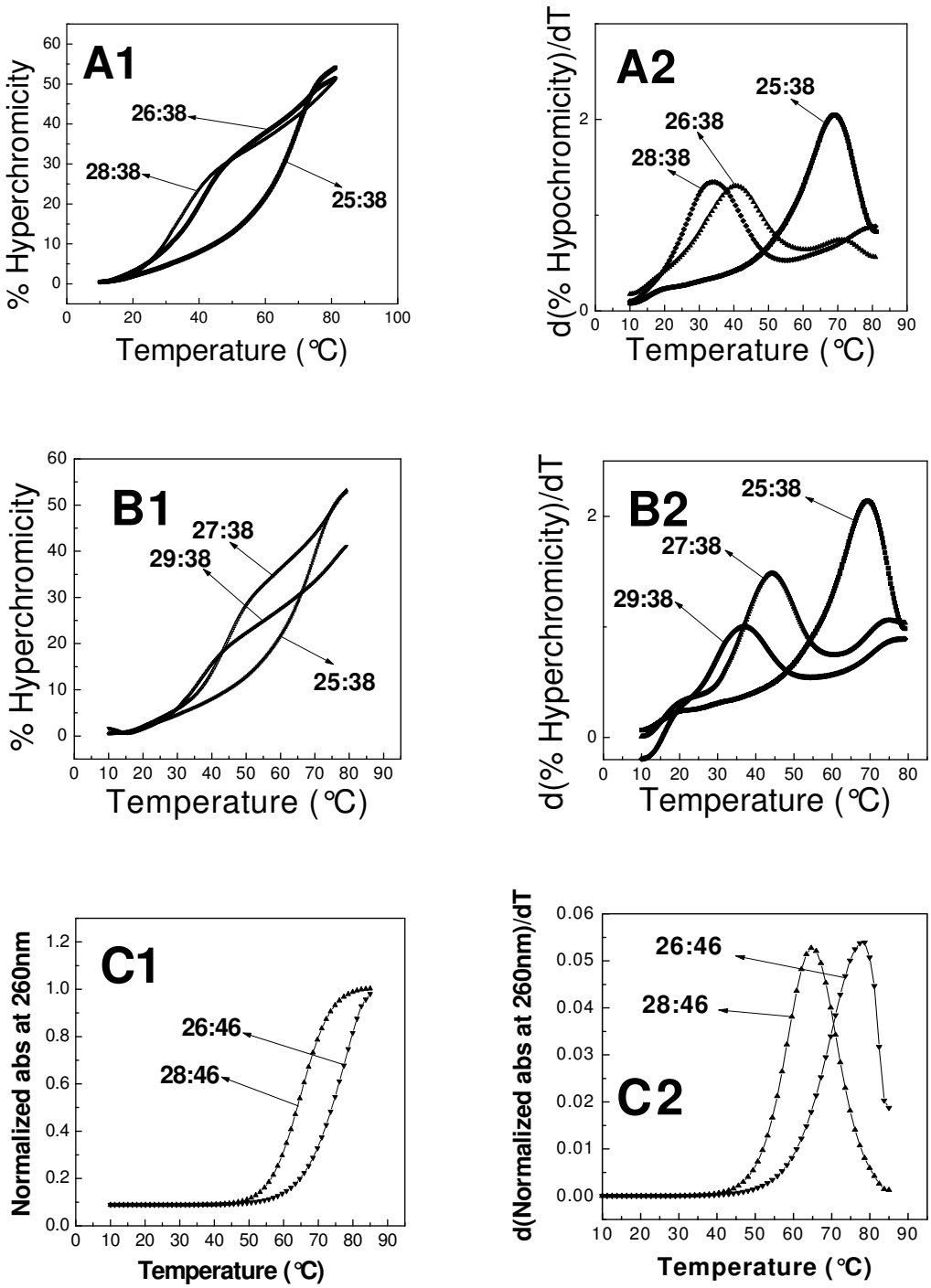

Figure 20a. **A1**-**B1**: Melting curves for PNA:DNA complexes of *aeg*PNA **25**, *SR*-*ch*PNA **26**, *RS*-*ch*PNA **27**, *SR*-*ch*PNA **28** and *RS*-*ch*PNA **29** with DNA **38**. **C1**: Melting curves for PNA:RNA complexes of *SR*-*ch*PNA **26** and *SR*-*ch*PNA **28** with RNA **46**. **A2**-**C2**: corresponding first derivative curves. DNA **38** = $CGC(A)_{10}CGC$, RNA **46** = poly **rA**. (10 mM sodium phosphate buffer, pH=7.0, 100 mM NaCl, 0.1 m M EDTA).

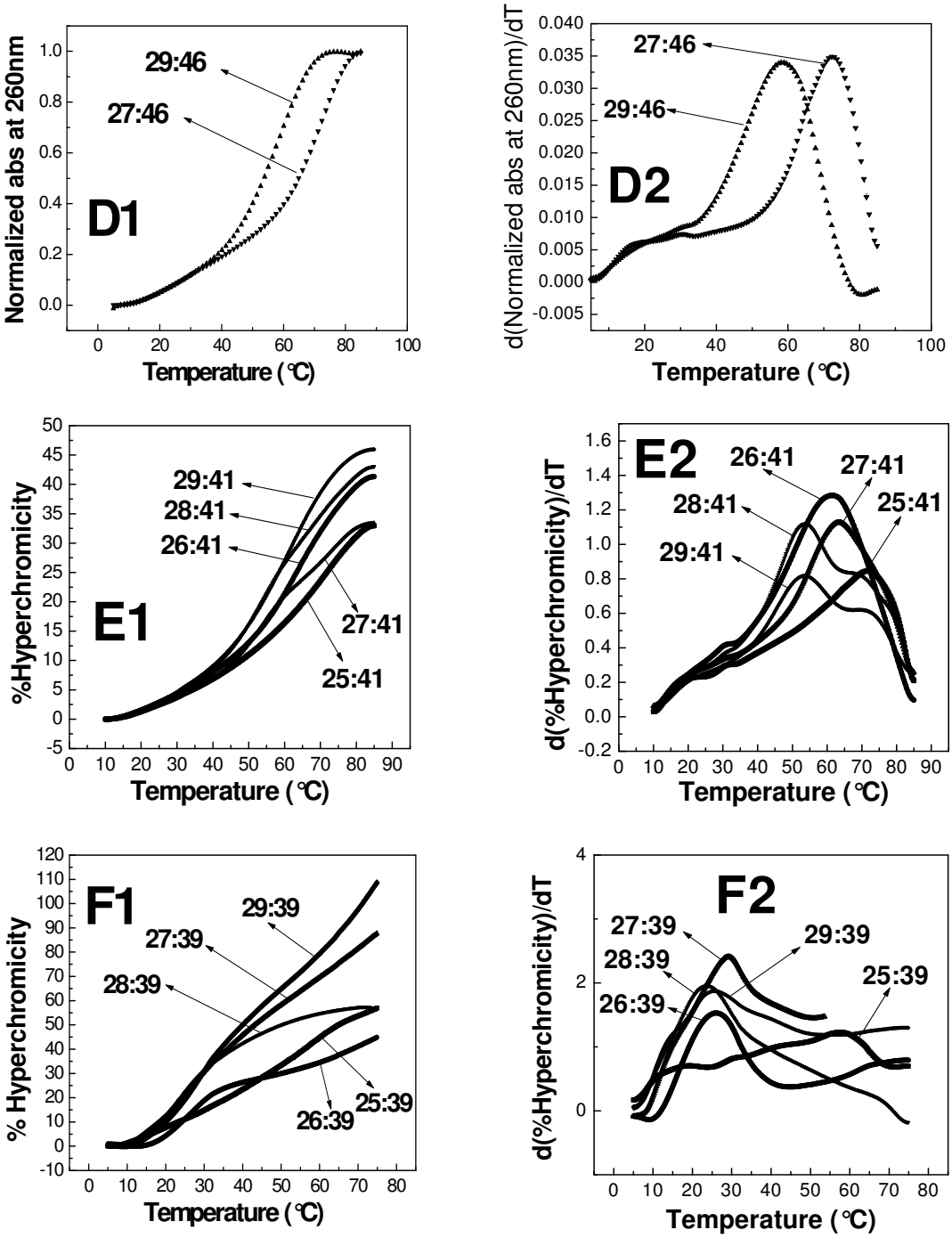

Figure 20b. **D1**: Melting curves for PNA:RNA complexes of *RS-ch*PNA **27** and *RS-ch*PNA **29** with RNA **46**. Melting curves for PNA:DNA complexes of *aeg*PNA **25**, *SR-ch*PNA **26**, *RS-ch*PNA **27**, *SR-ch*PNA **28** and *RS-ch*PNA **29** with DNA **41** (**E1**) and DNA **39** (**F1**, mismatch complexes). **D2**-**F2**: corresponding first derivative curves. RNA **46** = poly **rA**, DNA **41** = poly **dA**, DNA **39** = CGCAAAAA*C*AAAACGC. (10 mM sodium phosphate buffer, pH=7.0, 100 mM NaCl, 0.1 m M EDTA).

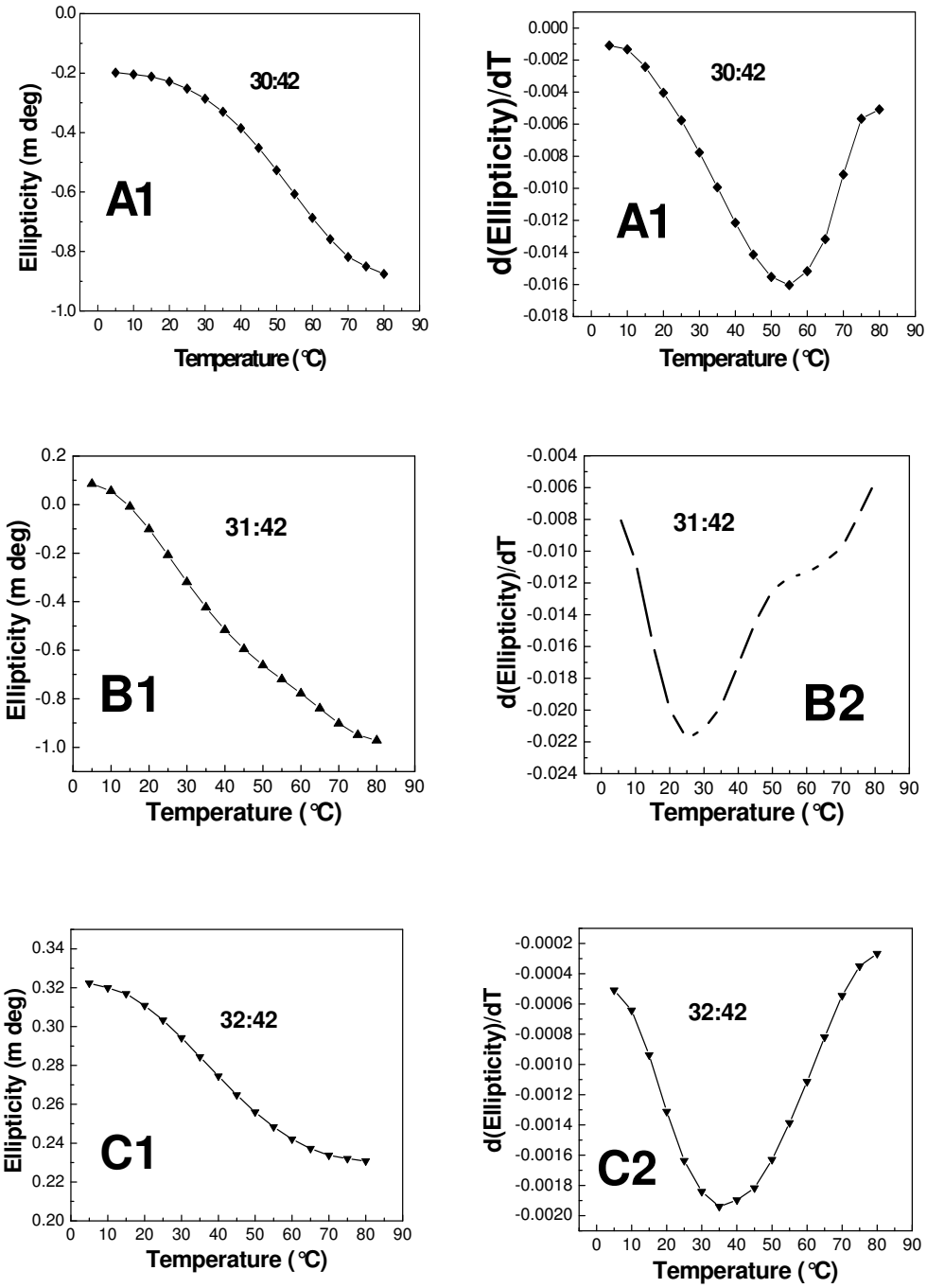

Figure 21. CD-*T*m curves for duplexes of *aeg*PNA **30**, *SR-ch*PNA **31**, *RS-ch*PNA **32** with DNA **42** (antiparallel) (**A1**, **B1**, **C1** respectively) and their corresponding derivative (**A2**, **B2**, **C2**). DNA **42** = 5' AGTGATCTAC 3' (10 mM sodium phosphate buffer, pH=7, 100 mM, NaCl, 0. 1 mM EDTA)

Data in Table 13 shows that the reference *aeg*-PNA **30** (entry 1 and 4) forms *ap*-duplexes with complementary DNA **42** and RNA **44** with equal stability. Compared to T_m of *aeg*-PNA:DNA duplex, the T_m values of *ch*-PNA:DNA duplexes (entry 2 and 3) are lower (ΔT_m = -30°C for *SR* and -20°C for *RS*). The thermal stability of *ch*-PNA/*cp*-PNA duplexes with complementary DNA/RNA oligonucleotides is stereochemistry dependent with T_m of *RS* duplexes more than that of *SR* duplexes. *ch*-PNAs **31** and **32** having low binding affinity with *ap*-DNA **42** were ineffective in forming parallel duplexes with DNA **43.** In the case of PNA:RNA duplexes, *ch*-(*SR*)-PNA **32** (entry 6) had a large stabilizing effect (ΔT_m>50°C) over that of control *aeg*-PNA. *ch*PNA:RNA antiparallel duplex (**32:44**) having T_m values >85°C did not dissociate completely, whereas parallel duplex (**32:45**) with a lower stability showed complete melting (Figure 21b). The most important feature of the data in Table 13 is that *SR*/*RS*-*ch*-PNAs destabilize the DNA duplex but enormously stabilize the RNA duplex. In the process, the *ch*-PNAs induce remarkable differences in duplex stabilities among their DNA and RNA complexes, with ΔT_m (RNA-

Table 13. UV-Melting temperatures (T_m values)[a] of *ch*PNA:DNA duplexes.

Entry	Duplexes (**antiparallel**)	T_m (°C)	Duplexes (**parallel**)	T_m (°C)
	PNA:DNA		**PNA:DNA**	
1	*aeg*PNA **30**:DNA **42**	55.0[b]	*aeg*PNA **30**:DNA **43**	40.0[b]
2	*ch*PNA **31**:DNA **42**	25.0[b]	*ch*PNA **31**:DNA **43**	[c]
3	*ch*PNA **32**:DNA **42**	35.0[b]	*ch*PNA **32**:DNA **43**	[c]
	PNA:RNA		**PNA:RNA**	
4	*aeg*PNA **30**:RNA **44**	55.4	*aeg*PNA **30**:RNA **45**	[c]
5	*ch*PNA **31**:RNA **44**	58.0	*ch*PNA **31**:RNA **45**	[c]
6	*ch*PNA **32**:RNA **44**	>85.0	*ch*PNA **32**:RNA **45**	80.0

[a]All values are an average of at least 3 experiments and accurate to within ± 0.5°C. Buffer. Sodium phosphate (10 mM), pH 7.0 with 100 mM NaCl and 0.1 mM EDTA; [b]Measured by CD to avoid interference from thermal transitions of single stranded PNAs. A, T, G, C are *aeg*PNA bases, $\mathbf{t}_{SR/RS}$ *ch*-PNA-T. DNA **42**, 5'-AGTGATCTAC-3'(*ap*); DNA **43,** 5'-CATCTAGTGA-3'(*p*); RNA **44**, 5'-AGUGAUCUAC-3'(*ap*); RNA **45,** 5'-CAUCUAGUGA-3' (*p*).

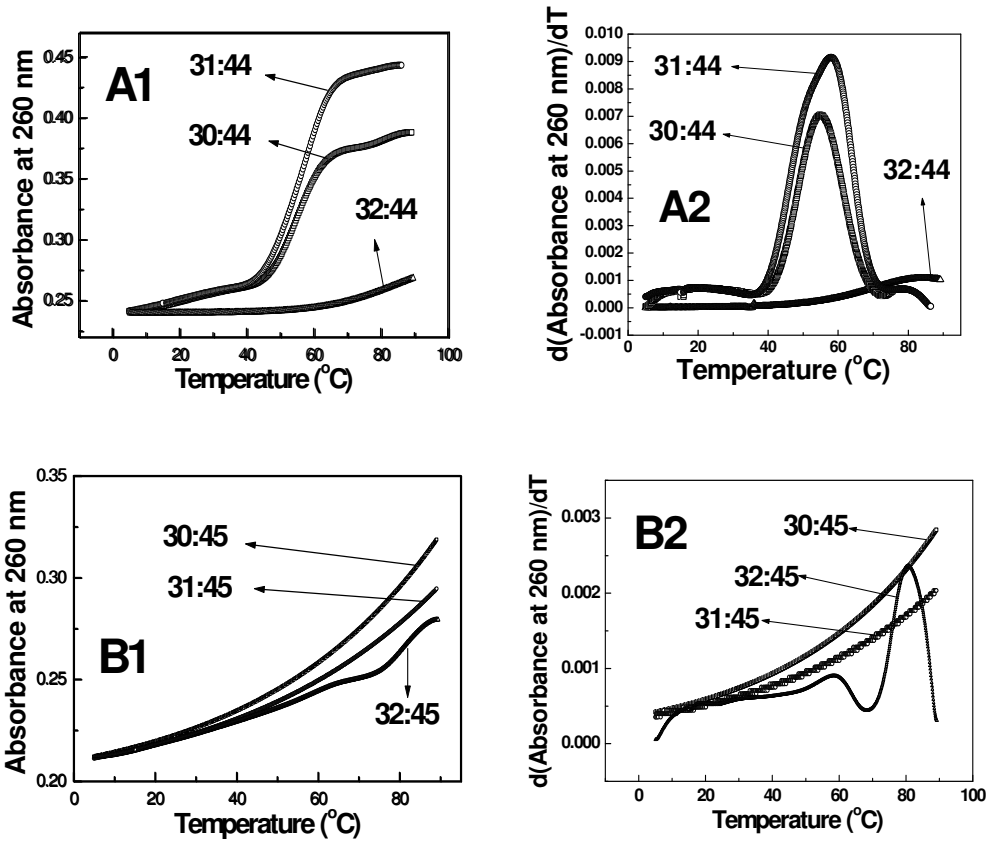

Figure 21b. Melting-curves for PNA:RNA duplexes of *aeg*PNA **30**, *ch*PNA **31**, *ch*PNA **32**; **A1**: with RNA **44** (antiparallel); **B1**: with RNA **45** (parallel). **A2**, **B2**: corresponding first derivative curves. RNA **44** = 5' AGUGAUCUAC 3', RNA **45** = 5' CAUCUAGUGA 3', (10 mM sodium phosphate buffer, pH=7, 100 mM, NaCl, 0.1 mM EDTA).

DNA) =+33°C for *SR-ch*-PNA **31** and +50°C for *RS-ch*-PNA **32**. This is a highly significant, exceptional binding selectivity of PNA to RNA over same DNA sequence.

Table 14: T_m (°C) values of PNA:DNA and PNA:RNA duplexes

Entry	PNA sequence		DNA **47**	RNA **49**	$\Delta T_{m\ (RNA-DNA)}$
1	GGCAGTGCCT-LysNH_2	**33**	59.5 (56.5)	64.0 (59.5)[a]	4.5
2	GGCAGT$_{SR}$GCCT-LysNH_2	**34**	58.5[b]	74.5[b]	16.0
3	GGCAGT$_{SR}$GCCT$_{SR}$-LysNH_2	**35**	55.5[b]	>85.0 (80.0)[a]	>40.0
4	GGCAGT$_{RS}$GCCT-LysNH_2	**36**	57.0[b]	83.0[b]	26.0
5	GGCAGT$_{RS}$GCCT$_{RS}$-LysNH_2	**37**	56.0[b]	>85.0 (~83.0)[a]	>40.0

[¶]All values are an average of at least 3 experiments and accurate to within ± 0.5°C. Buffer. Sodium phosphate (10 mM), pH 7.0 with 100 mM NaCl and 0.1 mM EDTA; A, T, G, C are *aeg*PNA bases, $\mathbf{T}_{SR/RS}$ *ch*PNA-T (**34-37**); DNA **47**, 5'-AGGCACTGCC-3'(*ap*); RNA **49**, 5'- AGGCACUGCC -3'(*ap*), DNA **48** (parallel) = 5'-CCGTCACGGA-3', RNA **50** (parallel) = 5'-CCGUCACGGA-3'. [a]Values in brackets are T_m for parallel PNA:DNA and PNA:RNA duplexes. [b] do not form corresponding PNA:DNA/RNA parallel complexes.

In order to study the generality of the RNA selectivity effect, a PNA sequence was constructed that is complementary to a portion of DNA/RNA encoding a mutant p53

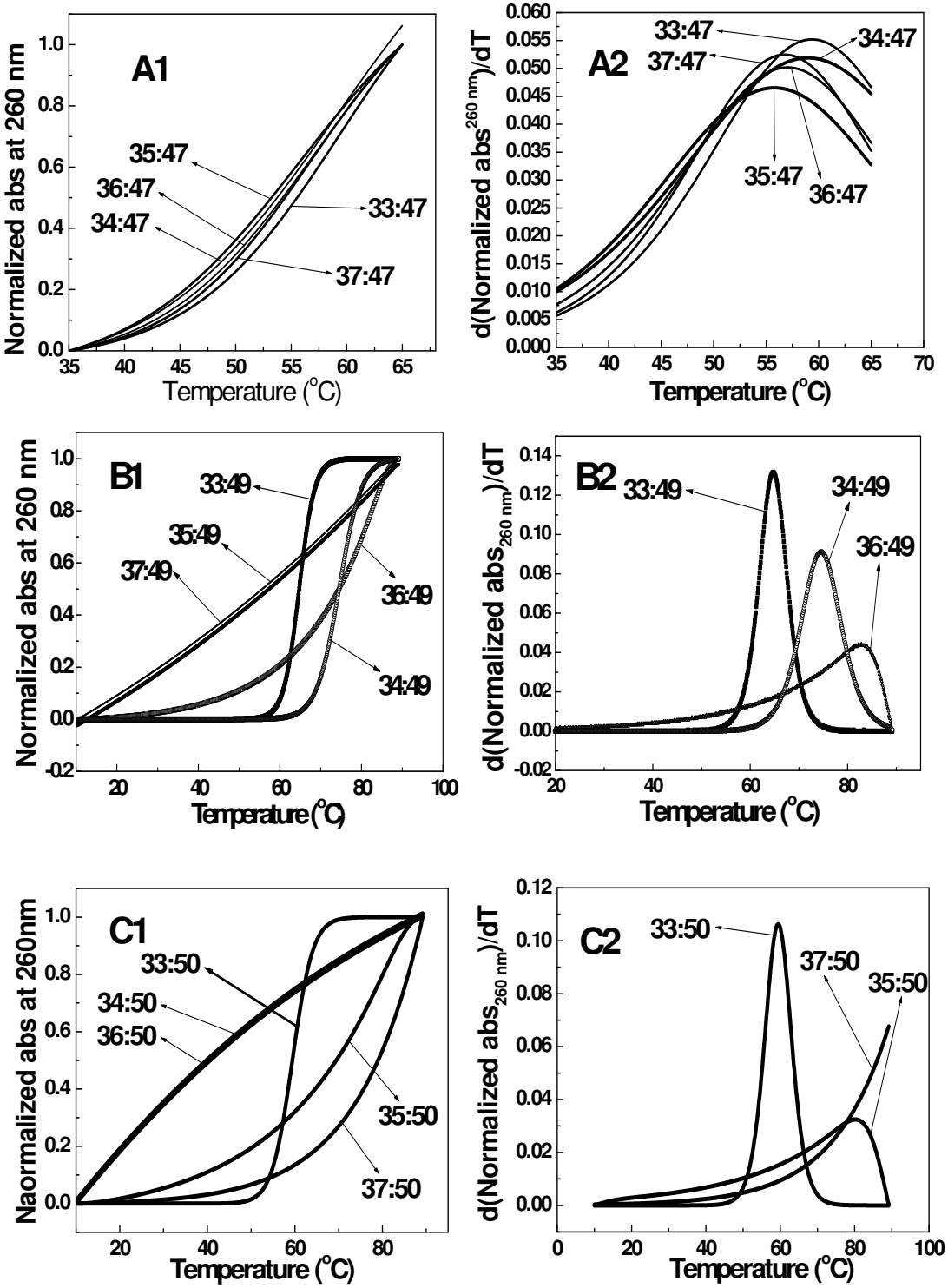

Figure 22. UV-T_m curves for PNA:DNA/RNA antiparallel duplexes of *aeg*PNA **33**, *SR-ch*PNA **34**, *SR-ch*PNA **35,** *RS-ch*PNA **36,** and *RS-ch*PNA **37** with DNA **47** (**A1**) and RNA **49** (**B1**). **C1**: melting curves of PNA:RNA Parallel duplexes. **A2, B2, C2**: corresponding derivative. DNA **47** (antiparallel) = 5'-AGGCACTGCC-3', RNA **49** (antiparallel) = 5'-AGGCACUGCC-3', RNA **50** (parallel) = 5'-CCGUCACGGA-3' (10 mM sodium phosphate buffer, pH=7, 100 mM, NaCl, 0. 1 mM EDTA)

protein that is prevalent in many different cancer cell lines.[200] The *ch*PNAs **34**-**37** were synthesized by incorporating one or two *cis*-cyclohexyl modified units at thymine positions. Data in Table 14 (Figure 22) shows that the effect is sequence independent, as the *ch*PNA **34**-**37** destabilize duplex with DNA while stabilizing RNA hybrids compared to *aeg*PNA **33**. The *ch*PNA **34** and **35** (entry 2 and 3) stabilizes duplexes with RNA **49** (ΔT_m = +16°C for *SR*-*ch*PNA **34** and +~40°C for *RS*-*ch*PNA **35**) by destabilizing the corresponding hybrids with DNA **47**. It is remarkable that a single substitution of *RS*-*ch*-PNA-T in a 10-mer *ch*PNA **36** shows ΔT_m (RNA-DNA) of 26^o (entry 4) while double substitution (entry 5, *ch*PNA **37**) makes the *ch*PNA:RNA hybrid even more stable with ΔT_m (RNA-DNA) > 40^o (Table 13, the ΔT_m (RNA-DNA) is > 50^o for *ch*PNA **32** having 3 x *RS*-*ch*-substitutions). Further, as observed for the *ch*PNA sequence **32**, the *RS* isomers are better than *SR* isomer in achieving discrimination. Increasing the number of substitution from one to two also destabilizes the corresponding DNA hybrids (ΔT_m = -1 to 5°C), while stabilizing the analogous RNA hybrids (ΔT_m = +16 to 40°C). The *ch*PNAs **34**-**37** binds DNA in antiparallel orientation and did not bind to parallel DNA **48**. PNAs **34** and **35** with single modification bind RNA only in antiparallel mode but not in parallel mode, while the PNAs **36** and **37** with two modified units formed PNA:RNA hybrid (parallel) with T_m lower than antiparallel hybrid.

2.3.10.4 Gel shift assay and competition binding experiments

Electrophoretic gel shift assay[195] was used to establish the binding of different PNAs to the complementary DNA. The PNAs modified with one or two units of *SR*/*RS* cyclohexyl units and the control PNA **25** were individually treated with oligonucleotide **38** (see Figure 23 legend for experimental conditions) and the complexations were monitored by non-denaturing gel electrophoresis at 10^{o}C. The spots were visualized on a

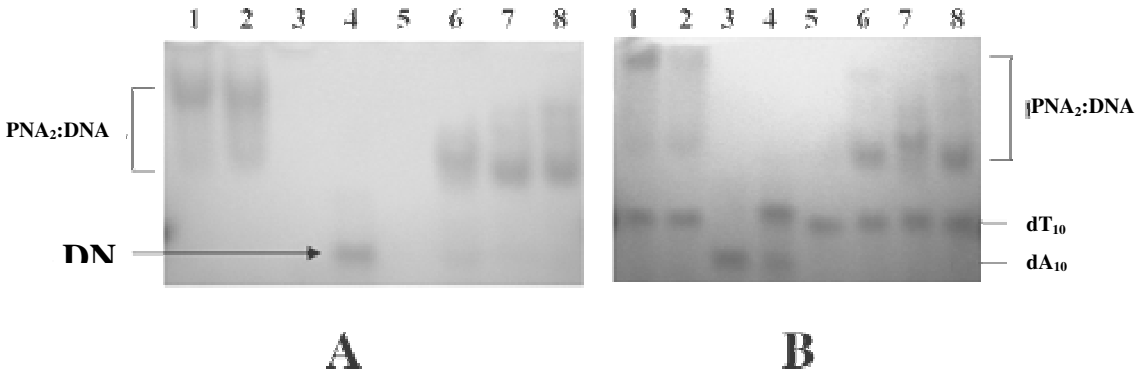

Figure 23. PNA/DNA complexation. (A) **Gel shift assay**: lane 1, *ch*PNA **28** + DNA **I**; lane 2, *ch*PNA **29** + DNA **I**; lane 3, ss*aeg*PNA-**25**; lane 4, DNA **I**; lane 5, ss*ch*PNA **26**; lane 6, *ch*PNA **26** + DNA **I**; lane 7, *ch*PNA **27** + DNA **I**; lane 8, *aeg*PNA **25** + DNA **I**. (B) **Competition binding experiments**: lane 1, DNA **I** + DNA **III** + *ch*PNA **28**; lane 2, DNA **I** + DNA **III** + *ch*PNA **29**; lane 3, ssDNA **I**; lane 4, DNA duplex (**I** + **III**); lane 5, ssDNA **III**; lane 6, DNA I + DNA **III** + *ch*PNA **26**; lane 3, ssDNA **I**; lane 4, DNA duplex (**I** + **III**); lane 5, ssDNA **III**; lane 6, DNA **I** + DNA **III** + *ch*PNA **26**; lane 7, DNA **I** + DNA **III** + *ch*PNA **27**; lane 8, DNA **I** + DNA **III** + *aeg*PNA **25**; DNA **I** = $CGCA_{10}CGC$ (DNA **38**, $\mathbf{dA}_{10}$), DNA **III** = $GCGT_{10}GCG$ (DNA **40**, dT_{10}). 0.5X, TBE, pH 8.0.

fluorescent TLC background and the results are shown in Figure 23. The formation of PNA_2:DNA complexes were accompanied by the disappearance of the single strand DNA **38** and appearance of a lower migrating band due to PNA:DNA complexes. The single modified PNA_2:DNA complexes migrated about the same as the unmodified PNA:DNA complex but lower than that of DNA **38** (Figure 23A, lane 6-8)**,** while the doubly modified PNA:DNA complexes showed more retardation (Figure 23A, lane 1-2). The different mobility retardation shifts of cyclohexyl PNA:DNA complexes may arise from the increased molecular weight upon formation of the complexes, a rigid geometry imposed by the cyclohexyl ring on the derived complexes or from an enhanced hydrophobicity due to cyclohexyl rings. Under the electrophoretic conditions employed, the single stranded PNAs that carry a net positive charge did not move out of the well (Figure 23A, lanes 3 and 5).

Competition binding: The competition binding experiments carried out by adding PNAs to the DNA duplex (**38**:**40**) followed by annealing and gel electrophoresis is shown in Figure 23B. Due to a higher binding affinity of PNA:DNA complexes compared with

DNA:DNA complexes, the added PNA binds to the complementary DNA **38** in the DNA duplex, releasing the DNA strand **40** (Equation 2). This is clearly seen in the gel electrophoresis in which the DNA duplex band (Figure 23B, lane 4) is converted into PNA:DNA complex seen as retarded band and the released DNA strand (Figure 23B, lane 6-8) showing as a faster moving band. The results indicate that the modified PNAs are as good as the unmodified PNA in successfully competing for binding with the complementary DNA strand.

Electrophoretic gel shift assay

Equation. 1: 2*ch*PNA + DNA **38** = [(*ch*PNA)$_2$ + DNA **38**]
*ch*PNA-DNA triplex

Competitive binding Experiment

Equation. 2: 2*ch*PNA + [DNA **38** + DNA **40**] = [(*ch*PNA)$_2$ + DNA **38**] + DNA **40**
DNA complex; *ch*PNA-DNA triplex; displaced ss DNA T_{10}

*where ch*PNA = *SR-chPNA* **26** and **28**
*RS-ch*PNA **27** and **29**

DNA **38** = 5' CGCAAAAAAAAAACGC 3'
DNA **40** = 5' GCGTTTTTTTTTGCG 3'

(*SR/RS*)-*ch*PNA: Duplex stability and selectivity. Classical *aeg*-PNA being flexible can easily attain competent conformation to hybridize with DNA as well as RNA and hence has near equal binding affinity to both as measured by T_m. In (*SR/RS*)-*ch*-PNA, the monomer dihedral angle β matches the range (65^o) found in PNA:RNA duplex rather than that in PNA:DNA duplex (141^o). The derived *ch*-PNAs thus exhibit a higher affinity to RNA and destabilize the complex with DNA. The inherently rigid six membered ring of *ch*-PNAs forbids structural adjustments to hybridize to DNA as well as RNA and consequently destabilize its binding with DNA. Thus the rigid (*SR/RS*)-*ch*-PNA imparts

an unparalleled selectivity for binding to RNA over DNA for duplex formation (>30°-50°C).

The present results on strong preferences of (*RS*)-*ch*-PNA for binding to RNA over DNA is in consonance with our strategy of adjusting dihedral angle β through chemical modifications to achieve structure based selectivity in PNAs. To our knowledge, this is the first-time report of any PNA analogues in a mixed base sequence that overwhelmingly discriminates identical sequences of DNA and RNA. The modification or conjugation of PNAs with cell penetrating ligands may also prompt their nuclear entry and induction of binding specificity for DNA/RNA complement would be highly desirable to improve the efficiency of nucleic acid based drugs.

2.4 Conclusion

On the basis of a rational design, the (1*S*,2*R*)- and (1*R*,2*S*)-amino cyclohexyl glycyl PNA monomers have synthesized, in which the torsion angle β is restricted to 60-70° by virtue of a *cis* axial-equatorial disposition of the backbone substituents. The designed monomers were built into PNA oligomers by solid phase synthesis using Boc protection strategy. The UV melting temperatures of the modified oligomers with the complementary/mismatched DNA and RNA were measured. The imposed stereochemistry of the PNA oligomer having (1*S*,2*R*)-isomer preferred to bind RNA and the oligomer having (1*R*,2*S*) isomer showed higher affinity towards DNA in homothymine oligomers, leading to a stereodiscrimination in recognition of DNA and RNA. Surprisingly the binding preference reverses from homothymine PNAs to mix PNAs. These results indicate that The PNA with (1*S*,2*R*)-amino cyclohexyl unit favors the RNA binding, while (1*R*,2*S*)-aminocyclohexyl unit favors the DNA binding.

The gel shift experiments indicated that the modifications retain the competitive binding attributes of PNA towards DNA duplex. The preorganization of the PNA backbone by chemical modifications such that the torsion angle β is restricted in a range found by NMR and crystal structure data may lead to the induction of substantial selectivity (discrimination) in DNA/RNA recognition. On the basis of this design, in order to study the actual effect of the binding affinity *via* entropic gains and efficient DNA/RNA discrimination, fully modified homooligomeric *ch*PNA sequences, both homopyrimidine and homopurine sequences need to be studied.

Summary

- ***cis*-Cyclohexyl PNAs (*ch*PNA) were designed, synthesized and the purpose of the design is clearly demonstrated.**
- **Triplex formation: *ch*PNA discriminates DNA from RNA. Stability-*SR*>*RS* with RNA.**
- **Duplex formation: *ch*PNA binds strongly to RNA discriminating DNA. Stability-*RS*>*SR***
- ***ch*PNAs successfully competing for binding with the complementary DNA strand.**

2.5 Experimental

***General*:** The chemicals used were of laboratory or analytical grade. All solvents used were purified according to the literature procedure. Reactions were monitored by TLC. Usual reaction work up involved sequential washing of the organic extract with water and brine followed by drying over anhydrous sodium sulfate and evaporation of the solvent under vacuum. Melting points of samples were determined in open capillary tubes using Buchi Melting point B-540 apparatus and are uncorrected. IR spectra were recorded on an infrared Fourier Transform spectrophotometer using KBr pellets or neat. Column chromatographic separations were performed using silica gel 60-120 mesh (Merck), solvent systems gradient 10-25% EtOAc/Pet ether and pure DCM to 3% MeOH/DCM. TLCs were carried out on pre-coated silica gel GF_{254} sheets (Merck 5554). TLCs were run in either petroleum ether with appropriate quantity of ethyl acetate or dichloromethane with an appropriate quantity of methanol for most of the compounds. TLCs were visualized with UV light and iodine spray and/or by spraying with Ninhydrin reagent after *t-Boc* deprotection (exposing to HCl vapors) and heating.

^{1}H and ^{13}C spectra were obtained using Bruker AC-200 (200 MHz) and 500 MHz NMR spectrometers. The chemical shifts are reported in delta (δ) values and referred to internal standard TMS for ^{1}H and deuterated NMR solvent chloroform-*d* itself for ^{13}C. The optical rotation values were measured on Bellingham-Stanley Ltd, ADP220 polarimeter. Mass spectra were obtained either by FAB (Finnigan-Matt mass spectrometer) or LCMS techniques. Oligomers were characterized by RP HPLC (Hewlett Packard) C18 column and MALDI-TOF mass spectrometry. The MALDI-TOF spectra were recorded on KRATOS PCKompact instrument and sinapinic acid as matrix. CD spectra were recorded on a JASCO J715 spectropolarimeter. UV-melting experiments

were carried out on Perkin-Elmer *Lambda-35* UV-spectrophotometer. The enzyme Amano-PS was obtained as a gift from Amano Pharmaceuticals, Japan.

Enzymatic Resolution of *Racemic* alcohol (1*R/S,*2*R/S*) 2 with Lipase *Pseudomonas cepacia*: To a solution of Lipase Amano-PS (500 mg) in Phosphate buffer (150 ml, pH = 7.2) was added the *racemic* butyrate (1*R/S,*2*R/S*)-2 (10 g). The mixture was stirred vigorously for 2.5 h, which accomplished 40% conversion for alcohol (-) (1*R,*2*R*)-**2a**. The enzyme was separated by filtration and the filtrate was extracted into DCM. The solvent was evaporated and the column chromatographic separation of the residue afforded chirally pure alcohol (1*R.*2*R*)-**2a** and the optically enriched butyrate (1*S,*2*S*)-**3**. The later was again subjected to enzyme hydrolysis as described to yield the optically pure butyrate (1*S,*2*S*)-**3a** after purification. From this the alcohol (1*S,*2*S*)-**2b** was obtained by methanolysis with catalytic amount of NaOMe in MeOH in 35% overall yield. The enantiomeric purity was confirmed by comparison with known values of the optical rotations of alcohols (1*R,*2*R*)-**2a** and (1*S,*2*S*)-**2b** from literature [for alcohol (*1R,2R*)- **2a;** $[\propto]_D^{20}$ **=** - 69.33° (lit[8].- 66.9°, c. 1.5, CH_2Cl_2); alcohol (1*S,*2*S*)-**2b;** $[\propto]_D^{20}$ **=** + 68.7° (lit.[8] + 66.3.°, c. 1.6, CH_2Cl_2)].

(1*R,*2*R*)–2-(*N-t*-butyloxycarbonylamino)-cyclohexanol [(1*R,*2*R*)- 4]: To a solution of (1*R,*2*R*)-2-azido cyclohexanol (5.6 g, 39.7 mmol) in dry ethyl acetate (10 ml) placed in a hydrogenation flask was added di-*t*-butyl dicarbonate (10.4 g, 47.6 mmol) and Adams catalyst (2 mol%). The mixture was hydrogenated in Parr apparatus (rt, 35-40 psi 3 h). The catalyst was filtered, solvent in filtrate was evaporated under reduced pressure and the residue was purified by column chromatography (EtOAc/Petroleum ether) to afford a white solid of the alcohol (1*R,*2*R*)

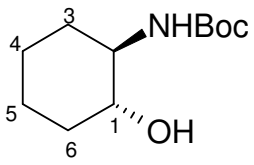

(1R,2R)-**4**

4. Yield (7.9g, 92.6%); m.p. 111°C; $[\alpha]_D^{20}$ +5.0° (*c* 0.6, CH_2Cl_2); ^{1}H-NMR ($CHCl_3$-*d*, 500 MHz); δ_H 1.04- 1.34 (m, 4H, 4-CH_2, 5-CH_2), 1.42 (s, 9H, *t*-Boc), 1.61- 1.73 (m, 2H, 3-CH_2), 1.89- 2.06 (m, 2H, 6-CH_2) 3.2- 3.36 (m, 2H, 1-CH, 2-CH) 2.8-3.5 (bd, 1H, -OH), 4.0-5.0 (bd, 1H, carbamate NH); ^{13}C-NMR ($CHCl_3$-*d*, 500 MHz): δ_C 23.9 (C-4), 24.6 (C-5), 28.3 (*t*Boc), 31.7 (C-3), 34.0 (C-6), 56.5 (C-2), 75.2 (C-1), 79. (*t*Boc), 160.0 (Carbamate C=O); Anal Calcd (%) for $C_{11}H_{21}NO_3$: C, 61.39; H, 9.76; N, 6.51; Found C, 61.17; H, 9.71; N, 6.33; MS (FAB^+): 216 [M+1] (50%), 116 (30%) [M+1- Boc].

(1*S*,2*S*)–2-(*N*-*t*-butyloxycarbonylamino)-cyclohexanol [(1*S*,2*S*)- 4]:This compound is prepared from the azido alcohol (*1S,2S*)-**2b** using the similar procedure as the one described for the alcohol (1*R*,2*R*)-**4**. m.p. 111°C, $[\alpha]_D^{20}$ -6.6° (*c* 0.6, CH_2Cl_2). ^{1}H-NMR ($CHCl_3$-*d*, 500 MHz); δ_H 1.04- 1.34 (m, 4H, 4-CH_2, 5-CH_2), 1.42 (s, 9H, *t*-Boc), 1.61- 1.73 (m, 2H, 3-CH_2), 1.89- 2.06 (m, 2H, 6-CH_2) 3.2- 3.36 (m, 2H, 1-CH, 2-CH) 2.8-3.5 (bd, 1H, -OH), 4.0-5.0 (bd, 1H, carbamate NH); ^{13}C-NMR ($CHCl_3$-*d*, 500 MHz): δ_C 23.9 (C-4), 24.6 (C-5), 28.3 (*t*Boc), 31.7 (C-3), 34.0 (C-6), 56.5 (C-2), 75.2 (C-1), 79.9 (*t*Boc), 160.0 (Carbamate C=O); Anal Calcd (%) for $C_{11}H_{21}NO_3$: C, 61.39; H, 9.76; N, 6.51; Found C, 61.56; H, 10.01; N, 6.40; MS (FAB^+): 216 [M+1] (50%), 116 (30%) [M+1- Boc].

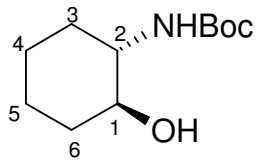

(*1S,2S*)-**4**

(1*R*,2*R*)-2-(*N*-*t*-butyloxycarbonylamino)-cyclohexan-1-methyl sulfonate [(1*R*,2*R*)-5]: To a stirred solution of alcohol (1*R*,2*R*)-**4** (6.0 g, 27.9 mmol) and DMAP (0.05 g) in dry pyridine (100 ml) at 0°C under nitrogen was added methanesulfonyl chloride (4.16 g, 36.3 mmol) over a period of 20 min. The mixture was stirred for 1 h and then refrigerated overnight. Pyridine was evaporated under reduced

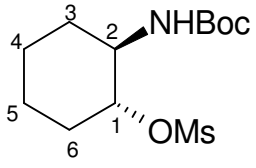

(*1R,2R*)-**5**

pressure and the residue was purified by column chromatography (EtOAc/Pet. ether) affording mesylate (1*R,*2*R*)-**5** as a white crystalline solid. Yield (8.0g, 97.9%); m.p. 121°C; $[\alpha]_D^{20}$ – 10.67° (*c* 1.5, CH_2Cl_2): ^{1}H-NMR ($CHCl_3$-*d*, 500 MHz); δ_H 1.15-1.34 (m, 3H, 4-CH_2, 3-CH), 1.41 (s, 9H, *t*Boc), 1.52-1.86 (m, 3H, 5-CH_2, 6-CH), 1.92-2.09 (m, 1H, 6-CH'), 2.1-2.2 (m, 1H, 3-CH'), 3.0 (s, 3H, mesyl-CH_3), 3.45-3.65 (bd, 1H, 2-CH), 4.3-4.5 (bd, 1H, 1-CH), 4.6-4.8 (bd, 1H, Carbamate NH); ^{13}C-NMR ($CHCl_3$-*d*, 500 MHz): δ_C 23.5 (C-4), 23.7 (C-5), 28.2 (*t*Boc), 31.6 (C-3), 32.0 (C-6), 38.3 (mesly-CH_3), 51.8 (C-2), 79.3 (*t*Boc), 82.4 (C-1), 155.2 (carbamate C=O): Anal Calcd (%) for $C_{12}H_{23}NO_5S$: C, 49.0; H, 7.80; N, 4.77; S, 10.92; Found C, 49.30; H, 7.86; N, 4.50; S, 10.55; MS (FAB$^+$): 294 [M+1] (5%), 194 (85%) [M+1-Boc].

(1*S,*2*S*)-2-(*N-t*-butyloxycarbonylamino)-cyclohexan-1-methyl sulfonate [(1*S,*2*S*)-5]: The compound (1*S,*2*S*)-**5** prepared from the alcohol (1*S,*2*S*)-**4** using the similar procedure as the one described for the mesylate (1*R,*2*R*)-**5**. m.p.121°C, $[\alpha]_D^{20}$ +

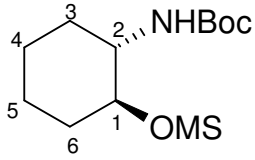

(*1S,2S*)-**5**

13.33° (*c* 1.5, CH_2Cl_2). ^{1}H-NMR ($CHCl_3$-*d*, 500 MHz); δ_H 1.15-1.34 (m, 3H, 4-CH_2, 3-CH), 1.41 (9H, s, *t*Boc), 1.52-1.86 (m, 3H, 5-CH_2, 6-CH), 1.92-2.09 (m, 1H, 6-CH'), 2.1-2.2 (m, 1H, 3-CH'), 3.0 (s, 3H, mesyl-CH_3), 3.45-3.65 (bd, 1H, 2-CH), 4.3-4.5 (bd, 1H, 1-CH), 4.6-4.8 (bd, 1H, Carbamate NH); ^{13}C-NMR ($CHCl_3$-*d*, 500 MHz): δ_C 23.5 (C-4), 23.7 (C-5), 28.2 (*t*Boc), 31.6 (C-3), 32.0 (C-6), 38.3 (mesly-CH_3), 51.8 (C-2), 79.3 (*t*Boc), 82.4 (C-1), 155.2 (carbamate C=O): Anal Calcd (%) for $C_{12}H_{23}NO_5S$: C, 49.0; H, 7.80; N, 4.77; S, 10.92; Found C, 49.21; H, 7.81; N, 4.56; S, 10.67; MS (FAB$^+$): 294 [M+1] (5%), 194 (85%) [M+1-Boc].

(1*S,*2*R*)-2-(*N-t*-butyloxycarbonylamino)-1-azidocyclohexane [(1*S,*2*R*)-6]: A stirred mixture of the mesylate (1*R,*2*R*)-**5** (8.0 g, 33.33 mmol) and NaN_3 (17.3 g, 0.26

mol) in DMF (80 ml) under nitrogen was heated at 65-70°C for 12 h. After cooling, the

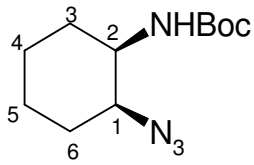

(*1S,2R*)-**6**

solvent was evaporated under reduced pressure and the residue was purified by column chromatography (EtOAc/Pet ether) to afford a white solid of azide (1*S,*2*R*)-**6**. Yield (5.7g, 87%): m.p. 69-70°C; IR, ν (cm^{-1}) (KBr); 3359, 2954, 2104, 1720, 1681, 1367, 1319 and 1166 cm^{-1}: $[\alpha]_D^{20}$ + 102° (*c* 1.5, CH_2Cl_2); ^{1}H-NMR ($CHCl_3$-*d*, 500 MHz); δ_H 1.21-1.35 (m, 1H, 5-CH'), 1.35-1.51 (12H, *t*Boc, 3-CH_2, 6-CH), 1.52-1.64 (m, 2H, 4-CH_2), 1.65-1.77 (m, 1H, 6-CH'), 1.89-2.01 (m, 1H, 3-CH'), 3.5-3.65 (bd, 1H, 1-CH), 3.8-4.0 (bd, 1H, 2-CH), 4.56-4.8 (bd, 1H, carbamate NH): ^{13}C-NMR ($CHCl_3$-*d*, 500 MHz): δ_C 19.6 (C-5), 24.2 (C-4) 27.5 (C-6), 28.2 (*t*Boc), 28.6 (C-3), 51.0 (C-1), 61.5 (C-2), 79.4 (*t*Boc), 154.9 (carbamate C=O): Anal Calcd (%) for $C_{11}H_{20}N_4O_2$: C, 55.00; H, 8.33; N, 23.33; Found C, 55.18; H, 8.00; N, 23.14;MS (FAB+) 241 (35%), [M+1], 141 (15%) [M+1-Boc].

(1*R,*2*S*)-2-(*N-t*-butyloxycarbonylamino)-1-azidocyclohexane [(1*R,*2*S*)-6]: The similar procedure as the one described for (1*S,*2*R*)-**6** was used to prepare (*1R,2S*)-**6** from (1*S,*2*S*)-**5.** m.p. 69-70°C; IR, ν (cm^{-1}) (KBr); 3359, 2954, 2104, 1720, 1681, 1367, 1319 and 1166 cm^{-1}: $[\alpha]_D^{20}$ -105.33° (*c* 1.5, CH_2Cl_2); ^{1}H-NMR ($CHCl_3$-*d*, 500 MHz); δ_H 1.21-1.35 (m, 1H, 5-CH'), 1.35-1.51 (12H, *t*Boc, 3-CH_2, 6-CH), 1.52-1.64 (m, 2H, 4-CH_2), 1.65-1.77 (m, 1H, 6-CH'), 1.89-2.01 (m, 1H, 3-CH'), 3.5-3.65 (bd, 1H, 1-CH), 3.8-4.0 (bd, 1H, 2-CH), 4.56-4.8 (bd, 1H, carbamate NH): ^{13}C-NMR ($CHCl_3$-*d*, 500 MHz): δ_C 19.6 (C-5), 24.2 (C-4) 27.5 (C-6), 28.2 (*t*Boc), 28.6 (C-3), 51.0 (C-1), 61.5 (C-2), 79.4 (*t*Boc), 154.9 (carbamate C=O): Anal Calcd (%) for

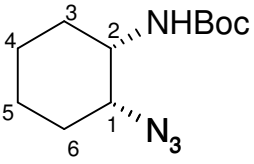

(*1R,2S*)-**6**

$C_{11}H_{20}N_4O_2$: C, 55.00; H, 8.33; N, 23.33; Found C, 55.11; H, 8.07; N, 23.21; MS (FAB+) 241 (35%) [M+1], 141 (15%) [M+1-Boc].

(1*S*,2*R*)-2-(*N*-t-butyloxycarbonylamino)-1-aminocyclohexane [(1*S*,2*R*)-7]: To a solution of the azide (1*S*,2*R*)-**6** (4.0 g, 16.7 mmol) in Methanol (5 ml) taken in hydrogenation flask was added Adam's catalyst (2 mol%). The reaction mixture was hydrogenated in a Parr apparatus for 3 h at rt and H_2 of pressure 35-40 psi. The catalyst was filtered off and then solvent was removed under reduced pressure to yield a residue of the amine (1*S*,2*R*)-**7** as a colorless oil. Yield (3.45g, 96.9%); This compound was used for the further reaction without any purification.

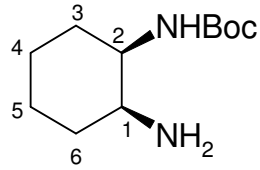

(1*S*,2*R*)-**7**

(1*R*,2*S*)-2-(*N*-t-butyloxycarbonylamino)-1-aminocyclohexane [(1*R*,2*S*)-7]: The amine (1*R*,2*S*)-**7** was obtained on hydrogenation of the azide (*1R,2S*)-**6** following the procedure as the one described for the synthesis of the amine (1*S*,2*R*)-**7**.

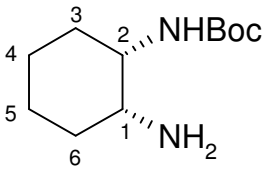

(1*R*,2*S*)-**7**

***N*-[(2*R*)-*t*Boc-aminocyclohex-(1*S*)-yl]-glycine ethyl ester [(1*S*,2*R*)]-8:** To a stirred mixture of amine (1*S*,2*R*)-**7** (3.4 g, 15.9 mmol), and freshly prepare KF-celite (5.52 g, 47.66 mmol) in dry acetonitrile (150 ml), ethyl bromoacetate (2.38 g, 14.3 mmol) was added dropwise for 30 min. at rt under nitrogen atmosphere. After 3.5 h the celite was filtered off and the solvent in the filtrate was evaporated under reduced pressure which on column chromatographic purification (EtOAc) afforded the ethyl ester (1*S*,2*R*)-**8** as colorless oil. Yield (3.63g, 76.6%): $[\alpha]_D^{20}$ -

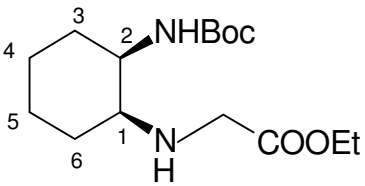

(1*S*,2*R*)-**8**

9.15° (*c* 1.42, CH_2Cl_2); ^{1}H-NMR ($CHCl_3$-*d*, 200 MHz); δ_H 1.24 (*t*, 3H, ester-CH_3), 1.41 (*t*Boc), 1.6-1.85 (m, 2H, 4-CH_2), 2.0-2.35 (m, 2H, 5-CH_2), 2.35-2.7 (m, 3H, 6-CH_2, 3-CH), 2.75-3.52 (m, 5H, 1-CH, 2-CH, 3-CH', N-CH_2), 3.67 (bd, 1H, NH), 4.0-4.5 (m, 2H, ester CH_2), 4.9-5.75 (bd, 1H, carbamate NH); ^{13}C-NMR ($CHCl_3$-*d*, 200 MHz): δ_C 13.9 (ester CH_3), 28.1 (*t*Boc), 33.7 (C-4), 37.7 (C-5), 40.7 (C-6), 49.1 (C-3), 60.2 (N-CH_2), 61.3 (C-2), 61.6 (ester-CH_2), 69.2 (C-1), 78.7 (*t*Boc), 156.3 (carbamate C=O), 172.4 (ester C=O); MS (FAB^+); 301 [M+1] (100%), 201 (12%) [M+1-Boc].

***N*-[(2*S*)-*t*Boc-aminocyclohex-(1*R*)-yl]-glycine ethyl ester [(1*R*,2*S*)]-8:** A similar procedure as the one described for the ethyl ester (1*S*,2*R*)-**8** afforded (1*R*,2*S*)-**8** starting

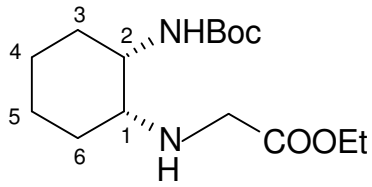

(1*R*,2*S*)-**8**

from the amine (1*R*,2*S*)-**7.** $[\alpha]_D^{20}$ + 10.56° (*c* 1.42, CH_2Cl_2); ^{1}H-NMR ($CHCl_3$-*d*, 200 MHz); δ_H 1.24 (*t*, 3H, ester-CH_3), 1.41 (*t*Boc), 1.6-1.85 (m, 2H, 4-CH_2), 2.0-2.35 (m, 2H, 5-CH_2), 2.35-2.7 (m, 3H, 6-CH_2, 3-CH), 2.75-3.52 (m, 5H, 1-CH, 2-CH, 3-CH', N-CH_2), 3.67 (bd, 1H, NH), 4.0-4.5 (m, 2H, ester CH_2), 4.9-5.75 (bd, 1H, carbamate NH); ^{13}C-NMR ($CHCl_3$-*d*, 200 MHz): δ_C 13.9 (ester CH_3), 28.1 (*t*Boc), 33.7 (C-4), 37.7 (C-5), 40.7 (C-6), 49.1 (C-3), 60.2 (N-CH_2), 61.3 (C-2), 61.6 (ester-CH_2), 69.2 (C-1), 78.7 (*t*Boc), 156.3 (carbamate C=O), 172.4 (ester C=O); MS (FAB^+); 301 [M+1] (100%), 201 (12%) [M+1-Boc].

***N*-[(2*R*)-*t*Boc-aminocyclohexan-(1*S*)-yl]-*N*-(chloroacetyl)-glycine ethyl ester [(1*S*,2*R*)-9**: To a stirred solution of the amine (1*R*,2*S*)-8 (3.6 g, 12 mmol) in 10% Na_2CO_3 (90 ml) and 1,4-dioxan (90 ml) cooled to 0°C, was added chloroacetyl chloride (6.78 g, 60 mmol) in two additions. After 30 min the dioxan was removed under reduced pressure and the residue was extracted into EtOAc (2 x 100 ml), dried over Na_2SO_4. The solvent was evaporated under reduced pressure and the residue was purified by column

chromatography (MeOH/ CH_2Cl_2) affording chloro compound (1*S,*2*R*)-**9** as white solid.

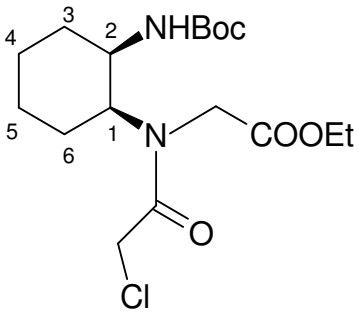

(*1S,2R*)-**9**

Yield (3.3g, 73%); m.p. 65-68°C. $[\alpha]_D^{20}$ - 89.54° (*c* 2.2, CH_2Cl_2); ^{1}H-NMR ($CHCl_3$-*d*, 200 MHz); δ_H 1.0-2.0 (m, 20H, $4CH_2$ cycl, 9H- *t*Boc, 3H- ester CH_3), 3.65-4.5 (m, 8H, 1-CH, 2-CH, N-CH_2, -$COCH_2Cl$, -$COOCH_2$), 4.7-5.2 (bd, 1H, carbamate NH); ^{13}C-NMR ($CHCl_3$-*d*, 200 MHz): δ_C 13.9 (ester CH_3), 19.8 (C-4), 23.7 (C-5), 25.2 (C-3), 28.2 (*t*Boc), 30.9 (C-6), 41.4 (-CH_2Cl), 45.8 (N-CH_2), 49.0 (C-2), 57.0 (C-1), 61.0 (ester CH_2), 79.5 (*t*Boc), 155.5 (carbamate C=O), 167.0 (acyl C=O), 169.0 (ester C=O); MS LCMS; 377 [M+1], 277 [M+1-Boc].

***N*-[(2*S*)-*t*Boc-aminocyclohexan-(1*R*)-yl]-*N*-(chloroacetyl)-glycine ethyl ester [(1*R,*2*S*)-9:** This compound was prepared from the amine (1*R,*2*S*)-**8** following the procedure described for the chloro compound (1*S,*2*R*)-**9**. m.p. 65-68°C; $[\alpha]_D^{20}$ + 91.36° (*c* 2.2, CH_2Cl_2); ^{1}H-NMR ($CHCl_3$-*d*, 200 MHz); δ_H 1.0-2.0 (m, 20H, $4CH_2$ cycl, 9H-

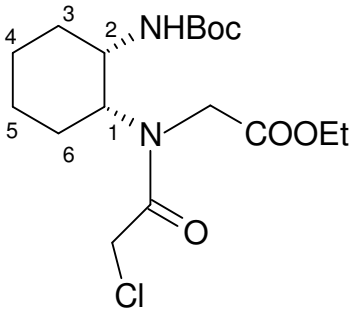

(*1R,2S*)-**9**

*t*Boc, 3H- ester CH_3), 3.65-4.5 (m, 8H, 1-CH, 2-CH, N-CH_2, -$COCH_2Cl$, -$COOCH_2$), 4.7-5.2 (bd, 1H, carbamate NH); ^{13}C-NMR ($CHCl_3$-*d*, 200 MHz): δ_C 13.9 (ester CH_3), 19.8 (C-4), 23.7 (C-5), 25.2 (C-3), 28.2 (*t*Boc), 30.9 (C-6), 41.4 (-CH_2Cl), 45.8 (N-CH_2), 49.0 (C-2), 57.0 (C-1), 61.0 (ester CH_2), 79.5 (*t*Boc), 155.5 (carbamate C=O), 167.0 (acyl C=O), 169.0 (ester C=O); MS LCMS; 377 [M+1], 277 [M+1-*t*Boc].

***N*-[(2*R*)-*t*-Boc-Aminocyclohex-(1*S*)-yl]-*N*-(thymin-1-acetyl)-glycine ethyl ester [(1*S*,2*R*)-10a]:** A mixture of chloro- compound (1*S*,2*R*)-**9** (1.5 g, 4.0 mmol), thymine (0.55 g, 4.38 mmol) and anhydrous K_2CO_3 (0.66 g, 4.8 mmol) in dry DMF (10 ml) under nitrogen was heated with stirring at 65°C for 3.5 h. After cooling, the solvent was removed under reduced pressure to leave a residue, which was extracted into DCM (2x 25 ml) and dried over Na_2SO_4. The solvent evaporated and the crude compound was purified by column chromatography (MeOH/DCM) to afford a White solid of thymine monomer ethyl ester (1*S*,2*R*)-**10a**. Yield (1.3g, 70.2%): m.p. 115-119°C. $[\alpha]_D^{20}$ - 85.33° (*c* 1.5, CH_2Cl_2); ^{1}H-NMR ($CHCl_3$-*d*, 500 MHz); δ_H 1.17-1.8 (17H, *t*Boc, $4CH_2$), 1.82 (s, 3H, thymine CH_3), 3.5-5.0 (8H, 1-CH, 2-CH, N-CH_2, -$COCH_2$, -$COOCH_2$), 5.0-5.5 (bd, 1H, carbamate), 7.1 (s, 1H, thymine –CH=C-), 8.3-8.5 (bd, 1H, thymine NH); ^{13}C-NMR ($CHCl_3$-*d*, 500 MHz): δ_C 12.0 (thymine-CH_3), 14.1 (ester CH_3), 19.8 (C-4), 23.5 (C-5), 25.0 (C-3), 28.1 (*t*Boc), 30.1 (C-6), 36.6 (-CH_2-thymine), 45.3 (N-CH_2), 47.5 (C-2), 55.6 (C-1), 61.0 (ester CH_2),79.4 (*t*Boc), 111.0 (thymine C), 141.1 (thymine –CH), 151.0 (thymine C=O), 155.5 (carbamate C=O), 164.4 (thymine C=O), 167.4 (N-C=O), 169.3 (ester C=O): Anal Calcd (%) for $C_{22}H_{34}N_4O_7$: C, 56.65; H, 7.29; N, 12.01; Found C, 56.81; H, 7.31; N, 11.97; MS (FAB^+); 467 [M+1] (10%), 367 (100%) [M+1-*t*Boc].

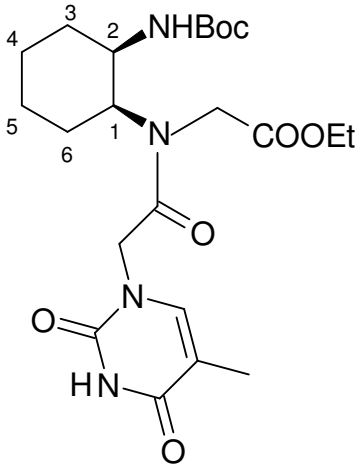

(*1S,2R*)-**10a**

***N*-[(2*S*)-*t*-Boc-Aminocyclohex-(1*R*)-yl]-*N*-(thymin-1-acetyl)-glycine ethyl ester [(1*R*,2*S*)-10b]:** A similar procedure as the one described for the monomer (1*S*,2*R*)-**10a** afforded (1*R*,2*S*)-**10b** from (1*R*,2*S*)-**9**. m.p.115-119°C. $[\alpha]_D^{20}$ + 86.67° (*c* 1.5, CH_2Cl_2): -

^{1}H-NMR ($CHCl_3$-*d*, 500 MHz); δ_H 1.17-1.8 (17H, *t*Boc, $4CH_2$), 1.82 (s, 3H, thymine CH_3), 3.5-5.0 (8H, 1-CH, 2-CH, N-CH_2, -$COCH_2$, -$COOCH_2$), 5.0-5.5 (bd, 1H, carbamate NH), 7.1 (s, 1H, thymine –CH=C-), 8.5-8.5 (bd, 1H, thymine NH); ^{13}C-NMR ($CHCl_3$-*d*, 500 MHz): δ_C 12.0 (thymine-CH_3), 14.1 (ester CH_3), 19.8 (C-4), 23.5 (C-5), 25.0 (C-3), 28.1 (*t*Boc), 30.1 (C-6), 36.6 (-CH_2-thymine), 45.3 (N-CH_2), 47.5 (C-2), 55.6 (C-1), 61.0 (ester CH_2),79.4 (*t*Boc), 111.0 (thymine –C), 141.1 (thymine CH), 151.0 (thymine C=O), 155.5 (carbamate C=O), 164.4 (thymine C=O), 167.4 (N-C=O), 169.3 (ester C=O):Anal Calcd (%) for $C_{22}H_{34}N_4O_7$: C, 56.60; H, 7.22; N, 12.23; Found C, 56.81; H, 7.31; N, 11.97; MS (FAB^+); 467 [M+1] (10%), 367 (100%) [M+1-*t*Boc].

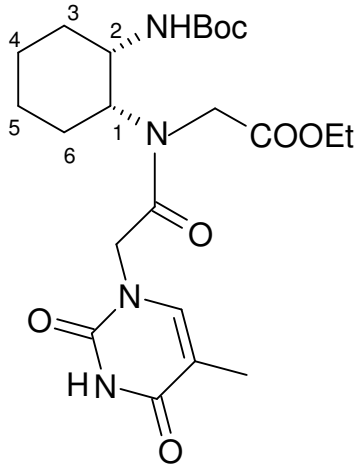

(*1R,2S*)-**10b**

***N*-[(2*R*)-*t*-Boc-Aminocyclohex-(1*S*)-yl]-*N*-(thymin-1-acetyl)-glycine [(1*S*,2*R*)-11a]:** To the monomer ester (1*S*,2*R*)-**10a** (1.0 g, 2.283 mmol) suspended in THF (10 ml), a solution of 0.5 M LiOH (10ml, 5.1 mmol) was added and mixture was stirred for 30 mins. The mixture was washed with EtOAc (2 X 10 ml). The aqueous layer was acidified to pH 3 and extracted with EtOAc (3 X 50 ml). The EtOAc layer was dried over sodium sulfate and evaporated under reduced pressure to afford monomer (1*S*,2*R*)-**11a** as a white solid. Yield: 0.92 g (97.8 %). m.p. 172-177°C; $[\alpha]_D^{20}$ -107° (*c* 1.06, CH_2Cl_2): ^{1}H-NMR ($CHCl_3$-*d*, 200 MHz); δ_H 0.5-1.8 (m, 17H, *t*-Boc, $4CH_2$), 1.88 (s, 3H, thymine CH_3), 3.3-5.5 (m, 7H, N-CH_2, acyl CH_2, 1-CH, 2-CH,

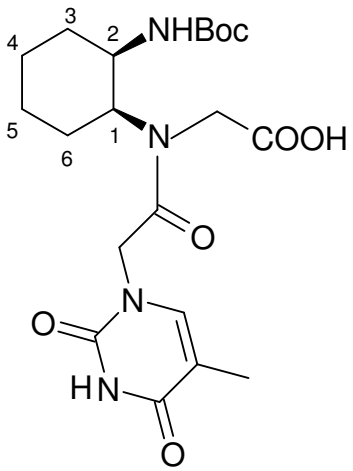

(*1S,2R*)-**11a**

carbamate NH), 7.18 (s, 1H, thymine-H), 10.0-11.0 (bd, 2H, thymine NH and -COOH); ^{13}C-NMR (DMSO-d_6, 200 MHz): δ_C 12.2 (thymin-CH_3), 19.7 (C-4), 23.1 (C-5), 25.5 (C-3), 28.6 (*t*-Boc), 31.0 (C-6), 40.3 (C-1), 47.7 (*N*-CH2, $\underline{CH_2}$-CO), 55.7 (C-1), 78.1 (*t*-Boc), 108.5 (thymine-C , 142.3 (thymine CH), 151.4 (thymine C=O), 156.1 (carbamate C=O), 164.7 (Thymine C=O), 167.7 (N-C=O), 174.0 (-COOH) : Anal Calcd (%) for $C_{20}H_{30}N_4O_7$: C, 54.78; H, 6.84; N, 12.77; Found C, 54.61; H, 7.01; N, 12.61; MS (FAB$^+$); 439 [M+1] (6 %), 339 (100%) [M+1-*t*Boc].

***N*-[(2*S*)-*t*-Boc-Aminocyclohex-(1*R*)-yl]-*N*-(thymin-1-acetyl)-glycine [(1*R*,2*S*)-11b]:** To the monomer ester (1*R*,2*S*)-**10b** (1.0 g, 2.283 mmol) suspended in THF (10 ml), a solution of 0.5 M LiOH (10ml, 5.1 mmol) was added and mixture was stirred for 30 mins. The mixture was washed with EtOAc (2 X 10 ml). The aqueous layer was acidified to pH 3 and extracted with EtOAc (3 X 50 ml). The EtOAc layer was dried over sodium sulfate and evaporated under reduced pressure to afford monomer (1*R*,2*S*)-**11a** as a white solid. Yield: 0.92 g (97.8 %). m.p. 172-177°C; $[\alpha]_D^{20}$ +110° (*c* 1.06, CH_2Cl_2): ^{1}H-NMR ($CHCl_3$-*d*, 200 MHz); δ_H 0.5-1.8 (m, 17H, *t*-Boc, 4CH_2), 1.88 (s, 3H, thymine CH_3), 3.3-5.5 (m, 7H, N-CH_2, acyl CH_2, 1-CH, 2-CH, carbamate NH), 7.18 (s, 1H, thymine-H), 10.0-11.0 (2H, bd, thymine NH and -COOH); ^{13}C-NMR (DMSO-d_6, 200 MHz): δ_C 12.2 (thymin-CH_3), 19.7 (C-4), 23.1 (C-5), 25.5 (C-3), 28.6 (*t*-Boc), 31.0 (C-6), 40.3 (C-1), 47.7 (*N*-CH2, $\underline{CH_2}$-CO), 55.7 (C-1), 78.1 (*t*-Boc), 108.5 (thymine-C , 142.3 (thymine CH), 151.4 (thymine C=O), 156.1 (carbamate C=O), 164.7 (Thymine C=O), 167.7 (N-C=O), 174.0 (-COOH) : Anal Calcd (%) for $C_{20}H_{30}N_4O_7$: C, 54.78; H,

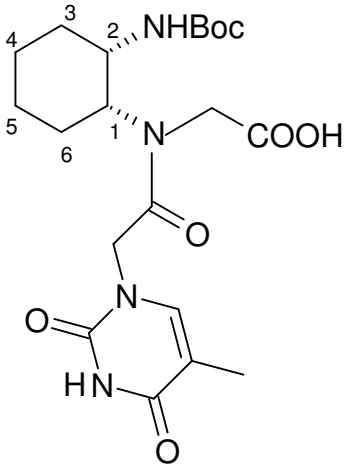

(*1R,2S*)-**11b**

6.84; N, 12.77; Found C, 54.67; H, 7.13; N, 12.8; MS (FAB^+); 439 [M+1] (6 %), 339 (100%) [M+1-Boc].

***N*1-(*t*-Boc)-1,2-diaminoethane (13)**: 1,2-diaminoethane (20 g, 0.33 mol) was taken in dioxane: water (1:1, 500 ml) and cooled in an ice-bath. Boc-azide (5 g, 35 mmol) in dioxane (50 ml) was slowly added with stirring and the pH was maintained at 10.0 by continuous addition of 4N NaOH. The mixture was stirred for 8 h and the resulting solution was concentrated to 100 ml. The *N*1, *N*2-di-Boc derivative not being soluble in water, precipitated, and it was removed by filtration. The corresponding *N*1-mono-Boc derivative was obtained by repeated extraction from the filtrate in ethyl acetate. Removal of solvents yielded the mono-Boc-diaminoethane **13** (3.45 g, 63%, Rf = 0.25, DCM: MeOH; 9:1). ^{1}H NMR ($CDCl_3$) δ_H: 5.21 (br s, 1H, NH), 3.32 (t, 2H, *J*=8 Hz), 2.54 (t, 2H, *J*=8 Hz), 1.42 (s, 9H).

Ethyl *N*-(2-Boc-aminoethyl)-glycinate (14): The *N*1-(Boc)-1,2-diaminoethane **13** (3.2 g, 20 mmol) was treated with ethylbromoacetate (2.25 ml, 20 mmol) in acetonitrile (100 ml) in the presence of K_2CO_3 (2.4 g, 20 mmol) and the mixture was stirred at ambient temperature for 5 h. The solid that separated was removed by filtration and the filtrate was evaporated to obtain the ethyl *N*-(2-Boc-aminoethyl)-glycinate **14** (4.3 g, Yield, 83%; Rf = 0.3, EtOAc) as a colourless oil. ^{1}H NMR ($CDCl_3$) δ_H: 5.02 (br s, 1H, NH), 4.22 (q, 2H, *J*=8Hz), 3.35 (s, 2H), 3.20 (t, 2H, *J*=6Hz), 2.76 (t, 2H, *J*=6Hz), 1.46 (s, 9H), 1.28 (t, 3H, *J*=8Hz).

Ethyl *N*-(Boc-aminoethyl)-*N*-(chloroacetyl)-glycinate (15): The ethyl *N*-(2-Boc-aminoethyl)-glycinate 14 (4.0 g, 14 mmol) was taken in 10% aqueous Na_2CO_3 (75 ml) and dioxane (60 ml). Chloroacetyl chloride (6.5 ml, 0.75 mmol) was added in two portions with vigorous stirring. The reaction was complete within 5 min. The reaction

mixture was brought to pH 8.0 by addition of 10% aqueous Na_2CO_3 and concentrated to remove the dioxane. The product was extracted from the aqueous layer with dichloromethane and was purified by column chromatography to obtain the ethyl *N*-(Boc-aminoethyl)-*N*-(chloroacetyl)-glycinate **15** as a colourless oil in good yield (4.2 g, Yield, 80%; Rf = 0.3, EtOAc:petroleum ether; 2:8). ^{1}H NMR ($CDCl_3$) δ_H: 5.45 (br s, 1H), 4.1-4.9 (S, 2H), 4.00 (s, 2H), 3.53 (t, 2H), 3.28 (q, 2H), 1.46 (s, 9H), 1.23 (t, 3H, *J*=8Hz).

***N*-(Boc-aminoethylglycyl)-thymine ethyl ester (16)**: Ethyl *N*-(Boc-aminoethyl)-*N*-(chloroacetyl)-glycinate **15** (1.0 g, 3.1mmol) was stirred with anhydrous K_2CO_3 (0.47 g, 3.4 mmol) in DMF with thymine (0.41 g, 3.25 mmol) to obtain the desired compound **16** in good yield. DMF was removed under reduced pressure and the oil obtained was purified by column chromatography to afford **16**. (1 g, Yield 83%; Rf = 0.2, MeOH:DCM; 5:95). ^{1}H NMR ($CDCl_3$) δ_H: 9.00 (br s, 1H, T-NH), 7.05 (min) & 6.98 (maj) (s, 1H, T-H6), 5.65 (maj) & 5.05 (min) (br s, 1H, NH), 4.58 (maj) & 4.44 (min) (s, 1H, T-CH_2), 4.25 (m, 2H, OCH_2), 3.55 (m, 2H), 3.36 (m, 2H), 1.95 (s, 3H, T-CH_3), 1.48 (s, 9H), 1.28 (m, 3H); ^{13}C NMR ($CDCl_3$) δ_C: 170.8, 169.3, 167.4, 164.3, 156.2, 151.2, 141.1, 110.2, 79.3, 61.8, 61.2, 48.5, 48.1, 47.7, 38.4, 28.1, 13.8, 12.2.

***N*^{4}-Benzyloxycarbonyl cytosine (17)**: Over a period of about 15 min, 50% solution of bezyloxycarbonyl chloride in toluene (12.3 ml, 36 mmol) was added dropwise to suspension of cytosine (2 g, 18 mmol) in dry pyridine (100 ml) at 0^{o}C under anhydrous conditions. The solution then was stirred vigorously for 20 h, after which the pyridine suspension was evaporated to dryness, under vacuum. To the residue, an ice cold water (20 ml) followed acidification by adding 2 N HCl to reach pH ~2.0. The resulting white precipitate was filtered off, washed with water and partially dried by air section. The still-wet precipitate was boiled with absolute ethanol (50 ml) for 10 min, cooled to 0^{o}C,

filtered, washed thoroughly with ether and vacuum dried to obtain 17 (2.9 g, yield 65%, Rf = 0.3, MeOH:DCM 1:9), mp = 256.0 ^{o}C. ^{1}H NMR (DMSO-d_6): δ_H, 7.71-7.67 (d, 1H, *J* = 7.32 Hz, C6H-Cyt), 7.28 (s, 5H, C_6H_5, Cbz), 6.84-6.6 (d 1H, *J* = 7.32, C5H-Cyt), 5.02 (s, 2H, OCH_3).

***N*-(Boc-aminoethylglycyl)-(*N*4-benzyloxycarbonyl cytosine)ethyl ester (18)**: A mixture of NaH (0.25 g, 6.2 mmol) and N4-benzyloxycarbonyl cytosine **17** (1.24 g, 6.2 mmol) was taken in DMF and stirred at 75^{o}C till the effervescence ceased. The mixture was cooled and ethyl *N*-(Boc-aminoethyl)-*N*-(chloroacetyl)-glycinate **15** (2.0 g, 6.2 mmol) was added. Stirring was then continued at 75^{o}C to obtain the cytosine monomer, *N*-(Boc-aminoethylglycyl)-(*N*4-benzyloxycarbonyl cytosine)ethyl ester **18**, in moderate yield (1.75 g, 69%;). ^{1}H NMR ($CDCl_3$) δ_H: 7.65 (d, 1H, C-H6, J=8Hz), 7.35 (s, 5H, Ar), 7.25 (d, 1H, C-H5, *J*=8Hz), 5.70 (br s, 1H, NH), 5.20 (s, 2H, Ar-CH2), 4.71 (maj) & 4.22 (min) (br s, 2H), 4.15 (q, 2H), 4.05 (s, 2H), 3.56 (m, 2H), 3.32 (m, 2H), 1.48 (s, 9H), 1.25 (t, 3H).

***N*-(Boc-aminoethylglycyl)-adenine ethyl ester (19)**: NaH (0.25 g, 6.1 mmol) was taken in DMF (15 ml) and adenine (0.8 g, 6.1 mmol) was added. The mixture was stirred at 75^{o}C till the effervescence ceased and the mixture was cooled before adding ethyl *N*-(Boc-aminoethyl)-*N*-(chloroacetyl)-glycinate **15** (2.0 g, 6.1mmol). The reaction mixture was heated once again to 75^{o}C for 1 h, when TLC analysis indicated the disappearance of the starting ethyl *N*-(Boc-aminoethyl)-*N*-(chloroacetyl)-glycinate. The DMF was removed under vacuum and the resulting thick oil was taken in water and the product, extracted in ethyl acetate. The organic layer was then concentrated to obtain the crude product, which was purified by column chromatography to obtain the pure *N*- (Boc-aminoethylglycyl)-adenine ethyl ester **19**. (Yield 75%; Rf = 0.2, MeOH:DCM; 5:95). ^{1}H

NMR ($CDCl_3$) δ_H: 8.32 (s, 1H), 7.95 (min) & 7.90 (maj) (s, 1H), 5.93 (maj) & 5.80 (min) (br, 2H), 5.13 (maj) & 4.95 (min), 4.22 (min) & 4.05 (maj) (s, 2H), 4.20 (m, 2H), 3.65 (maj) & 3.55 (min) (m, 2H), 3.40 (maj) & 3.50 (min) (m, 2H), 1.42 (s, 9H), 1.25 (m, 3H).

***N*-(Boc-aminoethylglycyl)-2-amino-6-chloropurine ethyl ester (20)**: A mixture of 2-amino-6-chloropurine (1.14 g, 6.8 mmol), K_2CO_3 (0.93 g, 7.0 mmol) and ethyl *N*-(Boc-aminoethyl)-*N*-(chloroacetyl)-glycinate 15 (2.4 g, 7.0 mmol) were taken in dry DMF (20 ml) and stirred at room temperature for 4 h. K_2CO_3 was removed by filtration, and the DMF, by evaporation under reduced pressure. The resulting residue was purified by column chromatography to obtain the *N*-(Boc-aminoethylglycyl)-2-amino-6-chloropurine ethyl ester (**20**) in excellent yield (2.55 g, 90%; Rf = 0.25, MeOH:DCM; 5:95). ^{1}H NMR ($CDCl_3$) δ_H: 7.89 (min) & 7.85 (maj) (s, 1H), 7.30 (s, 1H), 5.80 (br s, 1H, NH), 5.18 (br, 2H), 5.02 (maj) & 4.85 (min) (s, 2H), 4.18 (min) & 4.05 (maj) (s, 2H), 3.65 (maj) & 3.16 (min) (m, 2H), 3.42 (maj) and 3.28 (min) (m, 2H), 1.50 (s, 9H), 1.26 (m, 3H).

Hydrolysis of the ethyl ester functions of PNA monomers (General method): The ethyl esters were hydrolyzed using 2N aqueous NaOH (5ml) in methanol (5ml) and the resulting acid was neutralized with activated Dowex-H^+ till the pH of the solution was 7.0. The resin was removed by filtration and the filtrate was concentrated to obtain the resulting Boc-protected acids (21 - 24) in excellent yield (>85%). In case of cytosine monomer ethyl ester, mild base 0.5 M LiOH was used to avoid deprotection of the exocyclic amine-protecting group by strong bases.

Functionalization and Picric acid estimation of the MBHA [(4-methyl benzhydryl) amine] Resin: The loading value (amine function) 0.85 mmol/g of the MBHA resin (Sigma, 100-200 mesh) was lower to 0.25 mmol/g by capping the excess 0.6

mmol/g of amine functionalities in dry DMF/DCM using acetic anhydride and pyridine as a base. The loading value of 0.25 mmol/g was found to be optimum for the synthesis of oligomers. The MBHA resin with loading value 0.25 mmol/g, was functionalized by coupling di-protected L-lysine carboxylic group (N^{α}–amino group protected with Boc and N^{ω}– amino group by Cl-Cbz) to the free amines on the resin using coupling reagents. Then the final loading value of the so functionalized resin was estimated using picric acid. The procedure for estimation of the loading value of the resin was carried out with 5 mg of the resin and comprised the following steps:

The resin was swollen in dry DCM for at least 30 min. The DCM was drained off and a 50% solution of TFA in DCM was added (1 ml X 3), 10 min each. After washing thoroughly with DCM, the TFA salt was neutralized with a 5% solution of DIPEA in DCM (1 ml X 2, 2 min each). The free amine was treated with a 0.1 M picric acid solution in DCM (2 ml X 2, 3 min each). The excess picric acid was washed away with DCM. The adsorbed picric acid was displaced from the resin by adding a solution of 5% DIEA in DCM. The eluent was collected and the volume was made up to 10 ml with DCM in a standard volumetric flask. The absorbance was recorded at 358 nm in ethanol and the concentration of the amine groups on the resin was calculated using the molar extinction coefficient of picric acid 14,500 cm^{-1} M^{-1} at 358 nm.

Kaiser's Test: Kaiser's test was used to monitor the *t*-Boc-deprtection and amide bond (peptide bond) formation steps in the solid phase peptide synthesis. The Three solutions were used, viz., 1) ninhydrin (5.0 g) dissolved in ethanol (100 ml), 2) Phenol (80.0 g) dissolved in ethanol (20 ml) and 3) KCN; 2 ml of a 0.001 M aqueous solution of KCN in 98 ml pyridine.

To a few beads of the resin to be tested taken in a test tube, were added 3-4 drops of each of the three solutions described above. The tube was heated at 100^{o}C for ~2 min, and the color of the beads was noted. A blue color on the beads, which slowly comes in solution, indicated successful deprotection, while colorless beads and the solution confirmed the completion of the amide coupling reaction. The blank solution should remain yellow.

Synthesis of PNA-oligomers incorporating *cis*-(1*S*,2*R*)- and (1*R*,2*S*)-aminocyclohexyl PNA monomers: The modified PNA monomers were built into PNA oligomers using standard procedure on a L-lysine derivatized (4-methylbenzhydryl) amine (MBHA) resin (initial loading 0.25 meqg^{-1}) with HBTU/HOBt/DIEA in DMF/DMSO as a coupling reagent. The PNA oligomers were cleaved from the resin with TFMSA. The oligomrs were purified by RP HPLC (C18 column) and charecterized by MALDI-TOF mass spectrometry. The overall yields of the raw products were 35-65%. The normal PNAs were prepared similarly as discussed above.

Cleavage of the PNA oligomers from the resin*:* The MBHA resin (20 mg), oligomer attached it was stirred with thioanisole (40 µl) and 1,2-ethanedithiol (32 µl) in an ice bath for ten minutes. TFA (240 µl) was added, and after equilibrium for 10 min, TFMSA (32 µl) was added slowly. The reaction mixture stirred for 2.5 h at room temperature, filtered and concentrated under vacuum. The product was precipitated with dry ether from methanol and the precipitate was dissolved in water (200 µl) and loaded over sephadex G25 column. Fractions of 0.5 ml were collected and the presence of oligomer was detected by measuring the absorbance at 260 nm. The fractions containing oligomer were freeze-dried and the purity of the fractions was assessed by analytical RP-HPLC. If the purity is less than 90%, oligomers were purified by preparative HPLC.

Gel Filtration*:* The crude PNA oligomer obtained after ether precipitation was dissolved in water (~0.5 ml) and loaded on a gel filtration column. This column consisted of G25 Sephadex and had a void volume of 1ml. The oligomer was eluted with water and ten fractions of 1ml volume each were collected. The presence of the PNA oligomer was detected by measuring the absorbance at 260 nm. The fractions containing the oligomer were freeze-dried. The purity of the cleaved crude PNA oligomer was determined by RP HPLC on a C18 column. If the purity of the oligomers found to be above 96%, the oligomers were used as such for experiments without further purification. If the purity was not satisfactory, the oligomers were purified by HPLC.

HPLC (High Performance Liquid Chromatography) purification of PNA-oligomers: Peptide purifications were performed on a waters DELTAPAK-RP semi preparative C18 column attached to a Hewlett Packard 1050 HPLC system equipped with an auto sampler and Jassco-UV970 variable-wavelength detector. An isocratic elution method with 10% CH_3CN in 0.1% TFA/H_2O was used with flow rate 1.5 ml/min. and the eluent was monitored at 260 nm. The purity of the oligomers was further assessed by RP-C18 analytical HPLC column (25x 0.2 cm. 5 μm) with gradient elution: A to 50% B in 30 min, A = 0.1% TFA in H_2O, B = 0.1% TFA in CH_3CN:H_2O 1:1 with flow rate 1 ml/min. The purities of the so purified oligomers were found to be >98%.

MALDI-TOF Mass Spectrometry*:* Literature reports the analysis of PNA purity by MALDI-TOF mass spectrometry in which several matrices have been explored, *viz*. sinapinic acid (3,5-dimethoxy-4-hydroxycinnamic acid), CHCA (α-cyano-4-hydroxycinnamic acid) and DHB (2,5-dihydroxybenzoic acid). Of these, sinapinic acid was found to give the best signal to noise ratio with all the other matrices typically producing higher molecular ion signals. For all the MALDI-TOF spectra recorded for the

PNAs reported in this Chapter, sinapinic acid was used as the matrix and was found to give satisfactory results.

Binding Stoichiometry: Eleven mixtures of PNA:DNA with different ratios to each other such as 0:100, 10:90, 20:80, 30:70, 40:60, 50:50, 60:40, 70:30, 80:20, 90:10 and 100:0; all of the same total strand concentration (2 mM) in sodium phosphate buffer (100 mM NaCl, 0.1 mM EDTA, pH 7.0). The samples are heated to 85°C in water bath for 5 min., allowed to cool to room temperature and then cooled further in a refrigerator overnight. CD spectra for all the samples were recorded at 10°C with wavelength range from 350-190 nm with scan speed 100 nm/min, accumulation-8, response time-4 sec, band width-1 nm and sensitivity-10 mdeg. CD cell for all the studies was of 10 mm path length. Base line was subtracted from all the CD spectra.

UV-*T*m measurements: The concentration was calculated on the basis of absorbance from the molar extinction coefficients of the corresponding nucleobases (i.e., T, 8.8 cm^2/μmol; C, 7.3 cm^2/μmol; G, 11.7 cm^2/μmol and A, 15.4 cm^2/μmol). The complexes were prepared in 10 mM sodium phosphate buffer, pH 7.0 containing NaCl (100 mM) and EDTA (0.1 mM) and were annealed by keeping the samples at 85°C for 5 minutes followed by slow cooling to room temperature (annealing). Absorbance versus temperature profiles were obtained by monitoring at 260 nm with Perkin-Elmer *Lambda 35 UV-VIS* spectrophotometer scanning from 5 to 85/90°C at a ramp rate of 0.2°C per minute. The data were processed using Microcal Origin 5.0 and *T*m values derived from the derivative curves.

Circular Dichroism: CD spectra were recorded on a JASCO J-715 spectropolarimeter. The CD spectra of the PNA:DNA complexes and the relevant single strands were recorded in 10 mM sodium phosphate buffer, 100 mM NaCl, 0.1 mM

EDTA, pH 7.0. The temperature of the circulating water was kept below the melting temperature of the PNA:DNA complexes, i.e., at 10°C. The CD spectra of the homothymine T single strands were recorded as an accumulation of 10 scans from 320 to 195 nm using a 1 cm cell, a resolution of 0.1 nm, band-width of 1.0 nm, sensitivity of 2 mdeg, response 2 sec and a scan speed of 50 nm/min. for the PNA_2:DNA complexes, spectra were recorded as an accumulation of 8 scans, response of 1 sec and a scan speed of 200 nm/min. The CD spectra of the mixed base PNAs and the derived PNA:DNA duplexes were recorded as an accumulation of 5 scans and a scan speed of 200 nm/min.

Gel mobility shift assay: The PNAs (**25**-**29**, Table 8) were individually mixed with DNA (**38** or **40**) in 2:1 ratio (PNA strand, 0.4 mM and DNA **38** or **40**, 0.2 mM) in water. The samples were lyophilized to dryness and re-suspended in sodium phosphate buffer (10 mM, pH 7.0, 10µl) containing EDTA (0.1 mM). The samples were annealed by heating to 85°C for 5 min followed by slow cooling to RT and refrigeration at 4°C overnight. To this, 10µl of 40% sucrose in TBE buffer pH 8.0 was added and the sample was loaded on the gel. Bromophenol blue (BPB) was used as the tracer dye separately in an adjacent well. Gel electrophoresis was performed on a 15% non-denaturing polyacrylamide gel (acrylamide:bis-acrylamide, 29:1) at constant power supply of 200 V and 10 mA, until the BPB migrated to three-fourth of the gel length. During electrophoresis the temperature was maintained at 10°C. The spots were visualized through UV shadowing by illuminating the gel placed on a fluorescent silica gel plate, GF_{254} using UV-light.

2.6 Appendix

- Compound **4**, ^{1}H, ^{13}C NMR and DEPT
- Compound **5**, ^{1}H, ^{13}C NMR and DEPT
- Compound **8**, ^{1}H, ^{13}C NMR and DEPT
- Compound **9**, ^{1}H, ^{13}C NMR and DEPT
- Compound **10**, ^{1}H, ^{13}C NMR, DEPT and FAB mass
- Compound **11**, ^{1}H, ^{13}C NMR, DEPT and FAB mass

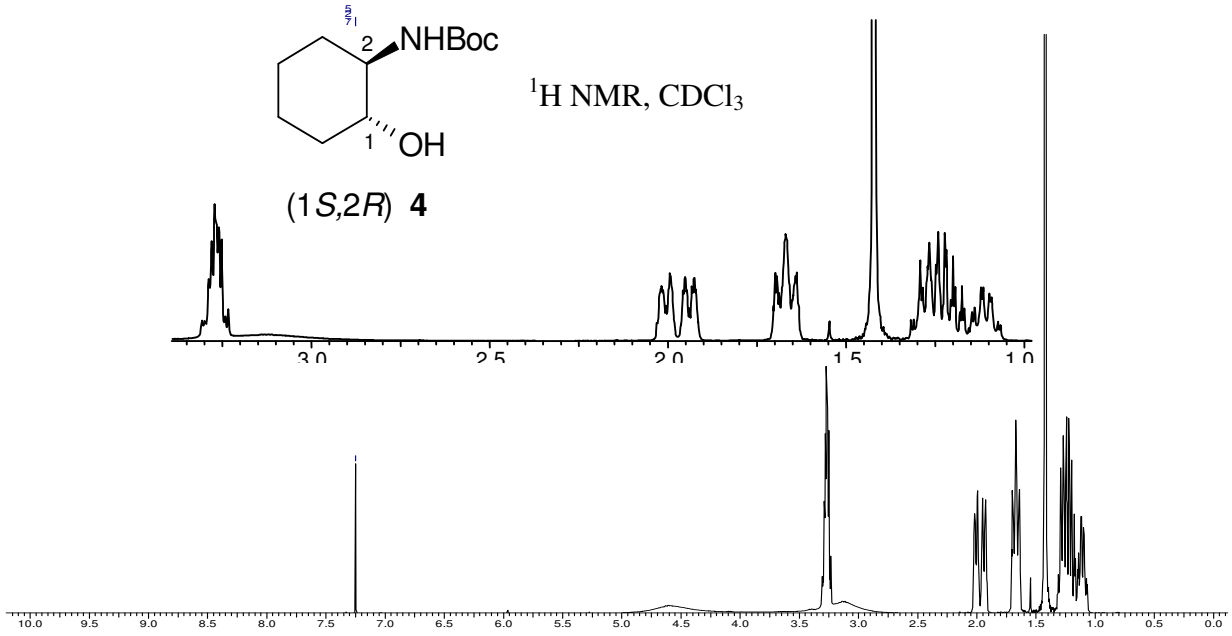
2
NHBoc
1
OH
(1S,2R) 4
1H NMR, CDCl3

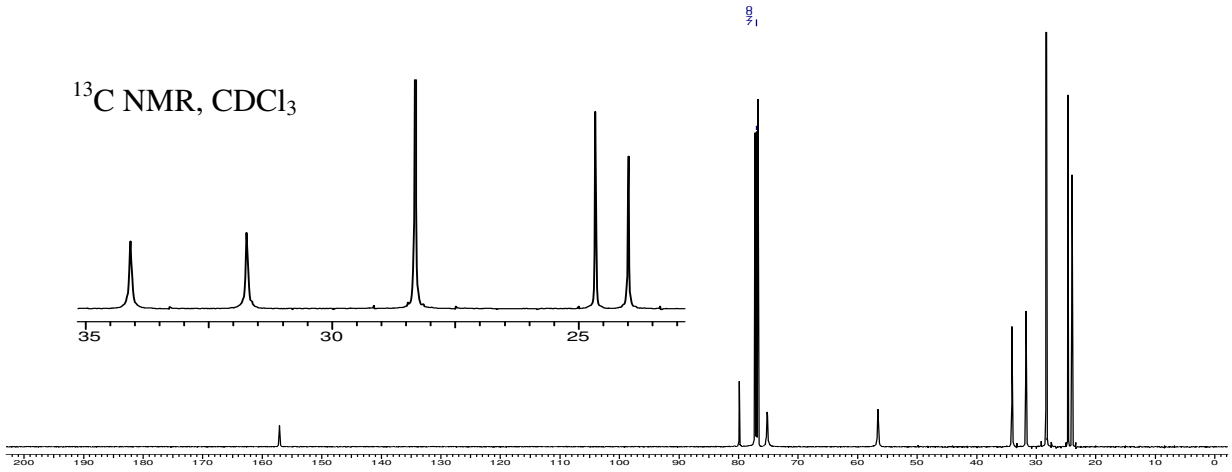
13C NMR, CDCl3

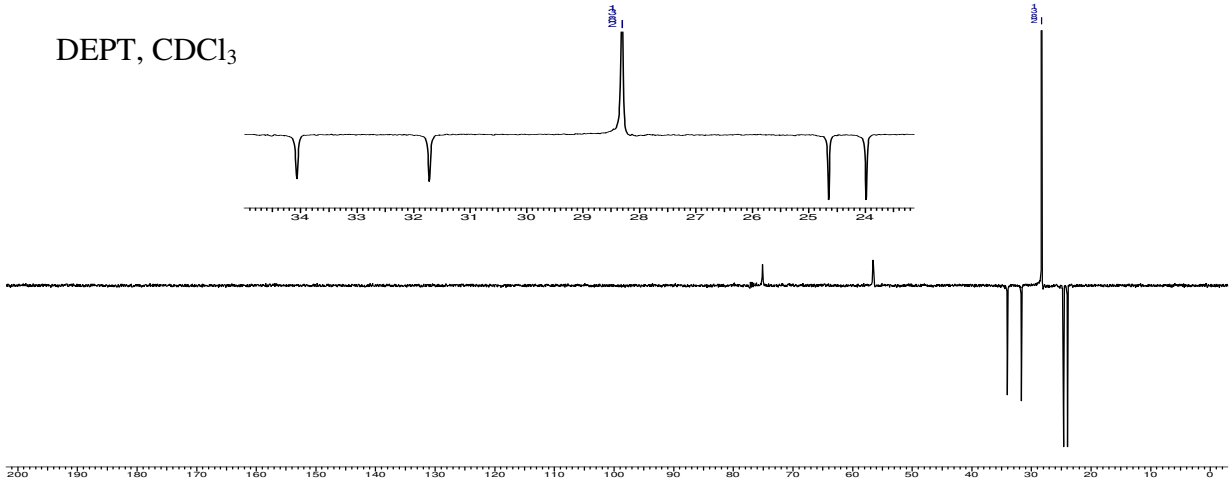
DEPT, CDCl3

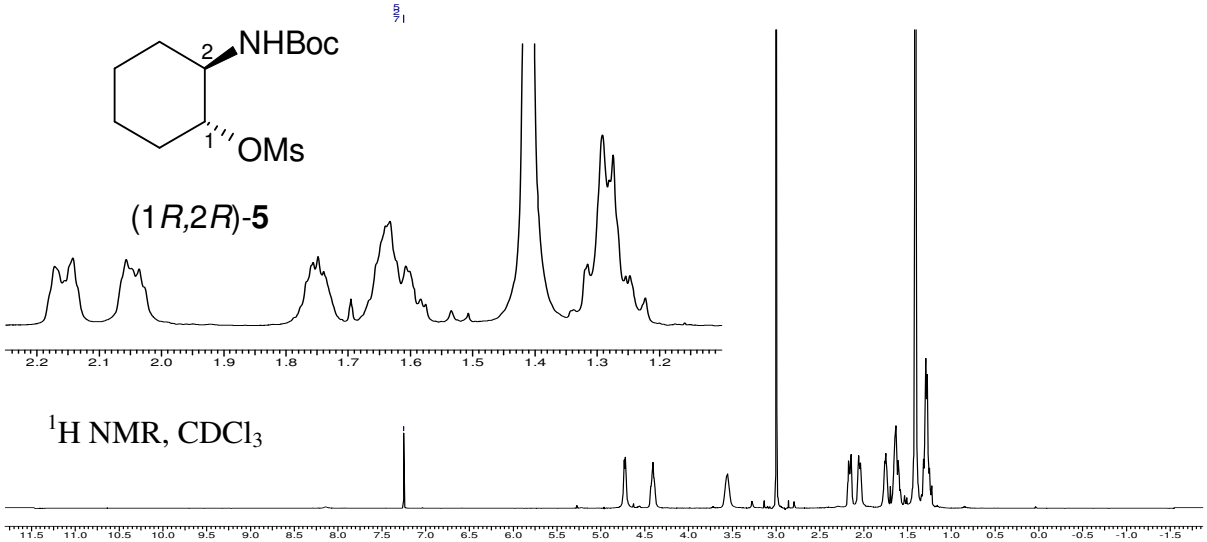
NHBoc
2
1
OMs
(1R,2R)-5
1H NMR, CDCl3

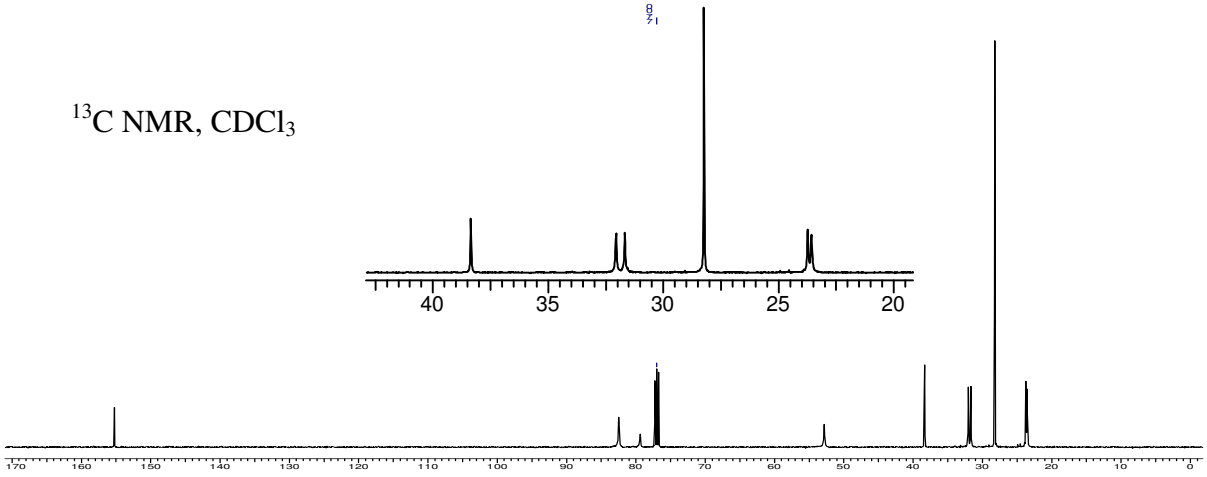
13C NMR, CDCl3

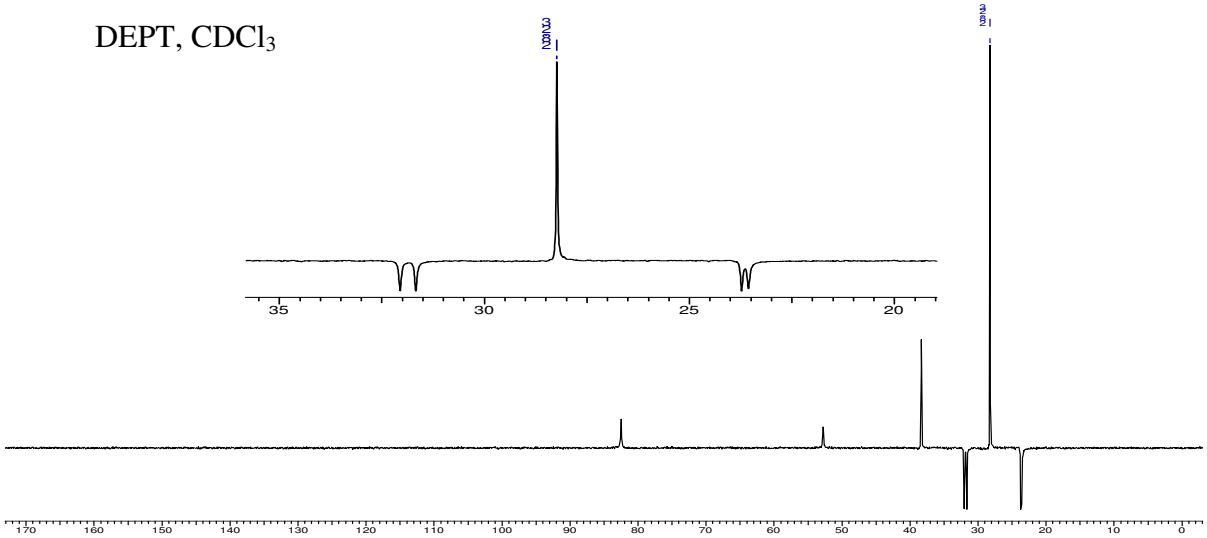
DEPT, CDCl3

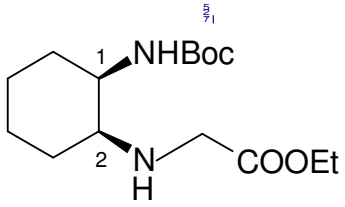

(1*R*,2*S*)-**8**

^{1}H NMR, $CDCl_3$

^{13}C NMR, $CDCl_3$

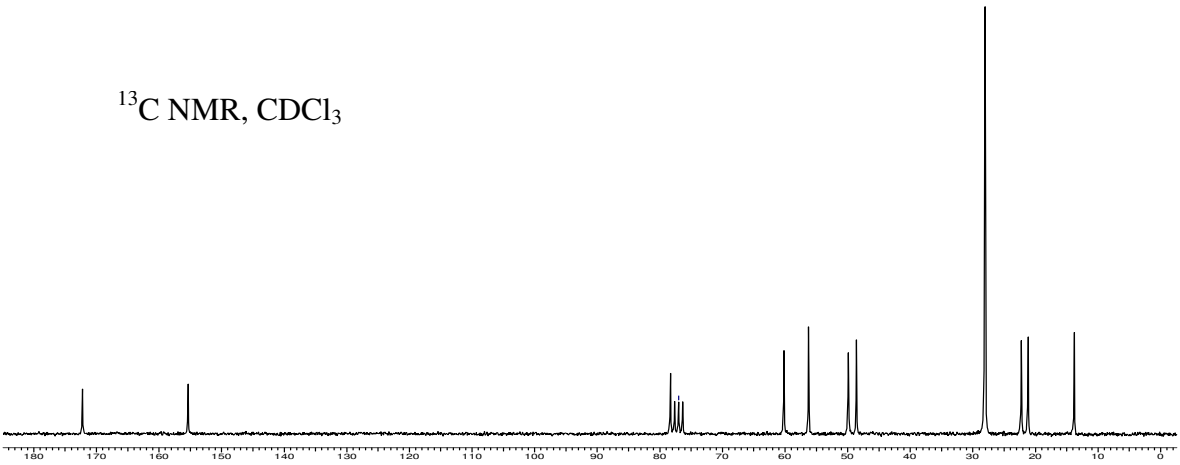

DEPT, $CDCl_3$

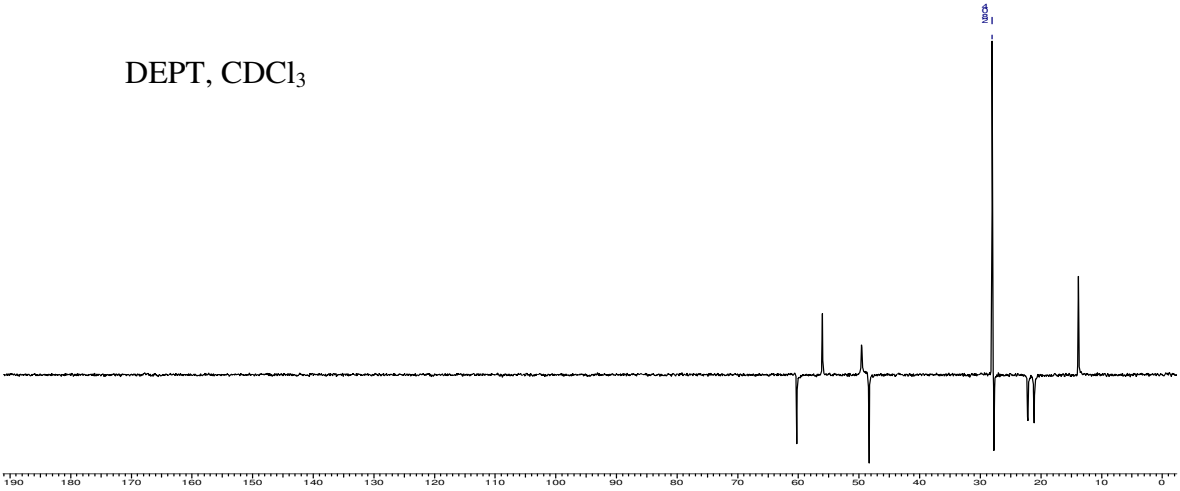

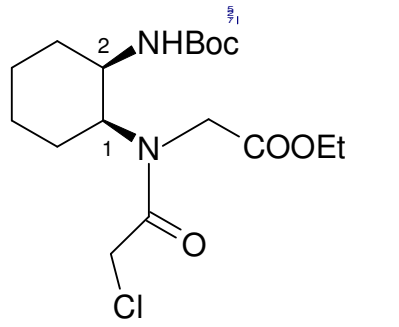

(1*S*,2*R*)-**9**

^{1}H NMR, $CDCl_3$

^{13}C NMR, $CDCl_3$

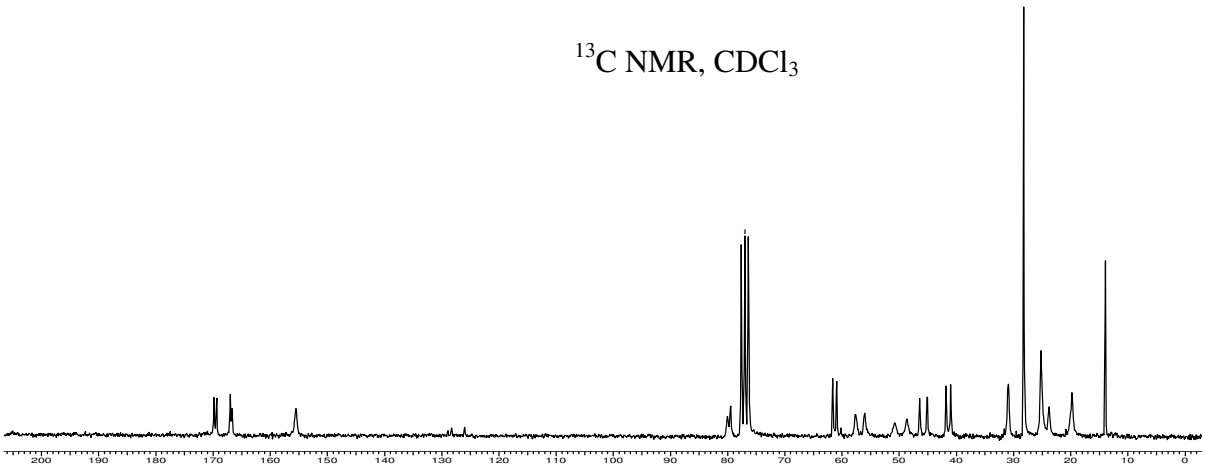

DEPT, $CDCl_3$

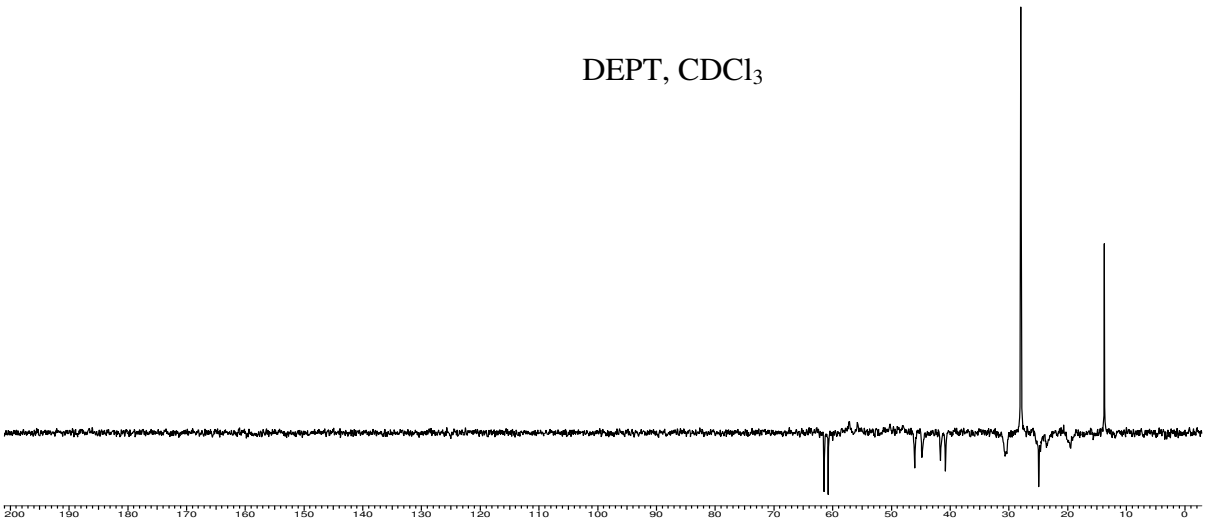

^{1}H NMR, $CDCl_3$

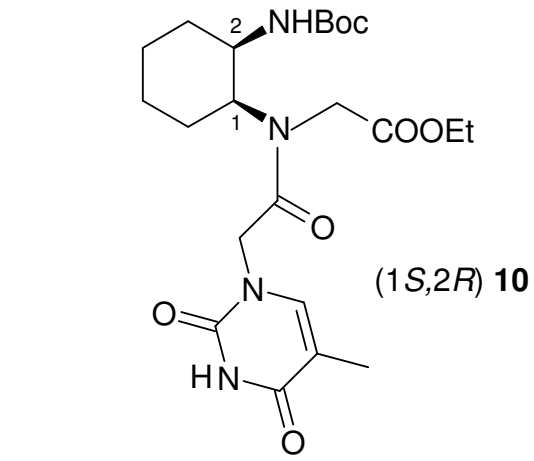

(1*S*,2*R*) **10**

^{13}C NMR, $CDCl_3$

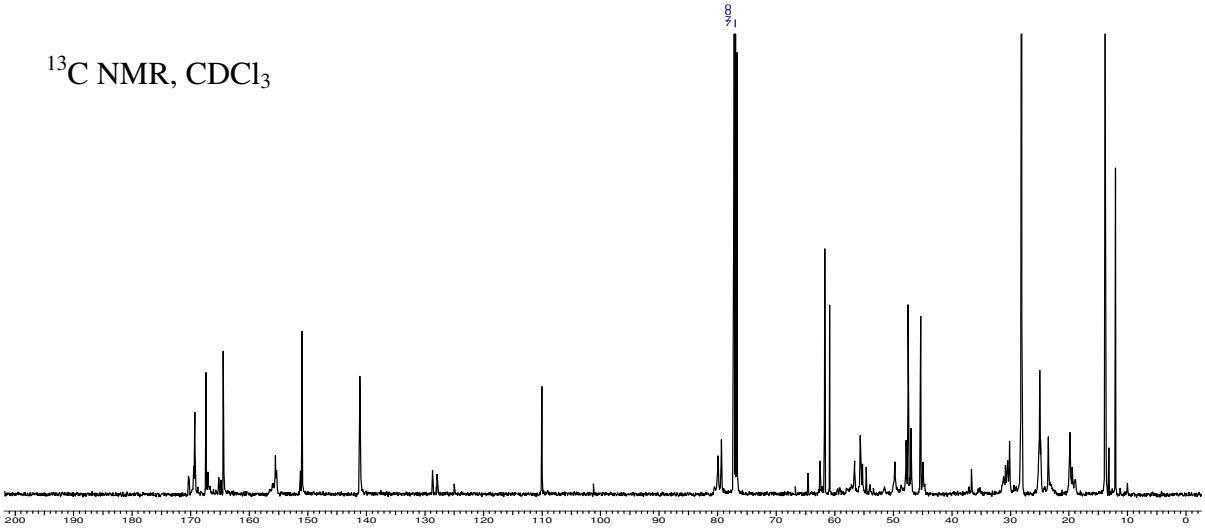

DEPT, $CDCl_3$

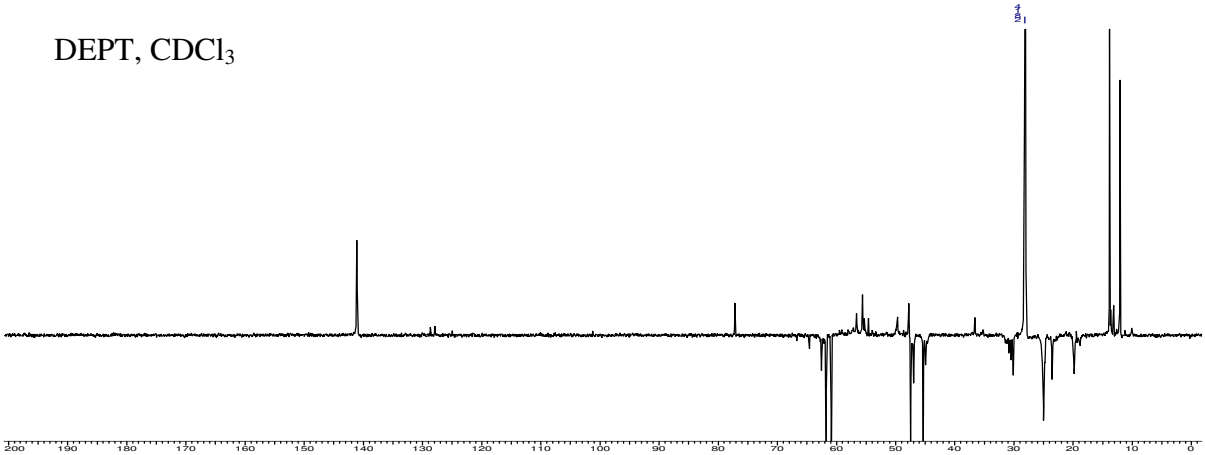

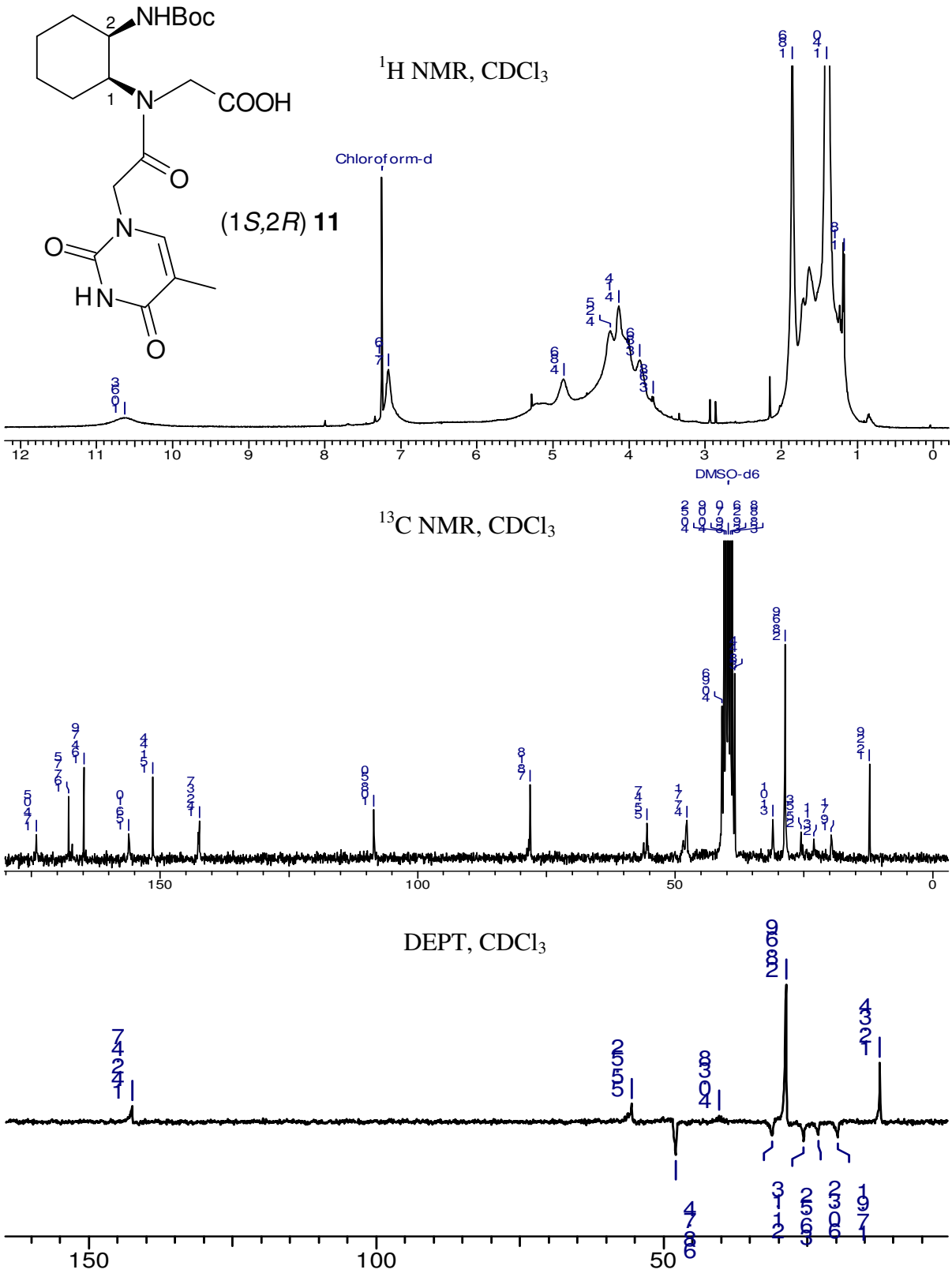
NHBoc
COOH
(1S,2R) 11
1H NMR, CDCl3
Chloroform-d
DMSO-d6
13C NMR, CDCl3
DEPT, CDCl3

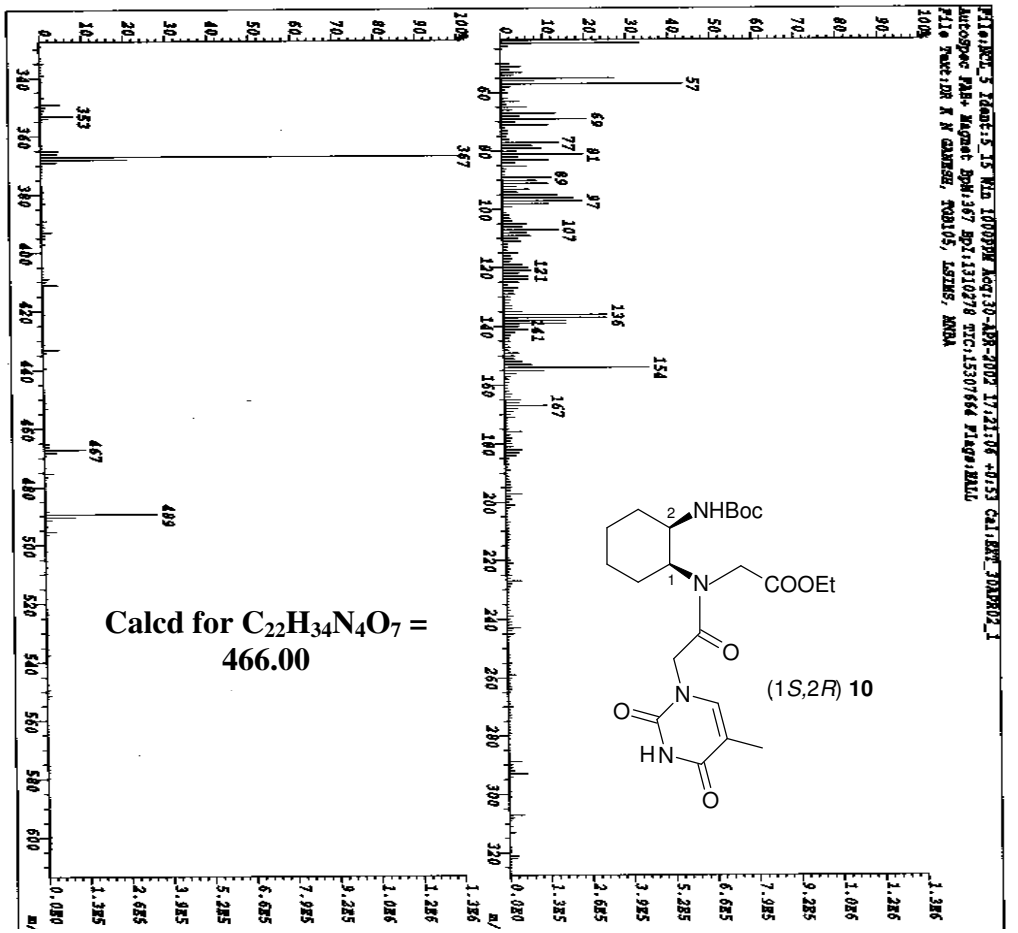
Calcd for $C_{22}H_{34}N_4O_7$ = 466.00
(1S,2R) 10

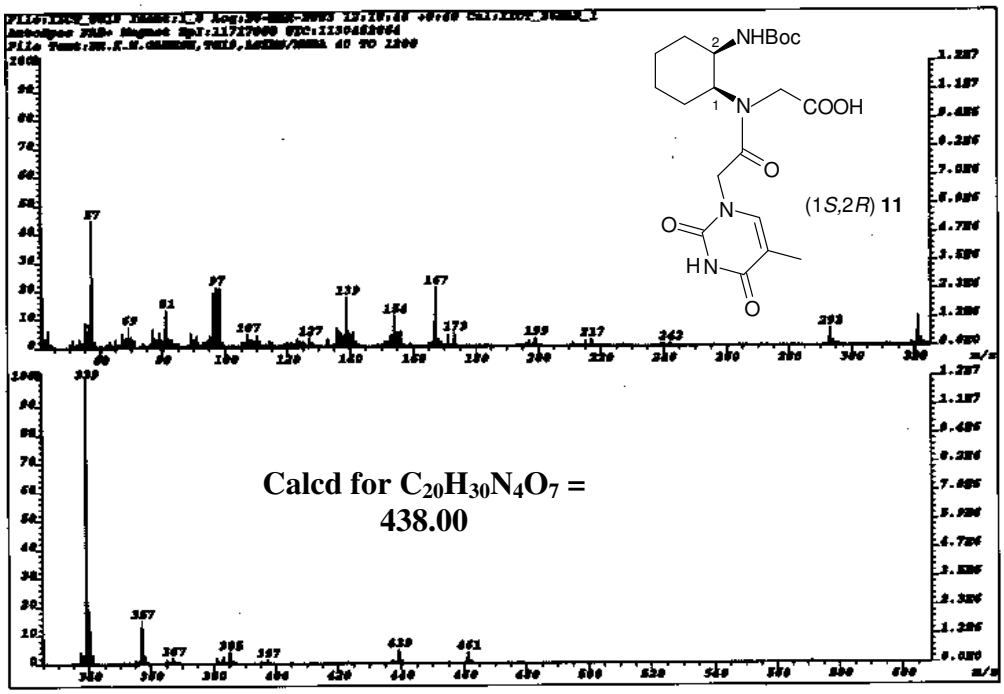
Calcd for $C_{20}H_{30}N_4O_7$ = 438.00
(1S,2R) 11

Chapter-3

(1*S*,2*R*)-and (1*R*,2*S*)-*cis*-Aminocyclopentylglycyl PNAs (*cp*PNA) as Conformationally Constrained analogues: Synthesis and Evaluation of *aeg*PNA-*cp*PNA chimera and Stereopreferences in Hybridization with DNA/RNA

3.1 Introduction

An analysis of the X-ray structural data of PNA_2:DNA triplex,[108] PNA:DNA duplex[106] and NMR data of PNA:RNA duplex[107] suggested that the dihedral angle β (Table 1) could be a key factor for rational design of pre-organized PNA structure. The preferred values of β for the PNA_2:DNA triplex and PNA:RNA duplex is in the range 65-70° while that for the PNA:DNA duplex is about ~140°, suggesting that it may be possible to impart DNA/RNA binding selectivity if β is restricted to 65-70° range through suitable chemical modifications. With such a rationale, *cis*-cyclohexyl PNA (*ch*PNA) (chapter 2), in which the axial-equatorial disposition of *cis*-1,2 substituents with β in the range 63-66° (opposite in sign for the two enantiomers 1*S*,2*R* and 1*R*,2*S*) was designed and shown to have a stereochemistry dependent preferential binding of the derived *ch*PNA oligomers to RNA as compared to DNA. This was interesting in comparison to the earlier report[126] on *trans*-1,2 diaxial substituted cyclohexyl system in which the dihedral angle β is 180°. This was unsuitable for forming hybrids with either DNA or RNA in agreement with X-ray data. However, a slightly lower binding affinity for triplex formation was seen with *cis*-1,2-*ch*PNA in comparison to unmodified *aeg*PNA. This suggested that inspite of a favorable β, the substituted cyclohexyl ring is inherently too rigid as it gets locked up in either of the chair conformations. A relatively flexible system would be a cyclopentyl ring in which the characteristic interconvertible *endo-exo*

puckering that dictates the pseudoaxial/pseudoequatorial dispositions of substituents[196] may allow better torsional adjustments to attain the necessary hybridization competent conformations.

Cyclohexane vs. cyclopentane Ring conformation: The chair conformation of cyclohexane ring system relieves all the strains, which are inherent with other smaller and larger rings or 'nothing is comparable to cyclohexanes energy minimum'. There are two chair conformers possible by ring flipping action and this depends on the nature of the substituents (Figure 1A). As the number and size (bulkiness and energy barrier for flipping) of the substituents increases, the rigidity of the system also increases and freezes to one of the chair conformation, with no more flipping of the ring. In contrast, cyclopentane ring system can assume two different conformations- i) envelope and ii)

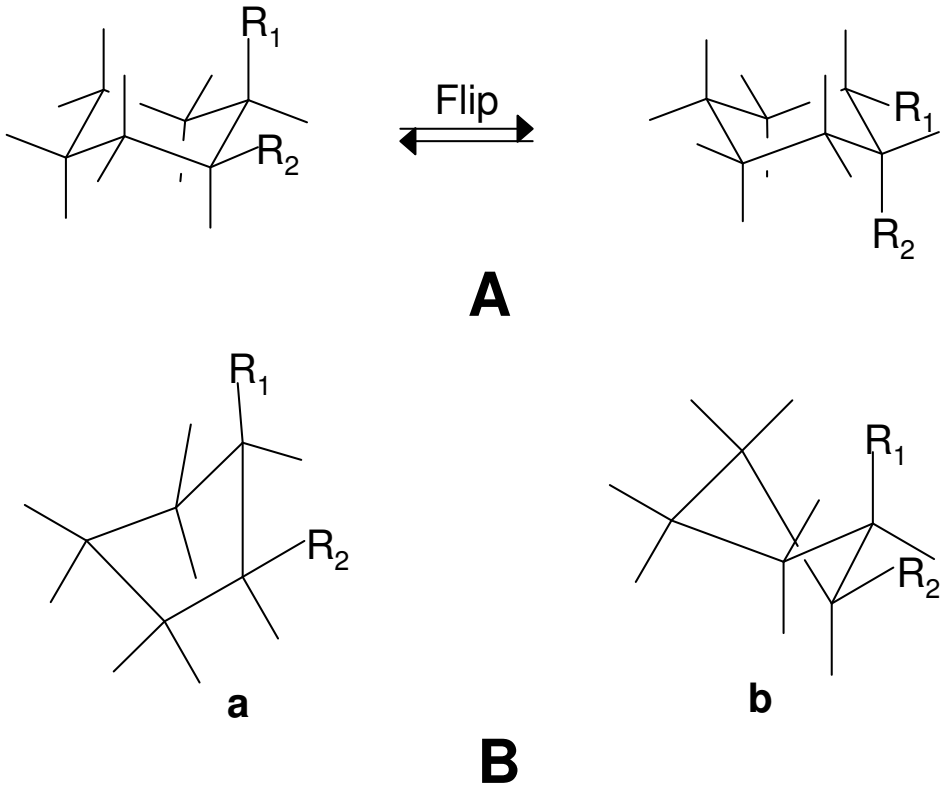

Figure 1. Interconvertible **A**. Cyclohexyl chair conformations and **B**. Cyclopentyl envelope (a) and half-chair (or twist) (b) conformations

half-chair (twist) conformations, neither form is static and possess rapid interconversion between several intermediate conformations amongst each of the two conformations, leading to pseudorotation cycle.[196] The energy barrier between the conformations is very small with cyclopentane ring being 'in a conformational flux between the two or more stable conformations and also among other in-between structures' (puckering).[196]

3.2 Rationale and Objective of the present work

There are several nucleic acid analogues for gene therapy and nucleosides as drug molecules for various diseases, where the five membered sugar rings (furanose) have been replaced by carbocyclic cyclopentane ring as discussed in chapter 1. Leumann *et al* evaluated carbocyclic furanose analogues in different contexts of study. Few related ones are Bicyclo[3.2.1]-DNA,[197] bca-DNA[198] and cpa-DNA[198] (Figure 2). These analogues possess cyclopentane ring in their structures with variation in the distance between sugar and the backbone. Bicyclo[3.2.1]-DNA is competent, but less effective partner for the complexation with DNA, RNA and for itself[197] and showed a strong discrimination of RNA relative to DNA in random sequences.[198] Structurally simpler analogue of bca-DNA is cyclopentane amide DNA (cpa-DNA), in which the fully modified cpa-oligoadenylates form complexes with complementary DNA that are less stable. The corresponding cpa-oligothymidylates do not participate in complementary base pairing with DNA/RNA.[199]

While the present work was in progress a five membered carbocyclic analogue of PNA was reported by Appella *et al*[200] and DNA binding studies on *trans*-(1*S*,2*S*) cyclopentane PNA (Figure 2) that showed stabilization of the derived PNA:DNA complexes. The synthetic route described for this *trans*-cyclopentane PNA analogue allows access to only one of the enantiomers.

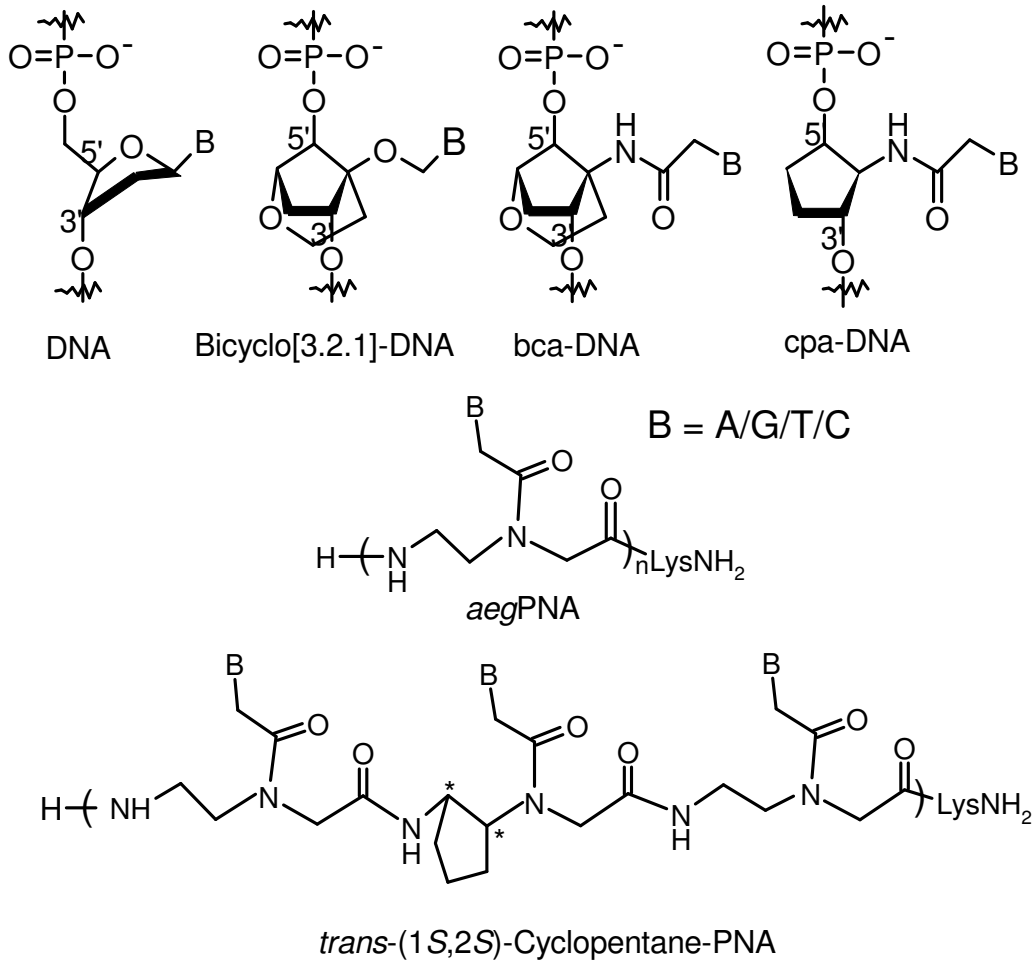

Figure 2. Cyclopentane derived DNA and PNA analogues.

In an attempt to tune the dihedral angle β according to our hypothesis and to strike a balance between "flexibility and rigidity", *cis*-(1*S*,2*R*/1*R*2*S*)-cyclopentyl PNAs (*cp*PNA) have been designed. The flexible *cis*-cyclopentane ring in the pre-organized PNA structure may bind complementary DNA/RNA sequence without much loss in the entropy of the PNA strand during the complexation. The *cp*PNA is derived by constraining the ethylene diamine portion of the *aeg*PNA with a hydrocarbon linker having three methylenes and one less than that in *ch*PNA (Figure 3), this imposing a conformational constraint on flexible aminoethylglycyl PNA with *cis*-cyclopentane ring. This study also provides a comparison of six membered pyranose conformation versus

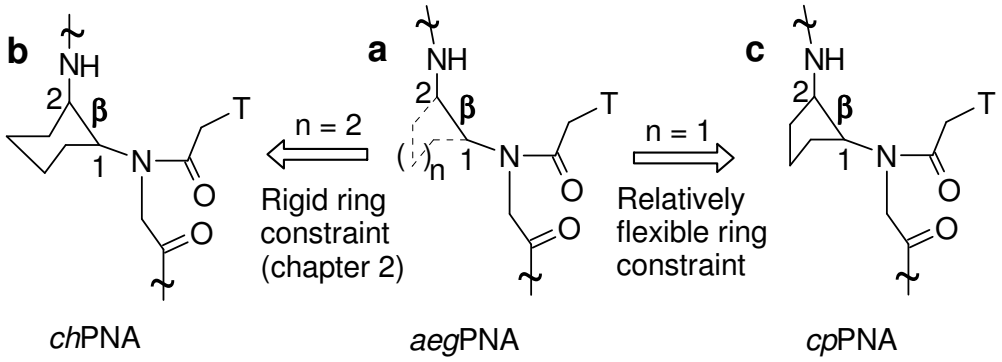

Figure 3. Dihedral angle and ring flexibility based design of *cp*PNA (c).

five membered furanose conformations, similar to pRNA and TNA in sugar nucleic acids by Eschenmoser.[81,82]

The objectives of this chapter are,

i) Synthesis of (1*S*,2*R*) and (1*R*,2*S*)-aminocyclopentylglycyl PNA monomers (Figure 4) involving chemo-enzymatic resolution of one of the key racemic intermediates.

ii) Solid phase synthesis of *cp*PNA-*aeg*PNA chimeras and *cp*PNA oligomers incorporating *aeg*PNA (T/A/G/C) monomers and *cp*PNA (T) monomer.

iii) Cleavage from the solid support and purification, characterization of the oligomers.

iv) Binding studies of *cp*PNA-*aeg*PNA chimeras and *cp*PNA with DNA/RNA using various biophysical techniques.

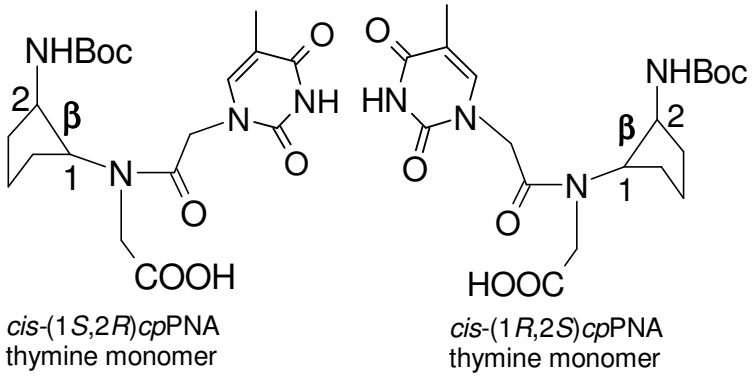

Figure 4. Structures of target *cp*PNA monomers.

v) Comparison of the results from *cp*PNA hybridization studies with that of *ch*PNA.

3.3 Results and Discussion

The *cis*-cyclopentyl PNA monomer can be synthesized as two different enantiomers in their highest optical purity. The two enantiomers of the *cis*-cyclopentyl PNA monomer (Figure 4) were synthesized in their optically pure form starting from the chirally pure (1*S*,2*R*) and (1*R*,2*S*)-cyclopentyl-1,2-diamines. These *cis*-cyclopentyl-1,2-diamines are not available commercially and there are no practical synthesis in literature to obtain these in optically pure form. These diamines can be obtained from the chirally pure 1,2-amino alcohols *via* stereospecific chemical transformations. The enantiomerically pure 1,2-amino alcohols can be obtained from the ring opening of the meso-epoxide cyclopentane-1,2-epoxide using sodium azide followed by chemoezyamtic resolution of the racemate product and reduction of the azide functionality. The optical

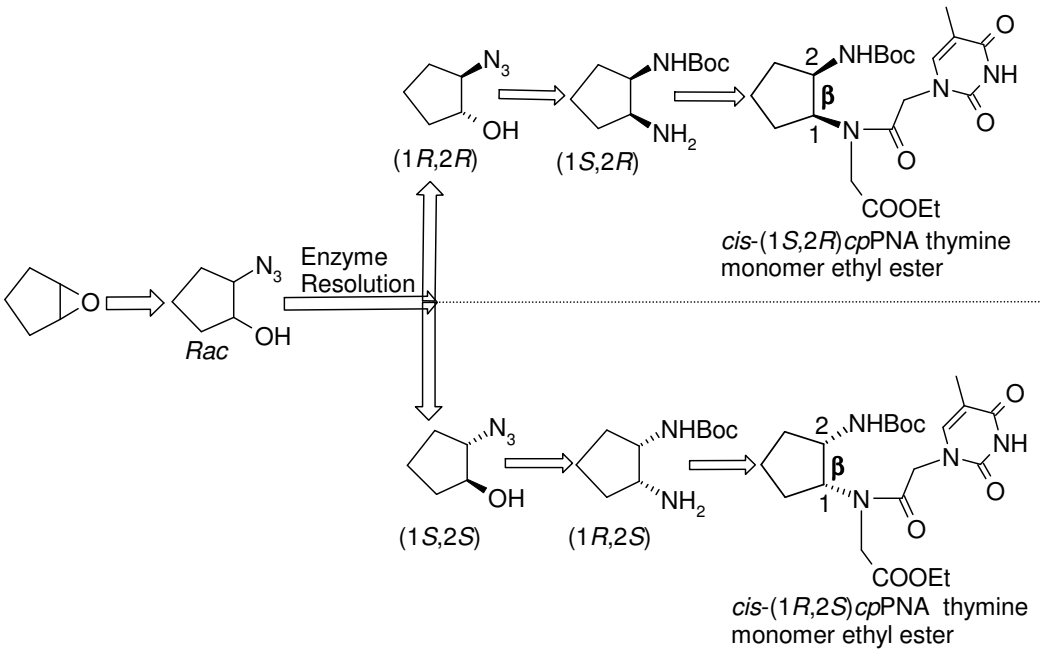

Figure 5. Schematic representation of synthesis of *cp*PNA monomer esters.

purities of enantiomers obtained from the enzymatic resolution are always better than that from any other method. This is an added advantage to get the target monomers in very high optical purity compared to chemical methods that are hardly available to access these *cis*-1,2-diamines. This helps in studying the effect of *cp*PNA stereochemistry on PNA backbone conformation and leads to a proper comparison of the results with respect to ring size and stereochemistry dependent factors on PNA:DNA/RNA hybridization. The target monomers were synthesized starting from simple cyclopentane-epoxide as represented schematically in the Figure 5.

3.3.1 Enzyme hydrolysis

The resolution of *trans*-1,2-azidocyclopentanol was reported using *Pseudomonas sp*., but it is not clear as to which particular enzyme was involved. However, here the enzyme from *Pseudomonas cepacia* obtained from Amano Pharmaceuticals, Japan, was used effectively for the resolution of butyrate ester of racemic *trans*-2-azido cyclopentanol and was found to be very efficient. The enzyme exhibited more selectivity for butyrate ester and poor selectivity was seen for esters like acetate and iso-butyrate. So the lipase *Pseudomonas cepacia* is effective in the hydrolysis (resolution) of butyrate esters of both *trans*-cyclohexyl (chapter 2) and cyclopentyl azido alcohols, whereas *Candida cylindracea* (*rugosa*) is effective only for butyrate ester of azido cyclohexanol and not for azido pentanol. It should be pointed out that the synthetic route involving enzymatic resolution steps permits synthesis of both the enantiomers.

3.3.2 Chemo-enzymatic resolution of *Racemic*, *trans*-2-azido-cyclopentanol

The resolution of title compound was achieved by the enzyme hydrolysis of mixture of (+) and (-)-*trans*-2-azido cyclopentanoate **3** using lipases well known in literature[169]. The butyrate ester of racemic *trans*-2-azido cyclopentanol was synthesized by oxirane ring opening of the commercially available meso epoxide **1** with sodium azide[170] followed by esterification with butyric anhydride (Scheme 1). The racemic butyrate ester **3** was resolved by enzymatic enantioselective hydrolysis using the lipase from *Pseudomonas cepacia* (Amano-PS)[169] in sodium phosphate buffer (pH = 7.2) which proceeded with 40% conversion. This was followed by chromatography, to obtain the

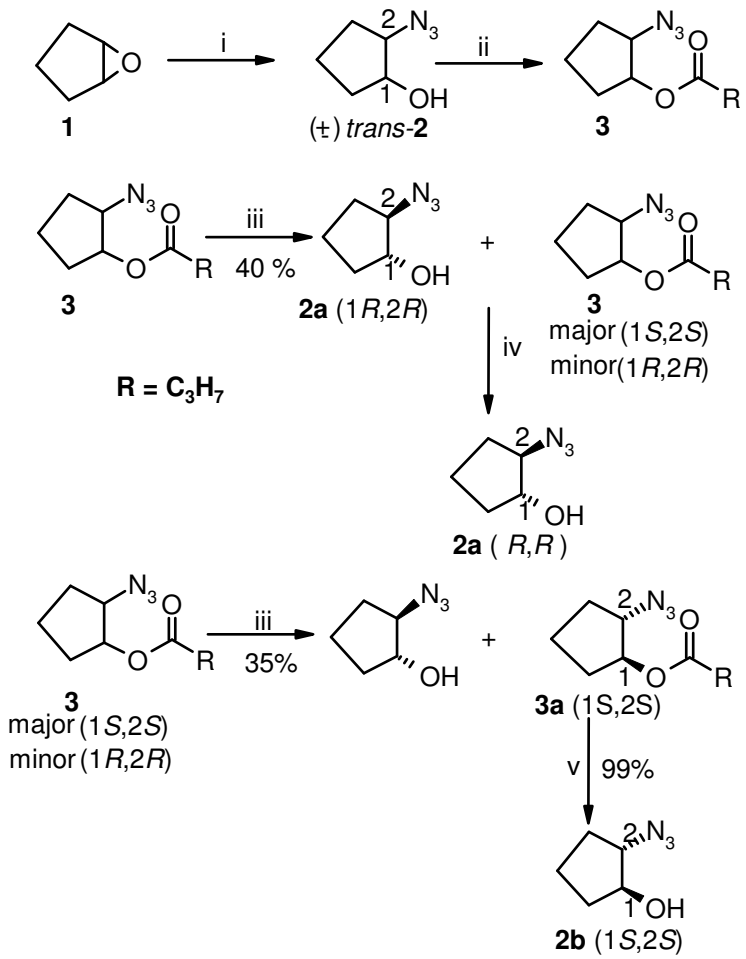

Scheme 1: Reagents and conditions: (i) NaN_3, NH_4Cl, Ethanol: Water (8:2), reflux, 16 h. (ii) n-Butyric anhydride, dry pyridine, DMAP (cat), rt, 16 h. (iii) *Pseudomonas cepacia* (Lipase), phosphate buffer, pH 7.2, 1.5 h. (iv) Column chromatography separation (v) NaOMe in MeOH 0.5 h.

optically pure (1*R*,2*R*) azido alcohol **2a**. *Pseudomonas cepacia* lipase (Amano-PS, LPSAA0852814) was found to be very effective for the resolution of *racemic-trans* cyclopentanaote, but lipase from *Candida cylinderacea* was totally ineffective as reported. We found that the Amano-PS also gave a slightly better enantiomeric purity and yield for the azido alcohols **2a** and **2b** than the reported ones under identical reaction conditions and in less reaction time. Further, the enzymatic treatment of the mixture of minor (1*R*,2*R*) and major (1*S*,2*S*) butyrate esters **2** a the second time followed by column purification and subsequent methanolysis of the (1*S*,2*S*) **3** ester using NaOMe in methanol gave pure (1*S*,2*S*) **2b** in 35% overall yield.

The enantiopurity of both (1*R*,2*R*) **2a** and (1*S*,2*S*) **2b** isomers was confirmed by comparing with the known values of optical rotations reported in the literature[169] and by ^{1}H NMR using the chiral chemical shift reagent Eu*(hfc)*$_3$.[172] The enantiomeric purity of alcohols (1*R*,2*R*)-**2a** and (1*S*,2*S*)-**2b** were confirmed from ^{1}H NMR measurement of their acetyl derivatives utilizing a chiral chemical shift reagent, (+)-*tris*-[3-(heptafluoropropylhydroxymethylene)-d-camphorato]europium (III) [Eu(hfc)$_3$]. (8.0 mole%). Examination of the ^{1}H NMR spectrum of the acetyl derivatives of racemic (1*R*/*S*,2*R*/*S*)-**2** shows the splitting in the methyl protons signal into clear doublet. But in the corresponding spectra of acetyl derivatives of (1*R*,2*R*)-**2a** and (1*S*,2*S*)-**2b**, the above mentioned signal was singlet and identical to corresponding signal in the spectrum of their racemate. Integration of the methyl signal (doublet) in the racemate and that of the pure (1*R*,2*R*)-**2a** and (1*S*,2*S*)-**2b** (singlet) shows that the enantiomeric excess will be >98% for both isomers (Figure 6).

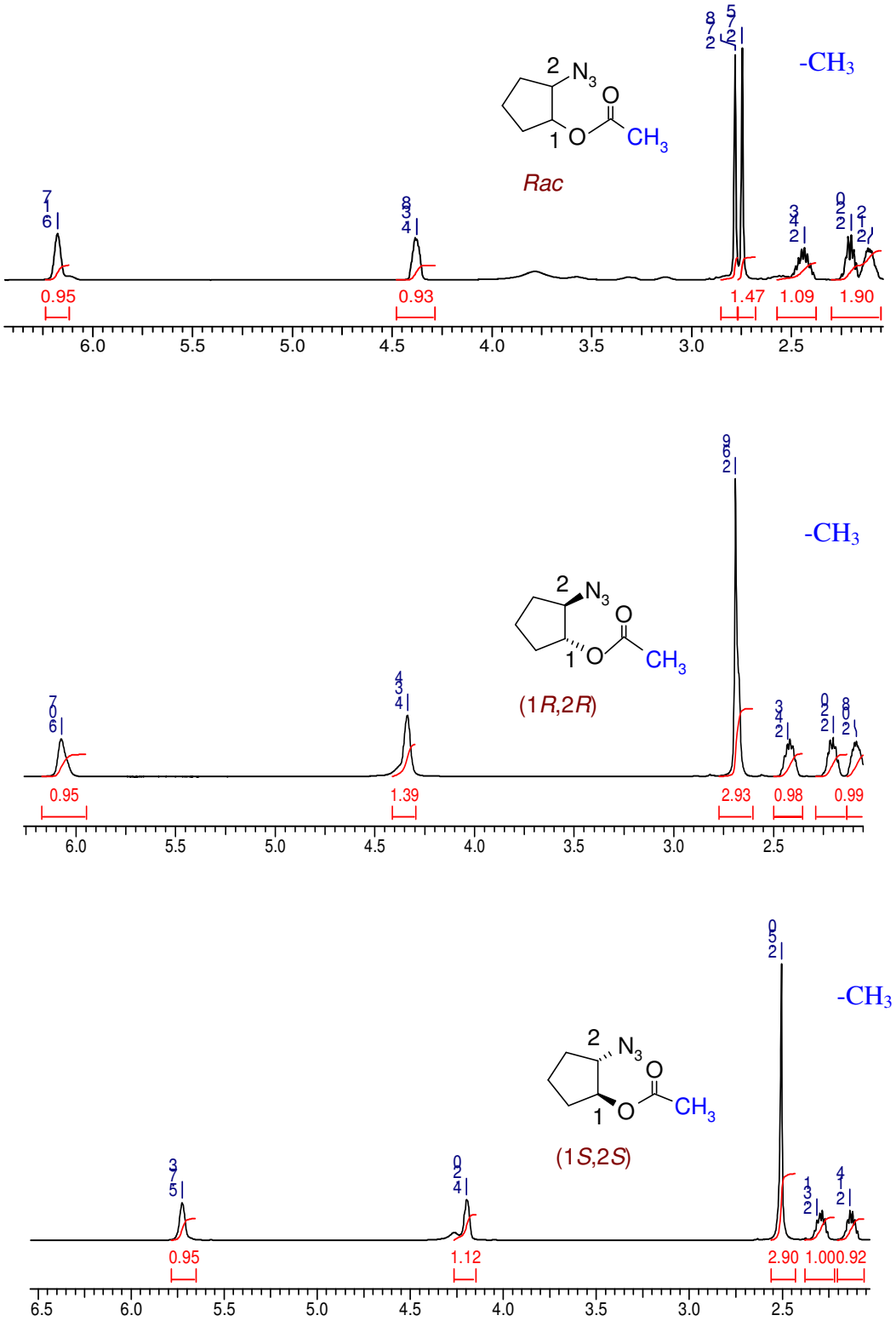

Figure 6. Enantiomeric purity determination from ^{1}H NMR of acetyl derivatives of *rac*, pure (1*R*,2*R*) and (1*S*,2*S*)-azido cyclopentanols with Eu(*hfc*)$_3$ reagent (8.0 mol%)

3.3.3 *N*-[(2*R*)-*t*-Boc-Aminocyclopent-(1*S*)-yl]-*N*-(thymin-1-acetyl)-glycine ethyl ester 10a.

The synthesis of the compound **10a** started with the reduction of the azide function in (1*R*,2*R*) **2a** by hydrogenation using Adam's catalyst[173] and *in situ* *t*-Boc protection of the resulting amine function to yield the Boc-protected amino alcohol (1*R*,2*R*) **4** (Scheme 2). Attempts to convert the alcohol **4** to the corresponding mesylate (1*R*,2*R*) **5** using mesyl chloride in pyridine with DMAP as a catalyst was unsuccessful. The mesylate **5** was obtained by using triethyl amine (2.5 eq.) in dry dichloromethane at rt in less than 30 min. The resulting mesylate **5** is very unstable to acidic conditions and decomposed on silica gel during purification and hence was directly used for further

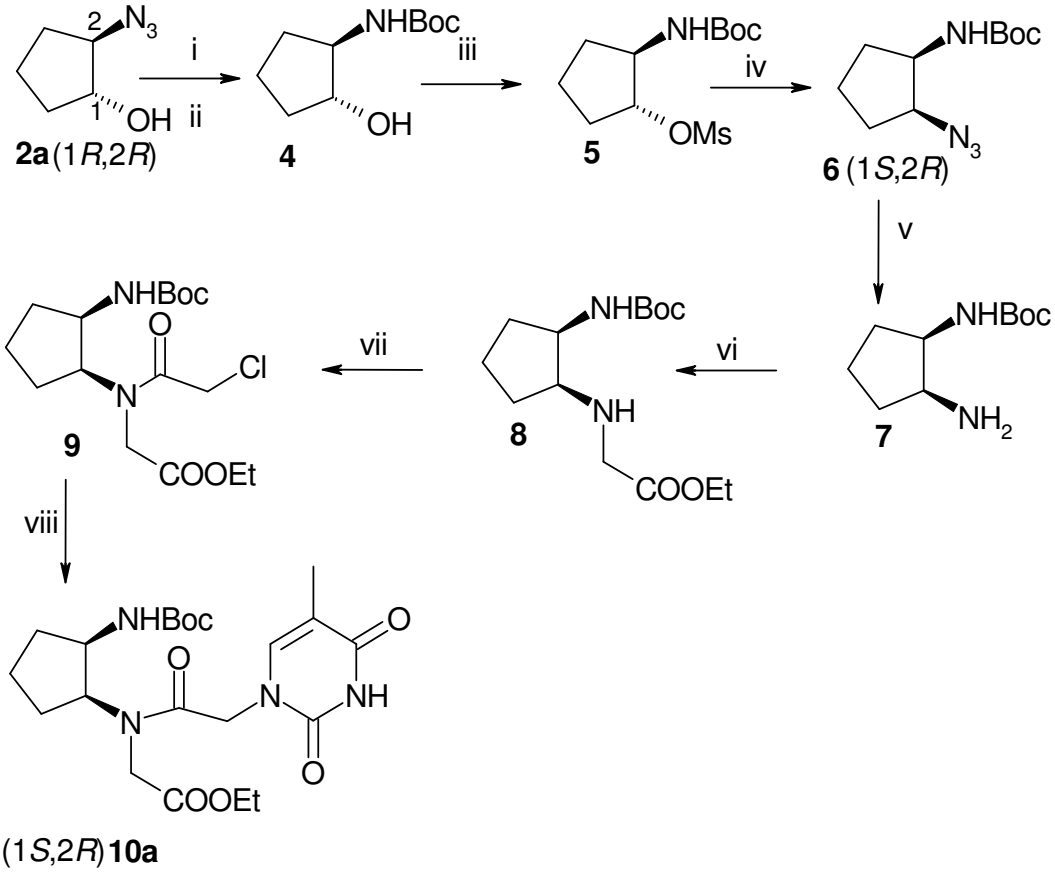

Scheme 2. Reagent and conditions. (i) PtO_2, dry EtOAc, H_2, 35-40 psi, rt, 3.5 h; (ii) $(Boc)_2O$ (iii) MsCl, dry triethyl amine, rt, 0.5 h; (iv) NaN_3, dry DMF, 70°C, 5 h; (v) PtO_2, MeOH, H_2, 35-40 psi, rt, 3.5 h; (vi) $BrCH_2COOEt$, KF-Celite, dry CH_3CN, 65°C, 4 h; vii) $ClCH_2COCl$, Na_2CO_3, Dioxan: H_2O (1:1), 0°C, 5 min.; (viii) Thymine, K_2CO_3 dry DMF, 65°C, 4 h.

reaction without any purification. The mesylate was treated with NaN_3 in dry DMF to yield the azide (1*S*,2*R*) **6**, and the reaction was accompanied by inversion of configuration at C1. During this conversion, a thermally rearranged product identified as urea derivative (**6c**) was obtained in 7% yield (Figure 7c). The azide (1*S*,2*R*) **6** was hydrogenated using Adam's catalyst to give the amine (1*S*,2*R*) **7**, which without further purification was alkylated with ethyl bromoacetate in the presence of KF-Celite.[178] This resulted in the monosubstituted *cis*-1,2 diamine (1*S*,2*R*) **8** which on acylation with chloroacetyl chloride gave the compound (1*S*,2*R*) **9.** The condensation of (1*S*,2*R*) **9** with thymine in presence of K_2CO_3 in DMF yielded the desired (1*S*,2*R*) aminocyclopentyl (thymin-1-yl-acetyl) glycyl PNA monomer ethyl ester **10a** and was confirmed by X-ray crystal structure (Figure 7a, Table 2). All new compounds were characterized by ^1H, ^{13}C NMR and mass spectral data and elemental analysis.

3.3.4 *N*-[(2*S*)-*t*-Boc-Aminocyclopent-(1*R*)-yl]-*N*-(thymin-1-acetyl)-glycine ethyl ester 10b.

The synthesis of the target monomer ester **10b** started with the reduction of the azide function in (1*S*,2*S*) **2b** by hydrogenation using Adam's catalyst[173] and in *situ t-Boc* protection of the resulting amine function yielded the *Boc*-protected amino alcohol (1*S*,2*S*) **4** (Scheme 3). Following a similar set of reactions as for the synthesis of isomer **10a**, *viz.*, mesylation of the alcohol (1*S*,2*S*) **4** and azidation of the mesylate **5** yielded the azide (1*R*,2*S*) **6** and a side product **6c** (Figure 7c, Table 1). The reduction of the azide was followed by alkylation with ethyl bromoacetate and acylation of the amine to yield the chloro compound (1*R*,2*S*) **9**. The condensation of chloro compound with nucleobase thymine to afford the monomer ethyl ester (1*R*,2*S*) **10b** in very good yield. The structure of **10b** was confirmed by X-ray crystal structure (Figure 7b, Table 3). All new

compounds were characterized by ^{1}H, ^{13}C NMR and mass spectral data and elemental analysis. The characteristic mirror image CD signatures for monomers **10a** and **10b** also confirmed their enantiomeric purities (Figure 7d).

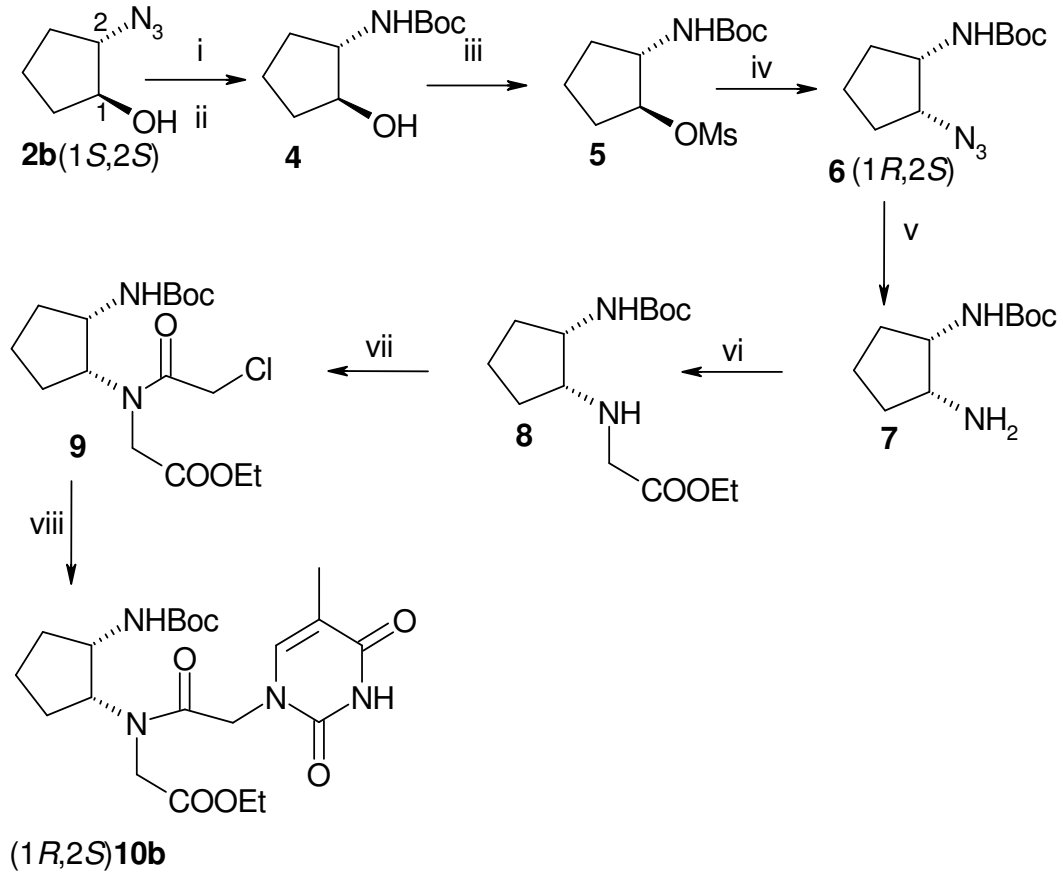

Scheme 3. Reagent and conditions. (i) PtO_2, dry EtOAc, H_2, 35-40 psi, rt, 3.5 h; (ii) $(Boc)_2O$ (iii) MsCl, dry triethyl amine, rt, 0.5 h; (iv) NaN_3, dry DMF, 70°C, 5 h; (v) PtO_2, MeOH, H_2, 35-40 psi, rt, 3.5 h; (vi) $BrCH_2COOEt$, KF-Celite, dry CH_3CN, 65°C, 4 h; vii) $ClCH_2COCl$, Na_2CO_3, Dioxan: H_2O (1:1), 0°C, 5 min.; (viii) Thymine, K_2CO_3 dry DMF, 65°C, 4 h.

3.3.5 Crystal structures of *cp*PNA thymine monomer esters 10a and 10b: Comparison of the dihedral angles with that of known values of PNA complexes.

Single crystals of both **10a** and **10b** were obtained by crystallization from chloroform (with petroleum ether as less polar solvent) and few drops of ethanol. X-ray intensity data were collected on a Bruker SMART APEX CCD diffractometer at low

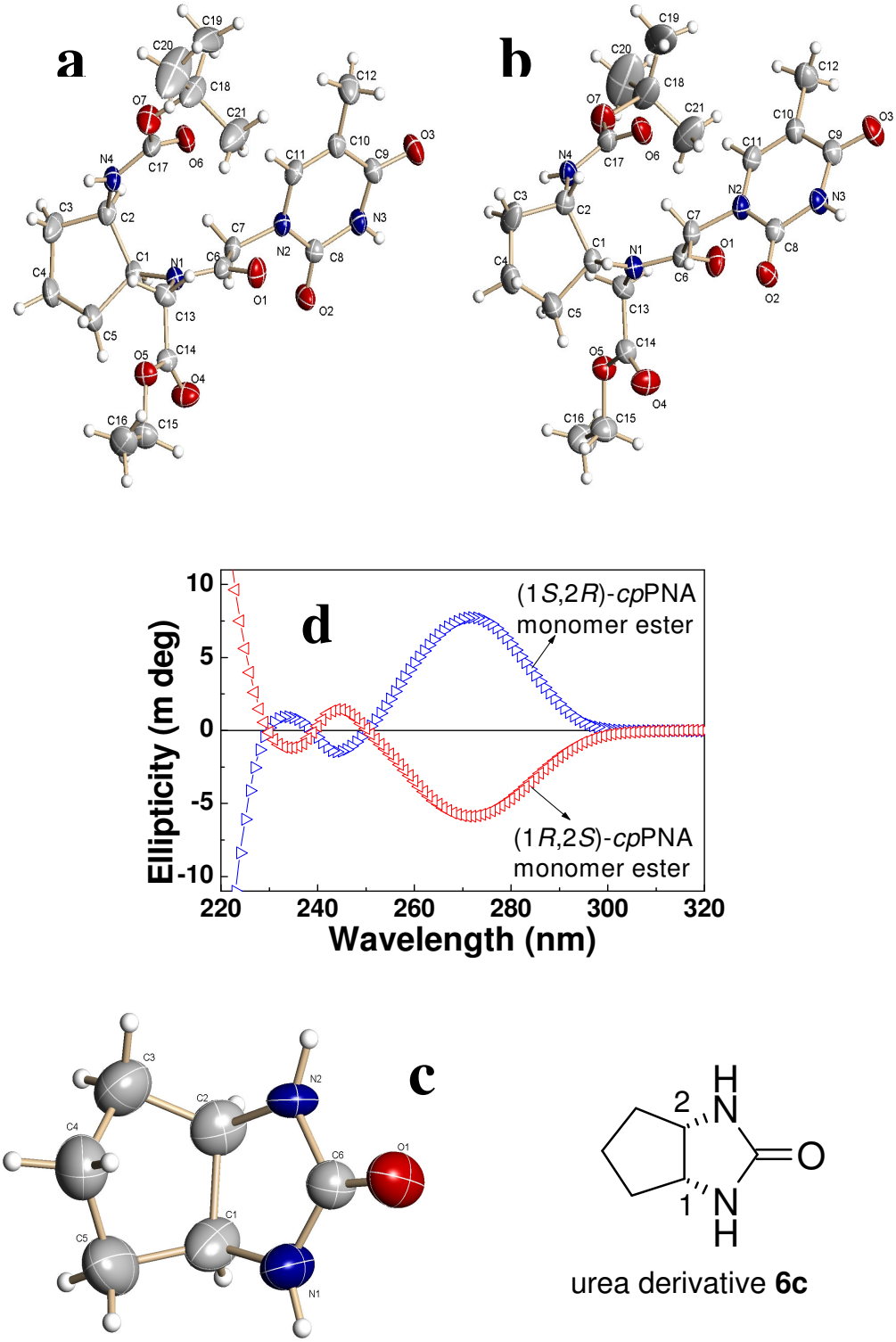

Figure 7. Crystal structures (a and b) of **10a** and **10b**, urea derivative **6c** (c), CD of **10a** and **10b** (d).

Table 1.Crystal data and structure refinement for Urea tive 6c.

Identification code	6c
Empirical formula	C12 H20 N4 O2
Formula weight	252.32
Temperature	293(2) K
Wavelength	0.71073 Å
Crystal system, space group	Monoclinic, $P2_1$
Unit cell dimensions	a = 10.322(3) Å alpha = 90°. b = 5.5641(18) Å beta = 5)°. c = 11.284(4) Å gamma = 90°.
Volume	643.5(4) $Å^3$
Z, Calculated density	2, 1.302 Mg/m^3
Absorption coefficient	0.091 mm^{-1}
F(000)	272
Crystal size	0.75 x 0.14 x 0.13 mm
Theta range for data collection	1.82 to 24.99 deg.
Limiting indices	-11<=h<=12, -6<=k<=6, -12<=l<=13
Reflections collected / unique	3144 / 2089 [R(int) = 0.0225]
Completeness to theta = 24.99	99.4 %
Max. and min. transmission	0.9882 and 0.9347
Refinement method	Full-matrix least-squares on F^2
Data / restraints / parameters	2089 / 1 / 163
Goodness-of-fit on F^2	1.120
Final R indices [I>2sigma(I)]	R1 = 0.0598, wR2 = 0.1555
R indices (all data)	R1 = 0.0645, wR2 = 0.1605
Absolute structure parameter	-1(3)
Largest diff. peak and hole	0.325 and -0.335 e $Å^{-3}$

Table 2. Crystal data and structure refinement for (1*S*2*R*)-10a.

Identification code	(1*S*2*R*)-10a
Empirical formula	C21 H32 N4 O7
Formula weight	452.51
Temperature	293(2) K
Wavelength	0.71073 Å
Crystal system, space group	Tetragonal, P4(3)2(1)2
Unit cell dimensions	a = 10.6505(7) Å α = 90°. b = 10.6505(7) Å β = 90°. c = 43.402(4) Å γ = 90°.
Volume	4923.3(6) $Å^3$
Z, Calculated density	8, 1.221 Mg/m^3
Absorption coefficient	0.092 mm^{-1}
F(000)	1936
Crystal size	0.63 x 0.60 x 0.24 mm
Theta range for data collection	1.97 to 25.00 deg.
Limiting indices	-12<=h<=12, -12<=k<=12, -51<=l<=51
Reflections collected / unique	34716 / 4339 [R(int) = 0.0362]
Completeness to theta = 25.00	99.7 %
Absorption correction	Multiscan
Max. and min. transmission	0.9786 and 0.9438
Refinement method	Full-matrix least-squares on F^2
Data / restraints / parameters	4339 / 0 / 317
Goodness-of-fit on F^2	1.370
Final R indices [I>2sigma(I)]	R1 = 0.0733, wR2 = 0.1537
R indices (all data)	R1 = 0.0746, wR2 = 0.1543
Absolute structure parameter	0(2)
Largest diff. peak and hole	0.201 and -0.161 e $Å^{-3}$

Table 3. Crystal data and structure refinement for(1*R*2*S*)-10b.

Identification code	(1R,2S)-10b
Empirical formula	C21 H32 N4 O7
Formula weight	452.51
Temperature	293(2) K
Wavelength	0.71073 Å
Crystal system, space group	Tetragonal, P4(3)2(1)2
Unit cell dimensions	a = 10.6483(4) Å α = 90° b = 10.6483(4) Å β = 90° c = 43.318(3) Å γ = 90°
Volume	4911.7(4) $Å^3$
Z, Calculated density	8, 1.224 Mg/m^3
Absorption coefficient	0.092 mm^{-1}
F(000)	1936
Crystal size	0.66 x 0.33 x 0.11 mm
Theta range for data collection	1.88 to 25.00 deg.
Limiting indices	-12<=h<=12, -12<=k<=8, -44<=l<=51
Reflections collected / unique	24647 / 4333 [R(int) = 0.0425]
Completeness to theta = 25.00	99.8 %
Absorption correction	Multiscan
Max. and min. transmission	0.9903 and 0.9416
Refinement method	Full-matrix least-squares on F^2
Data / restraints / parameters	4333 / 0 / 326
Goodness-of-fit on F^2	1.123
Final R indices [I>2sigma(I)]	R1 = 0.0537, wR2 = 0.1164
R indices (all data)	R1 = 0.0693, wR2 = 0.1224
Absolute structure parameter	1.1(15)
Largest diff. peak and hole	0.220 and -0.125 e $Å^{-3}$

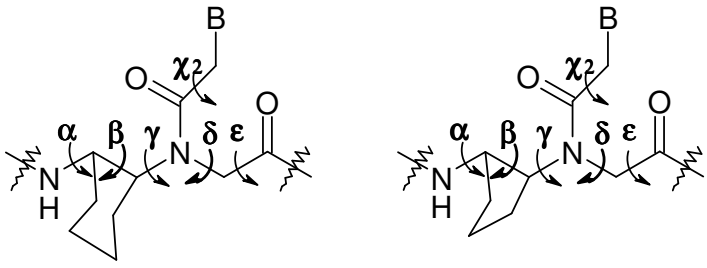

***ch*PNA** ***cp*PNA**

Table 4. Dihedral angles (°) in PNA and PNA:DNA/RNA complexes

Compound	α	β	γ	δ	χ_1	χ_2
PNA_2:DNA[9a]	-103	73	70	93	1	-175
PNA:DNA[9b]	105	141	78	139	-3	151
PNA:RNA[9c]	170	67	79	84	4	-171
*ch*PNA(1*S*,2*R*)*	128	-63	76	119	1.02	-175
*ch*PNA(1*R*,2*S*)*	-129	66	-78	-119	-0.87	174
*cp*PNA(1*S*,2*R*)*	84	-24	86	90	0.89	165
*cp*PNA(1*R*,2*S*)*	-84	25	-86	-90	1.2	-165

* dihedral angles from monomer crystal structures.: *ch*PNA, *cp*PNA

temperature. In contrast, though the same solvent system was used as in the case of *ch*PNA monomers for the crystallization, there were no solvent molecules in the crystals of *cp*PNA monomers. The torsion angles **β** as deduced from the X-ray crystal structures for **10a** (1*S,*2*R*) and **10b** (1*R*,2*S*) are –24° and +25° respectively (Table 4), which are much less than that found in PNA_2:DNA and PNA:RNA complexes and *cis*-cyclohexyl systems and are in opposite signs as expected for the enantiomeric pairs. In solution, the tertiary amide bond in PNA is known to exist as a rotameric mixture.[106-108] In the present structures, the amide bond is *trans* with carbonyl pointing towards the *C*-terminus, similar to that previously seen in cyanuryl PNA monomer[174] and to that seen in the recently reported crystal structure of the D-lysine based chiral PNA-DNA duplex.[109] The crystal structure data also shows pseudoaxial-psuedoequatorial dispositions for the *cis*-1,2-

substituents in (1*S*,2*R*/1*R*,2*S*)-cyclopentyl PNA monomers, with the bulky substituent carrying the nucleobase directed into a pseudo-equatorial position.

3.3.6 Hydrolysis of *cp*PNA monomer esters.

To synthesize the *cp*PNA oligomers, the monomer esters were hydrolysed to get amino group protected free acid. The *cp*PNA thymine monomer ethyl esters **10a** and **10b** were subjected to ester hydrolysis using very mild base 0.5 M LiOH in THF:Water. The reaction mixture was acidified to pH 3.0 and extracted to ethyl acetate. The organic solvent was evaporated to afford free acids **11a** and **11b** in quantitative yields (Scheme 4). This hydrolysis was done under mild condition to avoid racemization.

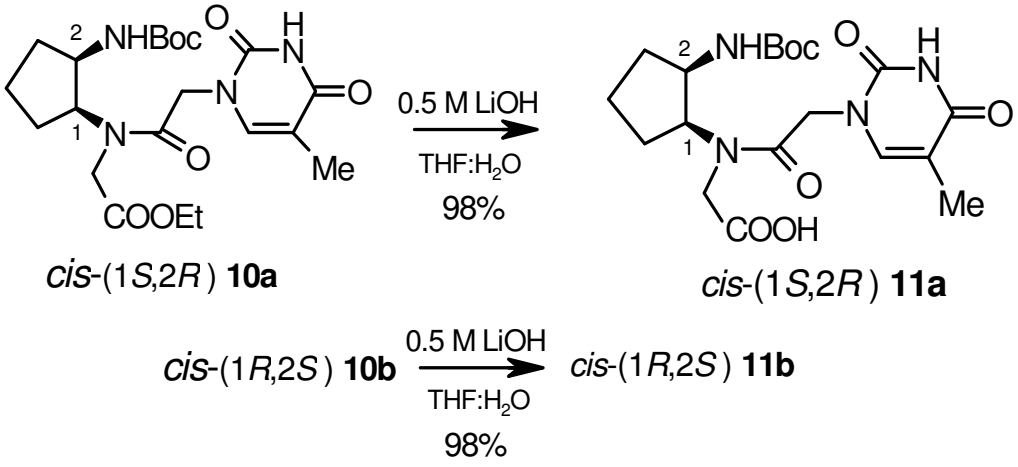

Scheme 4. Hydrolysis of ethyl esters of *cp*PNA monomers

3.3.7 Synthesis of *aeg*PNA, *cp*PNA-*aeg*PNA chimeras and *cp*PNA oligomers.

MBHA resin (4-methyl –benzhydryl amine resin) was used as the solid support on which the oligomers were built and the monomers were coupled by *in situ* activation with HBTU / HOBt.[172] In the synthesis of all oligomers, orthogonally protected (*Boc*/Cl-Cbz) L-lysine was selected as the *C*-terminal spacer-amino acid and it is linked to the resin through amide bond. The amine content on the resin was determined by the picrate

assay and found to be 0.85 mmol/g and the loading was suitably lowered to approximately 0.250 mmol/g by partial acetylation of amine content using calculated amount of acetic anhydride. The amount of free -NH_2 groups on the resin available for coupling was again estimated before starting synthesis.[185,186] The PNA oligomers were synthesized using repetitive cycles (Figure-8), each comprising the following steps:

(i) Deprotection of the *N*-*t*-Boc group using 50% TFA in CH_2Cl_2.

(ii) Neutralization of the trifluoroacetate salt of amine with diisopropyl ethylamine (DIPEA) to liberate the free amine.

(iii) Coupling of the free amine with the free carboxylic acid group of the incoming monomer (3 to 4 equivalents). The coupling reaction was carried out in DMF/ DMSO with HBTU a coupling reagent in the presence of DIPEA and HOBt as catalysts. The deprotection of the *N*-*t*-Boc protecting group and the coupling reactions were monitored by Kaiser's test.[187] The *t-Boc*-deprotection step leads to a positive kaiser's test, in which the resin beads as well as the solution are blue in color (Rheumann's purple). On the other hand, upon completion of the coupling reaction leads to negative Kaiser's test is negative, the resin beads remaining colorless.

(iv) Capping of the unreacted amino groups using Ac_2O / Pyridine in CH_2Cl_2 in case coupling does not go to completion. Figure 8 represents a typical solid phase peptide synthesis cycle.

The modified *cis*-(1*S*,2*R*/1*R*,2*S*)-aminocyclopentylglycyl thymine monomers **11a** and **11b** were incorporated into PNA sequences using Boc chemistry on L-lysine-derivatized (4-methylbezhydryl)amine (MBHA) resin as reported before, using HBTU/HOBt/DIEA in DMF as the coupling reagent.[173] Various homothymine PNA oligomers (**12**-**20**, Table 5) incorporating modified monomers at the middle (**14** and **17**),

N-terminus (**15** and **18**), *C*-terminus (**13** and **16**) and over the entire sequence (homooligomers **19**, **20**) were synthesized in order to study their triplex formation and stability with DNA/RNA. In order to study the duplex formation potential and in particular DNA/RNA discrimination of the *cp*PNA monomeric units, it was imperative to synthesize mixed sequences incorporating both, purines and pyrimidines. Mixed sequences *aeg*PNA **21**, *cp*PNA **22** and *cp*PNA **23** were also synthesized by incorporating *aeg*PNA (A/G/C/T) monomers and *cp*PNA (T) monomers (Table 5). The oligomers were cleaved from the resin using 'low-high TFMSA' procedure[191] followed by RP-HPLC purification and characterized by mass spectrometry (MALDI-TOF).

Cleavage of the PNA oligomers from the Solid Support: The oligomers are cleaved from the solid support, using strong acid trifluoromethane sulphonic acid (TFMSA) in the presence of trifluoro acetic acid (TFA) ('Low, High TFMSA-TFA

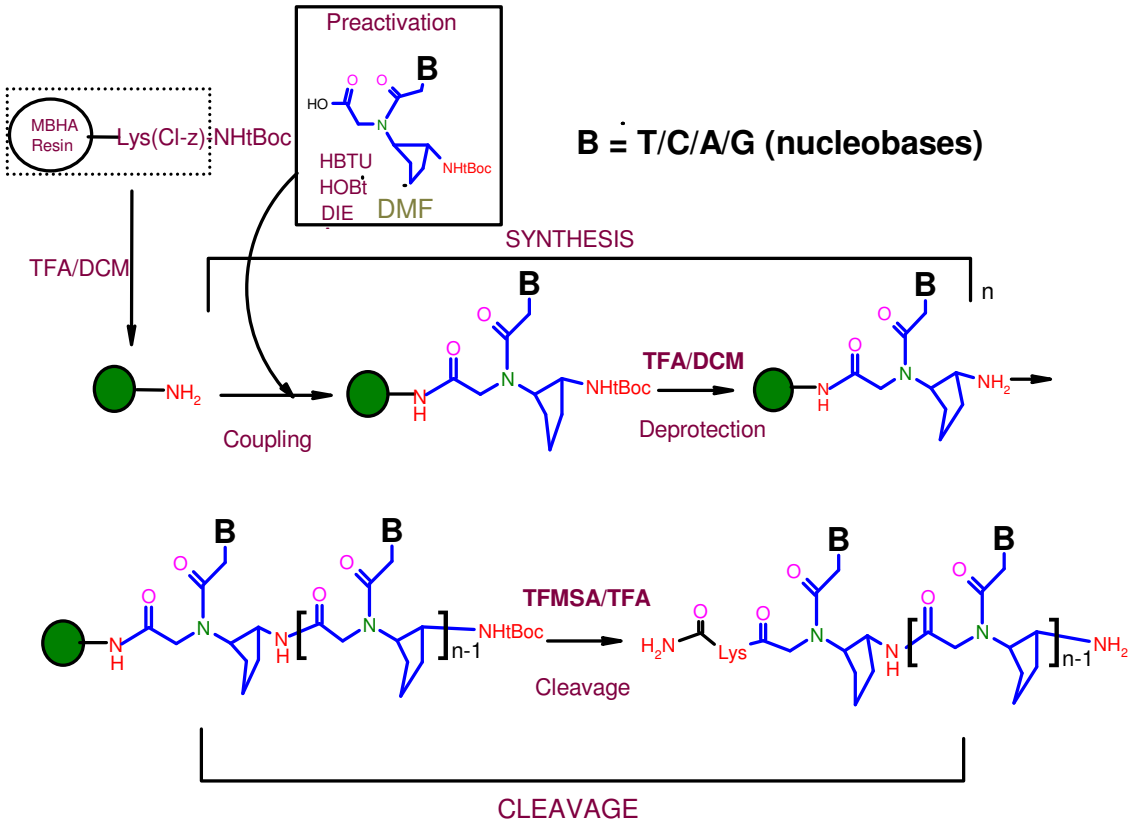

Figure-8. Solid phase peptide Synthesis

Table 5. PNA sequences synthesized in the present study

Entry	Sequnce code	PNA Sequences
		Homothymine sequences
1	*aeg*PNA **12**	H-T T T T T T T T -LysNH_2
2	*cp*PNA **13**	H-T T T T T T T t_{SR} -LysNH_2
3	*cp*PNA **14**	H- T T T t_{SR} T T T T -LysNH_2
4	*cp*PNA **15**	H- t_{SR} T T T T T T T -LysNH_2
5	*cp*PNA **16**	H- T T T T T T T t_{RS}-LysNH_2
6	*cp*PNA **17**	H- T T T t_{RS} T T T T -LysNH_2
7	*cp*PNA **18**	H- t_{RS} T T T T T T T -LysNH_2
8	*cp*PNA **19**	H-(t t t t t t t t)$_{SR}$ -LysNH_2
9	*cp*PNA **20**	H-(t t t t t t t t)$_{RS}$ -LysNH_2
		Mixed Sequences
6	*aeg*PNA **21**	H-G T A G A T C A C T-LysNH_2
7	*cp*PNA **22**	H-G t_{SR} A G A t_{SR} C A C t_{SR}-LysNH_2
8	*cp*PNA **23**	H-G t_{RS} A G A t_{RS} C A C t_{RS}-LysNH_2

A/G/C/T = *aeg*PNA Adenine/Guanine/Cytosine/Thymine monomers, t_{SR} = (1*S*,2*R*)-cpPNA Thymine monomer, t_{RS} = (1*R*,2*S*)-*cp*PNA Thymine monomer.

method"),[191] which yields oligomer with amide at their *C*-terminus. The synthesized PNA oligomers were cleaved from the resin (oligomer attached to L-lysine derivatized MBHA resin) using this procedure to obtain sequences bearing L-lysine-amide at their C-termini (Table 5). A cleavage time of 2-2.5 h at room temperature was found to be optimum. The side chain protecting groups are also cleaved during this cleavage process. After cleavage reaction, the oligomer was precipitated from methanol with dry diethyl ether.

Purification of the PNA Oligomers: All the cleaved oligomers were subjected to initial gel filtration. The purity of the so obtained oligomers were checked by analytical RP HPLC (C18 column, CH_3CN:H_2O system), which shows more than 65-78% purity. These were subsequently purified by reverse phase HPLC on a semi preparative C18 column. The purity of the oligomers was again ascertained by analytical RP-HPLC and

HPLC profile for *cp*PNA **13**

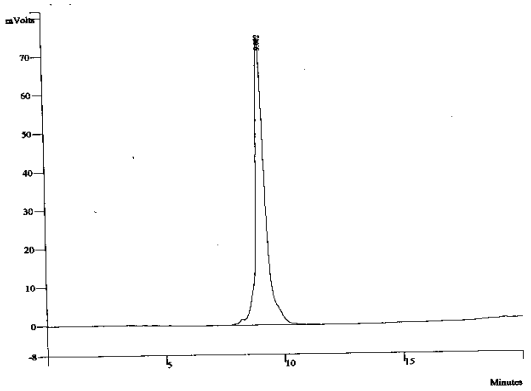

Peak No	Result ()	Ret Time (min)	Peak Area (counts)	Width 1/2 (sec)
1	100.0000	9.082	2109067	23.9
	100.0000		2109067	

HPLC profile for *cp*PNA **14**

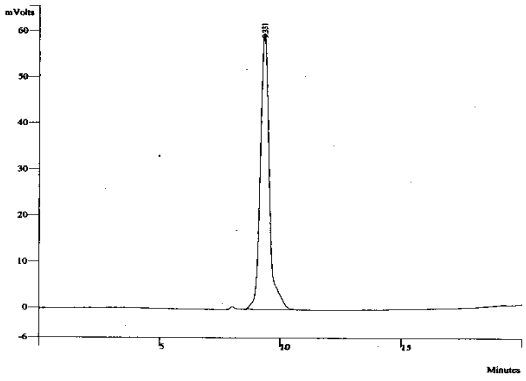

Peak No	Result ()	Ret Time (min)	Peak Area (counts)	Width 1/2 (sec)
1	100.0000	9.331	1561557	23.1
	100.0000		1561557	

HPLC profile for *cp*PNA **15**

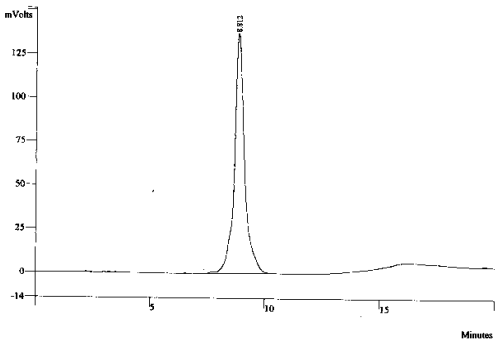

Peak No	Result ()	Ret Time (min)	Peak Area (counts)	Width 1/2 (sec)
1	100.0000	8.812	4282007	24.3
	100.0000		4282007	

HPLC profile for *cp*PNA **16**

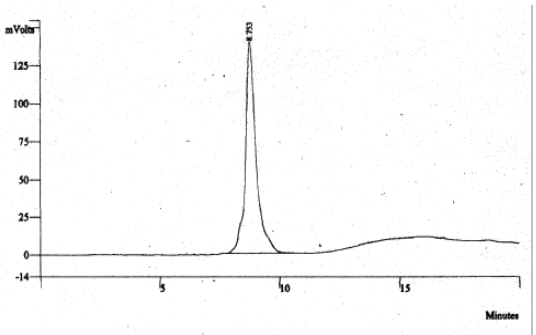

Peak No	Result ()	Ret Time (min)	Peak Area (counts)	Width 1/2 (sec)
1	100.0000	8.753	4364762	24.3
	100.0000		4364762	

HPLC profile for *cp*PNA **17**

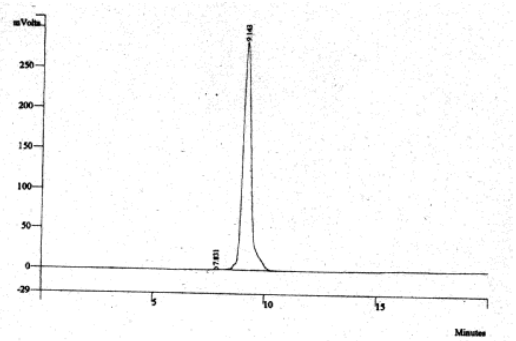

Peak No	Result ()	Ret Time (min)	Peak Area (counts)	Width 1/2 (sec)
1	0.4341	7.831	32067	8.6
2	99.5659	9.143	7355399	23.0
	100.0000		7387466	

HPLC profile for *cp*PNA **18**

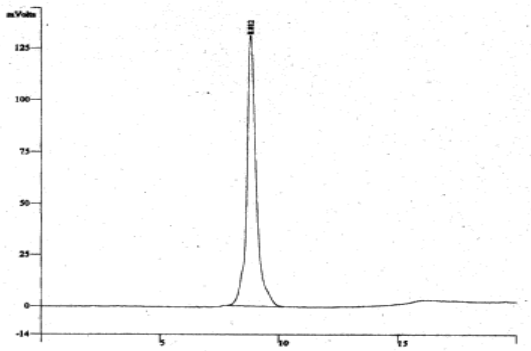

Peak No	Result ()	Ret Time (min)	Peak Area (counts)	Width 1/2 (sec)
1	100.0000	8.812	3652684	22.4
	100.0000		3652684	

Figure 9a. Reverse phase HPLC profiles for *cp*PNAs. (For HPLC conditions, see experimental section)

their integrity was confirmed by MALDI-TOF mass spectrometric analysis (see Appendix). Some representative HPLC profiles and mass spectra are shown in Figures 9 (Table 6).

Table 6. HPLC and MALDI-TOF mass spectral analysis of modified PNAs.

Entry.	PNA Strand	Retention, Time (mins), HPLC	Calculated MW (mol.formula)	Measured MW[a]
1	*aeg*PNA **12**	8.21	2274.0 ($C_{94}H_{126}N_{34}O_{34}$)	2279.0 $[M+5H]^+$
2	*cp*PNA **13**	9.08	2314.0 ($C_{97}H_{130}N_{34}O_{34}$)	2320.0 $[M+6H]^+$
3	*cp*PNA **14**	9.33	2314.0 ($C_{97}H_{130}N_{34}O_{34}$)	2321.0 $[M+7H]^+$
4	*cp*PNA **15**	8.81	2314.0 ($C_{97}H_{130}N_{34}O_{34}$)	2321.0 $[M+7H]^+$
5	*cp*PNA **16**	8.75	2314.0 ($C_{97}H_{130}N_{34}O_{34}$)	2316.0 $[M+2H]^+$
6	*cp*PNA **17**	9.14	2314.0 ($C_{97}H_{130}N_{34}O_{34}$)	2321.0 $[M+7H]^+$
7	*cp*PNA **18**	8.81	2314.0 ($C_{97}H_{130}N_{34}O_{34}$)	2321.0 $[M+7H]^+$
8	*cp*PNA **19**	13.36	2594.0 ($C_{118}H_{158}N_{34}O_{34}$)	2596.0 $[M+2H]^+$
9	*cp*PNA **20**	13.41	2594.0 ($C_{118}H_{158}N_{34}O_{34}$)	2596.0 $[M+2H]^+$
10	*aeg*PNA **21**	10.50	2852.0 ($C_{114}H_{147}N_{60}O_{31}$)	2853.0 $[M+H]^+$
11	*cp*PNA **22**	9.69	2972.0 ($C_{123}H_{159}N_{60}O_{31}$)	2974.0 $[M+2H]^+$
12	*cp*PNA **23**	9.73	2972.0 ($C_{123}H_{159}N_{60}O_{31}$)	2974.0 $[M+2H]^+$

3.3.8 Synthesis of Complementary Oligonucleotides

The DNA oligonucleotides **24**-**31** (Table 7) were synthesized on Applied Biosystems ABI 3900 high throughput DNA synthesizer using standard β-cyanoethyl phosphoramidite chemistry. The oligomers were synthesized in the 3' to 5' direction on polystyrene solid support, followed by ammonia treatment.[192] The oligonucleotides were desalted by gel filtration, their purity ascertained by RP HPLC on a C18 column to be more than 98% and were used without further purification in the biophysical studies of PNAs. The RNA oligonucleotides **29, 30** and **31** (Table 7) were obtained commercially.

HPLC profile for *cp*PNA **19** HPLC profile for *cp*PNA **20**

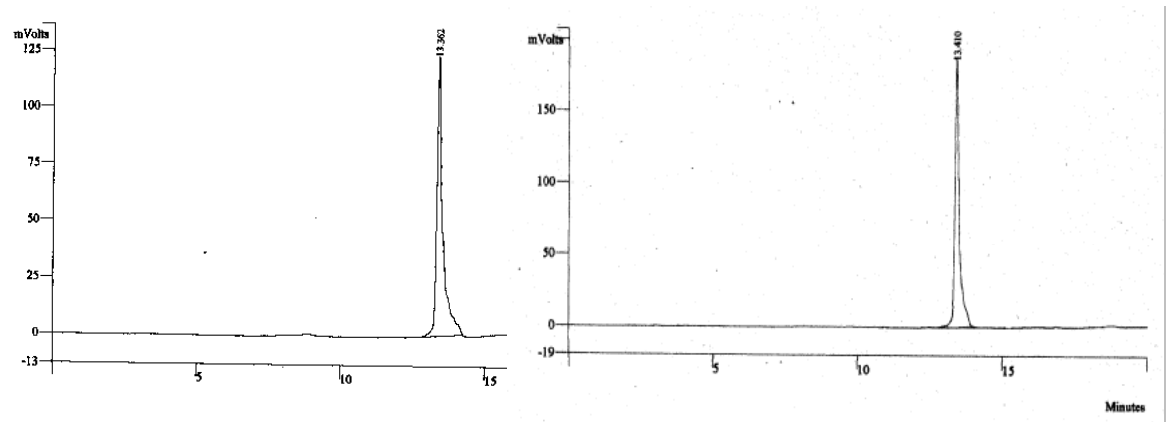

Peak No	Result ()	Ret Time (min)	Peak Area (counts)	Width 1/2 (sec)
1	100.0000	13.362	1761543	9.2
	100.0000		**1761543**	

Peak No	Result ()	Ret Time (min)	Peak Area (counts)	Width 1/2 (sec)
1	100.0000	13.410	2079059	8.6
	100.0000		**2079059**	

HPLC profile for *cp*PNA **22** HPLC profile for *cp*PNA **23**

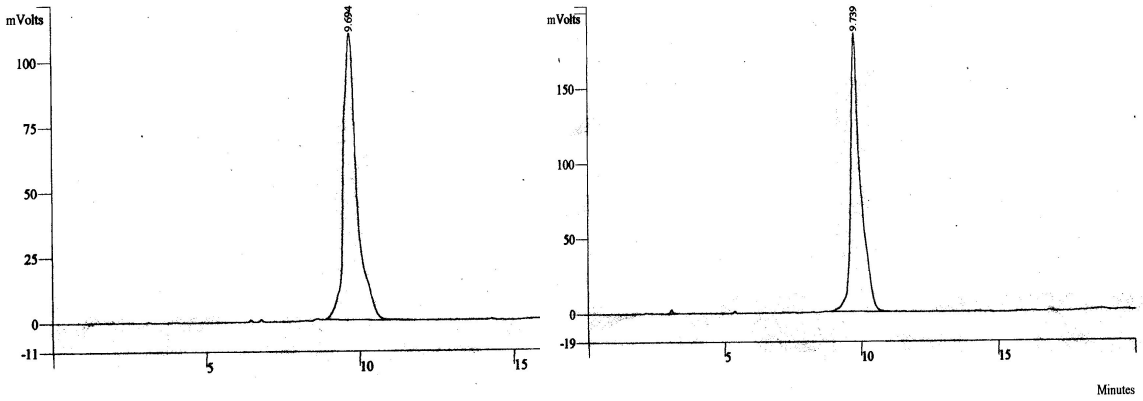

Peak No	Result ()	Ret Time (min)	Peak Area (counts)	Width 1/2 (sec)
1	100.0000	9.694	3326913	25.4
	100.0000		**3326913**	

Peak No	Result ()	Ret Time (min)	Peak Area (counts)	Width 1/2 (sec)
1	100.0000	9.739	4632538	19.2
	100.0000		**4632538**	

Figure 9b. RP HPLC profiles for *cp*PNAs.

3.3.9 Biophysical Studies of *cp*PNA:DNA/RNA Complexes

To investigate the binding selectivity, specificity and discrimination of *cp*PNAs towards complementary DNA and RNA, first the stoichiometry of the *cp*PNA:DNA was determined using Job's method.[193] The UV-melting studies were carried out with all the

synthesized oligomers and the T_m data was compared with the control *aeg*PNA T_8. The stability of the *cp*PNA duplexes with DNA/RNA was also studied. The CD spectra of single strands and corresponding complexes with complementary DNA were recorded. Finally the complexation of these *cp*PNAs to complementary DNA was confirmed by Gel electrophoretic shift assay.

Table 7. DNA/RNA Oligonucleotides used in the present work

Entry	Sequence code	Sequences	Type (corresponding PNA)
		DNA sequence 5' to 3'	
1	DNA **24**	C G C A A A A A A A A C G C	Match (**12**-**20**)
2	DNA **25**	C G C A A A A C A A A C G C	Mismatch (**12**-**20**)
3	DNA **26**	G C G T T T T T T T T G C G	Match (**25**)
4	DNA **27**	A G T G A T C T A C	Antiparallel (**21**-**23**)
5	DNA **28**	C A T C T A G T G A	Parallel (**21**-**23**)
		RNA sequences 5' to 3'	
6	RNA **29**	A G U G A U C U A C	Antiparallel (**21**-**23**)
7	RNA **30**	C A U C U A G U G A	Parallel (**21**-**23**)
8	RNA **31**	Poly rA	Match (**12**-**20**)

3.3.9.1 Binding Stoichiometry: CD and UV-mixing Curves

The stoichiometry of the paired strands may be obtained from the mixing curves, in which the optical property at a given wavelength is plotted as a function of the mole fraction of each strand from isodichoric and isoabsortive points.[193] The combination of absorption and CD spectra provides unambiguous determination of the complex formation and strand stoichiometry than is provided by absorption spectra alone.

Various stoichiometric mixtures of *cp*PNA **14** and DNA **24** were made with relative molar ratios of (*cp*PNA **14**:DNA **24**) strands of 0:100, 10:90, 20:80, 30:70, 40:60, 50:50, 60:40, 70:30, 80:20, 90:10, 100:0, all at the same strand concentration 2 μM in sodium phosphate buffer, 100 mM NaCl, 0.1 mM EDTA (10 mM, pH 7.2). The samples

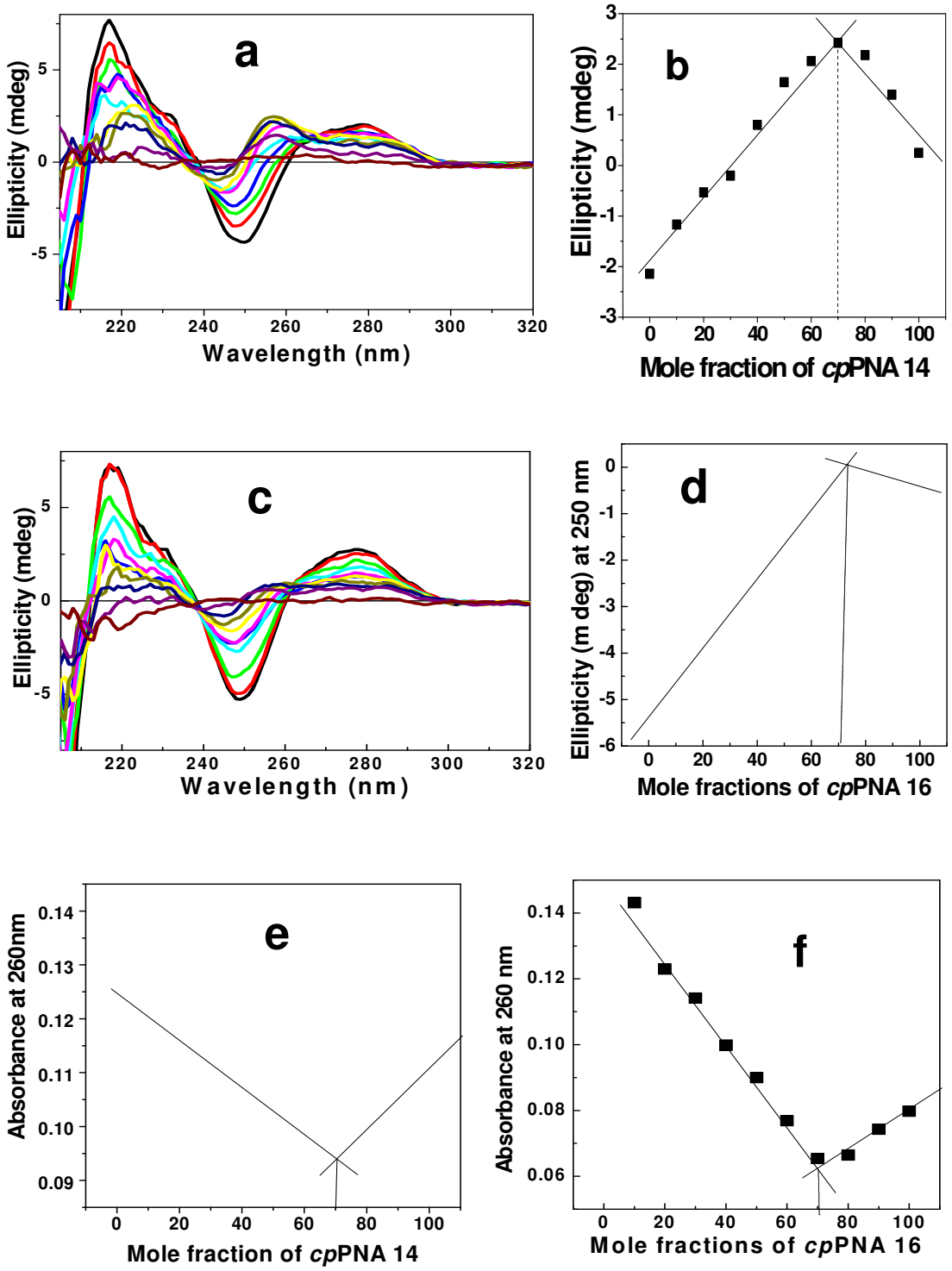

Figure 10. **a**) CD-curves for *cp*PNA **14** and the complementary DNA **33** d($CGCA_8CGC$) mixtures in the molar ratios of 0:100, 10:90, 20:80, 30:70, 40:60, 50:50, 60:40, 70:30, 80:20, 90:10, 100:0 (Buffer, 10 mM Sodium phosphate pH 7.0, 100 mM NaCl, 0.1 mM EDTA), **b**) CD-job plot corresponding to 255 nm, **e**) UV-job plot corresponding to above mixtures of different molar ratios, absorbance recorded at 260 nm and **c**, **d**, **f** are corresponding to that of *cp*PNA **16.**

with the individual strands were annealed and the CD spectra were recorded (Figure 10a). The CD spectra at different molar ratios shown a isodichoric point at around 265 nm (wavelength of equal CD magnitude). CD values around such wavelengths are useful for plotting mixing curves. This systematic changes in the CD spectral features upon variable stoichiometric mixing of PNA and DNA components can be used to generate Job's plot which also indicated a binding ratio of 2:1 for the cyclopentyl PNA:DNA complexes, confirming the formation of triplexes. The mixing curve in Figure 10b was plotted using the CD data at 260 nm from the spectra in Figure 10a, which indicated the formation of 2:1 triplex of *ch*PNA **14**:DNA **24**. Absorbance spectra were also recorded for the mixtures of *cp*PNA **14**:DNA **24** in different proportions as mention above. A mixing curve was plotted with absorbance at fixed wavelength (λ_{max} 260 nm) against mole fractions of *cp*PNA **14**. Figure 10c shows the change in λ_{max} observed for the mixtures of different molar fractions. There is a drastic shift in the λ_{max} value when the concentration of *cp*PNA **14** in the mixtures increased to 60 to 70%, absorbance further increased behind that proportions. This supports the formation of (*cp*PNA **14**)$_2$:DNA **24** triplexes.

Similarly, Job's plots were generated from stoichiometric mixtures of *cp*PNA **16** and DNA **24** with relative molar ratios of (*cp*PNA **16**:DNA **24**) strands of 0:100, 10:90, 20:80, 30:70, 40:60, 50:50, 60:40, 70:30, 80:20, 90:10, 100:0, both from CD (recorded at 10^{o}C) and UV-absorbance method. A PNA:DNA 2:1 stoichiometry for complex formation was obtained, confirming the formation of *cp*PNA$_2$:DNA triplex (Figure 10d-f).

3.3.9.2 CD spectroscopic studies of PNA:DNA complexes

PNA being non chiral, does not show any CD signatures. However, PNA:DNA complexes exhibit characteristic CD signatures due to chirality induced by DNA

component. It is known that formation of PNA triplexes[109] is accompanied by appearance of positive CD bands at 258 nm and 285 nm that are not present in DNA. The presence of chiral centers in cyclopentyl PNAs should further influence the CD patterns of the derived PNA:DNA triplexes. Figure 11 shows the CD spectra of complexes of *cp*PNAs **13-20** with DNA **24.** The single stranded cyclopentyl PNAs (**13**-**18**) show weak CD bands in the 250-290 nm region (Figure 11A and 11B) and all *cp*PNA:DNA triplexes show the expected positive bands at 258 and 285 nm. The relative ratios of 258/285 nm are different for the cyclopentyl PNA:DNA triplexes as compared to the control PNA:DNA triplex. These results imply that the cyclopentyl modifications alter base stacking patterns in PNA:DNA complexes. Systematic changes in the CD spectral features also occur in continuous variation mixing of *cp*PNA and DNA components to

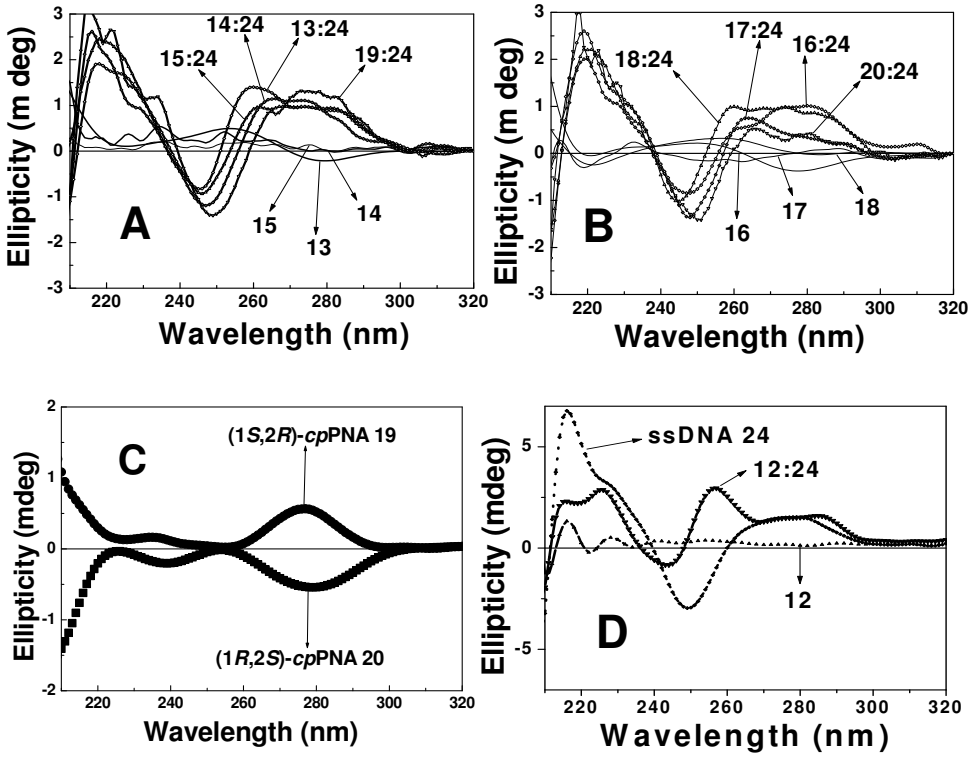

Figure 11. A-**D**: CD spectra of *aeg*PNA **12**, *cp*PNA **13**, *cp*PNA **14**, *cp*PNA **15**, *cp*PNA **16**, *cp*PNA **17**, *cp*PNA **18**, *cp*PNA **19**, *cp*PNA **20** and corresponding *cp*PNA:DNA **24** triplexes. (Buffer, 10 mM Sodium phosphate pH 7.0, 100 mM NaCl, 0.1 mM EDTA, 20°C)

generate Job's plot for determining the binding ratio which corresponded to 2:1 for the cyclopentyl PNA:DNA complexes. Fully modified single stranded *cp*PNAs containing (1*S*,2*R*)- or (1*R*,2*S*)- cyclopentyl thymines show weak but distinct CD spectra (Figure 11C), which are near mirror images of each other and similar to that of monomers (Figure 7d).

The CD profiles of *cp*-PNA:DNA duplexes (Figure 12A) show a higher intensity positive band at 275 nm and a negative band (250nm). The CD profiles of *cp*-PNA:RNA duplexes (Figure 12B) consisting of a high intensity positive band (260-270 nm) and a low intensity negative band (245 nm) like that of *aeg*-PNA:RNA duplex, suggests a high degree of helical identity among the *aeg/cp*-PNA:RNA duplexes. The CD spectra of *cp*PNA **22** and *cp*PNA **23** show that there is no epimerization during the synthesis, because they are related as mirror image spectra, though exact mirror image spectra was not expected due to the presence of L-lysine at *C*-terminus. The CD features of *cp*-PNA:DNA duplexes are akin to their RNA complexes implying that *cp*-PNA:DNA duplexes can adopt a more RNA-like structure with higher stability. The larger elliptic intensities seen in *cp*-PNA:RNA duplexes are indicative of a better base stacking in these compared to *ch*-PNA:DNA duplexes. Due to the dominant CD contributions from

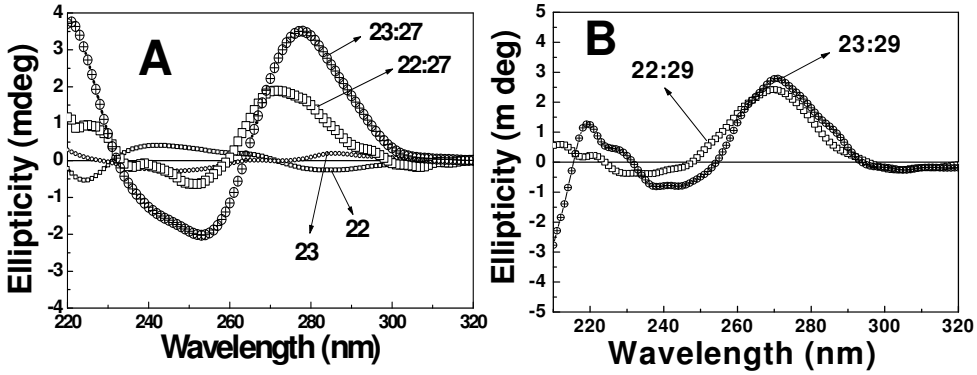

Figure 12. CD spectra of *cp*PNA **22**, *cp*PNA **23** and corresponding *cp*PNA:DNA **27** (**A**), *cp*PNA:RNA **29** (**B**) duplexes. (10 mM sodium phosphate buffer, pH=7, 100 mM NaCl, 0.1 m M EDTA, 20°C).

DNA/RNA strands in the complexes, differences due to *SR*/*RS* are not apparent, although the CD of the two enantiomeric *cp* monomers are mirror images.

3.3.9.3 UV-Melting studies of *cp*PNA:DNA/RNA complexes

The hybridization of various *cp*PNAs with complementary DNA **24** sequence was studied by temperature dependent UV-absorbance experiments. The stoichiometry for *aeg*-*cp*PNA:DNA complexation was established by Job's plot[193] of UV-absorbance data at 260 nm and found to be 2:1 (Figure 10). The thermal stabilities (T_m) of *aeg*-*cp*PNA_2:DNA triplexes (Table 8, Figure 13) were obtained for various *cp*PNAs with complementary DNA **24** and that having a single mismatch (DNA **25)** and poly rA to study the relative compatibility of the imposed stereochemistry constraints with deoxyribo and ribonucleic acids. In general, the PNA_2:DNA triplexes were found to be more stable for *cp*PNAs containing (1*S*,2*R*)- and (1*R*,2*S*)-cyclopentyl thymine units as compared to unmodified PNA. The *cp*PNA oligomers **14** and **17** having modifications in the center of the sequence showed contrasting binding stabilities as (1*S*,2*R*)-*cp*PNA **14** (entry 3) destabilized the complex with DNA **I** (ΔT_m = -23°C) whereas (1*R*,2*S*)-*cp*PNA

Table 8. UV-T_m of *cp*PNA:DNA/RNA triplexes*

Entry	PNA	DNA**24**	DNA **25** (ΔT_m)[a]	Poly rA
1	*aeg*PNA **12**, H-TTTTTTTT-$LysNH_2$	45.0	34.5 (10.5)	62.0
2	*Cp*PNA **13**, H-TTTTTTTt_{SR}-$LysNH_2$	51.0	27.8 (23.2)	73.5
3	*Cp*PNA **14**, H-TTTt_{SR}TTTT-$LysNH_2$	22.0	11.0 (11.0)	76.0
4	*Cp*PNA **15**, H-t_{SR}TTTTTTT-$LysNH_2$	44.5	26.4 (18.1)	66.0
5	*Cp*PNA **16**, H-TTTTTTTt_{RS}-$LysNH_2$	55.0	28.0 (27.0)	>85.0
6	*Cp*PNA **17**, H-TTTt_{RS}TTTT-$LysNH_2$	62.0	32.0 (30.0)	61.0
7	*Cp*PNA **18**, H-t_{RS}TTTTTTT-$LysNH_2$	48.7	27.8 (20.9)	69.0
8	*Cp*PNA **19**, H-(t t t t t t t t) $_{SR}$-$LysNH_2$	66.6	nd	>85.0
9	*Cp*PNA **20**, H-(t t t t t t t t) $_{RS}$-$LysNH_2$	72.0	nd	>85.0

*All values are an average of three independent experiments and accurate to within ± 0.5°. DNA **24,** d(CGCAAAAAAAACGC); DNA **25**, d(CGCAAAA*C*AAACGC). Buffer. Sodium phosphate (10 mM), pH 7.0 with 100 mM NaCl and 0.1 mM EDTA; nd, transition not detected; a, mismatch destabilization.

17 (entry 6) stabilized complex (ΔT = +17°C) in comparison to the control PNA **12** (entry 1). Thus a remarkable T_m difference of 40° was noticed between the two enantiomeric *cp*PNAs **14** and **17** in binding the complementary DNA. In case of *aeg-cp*PNAs (1*S*,2*R*) **13** (entry 2) and (1*R*,2*S*) **16** (entry 5) having single C-terminus modifications, both stabilized their complexes with DNA (ΔT = +6° and +10° respectively) as compared to *aeg*PNA **12,** with a mutual difference of only +4° between themselves. The N-terminus modified *aeg-cp*PNAs (1*S*,2*R*) **15** (entry 4) and (1*R*,2*S*) **18** (entry 7) showed T_ms almost comparable to the unmodified PNA, but lower compared to respective C-terminus modified PNAs.

Significantly, in contrast to singly modified analogues, the all-modified homo-oligomeric, homochiral *cp*PNAs (1*S,*2*R*)-**19** (entry 8) and (1*R,*2*S*)-**20** (entry 9) exhibited high thermal stabilities (ΔT_m =21° and +27°C, respectively) compared to the unmodified PNA **12**. The *cp*PNA sequence with one modification in the center with (1*S*,2*R*)-stereochemistry, **14**, largely destabilized the complex with DNA **24**. This could be a result of introduction of unfavored conformational discontinuity at the modification site. However, in the fully modified oligomer **19** with the same stereochemistry, the stability is regained perhaps due to the uniform conformational change over the entire backbone, without any sharp discontinuities. The singly and fully modified sequences with the other and probably favorable stereochemistry (1*R*,2*S*) in PNA sequences **17** and **20** show better binding affinity toward DNA **24**, suggesting that the effect of increased T_m could be additive (1.4°C per modification) from a single favorable modification to fully modified oligomer sequences.

Mismatch studies: The enhanced thermal stability observed for *aeg-cp*PNA and *cp*PNA complexes with DNA is not at the cost of losing base pairing specificities. This is

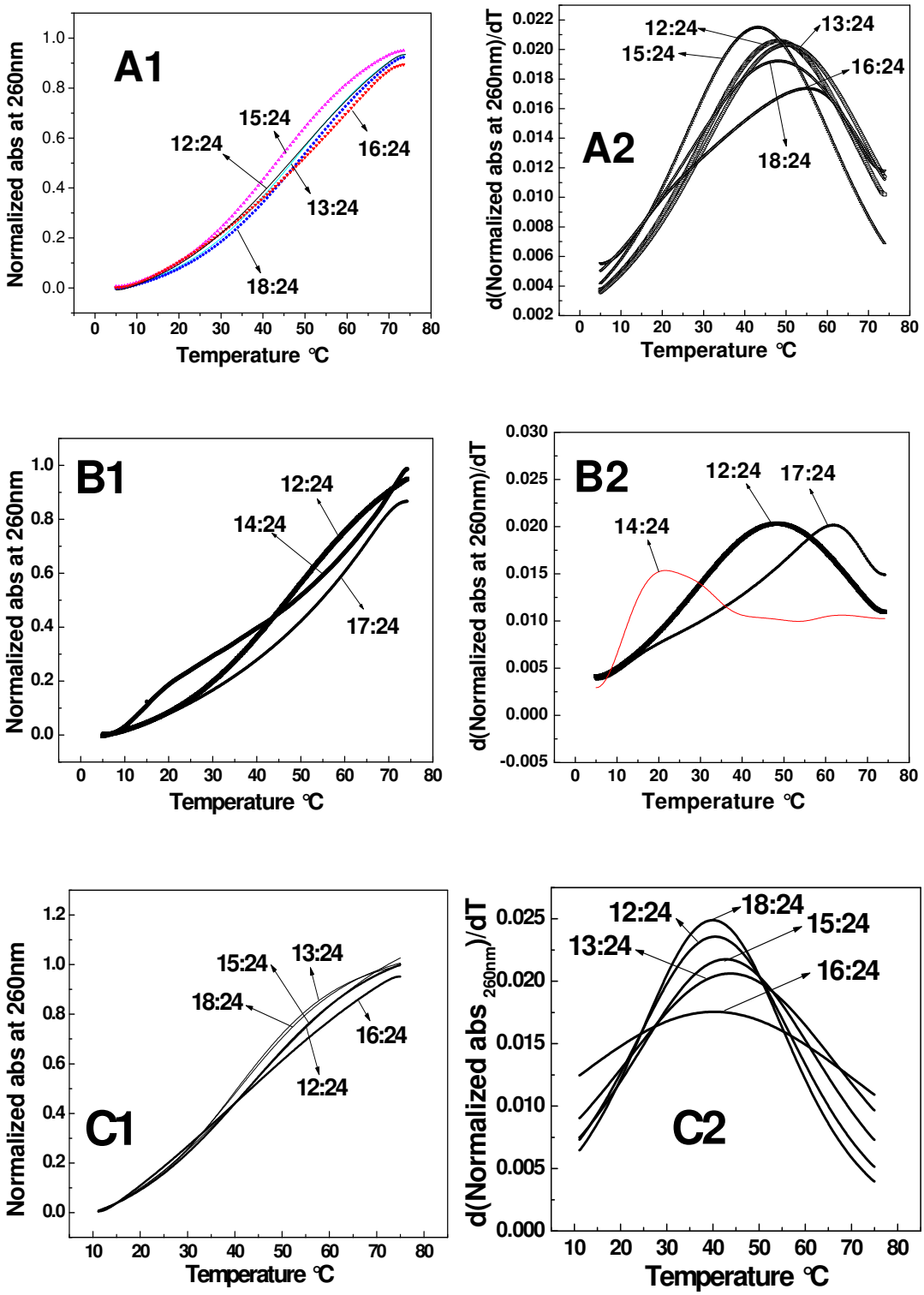

Figure 13a. **A1**, **B1**: Melting profiles for PNA:DNA triplexes of *aeg*PNA **12**, *cp*PNA **13** , *cp*PNA **14**, *cp*PNA **15**, *cp*PNA **16**, *cp*PNA **17** and *cp*PNA **18** with DNA **24** (heating). **C1**: Corresponding melting curves during cooling. **A2**-**C2**: Corresponding derivative curves. DNA 24 = 5' CGCAAAAAAAACGC 3'. (Buffer, 10 mM Sodium phosphate pH 7.0, 100 mM NaCl, 0.1 mM EDTA).

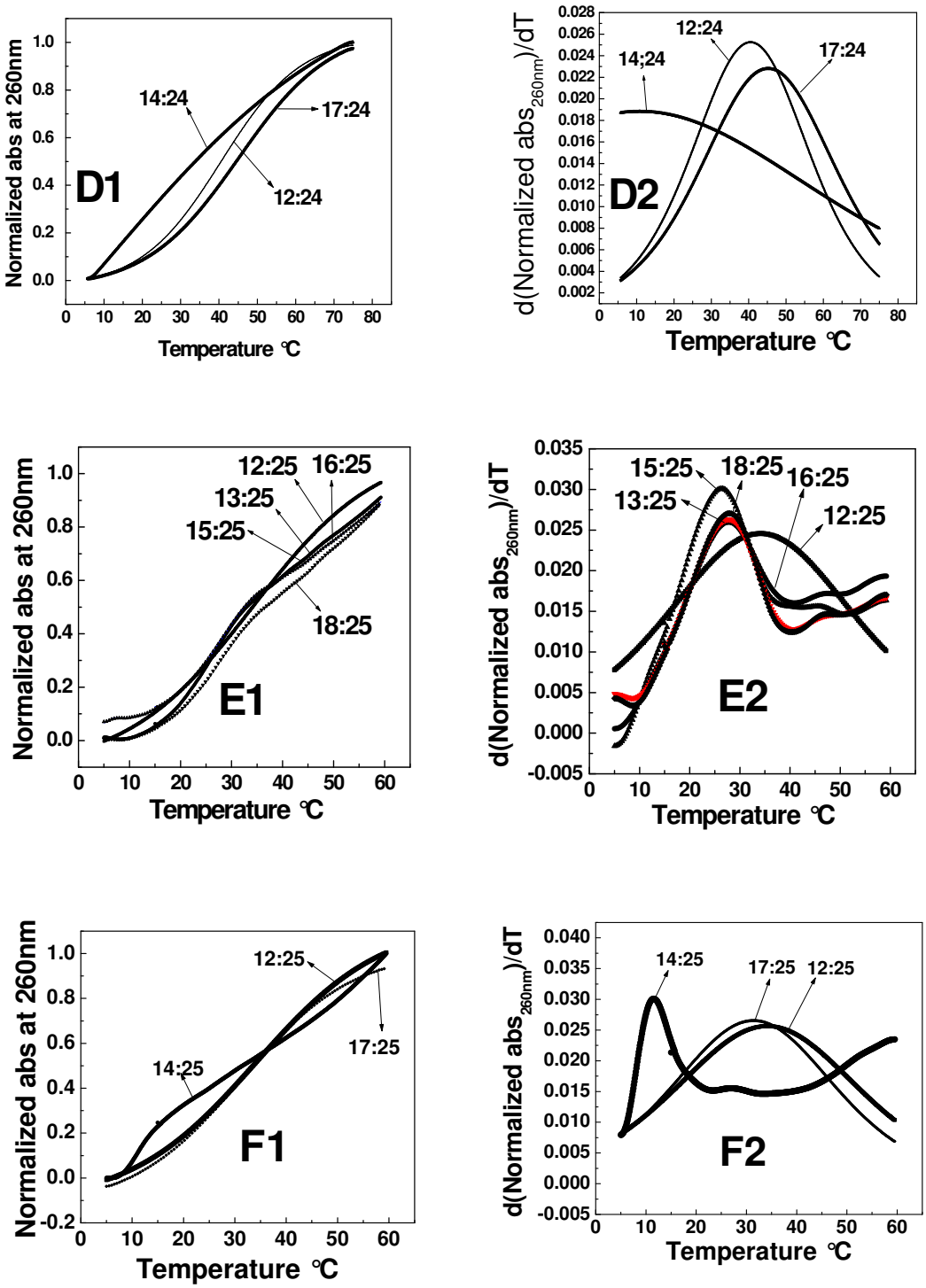

Figure 13b. **D1**: Melting profiles of *aeg*PNA **12**, *cp*PNA **14**, *cp*PNA **17** with DNA **24**, and **D2**: Corresponding derivative curves (cooling). **E1**, **F1**: Melting profiles for mismatch complexes of *aeg*PNA **12**, *cp*PNA **13**, *cp*PNA **14**, *cp*PNA **15**, *cp*PNA **16**, *cp*PNA **17**, *cp*PNA **18** with DNA **25** (mismatch). **E2**, **F2**: Corresponding derivative curves. DNA **24** = 5' CGCAAAAAAAACGC 3'; DNA **25** = 5' CGCAAAA*C*AAACGC 3' (mismatch). Buffer, 10 mM Sodium phosphate pH 7.0, 100 mM NaCl, 0.1 mM EDTA.

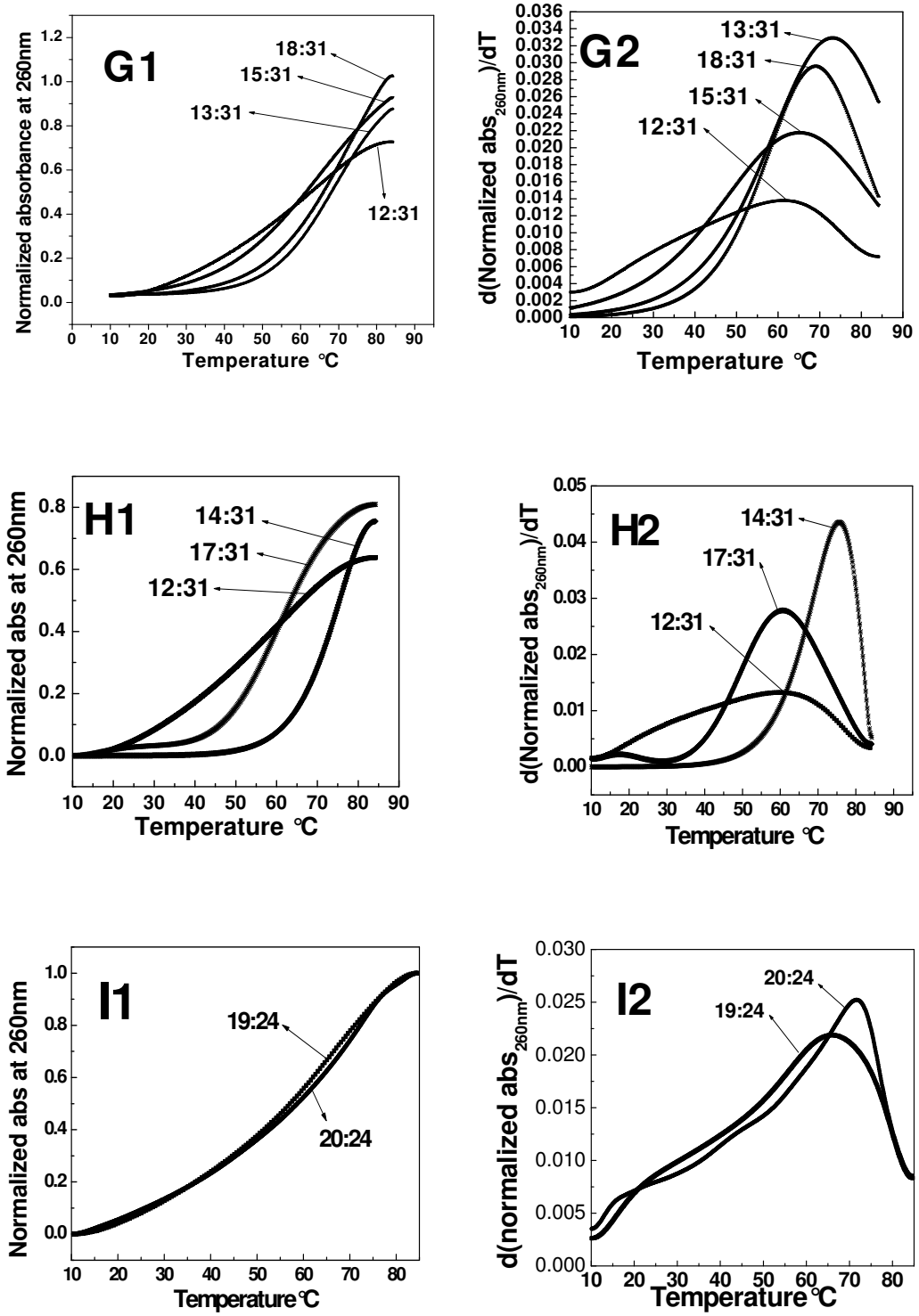

Figure 13c. **G1**, **H1**: Melting profiles for PNA:RNA complexes of *aeg*PNA **12**, *cp*PNA **13**, *cp*PNA **14**, *cp*PNA **15**, *cp*PNA **17** and *cp*PNA **18** with RNA **31**. **G2**, **H2**: Corresponding derivative curves. **I1**: Melting profiles of *cp*PNA **19**, *cp*PNA **20** with DNA **24** and **I2**: Corresponding derivative curves. (heating). RNA **31** = poly rA, DNA **24** = 5' CGCAAAAAAAACGC 3'. Buffer, 10 mM Sodium phosphate pH 7.0, 100 mM NaCl, 0.1 mM EDTA.

borne by data for their complexation with DNA **25** [dA_4CA_3] that carries a single mismatch at the middle position. The mismatch ΔT_m for control *aeg*PNA **12** was –10.5° (entry 1) while that for all *cp*PNAs were higher, except for (1*S*,2*R*) **14** which was as good. The mismatch destabilization was highest (-30°) for (1*R*,2*S*) **17** (entry 6) with-modification at the center. Other modified PNAs exhibited intermediate degrees of mismatch destabilization in the range 18-27°. The lower mismatch tolerance and higher binding affinities to matched complementary DNA **24** sequence reflects the sequence specific recognition of *cp*PNAs. The fully modified stereo oligomers **19** and **20** did not show any binding with mismatch DNA **25**. The complete inhibition of hybridization with fully modified sequences *cp*PNA **19** and *cp*PNA **20** with DNA **25** having a mismatch in the center of the sequence could be a result of mismatched hydrogen bonding in the center, in turn effecting steric incompatibility of fully modified sequences for DNA (mismatched) binding. The open-chain PNAs in other sequences do not impose the additional steric incompatibility and permit complex formation with DNA **25**, albeit reduced stability. In general, the (1*R*,2*S*)-cyclopentyl modified PNAs were better in binding and mismatch differentiation in complexing with complementary DNA.

In case of *aeg*-*cp*PNA complexation with poly rA, the presence of either *SR* or *RS* isomers at *C*/*N* terminus or internally, in general, stabilized the complexes compared to *aeg*PNA. The PNA oligomers **14** and **17**, modified at the center showed a reverse selectivity in binding to *aeg*-*cp*PNAs with **14** *SR* > **17** *RS* by 15°C as compared to binding with DNA **I** where **17** *RS* > **14** *SR* by 40°C. Unprecedented stabilization was observed for homo-oligomeric, homochiral **18** *SR*- and **19** *RS*- *cp*PNAs binding with poly rA, with no melting seen in range 5-85°C. The overall pattern of T_m values suggests that *cp*PNAs have high affinity to both RNA and DNA without much discrimination.

Thermal Stability of Duplexes: The thermal stability measurements of the duplexes (Table 9, Figure 14) formed between *cp*PNA **22** (entry 2) and *cp*PNA **23** (entry 3) with complementary DNA **27** strand (T_m= 77.1°C and 78.8°C respectively) indicate the enormous increase in the T_m (ΔT_m = +22°C and +24°C respectively). *cp*PNA **23**–DNA **27** duplex is slightly more stable than the *cp*PNA **22**-DNA **27** duplex (ΔTm = +2°C) (Table 9). More interestingly the modified mix backbone *cp*PNAs bind strongly compared to *aeg*PNA **21** (entry 4) to complementary RNA **29** (ΔT_m = 27 °C for *cp*PNA **22,** ΔT_m = >27 °C for *cp*PNA **23** and ΔT_m = 6°C for *cp*PNA **22,** ΔT_m = >6°C for *cp*PNA **23** between corresponding DNA and RNA). The *cp*PNA **23**:RNA **29** transition is not detected in 5-85°C heating range and will be >85°C, as confirmed by the decrease in T_m

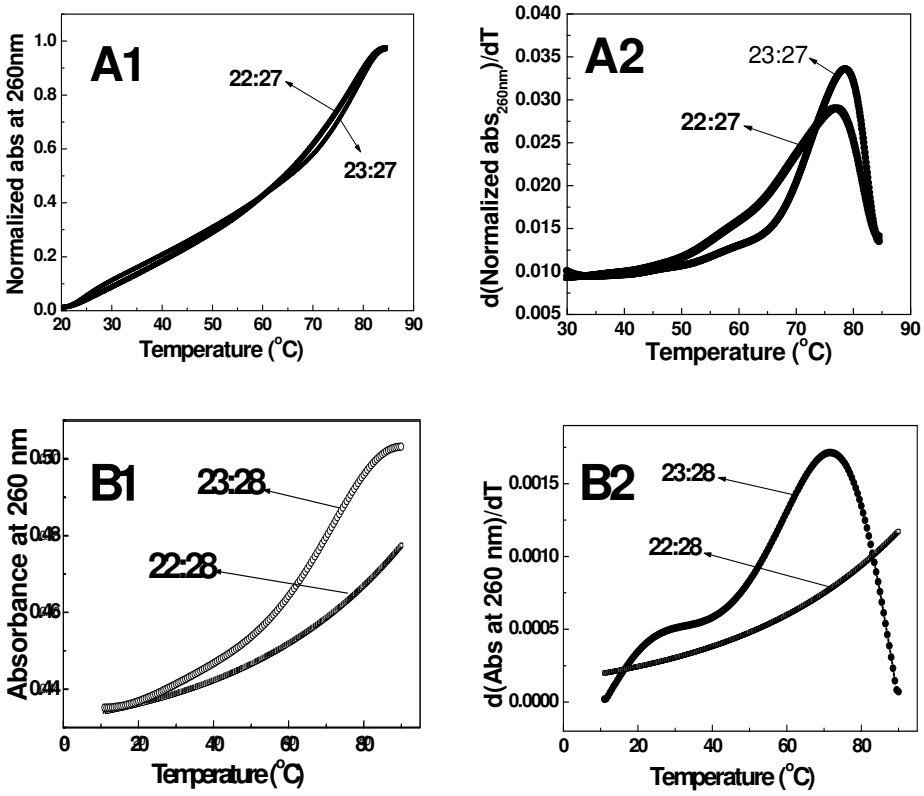

Figure 14a. Melting profiles for PNA:DNA duplexes of *cp*PNA **22**, *cp*PNA **23** with DNA **27** (**A1**), and DNA **28**. (**B1**). **A2**, **B2**: Corresponding derivative curves. DNA **27** = 5' AGTGATCTAC 3' (antiparallel); DNA **28** = 5' CATCTAGTGA 3' (parallel). Buffer, 10 mM Sodium phosphate pH 7.0, 100 mM NaCl, 0.1 mM EDTA.

Table 9. UV-T_m of *cp*PNA:DNA/RNA duplexes[a]

Entry	Duplexes (**antiparallel**)		Duplexes (**parallel**)	
	PNA:DNA	T_m (^{O}C)	**PNA:DNA**	T_m (^{O}C)
1	*aeg*PNA **21**:DNA **27**	55.0[b]	*aeg*PNA **21**:DNA **28**	40.0[b]
2	*cp*PNA **22**:DNA **27**	77.1	*cp*PNA **22**:DNA **28**	[c]
3	*cp*PNA **23**:DNA **27**	78.8	*cp*PNA **23**:DNA **28**	71.0
	PNA:RNA		**PNA:RNA**	
4	*aeg*PNA **21**:RNA **29**	55.4	*aeg*PNA **21**:RNA **30**	[c]
5	*cp*PNA **22**:RNA **29**	83.4	*cp*PNA **21**:RNA **30**	71.0
6	*cp*PNA **23**:RNA **29**	>85.0	*cp*PNA **23**:RNA **30**	84.0

[a]All values are an average of at least 3 experiments and accurate to within ± 0.5^{o}C. Buffer. Sodium phosphate (10 mM), pH 7.0 with 100 mM NaCl and 0.1 mM EDTA; [b]Measured by CD to avoid interference from thermal transitions of single stranded PNAs. A, T, G, C are *aeg*PNA bases, $\mathbf{t_{SR/RS}}$: *cp*-PNA-T (**4**, **5**); DNA **27**, 5'-AGTGATCTAC-3'(*ap*); RNA **29**, 5'-AGUGAUCUAC-3'(*ap*); DNA **28,** 5'-CATCTAGTGA-3'(*p*); RNA **30,** 5'-CAUCUAGUGA-3' (*p*). [c] A well-defined melting transition assignable to this complex could not be identified.

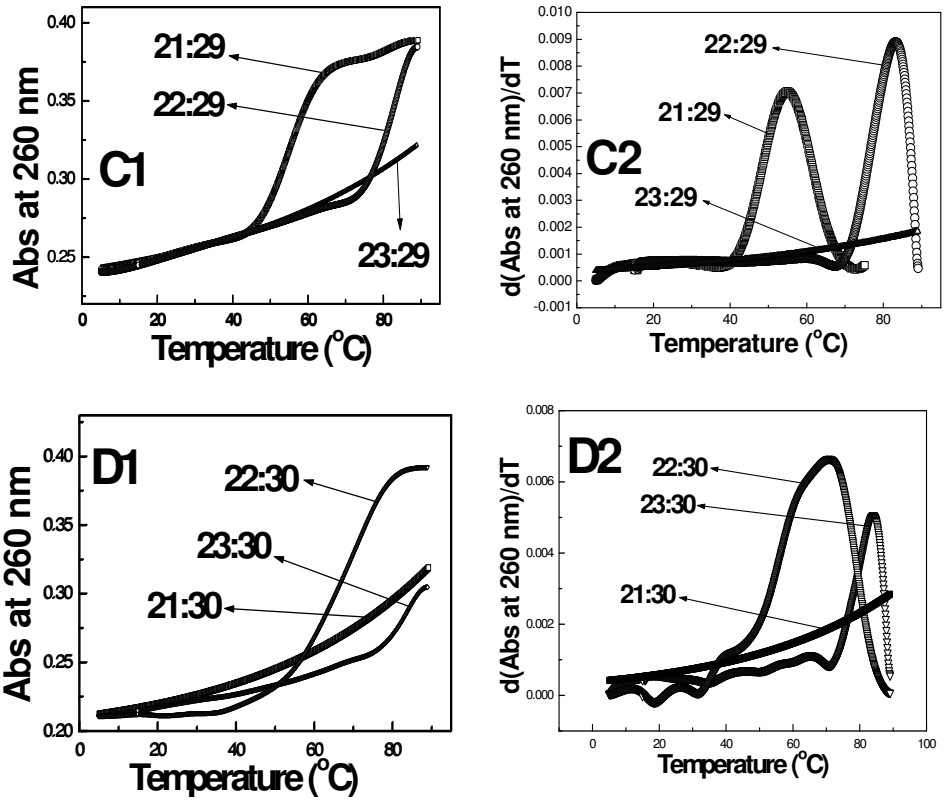

Figure 14b. Melting profiles for PNA:RNA duplexes of *cp*PNA **22**, *cp*PNA **23** with RNA **29** (**C1**), and RNA **30** (**D1**). **C2**, **D2**: Corresponding derivative curves. RNA **29** = 5' AGUGAUCUAC 3' (antiparallel); RNA **30** = 5' CAUCUAGUGA 3' (parallel). Buffer, 10 mM Sod. phosphate pH 7.0, 100 mM NaCl, 0.1 mM EDTA.

for parallel duplex (T_m = 80°C with RNA **30**, entry 6). But surprisingly, the binding preference reverses from homothymine PNAs to mix PNA. The *cp*PNA **23** showed low affinity to form parallel duplex with DNA **28** (ΔT_m = 8°C), while proper melting transition could not be assigned for *cp*PNA **22**:DNA **28**. The decreased melting temperature for *cp*PNA **22** (entry 5) and *cp*PNA **23** (entry 6) with parallel RNA **30** (T_m = 71°C and 84°C respectively) suggest that these *cp*PNAs prefer antiparallel mode of binding to complementary oligonucleotides.

3.3.9.4 Gel shift assay and competition binding experiments

Electrophoretic gel experiment[195] was used to establish the binding of modified PNAs to the complementary DNA **24** and mismatch DNA **25** (Figure 15). The various PNAs were individually mixed with DNA **24** in buffer (for conditions, see Figure 15 legend) and subjected to nondenaturing gel electrophoresis at 10°C and the bands were visualized on a fluorescent TLC background. The formation of PNA_2:DNA complexes was accompanied by the disappearance of the band due to single strand DNA **24** and

Electrophoretic gel shift assay

Equation. 1: 2*cp*PNA + DNA **24** = [(*cp*PNA)$_2$ + DNA **24**]
*cp*PNA-DNA triplex

Competitive binding Experiment

Equation. 2: 2*cp*PNA + [DNA **24** + DNA **26**] = [(*cp*PNA)$_2$ + DNA **24**] + DNA **26**
DNA complex; *ch*PNA-DNA triplex; displaced ss DNA T_8

*where cp*PNA = *SR-cpPNA* **13**, **14** and **15**
*RS-cp*PNA **16**, **17** and **18**

DNA **24** = 5' CGCAAAAAAAACGC 3'
DNA **26** = 5' GCGTTTTTTTTGCG 3'

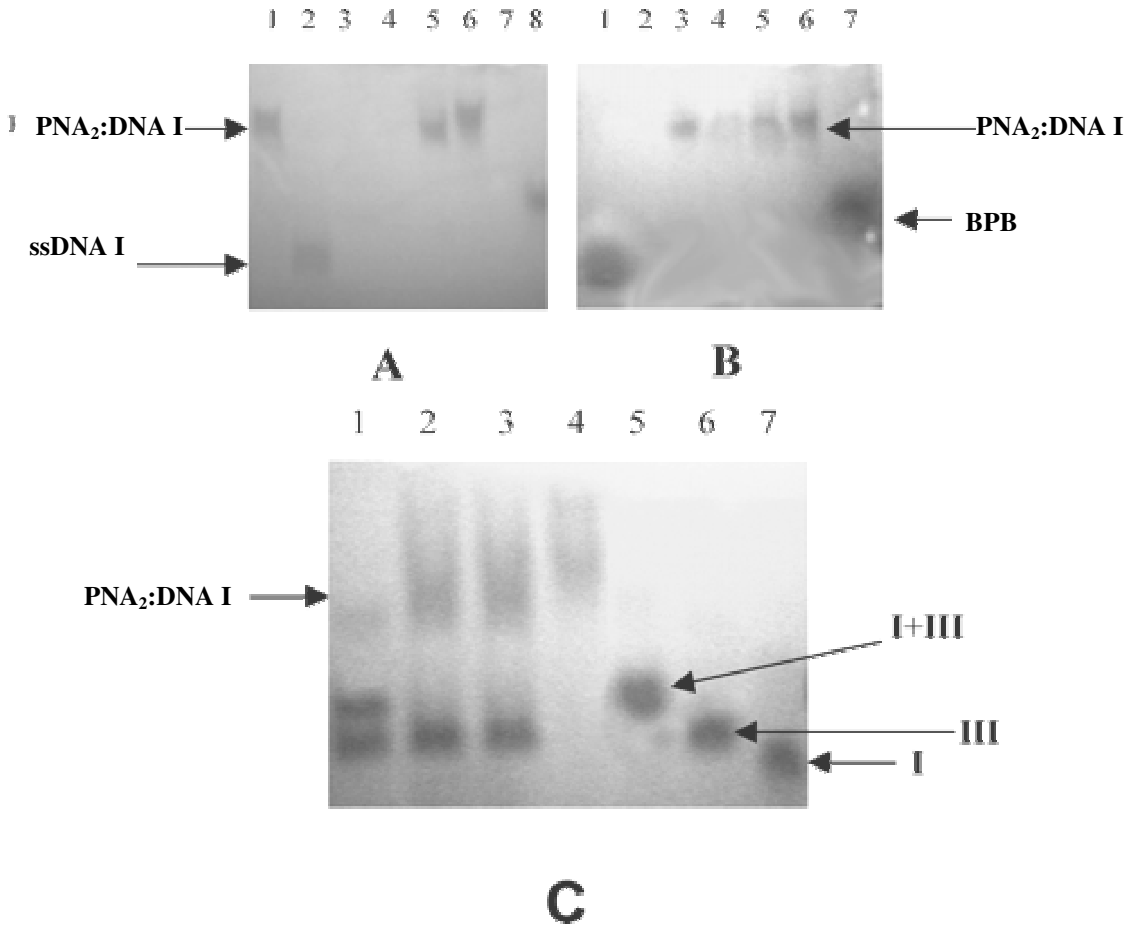

Figure 15. PNA:DNA Complexation. **A**: lane 1, *aeg*PNA **12** + DNA **I**; lane 2, ssDNA **I**; lane 3, ss*cp*PNA **12**; lane 4, ss*cp*PNA **14**; lane 5, *cp*PNA **14**:DNA **I**; lane 6, *cp*PNA **17** + DNA **I**; lane 7, ss*cp*PNA **17**; lane 8, marker bromophenol blue (BPB): **B**, lane 1, ssDNA **I**; lane 2, ss*cp*PNA **13**; lane 3, *cp*PNA **13** + DNA **I**; lane 4, *cp*PNA **15** + DNA **I**; lane 5, *cp*PNA **16** + DNA **I**; lane 6, *cp*PNA **18** + DNA **I**; lane 7, BPB. **C**: **Competition binding experiments**. Lane 1, DNA **I** + DNA **III** + *cp*PNA **14**; lane 2, DNA **I** + DNA **III** + *cp*PNA **15**; lane 3, DNA **I** + DNA **III** + *cp*PNA **17**; lane 4, DNA **I** + *cp*PNA **17**; lane 5, DNA duplex (**I** + **III**); lane 6, ssDNA **III**; lane 7, ssDNA **I**. Buffer, 0.5 X TBE, pH 8.0; DNA **I** = $CGCA_8CGC$ (DNA **24**), DNA **III** = $GCGT_8GCG$ (DNA **26**), BPB = bromophenol blue.

appearance of a lower migrating band of the complex. The singly modified PNAs **13**-**17** upon mixing with DNA **24** migrated about same as the unmodified PNA **12**:DNA **24** complex and much lower than that of DNA **24** (Figure 15A and 15B) clearly showing successful formation of *cp*PNA_2:DNA **24** triplexes. Under the conditions, the single stranded PNAs do not migrate from the well. The gel retardation experiments for singly modified *aeg*-*cp*PNAs with mismatch DNA **25** showed weaker and incomplete

complexation, as seen by presence of faster moving band due to unbound DNA **25** (Figure 16).

Competition binding: Competition binding experiments carried out by adding *aeg-cp*PNAs **15** or **17** separately to the DNA duplex (**23**:**26**) followed by annealing and gel electrophoresis (Figure 15C). Due to a higher stabilization of *aeg-cp*PNA:DNA **24** complexes compared with DNA:DNA duplex, the added PNA binds to the complementary DNA **24** in the DNA duplex, concomitantly releasing the DNA strand **26** (Figure 15C, Equation 2). This is clearly seen in the gel electrophoresis by the appearance of lower moving bands due to *aeg-cp*PNA:DNA **24** complex (Figure 15C, lanes 2 and 3), a faster moving band due to the released DNA strand **26** and the disappearance of the DNA (**24**:**26**) duplex band (as in lane 5). When the experiment is done with *aeg-cp*PNA**14**:DNA **24** complex that has a lower stability than DNA duplex, the competition binding is ineffective as seen by a weak band due to PNA:DNA complex and in efficient dissociation of DNA duplex **24:26** which is still persistent (Figure 15C, lane 1). Thus the modified *aeg-cp*PNAs are capable of successfully competing for binding with the complementary DNA **24** strand in a DNA duplex, just as in unmodified PNA.

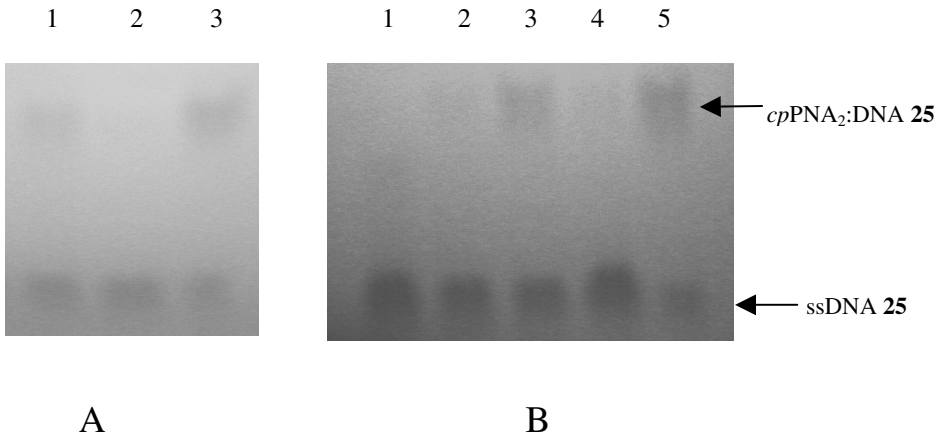

Figure 16. PNA:DNA (mismatch) complexation. **A.** lane 1, *cp*PNA **14** + DNA **II**; lane 2, ssDNA **25**; lane 3, *cp*PNA **17**+DNA **25**: **B.** lane 1, ssDNA **25**; lane 2, *cp*PNA **13**+DNA **25**; lane 3, *cp*PNA **15**+DNA **25**; lane 4, *cp*PNA **16**+DNA **25**; lane 5, *cp*PNA **18**+DNA **25**: DNA **25** = $CGCA_4CA_3CGC$.

3.3.9.5 Isothermal Titration Calorimetric analysis of the Thermodynamic parameters of *cp*PNA :DNA triplexes

Isothermal Titration Calorimetry (ITC): Isothermal titration calorimetry (ITC) is a thermodynamic technique that allows the study of the interactions of two species.[201] When these two species interact, heat is either generated or absorbed. By measuring these interaction heats, binding constants (K), reaction stoichiometry (n), and thermodynamic parameters including enthalpy (ΔH) and entropy (ΔS) can be accurately determined. In addition, varying the temperature of the experiment allows the determination of the heat capacity (ΔC_p) for the reaction. In ITC, a solution of a ligand is titrated against a solution of a binding partner at constant temperature. The heat released upon their interaction (ΔH) is monitored over time. As successive amounts of the ligand are titrated into the cell, the quantity of heat absorbed or released is in direct proportion to the amount of binding occurring. As the system reaches saturation, the signal diminishes until only heats of dilution are observed. A binding curve is then obtained from a plot of the heats from each injection against the ratio of ligand and binding partner in the cell.

Table 10. Thermodynamic parameters of the formation of PNA:DNA **24** complexes from Isothermal titration calorimetry at temperature 277 K.

First set of binding	K_1 (M^{-1})	$-\Delta H_1$ (kcal/mol)	ΔS_1 (Kcal/K/mol)	$-\Delta G_1$ (kcal/mol)	$T\Delta S_1$ (kcal/mol)	T_m°C
12:24	$3.57.\ 10^5$	13.27	-36.19	3.24	-10.02	45.0[b]
14:24	$5.84\ .\ 10^6$	14.43	-21.09	8.58	-5.84	22.0[b]
17:24	$8.71\ .\ 10^6$	68.64	-229.6	5.04	-63.6	62.0[b]
Second set of binding	K_2 (M^{-1})	$-\Delta H_2$ kcal/mol	ΔS_2 (Kcal/K/mol)	$-\Delta G_2$ kcal/mol	$T\Delta S_2$ kcal/mol	
12: 24	$4.0\ .\ 10^7$	17.54	-28.5	9.64	-7.89	
14:24	$7.04\ .\ 10^6$	43.97	-127.3	8.70	-35.26	
17:24	$1.11\ .\ 10^7$	67.17	274.6	143.23	76.06	

[a] for *aeg/cp*PNA-DNA triplex melting accompanied by single transition, unlike DNA-DNA triplexes which show two distinct transitions, one corresponds to triplex and other to duplex melting. [b] PNA:DNA triplexes melts to give single transition (T_m).

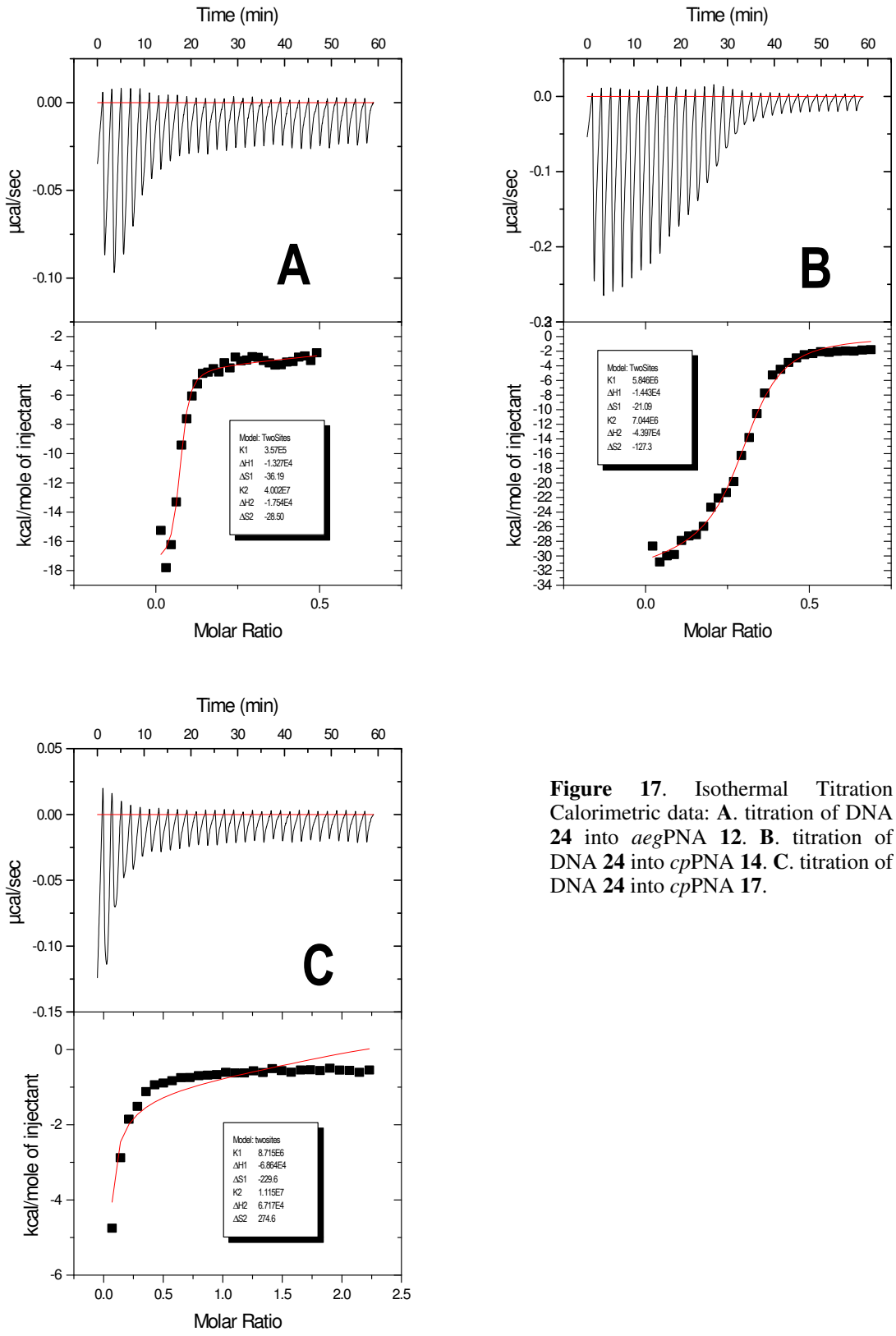

Figure 17. Isothermal Titration Calorimetric data: **A**. titration of DNA **24** into *aeg*PNA **12**. **B**. titration of DNA **24** into *cp*PNA **14**. **C**. titration of DNA **24** into *cp*PNA **17**.

A PC controlled Microcal VP ITC system was used. All samples used in the ITC experiments were performed in 10 mM Sodium phosphate buffer (100 mM NaCl, 0.1 mM EDTA, pH = 7.0). The temperatutre of the cell was held constant at 4°C for all experiments. A solution of one of the strands (PNA or DNA respectively), usually in these experiments 13.3 μ M PNA was placed in the cell (volume 1.43 mL) and the titrant solution (39.9 μM DNA, 300 μL) in the syringe, whose needle is designed as a peddle-shaped stirrer rotating at 400 rpm. The plunger is controlled by a stepping motor, allowing precise injections. Typically 30 injections of 10 μL each and 20 mins apart were made.[126,202] Two separate models are available for regression of the ITC data. I) a single set of identical binding and ii) two set of independent binding site. Here the second model, that is two binding site model is used to fit the data.[202]

The data (Table 10, Figure 17) clearly suggested that there is an over all increase in entropy for the binding of *cp*PNA **17** with DNA **33** when compared to *cp*PNA **14** and *aeg*PNA **25** (T_m = 45°C) which resulted in negative entropy of binding. As expected from their melting temperatures, even the enthalpy contribution was excellent in case of *cp*PNA **17**: DNA **24** (T_m = 62°C). Though the enthalpic contributionfor *cp*PNA **14**:DNA **24** (T_m = 22°C) complex formation is appreciable, but it is counter balanced the entropy loss. This again shows the stereochemistry dependent binding of *cp*PNA with complementary DNA.

3.4 Comaprison of *cis*-Cyclohexyl (*ch*PNA) and *cis*-cyclopentyl (*cp*PNA) PNA: Affinity versus selectivity

*ch*PNA and *cp*PNA are the result of the designs based on optimizing dihedral angle β to constrain PNA backbone for optimal DNA/RNA binding and discrimination *via* pre-organization mediated entropy gain. The UV-melting temperatures of the *ch*PNAs

with complementary DNA and RNA suggested a stereochemistry dependent discrimination, but the thermal stability of resultant cDNA/RNA complexes was reduced compared to *aeg*PNA. To improve the binding affinity and enhance the thermal stability of the complexes without losing the discrimination and stereospecificity, *cp*PNAs were designed based on the fact that the cyclopentyl ring is less rigid than the cyclohexyl ring and could provide a favorable conformation towards cRNA binding, although the dihedral angle β is much less (~25°) than the cyclohexyl system (~65°). *cp*PNAs showed a higher binding affinity to cDNA/RNA with stereochemistry dependent DNA/RNA discrimination. The binding of *cis*-cyclopentyl modifications reported here appear to be superior to the *trans*-cyclopentyl analogues reported recently.[200] The stereoselective binding was reflected from their lowering T_ms with mismatch cDNA (ΔT = -18°C to 30°C), which is more than that observed with *ch*PNAs. The relative ease of conformational adjustments in *cis*-cyclopentyl system seems to have significant consequences on the hybridization ability of *cp*PNA oligomers in spite of the less dihedral angle compared to *ch*PNAs.

(*SR/RS*)-*ch*-PNA/*cp*-PNA: Duplex stability and selectivity. Classical *aeg*-PNA being flexible can easily attain competent conformation to hybridize with DNA as well as RNA and hence has near equal binding affinity to both as measured by T_m. In (*SR/RS*)-*ch*-PNA, the monomer dihedral angle β matches the range (65^o) found in PNA:RNA duplex rather than that in PNA:DNA duplex (141^o). The derived *ch*-PNAs thus exhibit a higher affinity to RNA and destabilize the complex with DNA. (*SR/RS*)-*cp*-PNA with a lower dihedral angle β (25^o) binds to both RNA and DNA with a higher avidity compared to *aeg*-PNA and *ch*-PNA, but lack the differentiating ability of *ch*-PNA. In the five membered rings of *cp*-PNA and DNA, the flexible ring puckering allows better torsional

adjustments to attain hybridization competent conformation. The inherently rigid six membered ring of *ch*-PNAs forbids such structural adjustments and consequently destabilize its binding with DNA. Further, in *ch/cp*-PNAs, the favourable conformational features of the monomer seem to be co-operatively transmitted to the oligomer level even in a chimera. Thus the rigid (*SR/RS*)-*ch*-PNA imparts an unparalleled selectivity for binding to RNA over DNA for duplex formation (>30°-50°C), while the flexible (*SR/RS*)-*cp*-PNA binds both DNA and RNA with high affinity, but without any selectivity.

When biochemical recognitions are mediated by steric fit, higher binding affinity is accompanied by higher recognition specificities (positive correlation), which is the case for most enzyme-substrate interactions. A negative correlation is intrinsic to the nucleation-zipping model, which governs the sequence recognition between complementary nucleic acids strands.[203] Strategies to improve affinity of oligonucleotide analogues along with a corresponding increase in sequence fidelity could involve enhancing both hydrogen bonding interactions (to have enthalpic advantage) and steric fitting (to impart entropic advantage). In our previous studies that involved rational chemical modifications to induce preorganization of single stranded PNA backbone to match that of the DNA/RNA hybrids, higher affinities are mostly accompanied by a higher discrimination of single mismatches. In modified analogues with somewhat rigid structural features, incorrect hydrogen bonding recognition of DNA sequences with single base mismatch, would amplify destabilization effects due to steric interruption in zipping mechanism. The observed differences in DNA affinity between cyclohexyl and cyclopentyl PNAs may arise from differences in relative contributions of above factors and delineating these may help achieve optimal fine-tuning of PNA chemical modifications to achieve balanced affinity/selectivity towards target sequences.

3.5 Conclusion

In order to introduce PNA binding selectivity between DNA and RNA and higher affinity, we have synthesized *cp*PNAs incorporating optically pure *cis*-(1*S*,2*R*)- and *cis*-(1*R*,2*S*)-aminocyclopentylglycyl thymine monomers. These monomers were built into PNA oligomers by solid phase peptide synthesis and UV melting temperatures of the *cp*PNAs with complementary and mismatched DNA and RNA indicated that *cp*PNAs having (1*S*,2*R*) cyclopentyl unit have a higher binding affinity to RNA than DNA and PNA oligomers with (1*R*,2*S*)-cyclopentyl units showed relatively higher affinity towards DNA. The stereopreferences in *cp*PNA binding of DNA/RNA is accompanied by overall enhanced binding affinities compared to *aeg*PNA, unlike *ch*PNA where stereochemistry dependent discrimination of DNA/RNA was observed but with lower T_m-values. *cp*PNAs show high mismatch discrimination compared to *aeg*PNAs revealing base specific recognition. The torsional angle β in 1,2–disubstituted *cis*-cyclopentyl system is less than that in *ch*PNA but seems to have significant consequences on the hybridization ability of *cp*PNA oligomers.

The higher binding of cyclopentyl PNAs, is perhaps a consequence of the relative ease of conformational adjustments in a cyclopentyl ring as compared to rigid locking of cyclohexane systems. The favorable conformational features of the monomers are co-operatively transmitted to the oligomeric level. The results on *cis*-*cp*PNAs presented here support the idea of improving the stability and DNA/RNA binding selectivity *via* rational conformational tuning of classical PNA to achieve pre-organization. Further studies on sequence dependent and RNA/DNA discriminatory effects of *cp*PNA in mixed base *cp*PNA sequences having all modified *cp*PNA (A/G/C/T) monomers and their

thermodynamic studies to delineate entropic and enthalpic contributions are need to be carried out and also Molecular modeling or NMR Solution structure and X-ray crystal structure analysis of the corresponding triplexes and duplexes are very much necessary to understand the Structure-activity relation ships and the observed results.

Summary

- **Cyclopentyl PNAs (*cp*PNA) were designed, synthesized to study the effect of ring flexibility of cyclopentane.**
- **Triplex formation: *cp*PNAs forms stronger complexes with DNA and RNA without discrimination. Stability-*SR*>*RS* with RNA.**
- **Duplex formation: *cp*PNAs forms highly stable duplexes with both DNA and RNA attributed to flexibility of ring puckering. Stability-*RS*>*SR***
- ***cp*PNAs are successfully competing for binding with the complementary DNA strand and shown very high sequence discrimination with mismatch DNA.**

3.6 Experimental

General Experimental Procedure: Melting points of samples were determined in open capillary tubes using Buchi Melting point B-540 apparatus and are uncorrected. IR spectra were recorded on an infrared Fourier Transform spectrophotometer using KBr pellets. Column chromatographic separations were performed using silica gel 60-120 mesh, solvent systems gradient 10-25% EtOAc/Pet ether and pure DCM to 3% MeOH/DCM. ^{1}H and ^{13}C spectra were obtained using Bruker AC-200 (200 MHz) and 500 MHz NMR spectrometers. The chemical shifts are reported in delta (δ) values. The optical rotation values were measured on Bellingham-Stanley Ltd, ADP220 polarimeter. CD spectra were recorded on *JASCO-715* Spectropolarimeter. Mass spectra were obtained either by FAB or LCMS techniques. Oligomers were characterized by RP HPLC, C18 column and MALDI-TOF mass spectrometry. The enzyme Amano-PS was obtained as a gift from Amano Pharmaceuticals, Japan.

Enzymatic resolution of racemic butyrates (1*R/S,*2*R/S*) 3 with *Pseudomonas cepacia.* To a solution of enzyme *Pseudomonas cepacia* (500 mg) in phosphate buffer (150 ml, pH = 7.2) was added racemic butyrates (1*R/S,*2*R/S*)-**3** (10 g). The mixture was stirred vigorously for 1.5 h, which accomplished 40% conversion for alcohol (-) (1*R,*2*R*)-**2a.** The enzyme was separated by filtration and the filtrate was extracted into DCM. The solvent was evaporated and the column chromatographic separation of the residue afforded chiral pure alcohol (1*R.*2*R*)-**2a** and optically enriched butyrate (1*S,*2*S*)-**3.** The optically enriched butyrate (*1S,2S*)-**3** was subjected to second enzyme hydrolysis as described above to yield the optically pure butyrate (1*S,*2*S*)-**3** after column separation. From butyrate (1*S,*2*S*)-**2**, alcohol (1*S,*2*S*)-**2b** was obtained by methanolysis with catalytic amount of NaOMe in MeOH in 35% overall yield. The enantiomeric purity of **2a** and **2b**

was confirmed by their optical rotations: (*1R,2R*)- **2a** $[\propto]_{20}^{D}$ = -84.0° (lit[13].- 78.0°, c. 1.5, CH_2Cl_2); (1*S,*2*S*)-**2b;** $[\propto]_{20}^{D}$ = + 84.0° (lit.[13] + 84.1.°, c. 1.6, CH_2Cl_2)

(1*R,*2*R*)–2-(*N-t*-Boc-amino)-cyclopentanol (1*R,*2*R*) 4. To a solution of (1*R,*2*R*)-2-azido cyclopentanol (3.5 g, 27.55 mmol) in dry ethyl acetate (10 ml) placed in a hydrogenation flask was added di-*t*-butyl dicarbonate (7.21g, 33.06 mmol) and Adams catalyst (2 mol%). The mixture was hydrogenated in Parr apparatus (rt, 35-40 psi. 3.5 h). The catalyst was filtered, solvent in filtrate was evaporated under reduced pressure and the residue was purified by column chromatography (EtOAc/petroleum ether) to afford a white solid of the alcohol **4**(1*R,*2*R*)**.** Yield (4.6g, 83 %); m.p.87.0°; $[\alpha]_D^{20}$ +21.0° (*c* 1.0, CH_2Cl_2); ^{1}H-NMR ($CHCl_3$-*d*, 200 MHz); δ_H 1.00-1.45 (m, 10H, 4-CH, *t*-Boc), 1.45-1.8 (m, 3H, 4-CH, 3-CH_2), 1.8-2.15 (m, 2H, 5-CH_2), 3.4-3.7(m, 1H, 2-CH), 3.8-4.0 (m, 1H, 1-CH), 4.1-4.4 (bd, 1H, -OH), 4.6-5.0 (bd, 1H, carbamate NH); ^{13}C-NMR ($CHCl_3$-*d*, 200 MHz): δ_C 20.2 (C-4), 27.9 (*t*Boc), 29.5 (C-3), 31.5 (C-5), 59.5 (C-2), 78.2 (C-1), 78.9 (*t*Boc), 156.5 (Carbamate C=O); Anal: Calcd (%) for $C_{10}H_{19}NO_3$: C, 59.7; H, 9.45; N, 6.96; Found C, 59.63; H, 9.81; N, 6.86; LCMS: 202.05 [M+H].

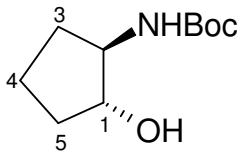

(1*R,*2*R*)-**4**

(1*S,*2*S*)–2-(*N-t*-Boc-amino)-cyclopentanol 4 (1*S,*2*S*). This was prepared from the azido alcohol (1*S,*2*S*)-**2b** using the similar procedure as the one described for the alcohol (1*R,*2*R*)-**4**. m.p. 87.0°; $[\alpha]_D^{20}$ -21.0° (*c* 1.0, CH_2Cl_2); ^{1}H-NMR ($CHCl_3$-*d*, 200 MHz); δ_H 1.00- 1.45 (m, 10H, 4-CH, *t*-Boc), 1.45-1.8 (m, 3H, 4-CH, 3-CH_2), 1.8-2.15 (m, 2H, 5-CH_2), 3.4-3.7(m, 1H, 2-CH), 3.8-4.0 (m, 1H, 1-CH), 4.1-4.4 (bd, 1H, -OH), 4.6-5.0 (bd, 1H, carbamate NH); ^{13}C-NMR ($CHCl_3$-*d*, 200 MHz): δ_C

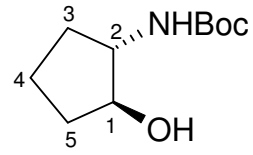

(*1S,2S*)-**4**

20.2 (C-4), 27.9 (*t*Boc), 29.5 (C-3), 31.5 (C-5), 59.5 (C-2), 78.2 (C-1), 78.9 (*t*Boc), 156.5 (Carbamate C=O); Anal Calcd (%) for $C_{10}H_{19}NO_3$: C, 59.7; H, 9.45; N, 6.96; Found C, 59.67; H, 9.89; N, 6.80; LCMS: 202.05 [M+H].

(1*R*,2*R*)-2-(*N*-*t*-Boc-amino)-cyclopentan-1-methyl sulfonate 5 (1*R*,2*R*). To a stirred solution of alcohol (1*R*,2*R*)-**4** (4.3 g, 21.39 mmol) and triethyl amine (6.49 g, 64.17 mmol) in dry CH_2Cl_2 (40 ml) at 0°C under nitrogen was added methanesulfonyl chloride (3.92 g, 34.22 mmol) over a period of 15 min. The mixture was stirred for another 20 mins at room temperature and the solvent was evaporated under reduced pressure. The residue was extracted with CH_2Cl_2, washed successively with $KHSO_4$ solution, water, brine and stored over Na_2SO_4. The organic layer was concentrated to afford mesylate (1*R*,2*R*)-**5.** Yield (5.6 g, 93%)**,** which was used without purification for further reaction.

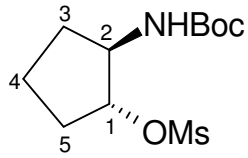

(*1R,2R*)-**5**

(1*S*,2*S*)-2-(*N*-*t*-Boc-amino)-cyclopentan-1-methyl sulfonate 5 (1*S*,2*S*). The compound (1*S*,2*S*)-**5** prepared from the alcohol (1*S*,2*S*)-**4** using the similar procedure as the one described for the mesylate (1*R*,2*R*)-**5** and the crude product was used for the further reaction without any purification.

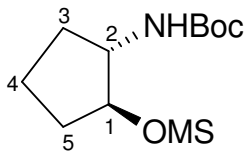

(*1S,2S*)-**5**

(1*S*,2*R*)-2-(*N*-*t*-Boc-amino)-1-azidocyclopentane 6 (1*S*,2*R*). A stirred mixture of the mesylate (1*R*,2*R*)-**5** (5.0 g, 17.92 mmol) and NaN_3 (9.3 g, 0.143 mol) in DMF (25 ml) under nitrogen was heated at 68-70°C for 5 h. After cooling, the solvent was evaporated under reduced pressure and the residue was extracted with EtOAc (25mlx2), stored over Na_2SO_4. The organic layer was removed

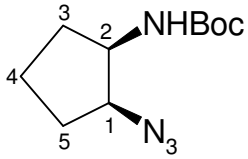

(*1S,2R*)-**6**

under reduced pressure and crude product was purified by column chromatography (EtOAc/petroleum ether) to afford a white solid of azide (1*S,*2*R*)-**6**. Yield (3.65g, 91.5%): m.p. 81.0°; IR, ν (cm^{-1}) (KBr); 3442.7, 3014.53, 2995.24, 2113.84, 1706.88 cm^{-1}: $[\alpha]_D^{20}$ + 116° (*c* 1.0, CH_2Cl_2); ^{1}H-NMR ($CHCl_3$-*d*, 200 MHz); δ_H 1.0-1.45(m, 11H, 4-CH_2, *t*-Boc), 1.65-2.0 (m, 4H, 5-CH_2, 3-CH_2), 3.7-4.1 (m, 2H, 1-CH, 2-CH), 4.6-5.0 (bd, 1H, carbamate NH): ^{13}C-NMR ($CHCl_3$-*d*, 200 MHz): δ_C 19.8 (C-4), 28.2 (*t*-Boc), 28.7 (C-5), 29.0 (C-3), 54.7 (C-1), 64.1 (C-2), 79.4 (*t*-Boc), 155.3 (carbamate C=O): Anal Calcd (%) for $C_{10}H_{18}N_4O_2$: C, 53.09; H, 7.96; N, 24.77; Found C, 52.55; H, 7.9; N, 24.8;MS (FAB+) 227 (35%) [M+1], 171 (100%) [M+1- N_3], 127 (15%) [M+1- *t*Boc].

(1*R,*2*S*)-2-(*N*-*t*-Boc-amino)-1-azidocyclopentane 6 (1*R,*2*S*). A similar procedure as the one described for (1*S,*2*R*)-**6** was used to prepare (1*R,*2*S*)-**6** from (1*S,*2*S*)-**5.** m.p. 81.0°; IR, ν (cm^{-1}) (KBr); 3442.7, 3014.53, 2995.24, 2113.84, 1706.88 cm^{-1}: $[\alpha]_D^{20}$ -116° (*c* 1.0, CH_2Cl_2); ^{1}H-NMR ($CHCl_3$-*d*, 200 MHz); δ_H 1.0-1.45(m, 11H, 4-CH_2, *t*-Boc), 1.65-2.0 (m, 4H, 5-CH_2, 3-CH_2), 3.7-4.1 (m, 2H, 1-CH, 2-CH), 4.6-5.0 (bd, 1H, carbamate NH): ^{13}C-NMR ($CHCl_3$-*d*, 200 MHz): δ_C 19.8 (C-4), 28.2 (*t*-Boc), 28.7 (C-5), 29.0 (C-3), 54.7 (C-1), 64.1 (C-2), 79.4 (*t*-Boc), 155.3 (carbamate C=O): Anal Calcd (%) for $C_{10}H_{18}N_4O_2$: C, 53.09; H, 7.96; N, 24.77; Found C, 52.55; H, 7.98; N, 24.71;MS (FAB+) 227 (35%) [M+1], 171 (100%) [M+1- N_3], 127 (15%) [M+1- *t*Boc].

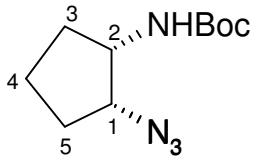

(*1R,2S*)-**6**

(1*S,*2*R*)-2-(*N*-*t*-Boc-amino)-1-aminocyclopentane 7 (1*S,*2*R*). To a solution of the azide (1*S,*2*R*)-**6** (3.0 g, 13.27 mmol) in methanol (5 ml) taken in hydrogenation flask was added Adam's catalyst (2 mol%). The reaction mixture was hydrogenated in a Parr apparatus for 3.5 h at rt and H_2 of pressure 35-40 psi. The catalyst was filtered off and

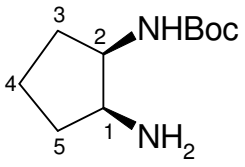

(1*S,2R*)-**7**

the solvent was removed under reduced pressure to yield a residue of the amine (1*S,*2*R*)-**7** as a colorless oil. Yield (2.6 g, 98.0%); this compound was used for the further reaction without any purification.

(1*R,*2*S*)-2-(*N*-*t*-Boc)-1-aminocyclopentane 7 (1*R,*2*S*). The amine (1*R,*2*S*)-**7** was obtained on hydrogenation of the azide (1*R,*2*S*)-**6** following the procedure as the one described for the synthesis of the amine (1*S,*2*R*)-**7**.

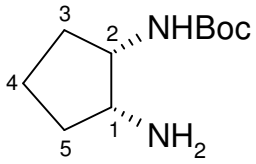

(1*R,*2*S*)-**7**

***N*-[(2*R*)-t-Boc-aminocyclopent-(1*S*)-yl]-glycine ethyl ester 8 (1*S,*2*R*).** To a stirred mixture of amine (1*S,*2*R*)-**7** (2.5 g, 12.5 mmol), and freshly prepare KF-celite (4.35 g, 37.5 mmol) in dry acetonitrile (150 ml), ethyl bromoacetate (1.87 g, 11.25 mmol) was added dropwise for 30 min. at rt under nitrogen atmosphere and then heated to 65°C. After 3.0 h the celite was filtered off and the solvent in the filtrate was evaporated under reduced pressure which on column chromatographic purification (EtOAc) afforded the ethyl ester (1*S,*2*R*)-**8** as colorless oil. Yield (2.81 g, 78.5%): $[\alpha]_D^{20}$ – 32.69° (*c* 1.0, CH_2Cl_2); ^{1}H-NMR ($CHCl_3$-*d*, 200 MHz); δ_H 0.62-2.1 (m, 18H, 4-CH_2, 3-CH_2, 5-CH2, *t*-Boc, ester-CH_3), 2.7-3.1 (bd, 1H, 2-CH), 3.1-3.4 (s, 2H, -CH_2-C=0), 3.5-3.9 (bd, 1H, 1-CH), 3.9-4.2 (q, 2H, ester-CH_2), 4.9-5.6 (bd, 2H, NH and carbamate-NH); ^{13}C-NMR ($CHCl_3$-*d*, 200 MHz): δ_C 13.5 (ester CH_3), 19.9 (4-CH_2), 27.8 (*t*-Boc), 29.3 (C-5), 30.2 (C-3), 48.6 (-CH_2-C=O), 52.5 (C-2), 59.5 (C-1), 60.1 (ester-CH_2), 78.4 (*t*-Boc), 155.5 (carbamate C=O), 171.2 (ester C=O); Anal Calcd (%) for

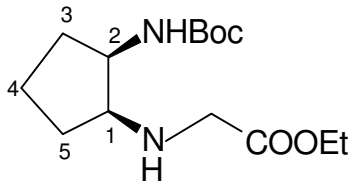

(1*S,*2*R*)-**8**

$C_{14}H_{26}N_2O_4$: C, 58.74; H, 9.09; N, 9.79; Found C, 58.85; H, 8.66; N, 9.50;LCMS; 287.05 [M+H], 187 [M+H-*t*Boc].

***N*-[(2*S*)-*t*-Boc-aminocyclopent-(1*R*)-yl]-glycine ethyl ester 8 (1*R*,2*S*).** A similar procedure as the one described for the ethyl ester (1*S*,2*R*)-**8** afforded (1*R*,2*S*)-**8** starting from the amine (1*R*,2*S*)-**7.** $[\alpha]_D^{20}$ +32.69° (*c* 1.0, CH_2Cl_2); ^{1}H-NMR ($CHCl_3$-*d*, 200 MHz); δ_H 0.62-2.1 (m, 18H, 4-CH_2, 3-CH_2, 5-CH_2, t-Boc, ester-CH_3), 2.7-3.1 (bd, 1H, 2-CH), 3.1-3.4 (s, 2H, -CH_2-C=0), 3.5-3.9 (bd, 1H, 1-CH), 3.9-4.2 (q, 2H, ester-CH_2), 4.9-5.6 (bd, 2H, NH and carbamate-NH); ^{13}C-NMR ($CHCl_3$-*d*, 200 MHz): δ_C 13.5 (ester CH_3), 19.9 (4-CH_2), 27.8 (*t*-Boc), 29.3 (C-5), 30.2 (C-3), 48.6 (-CH_2-C=O), 52.5 (C-2), 59.5 (C-1), 60.1 (ester-CH_2), 78.4 (*t*-Boc), 155.5 (carbamate C=O), 171.2 (ester C=O); Anal Calcd (%) for $C_{14}H_{26}N_2O_4$: C, 58.74; H, 9.09; N, 9.79; Found C, 58.87; H, 8.71; N, 9.72;LCMS; 287.05 [M+H], 187.05 [M+H-*t*Boc].

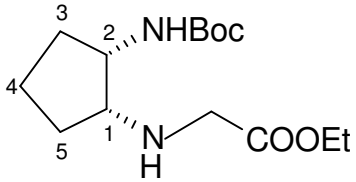

(1*R*,2*S*)-**8**

***N*-[(2*R*)-*t*-Boc-aminocyclopentan-(1*S*)-yl]-*N*-(chloroacetyl)-glycine ethyl ester 9 (1*S*,2*R*).** To a stirred solution of the amine (1*R*,2*S*)-**8** (2.5 g, 8.7 mmol) in 10% Na_2CO_3 (65 ml) and 1,4-dioxan (65 ml) cooled to 0°C, was added chloroacetyl chloride (4.93 g, 43.7 mmol) in two additions. After 30 min the dioxan was removed under reduced pressure and the residue was extracted into EtOAc (2 x 50 ml), dried over Na_2SO_4. The solvent was evaporated under reduced pressure and the residue was purified by column chromatography (MeOH/CH_2Cl_2) affording chloro compound (1*S*,2*R*)-**9** as white solid. Yield (2.4 g, 76%); m.p. 131.0°C. $[\alpha]_D^{20}$ +55.0° (*c* 1.0, CH_2Cl_2); ^{1}H-NMR

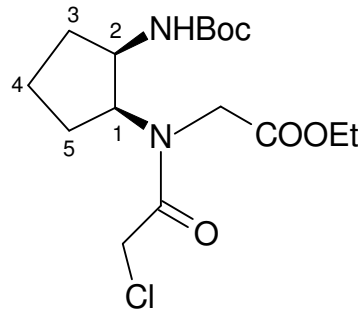

(*1S,2R*)-**9**

($CHCl_3$-*d*, 500 MHz); δ_H 1.0-2.4 (m, 18H, $3CH_2$ cycl, *t*Boc, ester CH_3), 3.5-4.5 (m, 8H, 1-CH, 2-CH, N-CH_2, -$COCH_2Cl$, -$COOCH_2$), 5.5-6.0 (bd, 1H, carbamate NH); ^{13}C-NMR ($CHCl_3$-*d*, 500 MHz): ^{13}C-NMR ($CHCl_3$-*d*, 500 MHz): δ_C 13.7 (ester CH_3), 20.8 (C-4), 27.8 (C-3), 28.0 (*t*Boc), 30.5 (C-5), 41.1 (-CH_2Cl), 46.0 (N-CH_2ester), 53.3 (C-2), 58.8 (C-1), 61.0 (ester CH_2), 78.2 (*t*Boc), 155.5 (carbamate C=O), 167.6 (acyl C=O), 169.5 (ester C=O); Anal Calcd (%) for $C_{16}H_{27}N_2O_5Cl$: C, 52.89; H, 7.43; N, 7.71; Cl, 9.77; Found C, 52.61; H, 7.91; N, 7.58; Cl, 9.72: MS LCMS; 363.05 [M+H], 263.05 [M+1-*t*Boc].

***N*-[(2*S*)-*t*-Boc-aminocyclopentan-(1*R*)-yl]-*N*-(chloroacetyl)-glycine ethyl ester [(1*R*,2*S*)-9:** This compound was prepared from the amine (1*S*,2*R*)-**8** following the procedure described for the chloro compound (*1S,2R*)-**9** m.p. 131.0°C. $[\alpha]_D^{20}$ -55.0° (*c* 1.0, CH_2Cl_2); ^{1}H-NMR ($CHCl_3$-*d*, 500 MHz); δ_H 1.0-2.4 (m, 18H, $3CH_2$ cycl, *t*Boc, ester CH_3), 3.5-4.5 (m, 8H, 1-CH, 2-CH, N-CH_2, -$COCH_2Cl$, -$COOCH_2$), 5.5-6.0 (bd, 1H, carbamate NH); ^{13}C-NMR ($CHCl_3$-*d*, 500 MHz): δ_C 13.7 (ester CH_3), 20.8 (C-4), 27.8 (C-3), 28.0 (*t*Boc), 30.5 (C-5), 41.1 (-CH_2Cl), 46.0 (N-CH_2ester), 53.3 (C-2), 58.8 (C-1), 61.0 (ester CH_2), 78.2 (*t*Boc), 155.5 (carbamate C=O), 167.6 (acyl C=O), 169.5 (ester C=O); Anal Calcd (%) for $C_{16}H_{27}N_2O_5Cl$: C, 52.89; H, 7.43; N, 7.71; Cl, 9.77; Found C, 52.73; H, 7.97; N, 7.61; Cl, 9.75: MS LCMS; 363.05 [M+H], 263.05 [M+1-*t*Boc].

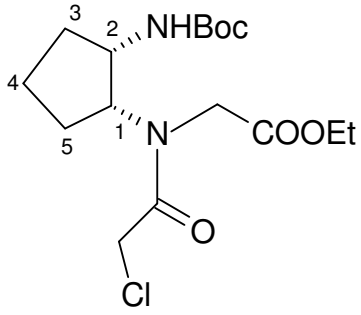

(*1R,2S*)-**9**

***N*-[(2*R*)-*t*-Boc-Aminocyclopent-(1*S*)-yl]-*N*-(thymin-1-acetyl)-glycine ethyl ester [(1*S,2R*)-10a]:** A mixture of chloro-compound (1*S,2R*)-**9a** (2.0 g, 5.52 mmol), thymine (0.70 g, 5.52 mmol) and anhydrous K_2CO_3 (0.91 g, 6.62 mmol) in dry DMF (10

ml) under nitrogen was heated with stirring at 65°C for 4.0 h. After cooling, the solvent was removed under reduced pressure to leave a residue, which was extracted into DCM (2x 25 ml) and dried over Na_2SO_4. The solvent evaporated and the crude compound was purified by column chromatography (MeOH/DCM) to afford a White solid of thymine monomer ethyl ester (1*S,*2*R*)-**10a**. Yield (1.8g, 72.2%): m.p. 211.0-215.0°C. $[\alpha]_D^{20}$ +32.64° (*c* 0.52, CH_2Cl_2); ^{1}H-NMR ($CHCl_3$-*d*, 500 MHz); δ_H 1.11-1.2 (t, 3H. ester CH_3), 1.26-1.4 (10H, *t*Boc, 4-CH), 1.4-1.53 (m, 1H, 4-CH), 1.6-1.7 (m, 1H, 5-CH), 1.7-1.78 (m, 1H, 3-CH),1.81(s, 3H, thymine CH_3), 2.02-2.15 (2H, 5-CH), 3.6-4.5 (m, 7H, 2-CH, N-CH_2, -$COCH_2$, -$COOCH_2$), 5.0-5.2 (d, 1H, 1-CH), 5.4-5.6 (bd, 1H, carbamate NH), 7.04 (s, 1H, thymine –CH=C-), 9.4-9.6 (bd, 1H, thymine NH); ^{13}C-NMR ($CHCl_3$-*d*, 500 MHz): δ_C 12.0 (thymine-CH_3), 13.8 (ester CH_3), 21.3 (C-4), 28.1 (C-3), 28.3 (*t*Boc), 31.1 (C-5), 46.0 (-CH_2-thymine), 47.8 (N-CH_2), 52.4 (C-2), 58.8 (C-1), 61.2 (ester CH_2),79.8 (*t*-Boc), 110.0 (thymine -C), 141.2 (thymine CH), 151.1 (thymine C=O), 155.7 (carbamate C=O), 164.3 (thymine C=O), 167.3 (*N*-C=O), 169.3 (ester C=O): Anal Calcd (%) for $C_{21}H_{32}N_4O_7$: C, 55.75; H, 7.07; N, 12.38; Found C, 55.63; H, 7.45; N, 12.08;MS (FAB^+); 453 [M+1] (42%), 353 (100%) [M+1-*t*Boc].

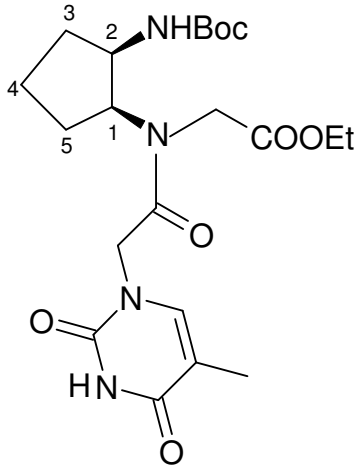

(*1S,2R*)-**10a**

***N*-[(2*S*)-*t*-Boc-aminocyclopent-(1*R*)-yl]-*N*-(thymin-1-acetyl)-glycine ethyl ester [(1*R,*2*S*)-10b]:**A similar procedure as the one described for the monomer (1*S,*2*R*)-**10** afforded (1*R,*2*S*)-**10b** from (1*R,*2*S*)-**9b**. m.p.211.0-215.0°C. $[\alpha]_D^{20}$ -32.64° (*c* 0.52, CH_2Cl_2); ^{1}H-NMR ($CHCl_3$-*d*, 500 MHz); δ_H 1.11-1.2 (t, 3H. ester CH_3), 1.26-1.4 (10H, *t*Boc, 4-CH), 1.4-1.53 (m, 1H, 4-CH), 1.6-1.7 (m, 1H, 5-CH), 1.7-1.78 (m, 1H, 3-

CH),1.81(s, 3H, thymine CH_3), 2.02-2.15 (2H, 5-CH), 3.6-4.5 (m, 7H, 2-CH, N-CH_2, -$COCH_2$, -$COOCH_2$), 5.0-5.2 (d, 1H, 1-CH), 5.4-5.6 (bd, 1H, carbamate NH), 7.04 (s, 1H, thymine –CH=C-), 9.4-9.6 (bd, 1H, thymine NH); ^{13}C-NMR ($CHCl_3$-*d*, 500 MHz): δ_C 12.0 (thymine-CH_3), 13.8 (ester CH_3), 21.3 (C-4), 28.1 (C-3), 28.3 (*t*Boc), 31.1 (C-5), 46.0 (-CH_2-thymine), 47.8 (N-CH_2), 52.4 (C-2), 58.8 (C-1), 61.2 (ester CH_2), 79.8 (*t*-Boc), 110.0 (thymine -C), 141.2 (thymine CH), 151.1 (thymine C=O), 155.7 (carbamate C=O), 164.3 (thymine C=O), 167.3 (*N*-C=O), 169.3 (ester C=O): Anal Calcd (%) for $C_{21}H_{32}N_4O_7$: C, 55.75; H, 7.07; N, 12.38; Found C, 55.69; H, 7.37; N,12.16; MS (FAB^+); 453 [M+1] (42%), 353 (100%) [M+1-*t*Boc].

(*1R,2S*)-**10b**

***N*-[(2*R*)-*t*-Boc-aminocyclopent-(1*S*)-yl]-*N*-(thymin-1-acetyl)-glycine [(1*S*,2*R*)-11a]:** To the monomer ester (1S,2*R*)-**10a** (1.0 g, 2.283 mmol) suspended in THF (10 ml), a solution of 0.5 M LiOH (10ml, 5.1 mmol) was added and mixture was stirred for 30 mins. The mixture was washed with EtOAc (2 X 10 ml). The aqueous layer was acidified to pH 3 and extracted with EtOAc (4 X 20 ml). The EtOAc layer was dried over sodium sulfate and evaporated under reduced pressure to afford monomer (1*S*,2*R*)-**11a** as a white solid. Yield: 0.92 g (97.8 %); m.p.139.0-141.0°C; $[\alpha]_D^{20}$ -17.0 ° (*c* 1.0, CH_2Cl_2); ^{1}H-NMR ($CHCl_3$-*d*, 200 MHz); δ_H 1.0-2.4 (m, 18H, *t*-Boc, thymine-CH_3,cypent 3CH_2), 3.5-4.8 (m, 5H, 2-CH, N-CH_2, -

(*1S,2R*)-**11a**

$COCH_2$), 5.13 and 5.31(bd, 1H, carbamate NH), 5.95 (s, 1H, 1-CH), 7.1-7.18 (1H, thymine –CH=C-), 9.9-10.2 (bd, 2H, thymine NH and -COOH); ^{13}C-NMR (DMSO-d_6, 200 MHz): δ_C 12.0 (thymine-CH_3), 21.8 (C-4), 28.6 (t-Boc), 28.3, 30.0 (C-3), 38.4 (C-5), 45.8 (C-2), 48.1 (acyl-CH_2-thymine), 50.5 (C-1), 59.0 (N-CH_2), 78.5 (*t*-Boc), 108.4 (thymine CH), 141.9 (thymine –C), 151.4 (thymine C=O), 156.0 (carbamate C=O), 164.6 (thymine C=O), 167.9 (N-C=O), 171.2 (-COOH): Anal Calcd (%) for $C_{19}H_{28}N_4O_7$: C, 53.77; H, 6.60; N, 13.20; Found C, 53.57; H, 6.91; N,13.11; MS (FAB$^+$); 425 [M+1] (6 %), 325 (100%), [M+1-*t*Boc].

***N*-[(2*S*)-*t*-Boc-aminocyclopent-(1*R*)-yl]-*N*-(thymin-1-acetyl)-glycine [(1*R*,2*S*)-11b].** To the monomer ester (1S,2*R*)-**10b** (1.0 g, 2.283 mmol) suspended in THF (10 ml), a solution of 0.5 M LiOH (10ml, 5.1 mmol) was added and mixture was stirred for 30 mins. The mixture was washed with EtOAc (2 X 10 ml). The aqueous layer was acidified to pH 3 and extracted with EtOAc (4 X 20 ml). The EtOAc layer was dried over sodium sulfate and evaporated under reduced pressure to afford monomer (1*S*,2*R*)-**11b** as a white solid. Yield: 0.92 g (97.8 %); m.p.139.0-141.0°C; $[\alpha]_D^{20}$ +17.0 ° (*c* 1.0, CH_2Cl_2); ^{1}H-NMR ($CHCl_3$-*d*, 200 MHz); δ_H 1.0-2.4 (m, 18H, *t*-Boc, thymine-CH_3,cypent 3CH_2), 3.5-4.8 (m, 5H, 2-CH, N-CH_2, -$COCH_2$), 5.13 and 5.31(bd, 1H, carbamate NH), 5.95 (s, 1H, 1-CH), 7.1-7.18 (1H, thymine –CH=C-), 9.9-10.2 (bd, 2H, thymine NH and -COOH); ^{13}C-NMR (DMSO-d_6, 200 MHz): δ_C 12.0 (thymine-CH_3), 21.8 (C-4), 28.6 (*t*-Boc), 28.3, 30.0 (C-3), 38.4 (C-5), 45.8 (C-2), 48.1 (acyl-CH_2-thymine), 50.5 (C-1), 59.0 (N-CH_2), 78.5 (*t*-Boc), 108.4 (thymine -C), 141.9 (thymine CH), 151.4 (thymine

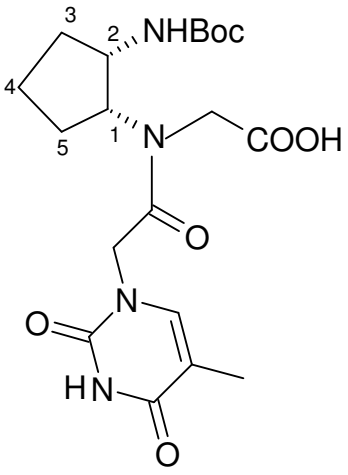

(*1R,2S*)-**11b**

C=O), 156.0 (carbamate C=O), 164.6 (thymine C=O), 167.9 (N-C=O), 171.2 (-COOH): Anal Calcd (%) for $C_{19}H_{28}N_4O_7$: C, 53.77; H, 6.60; N, 13.20.; Found C, 53.49; H, 6.93; N,13.17; MS (FAB^+); 425 [M+1] (6 %), 325 (100%)[M+1-*t*Boc].

Enantiomeric purity from ^{1}H NMR using chiral chemical shift Reagent: The enantiomeric purity of alcohols (1*R,*2*R*)-**2a** and (1*S,*2*S*)-**2b** were confirmed from ^{1}H NMR measurement of their acetyl derivatives utilizing a chiral chemical shift reagent, (+)-*tris*[3-(heptafluoropropylhydroxymethylene)-*d*-camphorato]europium (III) [$Eu(hfc)_3$]. (8.0 mol%). Examination of the ^{1}H NMR spectrum of the acetyl derivatives of racemic (1*R/S,*2*R/S*)-**3** shows the splitting in the methyl carbon signal into clear doublet. But in the corresponding spectra of acetyl derivatives of (1*R,*2*R*)-**2a** and (1*S,*2*S*)-**2b**, the above mentioned signal was singlet and corresponding to respective signal in the spectrum of their racemate. Integration of the methyl signal (doublet) in the racemate and that of the pure (1*R,*2*R*)-**2a** and (1*S,*2*S*)-**2b** (singlet) shows that the enatiomeric excess will be >98% for both isomers. (see supplementary information)

Synthesis of PNA-oligomers incorporating *cis*-(1*S*,2*R*)- and (1*R*,2*S*)-aminocyclopentyl PNA monomers. The modified PNA monomers were built into PNA oligomers using standard procedure on a L-lysine derivatized (4-methylbenzhydryl) amine (MBHA) resin (initial loading 0.25 $meqg^{-1}$) with HBTU/HOBt/DIEA in DMF/DMSO as a coupling reagent. The PNA oligomers were cleaved from the resin with TFMSA. The oligomers were purified by RP HPLC (C18 column) and characterized by MALDI-TOF mass spectrometry (Table 6). The overall yields of the raw products were 65-78%. The normal PNAs were prepared as described in literature.

UV-T_m measurements. The concentration of PNA and DNA was calculated on the basis of absorbance from the molar extinction coefficients of the corresponding

nucleobases. The complexes were prepared in 10 mM sodium phosphate buffer, pH 7.0 containing NaCl (100 mM) and EDTA (0.1 mM) and were annealed by keeping the samples at 95°C for 5 minutes followed by slow cooling to room temperature. The samples were cooled by keeping at 4°C for overnight. Absorbance versus temperature profiles were obtained by monitoring at 260 nm with Perkin-Elmer *Lambda 35 UV-VIS* spectrophotometer scanning from 5 to 85°C/90°C at a ramp rate of 0.2°C per minute. The data were processed using Microcal Origin 5.0 and T_m values derived from the derivative curves.

Electrophoretic gel mobility shift assay: The PNAs (**12**-**18**, Table 5) were individually mixed with DNA (**24** or **25**) in 2:1 ratio (PNA strand, 0.4 mM and DNA **25**, 0.2 mM or **24**) in water. The samples were lyophilized to dryness and re-suspended in sodium phosphate buffer (10 mM, pH 7.0, 10µl) containing EDTA (0.1 mM). The samples were annealed by heating to 85°C for 5 min followed by slow cooling to RT and refrigeration at 4^oC overnight. To this, 10µl of 40% sucrose in TBE buffer pH 8.0 was added and the sample was loaded on the gel. Bromophenol blue (BPB) was used as the tracer dye separately in an adjacent well. Gel electrophoresis was performed on a 15% non-denaturing polyacrylamide gel (acrylamide:bis-acrylamide, 29:1) at constant power supply of 200 V and 10 mA, until the BPB migrated to three-fourth of the gel length. During electrophoresis the temperature was maintained at 10°C. The spots were visualized through UV shadowing by illuminating the gel placed on a fluorescent silica gel plate, F_{254} using UV-light.

3.7 Appendix

- Compound **4**, ^{1}H, ^{13}C NMR and DEPT
- Compound **8**, ^{1}H, ^{13}C NMR and DEPT
- Compound **9**, ^{1}H, ^{13}C NMR and DEPT
- Compound **10**, ^{1}H, ^{13}C NMR, DEPT and FAB mass
- Compound **11**, ^{1}H, ^{13}C NMR and LC-TOF-MS
- MALDI-TOF spectra of *cp*PNAs **13**-**22**.

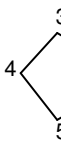

(1*R*,2*R*)-**4**

^{1}H NMR, $CDCl_3$

^{13}C NMR, $CDCl_3$

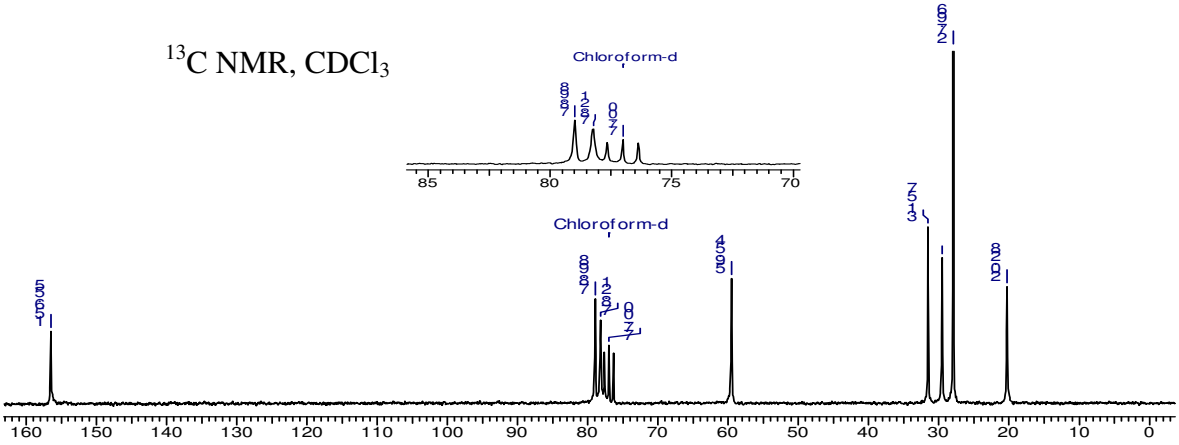

DEPT, $CDCl_3$

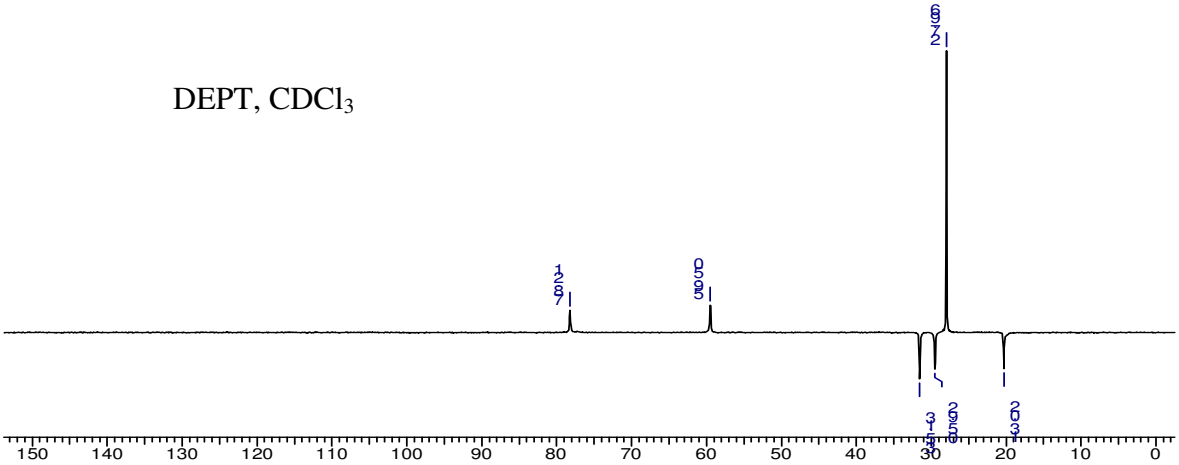

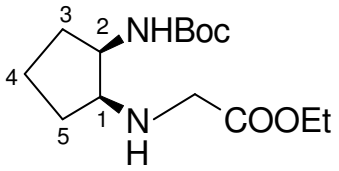

(1*S*,2*R*)-**8**

^{1}H NMR, $CDCl_3$

^{13}C NMR, $CDCl_3$

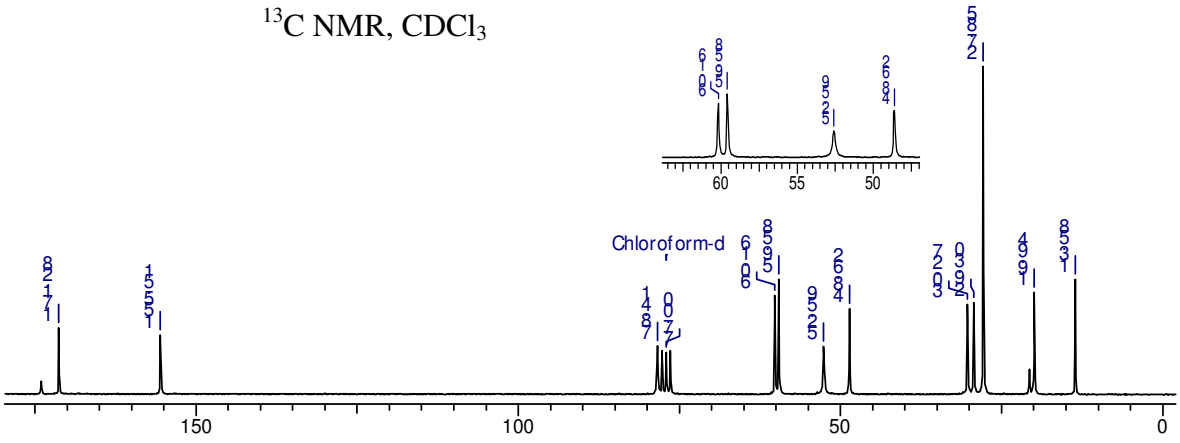

DEPT, $CDCl_3$

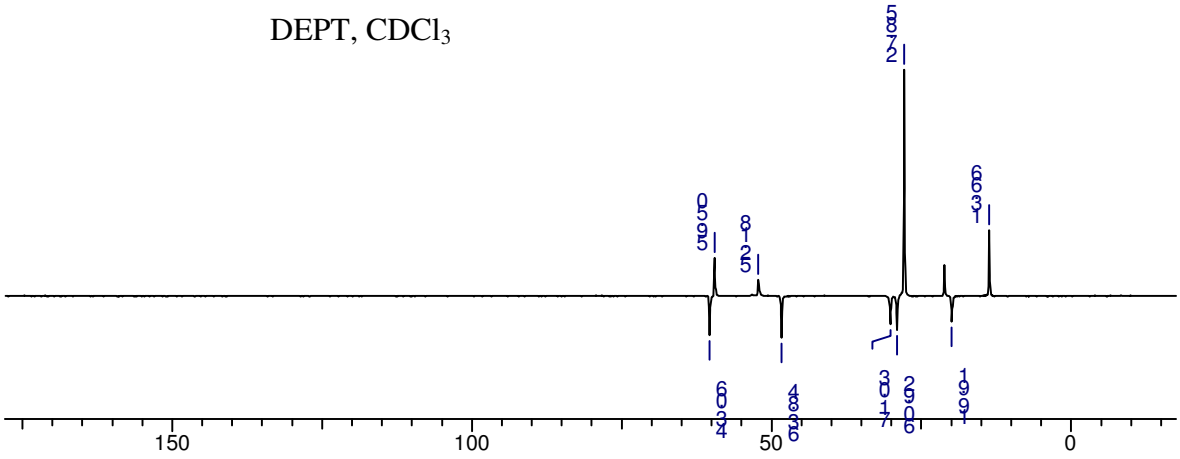

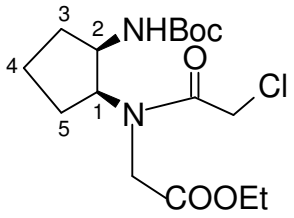

(1*S*,2*R*)-**9**

^{1}H NMR, $CDCl_3$

^{13}C NMR, $CDCl_3$

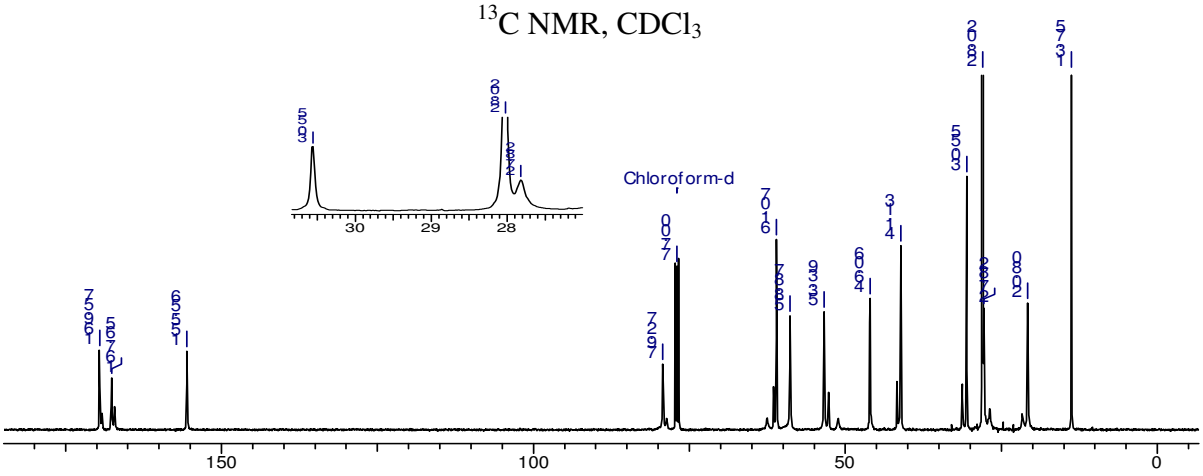

DEPT, $CDCl_3$

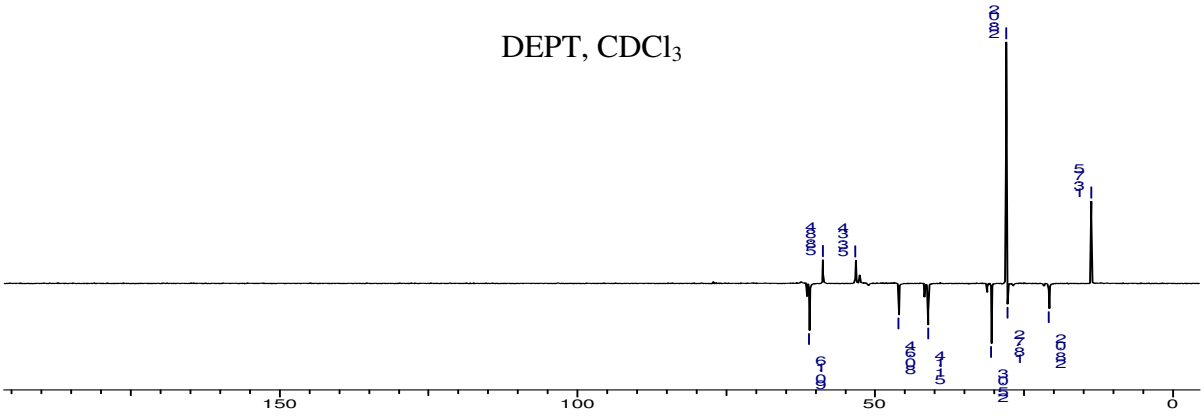

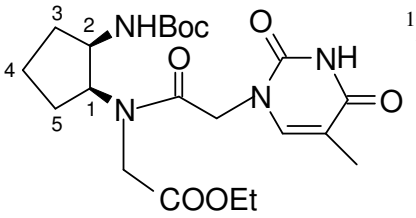

(1*S*,2*R*)-**10a**

^{1}H NMR, $CDCl_3$

^{13}C NMR, $CDCl_3$

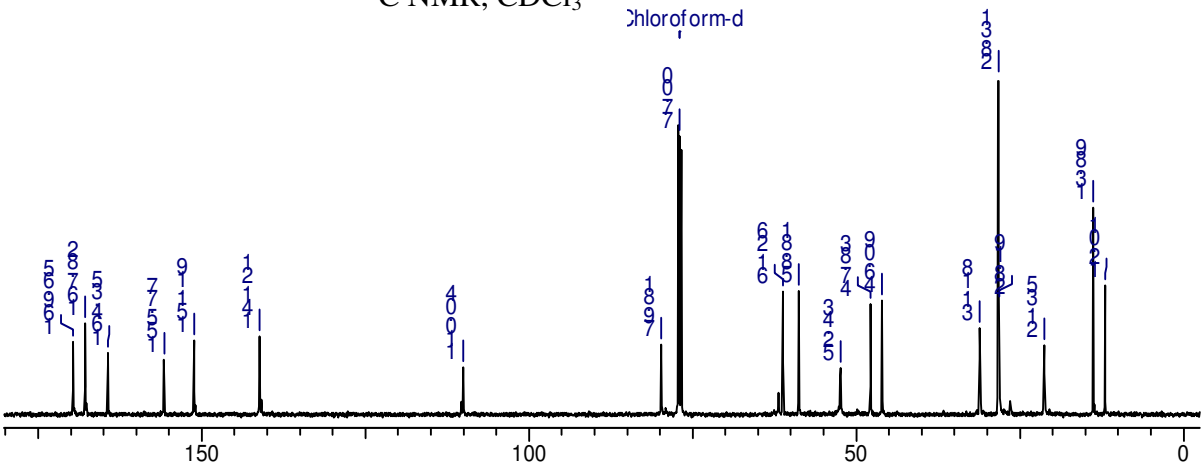

DEPT, $CDCl_3$

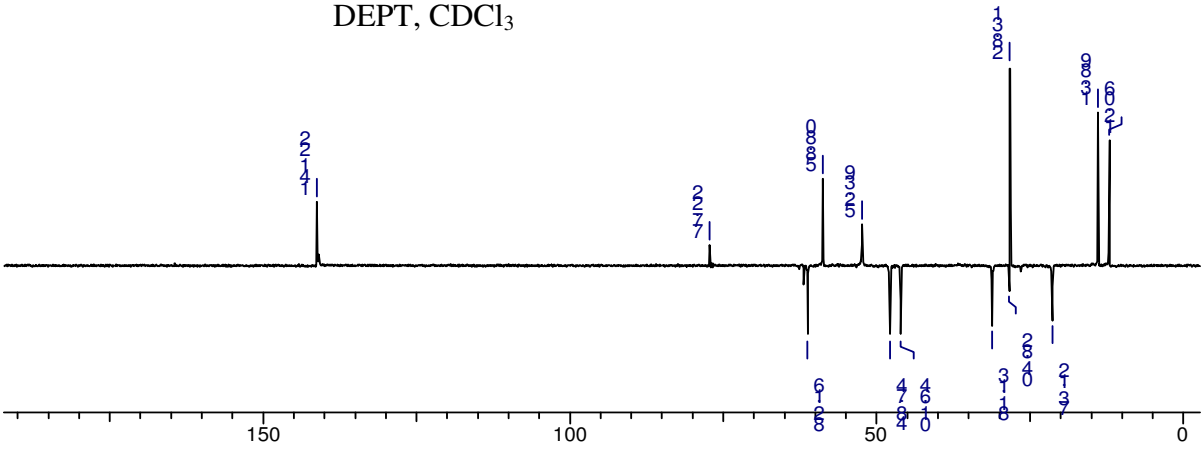

^{1}H NMR, $CDCl_3$

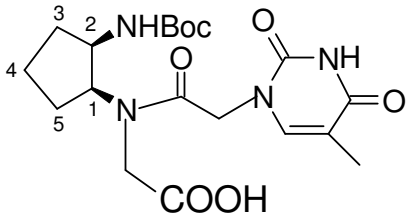

(1*S*,2*R*)-**11a**

^{13}C NMR, $CDCl_3$

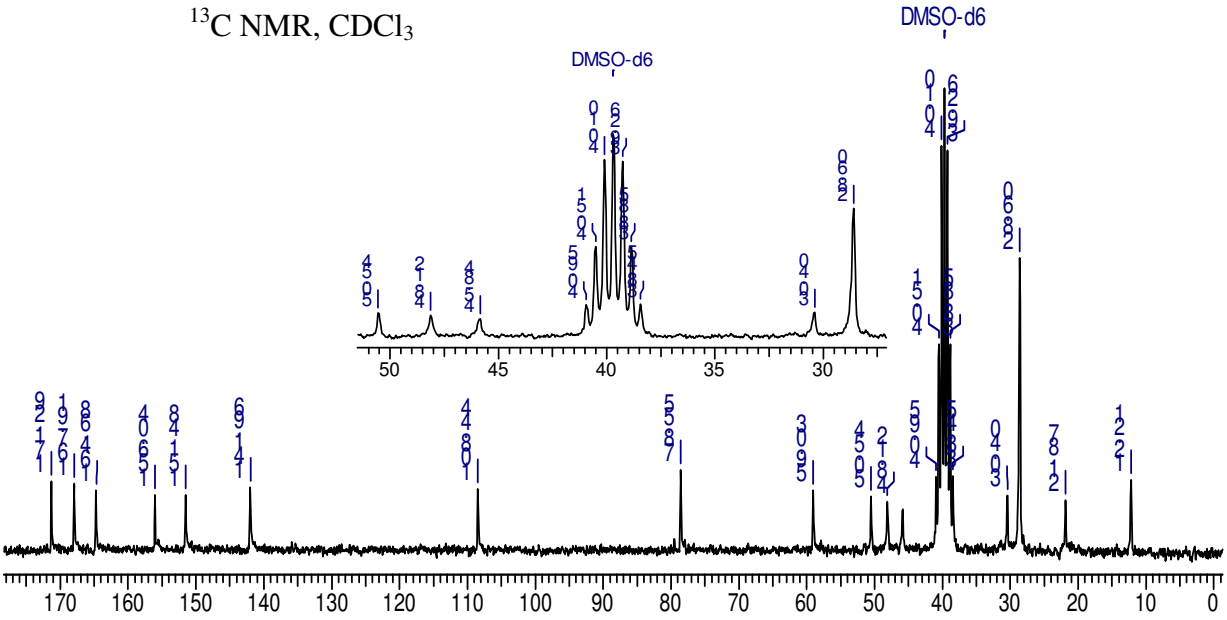

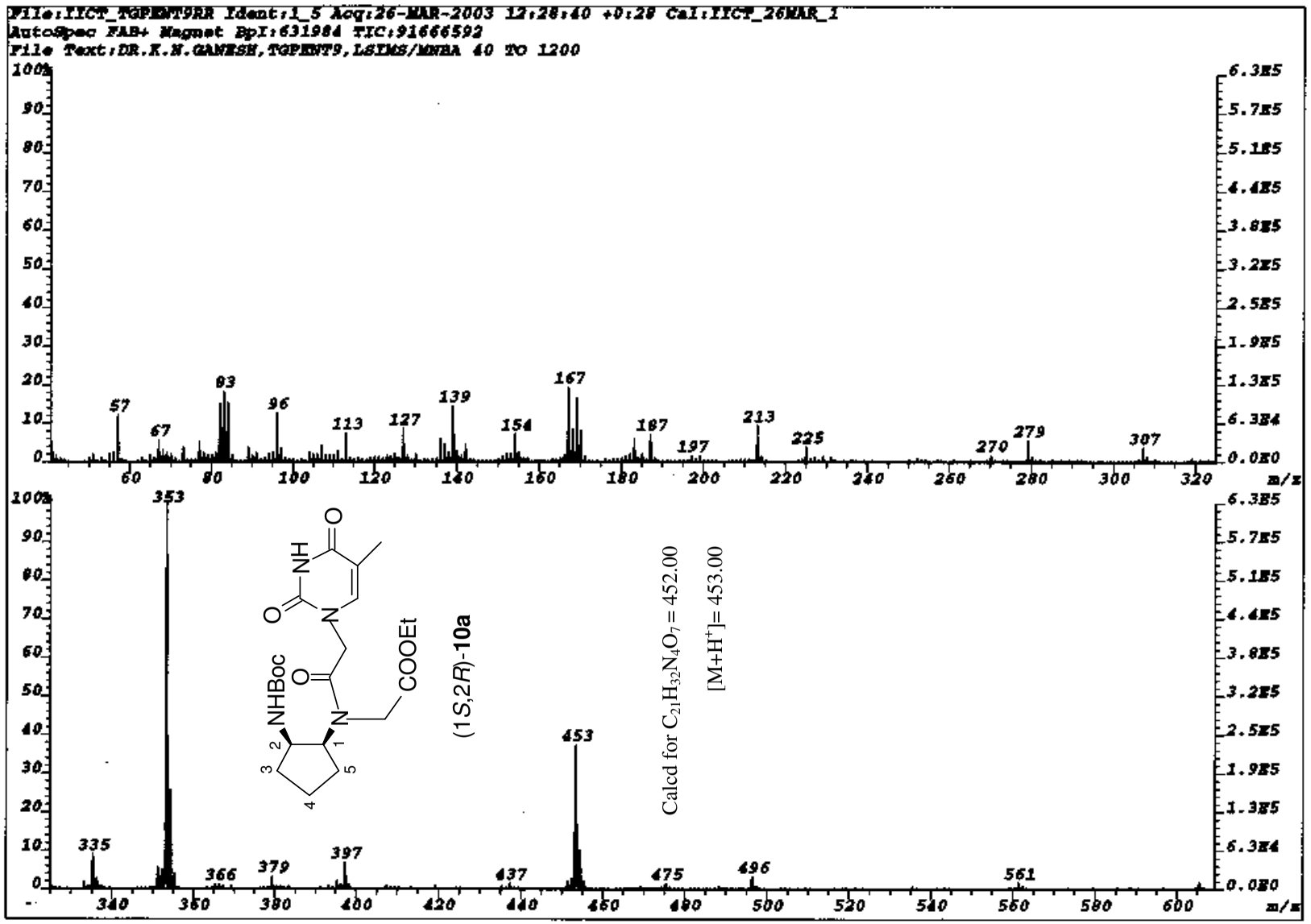
File:IICT_TGPENT9RR Ident:1_5 Acq:26-MAR-2003 12:28:40 +0:28 Cal:IICT_26MAR_1
AutoSpec FAB+ Magnet BpI:631984 TIC:91666592
File Text:DR.K.N.GANESH,TGPENT9,LSIMS/MNBA 40 TO 1200
m/z
NHBoc
COOEt
(1S,2R)-10a
Calcd for C21H32N4O7 = 452.00
[M+H+]= 453.00

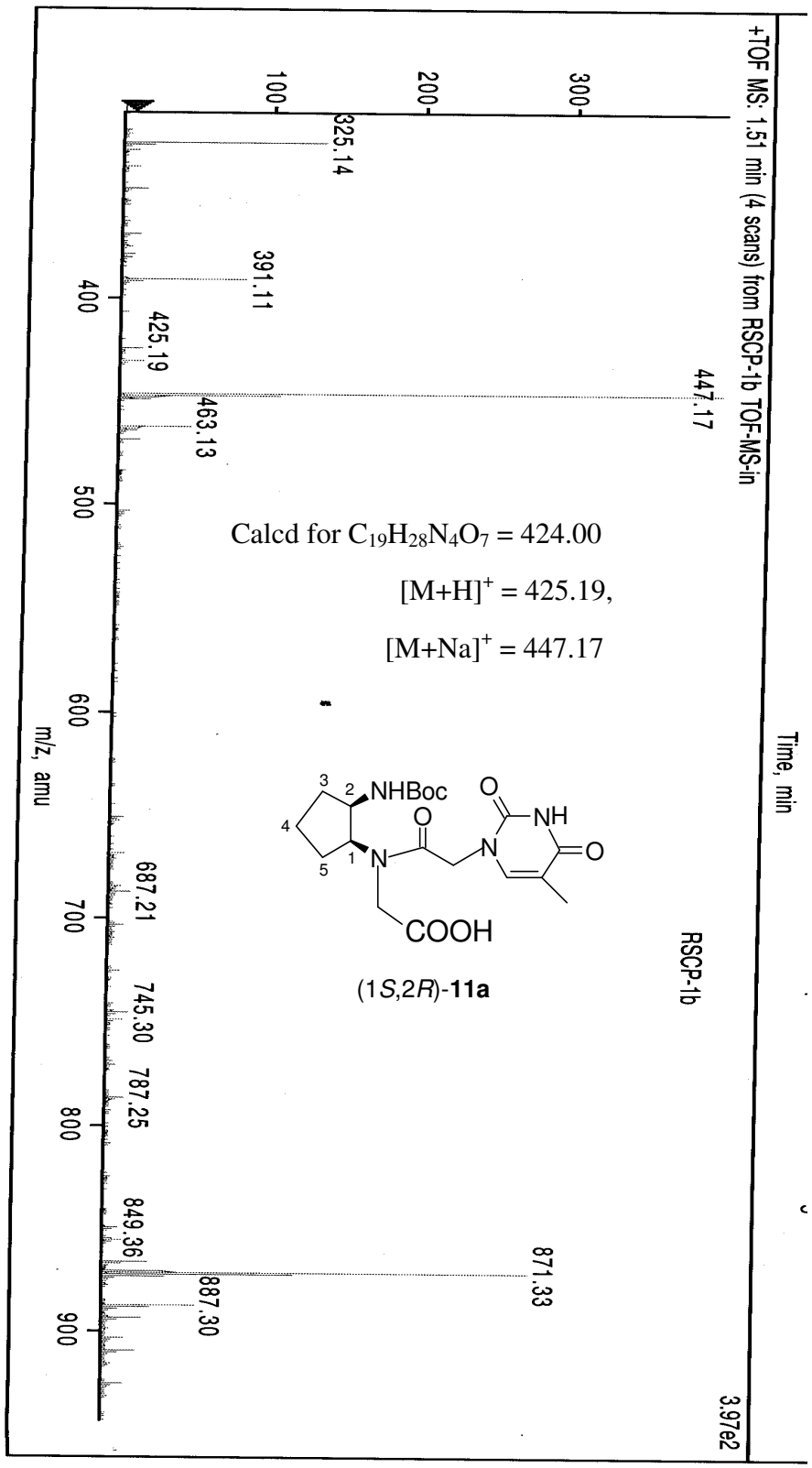
+TOF MS: 1.51 min (4 scans) from RSCP-1b TOF-MS-in
m/z, amu
Time, min
RSCP-1b
3.97e2
325.14
391.11
425.19
447.17
463.13
687.21
745.30
787.25
849.36
871.33
887.30
Calcd for C19H28N4O7 = 424.00
[M+H]+ = 425.19,
[M+Na]+ = 447.17
NHBoc
NH
COOH
(1S,2R)-11a

MALDI-TOF of *cp*PNA **15**

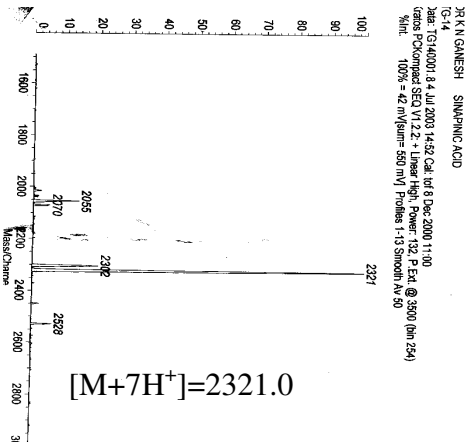

[M+7H$^+$]=2321.0

MALDI-TOF of *cp*PNA **16**

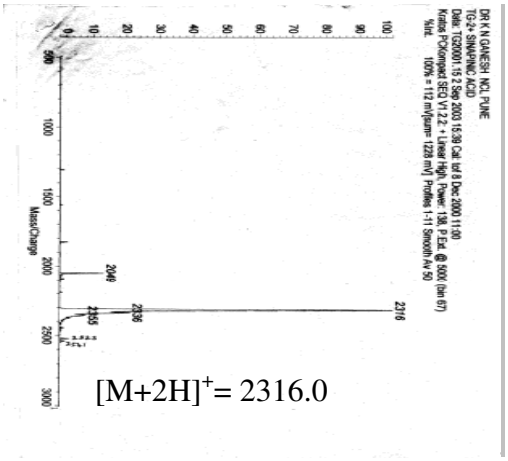

[M+2H]$^+$= 2316.0

MALDI-TOF of *cp*PNA **19**

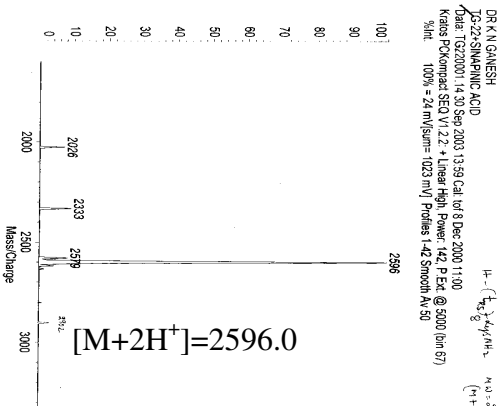

[M+2H$^+$]=2596.0

MALDI-TOF of *cp*PNA **22**

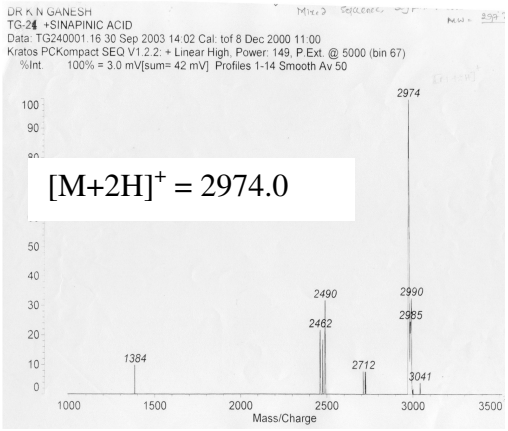

[M+2H]$^+$ = 2974.0

MALDI-TOF of *cp*PNA **13**

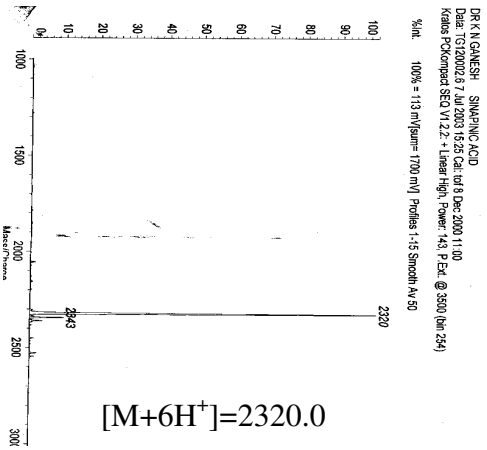

[M+6H$^+$]=2320.0

MALDI-TOF of *cp*PNA **14**

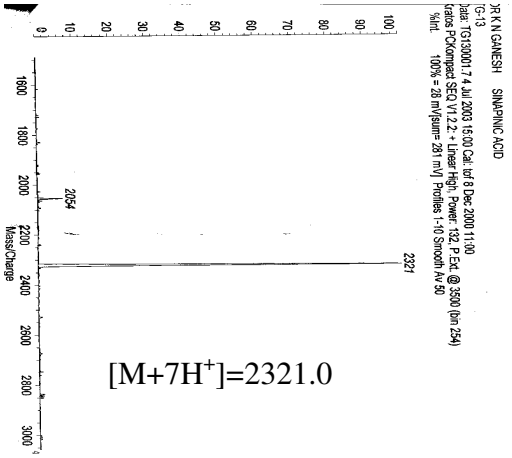

[M+7H$^+$]=2321.0

MALDI-TOF spectra of *cp*PNAs

Chapter-4

Backbone Extended Pyrrolidine PNA (*bep*PNA): Cationic, chiral PNA analogue with Optimized Inter-nucleobase distance and Geometry for Selective RNA Recognition

4.1 Introduction

In the previous chapters, where two complementary approaches namely tuning dihedral angle β around ethylene diamine segment of *aeg*PNA combined with constrained ring flexibility and chirality introduction were demonstrated to introduce RNA binding selectivity into classical PNA. The *ch*PNA (Chapter 2) showed RNA selectivity in forming duplexes and triplexes, though with lowered binding affinity in forming triplexes

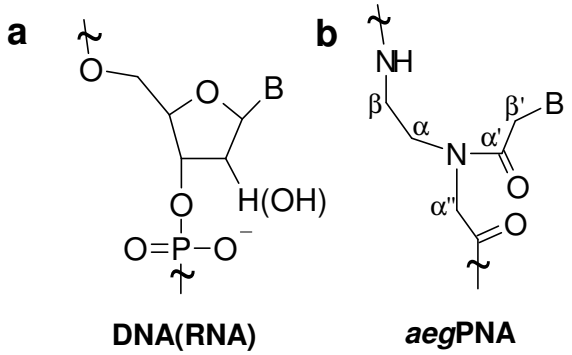

Figure 1. a) DNA (RNA) and b) *aeg*PNA-indicating the positions of carbon-atoms (Here α and β are used to denote the positions of carbon atoms and not for torsional angles).

and provided proof of design concept. In an attempt to increase the binding affinity in addition to RNA selectivity, *cp*PNA (Chapter 3) was designed to take the advantage of constrained flexibility through characteristic ring puckering of cyclopentane ring as opposed to conformationally locked cyclohexane ring. In fact *cp*PNA showed higher RNA binding affinity and unprecedented sequence specificity, but without DNA/RNA discrimination.

A different approach from those discussed above is designing a molecule that mimics DNA or PNA, (Figure 1) and also addresses PNA draw backs such as poor aqueous solubility and cellular uptake, in addition to ambiguity in parallel/antiparallel binding to complementary oligonucleotides and equal affinity for DNA and RNA. It was thought that properly preorganized PNA with five membered nitrogen heterocycle would satisfy the desired properties discussed above.

4.1.1 PNA With Five-membered Nitrogen Heterocycles

To overcome the drawbacks of *aeg*PNA, several rational modifications have been reported to date and five-membered nitrogen heterocyclic modifications represent a very important class among them. A number of neutral PNA analogues constrained with five membered pyrrolidine ring have been reported (Figure 1) from this laboratory[164] and elsewhere.[131,133, 205, 206] The chirality introduced in this way would make the resulting PNA to bind DNA/RNA in one direction either antiparallel or parallel. Aminoprolyl PNA (Figure 2**a**) was synthesized by bridging β -carbon atom of the aminoethyl segment and the α"-carbon of the glycine segment of *aeg*PNA, thus introducing two chiral centers.[132] All the four diastereomeric PNAs were synthesized. However, introduction of single chiral (2*R*,4*S*)- and (2*S*,4*R*)-aminoprolylPNA monomer at *N*-terminus showed some discrimination between parallel and antiparallel modes of binding towards the target DNA sequences. The homochiral thyminyl aminoprolyl PNAs did not bind to target sequences.[204] Perhaps the backbone-bridged structure of the monomers imparted high rigidity to the oligomers, making them structurally incompatible with the geometry of DNA for effective nucleobase recognition. A chimeric *aeg*PNA/(2*S*,4*R*)-aminoprolyl PNA backbone was shown to bind the target sequences with higher affinity as compared to the *aeg*PNA.[131] In another interesting modification, a methylene bridge was inserted

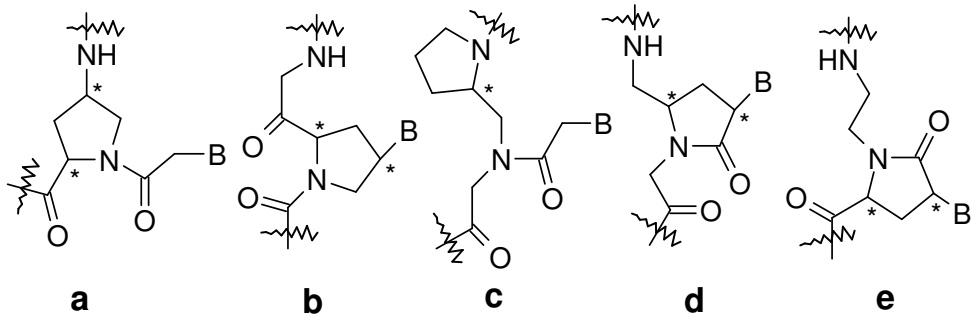

Figure 2. PNA Analogues with neutral five-membered pyrrolidine rings

between the α"–carbon atom of the glycine unit and β'-carbon atom of the nucleobase linker of the *aeg*PNA (Figure 2**b**).[133] The backbone so obtained consisted of alternating proline-glycine units, led to undesired rotameric populations arising from tertiary amide group. The oligomers with such a backbone were found to bind target sequences, with reduced binding affinity compared to *aeg*PNA.[131]

The introduction of a propyl hydrocarbon bridge between the amino nitrogen atom and the β-carbon atom of the aminoethyl segment of the *aeg*PNA afforded yet another PNA modification with a pyrrolidine ring (Figure 2**c**).[205] Incorporation of (*R*/*S*)-thymine monomer in the *aeg*PNA gave a constrained PNA, which bound to target oligonucleotide sequences with less efficiency than did the unmodified PNA. The PNA with a (2*R*)-pyrrolidine ring formed more stable complexes than did the PNA with (2*S*)-pyrrolidine ring. Methylene bridge inserted between the α-carbon of the aminoethyl segment and the β'-carbon atom of the acetyl linker to the nucleobase of *aeg*PNA (Figure 2**d**) lead to pyrrolidinone PNAs.[206] The methylene bridge prevented the rotation around the C-N bond of the acetyl segment connecting the nucleobase residue and pre-organized PNA in a rotameric conformation prevailing in complexes of PNA with target oligonucleotides as studied earlier.[207] The (3*S*,5*R*) isomer was shown to have the highest affinity towards RNA when compared to DNA. The fully modified decamer bound to rU_{10} with a small

decrease in the binding efficiency relative to *aeg*PNA. An alternative (2*S*,4*S*) *aepone*-PNA (Figure 2**e**) derived by insertion of a methylene bridge between β' and α'' carbons of *aeg*PNA stabilized DNA complex over RNA.[208]

Similarly a number of cationic PNAs constrained with pyrrolidine rings were also reported, where the tertiary nitrogen carries a positive charge, which causes easier solubility of the derived PNAs. A methylene bridge between α''-carbon of the glycine portion of the backbone and β'-carbon of the nucleobase-backbone linker, with carbonyl of the linker reduce to methylene results in aminoethylprolyl PNA (*aep*PNA) (Figure 3**a**).[209] Here the flexibility of the aminoethyl segment of *aeg*PNA was retained and the rotameric populations from the side chain were reduced. The oligomers of both (2*S*,4*S*) and (2*R*,4*S*) stereochemistries with nucleobase thymine showed very strong binding towards target sequences without compromising the sequence specificity. The *aep*PNA units carrying individual nucleobases: adenine, thymine, cytosine and guanine in a mixed purine/pyrimidine sequences exerted nucleobase-dependent binding efficacies and orientation selectivity towards target oligonucleotides.[210] Interestingly, a thymine homooligomer having (2*R*,4*R*) stereochemistry showed significant stabilization of the complexes with target poly rA.[211]

The possibility of the introduction of a β-α'-methylene bridge was also explored and gave another pyrrolidine based PNA modification (Figure 3**b**). This probably eases

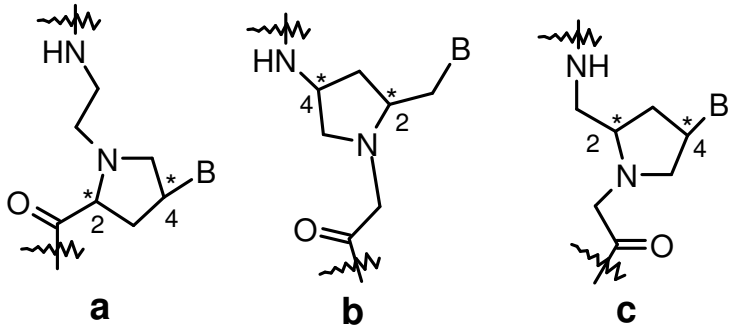

Figure 3. PNA Analogues with cationic five-membered pyrrolidine

the rigidity of the direct attachment of the nucleobase to the pyrrolidine ring. It was observed that the (2*R*,4*S*)-monomer, when incorporated in the center of *aeg*PNA T_8 sequence, was able to bind the target DNA, better than unmodified *aeg*PNA. Incorporation of the other isomer, with (2*S*,4*S*) stereochemistry, actually destabilized the complex with DNA. Three different research groups concurrently synthesized interesting structurally diastereomeric pyrrolidine PNAs (Figure 3**c**). A pentameric (2*R*,4*R*) pyrrolidine-amide oligonucleotide mimic (POM, Figure 3c), stabilized DNA/RNA with kinetic binding preference to RNA over DNA.[212] Pyrrolidine PNA having one (2*R*,4*S*)-modified unit (Figure 3c) showed destabilization against DNA and RNA and bind strongly when fully modified.[213] (2*S*,4*S*)-pyrrolidine PNA (Figure 3c) destabilized against both DNA and RNA.[214] In all the above pyrrolidine derived PNAs, the tertiary amine function with pKa ≈ 6.5-7.0 is partially protonated at physiological pH, and the PNAs are more water soluble even in the homo-oligomeric sequences.

The conformational strain in the alternating proline-glycine backbone (Figure 2**b**) was released by replacement of the α-amino acid residue by different β-amino acids spacers with appropriate rigidity (Figure 4).[215] β-Amino acids that gave favorable conformational freedom to the otherwise rigid backbone replaced the glycine unit in the prolyl-glycyl peptide backbone (**1**-**3**, Figure 4).[133,211] Novel pyrrolidinyl PNAs

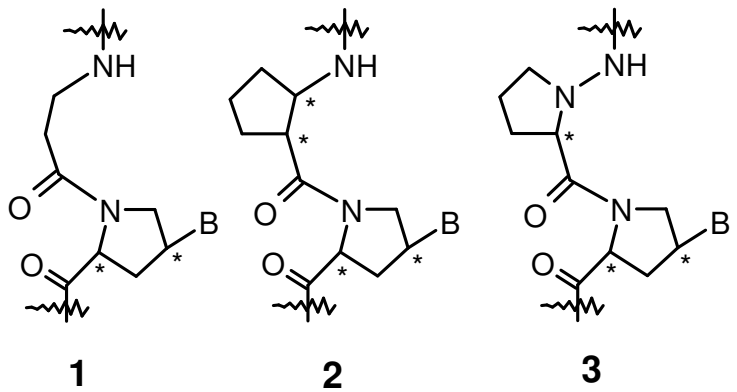

Figure 4. Prolyl-(β-amino acid) peptide PNAs.

comprising alternate units of nucleobase modified D-proline and either L-aminopyrrolidine-2-carboxylic acid, D-aminopyrrolidine-2-carboxylic acid (**3**, Figure 4), (1*R*,2*S*)-2-aminocyclopentanecarboxylic acid (**2**, Figure 4) or β-alanine (**1**, Figure 4)were synthesized. Gel binding shift assay revealed that only the homothymine PNA oligomer with D-aminopyrrolidine-2-carboxylic acid spacer could bind with the DNA target. The cyclic nature and the stereochemistry of the β–amino acid in the backbone geometry thus becomes an important feature of structural mimics of DNA.

Efforts directed towards the releasing the structural strain in aminoprolyl PNA (Figure 2**a**) also resulted in the synthesis of prolyl carbamate nucleic acids (Figure 5**a**), in which the amide bond was replaced by a carbamate linkage, extended by an additional atom in the repeating unit of the backbone in comparison to the unmodified *aeg*PNA oligomer.[216] Thymine or mixed pyrimidine oligomers of L-*cis*-prolyl carbamate nucleic acids were not attuned for binding with the target DNA. Another modification of prolyl PNA in which the internucleotide distance could be compatible to DNA was that formed by the replacement of the amide linkage by the phosphate linkage. No additional advantage was observed by the use either of 4-hydroxy-[143] or 3-hydroxyprolinol[217] derivatives (Figure 5**b** and 5**c** respectively).

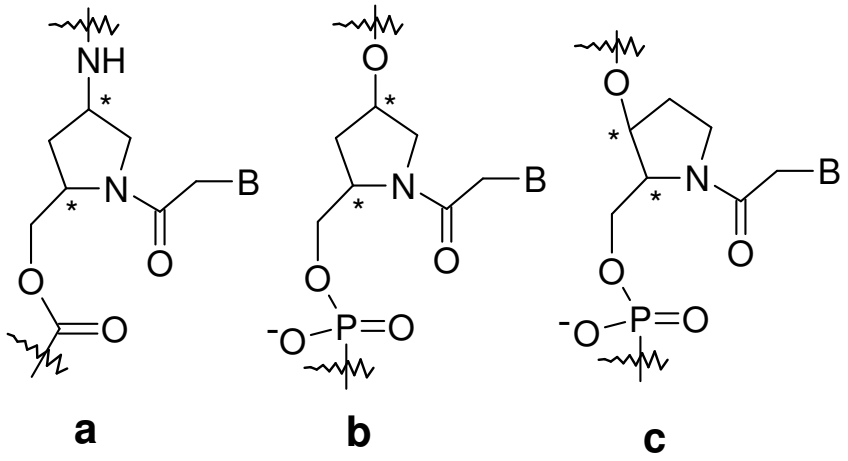

Figure 5. a) Prolyl carbamate NA; b) 4-hydroxyprolinol NA and c) 3-hydroxyprolinol

4.2 Rationale and Objective of the present work

Previous studies on DNA/RNA analogues have shown that the number of bonds in the repetitive DNA/RNA backbone can be varied to five or seven. As an example for five bond contracted backbone is TNA, an extraordinary oligonucleotide system introduced by Eschenmoser group.[82] TNA cross-pairs efficiently with complementary DNA and RNA, showing relatively high affinity to RNA over DNA. Matsuda *et al* studied the oligonucleotides containing an Oxetanocin A (Oxetanocin A, isolated from the culture filtrate of *Bacillus megaterium*), isomer of deoxyadenosine with an oxetane sugar moiety (Figure 6, **I**) and a higher analogue (Figure 6, **III**).[218] These analogues with extended seven-bond backbone cross-pair with RNA with high affinity compared to DNA.[218] Carbocyclic analogue of Oxetanocin A oligonucleotide system (Figure 6, **II**) also showed a tendency to form stronger complexes with ribonucleotide rather than with deoxyribonucleotide.[219]

In view of all these mixed results, it occurred to us that a pyrrolidine PNA with seven-bonds in the backbone (compared to six-bonds backbone of DNA, *aeg*PNA and other PNA analogues) being structurally analogues to DNA **III** (Figure 6), may have a

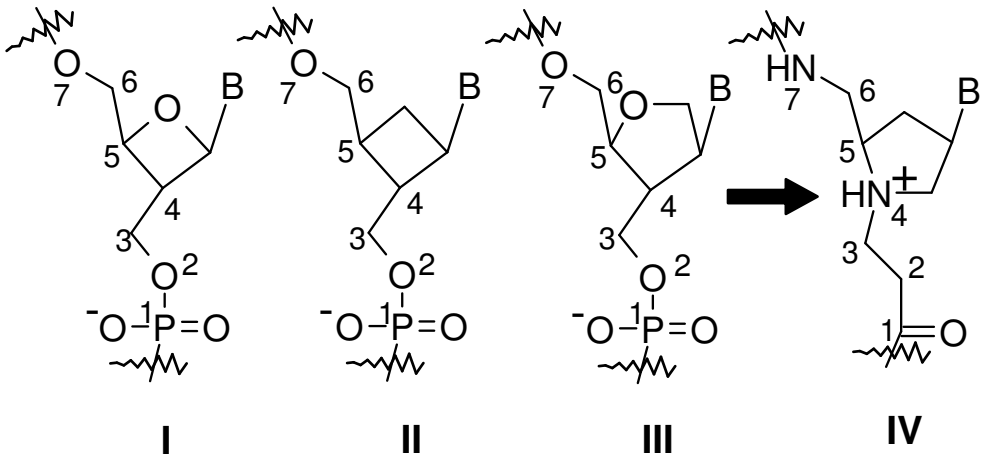

Figure 6. Design of *bep*PNA (**IV**) as DNA mimic. B = A/T

conformation with entropy advantages over *aeg*PNA to bind DNA/RNA.

There are examples in the literature suggesting that a five atom amide (linker) leading to a seven atom repeating backbone may be more useful because of the reduced conformational flexibility of the amide relative to phosphodiester backbone (Figure 7, Amide **I**, and Amide **II**).[220] This postulate has been supported by X-Ray studies.[220] Some of these analogues with extended seven-bond backbone cross-pair with RNA with higher affinity compared to DNA. The X-ray data indicated that the amide backbone has a *trans* conformation and that the distance between neighboring base pairs is not affected by incorporation of longer backbone.[220] In contrast, Lowe *et al* very effectively accomplished preferential DNA binding by replacing glycine with one atom extended β-amino acids in prolyl-glycyl PNA analogs (Figure 4).[211,215] Our preliminary results on the chimeric phosphate-amide extended backbone revealed that 2*R*,4*R* pyrrolidine-amide chimera were accommodated better in triplex forming sequences (Figure 7, Amide **III**).[221]

Based on these facts, we have designed pyrrolidine PNA (*bep*PNA **IV**, Figure 6 and 8) to achieve higher affinity and selectivity between DNA and RNA. This is homologues to pyrrolidine PNA, with increased length of the glycyl fragment to homoglycine. It may provide a hybridization-competent conformation with balanced

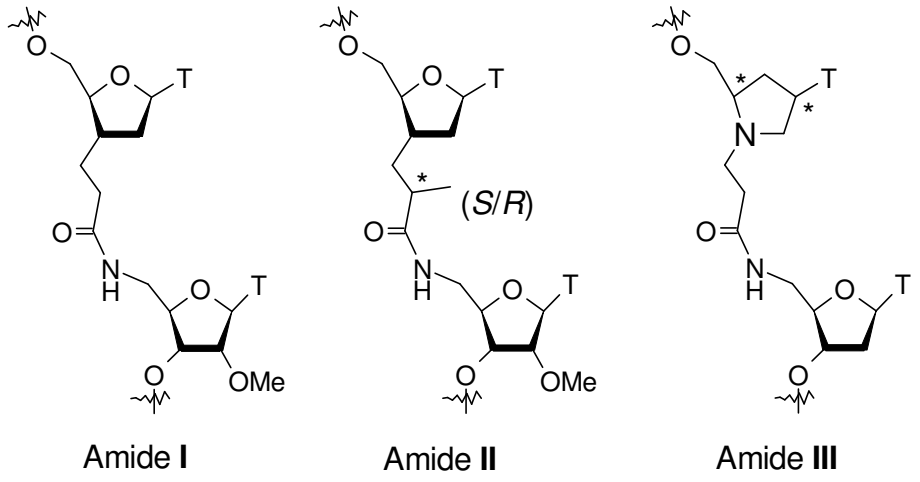

Figure 7. Oligonucleotide analogues with 5-atom amide backbone.

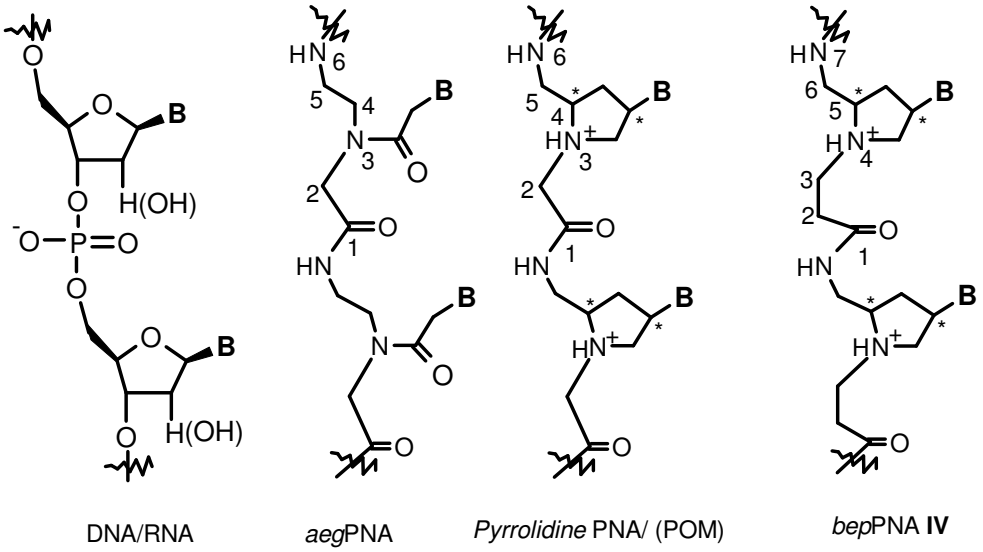

Figure 8. Chemical structures of DNA (RNA), *aeg*PNA, Pyrrolidine PNA and *bep*PNA

rigidity and flexibility to the modified PNA to bind DNA/RNA with a higher affinity and sequence selectivity. The cationic charge and the chirality will give additional advantage in terms of solubility and orientational selectivity.

The objectives of the present chapter are:

1) Synthesis of *bep*PNA monomer [(*2S,4S*)-2-(*tert*-butyloxycarbonylaminomethyl)-4-(thymin-1-yl)pyrrolidin-1-yl] propanoic acid (Figure 9).

2) Solid Phase Synthesis of oligomers incorporating *aeg*PNA (A/G/C/T) monomers or *bep*PNA (T) monomer.

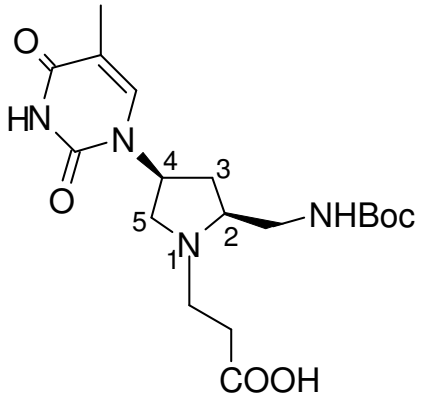

Figure 9. Target *cis*-(2*S*,4*S*)-*bep*PNA monomer

3) The binding studies of *bep*PNA with DNA/RNA using different biophysical techniques.

4.3 Results and Discussion

The naturally occurring amino acid *trans*-4-hydroxy-L-proline is a versatile starting material for the synthesis of various natural and unnatural organic compounds, as it possesses 3-site chemical diversity and 2-site stereochemistry that can be manipulated in a predictable way.[222] The (2*S*,4*R*)-isomer is the most abundant naturally occurring diastereomer.[223] That is commercially available in bulk amount. With two chiral centers at C-2 and C-4, trans-4-hydroxy-L-proline is a material of choice to access multi-functionalized pyrrolidine rings. Thus, the synthesis of (2*S*,4*S*)-*bep*PNA thymine monomer was achieved from hydroxy proline as represented in Figure 10.

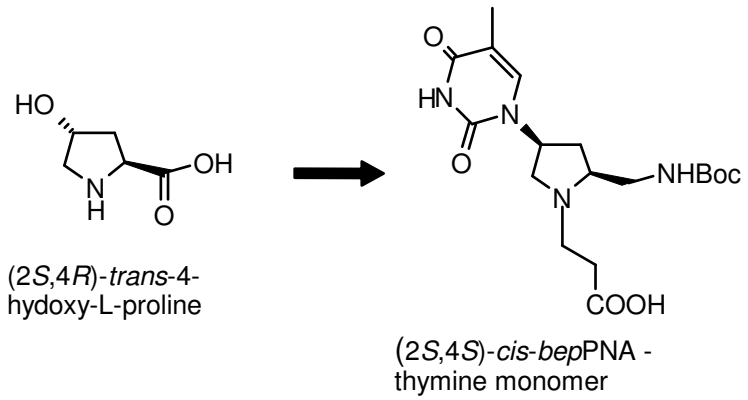

Figure 10. Schematic representation of synthesis of *bep*PNA monomer

4.3.1 Synthesis of *bep*PNA monomer [(*2S,4S*)-2-(*tert*-butyloxycarbonylaminomethyl)-4-(thymin-1-yl) pyrrolidin-1-yl] propanoic acid

The synthesis of monomer **12** started with the protection of ring nitrogen of the naturally occurring *trans*-4-hydroxy-L-proline (**1**) to give ring nitrogen protected compound **2**,[224] which was then converted to its methyl ester **3** on treatment with MeOH

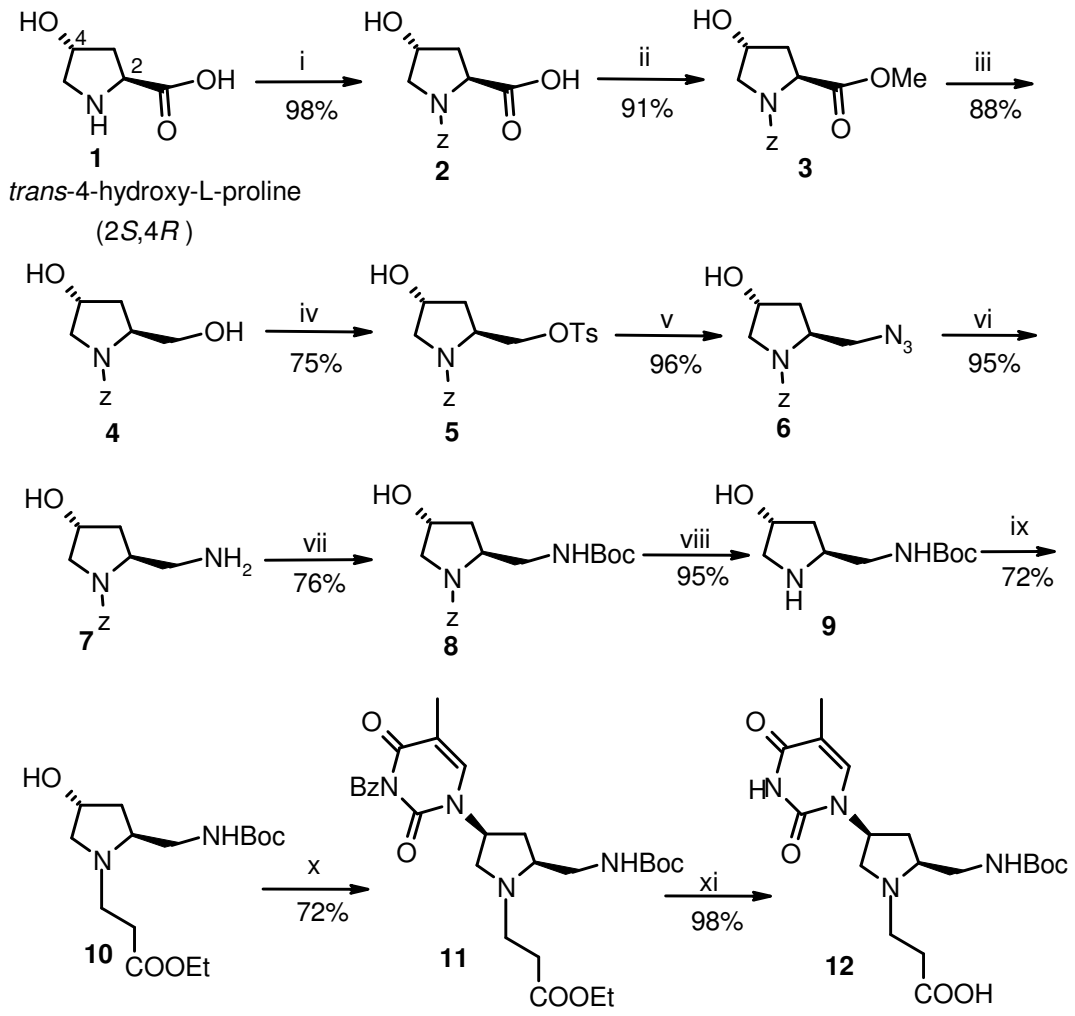

Scheme 1. *Reagents and conditions*: (i) Cbz-Cl (50% toluene soln.), Et_3N, $NaHCO_3$, water, rt, 8 h. (ii) $SOCl_2$, Et_3N, MeOH, rt, 7 h. (iii) LiCl, $NaBH_4$, ethanol:THF(4:3), rt, 7 h. (iv) TsCl, pyridine, rt, 7 h. (v) NaN_3, DMF, 70°C, 8 h. (vi) Raney Ni, H_2, MeOH, 35 psi, rt, 3 h. (vii) $BocN_3$, DMSO, 50°C, 5 h. (viii) H_2/Pd-C, MeOH, 60 psi, rt, 7 h. (ix) Ethyl acrylate, MeOH, rt, 2.5 h. (x) N3-benzoyl –Thymine, DEAD, PPh_3, benzene, rt, 4 h. (xi) 2N aq. NaOH, Dowex H^+,rt, 5 h.

/$SOCl_2$ as reported earlier.[214] The methyl ester in compound **3** was reduced using LiCl / $NaBH_4$ to yield diol **4** (Scheme 1)**.** Selective tosylation of the primary hydroxy group by controlled addition of *p*-TsCl in pyridine gave monotosylate **5** along with small amount of ditosylate, which was removed by column chromatography. The monotosylate **5** was treated with NaN_3 to obtain azido compound **6** and selective reduction of azide using Raney Ni in methanol yielded free amine **7**. The protection of free amine **7** using $BocN_3$

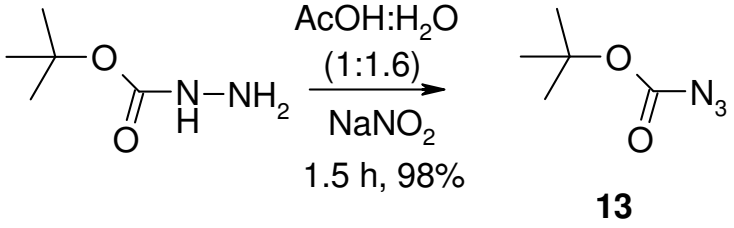

Scheme 2. Synthesis of $BocN_3$

in DMSO yielded compound **8.** The $BocN_3$ (**13**) was prepared by treating the *t*-butyl carbazate in glacial acetic acid and water with $NaNO_2$.

Azide compound **8** was subjected to hydrogenation using H_2/ Pd-C catalyst to remove benzyloxy carbonyl group to give free amine **9**, followed by its alkylation with ethyl acrylate in methanol to yield the alkylated product **10**. The secondary alcohol **10** was converted to protected thymine monomer ethyl ester **11** on treating with *N*3-benzoyl thymine under Mitsunobu conditions.[225] The retention of peaks in aromatic region integrating for five protons, indicated that benzoyl group on thymine was intact during the Mitsunobu reaction. It was observed that DIAD often delivered inferior yields in mitsunobu reactions especially while using poor nucleophiles such as *N*3-benzoyl thymine. Alternatively DEAD was used to obtain good yields. The hydrolysis of ethyl ester **11** and simultaneous *N*3 deprotection of thymine was achieved using 2N aq. NaOH in methanol. The sodium salt of the free acid in aqueous layer was washed with DCM to remove benzoic acid and then the aqueous layer was neutralized with a cation exchange resin (Dowex-H^+) to pH 7.0. The aqueous layer upon concentration yielded the required monomer [(*2S,4S*)-2-(*tert*-butyloxycarbonylaminomethyl)-4-(thymin-1-yl) pyrrolidin-1-yl] propanoic acid (**12**) in good yield (Scheme-1). All the compounds were characterized by NMR and mass spectroscopy.

One-step conversion of 4-OH in **10** to the corresponding thymin-1-yl derivative with an inversion of configuration can be achieved under Mitsunobu conditions. As the reactivities of *N*1 and *N*3 of thymine are comparable towards alkylation, this reaction results in both *N*1-alkylated and *N*1, *N*3-dialkylated products. Hence, *N*3 of the thymine was first protected as benzoyl derivative,[226] the synthesis of which is shown in scheme 3. *N*1, *N*3-di-benzoyl derivative **14** of thymine was prepared by treating thymine with 2.5 eq. of benzoyl chloride in pyridine. The treatment of *N*1,*N*3-dibenzoyl derivative **14** with K_2CO_3 in dioxane-water resulted in selective hydrolysis of *N*3-benzoyl group in **14** to yield the *N*1-benzoyl compound **15**.

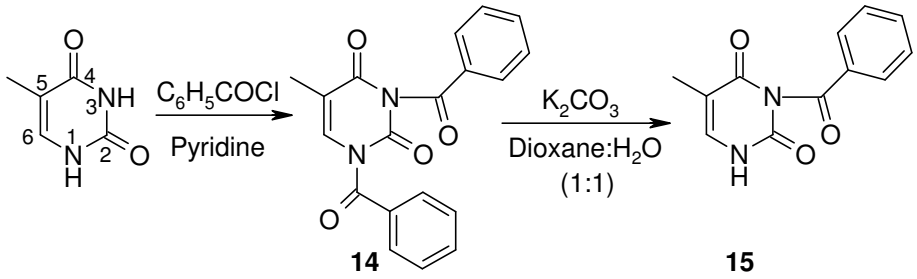

Scheme 3. *N*3-benzoyl protection of thymine

4.3.2 Determination of pKa of ring nitrogen (*N*1) of the *bep*PNA thymine monomer 12

The *bep*PNA monomer carry a tertiary amino group that can be protonated, and a pH titration experiments was carried out with NaOH to determine the exact pKa of the pyrrolidine ring nitrogen atom. A plot of pH versus volume of NaOH added gave three transitions; the first one corresponding to the carboxylic acid, second corresponding to the tertiary ring nitrogen and the third corresponding to the free amine group of the deprotected monomer. The *Boc* protected monomer **12** was deprotected using trifluoro acetic acid, which then titrated against 0.2N NaOH to find out the pKa values of free –

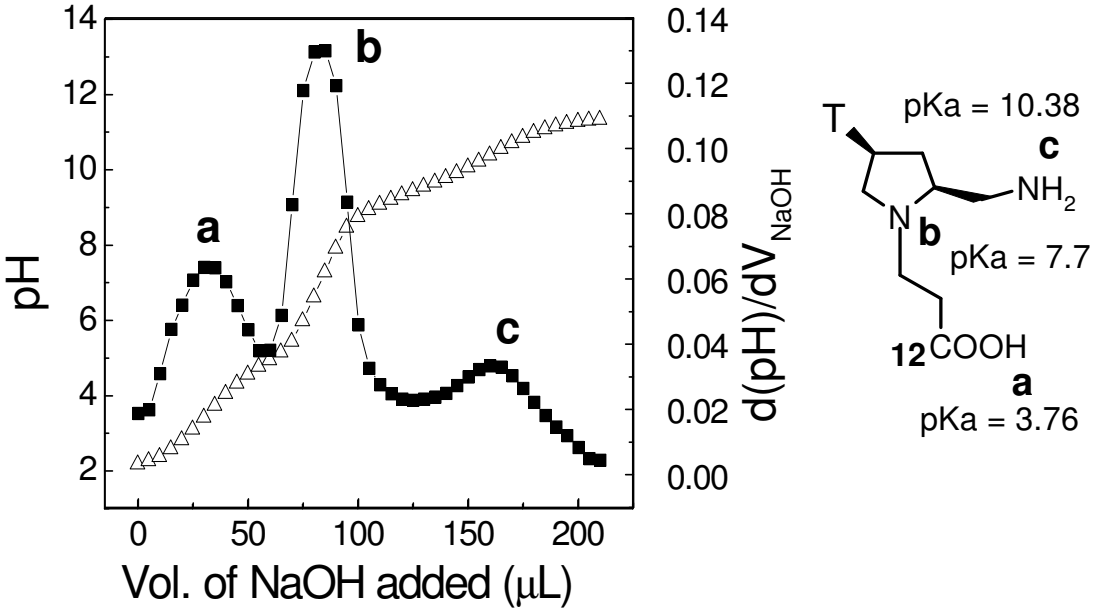

Figure 11. pH titration curve of (2*S*,4*S*)-*bep*PNA monomer **12** with NaOH and its derivative.

NH_2, -COOH and ring nitrogen. The pKa values for free -NH_2 and –COOH are found to be 3.76 and 10.38 respectively. The pKa of ring nitrogen was found to be 7.7 (Figure 11) and therefore indicate the partial protonation at physiological conditions (pH). This pKa (7.7) of the ring nitrogen is more than any other reported pyrrolidine PNA analogues and hence the derived PNA has potential to be more protonated at neutral pH.

4.3.3 Synthesis of *aeg*PNA monomers

Amino ethylglycyl PNA (A/G/C/T) monomers (Figure 12) were synthesized as discussed in Chapter 2,[175-178] these monomers were used for the synthesis of *aeg*PNA T_8 octamer for the control studies and to synthesize *bep*PNA-*aeg*PNA chimeras.

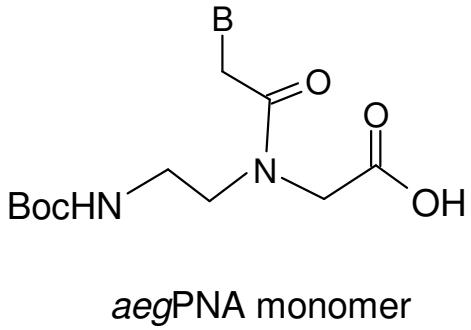

Figure 12. *aeg*PNA monomers, B = A/G/C/T

4.3.4 Solid phase peptide synthesis

In the synthetic strategy for the backbone extended pyrrolidine PNA monomer, the Boc-protecting group was utilized for the amino group and PNA oligomer synthesis was carried out from the '*C*' to '*N*' terminus using monomers with free carboxylic acid functions and amino functions protected as Boc derivatives that are cleavable with TFA at the beginning of every coupling cycle. The solid support used was MBHA (4-methyl benzhydryl amine) resin[172,173] that was derivatized with L-lysine using peptide coupling reagents. The loading value of the so derivatized resin was found to be 0.85 meq/g. L-lysine is linked to the resin via amide linkage enabling cleavage of the synthesized oligomer by strong acid like TFMSA in TFA to afford oligomer with *C*-terminal amide.

The resin, upon attachment of the L-lysine spacer amino acid, was suitably down loaded to attain a loading capacity of 0.25 m eq./g resin (Chapter 2), which is found to be suitable to build a peptide oligomer. The loading capacity of the resin was determined by the non-destructive picrate assay.[185,186] The synthesis was carried out by repetitive

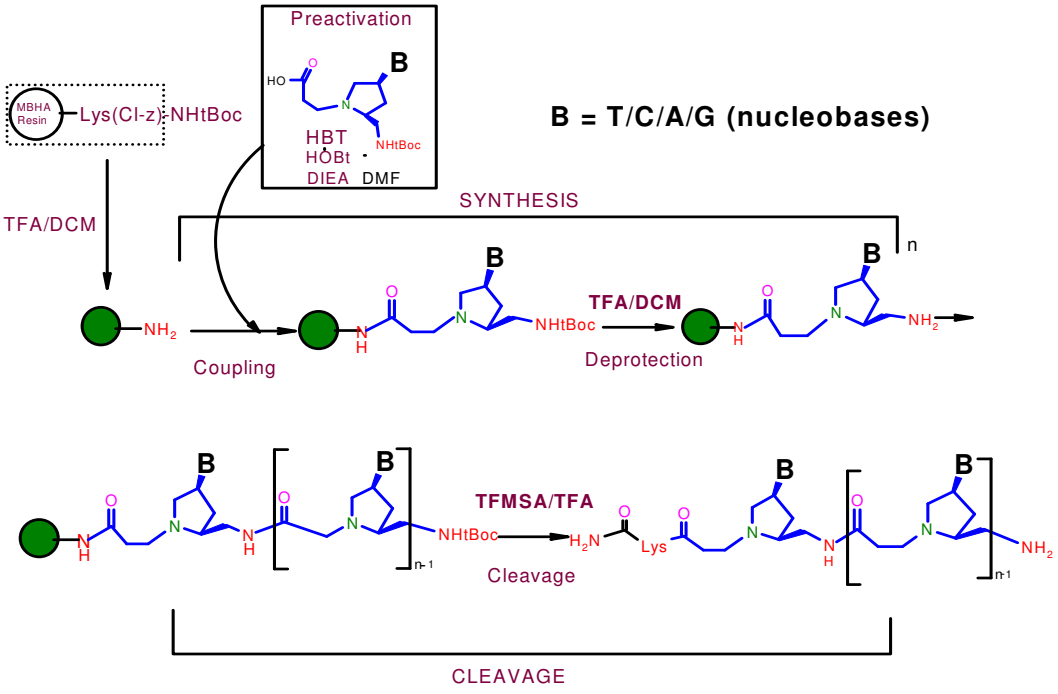

Figure 13. Solid Phase Peptide Synthesis of *bep*PNA

coupling cycles as shown in Figure 13, each cycle comprising i) deprotection of the *Boc*-amino group using 50% TFA in dichloromethane to generate the amine group as TFA salt, ii) neutralization of the resulting TFA salt by 5% DIEA to liberate the free amine, iii) coupling of the incoming *aeg*PNA/*bep*PNA monomer with the resin bound L-lysine α-amino groups using coupling reagents HBTU, HOBt and DIEA as a base in DMF/DMSO as a solvent. The deprotection and coupling steps were monitored by the ninhydrin method using Kaiser's test.[187] The coupling cycle is repeated according to the length of the required oligomer.

Synthesis of cationic backbone extended pyrrolidine Peptide Nucleic Acids (bep*PNA*): The modified *cis*-(2*S*,4*S*)-*bep*PNA thymine monomers **12** was incorporated into PNA sequences using Boc chemistry on L-lysine-derivatized (4-methylbezhydryl)amine (MBHA) resin as reported before, using HBTU/HOBt/DIEA in DMF as the coupling reagent. Various homothymine PNA oligomers (**17**-**20**, Table 1) incorporating modified monomers at the middle (**19**), *N*-terminus (**18**), *C*-terminus (**17**), at alternative positions (**20**) and through the entire sequence (homooligomer **21**) were-

Table 1. PNA sequences synthesized in the present study

Entry	Sequence code	PNA Sequences
		Homothymine sequences
1	*aeg*PNA **16**	H-T T T T T T T T -LysNH2
2	*bep*PNA **17**	H-T T T T T T T **t** -LysNH2
3	*bep*PNA **18**	H- T T T **t** T T T T -LysNH2
4	*bep*PNA **19**	H- **t** T T T T T T T -LysNH2
5	*bep*PNA **20**	H- T **t** T **t** T **t** T **t** -LysNH2
6	*bep*PNA **21**	H-(t t t t t t t t) -LysNH2
		Mixed Sequences
7	*aeg*PNA **22**	H-G T A G A T C A C T-LysNH2
8	*bep*PNA **23**	H-G **t** A G A **t** C A C **t**-LysNH2

A/G/C/T = *aeg*PNA Adenine/Guanine/Cytosine/Thymine monomers, **t** = (2*S*,4*S*)-*bep*PNA Thymine monomer

synthesized in order to study their triplex formation and stability with DNA/RNA Octamer (**16**) was also synthesized incorporating *aeg*PNA thymine monomer for the use of control studies. In order to study the duplex formation potential and in particular DNA/RNA discrimination of the *bep*PNA monomeric units, it was imperative to synthesize mixed sequences incorporating both, purine and pyrimidines. Mixed sequences *aeg*PNA **22** and *bep*PNA **23** were also synthesized by incorporating *aeg*PNA (A/G/C/T) monomers and *bep*PNA (**t**) monomers (Table 1).

Cleavage of the PNA Oligomers from The Solid Support: The oligomers are cleaved from the solid support, using strong acid trifluoromethane sulphonic acid (TFMSA) in the presence of trifluoro acetic acid (TFA) ('Low, High TFMSA-TFA method"),[191] which yields oligomer with amide at their *C*-terminus (Table 2). The side chain protecting groups are also cleaved during this process. After cleavage, the oligomers were precipitated from methanol with dry diethyl ether.

Purification of the PNA Oligomers: All the cleaved oligomers were subjected to initial gel filtration. The purity of the so obtained oligomers were checked by analytical RP HPLC (C18 column, CH_3CN-H_2O system), which shows more than 65-75% purity. These were subsequently purified by reverse phase HPLC on a semi preparative C18 column. The purity of the oligomers was again ascertained by analytical RP-HPLC and their integrity was confirmed by LC-TOF-MS mass spectrometric analysis. Some representative HPLC profiles and mass spectra are shown in Figures 14 (Table 2).

4.3.5 Synthesis of Complementary Oligonucleotides

The DNA oligonucleotides **24**-**29** (Table 3) were synthesized on Applied Biosystems ABI 3900 High Throughput DNA Synthesizer using standard β-cyanoethyl phosphoramidite chemistry. The oligomers were synthesized in the 3' to 5' direction on

HPLC profile of b*ep*PNA **17**

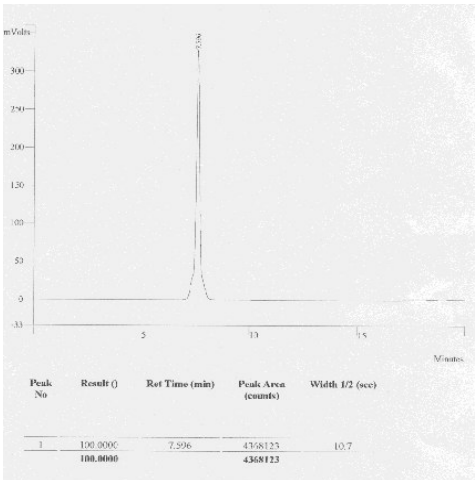

Peak No	Result ()	Ret Time (min)	Peak Area (counts)	Width 1/2 (sec)
1	100.0000	7.596	4368123	10.7
	100.0000		4368123	

HPLC profile of *bep*PNA **18**

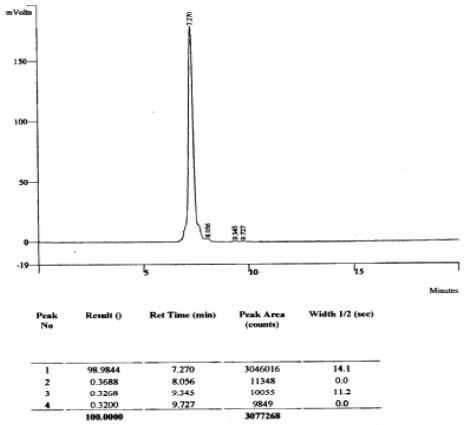

Peak No	Result ()	Ret Time (min)	Peak Area (counts)	Width 1/2 (sec)
1	98.9844	7.270	3046016	14.1
2	0.3688	8.056	11348	0.0
3	0.3268	9.345	10055	11.2
4	0.3200	9.727	9849	0.0
	100.0000		3077268	

HPLC profile of *bep*PNA **19**

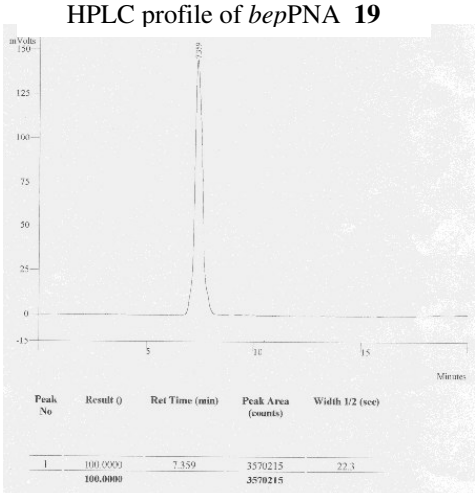

Peak No	Result ()	Ret Time (min)	Peak Area (counts)	Width 1/2 (sec)
1	100.0000	7.359	3570215	22.3
	100.0000		3570215	

HPLC profile of *bep*PNA **20**

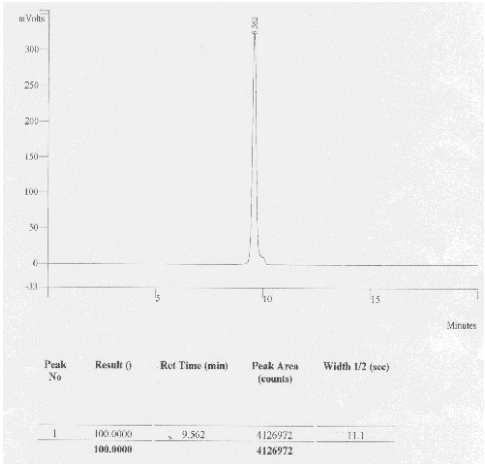

Peak No	Result ()	Ret Time (min)	Peak Area (counts)	Width 1/2 (sec)
1	100.0000	9.562	4126972	11.1
	100.0000		4126972	

HPLC profile of *bep*PNA **21**

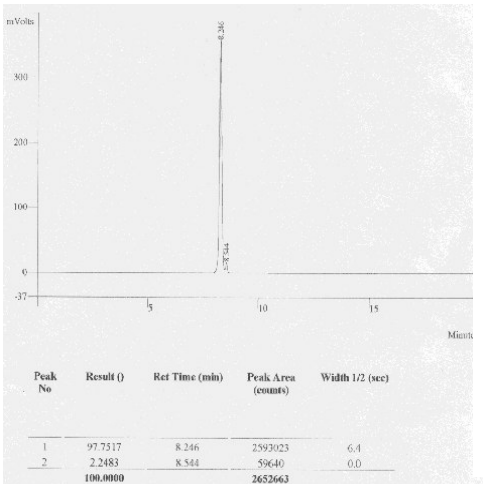

Peak No	Result ()	Ret Time (min)	Peak Area (counts)	Width 1/2 (sec)
1	97.7517	8.246	2593023	6.4
2	2.2483	8.544	59640	0.0
	100.0000		2652663	

HPLC profile of *bep*PNA **23**

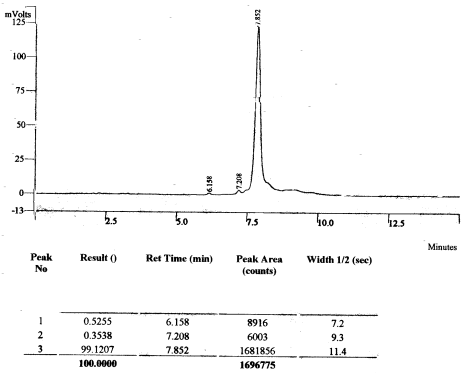

Peak No	Result ()	Ret Time (min)	Peak Area (counts)	Width 1/2 (sec)
1	0.5255	6.158	8916	7.2
2	0.3538	7.208	6003	9.3
3	99.1207	7.852	1681856	11.4
	100.0000		1696775	

Figure 14a. Reverse phase HPLC profiles of *bep*PNAs. (For HPLC conditions, see experimental section)

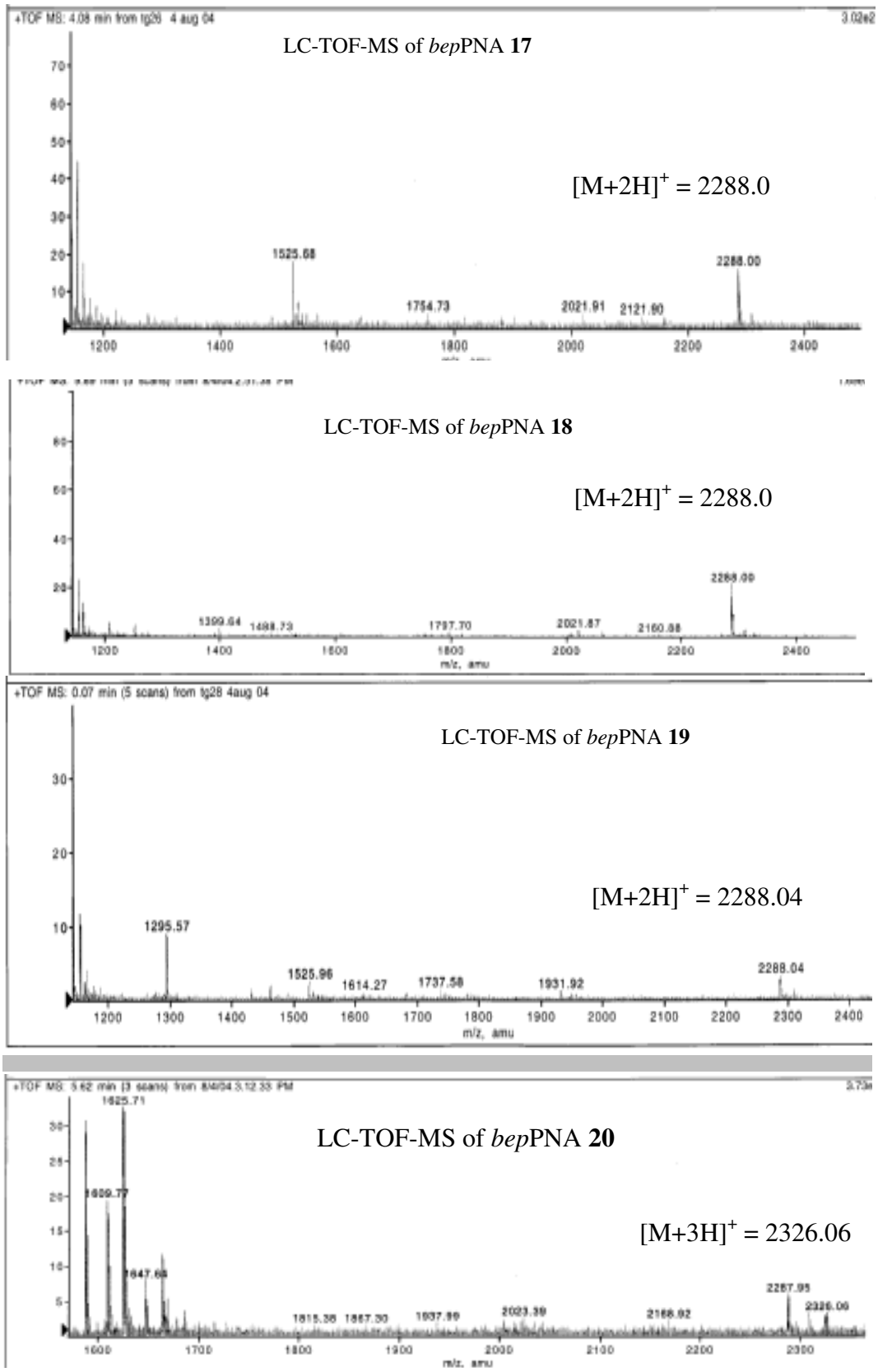

Figure 14b. Mass spectra of *bep*PNAs

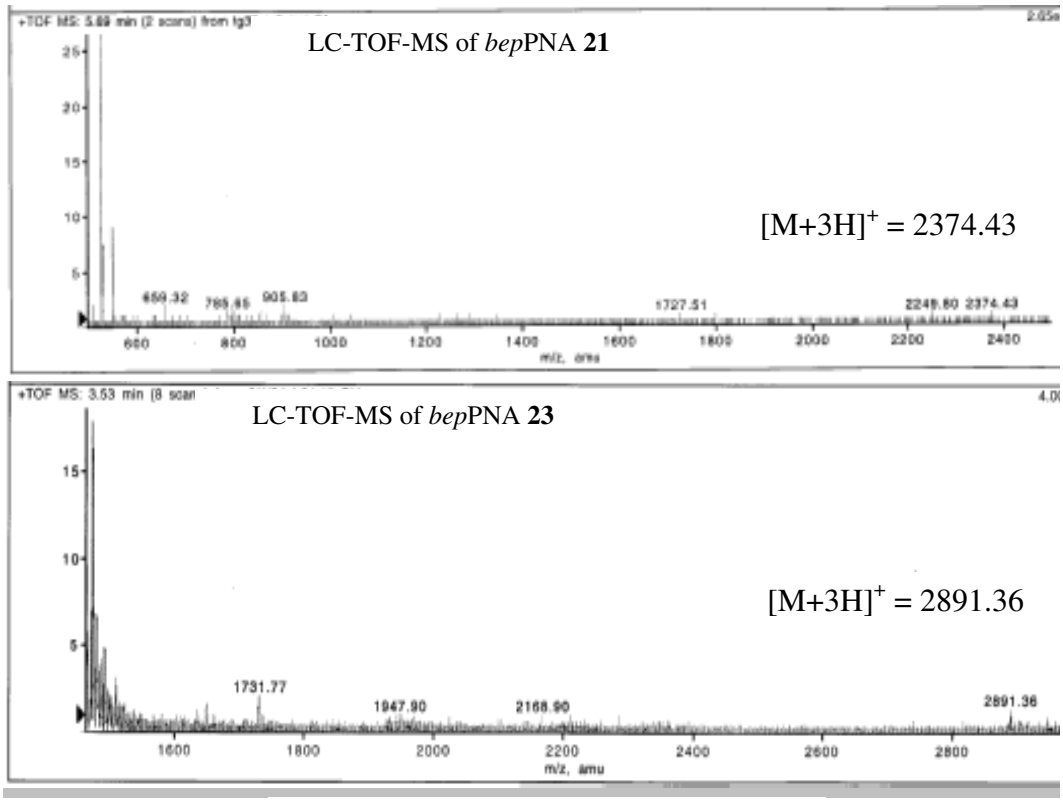

Figure 14c. Mass spectra of *bep*PNAs

Table 2. HPLC and Mass spectral analysis of synthesized PNAs.

Entry	PNA	HPLC (R.T, in mins.)	MW (Calcd)	MW (Found) [a]
1	*aeg*PNA **16**	7.53	2274.00 ($C_{96}H_{132}N_{35}O_{32}$)	2275.90 $[M+H]^+$
2	*bep*PNA **17**	7.59	2286.00 ($C_{96}H_{132}N_{35}O_{32}$)	2288.00 $[M+2H]^+$
3	*bep*PNA **18**	7.27	2286.00 ($C_{96}H_{132}N_{35}O_{32}$)	2288.00 $[M+2H]^+$
4	*bep*PNA **19**	7.35	2286.00 ($C_{96}H_{132}N_{35}O_{32}$)	2288.04 $[M+2H]^+$
5	*bep*PNA **20**	9.56	2323.00 ($C_{102}H_{144}N_{35}O_{29}$)	2326.06 $[M+3H]^+$
6	*bep*PNA **21**	8.24	2370.00 ($C_{110}H_{160}N_{35}O_{25}$)	2374.43 $[M+4H]^+$
7	*aeg*PNA **22**	10.50	2852.00 ($C_{114}H_{147}N_{60}O_{31}$)	2853.00 $[M+H]^+$
8	*bep*PNA **23**	7.85	2887.00 ($C_{120}H_{159}N_{60}O_{28}$)	2891.36 $[M+4H]^+$

[a] LC-TOF-MS, R.T = Retention time.

polystyrene solid support, followed by ammonia treatment.[192] The oligonucleotides were desalted by gel filtration, their purity ascertained by RP HPLC on a C18 column to be more than 98% and were used without further purification in the biophysical studies of PNAs. The RNA oligonucleotides **28, 29** and **30** (Table 3) were obtained commercially.

Table 3. DNA/RNA Oligonucleotides used in the present work

Entry	Sequence code	Sequences	Type (corresponding PNAs)
		DNA sequence 5' to 3'	
1	DNA **24**	C G C A A A A A A A A C G C	Match (**16**-**21**)
2	DNA **25**	G C G T T T T T T T T G C G	Match (**24**)
3	DNA **26**	A G T G A T C T A C	Antiparallel (**22**, **23**)
4	DNA **27**	C A T C T A G T G A	Parallel (**22**, **23**)
		RNA sequences 5' to 3'	
5	RNA **28**	A G U G A U C U A C	Antiparallel (**22**, **23**)
6	RNA **29**	C A U C U A G T G A	Parallel (**22**, **23**)
7	RNA **30**	Poly rA	Match (**16**-**21**)

4.3.6 Biophysical studies of *bep*PNA:DNA/RNA complexes

To investigate the binding selectivity, specificity and discrimination of *bep*PNAs towards complementary DNA and RNA, first the stoichiometry of the *bep*PNA:DNA/RNA was determined using Job's method.[193] The UV-melting studies were carried out with all the synthesized oligomers and the T_m data was compared with the control *aeg*PNA T_8. The stability of the *bep*PNA duplexes with DNA/RNA was also studied. The CD spectra of single strands and corresponding complexes with complementary DNA were recorded. Finally the complexation of these *bep*PNAs to complementary DNA was confirmed by Gel electrophoretic shift assay.

4.3.6.1 Binding Stoichiometry: CD and UV-mixing Curves

The stoichiometry of the paired strands may be obtained from the mixing curves, in which the optical property at a given wavelength is plotted as a function of the mole fraction of each strand[193] from isodichoric and isoabsortive points. Various stoichiometric mixtures of *bep*PNA **19** and RNA **30** were made with relative molar ratios of (*bep*PNA **19**: RNA **30**) strands of 0:100, 10:90, 20:80, 30:70, 40:60, 50:50, 60:40, 70:30, 80:20, 90:10, 100:0, all at the same strand concentration 2 μM in sodium phosphate buffer, 100

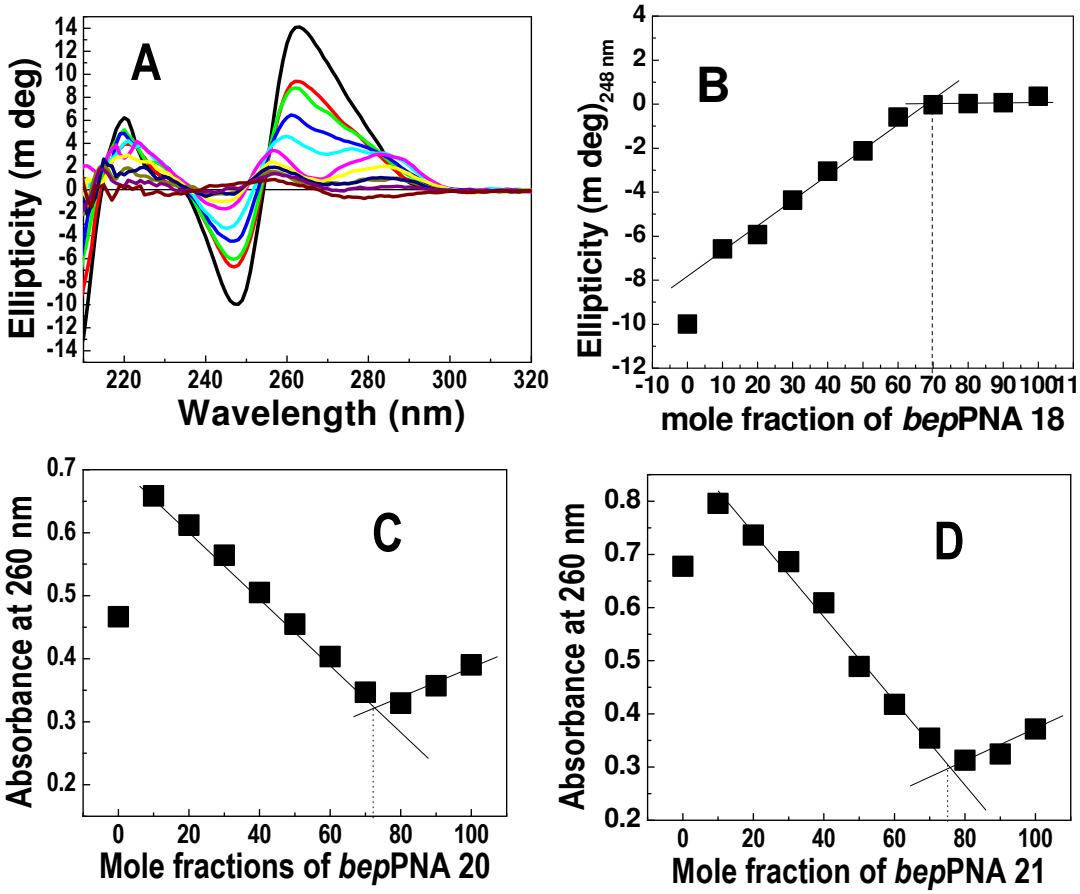

Figure 15. **A**: CD-curves for *bep*PNA **18** with RNA **30** (poly rA) mixtures in the molar ratios of 0:100, 10:90, 20:80, 30:70, 40:60, 50:50, 60:40, 70:30, 80:20, 90:10, 100:0 and **B**. Corresponding CD-Job plot at 248 nm; **C**. UV-Job plot for *bep*PNA **20** with RNA **30** and **D**. UV-Job plot for *bep*PNA **21** with RNA **30** (poly rA). (Buffer, 10 mM Sodium phosphate pH 7.0, 100 mM NaCl, 0.1 mM EDTA).

mM NaCl, 0.1 mM EDTA (10 mM, pH 7.2). The samples with the individual strands were annealed and the CD spectra were recorded (Figure 15A). The CD spectra at different molar ratios showed an isodichoric point at around 255 nm and 250 nm (wavelength of equal CD magnitude). CD values around such wavelengths are therefore especially useful for plotting mixing curves.[193] This systematic changes in the CD spectral features upon variable stoichiometric mixing of PNA and RNA components can be used to generate Job's plot which also indicated a binding ratio of 2:1 for the *bep*PNA:RNA **30** complexes, confirming the formation of triplexes. The mixing curve in Figure 15B was plotted using the CD data at 260 nm from the spectra in Figure 15A,

which indicated the formation of triplex of *bep*PNA **18**: RNA **30**. Similarly, UV-Job's plots of *bep*PNAs **20** and **21** with RNA **30** were also shown to form 2:1 triplexes (Figure 15C and 15D respectively).

4.3.6.2 CD spectroscopic studies of PNA:DNA/RNA complexes

Achiral *aeg*PNAs show very weak CD signatures due to the presence of chiral linker amino acid L-lysine. However, PNA:DNA complexes exhibit characteristic CD signatures due to chirality induced (ICD) by the DNA component. It is known that the formation of PNA_2:DNA triplexes[109] are accompanied by appearance of positive CD bands at 260 and 285 nm that are not present in DNA (Chapter 2). Unlike *aeg*PNA **16** the single stranded *bep*PNAs (**17**-**21**), exhibited distinct CD patterns depending the number and position of modified units present in the sequence (Figure 16C). Alternating *aeg*-bepPNA **20** show positive lower intensity bands at 245 nm, high intensity bands at 260 nm and negative intensity bands around 225 nm and 275 nm region (Figure 16A). The fully modified *bep*PNA homo-oligomer (**21**) gave a CD signature with maximum intensity positive band around 235 nm and a negative intensity band at 265 nm (Figure 16B). More interestingly, the CD signature of the *bep*PNA **21** is more pronounced than that of DNA **24** (Figure 16C). As expected the *C*- and *N*-terminus modified *bep*PNAs **17** and **19** with DNA show CD signatures similar to control PNA:DNA triplex whereas the CD signature of *bep*PNA **18** with DNA show broad band from 260–285 nm (Figure 16A) perhaps due to weak binding interaction.

Alternating *aeg-bep*PNA **20** and fully modified *bep*PNA **20** have contributed a completely different CD patterns (Figure 16A) from others and were found to be additive spectra of their corresponding CD signals of single stranded *bep*PNA and DNA **24** (Figure 16B). Subtraction of the CD spectra of single stranded *bep*PNA **20** and **21** from

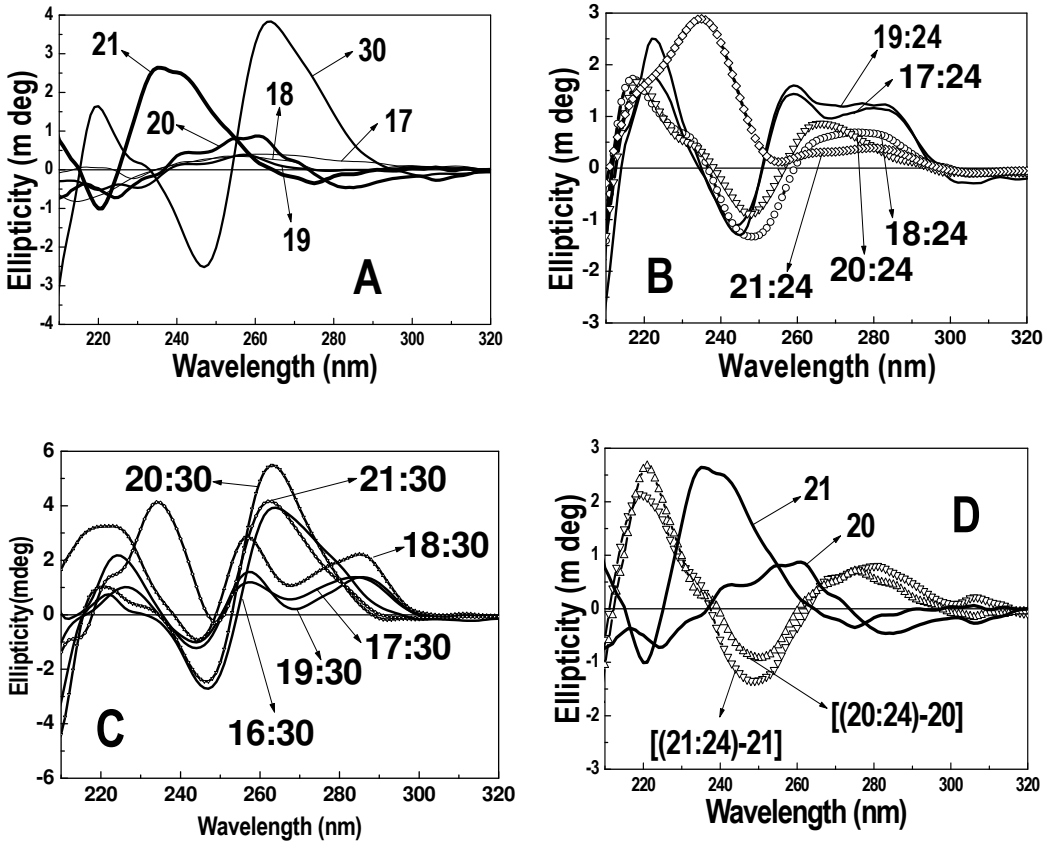

Figure 16. **A**: CD spectra of *bep*PNA **17**, *bep*PNA **18**, *bep*PNA **19**, *bep*PNA **20** and *bep*PNA **21** with DNA **24** (**B**) and with RNA **30** (**C**). **D**: Resultant spectra obtained by subtraction of Single stranded *bep*PNA **20** and *bep*PNA **21** from the spectra of [*bep*PNA **20**:DNA **24**] and [*bep*PNA **21**:DNA **24**]. DNA **24** = 5' CGCA8CGC 3', RNA **30** = poly rA. (Buffer, 10 mM Sodium phosphate pH 7.0, 100 mM NaCl, 0.1 mM EDTA, 20°C).

the CD spectra of [*bep*PNA **20**+DNA **24**] and [*bep*PNA **21**+DNA **24**] respectively gave the CD spectrum corresponding to single strand DNA **24**. CD spectra of *bep*PNA-RNA **30** complexes were recorded to study the structural changes after complexation in comparison with control *aeg*PNA **16**:RNA **30** complex (Figure 16D).

The CD signatures of singly modified *bep*PNAs **17**, **18**, and **19** with RNA **30** gave a different pattern compared to control *aeg*PNA **16**-RNA **30**, but similar to (*aeg*PNA **16**)$_2$-DNA **24** triplex CD profile with two characteristic bands at 260 nm and 285 nm (Figure 16D). The peak intensities in the CDs of *bep*PNA **18**-RNA **30** are much higher compare to corresponding terminally modified *bep*PNA complexes. As expected from the UV-T_ms of *aeg-bep*PNA **20** and *bep*PNA **21**, the CD patterns are also quite differ from

each other as well as to that of control *aeg*PNA **16**-RNA **30** (Figure 16D). The *aeg*-*bep*PNA **20**-RNA **30** complexation accompanied by the appearance of strong positive bands centered at 225 nm and 265 nm and a low negative intensity band at 245 nm compare to control with slight similarity. However, *bep*PNA **21**-RNA **30** shown quite different structure because of the dominance of single strand *bep*PNA **21** and accompanied by the strong positive bands at 235 nm and 265 nm and a very low intensity negative band at 248 nm. Thus, the CD spectral studies clearly shown the unprecedented RNA selectivity of *bep*PNAs attributed to their optimized inter-nucleobase distance and the geometry.

4.3.6.3 UV-Melting studies of *bep*PNA-DNA/RNA complexes

The T_m values of homopyrimidine PNAs **16**-**21**, hybridized with complementary DNA and RNA were obtained from temperature dependent UV-absorbance data (Figure 17, Table 4). The homopyrimidine *aeg*PNAs are known to form PNA_2:DNA triplexes.[109] The UV and CD Job's plots suggest the formation of 2:1 *bep*PNA_2:DNA and *bep*PNA_2:RNA triplexes and hence all the complementation studies were performed with 2:1 PNA:DNA stoichiometry. The UV-T_m values were obtained from the first derivatives of the normalized absorbance–temperature plots of the corresponding PNA:DNA/RNA complexes (Figure 17, Table 4).

Triplex studies: The *C*-terminal modified *bep*PNA **17** (entry 2) binds to DNA with slight decrease in T_m (ΔT_m= -1^oC) whereas *bep*PNA **19** (entry 4) modified at *N*-terminus stabilizes the complex (ΔT_m= +2^oC) compared to control *aeg*PNA **16** (entry 1). Surprisingly, *bep*PNA **18** (entry 3), modified at the center did not show any complexation with DNA. Alternate and homooligomeric *bep*PNAs (**20** and **21**, entry 5 and 6)) did not form complex with DNA as shown in UV-melting curves (Figure 17). When the

complexation studies were performed with RNA, chimeric PNAs with a single *bep*PNA unit were found to bind with approximately same T_m but slightly lower than that of control *aeg*PNA **16.** The *bep*PNA **20** with alternating *aeg-bep* units exhibited a very high binding affinity (ΔT_m= +4.5°C/mod) (Figure 17, Table 4).

Table 4. Melting temperatures (T_m) of PNA_2:DNA/RNA hybrids[a]

Entry	Sequence	DNA **24**	RNA **30**
1	*aeg*PNA **16**, H-TTTTTTTT-LysNH_2	51.5	65.8
2	*bep*PNA **17**, H-TTTTTTT**t**-LysNH_2	49.0	59.9
3	*bep*PNA **18**, H-TTT**t**TTTT-LysNH_2	nd	59.2
4	*bep*PNA **19**, H-**t**TTTTTTT-LysNH_2	53.0	59.0
5	*bep*PNA **20**, H-T**t**T**t**T**t**T**t**-LysNH_2	nd	84.4
6	*bep*PNA **21**, H-**t t t t t t t t**-LysNH_2	nd	58.9

a *T*m = melting temperature (measured in Buffer. 10 mM Sodium phosphate, pH 7.0 with 100 mM NaCl and 0.1 mM EDTA). Measured from 10 to 90° C at ramp 0.2° C/min. UV-absorbance measured at 260 nm. All values are an average of 3 independent experiments and accurate to within ± 0.5° C. **T** = *aeg*PNA unit and **t** = *bep*PNA monomeric unit, DNA **24** = d $CGCA_8CGC$; RNA **30**= poly rA; nd = not detected.

The observed transitions were very sharp with RNA compared to that with DNA. The sequence **21** comprised of only *bep*PNA backbone also recognized only RNA but with reduced strength compared to the alternating *aeg-bep*PNA. These results suggest that *bep*PNA monomer in chimeric and homooligomeric PNAs introduced binding selectivity

for RNA over DNA. Incorporation of the modified units at either terminus (*C-*/*N-*) seems to exert very weak effective preorganized conformation and allowed binding with DNA as well as RNA. When in the center of the sequence, the induced conformation allows recognition of RNA but that of DNA is suppressed. The high affinity binding of alternating *aeg-bep*PNA **20** with RNA suggests that the alternating *aeg-bep* units are uniformly spaced such that a balanced optimum conformation may be reached for recognition of RNA. The fully modified backbone in *bep*PNA **21** binds to RNA but with reduced strength compared with the alternating sequence **20**. This could perhaps arise

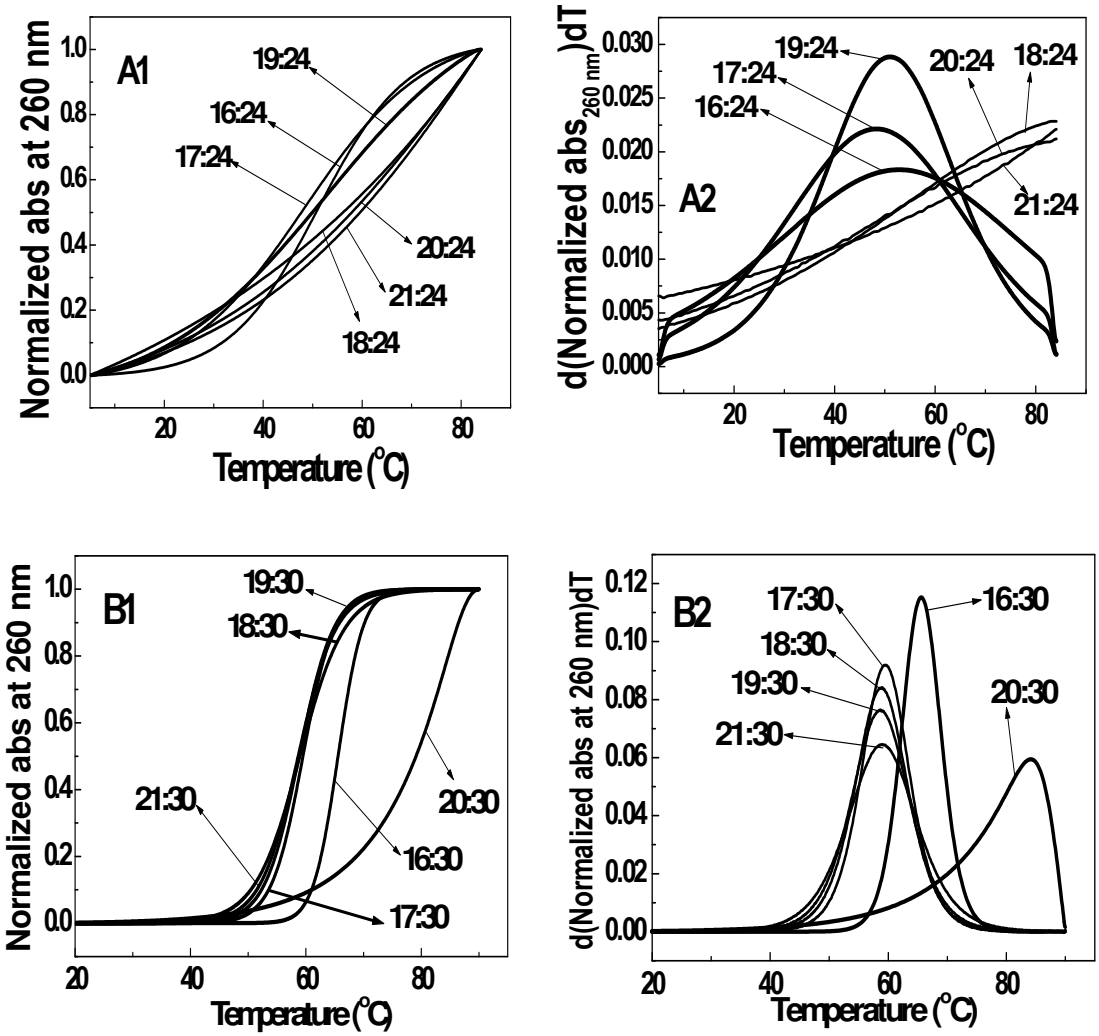

Figure 17. UV-T_m curves complexes of *aeg*PNA **16**, *bep*PNA **17**, *bep*PNA **18**, *bep*PNA **19**, *bep*PNA **20** and *bep*PNA **21** with DNA **24** (**A1**) and RNA **30** (**B1**). **A2**, **B2**: corresponding first derivative curves. DNA **26** = 5' CGCAAAAAAAACGC 3', RNA **30** = poly rA. (Buffer, 10 mM Sodium phosphate pH 7.0, 100 mM NaCl, 0.1 mM EDTA).

either from over-preorganization of single strand as seen with fully modified LNA[85] or higher positive charge concentration of two strands of *bep*-homooligomers in 2:1 binding mode. The 2:1 binding stoichiometry for *bep*PNA **20/21**:RNA was confirmed by UV-Job's plot (Figure 15). The charge-charge repulsions could be a possible reason for observed reduced T_m.

Table 5. Melting temperatures (T_m) of PNA:DNA/RNA duplexes[a]

Entry	Mix PNA sequence	DNA **26**	RNA **28**
1	*aeg*PNA **22**, H-GTAGATCACT-LysNH$_2$	55.0 (40.0) [b]	55.4
2	*bep*PNA **23**, H-G**t**AGA**t**CAC**t**-LysNH$_2$	nd	81.0 (74)

[a] T_m = melting temperature (measured in Buffer. 10 mM Sodium phosphate, pH 7.0 with 100 mM NaCl and 0.1 mM EDTA). Measured from 10 to 90° C at ramp 0.2° C/min. UV-absorbance measured at 260 nm. All values are an average of 3 independent experiments and accurate to within ± 0.5° C. A/G/C/T = aegPNA units and **t** = *bep*PNA monomeric unit, DNA **26**= 5' AGTGATCTAC (*ap*); DNA **27,** 5'-CATCTAGTGA-3'(*p*); RNA **28** = 5' AGUGAUCUAC (*ap*); RNA **29,** 5'-CAUCUAGUGA-3' (*p*). [b]Measured by CD to avoid interference from thermal transitions of single stranded PNAs.[130] nd = not detected. Values in brackets are T_m for parallel duplexes with DNA **27** and RNA **29**.

Duplex studies: To study the RNA binding selectivity of *bep*PNA in duplex formation, mix *bep*PNA decamer (**23)** was synthesized incorporating *bep*PNA-T monomer at three thymine positions in control *aeg*PNA **22**. The UV-thermal denaturation studies of *bep*PNA **23** with DNA and RNA were carried out (Figure 17, Table 5). Data in Table 5 shows that the reference *aeg*-PNA **22** forms *ap*-duplexes with complementary DNA **26** and RNA **28** with equal stability (Table 5, entry 1). Mixed *bep*PNA **23** did not bind to DNA (antiparallel and parallel, Table 5, entry 2), as there was no detectable transition assignable to the denaturation curve occured, whereas a high affinity binding was

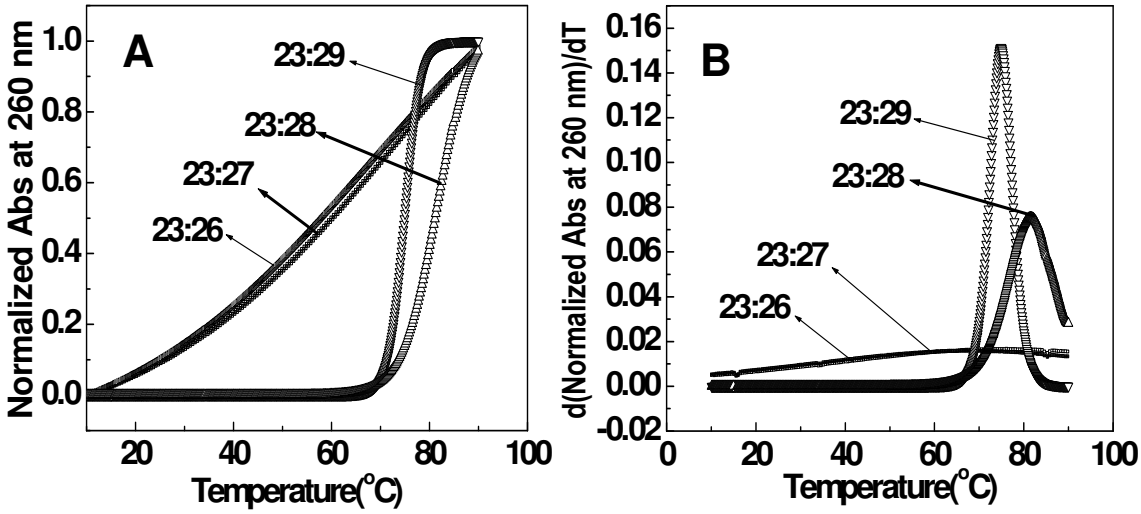

Figure 17. **A**: UV-T_m curves for duplexes of *bep*PNA **21** with DNA **26** (antiparallel), RNA **28** (antiparallel), DNA **27** (parallel), and RNA **29** (parallel). **B**: corresponding first derivative curves. DNA **26** = 5' AGTGATCTAC 3', DNA **27** = 5' CATCTAGTGA 3', RNA **28** = 5' AGUGAUCUAC 3', RNA **29** = 5' CAUCUAGUGA 3'. (Buffer, 10 mM Sodium phosphate pH 7.0, 100 mM NaCl, 0.1 mM EDTA).

observed with RNA **28** (antiparallel, ΔT_m = 26ºC, entry 2). A destabilization of (ΔT_m ~7ºC, entry 2) was observed for parallel *bep*PNA **23**:RNA **29** duplex, indicating the prefered for antiparallel mode of binding.

4.3.6.4 Electrophoretic Gel shift assay:

Electrophoretic gel shift experiment[195] was carried out to support the results obtained from UV-thermal denaturation studies of *bep*PNAs with complementary DNA **24** (Figure 18). The various PNAs were individually mixed with DNA **24** in buffer and subjected to non-denaturing gel electrophoresis at 10ºC, the bands were visualized on a fluorescent TLC background. The formation of PNA:DNA complex was accompanied by disappearance of band due to single stranded DNA **24** and appearance of a lower migrating band due to complex. The terminally modified *bep*PNAs **17** and **19** upon mixing with DNA **24** migrated about the same as the control *aeg*PNA **16**:DNA **24** complex (Figure 18, lane 1) and much lower than that of DNA **24** (Figure 18, lane 5 and

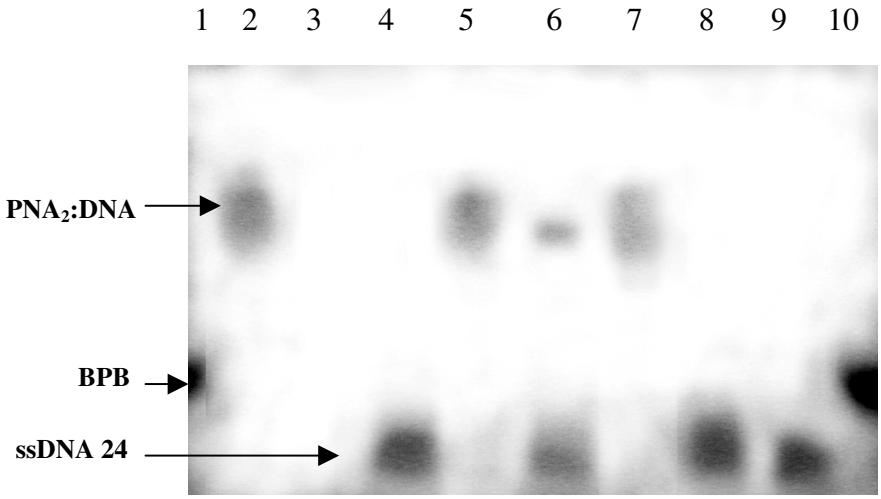

Figure 18. *bep*PNA-DNA complexation. Lane 1, BPB; lane 2, (*aeg*PNA **16**)$_2$:DNA ; lane 3, ss*bep*PNA **17**; lane 4, ssDNA **24**; lane 5, (*bep*PNA **17**)$_2$+DNA; lane 6, (*bep*PNA **18**)$_2$+DNA; lane 7, (*bep*PNA **19**)$_2$:DNA; lane 8, (*bep*PNA **20**)$_2$+DNA; lane 9, (*bep*PNA **21**)$_2$ + DNA; lane 10, BPB = bromophenol blue. DNA=CGCAAAAAAAACGC. 0.5X, TBE, pH 8.0.

7). The *bep*PNA **18** exhibited very weak binding interaction at lower temperature, though it was not seen during UV-T_m thermal denaturation (Figure 18, lane 6). Under the conditions used, the single stranded PNAs carrying positive charge do not migrate from the well. No complexation was observed in case of alternating *aeg*-*bep*PNA **20** and *bep*PNA **21** with DNA **24** as seen from faster moving band due to unbound single strand DNA, in consistence with data obtained from UV-T_m experiments.

4.4 Conclusion

In conclusion, we have designed and synthesized a novel class of cationic backbone extended pyrrolidine PNAs to improve the binding affinity and selectivity towards DNA/RNA recognition. The complementation studies with DNA/RNA reveals that these *bep*PNAs introduced unprecedented RNA binding selectivity which depends on the position and the number of modified monomeric units incorporated in the PNA sequences. From an application perspective, this chiral, cationic PNA analogue appears to have properties important for developing gene therapeutic drugs. Further studies on the mixed sequences having other than thymine monomer and other diastereomeric *bep*PNAs are necessary to draw clear conclusions. The NMR solution structure and molecular modeling studies are also necessary to elucidate the structure-activity relationship exhibited by *bep*PNA monomer and oligomers that is responsible for the unusual RNA recognition.

Summary

- **Cationic, chiral backbone extended pyrrolidine PNAs (*bep*PNA) were designed as DNA/PNA mimic**
- **The *bep*PNAs with preorganized geometry results in optimization of inter-nucleobase distance.**
- ***bep*PNAs introduced unprecedented RNA binding selectivity to form triplexes and duplexes**

4.5 Experimental

General spectroscopic and Experimental data: Melting points of samples were determined in open capillary tubes and are uncorrected. IR spectra were recorded on an infrared Fourier Transform spectrophotometer using KBr pellets. Column chromatographic separations were performed using silica gel 60-120 mesh, solvent systems 10-25% EtOAc/Pet ether and pure DCM to 3% MeOH/DCM. 1H, and 13C were obtained using Bruker AC-200 (200 MHz) and 500 MHz NMR spectrometers. The chemical shifts are reported in delta (δ) values. Mass spectra were obtained either by FAB or LCMS techniques. Oligomers were characterized by RP HPLC, C18 column and LC-TOF-MS spectrometry.

(2*S*,4*R*)-*N*1-(benzyloxycarbonyl)-4-hydroxyproline (2): To the solution of trans-4-Hydroxy-L-proline (5.0 g, 38 mmol) in water (25ml), Na_2CO_3 (8.0 g, 95 mmol) was added slowly in portions. To this mixture, benzylchloroformate (7.86 g, 45.8 mmol, 15.72 ml of 50% solution in toluene) added in one stretch and stirred for 8 h at rt. Toluene was removed under reduced pressure and the aqueous layer was washed with ether (25ml x 2). The ethereal layer was discarded and the aqueous layer was acidified to pH = 2, using 3N HCl with stirring, compound was extracted in to ethyl acetate (20 ml x 3). Ethyl acetate layer was washed with water, brine and then dried over Na_2SO_4 over night. Organic layer was concentrated to get white solid **2**, 10 g (yield 98%). (Rf = 0.3, MeOH:EtOAc, 5:95); $[\alpha]D_{20}$ +86.7° (c 0.53 , CH_2Cl_2); ^{1}H-NMR ($CHCl_3$-*d*, 200 MHz); δ_H 2.2-2.0 (m, 1H, C3H'), 2.2-2.4 (m, 1H, C3H), 3.5-3.65 (m, 2H, $C5H_2$), 4.35-4.5 (m, 2H, C4H, C2H), 5.1 (m, 2H, OCH_2), 6.3-6.6 (bd, 1H,OH), 7.15-7.4 (m, 5H, C_6H_5).

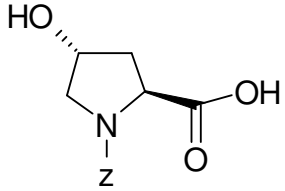

(2*S*,4*R*)-2

(2*S*,4*R*)-*N*1-(benzyloxycarbonyl)-4-hydroxyproline methyl ester (3): The *N*-protected compound **2** (10.0 g, 37.6 mmol) was dissolved in dry methanol (100 ml) and triethyl amine (9.89 g, 97.7 mmol) and cooled to 0°C. To the above ice cooled solution, Thionyl Chloride (5.367 g, 45 mmol) was added slowly over a period of 30 mins from dropping funnel. After the addition, the reaction mixture was stirred for 7 h at rt. The reaction mixture was evaporated to dryness, the residue was extracted into ethyl acetate (3 x 50 ml). The ethyl acetate layer was washed with water, brine and dried over anhydrous Na_2SO_4 and concentrated to get oily product **3** (9.6 g, yield 91%, Rf = 0.5, Ethyl acetate:petroleum ether-5:5). $[\alpha]_D^{20}$ +61.1° (*c* 0.93, CH_2Cl_2); ^{1}H-NMR ($CHCl_3$-*d*, 500 MHz); δ_H 1.8-2.1 (m, 1H, C3H'), 2.2-2.4 (m, 1H, C3H), 3.4-3.8 (m, 6H, OCH_3; two rotamers, C5H, C2H), 4.4-4.6 (m, 2H, C4H), 4.8-5.2 (m, 2H, OCH_2), 7.2-7.45 (m, 5H, C_6H_5). ^{13}C-NMR ($CHCl_3$-*d*, 500 MHz); δ_C 37.9 (C3), 51.7 (C2), 54.2 (C5), 57.4 (C4), 66.9 (OCH_3), 68.6 and 69.3 (OCH_2), 127.4, 127.7, 128.1, 135.8, 136.0 (Ar), 154.4 and 154.7 (*N*-C=O), 172.9 and 173.0 (-COOMe).

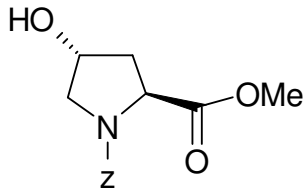

3

(2*S*,4*R*)-*N*1-(benzyloxycarbonyl)-4-hydroxy-2-(hydroxymethyl)-pyrrolidine (4): To a ice cooled solvent mixture dry THF (175 ml) and absolute Ethanol (250 ml) containing $NaBH_4$ (3.192 g, 84.3 mmol) in a 3 necked flask, LiCl (3.58 g, 84.3 mmol) was added slowly from the solid addition funnel for 30 mons. The above solution was stirred for 1.0 h and appearance of milky solution indicates the formation of LiBH4 in situ. To the above ice cooled milky solution, methyl ester **3** (9.45 g, 33.75 mmol) dissolved in absolute ethanol (50 ml) was added from dropping funnel over a period of 30 mins under nitrogen atmosphere and the reaction mixture was stirred over

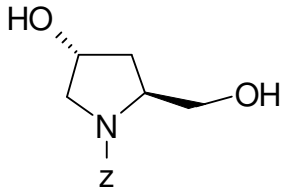

4

night at rt. Then the pH was adjusted to 7.0 by adding saturated solution of NH_4Cl. The solvent mixture was removed under vacuum and the residue was extracted into ethyl acetate (25 ml x 3). The organic layer was washed with water, brine solution, dried over anhydrous Na_2SO_4 and concentrated to afford oily product diol 4 (7.5 g, yield 88%, Rf= 0.3, Ethyl acetate: petroleum ether 5:5). $[\alpha]D_{20}$ +16.8° (c 3.26, CH_2Cl_2); ^{1}H-NMR ($CHCl_3$-*d*, 200 MHz); δ_H 1.65-1.9 (m, 1H, C3H'), 1.9-2.15 (m, 1H, C3H), 3.4-3.9 (m, 5H, $\underline{CH_2}OH$, C2H, C5H), 4.2 (m, 1H, C4H), 4.4 (bd, 1H, $CH_2\underline{OH}$, exchangeable), 5.2-5.75 (bd, 1H, C4-$\underline{OH}$), exchangeable), 7.4 (s, 5H, C6H5). ^{13}C-NMR ($CHCl_3$-*d*, 200 MHz); δ_C 37.1 (C3), 55.4 (C2), 58.9 (C5), 65.5 (CH_2OH), 87.2 and 89.0 (OCH_2), 127.7, 128.3, 136.2 (Aromatic), 159.5 (*N*-C=O): Anal Calcd (%) for $C_{13}H_{17}NO_4$: C, 62.15; H, 10.75; N, 5.57; Found C, 61.83; H, 10.91; N, 5.53; LCMS; 252.07 $[M+1]^+$.

(2*S*,4*R*)-*N*1-(benzyloxycarbonyl)-4-hydroxy-2-(*p*-toluenesulfonyloxymethyl)-pyrrolidine (5): The diol **4** (7.12 g, 28.36 mmol) dissolved in dry pyridine (200 ml) and cooled to 0°C. To the this ice cooled solution, freshly crystallized *p*-toluene sulfonyl chloride (5.95 g, 31.2 mmol) in pyridine was added from the dropping funnel over a period of 1.5 h under nitrogen atmosphere. The reaction mixture was stirred for 8 h at rt. Pyridine was removed under reduced pressure and co-evaporated with toluene (twice). The residue was extracted in to ethyl acetate (50 ml x 2), washed with water and dried over Na_2SO_4 and concentrated to yield crude oily residue. The residue was purified by column chromatography to get monotosylate **5**. (8.6 g, yield 75%, Rf = 0.36, Ethyl acetate: petroleum ether-5:5). $[\alpha]D_{20}$ +27.7° (c 4.43, CH_2Cl_2); ^{1}H-NMR ($CHCl_3$-*d*, 200 MHz); δ_H 1.7-2.15 (2H, C2H, C3H), 2.2-2.5 (s, 3H, OCH_3), 3.1-3.6 (m, 2H, $C5H_2$), 3.7-4.2 (m, 3H, CH_3), 4.25-4.65 (m, 2H, $\underline{CH_2}$-OTs), 4.7-5.5 (bd, 4H,

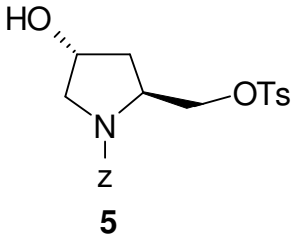

5

C4H, $COOCH_2$, OH), 7.26-7.4 (s, 7H, C_6H_5, two CH-Ts), 7.5-7.8 (m, 2H, two CH-Ts). ^{13}C-NMR ($CHCl_3$-*d*, 200 MHz); δ_C 21.0 (CH_3), 35.9 (C3), 54.5 (C2), 54.8 (C5), 66.4 ($O\underline{CH_2}Ts$), 68.7 (C4), 69.8 (OCH_2), 127.3, 128.0, 129.5, 132.3, 136.0, 144.5 (Aromatic), 154.6 (*N*-C=O); Anal Calcd (%) for $C_{20}H_{23}NO_6S$: C, 59.25; H, 5.67; N, 3.45; S, 7.90, Found C, 58.92; H, 5.77; N, 3.37; S, 7.67; MS LCMS; 405.00 $[M]^+$.

(2*S*,4*R*)-*N*1-(benzyloxycarbonyl)-4-hydroxy-2-(azidomethyl)-pyrrolidine (6): To the solution of monotosylate **5** (6.0 g, 14.8 mmol) in DMF (50 ml), NaN_3 (7.7 g, 118.4 mmol) was added. The reaction mixture was stirred at 55°C for 8 h. The solvent was removed under reduced pressure and the residue was extracted into ethyl acetate (25 ml x 3). The combined organic layer was washed with water, brine, dried over anhydrous Na_2SO_4 and then concentrated to yield azide **6**. (3.9 g, yield 96%, Rf = Ethyl acetate:petroleum ether-5:5). IR (neat) (ν) cm^{-1}. 3016, 2360, 2106, 1697, 1419. ^{1}H-NMR ($CHCl_3$-*d*, 200 MHz); δ_H 1.95-2.02 (m, 2H, $C3H_2$), 3.07-3.85 (m, 4H, C2H, $C5H_2$, OH), 3.97-4.45 (m, 2H, C5H, C4H), 5.09 (s, 2H, OCH_2), 7.31 (s, 5H, C_6H_5). ^{13}C-NMR ($CHCl_3$-*d*, 200 MHz); δ_C 36.9(C3), 51.9 (C5), 55.2, (CH_2N_3), 55.6 (C2), 66.6 (C4), 68.4 and 68.8 (OCH_2), 127.2, 127.5, 128.1, 136.2 (Ar), 162.5 (*N*C=O); LCMS; 277.00 $[M+1]^+$.

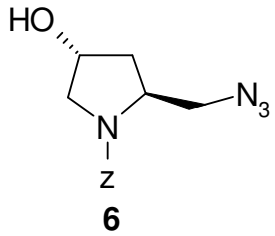

6

(2*S*,4*R*)-*N*1-(benzyloxycarbonyl)-4-hydroxy-2-(aminomethyl)-pyrrolidine (7): To a solution of the azide **6** (3.5 g, 12.7 mmol) in Methanol (5 ml) taken in hydrogenation flask was added Raney Nickel (1.5 ml). The reaction mixture was hydrogenated in a Parr apparatus for 3.5 h at rt and H_2 of pressure 35-40 psi. The catalyst was filtered off and then solvent was removed under reduced pressure to yield a residue of the amine **7** as colorless oil. Yield (3.0 g, 95.0%); this

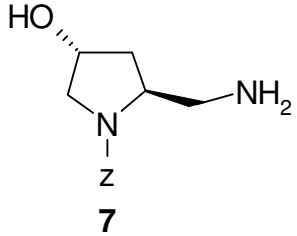

7

compound was used for the further reaction without any purification.

(2*S*,4*R*)-*N*1-(benzyloxycarbonyl)-2-(*tert*-butoxy carbonylaminomethyl)-4-hydroxy pyrrolidine (8): The amine **7** (3.0 g, 12.0 mmol) was taken in DMSO (10 ml), triethyl amine (1.58 g, 15.6 mmol) and $BocN_3$ (2.05 g, 14.4 mmol) were added. The reaction mixture was heated to 50°C for 8 h. The reaction mixture was poured into 150 ml of ice-cold water and the product extracted into ether (20 ml x 8). The combined ether layer was washed with water, brine and then concentrated to give Boc protected amine **8**. (3.2 g, yield 76%, Rf = 0.6, Ethyl acetate: petroleum ether). $[\alpha]D_{20}$ –12.74° (c 0.7, CH_2Cl_2); ^{1}H-NMR ($CHCl_3$-*d*, 200 MHz); δ_H 1.41 (s, 9H, Boc), 1.6-2.3 (m, 3H, C2H, $C3H_2$), 3.15-3.75 (m, 4H, $C5H_2$, $\underline{CH_2}NH$), 3.9-4.2 (m, 1H, C4-$\underline{OH}$), 4.3-4.5 (m, 1H, C4H), 5.11 (s, 2H, OCH_2), 5.4-5.6 (bd, 1H, carbamate NH), 7.33 (s, 5H, C_6H_5); ^{13}C-NMR ($CHCl_3$-*d*, 200 MHz); δ_C 28.3 (Boc), 38.04 (C3), 44.1 (C5), 54.9 (CH_2NH), 56.6 (C2), 67.0 (OCH_2), 69.2 (C4), 79.2 (Boc), 128.4 (Ar), 136.4 (Ar), 156.3 (carbamate C=O), 159.6 (-*N*-COO): Anal Calcd (%) for $C_{18}H_{26}N_2O_5$: C, 61.71; H, 7.42; N, 8.00; Found C, 61.68; H, 7.64; N, 7.78; LCMS; 351.21 $[M+1]^+$.

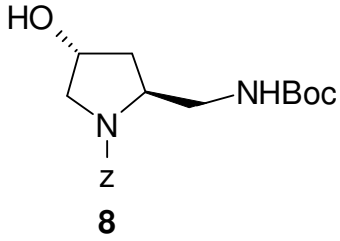

8

[(2*S*,4*R*)-2-(*tert*-butoxy carbonylaminomethyl)-4-hydroxy] pyrrolidine (9): To a solution of the ester **8** (3.2 g, 9.5 mmol) in Methanol (5 ml) taken in hydrogenation flask was added 10% Pd/C (0.32 g). The reaction mixture was hydrogenated in a Parr apparatus for 7 h at rt and H_2 of pressure 60 psi. The catalyst was filtered off and then solvent was removed under reduced pressure to yield a residue of the amine **9** as colorless oil. Yield (1.9 g, 95%); this compound was used for the further reaction without any purification.

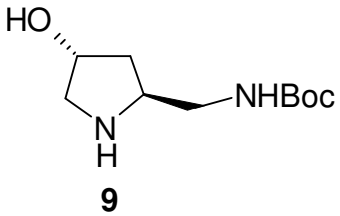

9

Ethyl-[(2*S*,4*R*)-2-(*tert*-butoxy carbonylaminomethyl)-4-hydroxy pyrrolidin-1-yl]-propeonate (10): The cyclic amine **9** (1.9 g, 8.8 mmol) taken in methanol (20 ml), added ethyl acrylate (0.97 g, 9.68 mmol) and stirred 3 h at rt. The reaction mixture was evaporated to dryness and was extracted into ethyl acetate (25 ml x 3). The organic layer was dried over Na_2SO_4 and concentrated to give crude residue, which on column chromatography afford ester **10**.

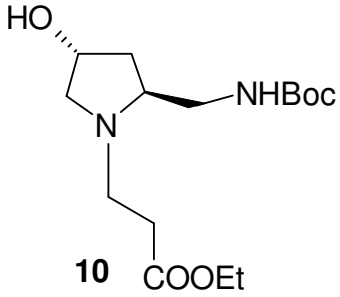

10

(2.0 g, yield 72%, Rf = 0.6, MeOH:CH_2Cl_2-1:9). ^{1}H-NMR ($CHCl_3$-*d*, 200 MHz); δ_H 1.24 (t, 3H, ester CH_3), 1.41 (s, 9H, Boc), 1.52-1.9 (m, 2H, C3H_2), 1.95-2.6 (m, 5H, -CH_2-CH_2-, C2H), 2.7-3.5 (m, 5H, C5H_2, CH_2NH, OH), 3.7-4.2 (m, 2H, ester CH_2), 4.25-4.4 (m, 1H, C4H), 4.75-5.45 (bd, 1H, NH). ^{13}C-NMR ($CHCl_3$-*d*, 200 MHz); δ_C 13.9 (ester CH_3), 28.1 (Boc), 33.7 (C3), 37.7 (*N*-$\underline{CH_2}$-CH_2-CO), 40.7 (CO$\underline{CH_2}$-CH_2-*N*), 49.1 (C5), 60.2 (CH_2NH), 61.3 (C2), 61.6 (ester CH_2), 69.2 (C4), 78.7 (Boc), 156.3 (carbamate C=O), 172.4 (ester C=O). Anal Calcd (%) for $C_{15}H_{28}N_2O_5$: C, 56.96; H, 8.86; N, 8.86, Found C, 56.65; H, 8.95; N, 8.71; LCMS; 317.00 $[M+1]^+$.

Ethyl-[(2*S*,4*S*)-2-(*tert*-butyloxycarbonylaminomethyl)-4-(*N*3-benzoyl thymin-1-yl)- pyrrolidin-1-yl]-propeonate (11): To a solution of alcohol **10** (1.5 g, 4.74 mmol), *N*3-benzoyl thymine and triphenyl phosphene in dry benzene cooled to 4^{o}C, added DEAD drop wise with syringe under nitrogen atmosphere. The reaction mixture was stirred for another 5 h at rt. The reaction mixture was evaporated to dryness and the residue

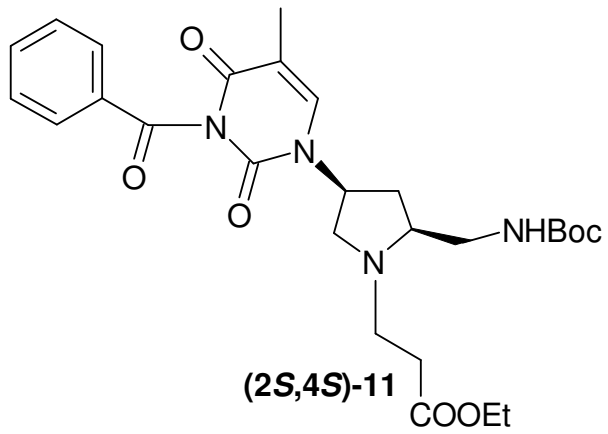

(2*S*,4*S*)-11

was purified by column chromatography to obtain monomer ethyl ester **11**. (1.8 g, yield 72%, Rf = 0.76, MeOH:CH_2Cl_2-1:9). $[\alpha]D_{20}$ –69.16° (c 0.50, CH_2Cl_2); ^{1}H-NMR ($CHCl_3$-*d*, 500 MHz); δ_H 1.29 (t, 3H, ester CH_3), 1.41 (s, 9H, Boc), 1.55-1.8 (m, 1H, C3H'), 1.96 (s, 3H, Thy CH_3), 2.15-2.3 (m, 1H, C3H), 2.35-2.7 (m, 5H, -CH_2-CH_2-, C2H), 3.0-3.2 (m, 3H, C5H', CH_2NH), 3.25-3.4 (m, 1H, C5H), 3.95-4.15 (m, 2H, ester CH_2), 4.95-5.15 (m, 1H, C4H), 5.2-5.3 (bd, 1H, NH), 7.15-7.25 (m, 2H, Ar), 7.25-7.35 (m, 1H, Ar), 7.35-8.00 (m, 3H, thy CH, Ar); ^{13}C-NMR ($CHCl_3$-*d*, 500 MHz); δ_C 12.1 (thy CH_3), 13.9 (ester CH_3), 28.0 (Boc), 33.2 (C3), 35.5 (*N*-$\underline{CH_2}$-CH_2-CO), 39.5 (CO-$\underline{CH_2}$-CH_2-*N*), 47.5 (C5), 57.3 (CH_2NH), 58.5 (C2), 60.4 (ester CH_2), 63.0 (C4), 79.0 (Boc), 110.6 (thy C5), 128.8, 130.0, 131.6 (Aromatic) 134.5 (thy CH),135.4 (thymine-C4=O), 149.6 (thymine –C2=O), 156 .0 (carbamate C=O), 162.2 (-$\underline{C}$OOEt), 168.9 (benzyl C=O), 172.2 (ester C=O). Anal Calcd (%) for $C_{27}H_{36}N_4O_7$: C, 61.36; H, 6.81; N, 10.60, Found C, 61.13; H, 6.97; N, 10.43; MS LCMS; 528.01 $[M]^+$, 428.01 $[M\text{-}tBoc]^+$.

[(2*S*,4*S*)-2-(*tert*-butyloxycarbonylaminomethyl)-4-(thymin-1-yl)- pyrrolidin-1-yl]-propeonic acid (12): The monomer ethyl ester **11** (1.5 g, 2.8 mmol) was dissolved in methanol (6 ml), 2N NaOH (6 ml) was added and stirred for 7 h. The reaction mixture was washed with ethyl acetate to remove benzoic acid. The aqueous layer was then neutralized with cation exchange resin (Dowex H+). After removal of the resin by filtration the aqueous layer was concentrated to a residue which on coevaporation with dichloromethane (10 ml x 2) afford monomer **12**. (1.1 g, yield 98%), mp, 119-121°C; $[\alpha]D_{20}$ –78.0° (c 0.5, CH_2Cl_2); ^{1}H-NMR (D_2O, 500 MHz); δ_H 1.39 (s, 9H, Boc), 1.82 (s, 3H, thy

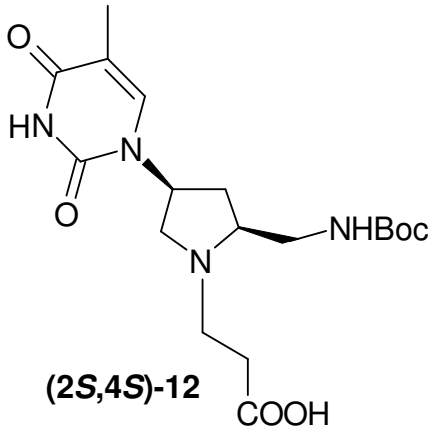

(2*S*,4*S*)-12

CH_3), 2.1-2.3 (m, 1H, C3H'), 2.45-2.75 (m, 2H, *N*-$\underline{CH_2}$-CH_2-CO), 2.8-2.9 (m, 1H, C2H), 2.95-3.15 (m, 1H, C5H'), 3.4-3.8 (m, 5H, CO$\underline{CH_2}$-CH_2-*N*, CH_2NH), 3.95-4.15 (m, 1H, C4H), 7.44 (s, 1H, thy CH). ^{13}C-NMR (D_2O, 500 MHz); δ_C 11.0 (thy CH_3), 27.45 (Boc), 31.9 (C3), 32.4 (*N*-$\underline{CH_2}$-CH_2-CO), 38.0 (CH_2NH), 50.3 (C5), 56.7 (CO$\underline{CH_2}$-CH_2-*N*), 57.5 (C2), 66.8 (C4), 81.4 (Boc), 110.4 (thy C5), 142.6 (thy C6), 157.6 (thymine-C4=O), 158.0 (thymine-C2=O), 168.5 (carbamate C=O), 177.7 (COOH). Anal Calcd (%) for $C_{18}H_{28}N_4O_6$: C, 54.54; H, 7.07; N, 14.14, Found C, 54.23; H, 7.29; N, 13.97; MS LCMS; 397.05 $[M+H]^+$, 297.05 $[M+1\text{-tBoc}]^+$.

***N*3-Benzoyl thymine (15)**: To a stirred solution of thymine (5.0 g, 40 mmol) in dry acetonitrile (50 ml) and dry pyridine (10 ml) in an ice bath, benzoyl chloride (10 ml, 88 mmol) was added drop wise. Stirring was continued at room temperature overnight, when di-benzoyl thymine (**14**) was found to be formed, the solvent was evaporated to obtain a crude yellow solid which was stirred with 0.25 M K_2CO_3 in dioxan:water (75 ml, 1:1) for 5 h, which gave suspension. The suspension was filtered and the solid was washed with ice-cold water and ether. The precipitate was first air dried and then dried under vacuum to obtain mono-benzoylated product (75 g, yield = 82%, RF = 0.3, EtOAc).

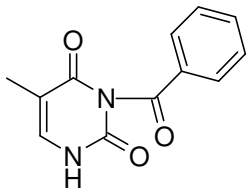

15

UV-T_m measurements: The complementary DNA oligomers were synthesized on an Applied Biosystems 3900 DNA Synthesizer. The poly rA and RNA mixed oligomers were obtained commercially. The concentration was calculated on the basis of absorbance from the molar extinction coefficients of the corresponding nucleobases. The complexes were prepared in 10 mM sodium phosphate buffer, pH 7.0 containing NaCl (100 mM) and EDTA (0.1 mM) and were annealed by keeping the samples at 90°C for 5 minutes

followed by slow cooling to room temperature. Absorbance versus temperature profiles were obtained by monitoring at 260 nm with Perkin-Elmer Lambda 35 spectrophotometer scanning from 5 to 90°C at a ramp rate of 0.2°C per minute. The data were processed using Microcal Origin 5.0 and Tm values derived from the derivative curves.

Circular Dichroism: CD spectra were recorded on a JASCO J-715 spectropolarimeter. The CD spectra of the PNA:DNA complexes and the relevant single strands were recorded in 10 mM sodium phosphate buffer, 100 mM NaCl, 0.1 mM EDTA, pH 7.0. The temperature of the circulating water was kept below the melting temperature of the PNA:DNA complexes, i.e., at 10^{o}C. The CD spectra of the homothymine T_8 single strands were recorded as an accumulation of 10 scans from 320 to 195 nm using a 1 cm cell, a resolution of 0.1 nm, band-width of 1.0 nm, sensitivity of 2 m deg, response 2 sec and a scan speed of 50 nm/min. for the PNA_2:DNA/RNA complexes, spectra were recorded as an accumulation of 8 scans, response of 1 sec and a scan speed of 200 nm/min.

Gel mobility shift assay: The PNAs **16**-**21** were individually mixed with DNA 24 in 2:1 ratio (*bep*PNA strand, 0.4 mM and DNA **24** 0.2 mM) in water. The samples were lyophilized to dryness and re-suspended in sodium phosphate buffer (10 mM, pH 7.0, 10µl) containing EDTA (0.1 mM). The samples were annealed by heating to 85°C for 5 min followed by slow cooling to RT and refrigeration at 4^{o}C overnight. To this, 10µl of 40% sucrose in TBE buffer pH 8.0 was added and the sample was loaded on the gel. Bromophenol blue (BPB) was used as the tracer dye separately in an adjacent well. Gel electrophoresis was performed on a 15% non-denaturing polyacrylamide gel (acrylamide:bis-acrylamide, 29:1) at constant power supply of 200 V and 10 mA, until the BPB migrated to three-fourth of the gel length. During electrophoresis the

temperature was maintained at 10°C. The spots were visualized through UV shadowing by illuminating the gel placed on a fluorescent silica gel plate, GF_{254} using UV-light.

4.6 Appendix

- Compound **5**, ^{1}H, ^{13}C NMR and DEPT
- Compound **8**, ^{1}H, ^{13}C NMR and DEPT
- Compound **10**, ^{1}H, ^{13}C NMR and DEPT
- Compound **11**, ^{1}H, ^{13}C NMR, DEPT and LC-MS
- Compound **12**, ^{1}H, ^{13}C NMR, DEPT and LC-MS

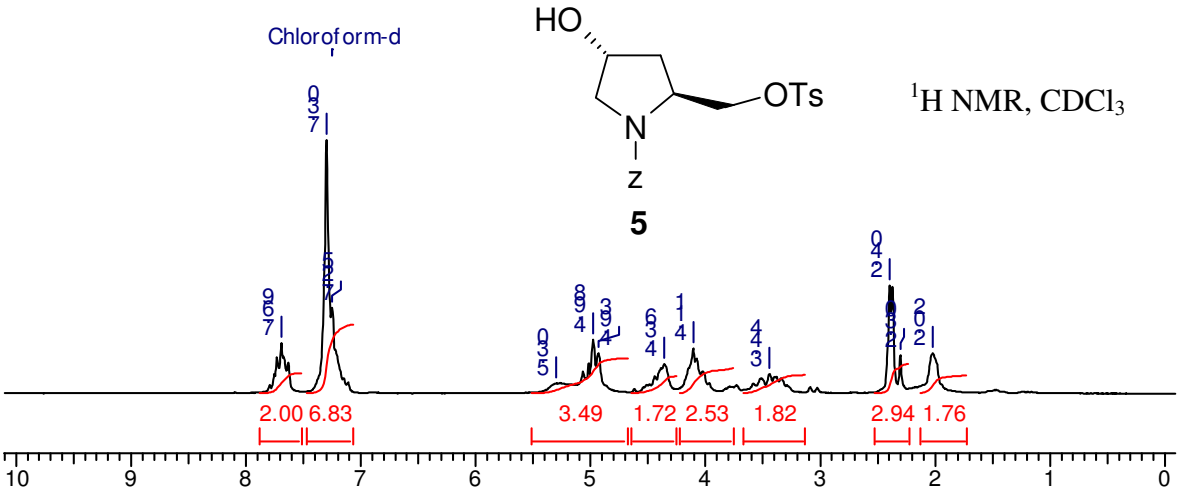

^{1}H NMR, $CDCl_3$

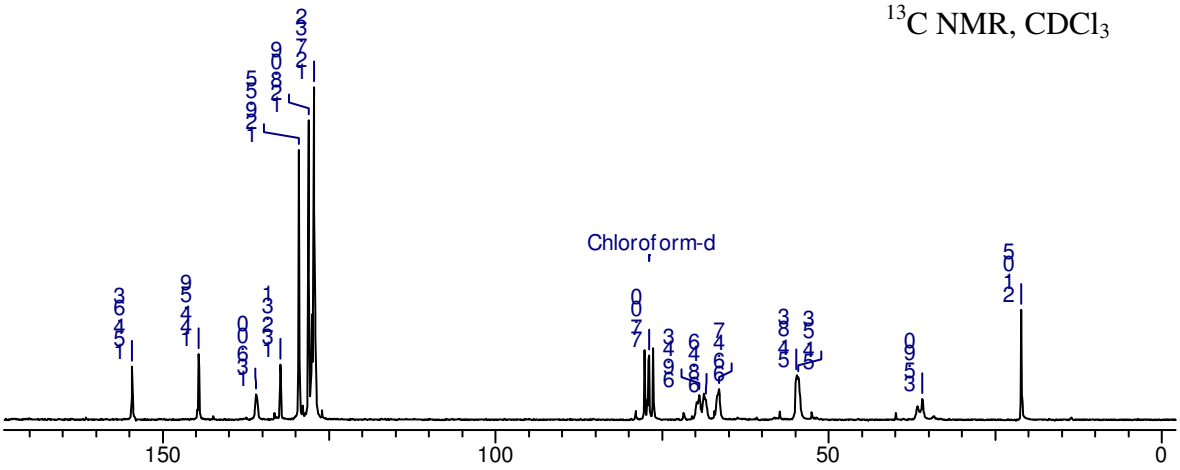

^{13}C NMR, $CDCl_3$

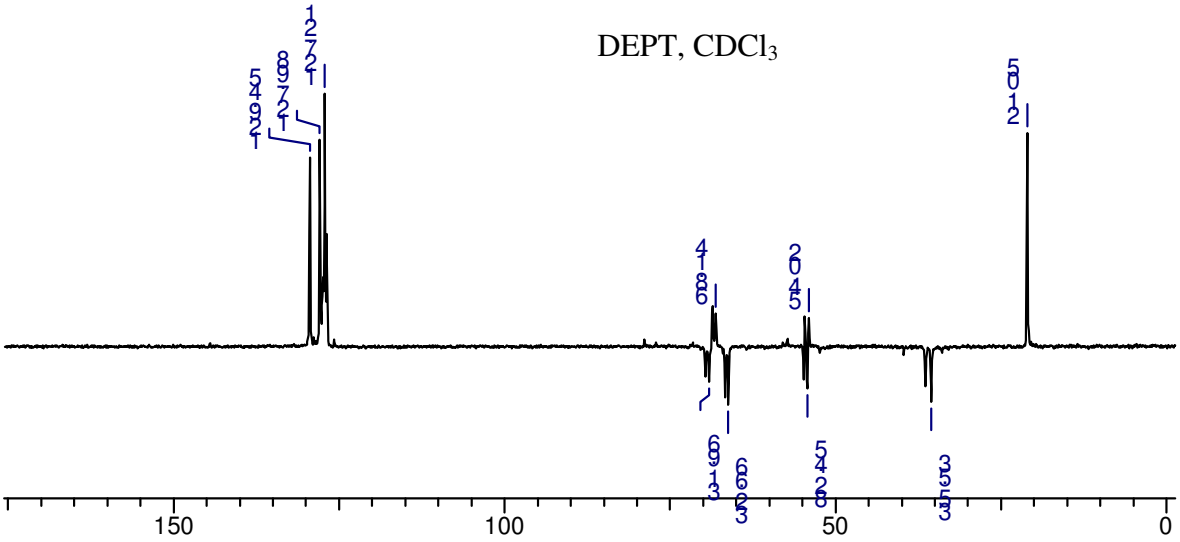

DEPT, $CDCl_3$

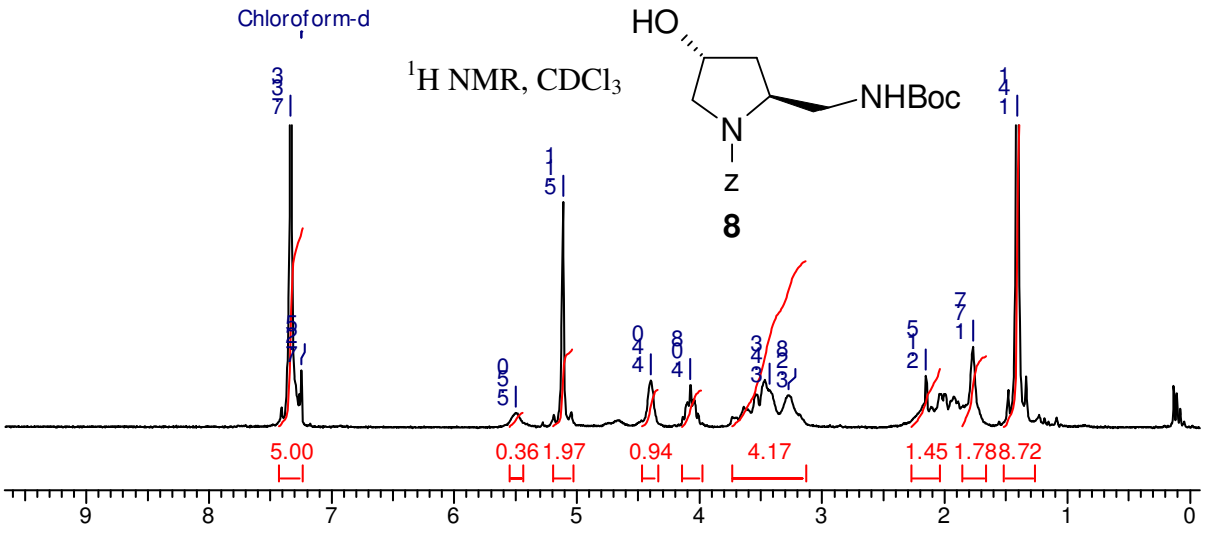
Chloroform-d
^{1}H NMR, CDCl$_3$
HO
NHBoc
N
Z
8
5.00
0.36
1.97
0.94
4.17
1.45
1.78
8.72

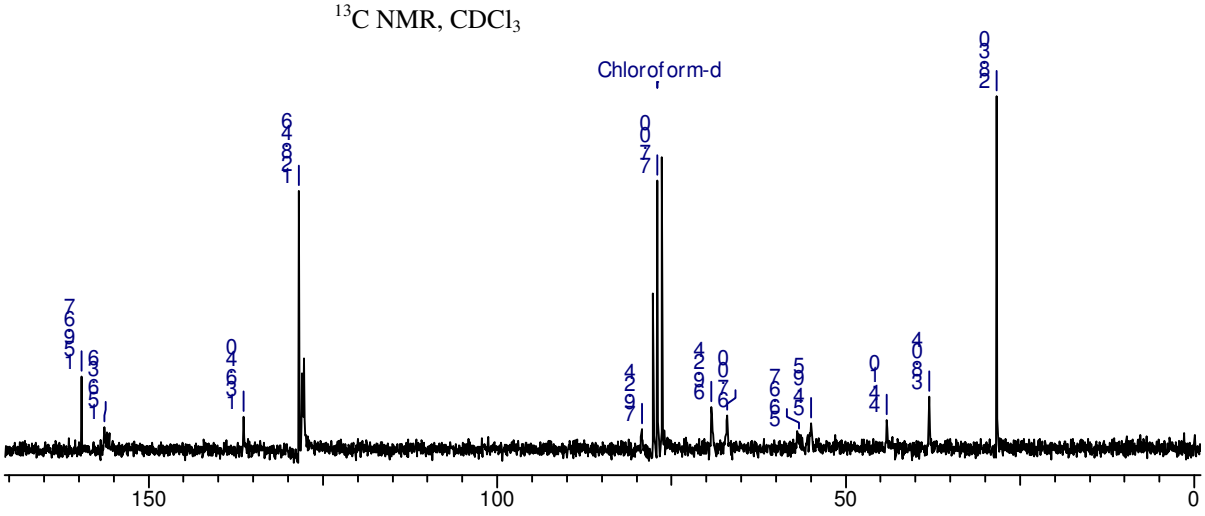
^{13}C NMR, CDCl$_3$
Chloroform-d

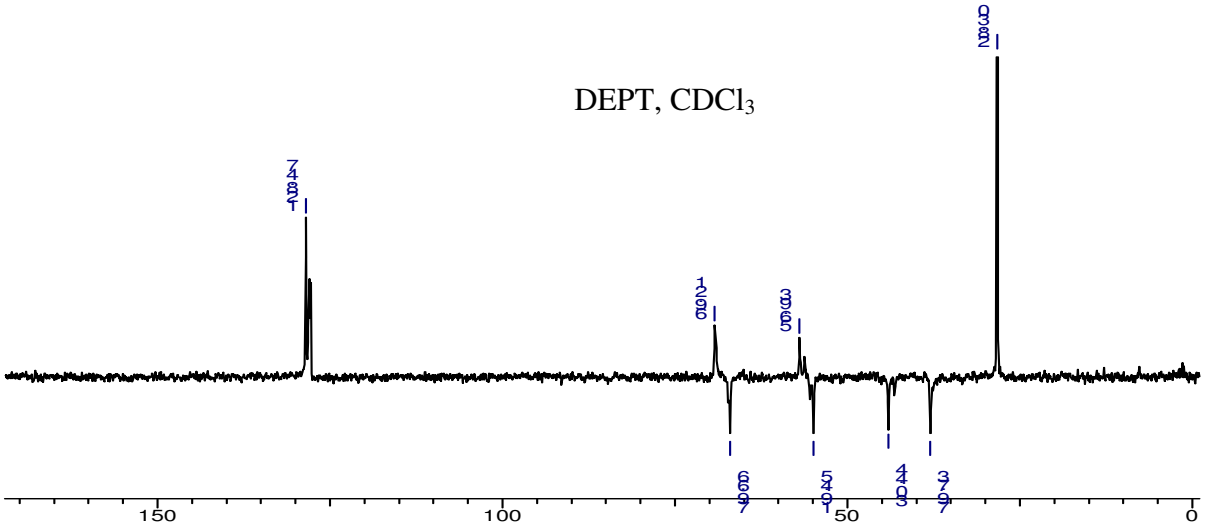
DEPT, CDCl$_3$

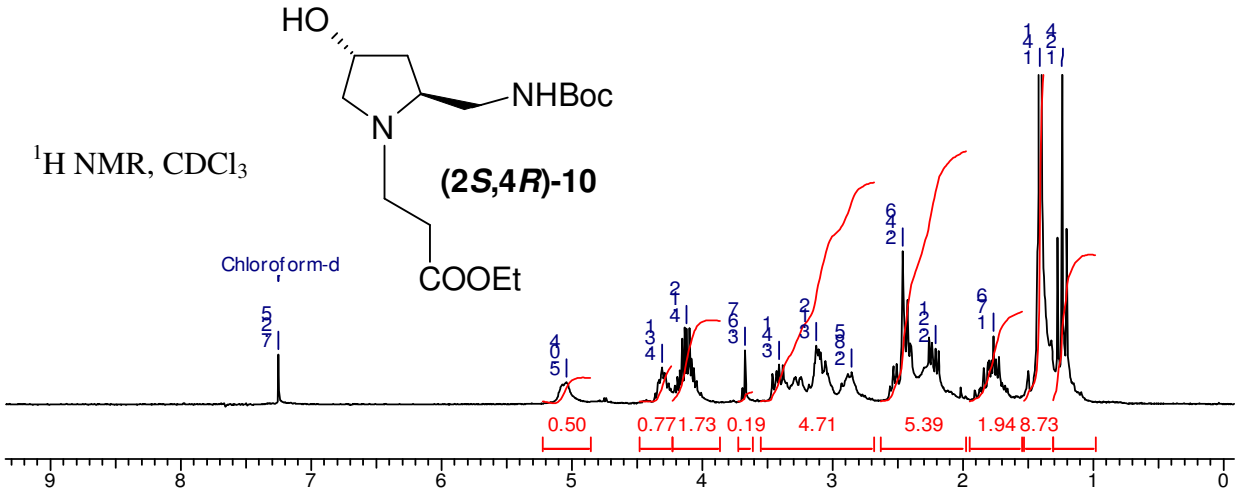
HO
NHBoc
N
COOEt
(2S,4R)-10
1H NMR, CDCl3
Chloroform-d
0.50
0.77
1.73
0.19
4.71
5.39
1.94
8.73

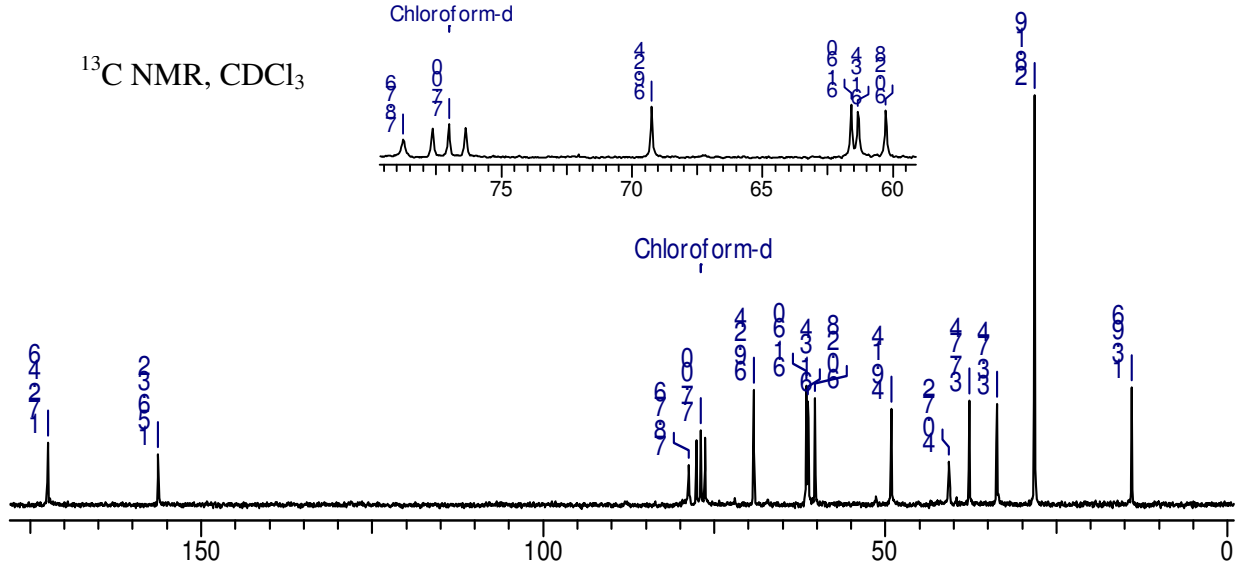
13C NMR, CDCl3
Chloroform-d

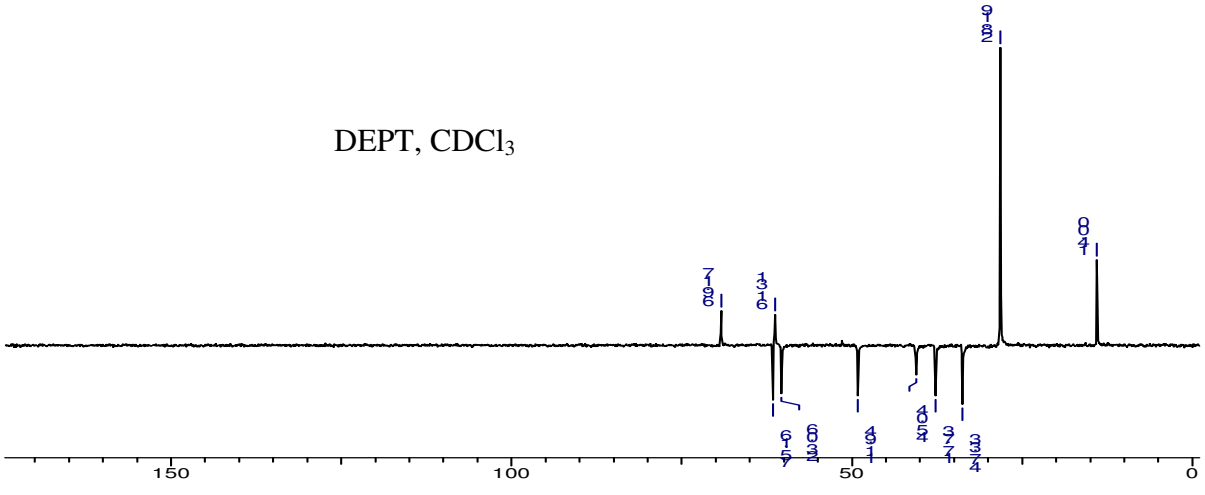
DEPT, CDCl3

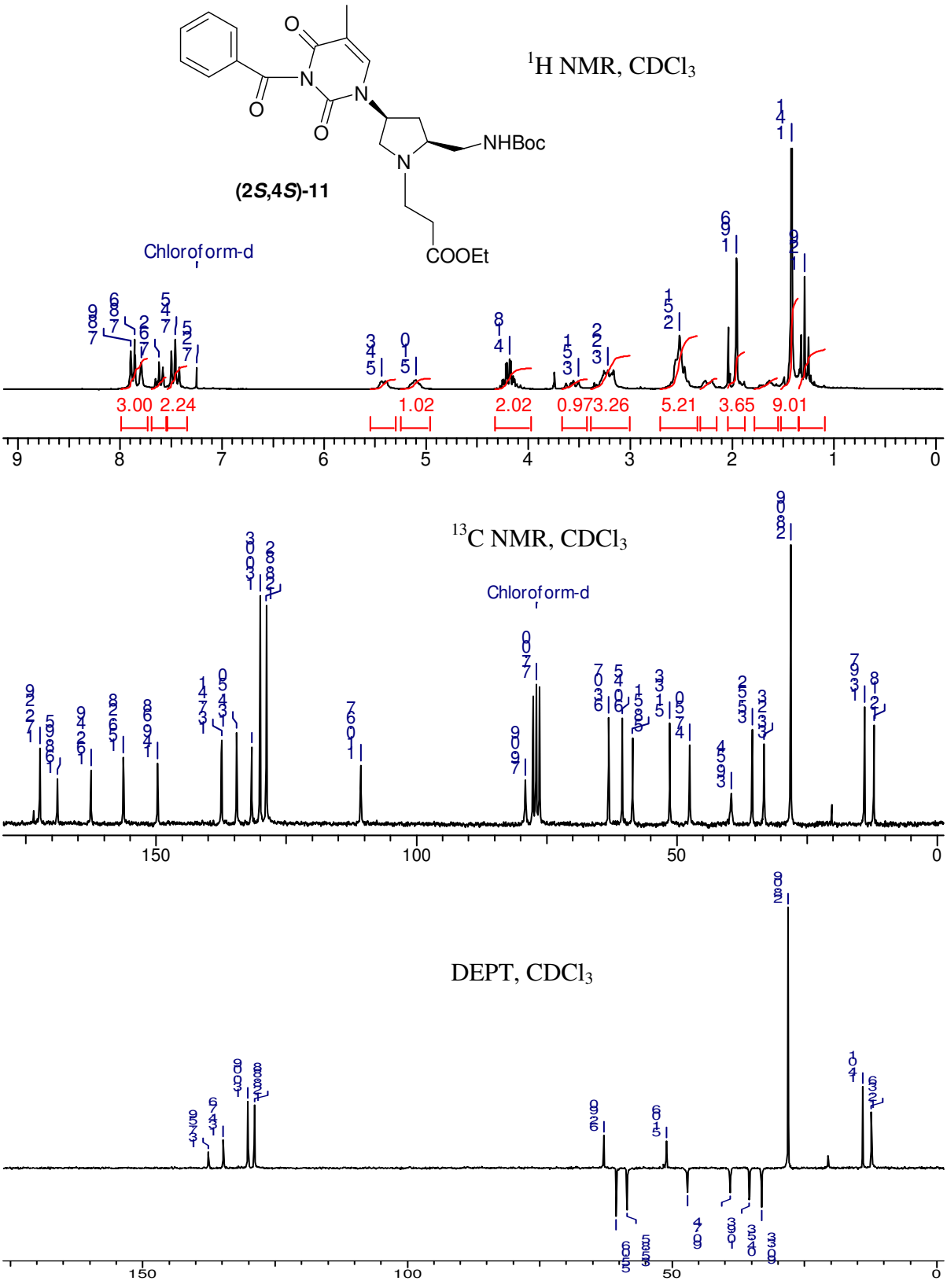
(2S,4S)-11
NHBoc
COOEt
^{1}H NMR, CDCl$_3$
Chloroform-d
3.00 2.24 1.02 2.02 0.973.26 5.21 3.65 9.01
^{13}C NMR, CDCl$_3$
Chloroform-d
DEPT, CDCl$_3$

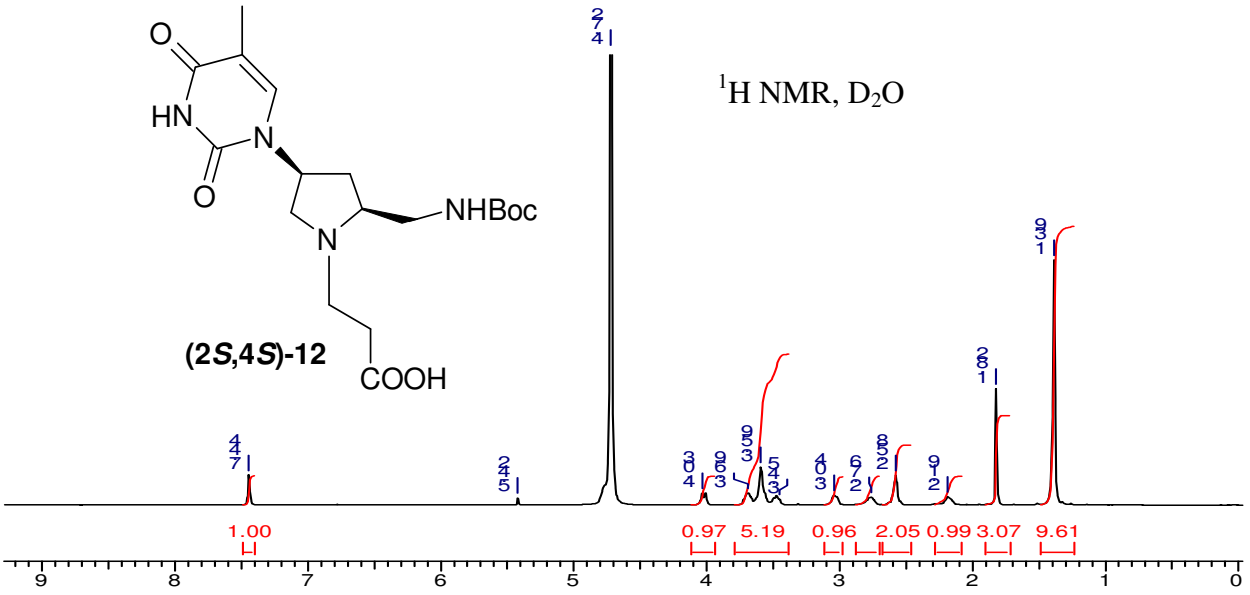
O
HN
N
O
NHBoc
N
COOH
(2S,4S)-12
^{1}H NMR, D$_2$O
1.00
0.97
5.19
0.96
2.05
0.99
3.07
9.61

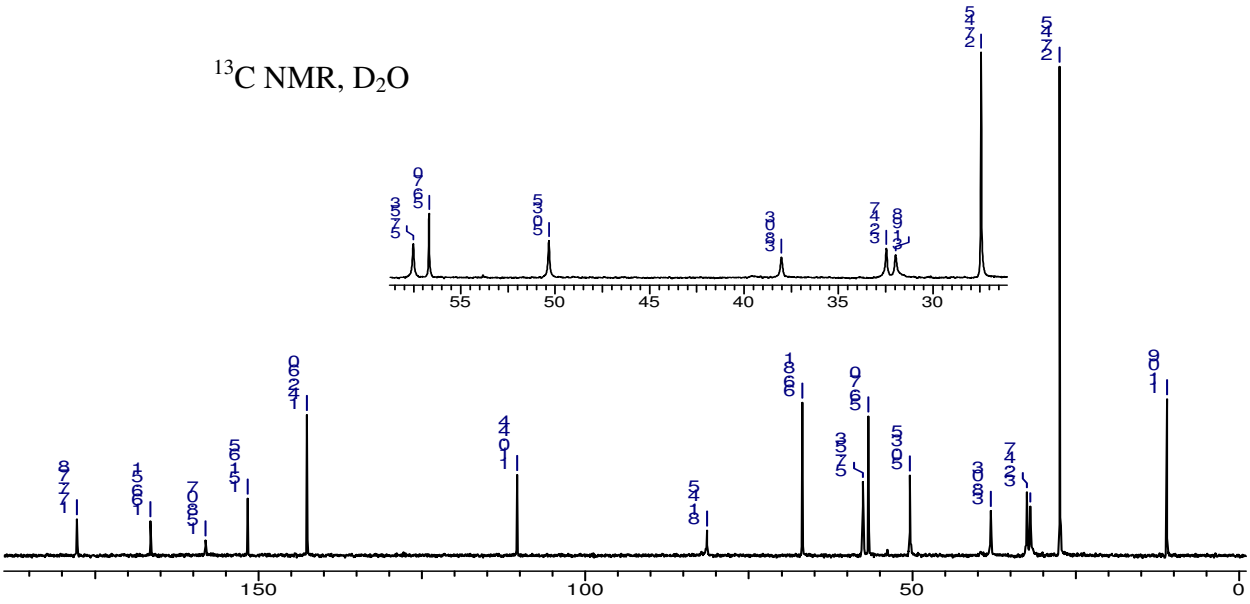
^{13}C NMR, D$_2$O

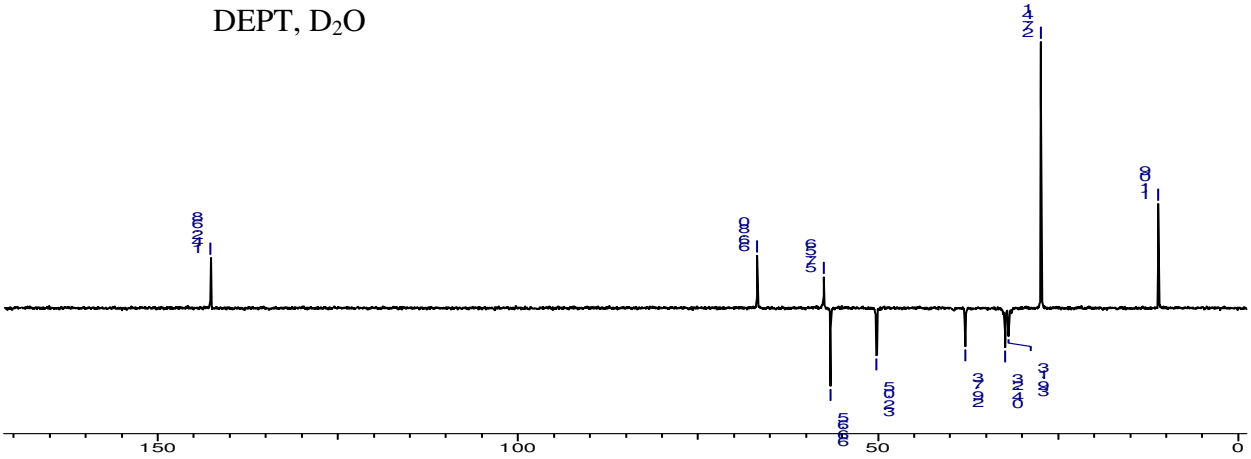
DEPT, D$_2$O

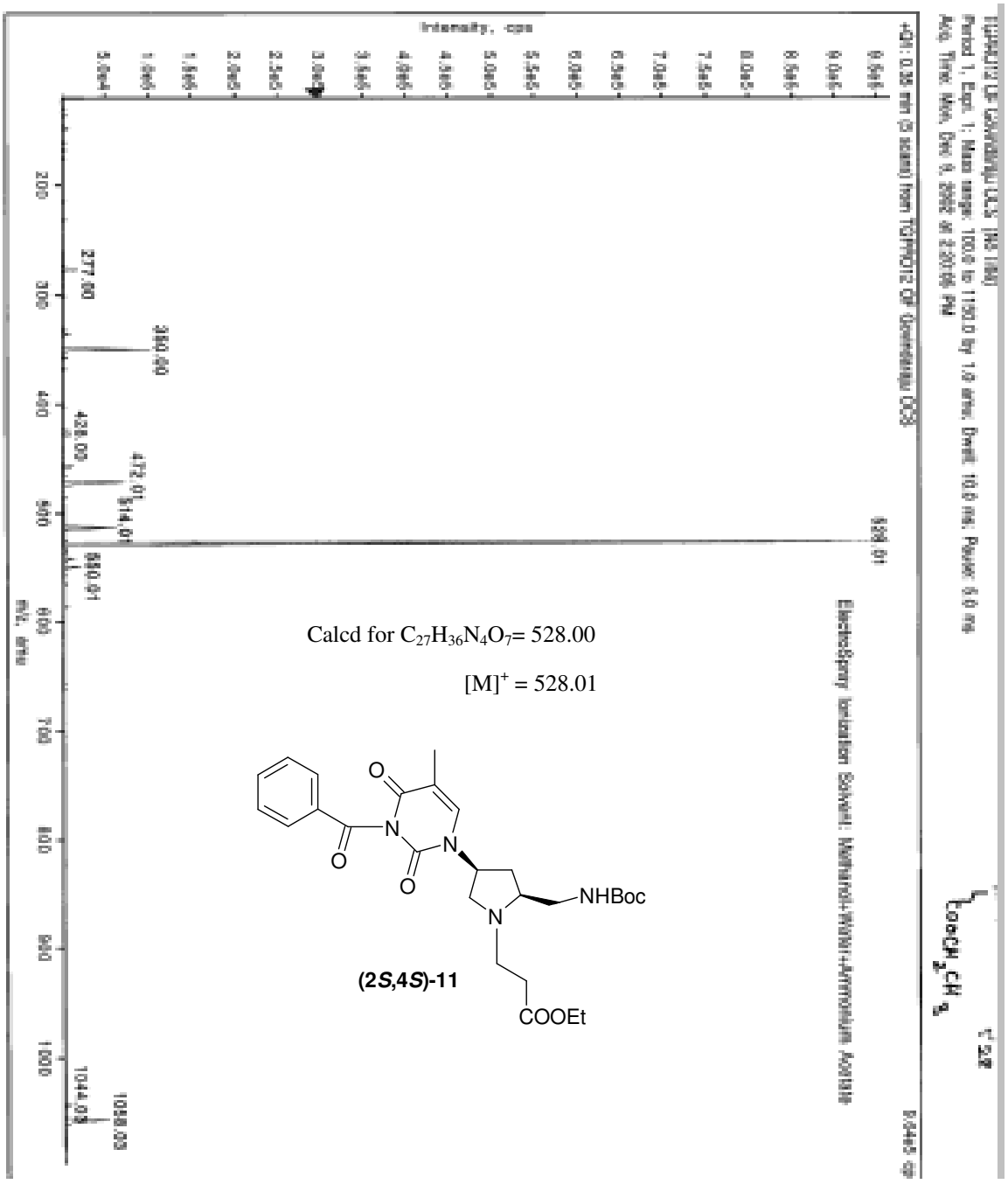

Calcd for $C_{27}H_{36}N_4O_7$= 528.00

$[M]^+$ = 528.01

(2*S*,4*S*)-11

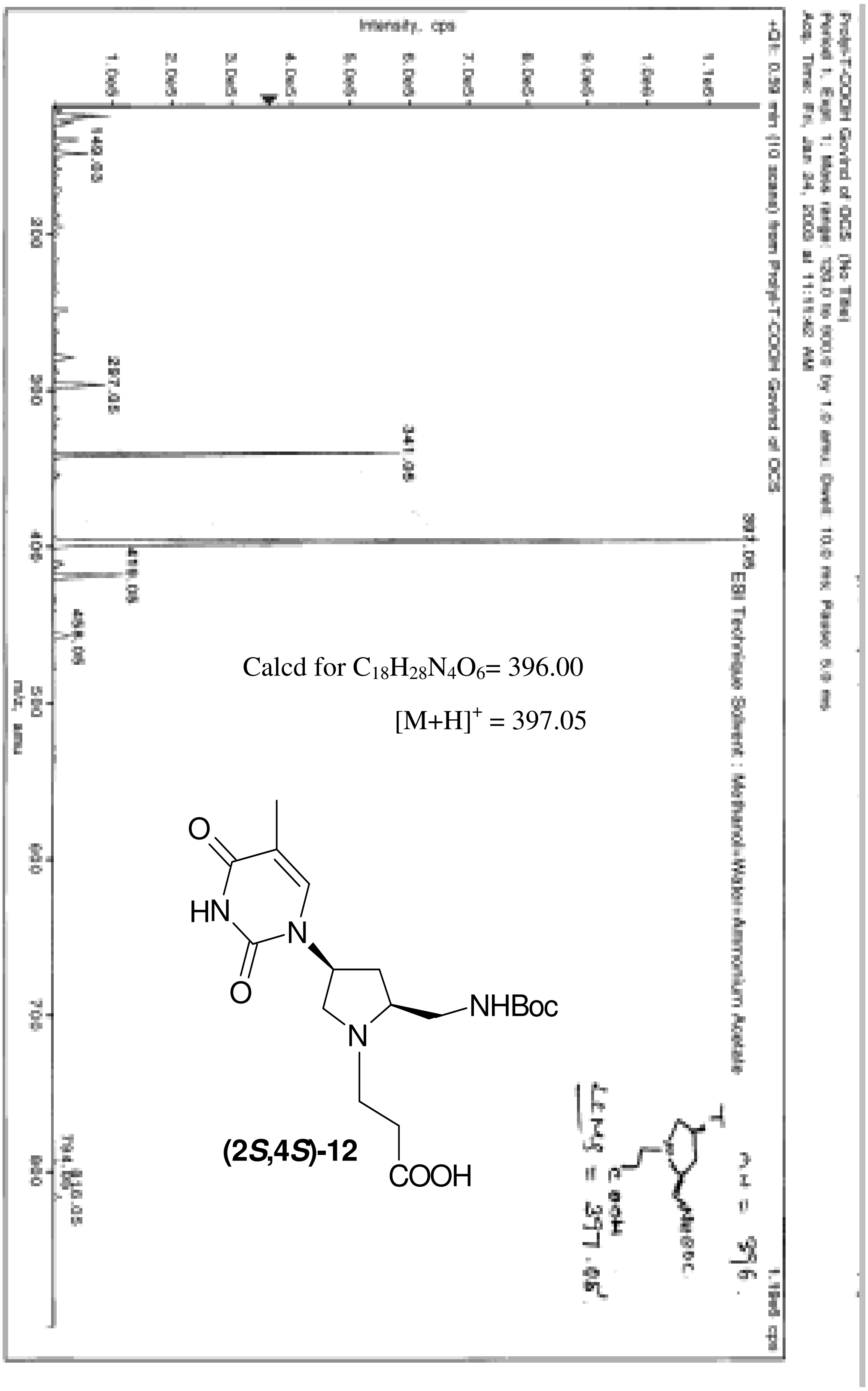

Calcd for $C_{18}H_{28}N_4O_6$= 396.00

$[M+H]^+$ = 397.05

(2*S*,4*S*)-12

Chapter-5

Microwave assisted fast and clean conversion of mesylate to azide: Synthesis of (1*S*,2*R*/1*R*,2*S*)-1-azido-2-carbocyclic amines as immediate precursors to versatile 1,2- *cis*-diamines

5.1 Introduction

In synthetic Organic chemistry, azido compounds are versatile precursors to access a variety of amino compounds such as 1,2-amino alcohols, 1,2-diamines and β-aminoacids.[227,228] Efficient methods available for the reduction of azide to amines has made the azide functionality a synthon of choice to access amino compounds and their potential derivatives.[229] Routine conversion of alcohol to azide functionality involves mesylation or tosylation followed by nucleophilic displacement by azide anion. A large variety of mesylates like primary, secondary and sterically hindered mesylates have been used to access azides. Mesylates react with azide nucleophile often very slowly, requiring prolonged reaction times and high temperatures. Under such circumstances, some reactive mesylates under go decomposition, rearrangement, intramolecular cyclizations and prolonged reaction times may cause racemization. In particular, conversion of hindered mesylate to azide requires very harsh conditions and even impossible in some cases. Thus an alternative rapid and efficient microwave assisted transformations of mesylate to azides will be of interest to many organic chemists and in a recent example, microwave irradiation was employed for the azidation of tosylate.[230] The microwave enhanced organic reactions are rapidly gaining acceptance and popularity since it provides opportunity to complete the reactions in minutes and have manifold application in academia and industry.[231,232]

5.2 Microwave assisted transformation of mesylate to Azide

During the course of our work, we were interested in making azides from sterically hindered mesylate substrates such as **1-11**, shown in Schemes 1 and 2. The conventional synthetic procedure involved heating of the mesylate with NaN_3 (8.0 eq.) in DMF for 5-12 h at 65-70°C. In microwave method, the reaction mixture was treated with microwave radiation in microwave reactor until complete conversion of the starting material. The temperature was maintained at 90°C and then allowed to cool to room temperature. The conversions monitored by thin layer chromatography (TLC), were very

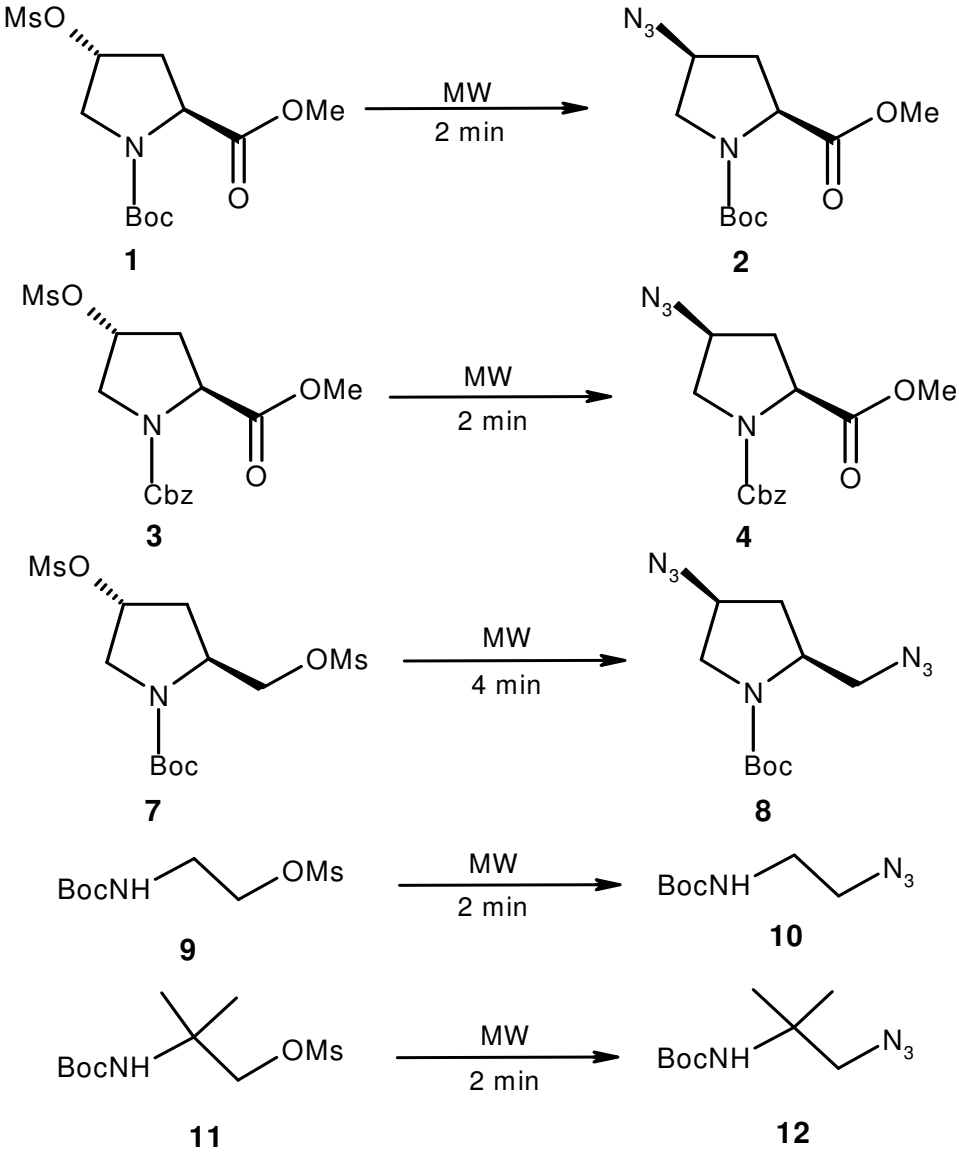

Scheme 1. Microwave assisted azidation of mesylates.

clean and no trace of impurities was found. DMF was a solvent of choice as in conventional method because of its high boiling point (153°C) and polarity resulting in very good microwave absorption medium. The results are summarized in Table 1 and 2. The nucleophile NaN_3 used was 1.5-2.0 eq. as compared to 8.0 eq. in conventional method. The products were easily purified by just filtration column chromatography to achieve high purity. Almost complete conversion was observed within short periods, leading to high enantiopurities of azide products and no recemization occurred. The optical rotations and other characterization data were in agreement with the reported data (Chapter 2 and 3).[233]

Table 1. Microwave assisted transformations (Scheme 1).

Entry	Product	Conventional method			Microwave irradiation		
		Time (h)	Yield (%)	$[\alpha]_D$	Time (min)	Yield (%)	$[\alpha]_D$
1	2	9	95	-27°[a]	2	99	-29°[a]
2	4	9	96	-24°[b]	2	99	-24°[b]
3	8	12	84	-10°[c]	4	99	-11°[c]
4	10	6	75	-	2	98	-
5	12	nt[d]	-	-	2	96	-

[a] for azides 2 (c 2.28, CH_2Cl_2) at 20°C.
[b] for azides 4 (c 1.37, CH_2Cl_2) at 20°C
[c] for azides 8 (c 0.52, $CHCl_3$) at 20°C
[d] no transformation

The mesylate **9** being unstable, underwent neighboring group assisted rearrangement to give slight amount of cyclic aziridine impurity. Interestingly, the inactive and sterically hindered mesylate **11** gave the azide **12** under microwave irradiation as the exclusive product, which was not possible by conventional method (Scheme 1, Table 1).

Conversion of carbocyclic mesylates such as *cp***5a**-*ch***5b** into corresponding azides by conventional methods was accompanied by formation of a side product, identified as

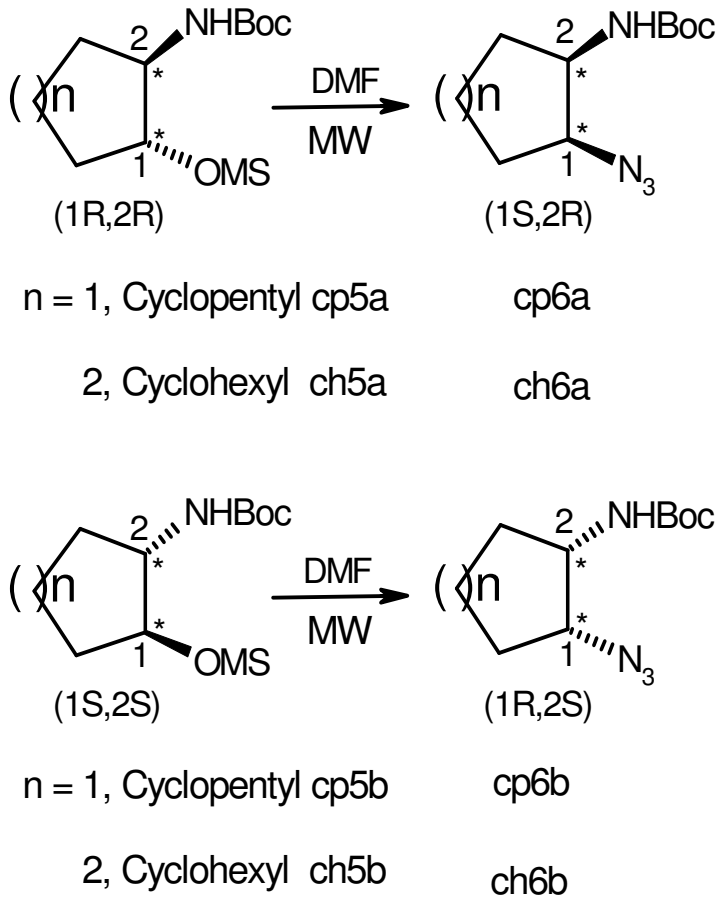

Scheme 2. Azidation of carbocyclic mesylates.

Table 2. Comparative results on (1*S*,2*R*/1*R*,2*S*)-azides (Scheme 2).

Entry	Product	Conventional method			Microwave irradiation		
		Time (h)	Yield (%)	[a][α]$_D$	Time (min)	Yield (%)	[a][α]$_D$
1	*cp***6a**	5	91	+116°	12	97	+117°
2	*ch***6a**	12	87	+102°	8	99	+104°
3	*cp***6b**	5	91	-116°	12	97	-117°
4	*ch***6b**	12	87	-105°	8	99	-105°

[a] for cyclopentyl azides (c 1.0, CH2Cl2) at 20°C.
for cyclohexyl azides (c 1.5, CH_2Cl_2) at 20°C.

the cyclic urea (Figure 1, **6c**) in 7% yield, where the structure was confirmed by NMR and X-ray crystallography (Figure 1). This is probably formed by the thermal decomposition of azide accompanied by the rearrangement with the adjacent carbamate

(Boc) functionality (Figure 2). However under microwave irradiation, no such impurities were observed. In general, conversions of *trans*-cyclohexyl (pentyl) mesylates are very rapid with slightly improved optical purities of the products (Scheme 2, Table 2). The carbocyclic 1,2-diamines were obtained by the reduction of these amino azides as reported (Chapter 2 and 3).

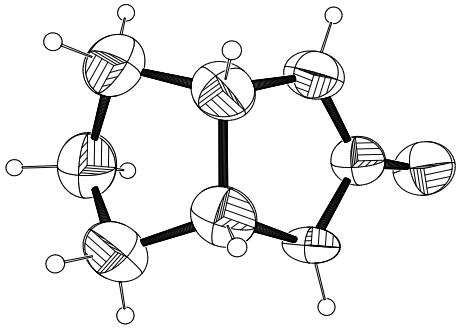

Figure 1. Ortep diagram of urea derivative **6c**

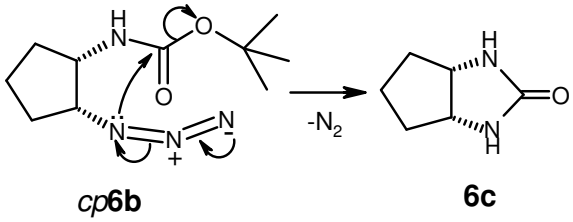

*cp***6b** **6c**

Figure 2. Thermal decomposition of azide *cp***6b**

1,2-Diamines are an important class of compounds, with applications as medicinal agents,[228,234] chiral auxiliaries[228] or as metal ligands in catalytic asymmetric synthesis.[235,236] They are also present in many natural products with potential biological properties.[228,237] Utilizations of the optically pure vicinal 1-azido-2-carbocyclic amines and their derivatives lead to the development of synthetic methods for the preparation of 1,2-diamines in their optically pure form. As compared to *trans*-1,2-cyclohexyl diamines, *cis*-1,2-cyclohexyl (pentyl) diamines have not been exploited to their full potential, in medicinal chemistry[238,239] and in catalytic asymmetric synthesis. In the design of opioid receptor N/OFQ antagonists, *cis*-and *trans*-1,2-cyclohexane diamine was used as a

hydrophobic handle for the manipulation of the pharmacological selectivity (**2**, Figure 3).[238c] The diaminocyclohexane derivatives have received increasing attention because of the discovery of the selective action of their diastereomers at κ or σ-receptor sites. Indeed, compound **1** (Figure 3), which is the *cis*-stereoisomer, has practically no affinity for κ-receptors, whereas its affinity for non-opioid σ-receptors is high.[238,239] The *cis*-carbocyclic-1,2-diamine and their derivatives have been used in the preparation of analogues of cisplatin (**4**-**6**, Figure 3) in their racemic form.[234,240] This is perhaps due to difficulty in obtaining chirally pure *cis*-1,2-cyclic diamines. We recently demonstrated the potential of these *cis*-1,2-diamines (both cyclohexyl and cyclopentyl) in designing constrained PNA analogues for DNA and RNA discrimination (Chapter 2 and 3). The microwave procedure discussed here would be helpful in access a variety of such optically pure azido precursors.

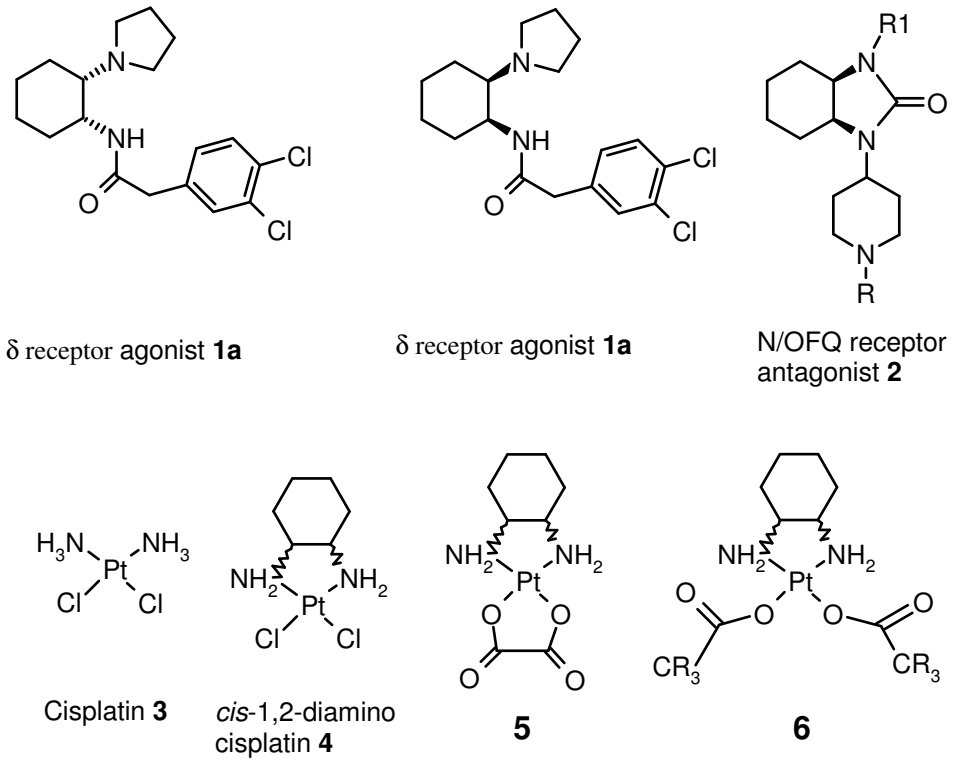

Figure 3. *cis*-1,2-Cyclohexane diamine derivatives used as therapeutics

In all the microwave irradiation experiments involving formation of azide products, no incidents have been observed. The sophisticated single mode microwave reactors enable the fine control of temperature and pressure during the microwave reactions, ensuring the safety.[241]

5.3 Conclusion

In summary, this report demonstrates the use of microwave-assisted synthesis of substituted azides, which are immediate precursors of amine functionality. This procedure is efficient, rapid, clean and high yielding process, and a better alternative to conventional method. Our synthesis provides an easy access to the optically pure enantiomers of *cis*-1,2-cyclohexyl and cyclopentyl diamines, which are otherwise difficult to obtain from other methods as compared to *trans*-diamines which are commercially available.

Summary

- **Microwave assisted conversion of unstable and sterically hindered mesylates to azides is demonstrated**
- **This Synthetic route provides an easy access to the optically pure enantiomers of *cis*-1,2-cyclohexyl (pentyl) diamines in high yield, which are otherwise difficult to obtain from other methods**

5.4 Experimental

General Procedure: Melting points of samples were determined in open capillary tubes on Bruker melting point apparatus B-540 and are uncorrected. IR spectra were recorded on an infrared Fourier Transform spectrophotometer using KBr pellets or as neat. Column chromatographic separations were performed using silica gel 60-120 mesh, solvent systems 10-25% EtOAc/Pet ether and pure DCM to 3% MeOH/DCM. ^{1}H and ^{13}C were obtained using Bruker 200 MHz and 500 MHz NMR spectrometers. The chemical shifts are reported in delta (δ) values. Mass spectra were obtained either by FAB or LCMS techniques.

Conventional method: A stirred mixture of the (1*S,*2*S*)-2-(*N*-*t*-Boc-amino)-cyclopentan-1-methyl sulfonate *cp***5b** (700 mg, 2.5 mmol) and NaN_3 (1.3 g, 20.0 mmol) in DMF (5 ml) under nitrogen atmosphere was heated at 68-70°C for 5-6 h. After cooling the reaction mixture, the solvent was evaporated under reduced pressure. The residue was extracted into ethyl acetate (10mlx2) and dried over Na_2SO_4. The organic layer was removed and the crude product was purified by column chromatography (EtOAc/pet.ether) to afford white solid of (1*R,*2*S*)-2-(*N*-*t*-Boc-amino)-1-azidocyclopentane (*cp***6b**). Yield, 91%, $[\alpha]_D^{20}$ - 116° (*c* 1.0, CH_2Cl_2), and the side product **6c** (yield, 7%). *cis-Cyclopentyl-1,3-Urea* **6c**: m.p. 143.0°; IR, ν (cm^{-1}) (KBr); 3280.69, 3016.46, 2970.17, 1745.46, 1409.87, 1244.0, 1215.07, 1114.78, 1039.56, 991.34, 946.98, 756.04; ^{1}H-NMR ($CDCl_3$-*d*, 200 MHz); δ_H 1.25-1.75 (m, 4H), 1.75-1.9 (s, 2H), 3.9-4.1 (s, 1H), 4.75-4.9 (s, 1H), 6.5-6.85 (bd, 2H): ^{13}C-NMR ($CDCl_3$-*d*, 200 MHz): δ_C 21.5 (C4), 33.7 (C3), 34.1 (C5), 56.5 (C1), 81.9 (C2), 160.3 (C=O): Anal Calcd (%)

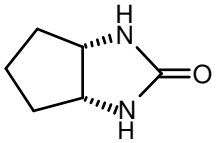

6c

for $C_6H_{10}N_2O$: C, 57.14; H, 7.93; N, 22.22; Found C, 56.91; H, 7.97; N, 21.87; MS, LCMS, 128.03 $[M+2]^+$.

Crystallographic data for compound 6c: Single crystal of *cis*-Cyclopentyl-1,3-Urea (**6c**) (colourless needles) was obtained from ethyl acetate and petroleum ether. X-ray intensity data was collected on a Bruker SMART APEX CCD diffractometer at room temperature. ¶*Crystal data: cis-Cyclopentyl-1,3-urea* (**6c**). Compound 19 was crystallized as colorless needles from ethyl acetate and petroleum ether (low polar solvent). $C_6H_{10}N_2O$, M = 126.16, Crystal system: Monoclinic, Crystal dimensions 0.75 x 0.14 x 0.13 mm, a = 10.322(3), b = 5.5641(18), c = 11,284(4) Å, space group P 2(1), V=643.5(4) Å3, Z = 4, Dc = 1.302 g cm^{-3}, μ (Mo-Kα) = 0.091 mm-1, T = 293(2) K, F(000) = 272, Max. and min. transmission 0.9882 and 0.9347, 3149 reflections collected, 2090 unique [I>2σ (I)], S= 1.116, R value 0.0595, *wR2* = 0.1559 (all data R = 0.0638, *wR2* = 0.1543). CCDC No. 249728 contains the crystallographic data for this compound (Chapter 3).

Microwave irradiation: The mixture of mesylate (1*S*,2*S*)- *cp***5b** (700 mg, 2.5 mmol) and NaN_3 (0.32 g, 5.0 mmol) in DMF (5 ml) was taken in a microwave reaction flask. The above reaction mixture was irradiated in a microwave reactor at 90°C for 12 mins. (To start with reaction periods were standardizing by irradiating the reaction mixtures in 1-6 cycles, each of 2 mins interval and 1 min rest. The progress of the reaction was monitored by TLC, in every 2 mins interval.) After cooling to room temperature, the solvent evaporated and the residue was extracted in to EtOAc (10 mlx2) and dried over Na_2SO_4. The organic layer was removed and passed through the silica gel column to gave the azide (1*R*,2*S*) *cp***6b**. Yield 97%. $[\alpha]_D^{20}$ -117° (*c* 1.0, CH_2Cl_2); m.p. 81.0°; IR, ν (cm^{-1}) (KBr); 3442.7, 3014.53, 2995.24, 2113.84, 1706.88 cm^{-1}: ^{1}H-NMR

($CDCl_3$-*d*, 200 MHz); δ_H 1.0-1.45(m, 11H, CH_2, *t*-Boc), 1.65-2.0 (m, 4H, $C5H_2$, $C3H_2$),

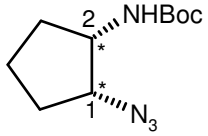

(1*R*,2*S*) *cp***6b**

3.7-4.1 (m, 2H, C1H, C2H), 4.6-5.0 (bd, 1H, carbamate NH): ^{13}C-NMR ($CDCl_3$-*d*, 200 MHz): δ_C 19.8 (C-4), 28.2 (*t*-Boc), 28.7 (C-5), 29.0 (C-3), 54.7 (C-1), 64.1 (C-2), 79.4 (*t*-Boc), 155.3 (carbamate C=O): Anal Calcd (%) for $C_{10}H_{18}N_4O_2$: C, 53.09; H, 7.96; N, 24.77; Found C, 52.55; H, 7.98; N, 24.71;MS (FAB+) 227 (35%) [M+1], 171 (100%) [M+1- N_3], 127 (15%) [M+1-*t*Boc].

(2*S*,4*S*)-4-azido-*N*1-butyloxycarbonyl proline methyl ester (2):

Yield 99%, IR, ν (cm^{-1}) (Neat); 3357, 2979, 2935, 2105, 1751, 1704, 1400, 1261, 1193, 1161; $[\alpha]_D^{20}$ –29.0° (*c* 2.28, CH_2Cl_2); ^{1}H-NMR ($CDCl_3$-*d*, 200 MHz); δ_H 1.2-1.6

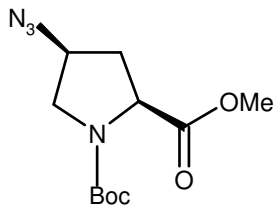

(d, 9H, Boc), 2.2-2.4 (m, 1H), 3.5-3.7 (m, 1H), 3.76 (s, 3H, OCH_3), 3.8-4.1 (m, 1H), 4.2-4.5 (bd, 1H): ^{13}C-NMR ($CDCl_3$-*d*, 300 MHz); δ_c 26.4 (C3), 28.1 (*t*Boc), 33.4 (C5), 49.1 (C4), 52.2 (C2), 81.0 (*t*Boc), 118.7 (ester CH_3), 152.9 (carbamate C=O), 171.6 (ester C=O): Anal Calcd (%) for $C_{11}H_{18}N_4O_4$: C, 48.88; H, 6.66; N, 20.74; Found C, 48.67; H, 6.71; N, 20.57; LCMS 271.0 [M+1], 171.0 [M+1-Boc].

(2*S*,4*S*)-4-azido-*N*1-benzyloxycarbonyl proline methyl ester (4):

Yield 99%, IR, ν (cm^{-1}) (Neat); 2953, 2106, 1753, 1711, 1499, 1416; $[\alpha]_D^{20}$ –24.0° (*c* 1.37, CH_2Cl_2); ^{1}H-NMR ($CDCl_3$-*d*, 200 MHz); δ_H 2.00-2.15 (m, 1H, C3'H),

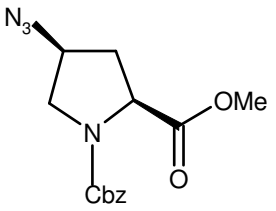

4

2.17-2.33 (m, 1H, C3H), 3.45-3.7 (m, 5H, C5H, -OCH_3), 4.04-4.16 (m, 1H, C4H), 4.43-4.31 (dd, J = 8, 16, 1H, C2H), 4.9 – 5.17 (m, 2H, -CH_2Ph), 7.23-7.27 (m, 5H, C_6H_5); ^{13}C-NMR ($CDCl_3$-*d*, 300 MHz); δ_c 34.9 (C2), 51.0 (C5), 52.2 (C4), 57.4 (C2), 58.1 (OCH_2Ar), 67.1 (ester CH_3), 125.1, 127.7, 127.9, 128.3, 128.8, 136.1

(Aromatic), 153.9 (N-C=O), 171.4 (ester C=O): Anal Calcd (%) for $C_{14}H_{16}N_4O_4$: C, 55.26; H, 5.26; N, 18.42; Found C, 55.19; H, 5.31; N, 18.19; LCMS 305.0 [M+1], 205.0 [M+1-Boc].

(2*S*,4*S*)-2-Azidomethyl-4-azido-*N*1-(*tert*-butyloxycarbonyl) pyrrolidine (8):

Yield, 99%, IR (neat, cm^{-1}): 3365.5, 2977.8, 2935.4, 2104.19, 1695.31, 1392.51, 1265.2, 1164.9, 1118.6, and 773.4. $[\alpha]_D^{20}$ -11.0 (c=0.52, $CHCl_3$); ^1H NMR ($CDCl_3$): δ_H

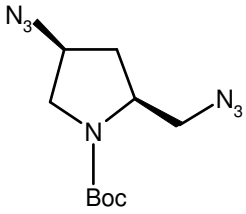

8

4.20-4.05 (m, 1H), 4.05-3.90 (m, 1H), 3.80-3.65 (m, 1H), 3.65-3.55 (m, 2H), 3.40-3.25 (m, 1H), 2.35-2.20 (m, 1H), 2.10-2.00 (m, 1H), 1.45 (s, 9H). ^{13}C NMR ($CDCl_3$): δ_C 27.9 (*t*Boc), 33.5 (C2), 51.3 (C5), 52.7 (-CH_2-N_3), 55.5 (C4), 58.6 (C2), 79.8 (*t*Boc), 153.4 (carbamate C=O); Anal Calcd (%) for $C_{10}H_{17}N_7O_2$: C, 44.94; H, 6.36; N, 11.98; Found C, 44.76; H, 6.71; N, 11.68; MS (FAB^+) 268 [M+1].

(1*S*,2*R*)-2-(*N*-*t*-Boc-amino)-1-azidocyclopentane (*cp*6a):

Yield 97%. $[\alpha]_D^{20}$ +117° (*c* 1.0, CH_2Cl_2); m.p. 81.0°; IR, ν (cm^{-1}) (KBr); 3442.7, 3014.53, 2995.24, 2113.84, 1706.88 cm^{-1}: ^1H-NMR ($CDCl_3$-*d*, 200 MHz); δ_H 1.0-1.45(m,

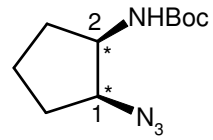

(1*S*,2*R*)-*cp*6a

11H, CH_2, *t*-Boc), 1.65-2.0 (m, 4H, C5H_2, C3H_2), 3.7-4.1 (m, 2H, C1H, C2H), 4.6-5.0 (bd, 1H, carbamate NH): ^{13}C-NMR ($CDCl_3$-*d*, 200 MHz): δ_C 19.8 (C-4), 28.2 (*t*-Boc), 28.7 (C-5), 29.0 (C-3), 54.7 (C-1), 64.1 (C-2), 79.4 (*t*-Boc), 155.3 (carbamate C=O): Anal Calcd (%) for $C_{10}H_{18}N_4O_2$: C, 53.09; H, 7.96; N, 24.77; Found C, 52.55; H, 7.98; N, 24.71;MS (FAB+) 227 (35%) [M+1], 171 (100%) [M+1- N_3], 127 (15%) [M+1- *t*Boc].

(1*S*,2*R*)-2-(*N*-*t*-butyloxycarbonylamino)-1-azidocyclohexane (*ch*6a):

Yield 99%: m.p. 69-70°C; IR, ν (cm^{-1}) (KBr); 3359, 2954, 2104, 1720, 1681, 1367, 1319 and 1166 cm^{-1}: $[\alpha]_D^{20}$ + 104° (*c* 1.5, CH_2Cl_2); ^1H-NMR ($CDCl_3$-*d*, 500

MHz); δ_H 1.21-1.35 (m, 1H), 1.35-1.51 (12H), 1.52-1.64 (m, 2H), 1.65-1.77 (m, 1H), 1.89-2.01 (m, 1H), 3.5-3.65 (bd, 1H), 3.8-4.0 (bd, 1H), 4.56-4.8 (bd, 1H): ^{13}C-NMR ($CDCl_3$-*d*, 500 MHz): δ_C 19.6 (C-5), 24.2 (C-4) 27.5 (C-6), 28.2 (*t*Boc), 28.6 (C-3), 51.0 (C-1), 61.5 (C-2), 79.4 (*t*Boc), 154.9 (carbamate C=O): Anal Calcd (%) for $C_{11}H_{20}N_4O_2$: C, 55.00; H, 8.33; N, 23.33; Found C, 55.18; H, 8.00; N, 23.14;MS (FAB^+) 241 (35%), [M+1], 141 (15%) [M+1- Boc].

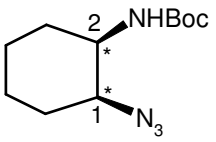

(1*S*,2*R*)-*ch***6a**

Crystallographic data for compound *ch***6a**: Single crystal of azide *ch***6a** (colorless tiny needles) was obtained from ethyl acetate and petroleum ether. X-ray intensity data was collected on a Bruker SMART APEX CCD diffractometer at room temperature. ¶Crystal data: (1*S,*2*R*)-2-(*N*-*t*-butyloxycarbonylamino)-1-azidocyclohexane (*ch***6a**): $C_{11}H_{20}N_4O_2$ *M* = 240.31, Crystal system: Tetragonal, Crystal dimensions 0.66 x 0.36 x 0.18 mm, *a* = 12.159(6), *b* = 12.159(6), *c* = 19.086(13) Å, space group *P* 4(3) 2(1) 2, *V*=2821(3) Å3, *Z* = 8, *Dc* = 1.31 g cm–3, μ (Mo-Kα) = 0.080 mm-1, *T* = 293(2) K, *F*(000) = 1040, Max. and min. transmission 0.9860 and 0.9491, 14080 reflections collected, 2493 unique [*I*>2σ (*I*)], *S*= 1.143, *R* value 0.0846, *wR2* = 0.2069 (all data *R* = 0.1179, *wR2* = 0.1610). CCDC No. 249729 contains the crystallographic data for this compound (Chapter 2).

(1*R*,2*S*)-2-(*N*-*t*-butyloxycarbonylamino)-1-azidocyclohexane (*ch*6b):

Yield 99%, m.p. 69-70°C; IR, ν (cm^{-1}) (KBr); 3359, 2954, 2104, 1720, 1681, 1367, 1319 and 1166 cm^{-1}: $[\alpha]_D^{20}$ -105.33° (*c* 1.5, CH_2Cl_2); ^{1}H-NMR ($CDCl_3$-*d*, 500 MHz); δ_H 1.21-1.35 (m,1H,), 1.35-1.51 (12H), 1.52-1.64 (m, 2H), 1.65-1.77 (m, 1H), 1.89-2.01 (m, 1H), 3.5-3.65 (bd, 1H), 3.8-4.0 (bd, 1H), 4.56-4.8 (bd, 1H): ^{13}C-NMR ($CHCl_3$-*d*, 500 MHz): δ_C

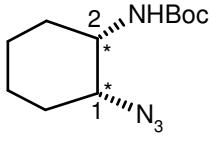

(1*R*,2*S*)-*ch***6b**

19.6 (C-5), 24.2 (C-4) 27.5 (C-6), 28.2 (*t*Boc), 28.6 (C-3), 51.0 (C-1), 61.5 (C-2), 79.4 (*t*Boc), 154.9 (carbamate C=O): Anal. Calcd (%) for $C_{11}H_{20}N_4O_2$: C, 55.00; H, 8.33; N, 23.33; Found C, 55.11; H, 8.07; N, 23.21; MS (FAB+) 241 (35%) [M+1], 141 (15%) [M+1-Boc].

4.6 Appendix

- Compound **6c**, ^{1}H, ^{13}C NMR, IR and LC-MS
- Compound *cp***6a**, ^{1}H, ^{13}C NMR, DEPT, IR and FAB-MS
- Compound *ch***6a**, ^{1}H, ^{13}C NMR, DEPT, IR and FAB-MS
- Compounds **2-12**, IR spectra

^{1}H NMR, $CDCl_3$

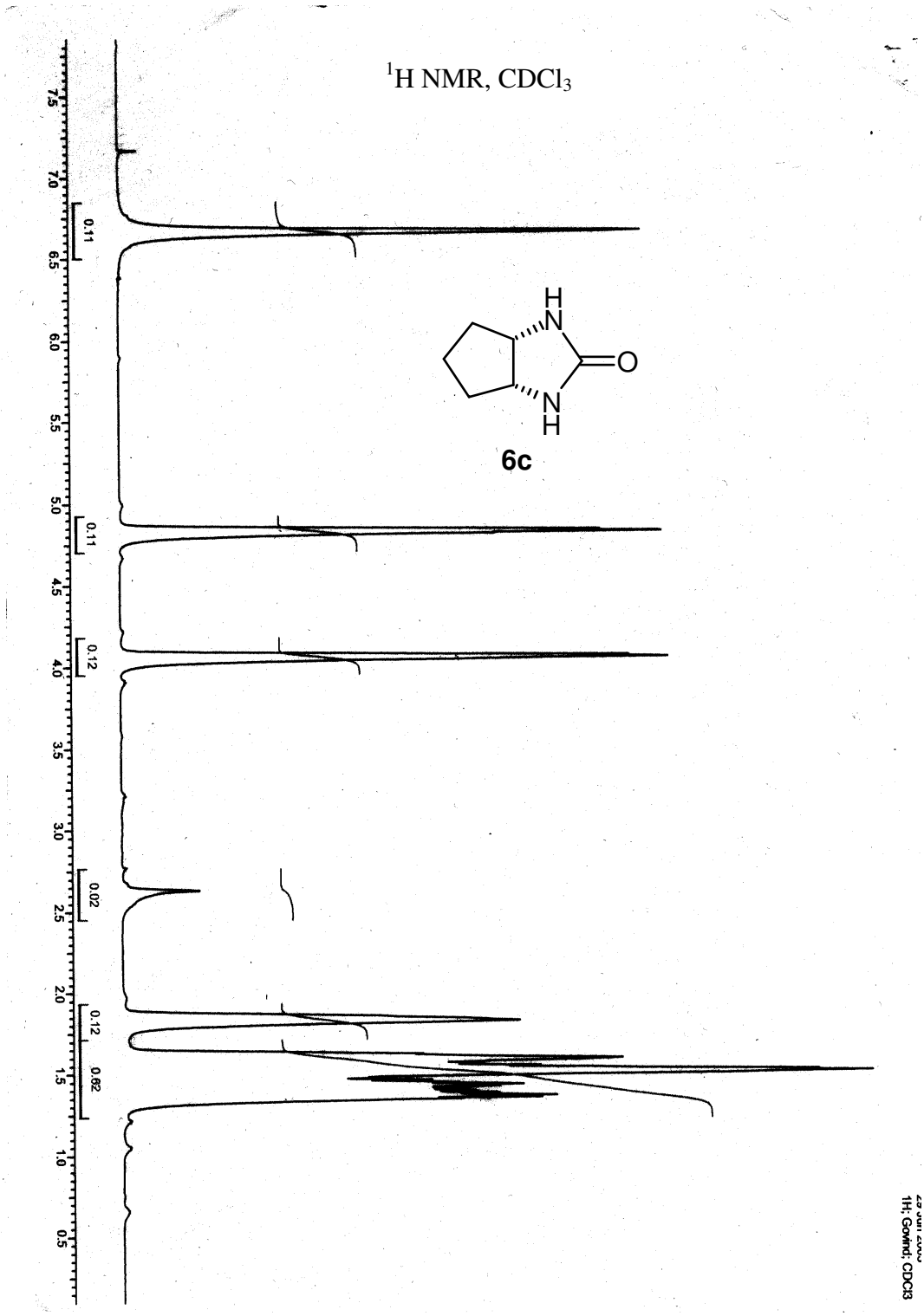

6c

^{13}C NMR, $CDCl_3$

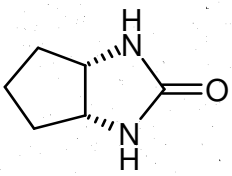

6c

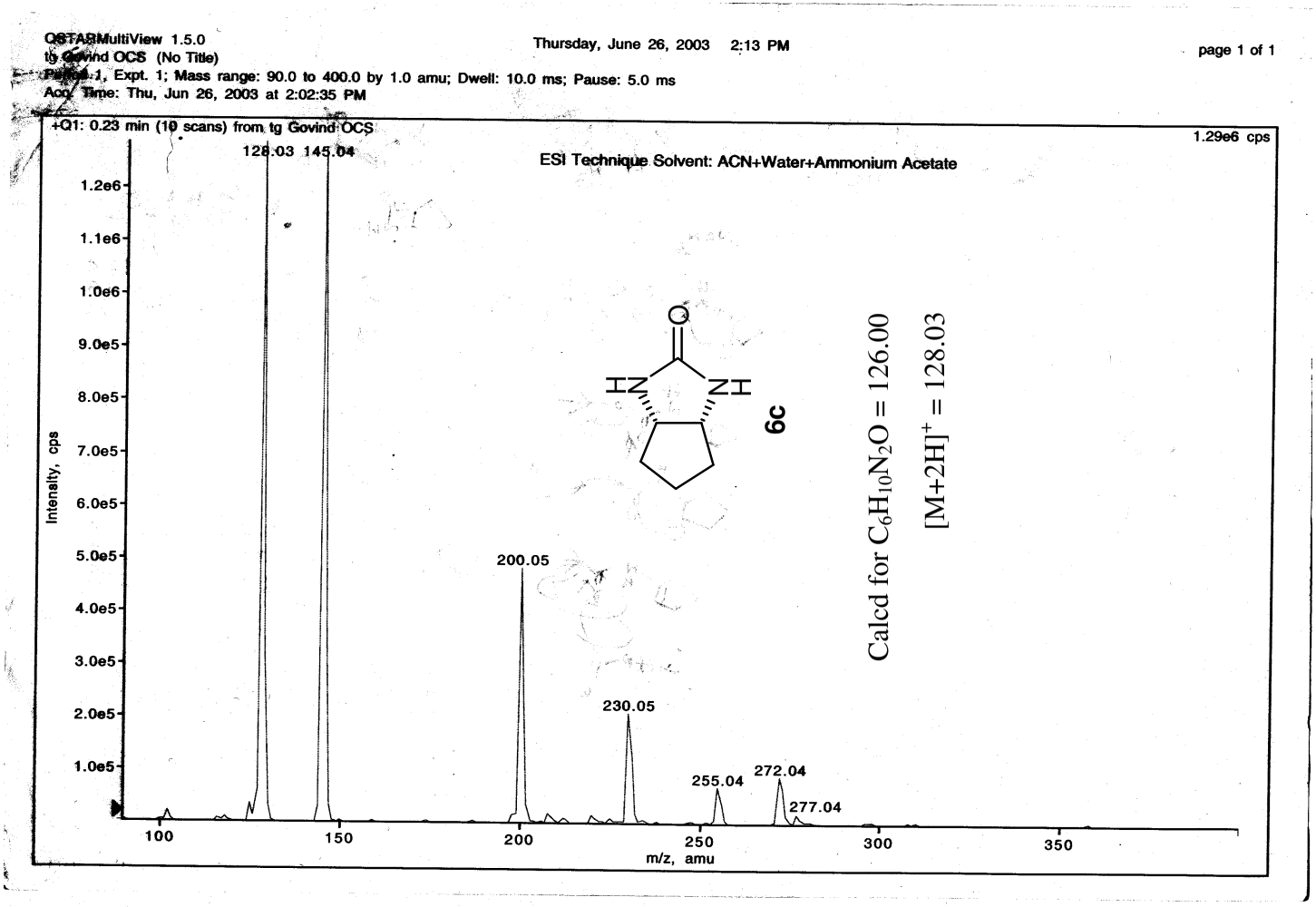
QSTARMultiView 1.5.0
tg Govind OCS (No Title)
Thursday, June 26, 2003 2:13 PM
page 1 of 1
Period 1, Expt. 1; Mass range: 90.0 to 400.0 by 1.0 amu; Dwell: 10.0 ms; Pause: 5.0 ms
Acq. Time: Thu, Jun 26, 2003 at 2:02:35 PM
+Q1: 0.23 min (10 scans) from tg Govind OCS
1.29e6 cps
ESI Technique Solvent: ACN+Water+Ammonium Acetate
128.03
145.04
200.05
230.05
255.04
272.04
277.04
Intensity, cps
m/z, amu
6c
Calcd for C6H10N2O = 126.00
[M+2H]+ = 128.03

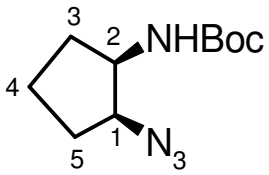

(1*S*,2*R*)-*cp***6a**

^{1}H NMR, $CDCl_3$

^{13}C NMR, $CDCl_3$

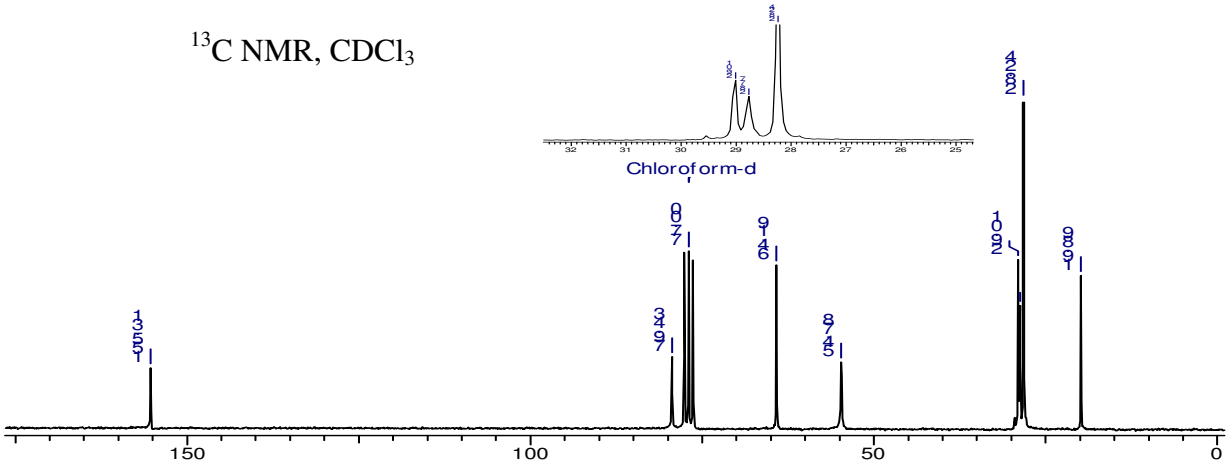

DEPT, $CDCl_3$

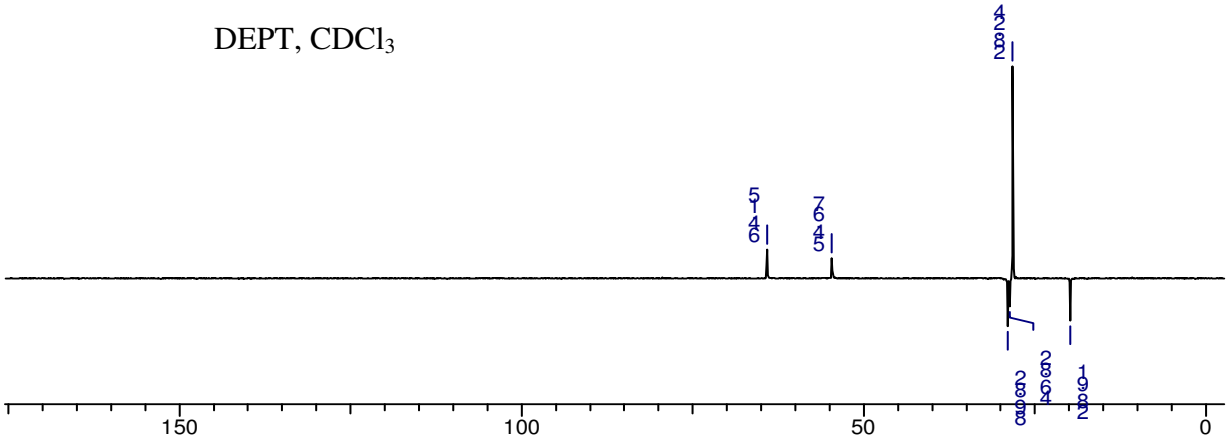

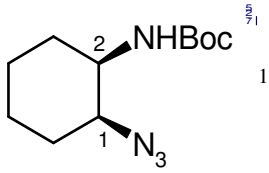

(1*S*,2*R*) *ch***6a**

^{1}H NMR, $CDCl_3$

^{13}C NMR, $CDCl_3$

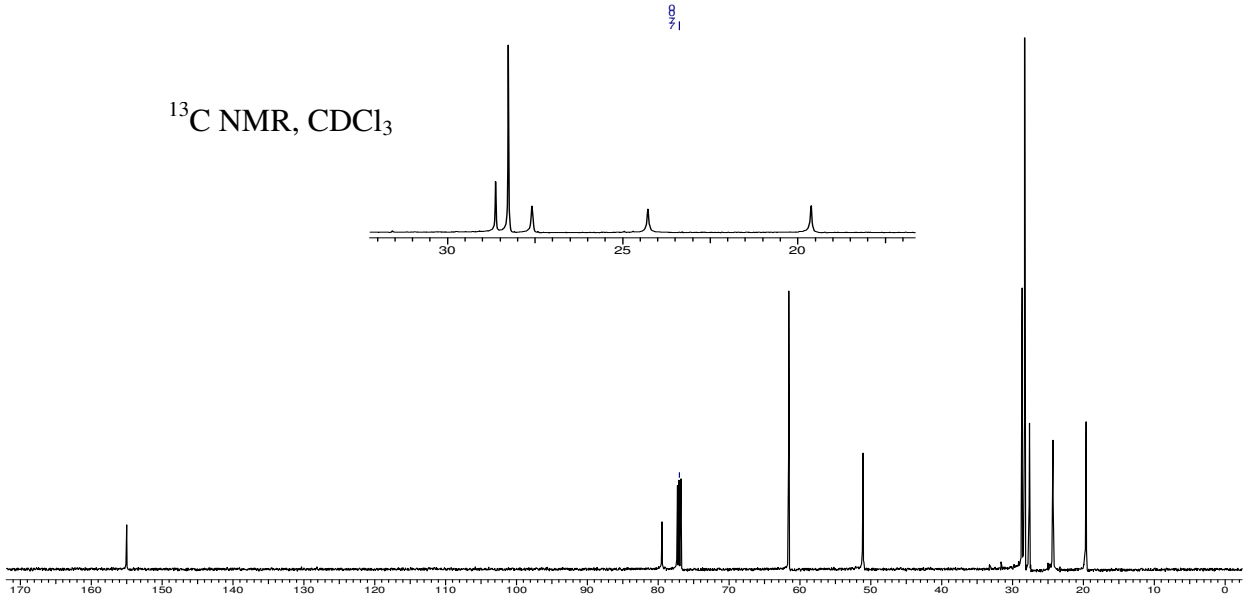

DEPT, $CDCl_3$

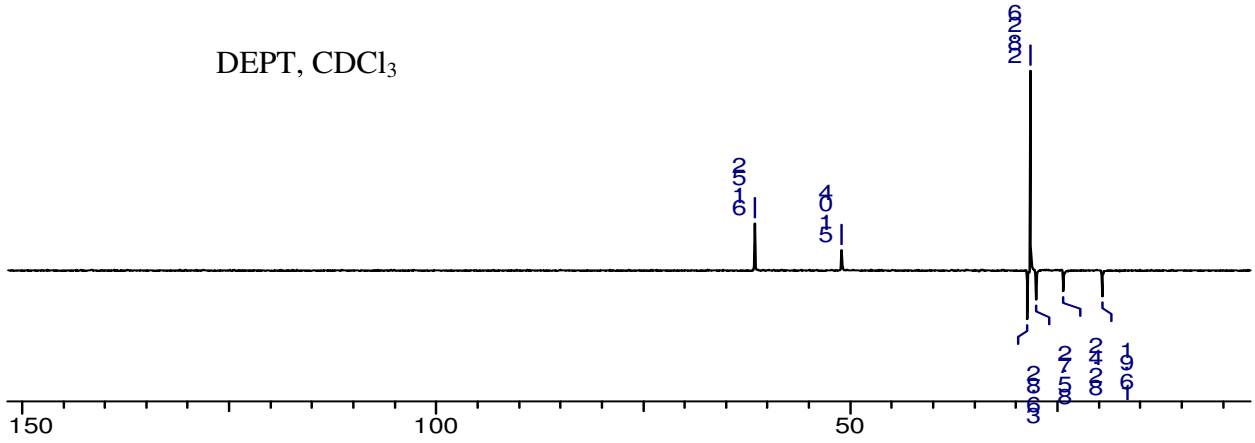

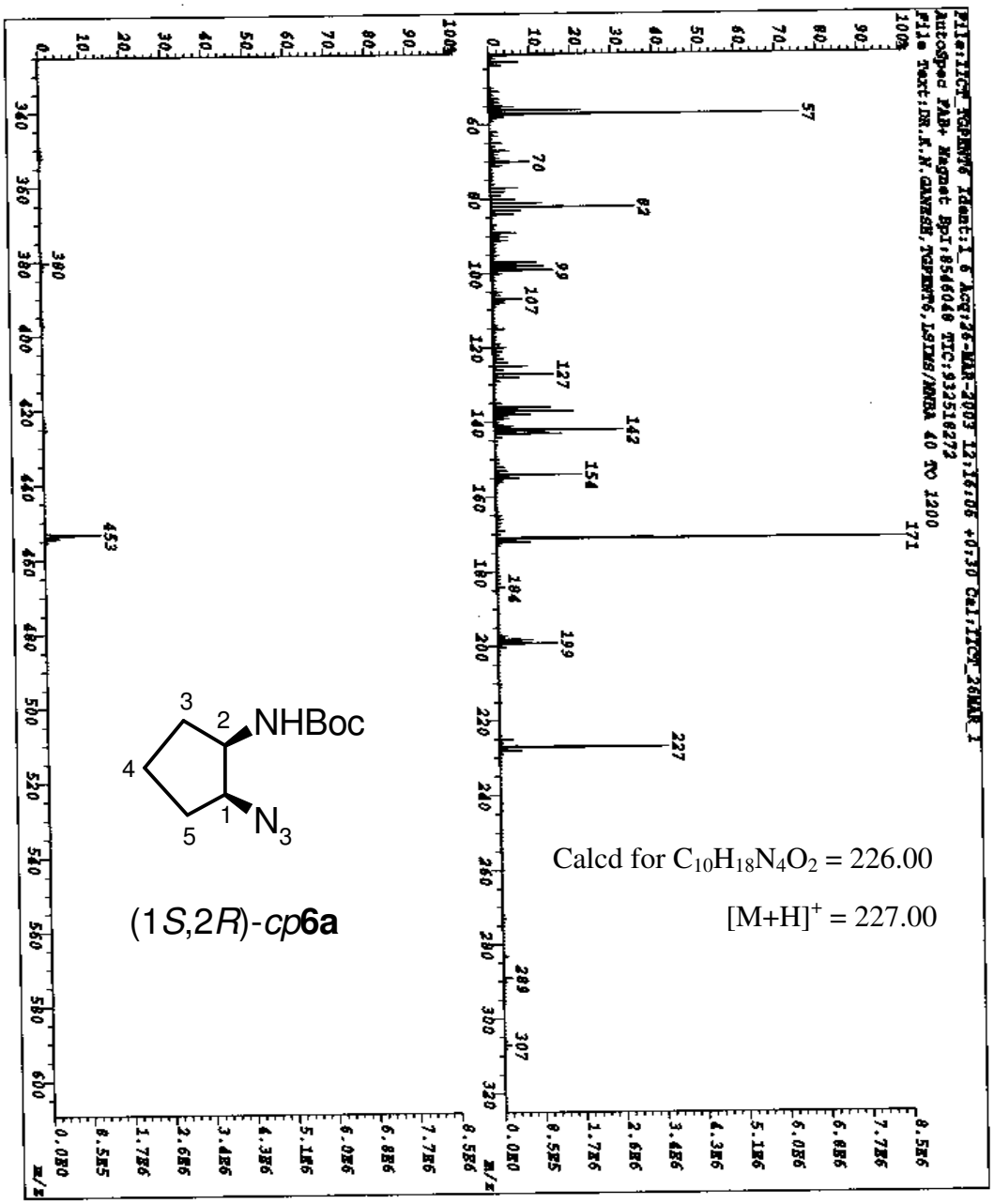
NHBoc
N3
1
2
3
4
5
(1S,2R)-cp6a
Calcd for C10H18N4O2 = 226.00
[M+H]+ = 227.00

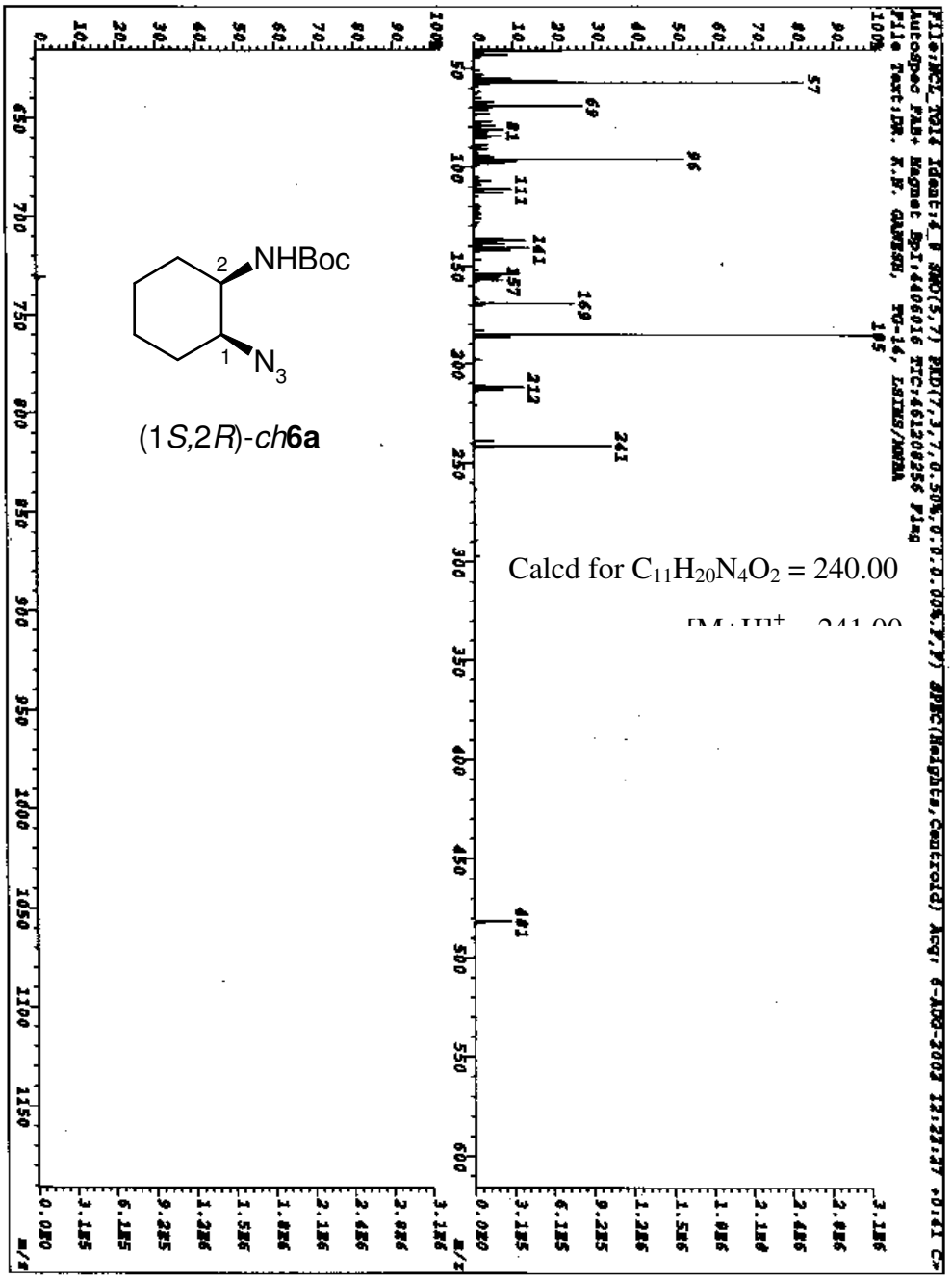
NHBoc
N3
(1S,2R)-ch6a
Calcd for C11H20N4O2 = 240.00

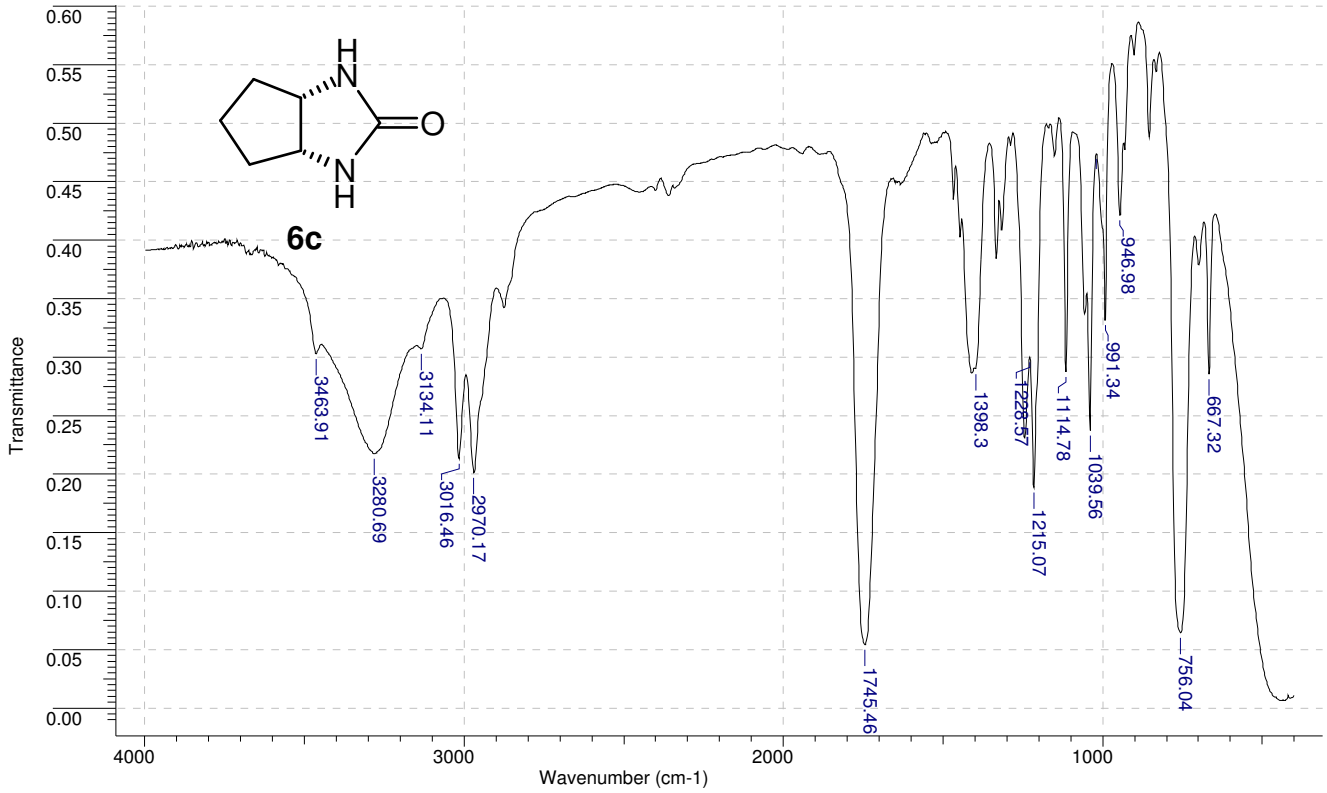
6c
Transmittance
Wavenumber (cm-1)
3463.91
3280.69
3134.11
3016.46
2970.17
1745.46
1398.3
1228.57
1215.07
1114.78
1039.56
991.34
946.98
756.04
667.32

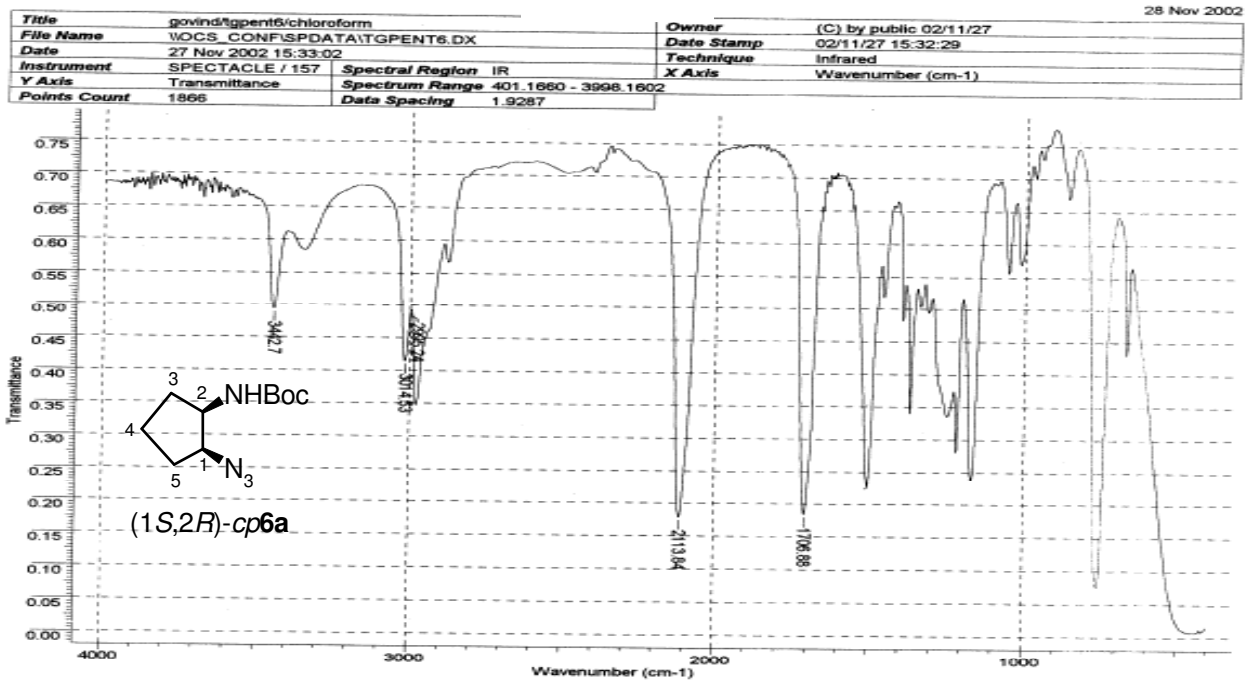
Title govind/tgpent6/chloroform
File Name \\OCS_CONF\SPDATA\TGPENT6.DX
Date 27 Nov 2002 15:33:02
Instrument SPECTACLE / 157
Y Axis Transmittance
Points Count 1866
Spectral Region IR
Spectrum Range 401.1660 - 3998.1602
Data Spacing 1.9287
Owner (C) by public 02/11/27
Date Stamp 02/11/27 15:32:29
Technique Infrared
X Axis Wavenumber (cm-1)
28 Nov 2002
NHBoc
N3
(1S,2R)-cp6a
Transmittance
Wavenumber (cm-1)
3442.7
2113.84
1706.88

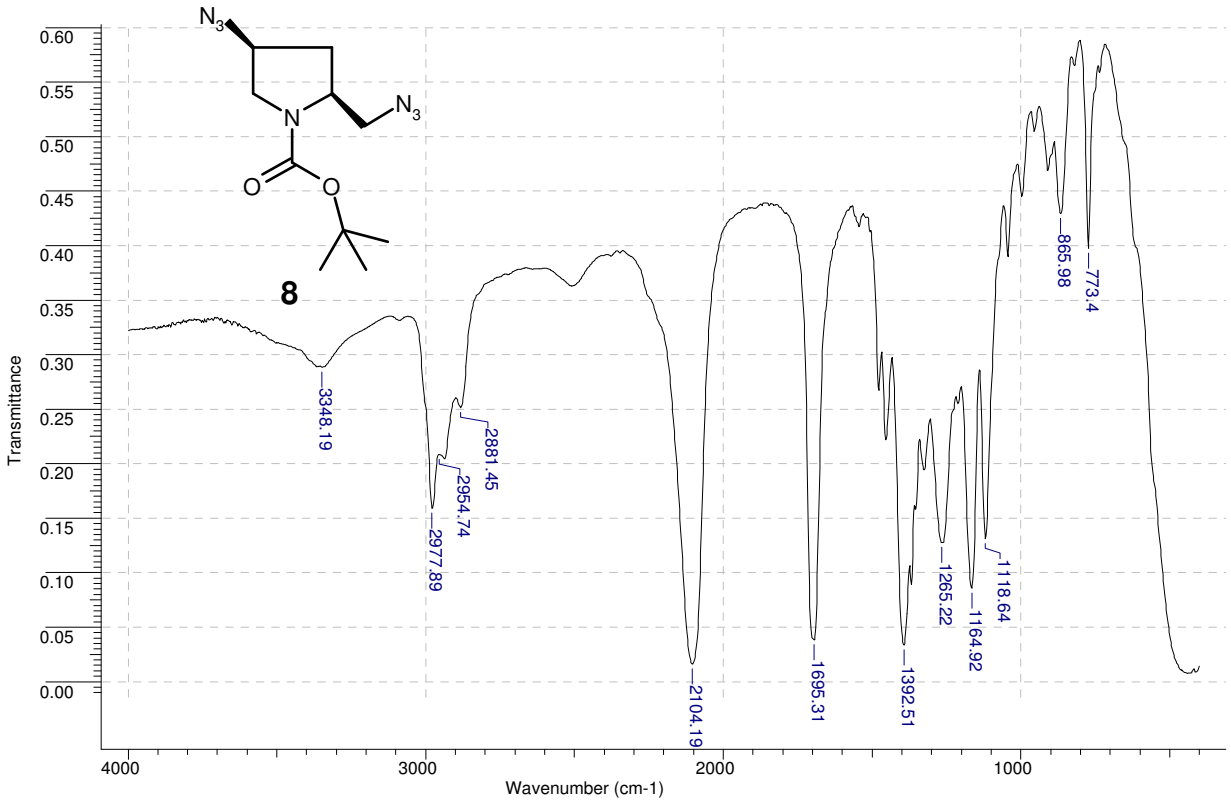
N3
N3
N
O
O
8
Transmittance
0.60
0.55
0.50
0.45
0.40
0.35
0.30
0.25
0.20
0.15
0.10
0.05
0.00
3348.19
2881.45
2954.74
2977.89
2104.19
1695.31
1392.51
1265.22
1164.92
1118.64
865.98
773.4
4000
3000
2000
1000
Wavenumber (cm-1)

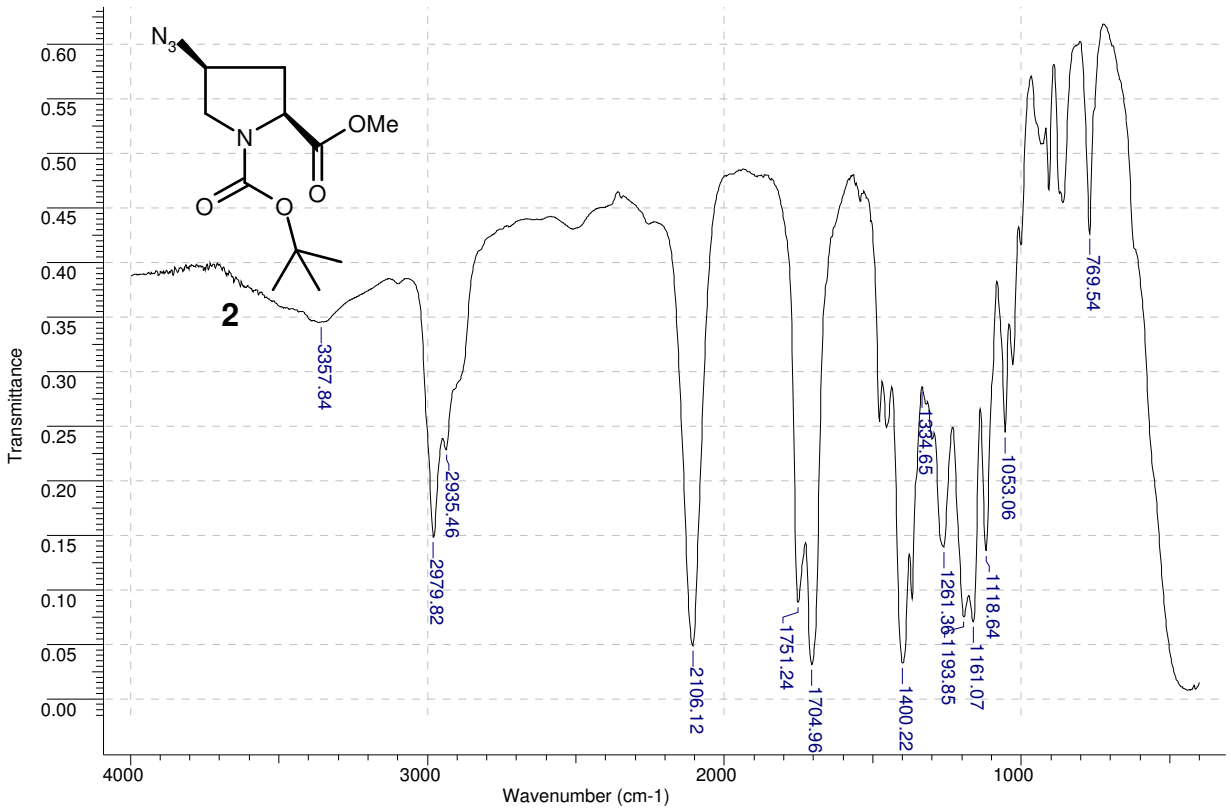
N3
OMe
N
O
O
O
2
Transmittance
0.60
0.55
0.50
0.45
0.40
0.35
0.30
0.25
0.20
0.15
0.10
0.05
0.00
3357.84
2935.46
2979.82
2106.12
1751.24
1704.96
1400.22
1334.65
1261.36
1193.85
1161.07
1118.64
1053.06
769.54
4000
3000
2000
1000
Wavenumber (cm-1)

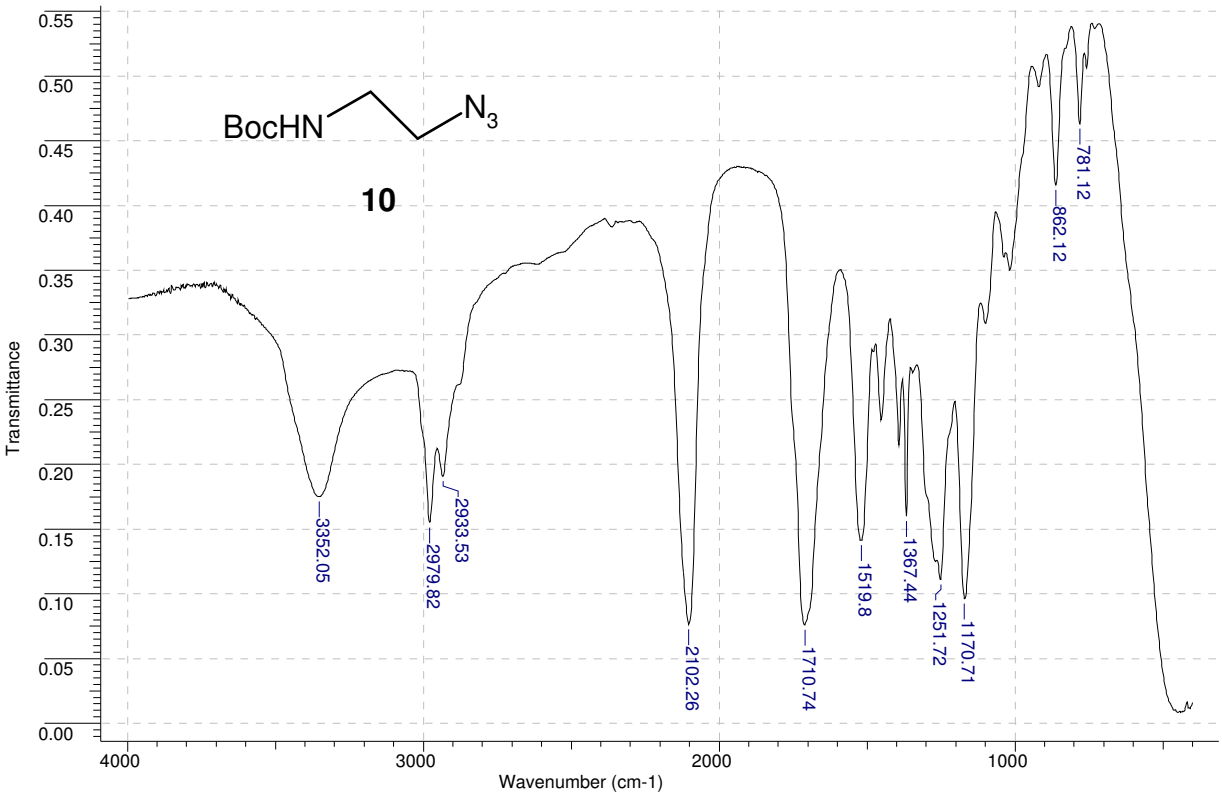
BocHN
N3
10
Transmittance
Wavenumber (cm-1)
3352.05
2979.82
2933.53
2102.26
1710.74
1519.8
1367.44
1251.72
1170.71
862.12
781.12

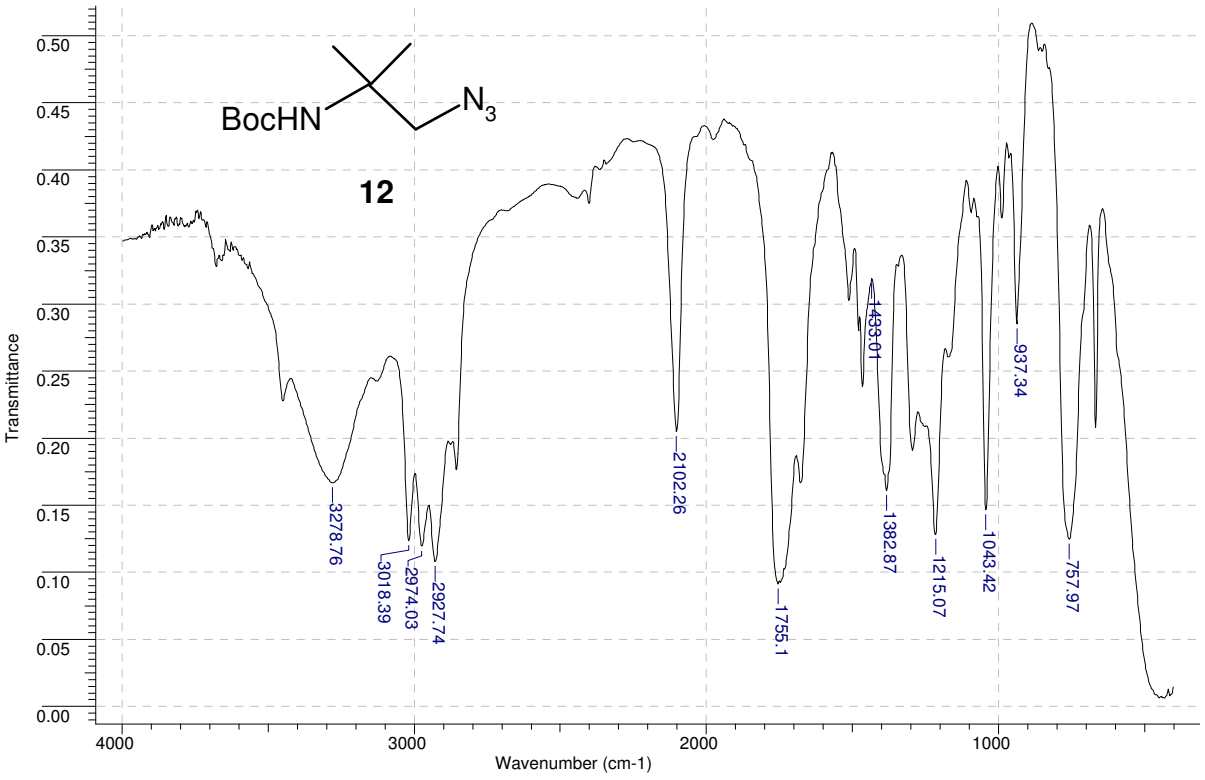
BocHN
N3
12
Transmittance
Wavenumber (cm-1)
3278.76
3018.39
2974.03
2927.74
2102.26
1755.1
1433.01
1382.87
1215.07
1043.42
937.34
757.97

References

1. Watson, J. D.; Crick, F. H. C: **Molecular structure of nucleic acid. A structure for deoxyribose nucleic acid**: *Nature*, **1953**, *171*, 737-738.

2. (a) Saenger, W. (1984). **Principles of nucleic acid structure**. Springer-Verlag, New York. (b) Lescrinier, E.; Froeyen, M.; Herdewijn, P: **Survey and summary: Difference in conformational diversity between nucleic acids with a six-membered 'sugar' unit and natural 'furanose' nucleic acids**. *Nucleic Acid. Res*. **2003**, *31*, 2975-2989.

3. (a) Hoogsteen, K: **The crystal and molecular structure of a Hydrogen-bonded complex between 1-methyl thymine and 9-methyl adenine**: *Acta. Cryst*. **1963**, *65*, 907. (b) Crick, F. H. C: **Codon-anticodon pairing. The Wobble hypothesis**: *J. Mol. Biol*. **1966**, *19*,548-555.

4. Seeman, N. C.; Rosenberg, J. M.; Rich, A: **Sequence specific recognition of double helical nucleic acids by proteins**. *Proc. Natl. Acad. Sci. USA*. 1**976**, *73*, 804-807.

5. (a) Brahms, J.; Mommaerts, W. F. H. M: **A study of conformation of nucleic acids in solution by means of circular dichroism**. *J. Mol. Biol*. **1964**, *10*, 73-85. (b) Fuller, W.; Wilkins, M. H. F.; Wilson, H. R.; Hamilton, L.; D: **The molecular configuration of deoxyribonucleic acid IV. X-ray diffraction study of the A-form**. *J. Mol. Biol*. **1965**, *12*, 60-80. (c) Dickerson, R. E: **DNA structure from A-Z.** *Methods in Enzymology*. **1992**, *211*, 67-111. (d) Saenger, W: (Ed) **Principles of Nucleic Acids structure**. Springer-Verlag, New York, **1984**.

6. Wang, A. H. J.; Quigley, G. J.; Kolpak, F. J.; Van der, M. G.; Van Boom, J. H.; Rich, A: **Left-Handed double helical DNA: Variations in the backbone conformations**. *Science* **1981**, *211*, 171-176.

7. Barawkar, D. A.; Rajeev, K. G.; Kumar, V. A.; Ganesh, K. N: **Triplex formation at physiological pH by 5-Me-dC-N^4-(spermine) [X] oligonucleotides: non protonation of N3 in X and X*G:C triad and effect of base mismatch/ionic strength on triplex stabilities**. *Nucleic Acid Res.* **1996**, *24*, 1229-1237.

8. Felsenfeld, G.; Davies, R. D.; Rich, A: **Formation of a three stranded polynucleotide molecule**. *J. Am. Chem. Soc*. **1957**, *79*, 2023-2024.

9. (a) Le Deon, T.; Perrouault, L.; Praseuth, D.; Habhoub, N.; Decout, J. L.; Thuong, N. T.; Lhomme, J.; Helene, C: **Sequence-specific recognition, photocrosslinking and cleavage of the DNA double helix by an oligo-[α]-thymidylate covalently linked to an azidoproflavine derivative**. *Nucleic Acid Res*. **1987**, *15*, 7749-7760. (b) Helene, C.; Toulene, J. J: **Oligonucleotides: Antisense Inhibitors of Gene Expression**, McMillan Press, London, **1989**.

10. (a) Moser, H. E.; Dervan, P. B: **Sequence specific cleavage of double helical DNA by triplex formation**. *Science* **1987**, *238*, 645-650. (b) Felsenfeld, G.; Rich, A: **Studies on the formation of two- and three-stranded polynucleotides**. *Biochem. Biophys. Acta* **1957**, *26*, 457-468.

11. Thuong, N. T.; Helene, C: **Sequence-specific recognition and modification of double helical DNA by oligonucleotides**. *Angew. Chem. Int. Ed*. **1993**, *32*, 666-690.

12. Beal, P. A.; Dervan, P. B**: Second structural motif for recognition of DNA by oligonucleotide-directed triple-helix formation**. *Science* 1991, 251, 1360-1363.

13. Hoogsteen, K: *Acta. Cryst*. **1959**, *12*, 822-823.

14. (a) Wells, R. D.; Harvey, S. C: in **Unusual DNA Structures**. **1988**, Springler-Verlag, New York. (b) Helene, C: *Anti-Cancer Drug Design* **1991**, *6*, 569-584. (c) Frank-Kamenetskii, M. D: **Protonated DNA structures**. *Methods in Enzymology* **1992**, *211*, 180-191. (d) Soyfer, V. N.; Potaman, V. N: **Triple Helical Nucleic Acids**, Eds **1996**, Springler-Verlag, New York.

15. Toule, J-J: in **Antisense oligonucleotides and antisense RNA: Novel Pharmacological and Therapeutic Agents**. (Weiss, B., ed), CRC press, 1997, pp. 1-16.

16. Belikova, A. M.; Zarytova, V. F.; Grineva, N. I: **Synthesis of ribonucleoside and deoxribonucleoside phosphates containing 2-chloroethylamine and nitrogen mustard residues**. *Tetrahedron Lett*. **1967**, *37*, 3557-3562.

17. Miller, P. S.; Braiterman, L. T.; Ts'o, P. O. P: **Inhibitory effect of complex formation with oligodeoxyriboncleotide ethyl-phophotriester on transfer ribonucleic acid aminoacylation**. *Biochemistry* **1977**, *13*, 4897.

18. (a) Zamecnik, P. C.; Stephenson, M. L: **Inhibition of Rous sarcoma virus replication and cell transformation by a specific oligonucleotide**. *Proc. Natl. Acad. Sci. U.S.A*. **1978**, *75*, 280-284.

19. Stephenson, M. L.; Zamecnik, P. C: **Inhibition of Rous sarcoma virus RNA translation by a specific oligonucleotides**. *Proc. Natl. Acad. Sci. U.S.A*. **1978**, *75*, 285-289.

20. (a) Akhtar, S.; Agrawal, S: **In vivo studies with antisense oligonucleotide**. *Trends in Pharmacol Sci.* **1997**, *18*, 12-18. (b) Bennet, C. F: **Antisense oligonucleotides: is the glass half full or half empty?**. *Biochem Pharmacol*. **1998**, *55*, 9-19. (c) Wickstrom, E: **Clinical Trials of Genetic Therapy with Antisense DNA and DNA vectors**. Eds. Marcel Dekker; New York, **1998**.

21. Lima, W. F: **Implication of RNA structure on antisense oligonucleotide hybridization kinetics**: *Biochemistry* **1992**, *31*, 12055.

22. Wyatt, J. R: **Combinatorially selected guanosine quartet structure is a potent inhibitor of human immunodeficiency virus, envelope mediated cell fusion**: *Proc. Natl. Acad. Sci. U.S.A*. **1994**, *91*, 1356-1360.

23. Ho, S. P: **Potent antisense oligonucleotides to human multi-drug resistance-1 mRNA are rationally selected by mapping RNA accessible sites with oligonucleotide libraries**: *Nucleic Acid Res*. **1996**, *24*, 1901-1907.

24. Miller, K. J.; Das, S. K: **Antisense oligonucleotides: Strategy for delivery**. *Pharmaceutical Science and Technology today* **1998**, *1*, 377-386.

25. (a) Liebhaber, S. A.; Cash, F. E.; Shakin, S. H: **Translationally associated helix-destabilizing activity in rabbit reticulocyte lyasate**. *J. Biol. Chem*. **1984**, *259*, 15597-15602. (b)

Shakin, S. H.; Liebhber, S. A: **Destabilization of messenger RNA/ complementary DNA duplexes by the elongating 80 S ribosome**. *J. Biol. Chem*. **1986**, *261*,16018-16025. (c) Crounch, R. J.; Dirksen, M.-L. **Ribonucleases H, in Nucleases**: Linn, S. M. and Roberts, R. J. eds, cold spring Harbor Laboratory press, Cold Spring Harbor, NY, **1985**, pp 211-241.

26. Mahon, E. X. et al. **Inhibition of chronic myelogenous leukemia cells harboring a BDR-ABL $B3A_2$ junction by antisense oligonucleotides targeted at the $B2A_2$ junction**. *Exp. Hematol*. **1995**, *23*, 1606-1611.

27. Dominski, Z.; Kole, : **Restoration of correct splicing in thalascemic pre-*m*-RNA by antisense oligonucleotides**. *Proc. Natl. Acad. Sci. U.S.A*. **1993**, *90*, 8673-8676.

28. Mcmanaway, M. E. et al. **Tumor-specific inhibition of lymphomia growth by an antisense oligodeoxynucleotides**. *Lancet* **1990**, *335*, 808-811.

29. (a) Agrawal et al, *Proc. Natl. Acad. Sci. U.S.A*. **1988**, *85*, 7079-7083. (b) Zheng, H. et al, *Proc. Natl. Acad. Sci. U.S.A*. **1989**, *86*, 1989-1993. (c) Crooke, S. T; *Adv. Pharmacol*. **1997**, *40*, 2-49.

30. Ecker, D. J. et al: **Pseudo-half-knot formation with RNA**. *Science* **1992**, *257*, 958-961.

31. Vickers, T. et. al: **Inhibition of HIV-LTR gene expression by oligonucleotide targeted to the TAR element**. *Nucleic Acid Res*. **1991**, *19*, 3359-3368.

32. (a) Chiang, M. Y. et al: **Antisense oligonucleotides inhibit intercellular adhesion molecule 1 expression by two distinct mechanisms**. *J. Biol. Chem*. **1991**, *266*, 18162-18171. (b) Baker, B. F.; Miraglia, L.; Hagedorn, C. H: **Modulation of eukyariotic initiation factor-4E binding to 5'-capped oligonucleotides by modified antisense oligonucleotides**. *J. Biol. Chem*. **1992**, *267*, 11495-11499.

33. Bishop, J. S. et al: **Intramolecular G-quartet motifs confer nuclease resistance to a potent anti-HIV oligonucleotide**. *J. Biol. Chem*. **1996**, *271*, 5698-5703.

34. Ornstein, R. L.; Macelroy, R. D: **Nucleic acid constituent interactions**. *Proc. Indian. Acad. Sci. Sect. B*, **1978**, *87b*, 135-145.

35. Tong, B. Y.; Leung, M. L. C: **Correlation between percentage guanine-cytosine content and melting temperature of deoxyribonucleic acid**. *Biopolymers* **1977**, *16*, 1223-1231.

36. Cantor, C. R.; Schimmel, P. R. (Eds) Biophysical Chemistry part III, **1971**, W. H. Freeman and Company, New Yok.

37. (a) Rodger, A.; Norden, B. in **Circular dichroism and Linear Dichroism 1997**, Oxferd university press. (b) Gray, D. M.; Ratliff, R. L. Vaughan, M. R: **Circular Dichroism spectroscopy of DNA** . *Methods in Enzymology* **1992**, *211*, 389-406. (c) Gray, D. M.; Hung, S.-H.; Johnson, K. H: **Absorption and circular dichroism spectroscopy of nucleic acid duplexes and triplexes.** in *Methods in Enzymology* **1995**, *246*, 19-34.

38. (a) Callis, P. R: **Electronic states and luminescence of nucleic acid systems**. *Ann. Rev. Phys. Chem*. **1983**, *34*, 329-357. (b) Ho, P. s.; Zhou, G.; Clark, L. B: **Polarized electronic spectra of Z-DNA single crystals**. *Biopolymers* **1990**, *30*, 151-163.

39. (a) Stryer, L. Biochemistry, 3rd ed.; New York: W. H. freeman and Company, 1988. (b) Egli, M.; williums, L. D.; Gao, Q.; Rich, A. *Biochemistry* **1991**, *30*, 11388. (c) Calladine, C. R.; Drew, H. R. **Understanding DNA, The molecule and how it works**; Cambridge: Academic Press LTd., **1992**. (d) Beveridge, D. L,; Jorgensen, W. L. Ann. NY Acad. Sci. 1986, 482. (e) Gassner, R. V.; Frederick, C. A.; Quigley, G. J.; Rich, A.; Wang, A. H.-J. J. **The molecular structure of the left handed Z-DNA double helix at 1.0 A atomic resolution. Geometry, conformation, and ionic interactions of d(CGCGCG)**. *Biol. Chem*. **1989**, *264*, 7921.

40. Williums, A. L. Jr.; Cheong, C.; Tinoco, I. Jr.; Clark, L. B: **Vacuum ultraviolet circular dichroism as indicator of helical handedness in nucleic acids**. *Nucleic Acid Res*. **1986**, *14*, 6649.

41. Anderson, P.; Bauer, W: **Supercoiling in closed circular DNA: dependence upon ion type and concentration**. *Biochemistry* **1978**, *17*, 594-601.

42. Sprecher, C. A.; Baase, W. A.; Johnson, W. C. Jr: **Conformation and circular dichroism of DNA**. *Biopolymers* **1979**, *8*, 1009-1019.

43. Ulhmann, E.; Peyman, A: **Antisense oligonucleotides: A new therapeutic principle**. *Chem. Rev*. **1990**, *90*, 543-584.

44. (a) Crooke, S. T.; Lebleu, B: **Antisense Research and Applications**. Boca Raton, FL: CRC Press, Inc. **1993**. (b) Crooke, S. T: **Progress in antisense therapeutics**. *Med. Res. Rev*. **1996**, *16*, 319-344. (c) Crooke, S. T.; Bennet, C. F: **Progress in antisense oligonucleotide therapeutics**. *Annu. Rev. Pharmacol. Toxicol*. **1996**, *36*, 107-129.

45. Milligan, J. F.; Matteucci, M. D.; Martin, J. C: **Current concepts in antisense drug design**. *J. Med. Chem*. **1993**, *36*, 1923-1937.

46. Pierga, J. –Y.; Magdelenat, H: **Applications of antisense oligonucleotides in oncology**. *Cell. Mol. Biol.* **1994**, *40*, 237-261.

47. Stein, C. A.; Cohen, J. S: **Phoshorothioate oligodeoxynucleotide analogues**. In Cohen, J. S. (ed.): Oligodeoxynucleotides-Antisense Inhibitors of Gene Expression. London: Macmillan Press, **1989**, p. 97.

48. Millar, P. S: Non-ionic antisense oligonucleotides. In Cohen, J. S. (ed.): **Oligodeoxynucleotides-Antisense Ihibitors of Gene Expression**. London: Macmillan Press, **1989**, p. 79.

49. Froehler, B.; Ng, P.; Matteucci, M: **Phosphoramidate analogs of DNA: Synthesis and thermal stabilities of heteroduplexes**. *Nucleic Acid Res*. **1988**, *16*, 4831-4839.

50. (a) Stec, W. J.; Zon, G.; Egan, W.; Stec, B: **Automated solid-phase synthesis, separation, and stereochemistry of phosphrothioate analogues of oligodeoxyribonucleotides**. *J. Am. Chem. Soc.* **1984**, *106*, 6077-6080. (b) Wagner, R. W: **The state of the art in antisense research**. *Nat. Med*. **1995**, *1*, 1116-1118. (c) Burgers, P. M. J.; Eckstein, F: **Synthesis of dinucleoside**

monophosphorotioates via addition of sulfur to phosphite trimesters. *Tetrahedron Lett*. **1978**, 3835-3838.

51. (a) Stec, W. J.; Zon, G: **Synthesis, separation, and stereochemistry of diastereomeric oligodeoxyribonucleotides having a 5'-terminal internucleotide phosphorothioates linkage**. *Tetrahedron Lett*. **1984**, *25*, 5275. (b) Stec, W. J.; Zon, G: **Stereochemical studies of the formation of chiral internucleotide linkages by phosphoramidite coupling in the synthesis of oligodeoxyribonucleotides**. *Tetrahedron Lett*. **1984**, *25*, 5279-5282.

52. Stein, C. A: **Does antisense exist?**. *Nat. Med*. **1995**, *1*, 1119-1121.

53. Summerton, J.; Stein, D.; Huang, S. B.; Matthews, P.; Weller, S.; Partridge, M: **Morpholino and phosphorothioates antisense oligomers compared in cell-free and in-cell systems**. *Antisense Nucleic Acid Drug Dev*. **1997**, *7*, 63-70.

54. (a) Checko, K. K.; Linder, K.; Saenger, W.; Miller, P. S: **Molecular structure of deoxyadenylyl-3'-methylphosphonate-5'-thymidine dihydrate, (d-ApT.2H_2O), a dinucleoside monophoshate with neutral phosphodiester backbone. An X-ray crystal study.** *Nucleic Acid Res.* **1983**, *11*, 2801-2814.

55. Miller, P. S.; Yano, J.; Yano, E.; Carroll, C.; Jayaraman, K.; Ts'o. P. O. P: **Nonionic nucleic acid analogues: Synthesis and characterization of dideoxyribonucleoside methylphosphonates**. *Biochemistry* **1979**, *18*, 5134-5142.

56. Kean, J. M.; Kipp, S. A.; Miller, P. S.; Kulka, M.; Aurelian, L: **Inhibition of herpes simplex virus replication by antisense oligo-2'-O-methylribonucleoside methylphosphonates**. *Biochemistry* **1995**, *34*, 14617-14620.

57. Letsinger, R. L.; Singman, C. N.; Histand, G.; Salunke, M: **Cationic oligonucleotides**. *J. Am. Chem. Soc*. **1988**, *110*, 4470-4471.

58. Jung, P. M.; Histand, G.; Letsinger, R. L: **Hybridization of alternating cationic/anionic oligodeoxyribonucleotides to RNA segments**. *Nucleosides Nucleotides* **1994**, *13*, 1597-1605.

59. Summers, M. F.; Powell, C.; Egan, W.; Byrd, R. A.; Wilson, W. D.; Zon, G: **Alkyl phospotriester modified oligodeoxyribonucleotides**. VI. **NMR and UV spectroscopic studies of ethyl phosphotriester (Et) modified Rp-Rp and Sp-Sp duplexes, (d(GGAA(Et)TTCC))2**. *Nucleic Acid Res*. **1986**, *14*, 7421-7437.

60. (a) Sood, S.; Shaw, B. R.; Spielvogel, B. F: **Boron-containing nucleic Acids. Synthesis of oligonucleoside boranophosphates**. *J. Am. Chem. Soc*. **1990**, *112*, 9000. (b) Shaw, B. R.; Madison, J.; sood, S.; Spielvogel, B. F; **Oligonucleotide boranophosphate (borane phosphate)**. In Agrawal, S. (ed): *Methods in Molecular biology*, vol *20*: Protocols for Oligonucleotides and Analogs. Synthesis and properties. Totowa, NJ. Humana Press, Inc., **1993**, pp. 225-243. (c) Sergueev, D. S.; Shaw, B. R: **H-phophonate approach for solid pase synthesis of oligodeoxyribinucleotide boranophosphates and their characterization**. *J. Am. Chem. Soc*. **1998**, *120*, 9417-9427.

61. Li, H.; Huang, F.; Shaw, B. R: **Conformational studies of dithymidine boranomonophosphate diastereoisomers**. *Bioorg. Med. Chem*. **1997**, *5*, 787-795.

62. (a) Higson, A. P.; Sierzchala, A.; Brummel, H.; Zhao, Z.; Caruthers, M. H: **Synthesis of an oligothymidylates containing boranophosphate linkages**. *Tetrahedron Lett*. **1998**, *39*, 3899-3902. (b) Rait, V. K.; Shaw, B. R: **Boranophosphates support the RNase H Cleavage of polyribonucleotides**. *Antisense Nucleic Acid Drug Dev*. **1999**, *9*, 53-60.

63. (a) Chin, D. J.; Green, G. A.; Zon, G.; szoka, Jr., F. C.; Straubinger, R. M: **Rapid nuclear accumulation of injected oligodeoxyribonucleotides**. *New Biologist* **1990**, *2*, 1091. (b) Leonetti, J. P.; Mechti, N.; Degols, G.; Gagnor, C.; Lebleu, B: **Intracellular distribution of microinjected antisense oligonucleotides**. *Proc. Natl. acad. Sci. USA*. **1991**, *88*, 2702.

64. Halford, M. H.; Jones, M. S: **Synthetic analogues of polynucleotides**. *Nature* **1968**, *217*, 638.

65. (a) Varma, R. S: **Synthesis of oligonucleotide analogues with modified backbones**. *Syn. Lett*. **1993**, *9*, 621. (b) Sanghvi, Y. S.; Cook, P. D: in **Carbohydrate Modifications in Antisense Research**. Washington, DC: American Chemical Society,**1994**, 1.

66. (a) Roughton, A. L.; Portmann, S.; Benner, S. A.; Egli, M: **Crystal structure of a dimethylene sulfone-linked ribonucleoside analog.** *J. Am. Chem. Soc*. **1995**, *117*, 7249. (b) McElroy, E. B.; Bandarn, R.; Huand, J.; Widlanski, T. S: **Synthesis and physical properties of sulfonamide-containing oligonucleotides**. *Bioorg. Med. Chem. Lett*. **1994**, *4*, 1071. (c) Huie, E. M.; Kirshenbaum, M.R.; Trainos, G. L: **Oligonucleotides with a nuclease resistant sulfur-based linkage**. *J. Org. Chem*. **1992**, *57*, 4569.

67. Veal, J. M.; Gao, X.; Brown, F. K: **A comparison of DNA-oligomer duplexes containing formacetal and phosphodiester linkers using molecular dynamics and quantum mechanics**. *J. Am .Chem. Soc*. **1993**, *115*, 7139.

68. Jones, R. J.; Lin, K. –Y.; Milligan, J. F.; Wadwani, S.; Matteucci, M. D: **Synthesis and binding properties of pyrimidines oligodeoxynucleoside analogs containing neutral phosphodiester replacements: The formacetal and 3'-thioformacetal internucleoside linkages**. *J. Org. Chem*. **1993**, *58*, 2983.

69. Vasseur, J. J.; Debart, F.; Sanghvi, Y. S.; Cook, P. D: **Oligonucleosides: Synthesis of a novel methylhydroxylamine-linked nucleoside dimer and its incarporation into antisense sequences**. *J. Am. Chem. Soc*. **1992**. *114*, 4006.

70. De Mesmaeker, A.; Lebreton, J.; Waldner, A.; Fritsch, V.; Wolf, R. M: **Replacement of the phosphodiester linkage in oligonucleotides: comparison of two structural amide isomers**. *Bioorg. Med. Chem. Lett*. **1994**, *4*, 873-878.

71. De Mesmaeker, A.; Lesueur, C.; Bevierre, M. -O.; Waldner, A.; Fritsch, V.; Wolf, R. M: **Increased affinity of modified oligonucleotides with conformationally constrained furanose rings to complemetary RNA strands**. *Angew. Chem*. **1996**, *108*, 2960.

72. (a) Stirchak, E. P.; Summerton, J. e.; weller, D. D: **Uncharged stereoregular nucleic acids analogs. Synthesis of a cytosine-containing oligomer with carbamateinternucleoside linkages**. *J. Org. Chem*. **1987**, *52*, 4202. (b) Coull, J. M.; Carlson, D. G.; Weith, H. L: **Synthesis and characterization of a carbamate linked oligonucleotide**. *Tetrahedron Lett*. **1987**, *28*, 745.

73. Wendeborn, s.; Jounno, C.; Wolf, R. M.; **De Mesmaeker, A: Replacement of the phosphodiester linkage in oligonucleotides by an acetylenic bond: Comparison between carbon-, sulfur, and oxygen containing analogs**. *Tetrahedron Lett*. **1996**, *37*, 5511.

74. (a) De Mesmaeker, a.; Waldner, A.; Lebreton, J.; Hoffmann, P.; Fritsch, V.; Wolf, R. M.; Freier, S. M: **Amides as a new type of backbone modification in oligonucleotides**. *Angew. Chem. Int. Ed.* **1994**, *33*, 226-229. (b) Idziak, I.; Just, G.; Damha, M. J.; Giannaris, P. A: **Synthesis and hybridization properties of amide-linked thymidine dimers incorporated into oligodeoxynucleotides.** *Tetrahedron Lett*. **1993**, *34*, 5417-5420.

75. Debart, F.; Vasseur, J.-J.; Sanghvi, Y.S.; Cook, P. D: **Synthesis and incarporation of a methyleneoxy(methylimino)-linked thymidine dimer into antisense oligonucleosides**. *Bioorg. Med. Che. Lett.* **1992**, *2*, 1479-1482.

76. (a) Browne, K. A.; Dempcy, R. O.; Bruice, T. C: **Binding studies of cationic thymidyl-deoxyribinucleic guanidine to RNA homopolynucleotides**. *Proc. Natl. Acad. Sci. U.S.A*. **1995**, *92*, 7051-7055. (b) Dempcy, R. O.; Browne, K. A.; Bruice, T. C: **Synthesis of the polycation thymidyl DNG, its fidelity in binding polyanionic DNA/RNA, and the stability and nature of the hybrid complexes**. *J. Am. Chem. Soc*.**1995**, *117*, 6140-6141.

77. (a) Inoue *et al* : **Synthesis and hybridization studies on twocomplemetary nona(2'-O-mehtyl)ribonucleotides**. *Nucleic Acid Res*. **1987**, *15*, 6131-6148. (b) Iribarren, A. M. et al: **2'-O-alkyl oligonucleotides as antisense probes**. *Proc. Natl. Acad. Sci. U.S.A*. **1990**, *87*, 7747-7751. (c) Lesnik, E. A. *et al*: **Oligonucleotides containing 2'-O-modified adenosine: Synthesis and effects on stability of DNA:RNA duplexes**. *Biochemistry* **1993**, *32*, 7832-7838.

78. Moulds, C. *et al*: **Site and mechanism of antisense inhibition by C-5 propyne oligonucleotides**. *Biochemistry*, **1995**, *34*, 5044-5053.

79. Monia, B. P. *et al*: **Evaluation of 2'-modified oligonucleotides containing 2'-deoxy gaps as antisense inhibitors of gene expression**. *J. Biol. Chem*. **1993**, *268*, 14514-14522.

80. Kawasaki, A. M. *et al*: **Uniformly modified 2'-doxy 2'-fluorophosphorothioate oligonucleotides as nuclease resistant antisense compounds with high affinity and specificity for RNA targets**. *J. Med. Chem*, **1993**, *36*, 831-841.

81. Pitsch, S.; Wendeborn, S.; Eschenmoser, A. *Helv. Chim. Acta*. **1993**, *76*, 2161-2183.

82. Schoning, K.; Scholz, P.; Guntha, S.; Wu, X.; Krishnamurthy, R.; Eschenmoser, A: **Chemical etiology of nucleic acid structure: The α-threofuranosyl-(3'-2') oligonucleotide system**. *Science*, **2000**, *290*, 1347-1351.

83. (a) Lescrinier, E.; Froeyen, M.; Herdewijn, P. **Differences in conformational diversity between nucleic acids with a six –membered 'sugar' unit and natural 'furanose' nucleic acids**. *Nucleic Acids Res.* **2003**, *31*, 2975-2989. (b) Hendrix, C.; Rosemeyer, H.; Verheggen, I.; Seela, F.; Arschot, A. V.; Herdewijn, P: **1',5'-Anhydrohexitol oligonucleotides: Synthesis, base pairing and recognition by regular oligodeoxyribonucleotides and oligoribonucleotides**. *Chem. Eur. J*. **1997**, *3*, 110-120.

84. Obika, S.; Nanbu, D.; Hari, Y.; Andoh, J. –I.; Mori, K. –I.; Doi, T.; Imanshi, T: **Stability and structural features of the duplexes containing nucleoside analogues with fixed type conformation, 2'-O, 4'-C-methyleneribonucleosides**. *Tetrahedron Lett*. **1998**, *39*, 5401-5404.

85. (a) Petersen, M.; Wengel, J. **LNA: A versatile tool for therapeutic and genomics**. *Trends Biotechnol*. **2003**, *21,* 74-81 (b) Koshkin, A.; Singh, S. K.; Nielsen, P.; Rajwanshi, V. K.; Kumar, R.; Meldgaard, M.; Olsen, C. E.; Wengel, J: **LNA (locked nucleic acid): synthesis of the adenine, cytosine, guanine, 5-methylcytosine, thymine and uracil bicyclonucleotide monomers, oligomerization and unprecedented nucleic acid recognition** . *Tetrahedron* **1998**, *54*, 3607-3630. (c) Singh, S. K.; Nielsen, P.; Koshkin, A. A.; Wengel, J: **LNA (locked nucleic acid): Synthesis and high affinity nucleic acid recognition**. *Chem. Commun*. **1998**, 455-456.

86. Wang, J.; Verbeure, B.; Luyten, I.; Lescrinier, E.; Froeyen, M.; Hendrix, C.; Rosemeyer, H.; Seela, F.; Arschot, A. V.; Herdewijn, P: Cyclohexene nucleic acids (CeNA): **Serum stable**

oligonucleotides that activate RNase H and increase duplex stability with complementary RNA. *J. Am. Chem. Soc*. **2000**, *122*, 8595-8602.

87. Mourinsh, Y.; Rosemeyer, H.; Esnouf, R.; Mevedovici, A.; Wang, J.; Ceulemans, G.; Lescrinier, E.; Hendrix, c.; Busson, R.; Sandra, P.; seela, F.; Aerschot, A. V.; Herdewijn, P: **Synthesis and purity properties of oligonucleotides containing 3-hydroxy-4-hydroxymethyl-1-cyclohexanyl nucleosides**. *Chem. Eur. J*. **1999**, *5*, 2139-2150.

88. Moser, H. E. (1993): **Strategies and chemical approaches towards oligonucleotide therapeutics**. In Testa B., Kyburz, E., Further, W.; Giger, R. (eds): *Perspectives Med. Chem*. **1993**, Basel: Verlag Helvitica Acta, pp. 275-297.

89. Altmann, K. –H.; Bevierre, M. –O.; De Mesmaeker, A.; Moser, H. E: **The evaluation of 2'- and 6'-substituted carbocyclic nucleosides as building blocks for antisense oligonucleotides**. *Bioorg. Med. Chem. Lett*. **1995**, *5*, 431-436.

90. Altmann, K.-H.; Kesselring, R.; Francotte, E.; Rihs, G: **4', 6'-Methano carbocyclic thymidine: A conformationally constrained building block for oligonucleotides**. *Tetrahedron Lett*, **1994**, *35*, 2331-2334.

91. Altmann, K.-H.; Martin, P.; Dean, N. M.; Monia, B. P: **Second generation antisense oligonucleotides-Inhibition of PKC-α and C-RAF kinase expression by chimeric oligonucleotides**. *Nucleosides Nucleotides* **1997**, 917-926.

92. Summerton, J.; Weller, D: **Morpholino antisense oligomers: Design, preparation, and properties**. *Antisense Nucleic Acid Drug Dev*. **1997**, *7*, 187-195.

93. Toyler, M. F. *et al*: **Effect of TNF-α antisense oligomers on cytokine production by primary murine alveolar macrophages**. *Antisense Nucleic Acid Drug Dev*. **1998**, *8*, 199-205.

94. Nielsen, P. E.; Egholm, M.; Berg, R. H.; Buchardt, O: **Sequence-selective recognition of DNA by strand displacement with a thymine-substituted polyamide**. *Science* **1991**, *254*, 1497-1501.

95. Egholm, M.; Buchardt, O.; Christensen, L.; Behrens, C.; Freier, S. M.; Driver, D. A.; Berg, R. H.; Kim, S. K.; Nordon, B.; Nielsen, P. E; **PNA hybridizes to complementary oligonucleotides obeying the Watson-Crick hydrogen-bonding rules**. *Nature*, **1993**, *365*, 566-568.

96. Jensen, K. K.; Qrum, H.; Nielsen, P. E.; Norden, B: **Hybridization kinetics of peptide nucleic acids (PNA) with DNA and RNA studied with BIAcore Technique**. *Biochemistry* **1997**, *36*, 5072-5077.

97. Demidov, V. V.; Potaman, V. N.; Frank-Kamenetskii, M. D.; Egholm, M.; Buchardt, O.; Sonnichsen, S. H.; Nielsen, P. E: **Stability of peptide nucleic acids in human serum and cellular extracts**. *Biochem. Pharmacol*. **1994**, *48*, 1310.

98. (a) Good, L.; Nielsen, P. E: **Progress in developing PNA as gene targeted drugs**. *Antisense Nucleic Acid Drug Dev*. **1997**, *7*, 431. (b) De Mesmaeker, A. et al: *Curr. Open. Struct. Biol*. **1995**, *5*, 343. (c) Uhlmann, E.; Peyman, A.; Breipohl, G.; Will, D. W: PNA: **Synthetic polyamide Nucleic Acids with Unusual Binding Properties**. *Angew. Chem. Int. Ed*. **1998**, *37*, 2796-2823.

99. Tomac, S.; Sarkar, M.; Ratilainen, T.; Wittung, P.; Nielsen, P. E.; Norden, B.; Graeslund, A: **Ionic effects on the stability and conformation of peptide nucleic acid (PNA) complexes**. *J. Am. Chem. Soc*. **1996**, *118*, 5544-5552.

100. Egholm, M.; Nielsen, P. E.; Buchardt, O.; Berg, R. H: **Peptide nucleic acids (PNA). Oligonucleotide analogues with an achiral peptide backbone**. *J. Am. Chem. Soc*. **1992**, *114*, 9677-9678.

101. Nielsen, P. E.; Christensen, L: **Strand displacement binding of a duplex forming Homopurine PNA to a homopyrimidine duplex DNA target**. *J. Am. Chem. Soc*. **1996**, *118*, 2287-2288.

102. (a) Bonham, M. A. *et al*, *Nucleic Acid Res*. **1995**, *23*, 1197-1203. (b) Knudsen, H.; Nielsen, P. E: **Antisense properties of duplex and triplex forming PNA**. *Nucleic Acid Res*. **1996**, *24*, 494-500.

103. Nielsen, P. E.; Egholm, M.; Berg, R. H.; Buchardt, O: **Peptide nucleic acids (PNA). DNA analogues with a polyamide backbone. In Antisense Research and Application**. Crook, S. and Lebleu, B. (eds). CRC Press, Boca Raton, **1993**, pp. 363-373.

104. (a) Praseuth, D. et al: **Peptide Nucleic Acids directed to the promoter of the α-chain of the interleukin-2-receptor**. *Biochim. Biophys. Acta*. **1997**, *1309*, 226-238. (b) Wittung, P.; Nielsen, P. E.; Norden, B: **Extended DNA-recognition repertoire of PNA**. *Biochemistry* **1997**, *36*, 7973-7979.

105. Lohse, J.; Dahl, O.; Nielsen, P. E: **Double duplex invation by peptide nucleic acid: A general principle for recognition of double stranded DNA**. *Proc. Natl. Acad. Sci. U.S.A*. **1999**, *96*, 11804. **106**. (a) Leijo, M. *et al*: **Structural characterization of PNA-DNA duplexes by NMR. Evidence for DNA in a B-like conformation**. *Biochemistry* **1994**, *22*, 9820-9825. (b) Eriksson, M.; Nielses, P. E: **Solution structure of a peptide nucleic acid-DNA duplex**. *Nat. Struct. Biol*. **1996**, *3*, 410-413.

107. Brown, S. C.; Thomson, S. A.; Veal, J. M.; Davis, D. G: **NMR Solution structure of a peptide nucleic acid complexed with RNA**. *Science* **1994**, *265*, 777-780.

108. Bets, L.; Josey, J. A.; Veal, J. M.; Jordan, S. R: **A nucleic acid triple helix formed by a peptide nucleic acid-DNA complex**. *Science* **1995**, *270*, 1838-1841.

109. Kim, S. K.; Nielsen, P.E.; Egholm, M.; Buchardt, O.; Berg, R. H.; Norden, B: **Right handed triple helix formed between peptide nucleic acid PNA-T_8 and poly dA shown by linear and circular dichroism spectroscopy**. *J. Am. Chem. Soc*. **1993**, *115*, 6477-6481.

110. Rasmussen, H.; Kastrup, J. S.; Nielsen, J. N.; Nielsen, J. M.; Nielsen, P. E: **Crystal structure of peptide nucleic acid (PNA) duplex at 1.7 A resolution**. *Nat. Struct. Biol*. **1997**, *4*, 98-101.

111. Hanvey, J. C. *et al*: **Antisense and antigene properties of peptide nucleic acids**. *Science*, **1992**, *258*, 1481.

112. (a) Gambacorti-Passerini, C. *et al*. *Blood* **1996**, *88*, 1411. (b) Mologni, L. *et al*: **Additive antisense effects of different PNAs on the in vitro translation of the PML/RARα gene**. *Nucleic Acid Res*. **1998**, *26*, 1934.

113. Nielsen, P. E.; Egholm, M.; Buchardt, O: **Evidence for PNA_2-DNA triplex structure upon binding to dsDNA by strand displacement**. *J Mol. Recogn*. **1994**, *7*, 165-170.

114. Egholm, M. *et al*: **Efficient pH independent sequence specific DNA binding by pseudoisocytosine-containing bis-PNA**. *Nucleic Acid Res*. **1995**, *23*, 217-222.

115. Nielsen, P. E.; Egholm, M.; Buchardt, O: **Sequence specific translation arrest by PNA bound to the template strand**. *Gene* **1994**, *149*, 139-145.

116. Tayler, R. W. *et al*: **Selective inhibition of mutant human mitochondrial DNA replication in vitro by peptide nucleic acids**. *Nature Genet*. **1997**, *15*, 212-215.

117. Vickers, T. A. *et al*. **Inhibition of NF-kB specific transcriptional activation by PNA strand invasion**. *Nucleic Acid Res*. **1995**, *23*, 3003-3008.

118. (a) Peffer, N. J. *et al*: **Strand-Invasion of duplex DNA by peptide nucleic acid oligomers**. *Proc. Natl. Acad. Sci. U.S.A*. **1993**, *90*, 10648-10652. (b) Griffith, M. C. et al.: **Single and bis-peptide nucleic acids as triplexing agents: binding and stoichiometry**. *J. Am. Chem. Soc*. **1995**, *117*, 831.

119. Dueholm, K. L.; Nielsen, P. E: **Chemistry, properties and applications of PNA (peptide nucleic acid)**. *New. J. Chem*. **1997**, *21*, 19-31.

120. Hyrup, B.; Egholm, M.; Rolland, M.; Nielsen, P. E.; Berg, R. H.; Buchardt, O: **Modification of the binding affinity of peptide nucleic acid (PNA). PNA with extended backbones consisting of 2-aminoethyl-β-6-γ-alanine or 3-aminopropylglycine units**. *J. Chem. Soc. Chem. Commun*. **1993**, 518-519.

121. Hyrup, B.; Egholm, M.; Nielsen, P. E.; Wittung, P.; Nordon, B.; Buchardt, O: **Structure-activity studies of the binding of modified peptide nucleic acids (PNA) to DNA**. *J. Am. Chem. Soc*. **1994**, *116*, 7964.

122. Hyrup, B.; Egholm, M.; Buchardt, O.; Nielsen, P. E: **A flexible and positively charged PNA analogue with an ethylene-linker to the nucleobase: Synthesis and hybridization properties**. *Bioorg. Med. Chem. Lett*. **1996**, *6*, 1083-1088.

123. Dueholm, K.; Peterson, K. H.; Jensen, D. K.; Egholm, M.; Nielsen, P. E.; Buchardt, O: **Peptide nucleic acid (PNA) with chiral backbone based on alanine**. *Bioorg. Med. Chem. Lett*. **1994**, *4*, 1077-1080.

124. Haaima, G.; Lohse, A.; Buchardt,O.; Nielsen, P. E: **Peptide nucleic acids (PNA) containing thymine monomers derived from chiral amino acids: Hybridization and solubility properties of D-lysine PNA**. *Angew. Chem. Int. Ed*. **1996**, *35*, 1939.

125. Puschl, A.; Sforza, S.; Haaima, G.; Dahl, O.; Nielsen, P. E: **Peptide nucleic acids (PNAs) with functional backbone**. *Tetrahedron Lett*. **1998**, *39*, 4707-4710.

126. Lagriffoule, P.; Buchardt, O.; Wittung, P.; Nordan, B.; Jensen, K. K.; Nielsen, P. E: **Peptide nucleic acids (PNAs) with conformationally constrained, chiral cyclohexyl derived backbone**. *Chem. Eur. J*. **1997**, *3*, 912-919.

127. Maison, W.; Schlemminger, I.; Westerhoff, O.; Martens, J. *Bioorg. Med. Chem. Lett*. **1999**, *9*, 581.

128. Kortz, A. H.; Larsen, S.; Buchardt, O.; Nielsen, P. E: **Retro-Inverse PNA: Structural implications for DNA binding**. *Bioorg. Med. Chem. Lett*. **1998**, *6*, 1983.

129. Almorsson, O.; Bruice, T. C: **Peptide nucleic acid (PNA) conformation and polymorphism in PNA-DNA and PNA-RNA hybrids**. *Proc. Natl. Acad. Sci. U.S.A*. **1993**, *90*, 9542-9546.

130. Lagriffoule, P.; Egholm, M.; Nielsen, P. E.; Buchardt, O: **The synthesis, co-oligomerization and hybridization of a thymine-thymine heterodimer containg PNA**. *Bioorg. Med. Chem. Lett*. **1994**, *4*, 1081-1084.

131. (a) Jordan, S.; Schwemler, C.; Kosch, W.; Kretschmer, a.; Schwemnner, E.; Stropp, U.; Mielke, B. **Synthesis of new building blocks for peptide nucleic acids containing monomers with variations in the backbone**. *Bioorg. Med. Chem. Lett*. **1997**, *7*, 681-686. (b) Jordan, S.; Schwemler, C.; Kosch, W.; Kretschmer, a.; Schwemnner, E.; Stropp, U.; Mielke, B: **New hetero-oligomeric peptide nucleic acids with improved binding properties to complementary DNA**. *Bioorg. Med. Chem. Lett*. **1997**, *7*, 687-692.

132. Gangamani, B. P.; Kumar, V. A.; Ganesh, K. N: **Synthesis of *N*-(purinyl/pyrimidinyl acetyl)-4-aminoproline diastereomers with potential use in PNA synthesis**. *Tetrahedron* **1996**, *52,* 15017.

133. (a) Lowe, G.; Vilaivan, T: **Amino acids bearing nucleobases for the synthesis of novel peptide nucleic acids**. *J. Chem. Soc. Perkin Trans 1* **1997**, 539-546. (b) Lowe, G.; Vilaivan, T: **Solid phase synthesis of novel peptide nucleic acids**. *J. Chem. Soc. Perkin Trans 1* **1997**, 555-560.

134. Haaima, G.; Hansen, H. F.; Christensen, L.; Dahl, O.; Nielsen, P. E: **Increased DNA binding and sequence discrimination of PNA upon incorporation of Diaminopurine**. *Nucleic Acid Res*. *1997*, *25*, 4639-4643.

135. (a) Gangamani, B. P.; Kumar, V. A.; Ganesh, K. N: **2-Aminopurine peptide nucleic acids (2*ap*PNA):Intrinsic fluorescent PNA analogs for probing PNA-DNA interaction dynamics**. *J. Chem. Soc. Chem. Commun*. **1997**, 1913-1914. (b) Gangamani, B. P.; Kumar, V. A.; Ganesh, K. N: *Biochem. Biophys. Res. Commun*. **1997**, *240*, 778.

136. Eldrup, A. B.; Dahl, O.; Nielsen, P. E: **A novel peptide nucleic acid monomer for recognition of thymine in triple helix structures**. *J. Am. Chem. Soc*. **1997**, *119*, 11116-11117.

137. Timar, Z.; Bottaka, S.; Kovacs, L.; Penke, B: **Synthesis and preliminary thermodynamic investigation of hypoxanthine containing peptide nucleic acids**. *Nucleosides Nucleotides* **1999**, *18*, 1131-1133.

138. Bergamann, F.; Bannwarth, W.; Tam, S: **Solid phase synthesis of directly linked PNA-DNA-hybrids**. *Tetrahedron Lett*. **1995**, *36*, 6823.

139. Petersen, K. H.; Buchardt, O.; Nielsen, P. E: **Synthesis and oligomerization of Nδ-Boc-Nα-) thymin-1-yl-acetyl)-ornithine**. *Bioorg. Med. Chem. Lett*. **1996**, *6*, 793-796.

140. Van der Laan, A. C. *et al*: **A convenient automated synthesis of PNA-(5')-DNA—(3')-PNA chimera**. *Tetrahedron Lett*. **1997**, *38*, 2249-2252.

141. Koch, T. et al: **PNA-peptide chimerae**. *Tetrahedron Lett*. **1995**, *36*, 6933-6936.

142. Qrum, H.; Nielsen, P. E.; Jorgensen, M.; Larsson, C.; Stanley, C. Koch, T: **Sequence specific purification of nucleic acids by PNA-controlled hybridization selection.** *Biotechniques* **1995**, *19*, 472.

143. Verheijen, J. C. *et al*.: **Incorporation of a 4-hydroxy-N-acetylprolinol nucleotide analogue improves the 3'-exonuclease stability of 2'—5'-oligoadenylate-antisense conjugates**. *Bioorg. Med. Chem. Lett*. **2000**, *10*, 801-804.

144. Harrison, J. G.; Frier, C. Laurant, R.; Dennis, R.; Rancy, K. D.; Balasubramanian, S. **Inhibition of human telomerase by PNA-cationic peptide conjugates**. *Bioorg. Med. Chem. Let*. **1999**, *9*, 1273-1278.

145. Knudsen, H. PhD. Thesis university of Cophenhagen, 1997: T. Ljungstrom, H.; Knudsen, H.; Nielsen, P. E.

146. (a) Derossi, D.; Joliot, A. H.; Chassaing, G.; Prochiantz, A: **The third helix of the Antennapedia Homeodomain translocates through biological membranes**. *J. Biol. Chem*. **1994**, *269*,10444-10450. (b) Richard, J. P. et al. **Cell-penetrating Peptides: A reevaluation of the mechanism of cellular uptake**. *J. Biol. Chem*. **2003**, *278*, 585-590.

147. Nagahara, H. *et al*: **Transduction of full-length TAT fusion proteins into mammalian cells: TAT-p27 (KiP1) induces cell migration**. *Nat. Med*. **1998**, *4*, 1449-1452.

148. (a) Pooga, M. *et al*. *Nature Biotechnol*. **1998**, *16*, 857. (b) de Koning, M. C. et al: **Synthetic developments towards PNA-peptide conjugates**. *Curr. Open. Chem.. Biol*. **2003**, *7*, 734-740. (c) Mier, W. *et al*: **Peptide-PNA conjugate: Targeted transport of antisense therapeutics in to tumors**. *Angew. Chem. Int. Ed*. **2003**, *42*, 1968-1971.

149. Zhou, P. *et al*: **Novel binding and efficient cellular uptake of guanidine-based peptide nucleic acids (GPNA)**. *J. Am. Chem. Soc*. **2003**, *125*, 6878-6879.

150. Nielsen, P. E.; Egholm, M.; Berg, R. H.; Buchardt, O: **peptide nucleic acids (PNAs): potential antisense and antigene agents**. *Anti-Cancer Drug Design* **1993**, *8*, 53-63.

151. Koppelhus, U. *et al*: **Efficient in vitro inhibition of HIV I *gag* reverse transcription by peptide nucleic acid (PNA) at minimal ratios of PNA/RNA**. *Nucleic Acid Res*. **1997**, *25*, 2167-2173.

152. Norton, J. C.; Piatyszek, M. A.; Wright, W. E.; Shay, J. W.; Corey, D. R: **Inhibition of human telomerase activity by peptide nucleic acids**. *Nat. Biotech*. **1996**, *14*, 615-620.

153. Hamilton, S. E.; Simmons, C. G.; Kathiriya, I. S.; Corey, D. R: **Cellular delivery of peptide nucleic acids and inhibition of human telomerase**. *Chem. Biol*. **1999**, *6*, 343-351.

154. Qrum, H.; Nielsen, P. E.; Egholm, M.; Berg, R. H.; Buchardt, O.; Stanley, C: **single base pair mutation analysis by PNA directed PCR clamping**. *Nucleic acid Res*. **1993**, *21*, 5332-5336.

155. Thiede, C.; Bayerdoerffer, E.; Blasczyk, R.; Wittig, B.; Neubauer, A: **Simple and sensitive detection of mutations in the ras proto-oncogenes using PNA-mediated PCR-clamping.** *Nucleic Acid Res*. **1996**, *24*, 983-984.

156. Demers, D. B.; Curry, E. T.; Egholm, M.; Sozer, A. C.; **Enhanced PCR amplification of VNTR locus DIS80 using peptide nucleic acid (PNA)**. *Nucleic Acid Res*.**1995**, *23*, 3050-3055.

157. Lansdrop, P. M. *et al*. *Hum. Mol. Genet*. **1996**, *5*, 685-691.

158. Weiler, J. *et al*. **Hybridization based DNA screening on Peptide nucleic acid (PNA) oligomer arrays**. *Nucleic Acid Res*. **1997**, *25*, 2792-2799.

159. Demidov, V. Frank-Kamenetskii, M. D.; Egholm, M.; Buchardt, O.; Nielsen, P. E: **Sequence selective double strand DNA cleavage by PNA targeting using nuclease S1**. *Nucleic Acid Res*. **1993**, *21*, 2103-2107.

160. Nielsen, P. E.; Egholm, M.; Berg, R. H.; Buchardt, O: **Sequence specific inhibition of restriction enzyme cleavage by PNA**. *Nucleic Acid Res*. **1993**, *21*, 197-200.

161. Veselkov, A. G.; Demidov, V.; Nielsen, P. E.; Frank-Kamenetskii, M. D. **A new class of genome rare cutters**. *Nucleic Acid Res*. **1996**, *24*, 2483-2487.

162. Strobel, S. A.; Dervan, P. B: **Single-site enzymatic cleavage of yeast genomic DNA mediated by triplex formation**. *Nature*, **1991**, *350*, 172-174.

163. (a) Uhlmann, E.; Peyman, A: **Antisense oligonucleotides: A new therapeutic principles**. *Chem. Rev*. **1990**, *90*, 543-584. (b) De Mesmaeker, A.; Haener, R.; Martin, P.; Moser, H. E: **Antisense oligonucleotides**. *Acc. Chem. Res*. **1995**, *28*, 366-374. (c) Micklefield, J: **Backbone modification of nucleic acids: Synthesis, structure and therapeutic applications**. **Curr. Med. Chem. 2001**, *8*, 1157-1179. (d) Frier, S. M.; Altmann, K. –H. *Nucleic Acid Res*. **1997**, *25*, 4429-4443. (d) Kool, E. T: **Preorganization of DNA: Design principles for improving nucleic acid recognition by synthetic oligonucleotides**. *Chem. Rev*. **1997**, *97*, 1473-1488.

164. (a) Ganesh, K. N.; Nielsen, P. E: **Peptide nucleic acids: analogs and derivatives**. *Curr. Org. Chem.* **2000**, *4*, 1931-1943. (c) Kumar, V. A: **Structural preorganization of peptide nucleic acids: Chiral cationic analogues with five- or six-membered ring structures**. *Eur. J. Org. Chem*. **2002**, 2021-2032.

165. Menchise, V.; Simone, G. D.; Tedeschi, T, Corradini, R.; Sforza, S.; Marchelli, R.; Capasso, D.; Saviano, M.; Pedone, C : **Insights into peptide nucleic acid (PNA) structural features :**

The crystal structure of a D-lysine-based chiral PNA-DNA duplex. *Proc. Natl. Acad. Sci (USA)*, **2003**, *100*, 12021-12026.

166. Drauz, K.; Waldmann, H; (eds): Enzyme Catalysis in Organic Synthesis. Vol. II, Wiley-VCH, 2002. (b) Bornscheuer, U. T.; Kazlauskas, R. J; (eds): **Hydrolases in Organic Synthesis: Regio- and stereoselective Biotransformations**. Wiley-VCH, **1999**.

167. (a) Francalanci, F.; Cesti, P.; Cabri, W.; Bianchi, D.; Martinengo, T.; Foa, M. *J. Org. Chem*. **1987**, *52*, 5079. (b) Gotor, V.; Brieva, R.; Rebolledo, F. *J. Chem. Soc. Chem. Commun*. **1988**, 957. (c) Fernandez, S.; Brieva, R.; Rebollendo, F.; Gotor, V. *J. Chem. Soc. Perkin Trans. 1*. **1992**, 2885. (d) Ader, U.; Schneider, M. P: **Enzyme assisted preparation of enantiomerically pure -adrenergic blockers and facile screening method for suitable biocatalysts**. *Tetrahedron: asymmetry* **1992**, *3*, 201. (e) Lundell, K.; Kanvera, L. T: **Enantiomers of ring substituted 2-amino-1-phenyl ethanols by *Pseudomonas cepacia* lipase**. *Tetrahedron: Asymmetry* **1995**, *6*, 2281.

168. Godchot, R. M.; Mousseron, M. *Compt. Rend*. **1932**, *194*, 981.

169. (a) Faber, K.; Honig, H.; Seufer-Wasserthal, P: **A novel and efficient synthesis of (+)- and (-)-*trans*-2-aminocyclohexanol by enzymatic hydrolysis**. *Tetrahedron Lett*. **1988**, *29*, 1903-1904. (b) Honig, H.; Seufer-Wasserthal, P: **Enzymatic resolutions of cyclic amino alcohol precursors**. *J. chem.. Soc. Perkin Trans. 1* **1989**, 2341-2345.

170. Swift, G.; Swern, D: **Stereospecific synthesis of *cis* and *trans*-1,2-diaminocyclohexanes and aliphatic vicinal diamines**. *J. Org. Chem*. **1967**, *32*, 511-517.

171. Hofle, G.; Steglich, W.; Vobruggen, H: **4-Dialkylaminopyridines as highly active acylation catalysts**. *Angew. Chem. Int. Ed*. **1978**, *17*, 569-583.

172. (a) Goering, H. L.; Eikenberry, J. N.; Koermer, G. S: **Tris-[(3-trifluromethylhydroxymethylene)-d-camphorato] europium (III). A chemical shift reagent for direct detrmination of enantiomeric compositions**. *J. Am. Chem. Soc*. **1971**, *93*, 5913-5914. (b) McCreary, M. D.; Lewis, D. W.; Wernick, D. L.; Whitesides, G. M: **The determination**

of enantiomeric purity using chiral lanthanide shift reagents. *J. Am. Chem. Soc*. **1974**, *96*, 1038. (c) Peterson, P. E.; Stepanian, M: **Methodology for analysis of products from asymmetric synthesis using chemical NMR shift reagents. Relative complexation constants of enantiomers**. *J. Org. Chem*. **1988**, *53*, 1907-1911. d) Gogte, V. N.; Pandit, V. S.; Natu, A. A.; Nanda, R. K.; Sastry, M. K. *Org. Magn. Res*. **1984**, *22*, 624-630.

173. Schaus, S. E.; Larrow, J. F.; Jacobsen, E. N: **Practical synthesis of enantiopure cyclic 1,2-amino alcohols via catalytic asymmetric ring opening of mesoepoxides**. *J. Org. Chem*. **1997**, *62*, 4197-4199.

174. Sanjayan, G. J.; pedireddi, V. R.; Ganesh, K. N: **Cyanuryl-PNA monomer: synthesis and crystal structure**. *Org. Lett*. **2000**, *2*, 2825-2828.

175. Egholm, M.; Buchardt, O.; Nielsen, P. E: **Peptide nucleic acids (PNAs): Oligonucleotide analogues with an achiral peptide backbone**. *J. Am. Chem. Soc*. **1992**, *114*, 1895-1897.

176. Egholm, M.; Nielsen, P. E.; Buchardt, O. Berg, R. H: **Recognition of guanine and adenine in DNA by cytosine and thymine containing peptide nucleic acids (PNAs)**. *J. Am. Chem. Soc*. **1992**, *114*, 9677-9678.

177. Dueholm, K. L.; Egholm, M.; Behrens, C.; Christensen, L.; Hansen, H. F.; Vulpius, T.; Petersen, K. H.; Berg, R. H.; Nielsen, P. E.; Buchardt, O: **Synthesis of peptide nucleic acid monomers containing the four natural bases: Thymine, cytosine, adenine, and guanine and their oligomerization.** *J. Org. Chem*. **1994**, *59*, 5767-5773.

178. Ando, T.; Yamawaki, J: **Potassium fluoride in Celite. A versatile reagent for C-, N-. O-, and S-alkylations**. *Chem. Lett*. **1979**, *1*, 45.

179. Merrifield, R. B: **Solid phase synthesis. I. The synthesis of a tetrapeptide**. *J. Am. Chem. Soc*. **1963**, *85*, 2149-2154.

180. (a) Mckay, F. C.; Albertson, N. F: **New amine-masking groups for peptide synthesis**. *J. Am. Che. Soc*. **1957**, *79*, 4686-4690. (b) Anderson, G. W.; McGreoger, A. C: ***t*-Butyloxycarbonyl aminoacids and their use in peptide synthesis**. *J. Am. Chem. Soc*. **1957**, *79*, 6180-6183.

181. Schlatter, J. M.; Mazur, R. H.; Goodmonson, O: **Hydrogenation in solid phase peptide synthesis. I. Removal of product from the resin**. **Tetrahedron Lett**. **1977**, 2851-2852.

182. Wright, D. E.; Agarwal, N. s.; Hruby, Victor, J: **Synthesis of protected secretin 16-27 on a Merrifield resin. Examination of ammonlysis conditions of preparing carboxamide terminal protected peptides suitable for fragment condensation**. *Int. J. Pept. Protein Res*. **1980**, *15*, 271-278.

183. Barn, D. R.; Richard, M. J.; David, C. R: **synthesis of an array of amides by aluminium chloride assisited cleavage of resin-bound esters**. *Tetrahedron Lett*. **1996**, *37*, 3213-3216.

184. Matsueda, G. R.; Stewart, J. M: **A *p*-methyl benzhydryl amine resin for improved solid-phase synthesis of peptide amides**. *Peptides* **1981**, *2*, 45-50.

185. Erickson, B. w.; Merrifield, R. B: **Solid Phase Peptide Synthesis**. In the Proteins Vol. II, 3rd ed.; Neurath, H. and Hill, R. L. eds.; Academic Press, New York, **1976**, pp 255.

186. Merrifield, R. B.; Stewart, J. M.; Jernberg, N: **Instrument for automated synthesis of peptides**. *Anal. Chem*. **1966**, *38*, 1905-1914.

187. (a) Kaiser, E.; Colescott, R. L.; Bossinger, C. D.; Cook, P. I: **Color test for the detection of free terminal amino groups in the solid phase synthesis of peptides**. *Anal. Biochem*. **1970**, *34*, 595-598. (b) Kaiser, E.; Bossinger, C. D.; Cplescott, R. L.; Olsen, D. B: **Color test for terminal prolyl residues in the solid phase synthesis of peptides**. *Anal. Chim. Acta*. **1980**, *118*, 149-151. (c) Sarin, V. K.; Kent, S. B. H.; Tam, J. P.; Merrifield, R. B: **Quantitative monitoring of solid phase peptide synthesis by ninhydrin reaction**. *Anal. Biochem*. **1981**, *117*, 147.

188. Christensen, T. *Acta, chem.. Scand*. **1979**, *34*, 594-598.

189. Madder, A.; Farcy, N.; Hosten, N. G. C.; De Muynck, H.; De Clereq, P.; Barry, J.; Davis, A. P: *Eur. J. Org. Chem*. **1999**, *11*, 2787-2791.

190. Pietta, P. G.; Marshall, G. R. *J. Chem. Soc. D*. **1970**, 650-651.

191. Christensen, L.; Fitzpatrick, R.; Gildea, B.; Petersen, K. H.; Hansen, H. F.; Koch, T.; Egholm, M.; Buchardt, O.; Nielsen, P. E.; Coull, J.; Berg, R. H. *J. Peptide Sci*. **1995**, *3*, 175.

192. (a) Gait, J. M: **Oligonucleotide synthesis: A practical approach**. IRL Press Oxford, Uk 217, 1984. (b) Agrawal, S: in **Protocols for oligonucleotides and analogs: Synthesis and properties**. *Methods in Molecular Biology*. Agrawal, S. (ed): vol 20: Totowa, NJ. Humana Press, Inc., **1993**.

193. (a) Job, P. *Ann. Chim*. **1928**, *9*, 113-203. (b) Cantor, C. R.; Schimmel, P. R. *Biophys. Chem. Part III* **1980**, 624.

194. Petersen, K. H.; Jensen, K. D.; Buchardt, O.; Nielsen, P. E: **A PNA-DNA linker synthesis of N-((4,4'-dimethoxytrityloxy)-ethyl)-N-(thymin-10ylacetyl)glycine.** *Bioorg. Med. Chem. Lett*. **1995**, *5*, 1119-1124.

195. Sambrook, J.; Fritsch, E. F.; Maniatis, T. In **Molecular Cloning: A Laboratory Manual**, 2; Cold Spring Harbor Laboratory Press: Cold Spring Harbor, NY. **1989**.

196. (a) Lambert, J. B.; Papay, J. J.; Khan, S. A.; Kappauf, K. A.; Magyar, E. S: **Conformational analysis of five membered rings**. *J. Am. Chem. Soc*. **1974**, *96*, 6112-6118. (b) Abraham, R. J.; Koniotou, R.; Sancassan, F: **Conformational analysis: part 39. A theoretical and lanthanide induced shift (LIS) investigation of the conformations of cyclopentanol and *cis* and *trans*-cyclopentane-1,2-diol**. *J. Chem. Soc. Perkin Trans*. **2002**, 2025-2030.

197. (a) Epple, C.; Leumann, C. J. *Chem. Biol*. **1998**, *5*, 209-216. (b) Robertc, C. D.; Epple, C.; Leumann, C. J: *Nucleosides Nucleotides* **1999**, *18*, 1413-1415. (c) Keller, B. M.; Leumann, C. J: **Bicyclo[3.2.1]DNA: On the structural and energetic role of the furanose subunit in complementary strand recognition of DNA**. *Angew. Chem. Int. Ed*. **2000**, *39*, 2278-2281.

198. (a) Egger, A.; Hunziker, J.; Rihs, G.; Leumann, C. *Helv. Chim. Acta* **1998**, *82*, 734-743. (b) Ahn, D. –R.; Egger, A.; Lehmann, C.; Pitsch, S.; Leumann, C: **Bicyclo[3.2.1]amide-DNA: A chiral, nonchiroselective base-pairing system**. *Chem. Eur. J*. **2002**, *8*, 5312-5322.

199. Ahn, D. R.; Mosimann, M.; Leumann, C: **Synthesis of cyclopentane amide DNA (cpa-DNA) and its pairing properties**. *J. Org. Chem*. **2003**, *68*, 7693-7699.

200. a) Myers, M. C.; Witschi, M. A.; Larionova, N. V.; Franck, J. M.; Haynes, R. D.; Hara, T.; Grajkowski, A.; Appella, D. H: **A cyclopentane conformational restraint for a peptide nucleic acid:Design, asymmetric synthesis, and improved binding affinity to DNA and RNA**. *Org. Lett*. **2003**, *5*, 2695-2698. (b) Pokorski, J. K.; Witschi, M. A.; Purnell, B. L.; Appella, D. H; **(*S*,*S*)-trans-cyclopentane-constrained peptide nucleic acids. A general backbone modification that improves binding affinity and sequence selectivity**. *J. Am. Chem. Soc*. **2004**, *126*, 15067-15073.

201. (a) Blandamer, M. J.; Cullis, P. M.; Engberts, J. B. F. N: **Titration microcalorimetry**. *J. Chem. Soc., Faraday Trans.* **1998**, *94*, 2261-2267. (b) Blandamer, M. J. **Biocalorimetry: Applications of calorimetry in biological sciences**. Ed., Ludbary, J.; Chowdhry, B. Z., Wiley, Chichester, **1998**. (c) Pierce, M. M.; Raman, C. S.; Nall, B. T: **Isothermal titration calorimetry of protein-protein interactions**. *Methods* **1999**, *19*, 213-221. (d) Malulis, D.; Rouzina, J.; Bloomfield, V. A: **Thermodynamics of DNA binding and condensation: Isothermal titration calorimetry and electrostatic mechanism**. *J. Mol. Biol*. **2000**, *296*, 1053-1063.

202. Shawrz, F. P.; Robinson, S.; Butler, J. M: **Thermodynamic comparison of PNA/DNA and DNA/DNA hybridization reactions at ambient temperature**. *Nucleic Acid. Res*. **1999**, *27*, 4792-4800.

203. Demidov, V. V.; Frank-Kamenetskii, M. D: **Two sides of the coin: affinity and specificity of nucleic acid interactions**. *Trends in Biochemical Sciences*. **2004**, *29*, 62-71.

204. (a) Gangamani, B. P.; Kumar, V. A.; Ganesh, K. N: **Chiral analogs of peptide nucleic acids: Synthesis of 4-aminoprolyl nucleic acids and DNA complementation studies using**

UV/CD spectroscopy. *Tetrahedron* **1999**, *55*, 177-192. (b) Gangamani, B. P.; De Costa, M.; Kumar, V. A.; Ganesh, K. N: **Conformationally restrained chiral PNA conjugates: synthesis and DNA complementation studies**. *Nucleosides and Nucleotides* **1999**, *18*, 1409-1411.

205. Slaitas, A.; Yeheskiely, E: **Synthesis and hybridization of novel chiral pyrrolidine based PNA analogue**. *Nicleosides, Nucleotides and Nucleic acids*. **2001**, *20*, 1377-1379.

206. Puschl, A.; Boesen, T.; Zuccarello, O.; Dahl, O.; Pitsch, S.; Nielsen, P. E: **Synthesis of Pyrrolidinone PNA: A novel conformationally restricted PNA analogues**. *J. Org. Chem*. **2001**, *66*, 707-712.

207. Schutz, R.; Cantin, M.; Roberts, C.; Greiner, B.; Uhlmann, E.; Leumann, C: **Olefinic peptide nucleic acids (OPAs). New aspects of the molecular recognition of DNA by PNA**. *Angew. Chem. Int. Ed*. **2000**, *39*, 1250-1253.

208. Sharma, N. K.; Ganesh, K. N: **Expanding the repertoire of pyrrolidinyl PNA analogues for DNA/RNA hybridization selectivity: aminoethylpyrrolidinone PNA (*aepone*-PNA)**. *Chem. Commumn*. **2003**, *19,* 2484-2485.

209. De Costa, M.; Kumar, V. A.; Ganesh, K. N: **Aminoethylprolyl peptide nucleic acids (*aep*PNA): Chiral PNA analogues that form highly stable DNA:*aep*PNA$_2$ triplexes**. *Org. Lett*. **1999**, *1*, 1513-1516.

210. (a) Kumar, V. A.; De Costa, M.; Ganesh, K. N. *Nucleosides, Nucleotides and Nucleic acids* 2001, 20, 1187-1191. (b) De costa, M.; Kumar, V. A.; Ganesh, K. N: **Aminoethylprolyl (*aep*) PNA: Mixed purine/pyrimidines oligomers and binding orientation preferences for PNA:DNA duplex formation**. *Org. Lett*. **2001**, *3*, 1281-1284.

211. Vilaivan, T.; Khongdeesameor, C.; Harnyuttanokorn, P.; Westwell, M. S.; Lowe, G.: **Synthesis and properties of chiral peptide nucleic acids with a N-aminoethyl-D-proline backbone**. *Bioorg. Med. Chem. Lett*. **2000**, *10*, 2541-2545.

212. (a) Hickman, D. T.; King, P. M.; Cooper, M. A.; Slater, J. M.; Micklefield, J: **Unusual RNA and DNA binding properties of a novel pyrrolidine-amideoligonucleotide mimic**. *Chem. Commun*. **2000**, 2251-2252. (b) Hickman D. T.; Tan, T. H. S.; Morral, J.; King, P. M.; Cooper, M. A.; Micklefield, J: **Design, synthesis, conformational analysis and nuclec acid hybridization properties of thymidyl pyrrolidine-amide oligonucleotide mimic (POM)**. *Org. Biomol. Chem*., **2003**, *1*, 3277-3292. (c) Hickman, D. T.; King, P. M.; Cooper, M. A.; Slater, J. M.; Micklefield, J: **Nucleic acid binding properties of thyminyl and adeninyl pyrrolidine-amide oligonucleotide mimics**. *Chem. Commun*. **2004**, 516-517.

213. Puschl, A.; Tedeschi, T.; Nielsen, P. E: **Pyrrolidine PNA: A novel conformationally restricted PNA analogue**. *Org. Lett*. **2000**, *2*, 4161-4163.

214. Kumar, V. A.; Meena: **Synthesis of *trans*-L/D-2-(*tert*-butyloxycarbonyl-aminomethyl)-4-(thymin-1-yl) pyrrolidin-1-yl acetic acid**. *Nucleosides. Nucleotides & Nucleic Acids*, **2003**, *22*, 1285-1288.

215. Vilaivan, T.; Khongdeesameor, C.; Harnyuttanokorn, P.; Lowe, G.: **Synthesis and properties of novel pyrrolidinyl PNA carrying β-amino acid spacers**. *Tetrahedron Lett*. **2001**, *42*, 5533-5536.

216. (a) Meena, Kumar, V. A.; Ganesh, K. N. *Nucleosides, Nucleotides and Nucleic Acids*. **2001**, 20, 1193-1196. (b) Meena; Kumar, V. A.: **Pyrrolidine carbamate nucleic acids: synthesis and DNA binding studies**. *Boorg. Med. Chem.* **2003**, *11*, 3393-3399.

217. Ceulemans, G.; Aerschot, A. V.; Rozenski, J.; Herdewijn, P.: **Oligonucleotides with 3-hydroxy-N-acetylprolinol as sugar substitute**. *Tetrahedron* **1997**, *53*, 14957-14974.

218. Kakefuda, A.; Masuda, A.; Ueno, Y.; Ono, A.; Matsuda, A.: **Nucleosides and Nucleotides. 147. Synthesis of DNA dodecamers containing Oxetanocin A and (2*R*,3*R*)-2-(adenin-9-yl)-1,4-anhydro-2,3-dideoxy-3-C-hydroxymethyl-D-arabitol**. *Tetrahedron* **1996**, *52*, 2863-2876.

219. (a) Katagiri, N.; Morishita, Y.; Yamaguchi, M.: **Highly regio- and enantio-selective deacylation of carbocyclic 3',5'-di-O-acyloxetanocins by lipases**. *Tetrahedron Lett*. **1998**, *39*,

2613-2616. (b) Katagiri, N.; Morishita, Y.; Oosawa, I.; Yamaguchi, M.: **Artificial oligonucleotides consisting of an analog of nucleoside antibiotics, carbocyclic axetanocins**. *Tetrahedron Lett*. **1999**, *40*, 6835-6840. (c) Honzawa, S.; Ohwada, S.; Morishita, Y.; Sato, K.; Katagiri, N.; Yamaguchi, M.: **Synthesis and hybridization property of oligonucleotides containing carbocyclic Oxetanocins**. *Tetrahedron* **2000**, *56*, 2615-2627.

220. C. J. Wilds, G. Minasov, F. Natt, P. Von Matt, K. –H. Altamann, M. Egli, *Nucleosides Nucleotides and Nucleic Acids,* 2001, **20**, 991-994.

221. (a) Meena, V. A. Kumar: **Pyrrolidine PNA-DNA chimeric oligonucleotides with extended backbone**. *Nucleosides. Nucleotides & Nucleic Acids*, **2003**, *22*, 1101-1104. (b) V. Kumar, P. S. Pallan, Meena, K. N. Ganesh: **Pyrrolidine nucleic acids: DNA/PNA oligomers with 2-hydroxy/aminomethyl-4-(thymin-1-yl) Pyrrolidine-N-acetic acid**. *Org. Lett*. **2001**, **3**, 1269-1272.

222. (a) Robinson, D. S.; Greenstein, J. P. J. Biol. Chem. 1952, 195, 383-388. (b) Webb, T. R.; Eigenbrot, C: **Conformationally restricted Arginine analogue**. *J. Org. Chem*. **1991**, *56*, 3009-3016.

223. Ramuzon, P: ***trans*-4-Hydroxy-L-Proline, a useful and versatile chiral starting block**. *Tetrahedron*, **1996**, *52*, 13803-13835.

224. Williums, M. A.; Rapport, H.: **Synthesis of conformationally constrained DTPA analogs. Incorporation of the ethylene diamine units as aminopyrrolidines**. *J. Org. Chem*. **1994**, *59*, 3616-3625.

225. Mitsunobu, O.: **The use of diethyl azodicarboxylate and triphenylphosphine in synthesis and transformation of natural products**. *Synthesis* **1981**, *1*, 1-28.

226. (a) Rabinowitz, J. L.; Gurin, S.: **Some pyrimidines derivatives**. *J. Am. Chem. Soc*. *1953*, *75*, 5758-5759. (b) Cruickshank, K. A.; Jiricny, F.; Reese, C. B.: **The benzylation of uracil and thymine**. *Tetrahedron Lett*. **1984**, *25*, 681-684.

227. Sheradsky, T. **In Chemistry of the Azido Group**; Patai, S., Ed.; Inter Science: New York, **1971**; p 331.

228. Lucet, D.; Le Gall, T.; Mioskowski, C: **The chemistry of vicinal diamines**. *Angew. Chem. Int. Ed*. **1998**, *37*, 2580.

229. (a) Butcher, J. W.; Liverton, N. J.; Selnick, H. G.; Elliot, J. M.; Smith, G. R.; Tebben, A. J.; Pribush, D. A.; Wai, J. S.; Claremon, D. A: **Preparation of 3-amino-1,4-benzodiazepin-2-ones via direct azidation with trisyl azide**. *Tetrahedron Lett*. **1996**, *37*, 6685-6688. (b) Reddy, G. V.; Rao, G. V.; Iyengar, D. S: **A novel, simple, chemoselective and practical protocol for the reduction of azides using In/NH_4Cl**. *Tetrahedron Lett*. **1999**, *40*, 3937-3938.

230. Park, S. H: **Acceleration of azidation by microwave irradiation**. *Bull. Korean Chem. Soc*. **2003**, *24*, 253-255.

231. (a) Caddick, S: **Microwave assisted organic reactions**. *Tetrahedron* **1995**, *51*, 10403-10432. (b) Varma, R. S: **Solvent-free organic synthesis using supported reagents and microwave reaction**. *Green Chemistry*, **1999**, 43-55. (c) Caddick, S.; Mccarroll, A. J.; Sandham, D. A: **A convenient and practical method for selective benzylation of primary hydroxyl groups using microwave heating**. *Tetrahedron* **2001***, 57*, 6305-6310. (d) Lidstrom, P.; Tierney, J.; Wathey, B.; Westman, J: **Microwave assisted organic synthesis-A review**. *Tetrahedron* **2001**, *57*, 9225-9283. (e) Wathey, B.; Tierney, J.; Lidstrom, P.; Westman, J: **The impact of microwave-assisted organic chemistry on drug discovery**. *Drug discovery Today*, **2002**, *7*, 373-380. (f) Hayes, B. L. **In *Microwave Synthesis: Chemistry at the Speed of Light***; Eds; CEM Publishing: NC, **2002**.

232. Banik, B. K.; Barakat, K. J.; Wagle, D. R.; Manhas, M. S.; Bose, A. K: **Microwave assisted rapid and simplified hydrogenation**. *J. Org. Chem*. **1999**, *64*, 5746-5753.

233. Nagamani, D.; Ganesh, K. N: **Pyrrolidinyl polyamines: Branched chiral poly amine analogues that stabilize DNA duplexes and triplexes**. *Org. Lett*. **2001**, *3*, 103-106.

234. (a) Rho, Y. S.; Kim, A. E.; Jung, J. C.; Shin, C. C; Chang, S. G: **Anticancer cytotoxicity and nephrotoxicity of the new platinum (II) complexes containing diaminocyclohexane and glycolic acid**. *International Journel of Oncology*, **2002**, *20*, 929-935. (b) Conner, T. A.; Jones, M.; Ross, W. C: **New platinum complexes with antitumor activity**. *Chem. Biol. Interact.* **1972**, *5*, 415-424. (c) Gale, G. R.; Walker, E. M.; Atkins, L. M: **Antileukemic properties of dichloro-(1,2-diamino cyclohexane) platinum (II)**. *Res. Commun. Chem. Pathol. Pharmacol*. **1974**, *7*, 529-534. (c) Rho, Y. S.; Lee, H. J.; Yoon, J. K.; Jung, J. C. *Bull. K. H. Pharma. Sci.* **2000**, *28*, 1. (d) Chang, S. G.; Kim, J. I.; Jung, J. C.; Rho, Y. S.; Lee, K. T.; Zilian, Wang, X.; Hoffman, R. M: **Antimetastatic activity of the new platinum analog {Pt (*cis*-dach) (DPPE). $2NO_3$}**. *Anticancer Research*. **1997**, *17*, 3239-3242. (e) Chang, S. G.; Jung, J. C.; Rho, Y. S.; Huh, J. s.; Kim, J. I.; Hoffman, R. M: **Efficacy of the platinum analog { Pt (*cis*-dach) (DPPE)-2 NO_3} on histocultured human patial bladder tumors and cancer cell lines**. *Anticancer Reasearch*, **1996**, *16*, 3423-3428. (f) Rosenberg, B.; Vancamp, L.; Trosko, J. E.; Mansour, V. H: **Platinum compounds: a new class of potent antitumor agents**. *Nature*, **1969**, *222*, 385-386. (g) Pasini, A.; Zunino, F: **New *cis*-platinum analogues- on the way to better antitumour agents**. *Angew. Chem. Int. Ed*. **1987**, *26*, 615-624. (h) Brunner, H.; Hankofer, P.; Holzinger, U.; Triettinger, B.; Schonenberger, H: **Synthesis and antitumour activity of platinum (II) complexes containing substituted thylene diamine ligands**. *Eur. J. Med. Chem.* **1990**, *25*, 35-44. (i) Kelland, L. R.; Abel, G.; Mekeage, M. J.; Jones, M.; Goddard, M.; Valenti, M.; Murrer, B. A.; Harrap, K. R: **Preclinical antitumour evaluation of bis-acetato-ammine-dichloro cyclohexylamine platinum (IV): An orally active platinum drug**. *Cancer Res*. **1993**, *53*, 2581-2586. (j) Khokhar, A. R.; Al-Baker, S.; Shamsuddin, S.; Siddik, Z. H: **Chemical and biological studies on a series of novel [*trans*-(1*R*,2*R*)-, *trans*-(1*S*,2*S*) and *cis*-1,2- diaminocyclohexane) platinum (IV) carboxylate complexes**. *Bioorg. Med. Chem. Lett.* **1997**, *40*, 112-116. (k) Miller, K. J.; McCarthy, S. L.; Krauss, M: Binding of cis-(1,2-diaminocyclohexane) platinum (II) and its derivatives to duplex DNA. J. Med. Chem. 1990, 33, 1043-1046.

235. (a) Blazis, V. J.; Koeller, K. J.; Spilling, C. D: **Asymmetric synthesis of α-hydroxy phosphonamides, phosphonates and phosphonic acids**. *Tetrahedron: Assymmetry*, **1994**, *5*,

499-502. (b) Togni, A.; Venanzi, L. M. *Angew. Chem. Int. Ed.* **1994**, *33*, 497. (c) Torneiro, M.; Still, W. C: **Simple synthetic receptors that bind peptides in water**. *Tetrahedron* **1997**, *53*, 8739-8787. (d) Whitesell, J. K. *Chem. Rev*. 1989, 89, 1581. (e) Brunner, H.; Schiessling, H. *Angew. Chem. Int. Ed*. **1994**, *33*, 125. (f) Tokles, M.; Snyder, J. K. *Tetrahedron Lett*. **1986**, *27*, 3951. (g) Arena, C. G.; Casilli, V.; Faraone, F: **New chiral amino-phosphoramidate and *bis*-phosphoramidite ligands derived from (*R*,*R*)-1,2-diaminocyclohexane: Application in Cu-catalyzed asymmetric conjugate addition of diethyl zinc to 2-cyclohexenone.** *Tetrahedron: Assymmetry*, **2003**, *14*, 2127-2131.

236. (a) Jacobsen, E. N. **In *Catalytic Assymmetric Synthesis;*** Ojima. I. Ed.; VCH; Weinheim, **1993**; Chapter 4.2. (b) Katsuki, T: **Catalytic asymmetric oxidation using optically active (salen) manganese (III) complexes as catalysts**. *Coord. Chem. Rev*. **1995**, 140, 189. (c) Jacobsen, E. N: **Asymmetric catalysis of epoxide ring opening reactions**. *Acc. Chem. Res*. **2000**, *33*, 421-431.

237. (a) Hale, K. J.; Domostoj, M. M.; Tocher, D. A.; Irving, E.; Sheinmann, F: **Enantiospecific formal total synthesis of the tumor and GSK-3β inhibiting alkaloid (-)- agelastatin A**. *Org. Lett*, **2003**, *5*, 2927-2930. (b) Luna, A.; Alfonso, I.; Gotor, V: **Biocatalytic approaches towards the synthesis of both enantiomers of *trans*-cyclopentane-1,2-diamine**. *Org. Lett*. **2002**, *4*, 3627-3629. and references there in. (c) Eisenberg, M. A. *in Escherichia coli and salmonella typhimurium*; Vol. 1; Ed.; Neidhardt, F. C. American Society for Microbiology, Washington DC, **1987**, p 544. (d) Marquet, A. *Pure Appl. Chem*. **1993**, *65*, 1249. (e) Baldwin,J. E.; Adlington, R. M.; Birch, D. J: **γ-Lactam analogues of carbapenicillinic acids**. *J. Chem. Soc. Chem. Commun*. **1985**, 256. (f) Dewar, J. H.; Shaw, G. *J. Chem. Soc*. **1962**, 583. (g) Bickel, A. F. *J. Am. Chem. Soc*. **1947**, *65*, 1805.

238. (a) De Costa, B. R.; Bowen, W. D.; Hellewell, S. B.; George, C.; Rothman, R. B.; Reid, R. A.; Walker, J. M.; Jacobsen, A. E.; Rice, K. C. *J. Med. Chem.* **1989**, *32*, 1996. (b) De Costa, B. R.; Rice, K. C.; Bowen, W. D.; Thurkauf, A.; Rothman, R. B.; Band, L.; Jacobsen, A. E.; Radesca, L.; Contreras, P. C.; Gray, N. M.; Daly, I.; Iyengar, S.; Finn, D. T.; Vazirani, S.; Walker,

J. M: **Synthesis and evaluation of N-substituted *cis*-N-methyl-2-(1-pyrrolidinyl) cyclohexyl amines as high affinity σ-receptor probes.** *J. Med. Chem*. **1990**, *33*, 3100-3110. (c) Chen, Z.; Goerying, R. R.; Valenzano, K. J.; Kyle, D. J: **Design and synthesis of novel small molecule N/OFQ receptor antagonists**. *Bioorg. Med. Chem. Lett*. **2004**, *14*, 1347-1351.

239. Kitagawa, O.; Yotsumoto, K.; Kohriyama, M.; Dobashi, Y.; Taguchi, T: **Catalytic asymmetric synthesis of vicinal diamine derivatives through enantioselective *N*-allylation using chiral π–allyl Pd-catalyst**. *Org. Lett*. **2004**, *6*, 3605-3607.

240. Gacheru, S. N.; Trackman, P. C.; Calaman, S. D.; Greenaway, F. T.; Kagan, H. N: **Vicinal diamines as pyrroloquinoline quinone directed irreversible inhibitors of lysyl oxidase**. *J. Biol. Chem*. **1989**, *264*, 12963-12969.

241. www. Cem.com